WHC-EP-0645

Performance Assessment for the Disposal of Low-Level Waste in the 200 West Area Burial Grounds

Prepared for the U.S. Department of Energy
Office of Environmental Management

Westinghouse
Hanford Company Richland, Washington

Hanford Operations and Engineering Contractor for the
U.S. Department of Energy under Contract DE-AC06-87RL10930

RECORD COPY

Approved for Public Release

LEGAL DISCLAIMER

This report was prepared as an account of work sponsored by an agency of the United States Government. Neither the United States Government nor any agency thereof, nor any of their employees, nor any of their contractors, subcontractors or their employees, makes any warranty, express or implied, or assumes any legal liability or responsibility for the accuracy, completeness, or any third party's use or the results of such use of any information, apparatus, product, or process disclosed, or represents that its use would not infringe privately owned rights. Reference herein to any specific commercial product, process, or service by trade name, trademark, manufacturer, or otherwise, does not necessarily constitute or imply its endorsement, recommendation, or favoring by the United States Government or any agency thereof or its contractors or subcontractors. The views and opinions of authors expressed herein do not necessarily state or reflect those of the United States Government or any agency thereof.

This report has been reproduced from the best available copy. Available in paper copy and microfiche.

Available to the U.S. Department of Energy
and its contractors from
Office of Scientific and Technical Information
P.O. Box 62
Oak Ridge, TN 37831
(615) 576-8401

Available to the public from the U.S. Department of Commerce
National Technical Information Service
5285 Port Royal Road
Springfield, VA 22161
(703) 487-4650

Printed in the United States of America

DISCLM-1.CHP (1-91)

WHC-EP-0645
UC-2050

Performance Assessment for the Disposal of Low-Level Waste in the 200 West Area Burial Grounds

M. I. Wood[2]
R. Khaleel[2]
P. D. Rittmann[2]
A. H. Lu[2]
S. H. Finfrock[2]
R. J. Serne1[1]
K. J. Cantrell[1]
T. H. DeLorenzo[2]

[1]Pacific Northwest Laboratory
[2]Westinghouse Hanford Company

Date Published
June 1995

Prepared for the U.S. Department of Energy
Office of Environmental Management

Westinghouse Hanford Company P.O Box 1970 Richland, Washington

Hanford Operations and Engineering Contractor for the
U.S. Department of Energy under Contract DE-AC06-87RL10930

Approved for Public Release

RELEASE AUTHORIZATION

Document Number:	WHC-EP-0645
Document Title:	Performance Assessment for the Disposal of Low-Level Waste in the 200 West Area Burial Grounds
Release Date:	3/30/95

This document was reviewed following the procedures described in WHC-CM-3-4 and is:

APPROVED FOR PUBLIC RELEASE

WHC Information Release Administration Specialist:

V. L. Birkland — V.L. Birkland

5/30/95 — Date

A-6001-400.2 (09/94) WEF256

EXECUTIVE SUMMARY

This document reports the findings of a performance assessment (PA) analysis for the disposal of solid low-level radioactive waste (LLW) in the 200 West Area Low-Level Waste Burial Grounds (LLBG) in the northwest corner of the 200 West Area of the Hanford Site. This PA analysis is required by U.S. Department of Energy (DOE) Order 5820.2A (DOE 1988a) to demonstrate that a given disposal practice is in compliance with a set of performance objectives quantified in the order. These performance objectives are applicable to the disposal of DOE-generated LLW at any DOE-operated site after the finalization of the order in September 1988. At the Hanford Site, DOE, Richland Operations Office (RL) has issued a site-specific supplement to DOE Order 5820.2A, DOE-RL 5820.2A (DOE 1993), which provides additional performance objectives that must be satisfied.

The general type of disposal facility under consideration is a shallow, unlined trench of variable width (~3 to 10 m), length (~50 to 100 m) and depth (~5 to 10 m). Waste is typically packaged in containers (drums or boxes) and placed in trenches to within 2 to 3 m from the surface. Once a trench is filled, a soil cover is placed over the waste. Trenches are typically arranged in parallel fashion with the long axis running due east-west. Two types of disposal facilities are considered in this analysis. The first facility (a Category 1 waste facility) is assumed to have no functional barriers and is intended to contain very low concentrations and quantities of radionuclides in the inventory. The second facility (a Category 3 waste facility) is assumed to have a cover that controls infiltration to the same degree as the natural soil and vegetation system. The option of using

waste-form physical and chemical properties to control radionuclide release in wastes containing high concentrations of long-lived mobile radionuclides (e.g., ^{99}Tc and ^{14}C) is also considered.

Types of waste include paper, plastics, wood, concrete rubble, activated metal, and sludges. A large number of generators provide waste streams with variable waste inventories. Commonly observed radionuclides in these wastes include ^{90}Sr, ^{137}Cs, and uranium. Lesser, but significant, activities of ^{14}C, ^{129}I, and ^{99}Tc are also recorded.

Evaluation of two facility types is being completed for three reasons. First, uncertainties in future waste inventory are extensive because of the large number of generators providing waste for disposal, variability in the types of waste streams among generators, and variability in the quality and completeness of the waste characterization data. Second, evaluation of the available data indicate that substantial quantities of waste to be disposed consist of very low-level inventories and should require minimal disposal requirements. Thus, it is desirable to differentiate those wastes that can be disposed at minimal expense from those wastes that require enhanced isolation at greater cost. Third, the ability of different disposal facility designs to satisfy performance objectives in the Hanford Site environment cannot be adequately determined without a PA analysis.

For each type of facility, a set of calculations was completed to estimate potential dose to man resulting from the release of radionuclides from the facility into the surrounding environment (i.e., soil, water, and air). Dose estimates were determined for radionuclide release scenarios that

were relevant to performance objectives (e.g., dose limits) stated in DOE Order 5820.2A. Comparison of dose estimates with performance objectives was then used to determine the effectiveness of these facilities in meeting the performance objectives. In this manner, compliance with the DOE Order 5820.2A was established.

As a result of the conditions under which waste is received at the 200 West Area LLBG, dose estimate calculations were applied in two ways to determine with reasonable assurance that compliance with the performance objectives would be satisfied. First, because the sources of waste are not restricted to a unique set of generators or a finite volume of waste, criteria were developed to ensure that waste accepted for disposal could not result in a potential dose in excess of the performance objectives. The primary waste acceptance criteria are radionuclide-specific concentration limits (Ci/m^3) for isotopes with half-lives greater than 5 yr and total activity limits (Ci) for long-lived environmentally mobile radionuclides. Second, compliance with the performance objectives was evaluated by estimating potential dose resulting from the disposal of the entire projected inventory of LLW in the 200 West Area LLBG. This evaluation was performed to demonstrate the adequacy of the disposal practices for the total quantity of waste expected to be disposed in the facility over time.

The following process was used to calculate potential dose: (1) identify performance objectives; (2) select radionuclide release scenarios that correspond to each performance objective; (3) quantify a set of parameters controlling radionuclide release and contamination of the environment for each

scenario, and (4) estimate radionuclide-specific doses that can be compared with each performance objective.

The performance objectives are summarized in Table S-1. The primary source of these objectives is DOE Order 5820.2A, which specifically identifies the all-pathways and intruder protection scenarios. The air emissions objectives are taken from the Clean Air Act (40 CFR 61). Proposed 10 CFR 834 contains limits on air and water contamination, including the radon surface flux limit. The general population performance objective is specified in DOE-RLID Order 5820.2A and 40 CFR 141. The drinking water objective is taken from DOE-RL 5820.2A. The times of compliance are not specified in the orders except for the minimum 100 yr for inadvertent intrusion and the drinking water objective in DOE-RL Order 5820.2A (1,000 yr). Selection of compliance times are believed to be sufficient to evaluate the effect of site conditions on the dose estimates.

Table S-1. Performance Objectives for the 200 West Area Low-Level Waste Burial Grounds.

Exposure pathway	Time period (yr)	Performance objective
General public protection		
All pathways*	≤10,000	25 mrem/yr
General population (ALARA)	≤10,000	500 person-rem/yr
Air emissions (excluding Rn)*	≤10,000	10 mrem/yr
Air emissions (Rn)*	≤10,000	20 pCi/m^2-s
Intruder protection		
Continuous exposure*	100 to 500	100 mrem/yr
Single acute exposure*	100 to 500	500 mrem/yr
Groundwater resource protection		
Drinking water*	≤10,000yr	4 mrem/yr

*Limits apply to the maximum exposed individual.

The performance objectives are interpreted to define two basic kinds of release scenarios: (1) inadvertent intrusion by man and (2) release of radionuclides from the facility by natural causes, the primary mechanism being leaching of radionuclides into the soil column with migration to groundwater. Intruder scenarios and their relationship to the development of intruder waste acceptance criteria are first summarized below. A similar discussion is then provided for the groundwater contamination scenarios and waste acceptance criteria.

To address the intruder objectives, three commonly occurring human activities were considered that could result in contact with buried radioactive waste: (1) building a home with a basement, (2) drilling a well for irrigation and drinking water, and (3) farming (crop growth and livestock). Irrigated farming is a major commercial activity in areas surrounding the semi-arid Hanford Site because of the plentiful supply of surface water and groundwater.

These three general activities were used to develop four intruder scenarios: two scenarios to consider acute exposure events and two scenarios to consider chronic exposure events. The acute exposure scenarios are excavation, during which waste is exhumed as part of construction of a home basement, and drilling a water well. Pathways of exposure include external exposure to gamma-emitting isotopes and inhalation of contaminated dust. The chronic exposure scenarios are postexcavation and postdrilling, during which the exhumed waste is mixed with soil, spread around the site, and subsequently used to grow crops for consumption. In addition to external exposure and

inhalation, dose is assumed to be received by ingestion of contaminated crops grown in the waste-soil mixture.

Doses from inadvertent intrusion are linearly proportional to initial radionuclide concentrations in the disposal facility. Thus, waste acceptance criteria based on intrusion scenario limits are defined as concentration limits. Radionuclide specific intruder concentration limits for each type of facility were determined by a three-step process. First, the set of scenarios appropriate for the facility characteristics was identified. Second, the scenario in the set that provided the largest ratio of potential dose to performance objective dose limit for the same initial radionuclide concentration was determined. Third, a unique set of site-specific parameter values was chosen to estimate radionuclide specific doses for that scenario. These parameter values are referred to as base case or best estimate values. By taking the ratio of the performance objective to the dose calculated for each radionuclide, a corresponding concentration limit was derived. Concentration limits were not estimated for radionuclides with half-lives $\leq$5yr because the minimum intrusion time is 100 yr. It is expected that these very short half-life radionuclides will have decayed to insignificant quantities after 100 yr.

For the Category 1 facility, it was assumed that all of the intruder scenarios could occur because the waste could be disposed at a shallow depth. The scenario that provided the maximum dose turned out to be the postexcavation scenario. It was assumed that intrusion occurred 100 yr postclosure. For the Category 3 facility, an assumed depth of burial of $\geq$5m

excludes excavation and postexcavation as a means of intrusion. Consequently, the postdrilling scenario provides the maximum dose. It was assumed that intrusion occurred 500 yr postclosure. Deterrence to the intruder is provided by a variety of methods, including public records, markers, and cover materials (e.g., rip rap) to alert the intruder to an unusual circumstance. Both the reduced quantity of waste exhumed (drilling versus basement excavation) and the additional time to intrusion increased the allowable concentration limits relative to Category 1 limits. For some radionuclides (e.g., ^{60}Co), the additional decay time was sufficient to allow no concentration limits.

To address the groundwater contamination performance objectives, three groundwater scenarios were assumed to provide dose to man. The all-pathways scenario was defined as a two-step process in which radionuclides are first leached from the disposal facility due to infiltration by precipitation into the waste material and subsequently transported down through the partially saturated or vadose zone into the unconfined aquifer. Subsequently, man drills a well into the aquifer and draws contaminated water for drinking, crop irrigation, and livestock consumption. Dose is received by direct exposure to gamma-producing radionuclides in the soil, inhalation of contaminated dust, and ingestion of contaminated crops, water, beef, and milk. In the Columbia River scenario, dose is received in essentially the same manner except that the source of contamination is the river water into which contaminated water from the unconfined aquifer has discharged. Additional sources of dose are swimming in the water and eating fish. The only source of dose in the drinking water scenario was ingestion of contaminated water from the unconfined aquifer.

Waste acceptance criteria for groundwater contamination were derived using the same process described above to determine intruder limits. Doses from groundwater contamination are linearly proportional to total activity in the disposal facility, unless solubility reactions are assumed to control the release of a radionuclide. Thus, waste acceptance criteria for groundwater contamination are defined for most radionuclides as activity limits (Ci). Uranium in a Category 3 facility was the only radionuclide for which solubility control was found sufficient to satisfy the dose limits. Of the three groundwater scenarios considered, the maximum dose relative to the performance objectives occurs for the drinking water scenario.

The dose calculations for groundwater contamination showed that the combination of environmental conditions and expected waste inventory limit the type of radionuclides that could provide a significant dose. These radionuclides are long-lived and nonsorbing (e.g., ^{14}C, ^{129}I, ^{99}Tc, and uranium). Low infiltration rates and a thick vadose zone caused a sufficiently long travel time to the unconfined aquifer below the 200 West Area LLBG such that short-lived poorly to moderately sorbing radionuclides decayed to insignificant activity before reaching the aquifer. Conversely, moderately and strongly sorbing long-lived radionuclides (Kd $\geq$10mL/g) were estimated to have very long travel times to the unconfined aquifer (in excess of 100,000 yr). Consequently, total activity limits are recommended only for the small set of long-lived, nonsorbing radionuclides.

Waste acceptance criteria for groundwater protection were based on potential doses received from peak groundwater concentrations that were predicted to occur at times of $\leq$10,000 yr or less. As with the intruder

scenarios, a unique set of parameters were selected for each type of facility to estimate peak doses considered to be base case values. The set of parameters is the same for each facility except for the assumption of infiltration rate (5 cm/yr and 0.5 cm/yr for Category 1 and 3 facilities, respectively) and for a subset of cases in the Category 3 facility where waste form performance via diffusional control of radionuclide release is assumed.

Larger activity limits were allowed for the Category 3 waste facility because of the assumption of lower infiltration rates. Also, within the Category 3 facility, the activity limits could be increased if waste form control of release was assumed. For example, a decrease in the assumed diffusion coefficient of material leaching from the waste form reduces the rate of release and the peak groundwater concentration, thus permitting an increase in the activity limit.

The final part of the PA analysis was to estimate potential dose to man assuming the entire projected inventory of LLW was ultimately disposed in the 200 West Area LLBG. To complete this evaluation, a total inventory was estimated. Burial ground inventory records for a 4-yr period (1989 to 1992) were coupled with 30-yr waste volume forecasts provided by the generators to project the entire inventory. It was assumed that the distribution of radionuclide concentrations and quantities per generator volumes would remain constant. The wastes were divided into Category 1 and Category 3 wastes using the waste acceptance criteria derived previously. Using this forecast and the dose estimates generated for the base case conditions, total doses were calculated. These are summarized in Table S-2.

Table S-2. Comparison of Dose Estimates from Disposal of Total Projected Low-Level Waste Inventory with Performance Objectives.

Performance objectives	Exposure pathway	Estimated dose or flux*	
		Category 1	Category 3
25 mrem/yr	Groundwater, irrigated farm	0.23	0.47
4 mrem/yr	Groundwater, drinking	0.13	0.35
100 mrem/yr (100 yr)	Postexcavation	44	NA
100 mrem/yr (500 yr)	Postdrilling	NA	0.7
20 pCi m^2/s	Radon emission	0.0012	0.15
10 mrem/yr	Atmospheric dispersion	1.1 E-06	0.012
500 person-rem/yr	Columbia River	0.017	1.6

NA = not applicable.
*The estimated values are in the same units as the performance objectives.

The comparison with performance objectives shows that all performance objectives are satisfied. In the projected inventory, the primary radionuclides contributing to dose for the intruders are ^{137}Cs and ^{90}Sr. The primary radionuclides contributing to dose from groundwater contamination are ^{14}C, ^{129}I, ^{99}Tc, and uranium, with the exception of uranium encapsulated in grout. No reliance is placed on waste form performance in making these calculations because no wastes were identified in the projected inventory that required waste form performance. With the exception of ^{222}Rn, all groundwater pathway doses are calculated from the peak groundwater concentrations that are predicted to occur $\leq$1,000yr after closure. The ^{222}Rn flux will increase over time until secular equilibrium with its parent ^{238}U occurs at about 1 million years. Based on the current projected average concentrations of ^{238}U, the estimated flux from ^{222}Rn is 5.8×10^{-4} and 1.0×10^{-3} pCi/m^2-s for Category 1 and 3 facilities, respectively at 100,000 yr.

The results of these calculations combined with the development of waste acceptance criteria to administratively control waste accepted for disposal indicate that performance objectives will be complied with in the 200 West Area LLBG for the foreseeable future.

This page intentionally left blank.

LIST OF TERMS

AAMS	Aggregate Area Management Study
AEC	Atomic Energy Commission
ALARA	As Low as Reasonably Achievable
CERCLA	Comprehensive Environmental Response, Compensation, and Liability Act
CFR	Code of Federal Regulations
DOE	U.S. Department of Energy
EDE	effective dose equivalent
EPA	U.S. Environmental Protection Agency
ERDF	Environmental Restoration Disposal Facility
FFTF	Fast Flux Test Facility
FUSRAP	Formerly Utilized Site Remedial Action Program
HDW-EIS	Hanford Defense Waste Environmental Impact Statement
HEHF	Hanford Environmental Health Foundation
HIC	high-integrity container
HMS	Hanford Meteorology Station
HWVP	High-Level Waste Vitrification Plant
KEH	Kaiser Engineers Hanford
LERF	Liquid Effluent Treatment Facility Liability Act
LLBG	low-level burial grounds
LLW	low-level waste
MW	mixed waste
ORNL	Oak Ridge National Laboratory
PA	performance assessment
PCG	Preconditioned Conjugate Gradient
PFP	Plutonium Finishing Plant
PNL	Pacific Northwest Laboratory
PRP	peer review panel
PUREX	Plutonium-Uranium Extraction (Plant)
RCRA	Resource Conservation and Recovery Act
RL	DOE, Richland Operations Office
RRMS	relative root mean square
SAR	safety analysis report
SGI	Silicon Graphics Inc.
SWITS	Solid Waste Information and Tracking System
SWOC	Solid Waste Operations Complex
TRU	transuranic
U Pond	216-U-10 Pond
WAC	Washington Administrative Code
WNP-2	Washington Nuclear Plant 2
WRAP	Waste Receiving and Processing

This page intentionally left blank.

CONTENTS

1.0 INTRODUCTION 1-1
1.1 PURPOSE AND SCOPE 1-1
1.2 HISTORICAL BACKGROUND AND STATUS OF THE DEVELOPMENT OF THE 200 WEST AREA LOW-LEVEL BURIAL GROUNDS PERFORMANCE ASSESSMENT ANALYSIS 1-2
1.3 APPROACH TO PERFORMANCE ASSESSMENT FOR THE 200 WEST AREA LOW-LEVEL BURIAL GROUNDS 1-3
1.4 REGULATIONS FOR THE DISPOSAL OF LOW-LEVEL WASTE 1-4
1.5 TREATMENT OF DOSE LIMIT PERFORMANCE OBJECTIVES IN THE PERFORMANCE ASSESSMENT ANALYSIS 1-6
1.6 POINTS AND TIMES OF COMPLIANCE RELATED TO DOSE LIMIT PERFORMANCE OBJECTIVES 1-7

2.0 DISPOSAL FACILITY DESCRIPTION 2-1
2.1 CHARACTERISTICS OF THE 200 WEST AREA LOW-LEVEL WASTE BURIAL GROUNDS 2-1
2.1.1 Site Geography and Demography 2-1
2.1.2 Site Climatology and Meteorology 2-3
2.1.3 Site Ecology 2-3
2.1.4 Regional and Site-Specific Land Use 2-3
2.1.5 Seismology 2-5
2.1.6 Radiation Background 2-5
2.1.7 Regional Hydrogeology 2-7
2.1.8 Hydrogeology of the 200 West Area Low-Level Waste Burial Grounds 2-9
2.1.9 Geochemistry of the Soil Column 2-16
2.2 TREATMENT OF ENVIRONMENTAL CHARACTERISTICS IN THE PERFORMANCE ASSESSMENT ANALYSIS 2-16
2.2.1 Meteorology and Climatology 2-16
2.2.2 Seismicity 2-17
2.2.3 Geology and Hydrology 2-19
2.2.4 Soil Column Geochemistry 2-19
2.2.5 Other Disposal Facility and Environmental Characteristics 2-19
2.3 LOW-LEVEL WASTE CHARACTERISTICS 2-20
2.3.1 Defense Waste Management Waste 2-21
2.3.2 Chemical Processing Waste 2-22
2.3.3 Other Onsite Generators 2-22
2.3.4 Offsite Generators 2-23
2.4 TREATMENT OF WASTE CHARACTERISTICS IN THE PERFORMANCE ASSESSMENT ANALYSIS 2-24
2.5 WASTE TREATMENT, CERTIFICATION, AND DISPOSAL 2-25
2.5.1 Waste Treatment and Certification 2-26
2.5.2 Low-Level Waste Disposal Practices and Facility Description 2-26
2.5.3 Planned Modifications to Current Low-Level Waste Disposal Practices 2-30
2.6 TREATMENT OF DISPOSAL FACILITY FEATURES IN THE PERFORMANCE ASSESSMENT ANALYSIS 2-32

CONTENTS (cont)

3.0 PERFORMANCE ASSESSMENT ANALYSIS METHODOLOGY 3-1
3.1 INTRUDER SCENARIO ANALYSIS 3-1
3.1.1 Conceptual Model of the Inadvertent Intruder Scenarios 3-1
3.1.2 Mathematical Simulation of Dose Estimates to the Inadvertent Intruder 3-3
3.1.3 Postexcavation and Postdrilling Base Case Parameter Selection 3-5
3.2 GROUNDWATER CONTAMINATION ANALYSIS 3-7
3.2.1 Overview of the Modeling Approach 3-8
3.2.2 Source Term Analysis 3-10
3.2.2.1 Conceptual Model of Source Term Release . . . 3-10
3.2.2.2 Mathematical Simulation of Radionuclide Release Mechanisms 3-12
3.2.2.2.1 Advection-Dominated Release Model 3-12
3.2.2.2.2 Diffusion-Dominated Release Model 3-13
3.2.2.2.3 Solubility-Limited Release Model 3-15
3.2.2.3 Base Case Parameter Selection 3-15
3.2.3 Contaminant Flux in the Vadose Zone and the Unconfined Aquifer 3-17
3.2.3.1 Conceptual Model of Mass Transport in the Hydrogeologic Environment 3-17
3.2.3.2 Mathematical Simulation of Contaminant Flux 3-19
3.2.3.3 Base Case Parameter Selection 3-23
3.2.3.3.1 Representation of the Soil Column Stratigraphy 3-24
3.2.3.3.2 Moisture Retention and Unsaturated Hydraulic Conductivity Curves . . 3-25
3.2.3.3.3 Saturated Media and Transport Properties 3-26
3.2.3.3.4 Geochemical Parameters 3-26
3.2.3.3.5 Disposal Facility Parameters . . . 3-27
3.2.3.3.6 Additional Modeling Parameters . . 3-27
3.2.4 Quality Control/Quality Assurance Practices for VAM3D-CG 3-29
3.2.5 Groundwater Pathway Dose Calculations 3-30
3.2.5.1 All-Pathways Irrigator Scenario 3-30
3.2.5.2 Groundwater Consumption 3-30
3.2.5.3 Population Dose Scenario 3-30
3.3 ADDITIONAL ANALYSES 3-31
3.3.1 Vapor Diffusion Pathway Analysis 3-31
3.3.2 Upward Diffusion 3-32

CONTENTS (cont)

4.0 ANALYTICAL RESULTS 4-1
4.1 ANALYTICAL RESULTS FOR INADVERTENT INTRUDER SCENARIOS 4-1
4.1.1 Dose Estimate Results 4-1
4.1.2 Intruder Dose Sensitivity Analysis 4-7
4.1.2.1 General Observations 4-7
4.1.2.2 Sensitivity Analysis of Parameters Affecting All-Intruder Pathways 4-9
4.1.2.3 Sensitivity Analysis of Ingestion Parameters 4-9
4.1.2.4 Inhalation Parameter Sensitivity Analysis . . 4-11
4.1.2.5 External Exposure Parameter Sensitivity Analysis 4-12
4.1.3 Intruder Scenario Uncertainty Analysis 4-12
4.1.3.1 Uncertainty Analysis of Parameters Affecting All-Intruder Pathways 4-12
4.1.3.2 Uncertainty Analysis of Ingestion Parameters 4-13
4.1.3.3 Inhalation Parameter Uncertainty Analysis . . 4-16
4.1.3.4 External Exposure Parameter Uncertainty Analysis 4-16
4.1.3.5 Summary of Uncertainty Analysis 4-17
4.2 ANALYTICAL RESULTS FOR THE GROUNDWATER PATHWAYS SCENARIOS . . 4-17
4.2.1 Peak Time and Concentration Results from the Release and Transport Analyses 4-17
4.2.1.1 Source Term Analysis for Base Case Conditions 4-18
4.2.1.2 Release And Transport Analysis for Base Case Conditions 4-26
4.2.1.2.1 Peak Concentration Estimates for a Category 1 Waste Disposal Facility 4-28
4.2.1.2.2 Peak Concentration Estimates for a Category 3 Waste Disposal Facility 4-28
4.2.2 Sensitivity Analyses for the Groundwater Pathway . . . 4-30
4.2.2.1 Sensitivity of Peak Concentration to Release Mechanism Versus Infiltration Rate 4-36
4.2.2.2 Sensitivity Analysis of Differential Infiltration Rates of the Disposal Facility Cover and Surrounding Area 4-36
4.2.2.3 Sensitivity Analyses of Other Natural Parameters Affecting Radionuclide Transport 4-38
4.2.2.3.1 Peak Concentration Response to Increased Permeability 4-38
4.2.2.3.2 Radionuclide Groundwater Concentration Response to Decreased Hydraulic Gradient . . . 4-39
4.2.2.3.3 Radionuclide Groundwater Concentration Response to Variability in Vadose Layer Hydrologic Properties 4-40

CONTENTS (cont)

4.2.2.3.4 Radionuclide Groundwater Concentration Response to Presence of a Clastic Dike 4-41

4.2.2.4 Sensitivity Analyses of Other Manmade Parameters Affecting Radionuclide Transport 4-42
4.2.2.4.1 Radionuclide Groundwater Concentration Response to Presence of High-Concentration Waste Packages 4-42
4.2.2.4.2 Radionuclide Groundwater Concentration Response to Variable Length Trenches 4-43
4.2.2.4.3 Radionuclide Groundwater Concentration Response to Pumping 4-44
4.2.3 Determination of Inconsequential Radionuclides in the Groundwater Pathway 4-45
4.2.4 Dose Estimates for Dose-Producing Radionuclides in Groundwater 4-47
4.2.5 Groundwater Concentration Uncertainty Analysis 4-49
4.3 ADDITIONAL ANALYSES 4-54
4.3.1 Analytical Result for Vapor Transport of Carbon-14, Tritium, and Radon-222 4-54
4.3.1.1 Tritium Analysis 4-54
4.3.1.2 ^{14}C Analysis 4-57
4.3.1.3 Radon-222 Analysis Results 4-58
4.3.2 Upward Transport of Radionuclides by Liquid Diffusion 4-58
4.3.3 Dose Effects from the Mixing of Contaminant Plumes . . 4-60
4.3.4 Large-Scale Commercial Irrigation Effects on Dose Estimates 4-63
4.4 INTEGRATION OF RESULTS 4-64
4.4.1 Determination of Inadvertent Intruder Concentration Limits 4-64
4.4.1.1 Summary of Parameters Affecting Dose Calculations and Quantification of Concentration Limits 4-64
4.4.1.2 Additional Considerations for Establishing Concentration Limits 4-67
4.4.1.3 Use of the Concentration Limits Table 4-68
4.4.2 Determination of Groundwater Pathway Inventory Limits 4-69
4.4.2.1 Summary of Parameters Affecting Dose Calculations and Quantification of Groundwater Pathway Inventory Limits 4-69
4.4.3 Dose Estimate for the Total Projected Inventory and Comparison with Performance Objectives 4-72
4.4.3.1 Estimate of Intruder Doses 4-72

CONTENTS (cont)

4.4.3.2 Estimate of Groundwater Contamination Doses 4-73
4.4.3.3 Estimates of Air Contamination Doses 4-77

5.0 PERFORMANCE EVALUATION 5-1
5.1 COMPARISON OF ESTIMATED DOSES WITH PERFORMANCE OBJECTIVES 5-1
5.2 DESIGN CHANGES REQUIRED TO MEET PERFORMANCE OBJECTIVES . . . 5-2
5.3 ADDITIONAL APPLICATIONS OF PERFORMANCE ASSESSMENT RESULTS IN WASTE MANAGEMENT 5-2
5.4 ADDITIONAL DATA AND ANALYSIS NEEDS 5-3

6.0 LIST OF PREPARERS 6-1

7.0 REFERENCES 7-1

LIST OF FIGURES

2-1 Map Showing Location of Hanford Site and the 200 Areas Low-Level Burial Grounds (Bjornstad 1990) 2-2

2-2 Topography of the Hanford Site 2-4

2-3 Historical Seismicity of the Columbia Plateau and Surrounding Areas 2-6

2-4 Hydrologic Basins Designated for the Washington State Portion of the Columbia Plateau 2-8

2-5 Stratigraphic Chart for the 200 West Area 2-11

2-6 Geomorphic Features in the West-Central Portion of the Hanford Site 2-13

2-7 Water Table Map for the 200 Areas, December 1987 2-14

2-8 Hanford Site Water Table Map, January 1944 2-15

2-9 Cold Creek Watershed Floodplain from the Probable Maximum Flood (DOE 1987) 2-18

2-10 Low-level Waste Burial Ground Locations in the 200 West Area . . 2-27

2-11 Topographic Map of Burial Ground 218-W-5 2-28

2-12 Topographic Map of Burial Ground 218-W-3A 2-29

2-13 Topographic Map of Burial Ground 218-W-3AE. 2-31

2-14 Topographic Map of Burial Ground 218-W-4C 2-33

2-15 Schematic Comparison of Analyzed Trench Section Used in Groundwater Flow and Transport Analyses versus Actual Trench Dimensions . . . 2-34

3-1 Finite Element Mesh With Material Type Table 3-21

4-1 Saturation Contours for 5 cm/yr Recharge 4-19

4-2 Velocity Plots for 5 cm/yr Recharge (Vadose Zone Blow-Up) 4-20

4-3 Velocity Plots for 5 cm/yr Recharge (Full Simulation Field) . . . 4-21

4-4 Release History for 5 cm/yr Recharge, Advection Dominated 4-22

4-5 Saturation Contours for 0.5 cm/yr Recharge 4-23

4-6 Velocity Plots for 0.5 cm/yr Recharge (Vadose Zone Blow-Up) . . . 4-24

4-7 Flux Release History, 0.5 cm/yr Recharge, Advection Dominated . . 4-25

LIST OF FIGURES (cont)

4-8 Flux Release History for 0.5 cm/yr Recharge, Diffusion with $D_e = 3.15 \times 10^{-5}$ m^2/yr (1×10^{-8} cm^2/s) 4-27

4-9a Plume Cross-Section for Cases 1a and 1b Assuming Advective Release 4-29

4-9b Plume Cross-Section for Cases 1c and 1K 4-31

4-10 Radionuclide Concentrations at the 100-m Well Assuming Advective Release for Category 1 Conditions 4-30

4-11 Radionuclide Concentrations at the 100-m Well Assuming Advective Release for Category 3 Conditions 4-33

4-12 Radionuclide Concentrations at the 100-m Well Assuming Diffusional Release for Category 3 Conditions 4-34

4-13 Radionuclide Concentrations at the 100-m Well Assuming Solubility Controlled Release for Category 3 Conditions 4-35

4-14 Relative Location of Existing and Potential Low-Level Waste Disposal Sites in the Vicinity of the 200 West Area Low-Level Burial Ground 4-62

LIST OF TABLES

2-1 30-Year Low-Level Waste Volume Forecast for Hanford Site and Offsite Generators 2-20

2-2 Radionuclide Inventory of Commonly Listed Isotopes in the Solid Waste Information Tracking System for Waste Accepted at the Hanford Burial Grounds from 1989 Through 1992 2-21

3-1 Calculation of the Inhalation Time for the Intruders 3-6

3-2 Human Food Consumption Parameters 3-7

3-3 Summary of Performance Assessment Methodology 3-9

3-4 Hydraulic Property Input Data to the Release and Transport Model 3-25

3-5 Radionuclide Sorption Coefficients in the Soil Column 3-26

4-1 Radionuclides Considered to be in Secular Equilibrium in the Dose Analysis 4-2

4-2 Radioactive Decay Chains Used in the Spreadsheet 4-4

4-3 Total Doses (mrem/yr per Ci/m^3) for the Post-Excavation Scenario Using Concentration Ratios 4-5

4-4 Total Doses (mrem/yr per Ci/m^3) for the Post-Drilling Scenario Using NUREG/CR-5512 Concentration Ratios 4-6

4-5 Comparison of Dose to the Intruder by Exposure Pathway at 100 Years Postclosure 4-8

4-6 Ratio of Total Doses: NUREG/CR-5512/ORNL-5785. 4-10

4-7 Ratio of Total Doses: NonLeaching and Leaching 4-10

4-8 Relative Contributions (%) to Ingestion Dose by Food Type 4-11

4-9 Ratios of GENII and EPA Internal Dose Factors to DOE Internal Dose Factors 4-14

4-10 Ratio of Pathway Doses for NUREG/CR-5512 and ORNL-5785 Parameters 4-15

4-11 Comparison of Advection and Diffusion Dominated Release Model, with De=10^{-6}, 10^{-8}, 10^{-9}, 10^{-10}, 10^{-12} cm^2/s 4-37

4-12 Comparison of Steady-State (Solubility Control) Release Rate and Infiltration Rate Effects on Peak Concentrations 4-37

LIST OF TABLES (cont)

4-13 Effect of Differential Cover and Soil Infiltration Rates on Peak Concentrations 4-38

4-14 Advection-Dominated release, K_{sat} = 10X 4-39

4-15 30% Decrease in Hydraulic Gradient, Advection-Dominated Release 4-40

4-16 Effects of Vadose Soil Hydrologic Property Variability on Estimated Peak Concentrations 4-41

4-17 Effect of Clastic Dike Underlying Disposal Facility on Peak Concentrations 4-42

4-18 Effect of High Concentration Waste Package on Peak Concentration 4-43

4-19 Effect of Varying Trench Size on Peak Concentrations 4-44

4-20 Effect of Pumping on Peak Concentrations 4-45

4-21 Radionuclides that Decay to Insignificant Quantities During Transport from the Disposal Facility to the Unconfined Aquifer 4-46

4-22 Radionuclide Dose Estimates for Groundwater Pathways 4-48

4-23 Upward Versus Downward Transport in the Soil Cover Resulting from Diffusion and Advection 4-59

4-24 Category 1 and 3 Concentration Limits Based on Intruder Scenarios 4-66

4-25 Inventory Limits (Ci) for Groundwater Pathway Performance Objectives 4-71

4-26 Radionuclide Specific Intruder Dose Estimates for Category 1 Waste 4-73

4-27 Current and Projected Inventories of Groundwater Contaminating Radionuclides 4-74

4-28 Radionuclide Specific Groundwater Dose Estimates for Category 1 and 3 Waste 4-75

5-1 Comparison of Dose Estimates with Performance Objectives 5-1

APPENDIXES

A Stratigraphic and Vadose Zone Hydrologic Properties A-1

B Detailed Listing of Radionuclide Inventories of Waste Disposed at the Hanford Burial Grounds (1989 to 1992) B-1

C Modeling Equations, Parameter Selection, and Parameter Values Used for the Exposure Pathway Analysis C-1

D Radionuclide Groundwater Concentration Versus Time Results From the Numerical Release and Transport Analysis--Summary Figures and Tables D-1

E Selected Solubility and Sorption Data E-1

F Waste Form Release Analysis and Data Collection F-1

G1 Calibration/Testing of VAM3D-CG Computer Code Using Injection Test Site Data at Hanford G1-1

G2 Verification and Benchmark Testing of the VAM3d-CG Flow and Transport Computer Code for Use in the Performance Assessment at Hanford G2-1

H Response to Peer Review Panel Comments H-1

1.0 INTRODUCTION

1.1 PURPOSE AND SCOPE

A site-specific performance assessment (PA) analysis is required by U.S. Department of Energy (DOE) Order 5820.2A (Chapter III, Section 3.b.[1]) to support disposal of low-level waste (LLW) after September 1988 at DOE waste management sites such as the Hanford Site. The DOE order has also established a peer review panel (PRP) to evaluate PA analyses for consistency and technical adequacy. To achieve compliance with DOE Order 5820.2A, the PA analysis must be reviewed by the PRP and be approved as technically adequate. This document provides a final analysis that evaluates the disposal of LLW radioactive waste in the 200 West Area low-level burial grounds (LLBG) at the Hanford Site. Before this analysis, a preliminary draft analysis was reviewed by the PRP. Their comments have been addressed in this report.

The primary purpose of this PA analysis is (1) to estimate potential dose to man resulting from the disposal of the projected LLW inventory in the 200 West Area LLBG and (2) to compare the estimated dose with dose limit performance objectives defined in the DOE Order (Chapter III, Section 3.a.[2] and [3]). If the projected doses can, with reasonable assurance, be shown to fall below the dose limits, then compliance is demonstrated. Consequences of the release of hazardous materials from the disposal facilities are not considered in this analysis except as such releases may influence radionuclide behavior. This analysis does not consider radiological releases from transuranic (TRU) wastes or LLW disposed before September 1988. TRU wastes are being stored and are not planned for disposal at this site. Wastes disposed before 1988 will be the focus of *Comprehensive Environmental Response, Compensation, and Liability Act* (CERCLA) remediation evaluations or *Resource Conservation and Recovery Act of 1976* (RCRA) closure.

The analysis evaluates the effects of site-specific characteristics of the Hanford Site and disposal facility features that influence radionuclide mobility. These features include the hydrogeologic and climatological characteristics of the site and the design features of the disposal unit. The Hanford Site is located in eastern Washington State where the climate is semiarid. Disposal of LLW at the Hanford Site occurs primarily in two burial ground areas, 200 East Area and 200 West Area, which are located on a plateau in the interior of the site. LLW disposal has been occurring at these sites for more than 40 years. Depth to the water table is about 200 ft (about 75 m). The standard method of disposal has been and continues to be placement of waste containers in shallow trenches that are subsequently covered with several feet of soil. This PA analysis considers the performance of this type of disposal facility (designated as a Category 1 waste facility) and also considers disposal in an enhanced facility with engineered barriers (designated as a Category 3 waste facility) which is intended to accept waste with more concentrated inventories of radioactive waste. This analysis is focused on waste disposed in the 200 West Area LLBG after September 1988.

Additional LLW sites that are active or potentially active in other areas on the Hanford Site are or will be the subjects of separate PA analyses. Other sites include the 200 East Area burial grounds, the proposed Environmental Restoration Disposal Facility (ERDF) which is intended to accept

wastes generated by Hanford Site remediation, and a site for the disposal of LLW generated by the remediation of liquid and sludge waste stored in underground tanks on the Hanford Site. These waste sites are only included in this PA in terms of potential for contaminant plume mixing with a potential release from the 200 West Area burial grounds.

It is anticipated that the environmental conditions and disposal methods in the 200 East Area LLBG and the ERDF are sufficiently similar to the 200 West Area LLBG such that the PA results from this analysis will be correspondingly similar.

1.2 HISTORICAL BACKGROUND AND STATUS OF THE DEVELOPMENT OF THE 200 WEST AREA LOW-LEVEL BURIAL GROUNDS PERFORMANCE ASSESSMENT ANALYSIS

A preliminary draft of the PA analysis was prepared in fiscal year 1993 and was reviewed internally before being presented to the PRP. The PRP provided a number of comments that are addressed in the text and in Appendix H. Two significant changes have been made in the scope of the analysis as a result of the review comments. First, it was noted in the preliminary draft review that only one of the burial grounds in the 200 West Area, 218-W-5, was considered while some adjacent burial grounds are being used or could be used for LLW disposal. Therefore, the analysis was expanded to include these burial grounds that have been used since September 1988 and any future burial grounds adjacent to the present ones that might be used for disposal of solid LLW. This approach is justified because the individual burial grounds share essentially the same environmental conditions leading to identical dose estimates. Also, it is unlikely that a plume from one burial ground could be distinguished from another in the aquifer. Second, an estimate of dose resulting from the disposal of the entire projected LLW inventory in the 200 West Area LLBG is provided and compared with the performance objectives.

Another PA analysis has been prepared at the Hanford Site to demonstrate compliance with DOE Order 5820.2A (Kincaid et al. 1993). The subject of this PA analysis is the disposal of low-level waste generated by remediation of liquid waste in underground double-shelled tanks at the Hanford Site. Estimates of dose are not expected to be identical for solid waste and liquid waste because of differences in radionuclide inventory and the proposed methods of disposal. However, because of the shared environmental conditions and performance objectives, the methods used to estimate dose and the selection of parameter values affecting dose should be consistent to the extent possible. Efforts have been made to ensure consistency in the following areas: (1) selection of the same set of performance objectives, (2) selection of similar radionuclide release scenarios, and (3) selection of similar parameter values that characterize hydrogeologic properties, radionuclide mobility, and inadvertent intruder dose estimates.

1.3 APPROACH TO PERFORMANCE ASSESSMENT FOR THE 200 WEST AREA LOW-LEVEL BURIAL GROUNDS

As described in Section 1.1, the primary task in the PA analysis is to estimate potential dose to man if radionuclides were released from the disposal facility. Compliance with the DOE Order 5820.2A is demonstrated if the doses estimated can reasonably be expected to fall below the dose limits defined in the performance objectives. The following steps were taken to estimate potential dose to man:

1. **Define Performance Objectives.** Performance objectives are most often quantified as dose limits and are provided primarily in DOE Order 5820.2A and are listed in Section 1.4. The performance objectives identify two primary means by which dose could be received. The first is contamination to the environment brought about by the release of radionuclides from the disposal facility by natural causes. The second is inadvertent intrusion by man.

2. **Select Radionuclide Release Scenarios.** The radionuclide release scenarios are largely driven by the type of performance objectives. Leaching of radionuclides from the disposal facility by infiltrating rainwater is the most significant source of environmental contamination due to natural causes. Intrusion scenarios were based on common activities in the Hanford Site region that could result in the exhumation of waste (i.e., digging and drilling).

3. **Define Scenario Parameters and Parameter Values.** For the scenarios involving the groundwater pathway, parameters are identified to characterize the aspects of the disposal facilities and the Hanford Site environment that influence radionuclide release and transport. For the scenarios involving inadvertent intrusion, parameters describing activities leading to dose (e.g., exhumation of waste) and disposal facility features affecting the type of intrusion expected to occur are quantified.

4. **Estimate Dose.** For each scenario, mathematical models were selected to simulate the radionuclide release conceptual model. These models were then applied to calculate dose estimates. For each scenario, a base case dose estimate was calculated using a unique set of parameter values. For each parameter, selection of the base case value was determined by evaluating the range of possible values and selecting the value that would lead to a reasonably conservative estimate of dose. This approach contrasts with the determination of a "best estimate" case in which parameter values are selected from the perspective of accuracy rather than reasonable conservatism. Thus, dose estimates for the base case exceed those of the best estimate case. A unit concentration or quantity in the facility for a given radionuclide (depending on the radionuclide release scenario) was assumed. The fact that dose estimates are proportional to radionuclide concentration or quantity allowed the results to be applied to the comparison of dose estimates with the performance objectives using actual radionuclide inventory estimates.

In addition to the base case analyses, a number of sensitivity analyses were also conducted to quantify the effects of uncertainties in the values of parameters that most critically affect dose estimates. From these analyses, the potential range of dose estimates was determined for each scenario.

5. **Compare Dose Estimates with Performance Objectives.** Dose estimates from the base case analyses were compared to performance objectives and used to (1) calculate waste acceptance criteria and (2) to estimate dose that could result from the disposal of the entire projected inventory (30 yr) in the 200 West Area LLBG. Frequently, only the latter estimate is made to evaluate compliance with the performance objectives. However, dose estimates are proportional to the total inventories of specific radionuclides and radionuclide concentrations. Because of the uncertainty in the complete waste inventories to be disposed in the 200 West Area LLBG (e.g., numerous generators, variable characterization, uncertain volumes of waste to be disposed), there is uncertainty in the dose estimates and consequently, the comparison of dose estimates with the performance objectives. By quantifying waste acceptance criteria that are related to performance objective dose limits, the receipt and disposal of future waste at the 200 West Area LLBG can be controlled such that potential dose from the facility is acceptable. In addition, the total dose estimate for the completed facility and comparison with the performance objectives provides an indication of the acceptability of the proposed facility.

Waste acceptance criteria are both concentration limits (Ci/m^3) for radionuclides with half-lives $\geq$5 yr and total inventory limits (Ci) for long-lived environmentally mobile radionuclides. The concentration limits are calculated to satisfy the inadvertent intruder performance objectives. The inventory limits are calculated to satisfy the groundwater contamination performance objectives.

Major topics that require discussion in the PA analysis in support of this PA approach are defined in two guidance documents (Case et al. 1989; Dodge et al. 1991). These topics are the major sections of this document. They include a description of the performance objectives applied to the LLW disposal facilities in the remainder of Chapter 1, a description of the site and its disposal facilities and waste characteristics (Chapter 2), a discussion of analytical methods and release pathways (Chapter 3), a discussion of the analytical results, sensitivity, and uncertainty analyses and an integration and interpretation of the results (Chapter 4), and a summary evaluation of the adequacy of site performance and a description of future work required to finalize the PA analysis and monitor performance of LLW disposal facilities (Chapter 5).

1.4 REGULATIONS FOR THE DISPOSAL OF LOW-LEVEL WASTE

DOE and U.S. Environmental Protection Agency (EPA) regulations are applicable to LLW disposal. The primary DOE order that relates to LLW is

DOE Order 5820.2A (DOE 1988a). The following performance objectives are stated in Chapter 3, Paragraph 3.a. of that order:

1. Protect public health and safety in accordance with standards specified in applicable Environmental and Health Orders and other DOE orders.

2. Ensure that external exposure to the waste and concentrations of radioactive material that may be released into surface water, groundwater, soil, plants, and animals results in an effective dose equivalent that does not exceed 25 mrem/yr to any member of the public. Releases to the atmosphere shall meet the requirements of 40 Code of Federal Regulations (CFR) 61. Reasonable effort should be made to maintain releases of radioactivity in effluents to the general environment as low as is reasonably achievable (ALARA).

3. Ensure that the committed effective dose equivalents received by individuals who inadvertently may intrude into the facility after the loss of active institutional control (100 yr) will not exceed 100 mrem/yr for continuous exposure or 500 mrem for a single acute exposure.

4. Protect groundwater resources, consistent with Federal, state, and local requirements.

At the Hanford Site, the U.S. Department of Energy, Richland Operations Office (RL) has generated a supplemental order, DOE-RLID 5820.2A, that provides additional or clarifying performance objectives in Chapter 3, Paragraph 3.a., as follows:

1. **General Public Protection.** Disposal systems shall be designed to ensure that exposure to any member of the public that results from disposal of solid LLW shall not exceed 25 mrem/yr effective dose equivalent (EDE) through all exposure pathways for at least 1,000 yr after disposal. The point of compliance shall be no further from the edge of the waste than the Hanford Site boundary during the period of active institutional control. After the active institutional control period (assumed to be not more than 100 yr), the point of compliance shall be not more than 100 m from the edge of the disposal site.

2. **Groundwater Protection.** Disposal systems shall be designed to ensure that disposal of LLW after September 26, 1988, does not result in concentrations of radionuclides (above existing levels) in groundwater exceeding those corresponding to an EDE of 4 mrem/yr to any person who might drink 2 L/d of water from a well drilled into the aquifer, for at least 1,000 yr after disposal. The point of compliance shall be no further than 100 m from the edge of the waste.

3. **As Low as Reasonably Achievable (Long-Term Protection).** Reasonable effort shall be made to design disposal systems in such a way that potential exposures are ALARA for all times up to the year of maximum exposure. If the predicted population exposure is less than

500 person-rem/yr in the year of maximum exposure, the ALARA requirement is defined to have been complied with.

4. **Intruder Protection.** Disposal closure systems shall be designed to ensure that exposure to individuals who inadvertently intrude on the closed facility after the active institutional control period shall not exceed 100 mrem/yr for continuous exposure, or 500 mrem for a single acute exposure. For wastes that may remain hazardous to inadvertent intruders beyond 100 yr, passive controls (e.g., long-term government ownership and control, appropriate markers, and barrier systems) shall be incorporated to provide reasonable assurance that inadvertent intruders will be warned and deterred from disturbing the site for up to 500 yr.

5. **Mixed-Waste Regulations.** Disposal systems shall be designed to meet the applicable requirements of 40 CFR 264 and 265 and Washington Administrative Code (WAC) 173-303 for the disposal of LLW-mixed waste (MW).

DOE has also issued a proposed rulemaking, 10 CFR Part 834, "Proposed Rule" (DOE 1993, *Radiation Protection of the Public and the Environment*). In the order, no requirements are provided that apply directly to LLW disposal except the 25 mrem/yr requirement (Section 834.109). However, protection of air and drinking water are also covered, both of which could be contaminated as a result of disposal (Sections 834.102 and 834.103). Proposed limits that could apply to disposal facilities include airborne release limits of 10 mrem/yr for all radionuclides excluding ^{222}Rn and a ^{222}Rn flux limit through the surface of the facility of 20 $pCi/m^2/s$. For DOE-managed drinking water systems, a 4-mrem/yr limit resulting from consumption of the water is proposed. Separate activity limits are recommended for ^{226}Ra and ^{228}Ra combined (5×10^{-9} μCi/mL) and gross alpha excluding radon and uranium (5.6×10^{-8} μCi/mL). Finally, for private or public drinking water systems downstream of the DOE facility, the radiological limits provided in 40 CFR 141 are recommended.

At present, no Washington State or local laws are in place to regulate radionuclide release from LLW disposal facilities. In 40 CFR 141, radiological limits are recommended for drinking water facilities. Limits include a 4-mrem/yr limit on beta- and gamma-emitting radionuclides. Separate limits are provided for individual alpha-emitting nuclides and total alpha radiation.

1.5 TREATMENT OF DOSE LIMIT PERFORMANCE OBJECTIVES IN THE PERFORMANCE ASSESSMENT ANALYSIS

The discussion in the previous section identified a mixture of clearly defined and proposed performance objectives. For the purposes of this analysis, the following criteria are selected:

1. The PA analysis shall only consider potential doses that could occur following closure of the Hanford Site LLW disposal facility. Potential doses received during the operational period of the facility shall be addressed in a SAR.

2. An inadvertent intruder into the Hanford Site LLW disposal facilities shall not receive an effective dose equivalent of more than 500 mrem/yr from a single acute exposure or 100 mrem/yr for continuous exposure. The PA analysis will compare estimated doses from plausible intruder scenarios with these dose limits and demonstrate with reasonable assurance that the disposal facility and site-specific conditions affecting radionuclide release are sufficient to satisfy these dose limits.

3. Any nonintruder member of a critical group shall not receive an effective dose equivalent of more than 25 mrem/yr from all exposure pathways resulting from radionuclide release from 200 West Area LLBG disposal facilities. The PA analysis will provide a comparison of all-pathways release estimates with this dose limit and demonstrate with reasonable assurance that the disposal facility and site-specific conditions affecting radionuclide release are sufficient to satisfy these dose limits.

4. To protect groundwater resources, predicted groundwater concentrations resulting from the leaching and transport of radionuclides from the 200 West Area LLBG to the water table shall be compared to concentrations that result in a 4-mrem/yr effective dose equivalent.

5. The effective dose equivalent to any individual resulting from airborne effluents released from the 200 West Area LLBG facilities shall not exceed 10 mrem/yr. The limit applies to all radionuclides except ^{222}Rn. For ^{222}Rn the surface flux limit of 20 $pCi/m^2/s$ averaged over the entire facility is selected.

6. The downstream population shall not receive more than 500 person-rem/yr in the year of maximum exposure as a result of radionuclide releases from the LLW disposal facility.

1.6 POINTS AND TIMES OF COMPLIANCE RELATED TO DOSE LIMIT PERFORMANCE OBJECTIVES

Two important aspects of the treatment of performance objectives are the point of compliance and the time of compliance. For the point of compliance, the following conditions are selected:

1. For intruder dose limits, the intruder contacts the waste directly.

2. For the drinking water pathway and the all-pathways scenarios, the point of compliance occurs at the place where the maximum dose can be received by an offsite individual. The minimum distance is 100 m from the edge of the waste (DOE-RL 1990). A well is constructed at this distance from which contaminated groundwater can be drawn for drinking and agricultural purposes.

Quantitative requirements on the time of compliance for any of the dose limit criteria are limited. The following conditions are selected:

1. DOE Order 5820.2A specifies that inadvertent intrusion cannot occur until loss of institutional control, which is defined as 100-yr postclosure. In addition, for those facilities containing wastes that are hazardous beyond 100 yr and incorporating passive controls for deterrence of intruders, a time of compliance of 500 yr is defined in DOE-RL Order 5820.2A.

2. For the drinking water pathway, a minimum time of compliance of 1,000 yr postclosure has been specified in DOE-RL Order 5820.2A. As a design goal, the time of compliance has been extended to 10,000 yr for potential doses received from the drinking water, all-pathways, and Columbia River scenarios. The 10,000-yr period is consistent with the compliance time specified in proposed EPA regulations for the disposal of high-level waste (58 FR 7924). The analyses generally show that peak doses occur at times less than 10,000 yr (e.g., about 1,000 yr or less). In cases where peak doses occur after 10,000 yr, the results and their impacts are discussed.

2.0 DISPOSAL FACILITY DESCRIPTION

This chapter provides background information to complete a site-specific PA analysis for disposal of LLW in the general vicinity of 200 West Area LLBG on the Hanford Site. Several topics are discussed that are pertinent to the completion of a PA analysis:

1. A description of the general environment of the disposal facility (Section 2.1)
2. The use of these environmental conditions in this PA analysis (Section 2.2)
3. A description of waste characteristics (Section 2.3)
4. The treatment of waste characteristics in the PA analysis (Section 2.4)
5. A description of current disposal facility practices and proposed modifications of disposal practices that are to be evaluated in the PA analysis (Section 2.5)
6. The treatment of disposal facility features in the PA analysis (Section 2.6).

The primary purpose of this section is to describe those aspects of the disposal practices and environmental conditions that control the release of radionuclides into the environment. Conversely, those aspects of the environment not considered in this PA analysis will be discussed along with the justification for each decision.

2.1 CHARACTERISTICS OF THE 200 WEST AREA LOW-LEVEL BURIAL GROUNDS (LLBG)

In this section, the environmental conditions that characterize the 200 West Area LLBG are summarized. A detailed discussion will not be provided because these topics have been discussed at length in other publications (e.g., the Hanford Defense Waste Environmental Impact Statement [HDW-EIS {DOE 1987}] and numerous safety analysis reports [SAR]). Much of the information in these documents has not been updated for several years but is considered valid for the purposes of this PA analysis. Environmental characteristics discussed include regional geography and demography, regional and site-specific geology, regional and site-specific hydrology, climatology, meteorology, ecology, and natural radiation background.

2.1.1 Site Geography and Demography

The 200 West Area LLBGs are located on the Hanford Site in the southeast corner of Washington State (Figure 2-1). The Hanford Site is located in a structural and topographic depression of the Columbia Plateau called the Pasco Basin. The northern and eastern boundaries of the site generally follow

Figure 2-1. Map Showing Location of Hanford Site and the 200 Areas Low-Level Burial Grounds (Bjornstad 1990).

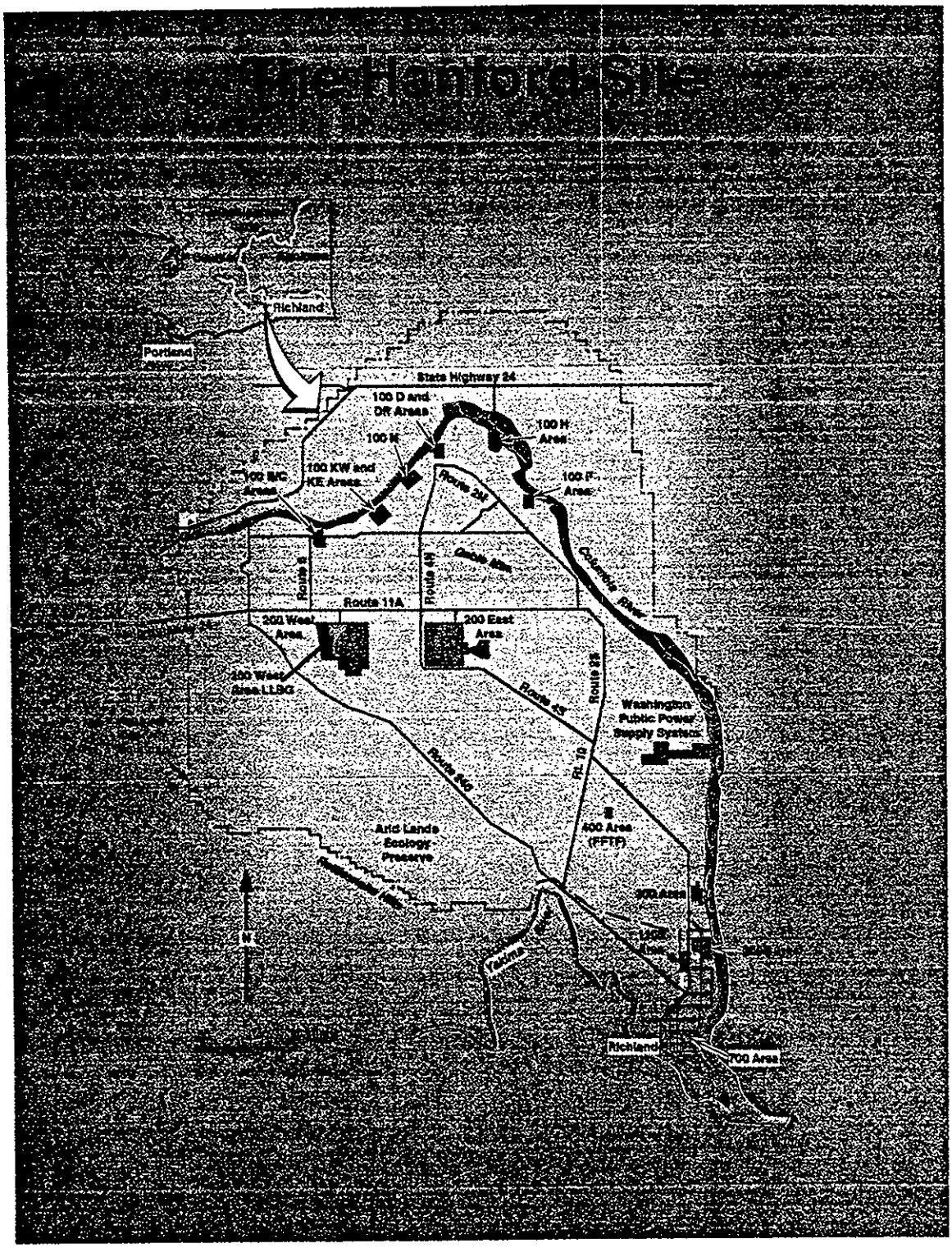

the Columbia River. The western boundary of the site is generally bounded by the Rattlesnake Hills and the southern boundary by the Yakima River. The Hanford Site covers an area of about 1,500 km^2. With the exception of a few natural basalt hills (e.g., Gable Butte and Gable Mountain), the site is relatively flat (Figure 2-2) with a topographical low at the Columbia River (about 100 to 120 m above sea level and a gradual increase in elevation toward the north-central part of the site). The 200 West Area LLBGs are located in this region, commonly referred to as the 200 Area Plateau. The elevation of the burial ground is about 225 m.

The nearest population center consists of three small cities (Richland, Kennewick, and Pasco) that are situated to the southeast of the site on the Columbia River. The population living within 80 km of the burial grounds is about 375,000 (Kincaid, et al 1993).

2.1.2 Site Climatology and Meteorology

Meteorological data have been collected at the Hanford Meteorology Station (HMS) since the year 1945. The HMS is located between the 200 East Area and the 200 West Area. Temperature and precipitation data have been recorded in the region since the year 1912. Generally, the Hanford Site climate is classified as semiarid with an average rainfall of about 16 cm/yr, nearly half of which occurs in the winter months of November through January.

The prevailing winds of the area are from the northwest and secondarily from the southeast. Average wind speeds are about 10 to 15 km/h. The area is subjected to occasional high winds (e.g., a peak gust wind of 130 km/h [80 mi/h] was recorded at the HMS in 1972). Only 24 tornado occurrences have been reported in the vicinity of the Hanford Site.

2.1.3 Site Ecology

Site ecology is thoroughly summarized in the HDW-EIS (DOE 1987). Dominant vegetation at the Hanford Site includes sagebrush, rabbit brush, and a variety of grasses, including cheatgrass and bunchgrass. Common mammals on the site include mule deer, elk, jack and cottontail rabbits, coyotes, badgers, raccoons, and a variety of rodents. Common birds on site include grouse, doves, falcons, hawks, owls, geese, and ducks. A wide variety of fish inhabit the Columbia River including salmon, trout, shad, bass whitefish, sturgeon, and catfish.

Endangered, threatened, or candidate species have been identified onsite. However, a review based on information from the Fish and Wildlife Service for the Department of the Interior suggests that these species are not directly at risk from waste management activities in the 200 Areas (DOE 1987).

2.1.4 Regional and Site-Specific Land Use

In the region surrounding the Hanford Site, commercial land use is typically agricultural which relies on irrigation to grow crops. The sources

Figure 2-2. Topography of the Hanford Site.

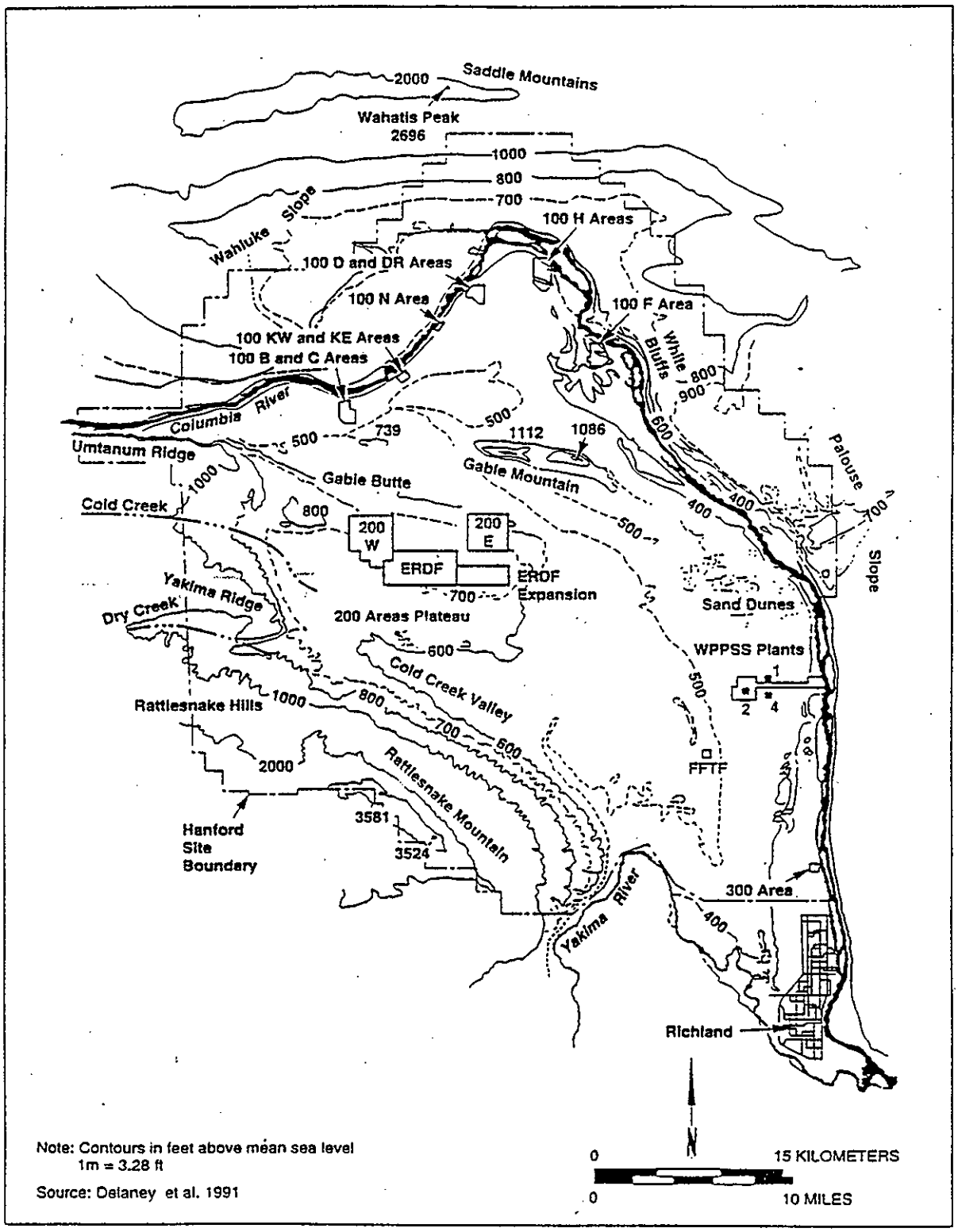

923 E412/48587/3-1-94

of irrigation are generally the Columbia and Yakima Rivers and confined aquifers (sediment layers between upper basalt flows). Several nuclear facilities are in operation on or adjacent to the Hanford Site including the Washington Nuclear Plant 2 (WNP-2), a commercial nuclear reactor operated by the Washington Public Power Supply System, and the Siemens Nuclear Power Corporation Fuel Fabrication Plant. In addition, a commercial LLW disposal facility operated by U.S Ecology is located adjacent to the 200 East Area.

On the Hanford Site, a large number of facilities including reactors and processing plants have been operated to produce nuclear materials. None of these facilities are currently operational and permanent shutdown is planned. Adjacent to the 200 West Area LLBG, the Solid Waste Operations Complex is operating for management of LLW. The complex consists of a number of active and inactive burial sites (shallow-land trenches), storage buildings (primarily for mixed waste), and administrative buildings. The Waste Receiving and Processing (WRAP) Facility is planned for construction and operation in this area to treat, package, and ship TRU waste and LLW for disposal. Also, a mixed LLW RCRA-compliant disposal facility is being constructed and operated in Burial Ground 218-W-5.

2.1.5 Seismology

The Hanford Site is in an area of low seismicity (Figure 2-3). Earthquakes typically occur at shallow depths (focal depth less than 6 km [Caggiano and Duncan 1983]) as multiple events or swarms at magnitudes of less than 3.5. Two moderate-size earthquakes have been recorded near the site, one in 1936 in the Milton-Freewater area (Modified Mercalli intensity VII) about 40 mi southeast of the Hanford Site and another in Corfu in 1918 (Modified Mercalli intensity IV to VI) about 118 mi north of the site. The Corfu earthquake is estimated to have produced peak ground accelerations of 0.01 to 0.03 g onsite. The epicenters of recorded earthquakes occur somewhat randomly and are not strongly associated with any geologic structural features.

2.1.6 Radiation Background

The natural environment of the Hanford Site is contaminated by radiation from two sources: Hanford Site nuclear production activities during the last 50 years and fallout from nuclear weapons testing in other parts of the world. Radiation measurements have been made for Columbia River water, groundwater (primarily the unconfined aquifer), local soil, and wildlife including mammals, birds, and fish. The HDW-EIS (DOE 1987) reports small quantities (less than 1 pCi/L) of ^{144}Ce, ^{60}Co, ^{137}Cs, ^{129}I, ^{131}I, ^{90}Sr, ^{95}Zr, plutonium, and uranium in the Columbia River. In Hanford Site soil, average quantities of ^{90}Sr, plutonium, and uranium of less than 1 pCi/g have been reported. Slightly higher concentrations of ^{137}Cs (about 2 pCi/g) have been measured. Quantities of ^{60}Co, ^{137}Cs, ^{90}Sr, plutonium, and uranium have also been reported in mammals, birds, fish, and vegetation generally at values less than 0.01 pCi/g.

Figure 2-3. Historical Seismicity of the Columbia Plateau and Surrounding Areas.

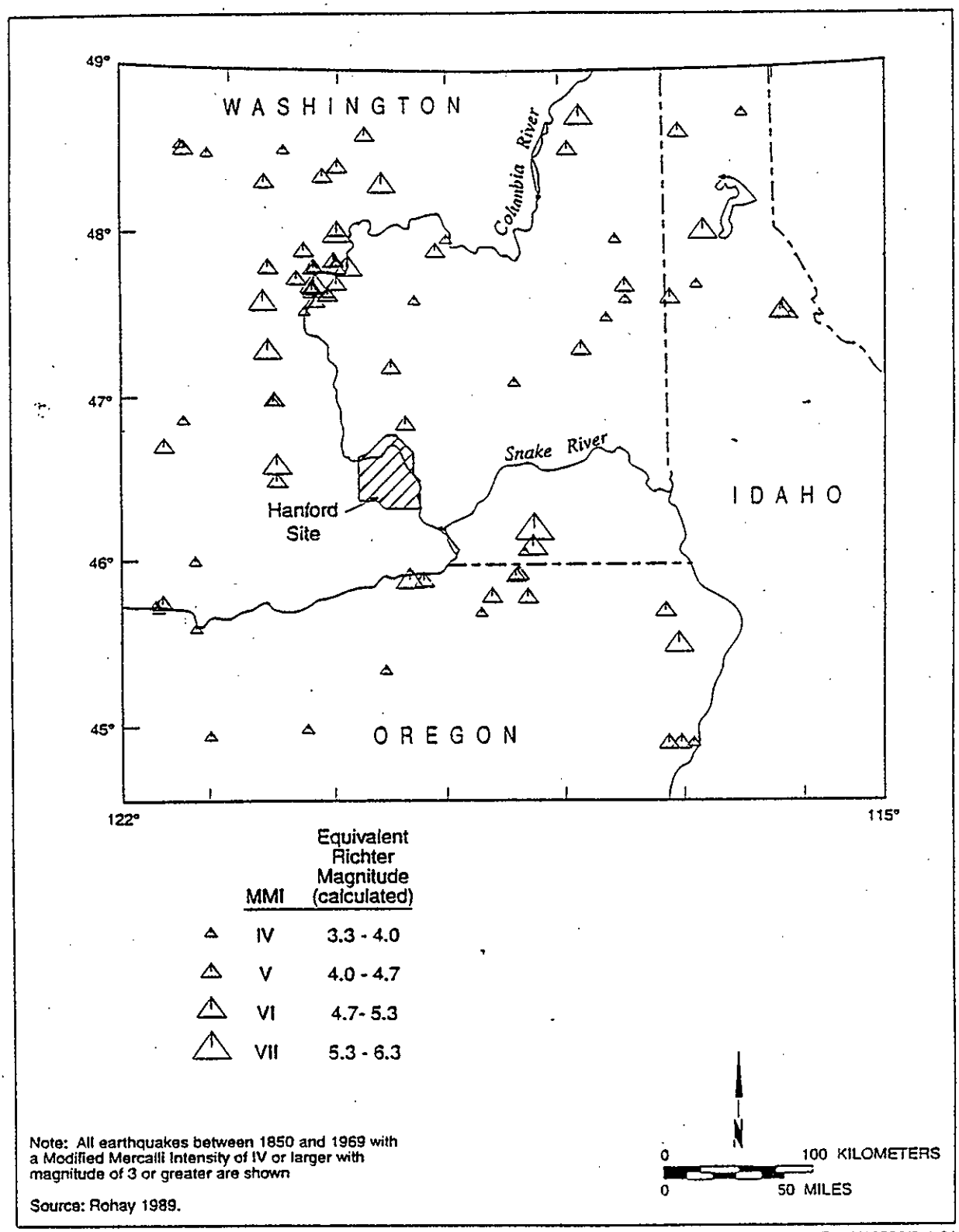

923 E412/48590/3-4-94

Numerous contaminant plumes are present in the unconfined aquifer beneath the 200 Area Plateau; these plumes resulted from the disposal of wastewater from various processing facilities into ponds, cribs, and ditches. Groundwater chemistry data was gathered and reviewed in 1992 as part of the 200 Aggregate Area Management Study (AAMS). The results of this groundwater sampling and analysis investigation are discussed in Ford (1993). Ford (1993) defines 18 contaminants whose groundwater concentrations can be mapped as a plume (i.e., at least one plume with multiple-well exceedances that are semicontiguous). All plumes identified by Ford (1993) emanated from facilities within the 200 Areas. Radionuclides present in the plumes include ^{3}H, ^{129}I, ^{106}Ru, ^{99}Tc, and uranium. Maps of the plumes are shown in Appendix A.

2.1.7 Regional Hydrogeology

The Hanford Site is located on a geologic province referred to as the Columbia Plateau. The Columbia Plateau covers much of eastern Washington, eastern Oregon, and parts of Idaho. It was formed by a massive upwelling of basalt magma during a time period of about 10,000,000 yr. Locally, the site is located in the Pasco Basin, a structural depression of the Columbia Plateau. About 10,000 ft (3,000 m) of basalt underlie a series of vadose sediments of variable thickness across the Hanford Site. The major sedimentary units are the Ringold Formation and the Hanford formation. The Ringold Formation overlies the uppermost basalt flow and was deposited by various erosional processes. The Hanford formation overlies the Ringold Formation and was deposited catastrophically in a series of major floods associated with glacial melting.

The hydrology of the Pasco Basin is characterized by a number of surface sources and aquifers, associated with both the basalts and the suprabasalt sediments. The basalt aquifers consist of the tholeiitic flood basalts of the Columbia River Basalt Group and relatively minor amounts of intercalated fluvial and volcaniclastic sediments. The uppermost aquifer system occurs within the fluvial, lacustrine, and glaciofluvial suprabasalt sediments. This aquifer is regionally unconfined and is contained largely within the Ringold Formation and the Hanford formation.

Surface drainage enters the Pasco Basin from several other basins (Figure 2-4), including the Yakima River Basin, Horse Heaven Basin, Walla Walla River Basin, Palouse/Snake Basin, and Big Bend Basin. Within the Pasco Basin, the Columbia River is joined by major tributaries including the Yakima, Snake, and Walla Walla Rivers. Two intermittent streams, Cold Creek and Dry Creek, cut through the Hanford Site. Water drains through these pathways during the wetter winter and spring months. No perennial streams originate within the Pasco Basin.

The total estimated precipitation over the Pasco Basin averages less than 6.3 in. (16 cm) per year. Mean annual runoff is estimated to be less than 2.5×10^{4} acre-ft per year, or approximately 3% of the total precipitation. The remaining precipitation is assumed to be lost through evapotranspiration, with a small component (perhaps less than 1%) contributing to recharging of the groundwater system (DOE 1988b, vol. 2, p. 3.1-6).

Figure 2-4. Hydrologic Basins Designated for the Washington State Portion of the Columbia Plateau (from Kincaid et al. 1993).

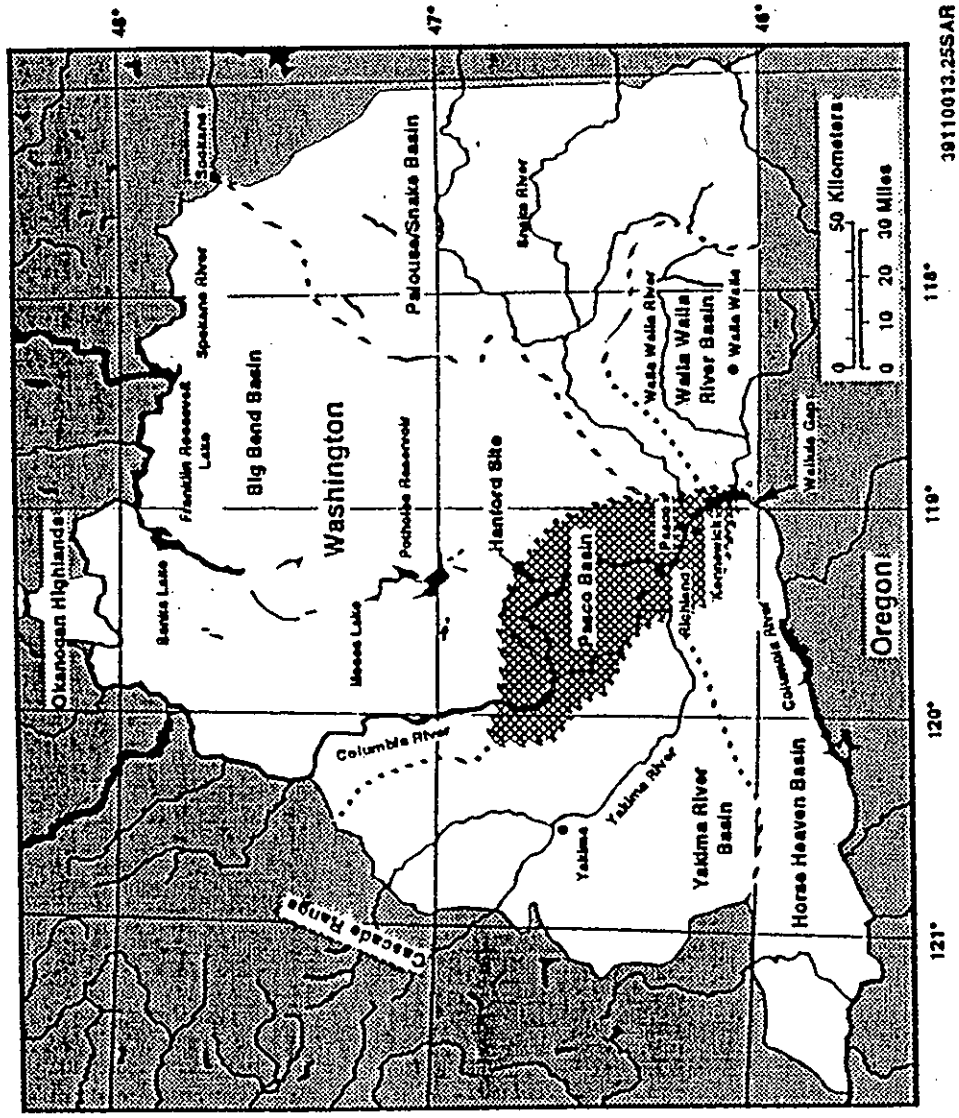

Primary surface water features associated with the Hanford Site are the Columbia and Yakima Rivers and their major tributaries, the Snake and Walla Walla Rivers. West Lake, about 10 acres (4.0 hectares) in size and <3 ft (0.9 m) deep, is the only natural lake within the Hanford Site. Wastewater ponds, cribs, and ditches are also associated with nuclear fuel reprocessing, and waste disposal activities are, of course, present on the Hanford Site.

Groundwater occurs both within the upper unconfined aquifer system and within a system of deeper confined to semiconfined aquifers in the basalt flow tops, flow bottom zones, and sedimentary interbeds (DOE 1988b, vol. 2, p. 3.6-1). These deeper aquifers are intercalated with aquitards, consisting of basalt flow interiors (colonnades and entablatures).

The general direction of groundwater flow is from the natural recharge areas west of the Hanford Site to discharge areas, primarily toward the Columbia River. Recharge of the confined basalt aquifers occurs through infiltration on the anticlinal ridges bounding the Pasco Basin and from westward flow in basalt aquifers beneath the Columbia Plateau. Sources of natural recharge to the uppermost (unconfined) aquifer system are infiltration and runoff of precipitation and runoff on the ridges bounding the Pasco Basin, infiltration from ephemeral streams, and from rivers along influent reaches of the Yakima and Columbia Rivers. The movement of precipitation through the vadose zone has been studied at several locations on the Hanford Site (Gee 1987; Routson and Johnson 1990; Rockhold et al. 1990; Fayer et al. 1991), with the general conclusions being that very little, if any, infiltration occurs where the soils are relatively fine grained and deep-rooted vegetation is present.

Principal sources of natural recharge to the unconfined aquifer, where precipitation and surface runoff infiltrate to the water table, occur west of the 200 West Area. Several small streams, such as Cold Creek and Dry Creek, that are located between the Rattlesnake Hills and Umptanum Ridge, drain the western slopes of the Pasco Basin, losing water to the subsurface as they spread across the lower valley plains. From here, groundwater moves through the sediments generally from west to east (DOE 1988b). Studies performed on the Hanford Site indicate that some recharge to the water table (0 to 10 cm/yr) may occur locally depending on surface conditions, especially during the winter months (Gee 1987); most precipitation, however, is returned to the atmosphere through evapotranspiration.

Artificial or synthetic recharge to the unconfined aquifer from liquid-waste disposal operations occurs at the Hanford Site, mainly in the 200 Areas. Recharge from the 200 Areas wastewater-disposal facilities is estimated to be approximately 10 times the natural recharge at the Hanford Site (Graham et al. 1981).

2.1.8 Hydrogeology of the 200 West Area LLBG

The source of the data described in this section is (1) a detailed summary of the geohydrology of the 200 West Area by Connelly et al. (1992) and (2) a detailed characterization of Burial Ground 218-W-5 by Bjornstad (1990). These reports represent the most recent synthesis of available data that have

been used to characterize the primary features of the vadose zone and unconfined aquifer that influence groundwater movement. Typical soil characterization data taken from the soil samples includes particle size distribution, ambient moisture content, calcium carbonate content and gross gamma radiation counts as a function of depth below the surface. The data base shows that Hanford Site soils are predominantly sandy with ambient moisture content in the range of 3 to 15 vol%. Calcium carbonate is generally present in sufficient quantity to control the pH of the groundwater solution.

Isopach maps (Connelly et al. 1992) of the major soil column units underlying the 200 West Area are shown in Appendix A. A generalized cross-section of the stratigraphic units is shown in Figure 2-5. Also, several cross sections (Bjornstad 1990) across Burial Ground 218-W-5 are shown in Appendix A. These drawings illustrate the spatial distribution of the major vadose zone units in a three-dimensional fashion. The bulk of the Hanford Site vadose zone comprises two formations: the Hanford formation and the underlying Ringold Formation. The Ringold Formation overlies the uppermost basalt flow of the Columbia Flood Basalts. The Ringold Formation consists of fluvial and lacustrine sediments while the Hanford Formation consists of catastrophic flood deposits. The total thickness of the vadose zone and the relative thickness of the two main formations vary depending on the location of interest on the Hanford Site.

Beneath the 200 West Area LLBG, four subunits of the Ringold are present, including the basal Ringold or Ringold A, the lower Ringold or Lower Mud Sequence, the middle Ringold or Ringold Unit E, and the upper Ringold. The basal Ringold contains a fine-grained and a coarse-grained subunit, the fine-grained unit being composed of sands and mud, and the coarse-grained unit containing larger quantities of gravel and gravelly sand. This unit pinches out just north of the burial grounds and thickens to the southwest, reaching a maximum thickness of about 50 ft beneath the burial grounds. The lower Ringold is a fine-grained unit consisting of relatively equal amounts of silt, sand, and clay. The unit is estimated at about 10 to 40 ft thick and pinches out just east of Burial Ground 218-W-5. The middle Ringold is a coarse-grained gravel sand unit which is up to 300 ft thick across Burial Ground 218-W-5. The water table and unconfined aquifer occur in this subunit. The upper Ringold is a sandy, medium- to fine-grained unit which is thickest to the north of the burial ground (about 35 ft) and pinches out completely to the south.

Between the Ringold and Hanford formations are two thin erosional layers that appear to be mostly continuous across the burial grounds. The Plio-Pleistocene layer that overlies the upper Ringold is a fine-grained sandy mud that has been reworked by plant and animal activity and is variably cemented with calcite. In some places, permeability is very low because of the cementing action. The unit thickness ranges from about 20 to 40 ft thick from south to north. It pinches out completely just south of the 200 West Area. Overlying the Plio-Pleistocene unit is the early Palouse soil unit, an unconsolidated, muddy sand layer that may have been deposited by wind erosion and then reworked by animal burrowing and root growth. This unit is about 10 ft thick across the burial grounds except where it thins, perhaps completely, in the southern parts of the burial grounds. The unit pinches out in all directions outside the 200 West Area.

Figure 2-5. Stratigraphic Chart for the 200 West Area (from Bjornstad 1990).

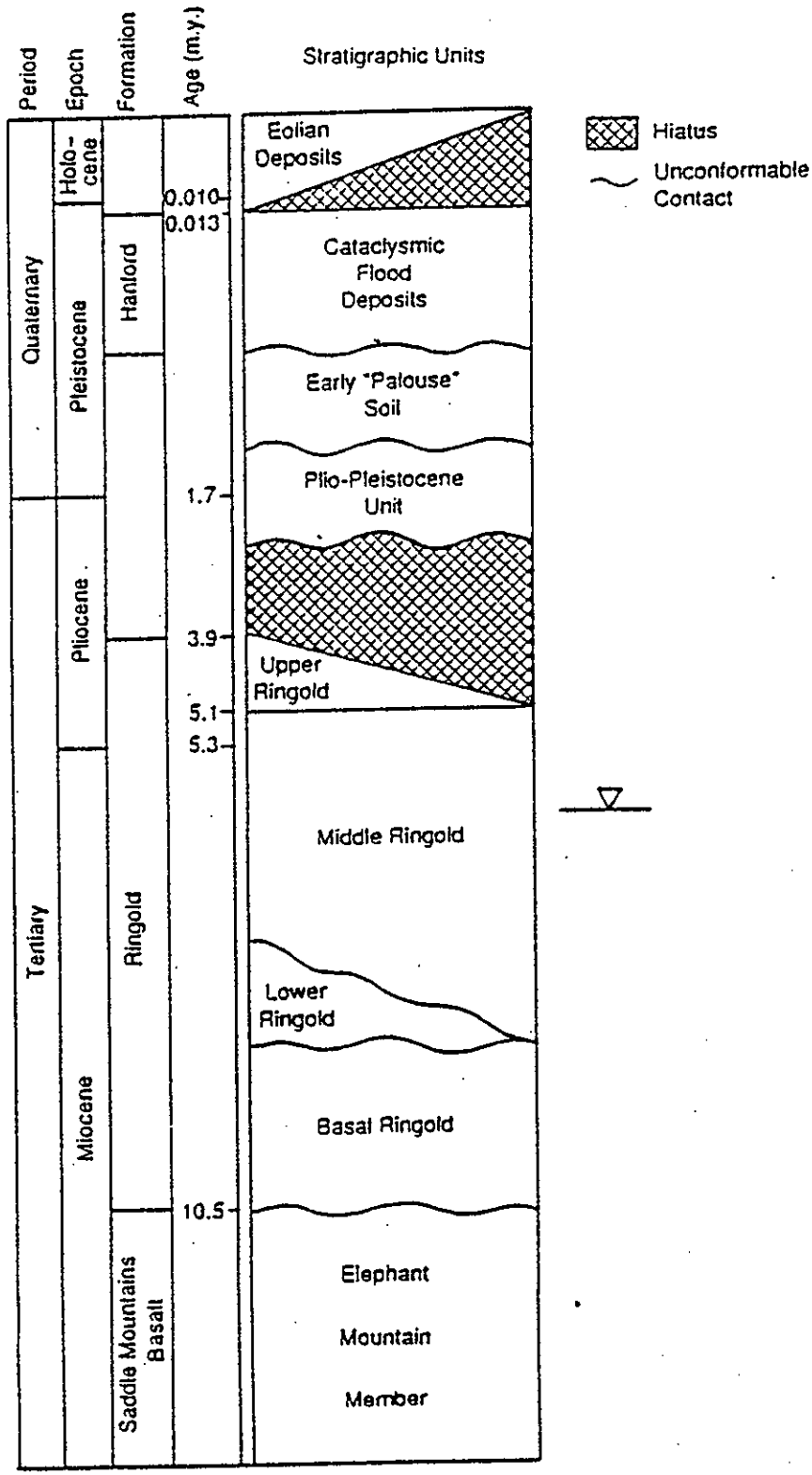

The Hanford formation consists of a variety of subfacies ranging from coarse gravels in the high-energy areas of deposition to fine-grained silts in low-energy deposits. Transition facies also exist which tend to be a mixture of coarse gravels and fine sands. Numerous cycles of flooding have apparently occurred leading to a chaotic distribution of subfacies units. As indicated by Figure 2-6, a secondary channel is indicated along the east side of the burial grounds by the high-energy deposition deposits of coarse gravelly sand in the Burial Grounds 218-W-3A and 218-W-3AE. In contrast, the burial grounds to the south and west (218-W-5 and 218-W-4C) are considered to be moderate energy areas of deposition as indicated by a larger component of finer sands and less gravel. The formation thickens from northeast (about 60 ft) to southwest (about 140 ft). The characterization of soil samples from wells in the vicinity indicate that small lenses of fine-grained material are interspersed in the Hanford formation that appear to be no more than 10 to 20 ft thick with a lateral extent of hundreds of feet or less.

Hydrologic flow patterns across the 200 West Area burial grounds were also estimated based on hydraulic conductivity data from sitewide soil samples and hydraulic head data from wells in the vicinity of the burial ground. As with the geologic interpretation, the hydrologic flow patterns were estimated in the context of our understanding of the Hanford Site hydrologic regime.

The present direction of groundwater flow in the vicinity of the 200 West Area is highly influenced by a groundwater mound associated with past artificial recharge at 216-U-10 Pond (U Pond) and with current recharge to the 216-U-14 Ditch, which lies just east of U Pond (Bjornstad 1990). The influence of the U Pond mound on groundwater flow beneath 200 West Area Burial Ground is demonstrated on a regional water table map that also indicates generalized groundwater flow direction (Figure 2-7). Artificial recharge at U Pond raised the level of the unconfined aquifer 55 ft between 1944, before the construction of U Pond, and 1987. Based on water-level measurements collected at well 299-W15-2, it appears that the water table has fluctuated as much as 15 ft over a 35-yr time period (Bjornstad 1990). The fluctuations are probably the result of varied volumes of process water being delivered to U Pond.

Even though U Pond has been decommissioned since 1984, the groundwater mound is expected to gradually decline for a number of years. Since about the time U Pond was decommissioned, water levels have in general declined, having fallen a total of about 7 ft in the last 6 yr at 299-W15-2. Hydrographs from the other wells located within 1,000 ft of 218-W-5 corroborate a general drop in water levels relative to those measured since the water levels have been measured at the site (Bjornstad 1990). As the groundwater mound dissipates, the direction of groundwater flow beneath 218-W-5 and the contiguous burial grounds will likely swing to the east, perhaps returning to the due-east regional groundwater flow direction recorded in 1944 (Figure 2-8).

The gradient across the burial ground is very slight (Figure 2-7). The general direction of flow is currently to the north-northeast. Saturated hydraulic conductivity data reported in the document show a reduction in hydraulic conductivity in the soils as a function of depth from 10^{-2} to

Figure 2-6. Geomorphic Features in the West-Central Portion of the Hanford Site (from Bjornstad 1990).

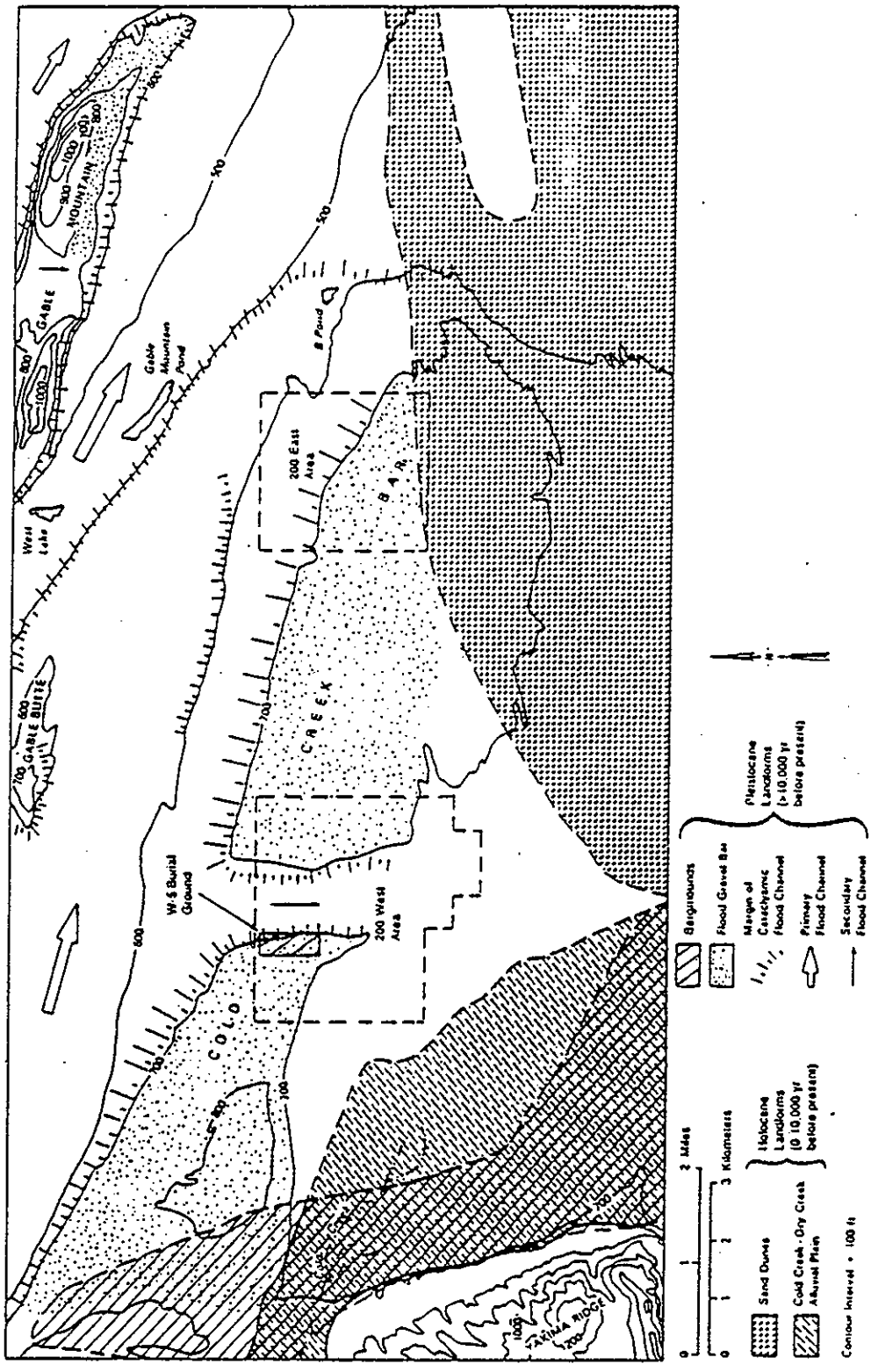

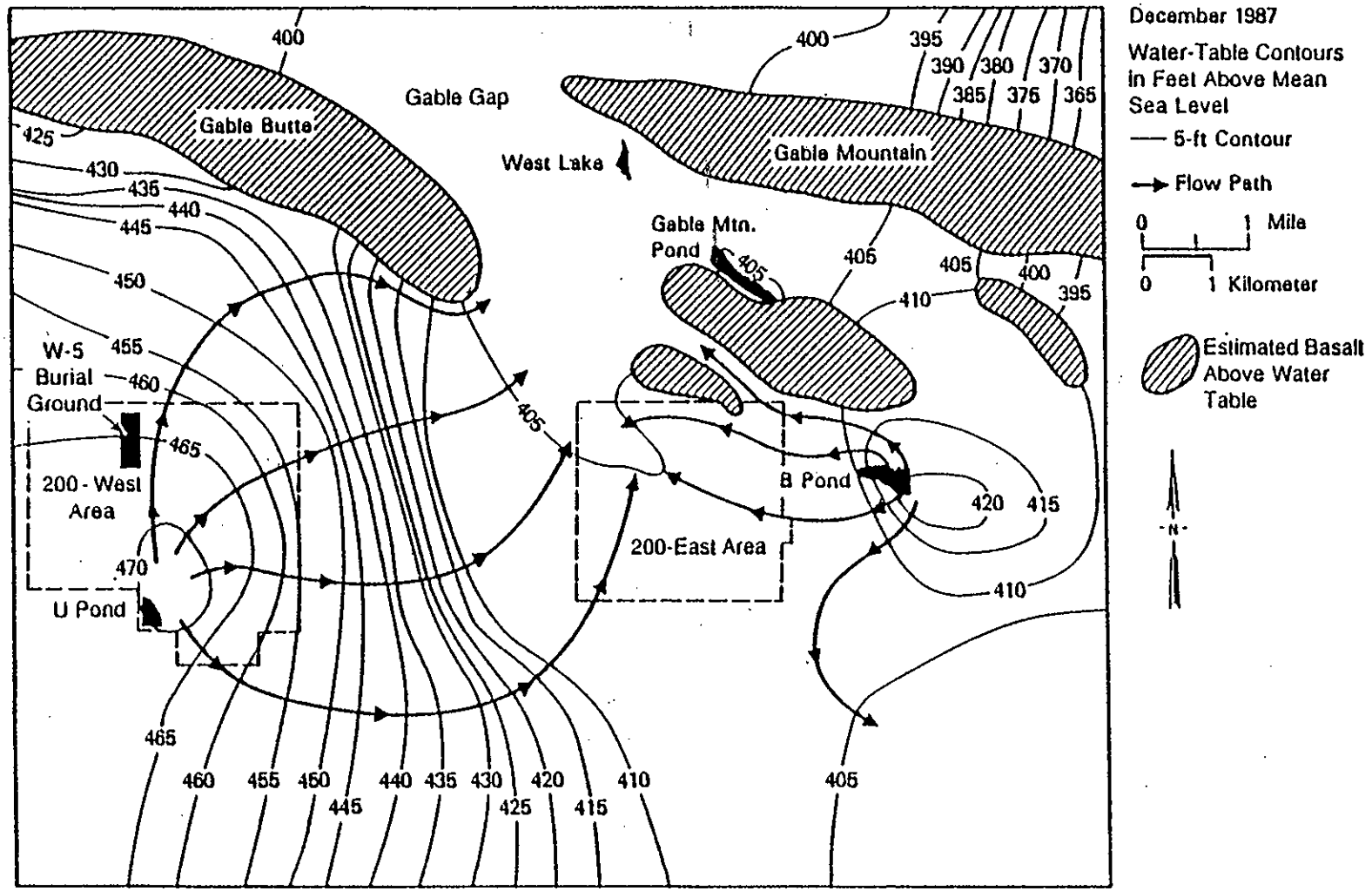

Figure 2-7. Water Table Map for the 200 Areas, December 1987 (from Bjornstad 1990).

Figure 2-8. Hanford Site Water Table Map, January 1944.

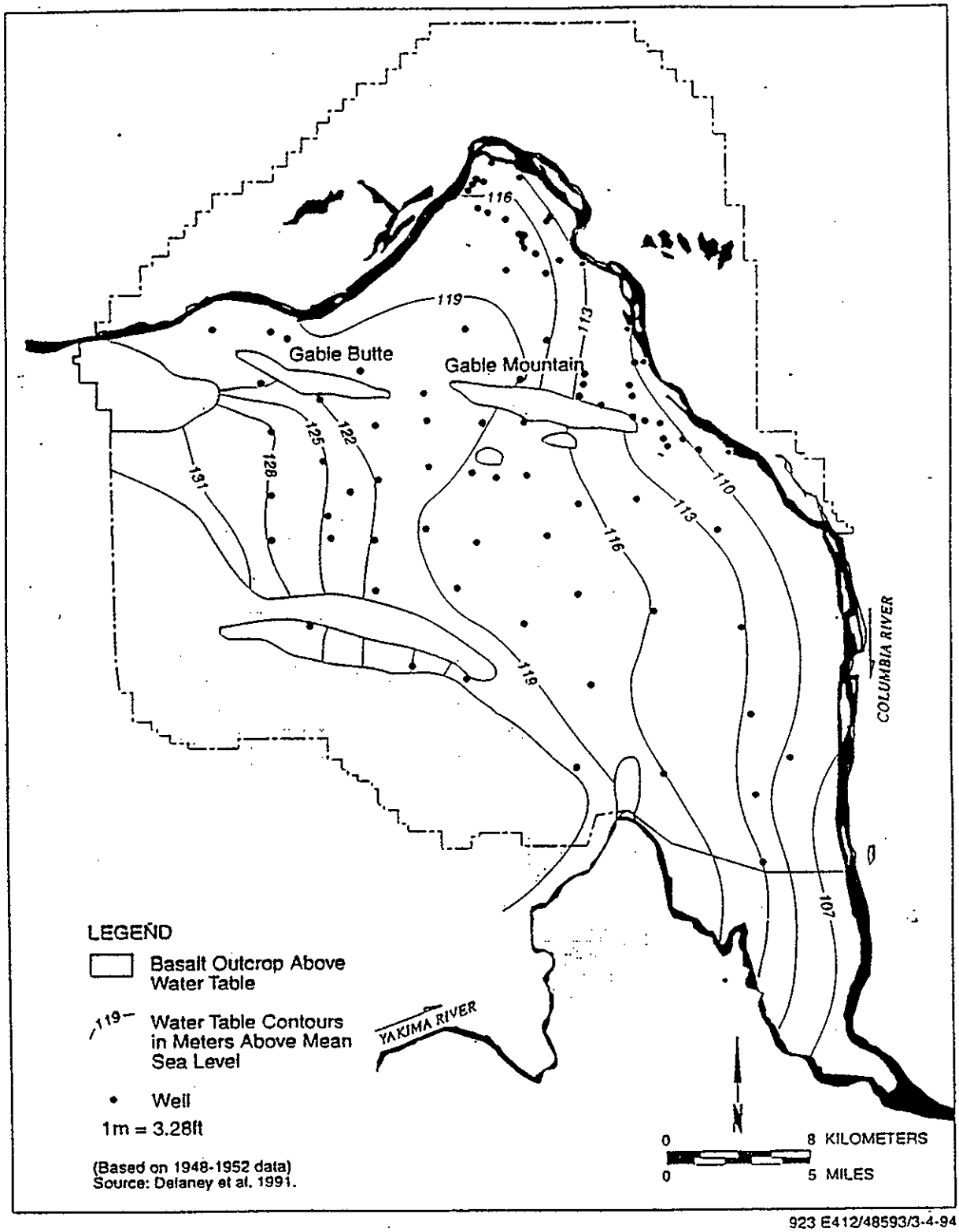

923 E412/48593/3-4-94

10^{-3} cm/s in the Hanford formation to 10^{-3} to 10^{-4} cm/s in the Ringold Formation. This trend is presumably the result of compaction by the soil column.

2.1.9 Geochemistry of the Soil Column

The general geochemical characteristics of the soil column are very consistent in the suprabasalt sediments across the Hanford Site. The soil phases are predominantly feldspar and quartz with minor quantities of smectite clay, hydrous oxides, and calcium carbonate that are consistently present. Measured quantities of soil phases from Burial Ground 218-W-5 (Serne et al. 1993) were about 31% feldspar, about 43% quartz, about 3% smectite clay, about 1% hydrous oxides, and about 2% calcium carbonate. Many analyses of the unconfined aquifer groundwater have been completed at the Hanford Site. Again, the data are very consistent. The groundwater is characterized as moderately alkaline (pH about 7.8 to 8.4), and oxidizing (Eh about 280 to 380 mv with moderate concentrations of aqueous species (about 5 meq/L). Analyses of moisture from vadose zone sediments (Serne et al. 1993) show essentially the same chemical characteristics.

2.2 TREATMENT OF ENVIRONMENTAL CHARACTERISTICS IN THE PERFORMANCE ASSESSMENT ANALYSIS

Of the environmental characteristics described above, some must be represented in the PA analysis and some do not require representation. For those characteristics that are represented, the manner in which they are represented is defined below. For those conditions that are not represented, a rationale for nonrepresentation in the PA analysis is given.

2.2.1 Meteorology and Climatology

At the Hanford Site, the meteorological conditions that require consideration are precipitation, flooding potential, high winds, and tornados. Of these, the most important process relative to PA analyses is the assumption of recharge rates resulting from precipitation. The actual percentage of recharge from precipitation is difficult to quantify precisely because of the semiarid climate (small annual amount of rainfall and the effectiveness of evapotranspiration that varies with the season, soil types, and vegetation types). This fractional value rather than the precipitation value has a direct impact on PA analyses because contaminant flux is proportional to rainwater infiltration flux through the waste material unless waste form characteristics exert a greater control over radionuclide release from the facility than infiltration. Because of this variability in actual infiltration rates, a range of rates is considered in this analysis as a function of assumed conditions (Section 3.2.3.3).

One other phenomenon, climatological change, is worth noting in connection with potential variability in recharge rate. A detailed discussion of past and potential changes in climate is found in Appendix B of the PA analysis for the disposal of LLW resulting from double-shell tank remediation at the Hanford Site (Kincaid et al. 1993). The evidence of past precipitation

has been inferred from pollen and tree ring studies that indicate periods of increases in precipitation over current conditions of about 30%. This inferred increase does not necessarily mean that recharge is proportionately increased because vegetation types and associated evapotranspiration rates will also respond to shifts in weather patterns due to glaciation processes. In the future, another glaciation event is predicted to occur in the next 50,000 to 100,000 yr. Quantitative predictions of changes in recharge resulting from glaciation are very uncertain and were not provided. However, there is no indication that drastic changes in recharge should occur because of the glaciation trend. It is concluded that the past 10,000-yr record is sufficient to presume that the present range of assumed values is reasonable for long-term future calculations.

The processes of flooding, tornados, and high winds are not evaluated in the PA analysis. A potential consequence of these events, the erosion of a disposal facility cover, is also not considered in this analysis. The most likely source of flooding in the vicinity of the 200 West Area is the Cold Creek Area (Figure 2-9), which is normally an ephemeral stream. The projected maximum flood would not reach the 200 West Area burial grounds. The other long-term source of flooding could occur as the result of glaciation events. It is assumed that man's activities will be sufficiently disrupted by associated climatic and geomorphic changes such that dose-to-man by displacement and dispersal of waste due to flooding is an unreasonable scenario to consider.

An evaluation of the historical occurrence of tornadoes (DOE 1987) suggests that the probability of a highly destructive event is very low (about 10^{-6}); therefore, it need not be considered a likely event. High wind events can be expected to occur on occasion. However, it is assumed that the type of disposal facilities being considered here will be underground and that soil covers can be designed to minimize the erosional effects of wind and the likelihood of airborne distribution of contamination. Several studies conducted by the Hanford Barrier program (see Appendix F of Kincaid et al. [1993] for a summary of the literature) have shown that the addition of pea gravel to the surface of a cover or planting natural vegetation on the surface should permit little or no erosion. The geomorphic features in the 200 Area plateau show no evidence of long-term erosion.

2.2.2 Seismicity

The nature of seismic events at the Hanford Site and the type of disposal facility being considered indicate that the potential for enhanced release and transport is not likely. First, there is no evidence that permanent displacement in the soil column has occurred nor is any expected as a result of the lack of structural rigidity in the soil column. The only evidence of displacement occurs in basalt. The normal low intensity of seismic activity makes the condition of displacement resulting from that activity unlikely and the geologic record suggests that permanent displacement is even more unlikely. Second, no large rigid features are planned for the LLW disposal facilities, such as vaults or large waste monoliths. These structures would

Figure 2-9. Cold Creek Watershed Floodplain from the Probable Maximum Flood (DOE 1987).

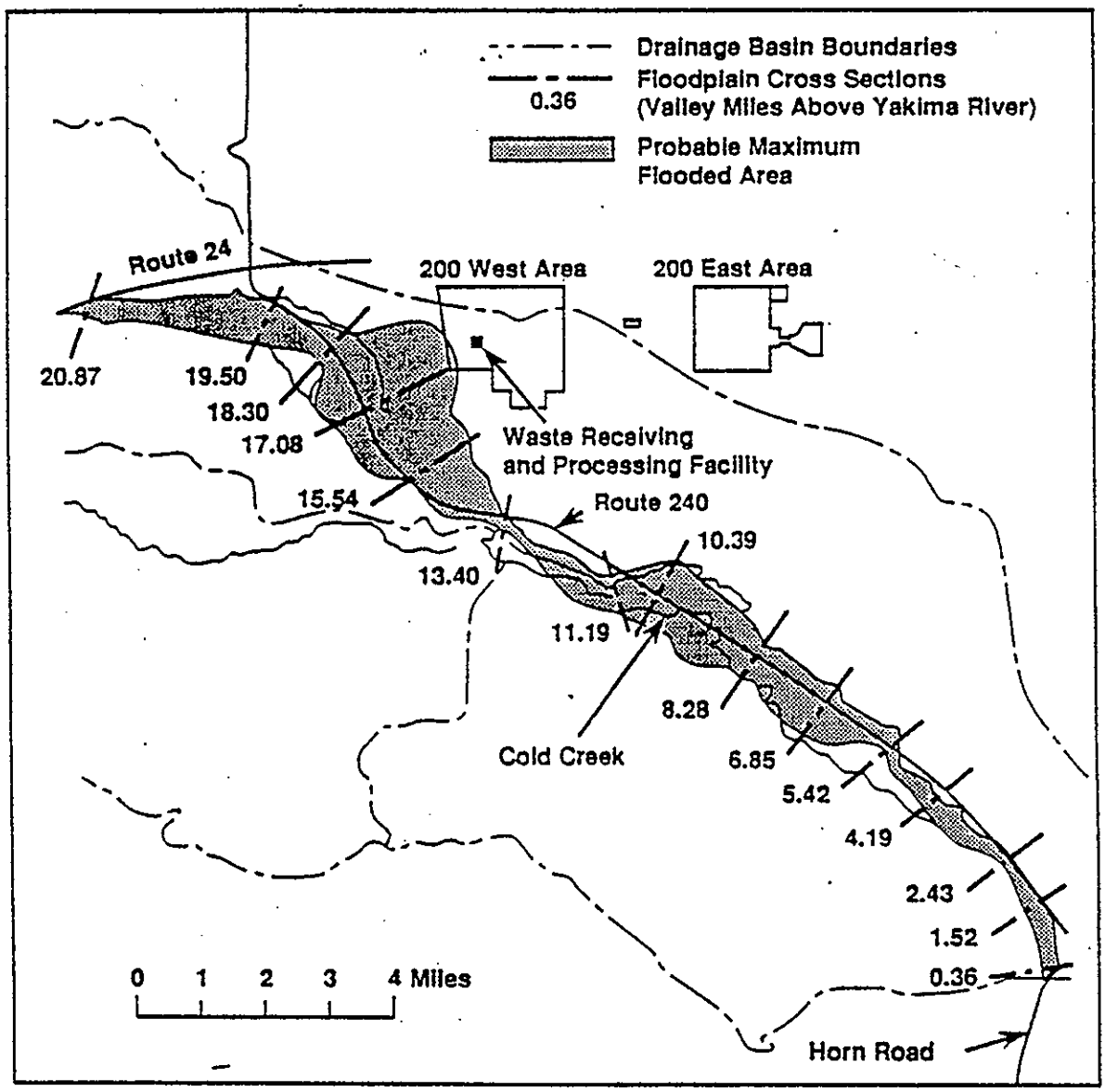

39103001.1C

be most susceptible to displacement. Relatively small stabilized waste materials such as grouted drums and boxes will be surrounded by loose soils which are expected to absorb the displacement energy in the unlikely event of such an occurrence.

2.2.3 Geology and Hydrology

For any geohydrological site, the conditions are sufficiently complex that completion of a mass transport modeling analysis can only be accomplished by assuming simplified representations of the real system. In the analysis, the four major units are assumed to be present underneath the disposal facility, each having distinct hydrologic properties. Preferential vertical pathways were not considered in the base case analysis, but sensitivity analyses were completed to evaluate the possible effect of features occurring in the area that could be potential pathways. Further discussion of geohydrologic parameters is provided in Section 3.2.3.3.

2.2.4 Soil Column Geochemistry

Properties of the soil column are not direct inputs into the computer modeling of the groundwater transport analysis. Rather, these characteristics are used to identify the appropriate sorption characteristics for radionuclides of interest. Selection of Kd values are provided in Section 3.2.3.3.4. For numerous radionuclides, Kd measurements have been collected in Hanford Site soil in the presence of typical groundwater. The same philosophy applies to the quantification of solubility limits for specific radionuclides in the soil column. However, the analyses indicate that solubility limits in the soil column are not significant factors in the control of radionuclide flux.

2.2.5 Other Disposal Facility and Environmental Characteristics

The existing radiation background results from past practices and world-wide nuclear testing events. Because DOE Order 5820.2A is focused on the consequences of future waste disposal, it is not required explicitly that the existing radiation background be added to the predicted radiation exposure from a new facility. Evaluation of land use around the disposal site in the PA analysis is considered in terms of the potential effect such use might have on the performance of the facility and the dose that might be received via exposure pathways from the disposal facility. Other facilities in the immediate vicinity of the 200 West Area burial grounds are storage and treatment facilities. It is expected that these facilities will not be operational during the postclosure period and will not influence the performance of a disposal facility. On the other hand, the prevalent use of well water in the area for agricultural purposes (drinking and irrigation) requires that well drilling and water use for drinking and farming be considered as a primary means of exposure. The assumption of well drilling is used in the development of inadvertent intruder scenarios and all-pathways scenarios. The effects of large-scale commercial irrigation on site are also considered as a sensitivity case.

2.3 LOW-LEVEL WASTE CHARACTERISTICS

LLW that is currently being disposed in the Hanford Site LLBG consist of many waste streams derived from numerous sources, both onsite and offsite. An annual report is prepared describing some of the characteristics of LLW being disposed onsite currently and projected to be disposed during the next 30 yr. Much of the information summarized here comes from the current report (Valero et al. 1993) and the report from the previous year (Duncan et al. 1992). The reports describe the physical and chemical makeup of the waste and the volumes of waste expected to be disposed at the Hanford Site. Uncertainties in the volume estimates and the potential for additional sources of waste are also discussed. A summary of generator groups and projected volumes of waste to be disposed through the year 2021 is provided in Table 2-1.

Table 2-1. 30-Year Low-Level Waste Volume Forecast for Hanford Site and Offsite Generators.*

Generator	Volume (m^3)		
	LLW	LLMW	Total
Defense waste management	72,600	121,900	194,500
Chemical processing	28,600	2,000	30,600
Other onsite facilities	14,700	500	15,200
Offsite facilities	171,700	29,600	201,300

*Volume estimates are taken from Valero et al. (1993).
LLW = low-level waste
LLMW = low-level mixed waste

Radionuclide inventory data is not provided in the annual report. Information discussed about radionuclide inventory is summarized from responses to waste characterization questionnaires provided by individual generators. Also, a computerized database, the Solid Waste Information and Tracking System (SWITS), provides inventory and waste volume data on a container-by-container basis. These records are somewhat limited because a complete listing of specific radionuclides has not been required until the last 2 yr. A summary of the radionuclide inventory characteristics over a 4-yr period (1989-1992) for the major generator groups is provided in Table 2-2.

The inventory and volume estimates provided below represent the best estimate of wastes disposed and future waste to be disposed after September 1988.

Table 2-2. Radionuclide Inventory of Commonly Listed Isotopes in the Solid Waste Information Tracking System for Waste Accepted at the Hanford Burial Grounds from 1989 Through 1992.

Generator	Radionuclides	Total quantity (Ci)	Range of concentration (log Ci/m^3)
Defense waste management	^{137}Cs	30	-7 to +1
	^{90}Sr	60	-7 to +1
	^{60}Co	7	-7 to -2
Chemical waste processing	^{137}Cs	2	-7 to -3
	^{90}Sr	2	-9 to -3
	^{60}Co	2	-15 to -3
Other onsite generators N Reactor	^{137}Cs	1,000	-12 to +1
	^{90}Sr	30	-12 to +1
	^{60}Co	0.8	-9 to -3
	^{152}Eu	0.01	-4 to -3
	^{154}Eu	0.05	-11 to -2
PNL	^{137}Cs	6,000	-10 to +1
	^{90}Sr	5,000	-8 to +1
	^{60}Co	2 E+4	-9 to +2
	^{152}Eu	2,000	-9 to +1
	^{154}Eu	2,000	-11 to +1
	U	10	-13 to -1
	Pu	0.8	-7 to -2
Offsite generators	U	0.5	-12 to -3
	^{232}Th	0.03	-15 to -4
	Pu	1	-9 to -3
	^{228}Ra	3	-9 to -2
	^{60}Co	50,000	-7 to +3

PNL = Pacific Northwest Laboratory

2.3.1 Defense Waste Management Waste

Several Hanford facilities are included in this group of waste generators including existing facilities, current tank farm operations and the B Plant Facility, and planned facilities, the Liquid Effluent Treatment Facility (LERF), the High-Level Waste Vitrification Plant (HWVP), and the Hanford Grout Facility (the grout facility is no longer planned but some replacement facility should be expected). The questionnaire information indicates that the breakdown of physical and chemical characteristics of the defense waste management waste are absorbed liquids and solids (about 34%), compactible solids (about 26%), metals (about 22%), and particulates (about 6%). Detailed radionuclide inventory records are listed in Appendix Table B-1.

Currently, the dominant user of the burial grounds in this group is the ongoing tank farms operation generator. The most frequently listed radionuclides are ^{60}Co, ^{137}Cs, and ^{90}Sr. Radionuclides that are listed less

frequently at lower activity include technetium (about 10^{-5} Ci), americium (about 10^{-5} Ci), plutonium (about 10^{-3} Ci), europium (about 10^{-2} Ci), and uranium (about 10^{-5} Ci).

The total volume of defense waste management waste deposited over the last 4 yr is about 11,000 m^3. This volume of generated waste is consistent with the waste volume forecast provided in Valero et al. (1993); therefore, some credence is lent to the long-term forecast.

2.3.2 Chemical Processing Waste

The generators in this group are the major nuclear material processing facilities at the Hanford Site, including the Plutonium-Uranium Extraction (PUREX) Plant, the Plutonium Finishing Plant (PFP), and the 222-S Laboratory. The questionnaire information indicates that the breakdown of physical and chemical characteristics of the environmental restoration waste are compactible solids (about 56%), metals (about 19%), and absorbed liquids and sludges (about 6%). The volume of waste is expected to decrease because the PUREX Plant is not going to be restarted and PFP restart plans are indefinite. Wastes are being generated and will be generated because of shutdown activities.

Detailed radionuclide inventory records are listed in appendix Table B-2, for waste disposed by chemical processing waste generators in the 200 Areas' burial grounds from 1989 to 1992. The most frequently listed radionuclides are ^{60}Co, ^{137}Cs, and ^{90}Sr. Radionuclides that are listed less frequently include technetium (about 1 x 10^{-5} Ci), americium (about 1 Ci), short-lived plutonium (about 1 Ci), long-lived plutonium (about 1 x 10^{-1} Ci), samarium (about 1 Ci), and uranium (about 1 x 10^{-5} Ci).

The total volume of chemical processing waste deposited during the last 4 yr is about 7,400 m^3. This volume of generated waste is consistent with the waste volume forecast provided in Valero et al. (1993).

2.3.3 Other Onsite Generators

The remainder of the Hanford Site generators who contribute or may contribute a minor but significant volume of waste for disposal at the burial grounds include Pacific Northwest Laboratory (PNL), and the 100-N Reactor. Additional generators who contribute smaller amounts of waste include onsite support services, the Hanford Environmental Health Foundation (HEHF), Kaiser Engineers Hanford (KEH), facility improvement projects, and the Fast Flux Test Facility (FFTF). The questionnaire information indicates that the breakdown of physical and chemical characteristics of the PNL, KEH, and HEHF waste are compactible solids (about 72%), and metals (about 11%). The questionnaire information indicates that the breakdown of physical and chemical characteristics of the 100-N Reactor waste are compactible solids (about 50%), metals (about 15%), spent resins (about 7%), and absorbed liquids and sludges (about 7%).

Detailed radionuclide inventory records are listed in appendix Table B-3 for waste disposed by other onsite waste generators in the 200 East and 200 West Areas' burial grounds from 1989 to 1992. The primary contributors are the N Reactor and PNL. The most frequently listed radionuclides for N Reactor waste are ^{60}Co, ^{137}Cs, ^{152}Eu, ^{154}Eu, and ^{90}Sr. Other radionuclides less frequently listed are nickel (about 1×10^{-8} Ci), uranium (about 0.01 Ci), and ^{238}Pu (about 10 Ci). The PNL wastes contains a wider variety of radionuclides because they are generated by research projects. Frequently listed radionuclides in PNL waste are ^{60}Co, ^{137}Cs, ^{152}Eu, ^{154}Eu, ^{90}Sr, plutonium, and uranium. Other radionuclides less frequently listed are ^{14}C (about 0.03 Ci), ^{59}Ni (about 0.007 Ci), and ^{99}Tc (about 0.06 Ci).

The total volume of N Reactor and PNL waste deposited during the last 4 yr is about 1,600 m^3 and about 2,200 m^3, respectively. This volume of generated waste is consistent with the waste volume forecast provided in Valero et al. (1993). N Reactor waste is expected to diminish as shutdown of the facility is completed. PNL is predicted to generate a relatively constant volume of waste for the foreseeable future.

2.3.4 Offsite Generators

Two types of offsite generators use or are proposing to use the Hanford Site burial grounds. The first are generators associated with cleanup of other DOE facilities. These include the Portsmouth Gaseous Diffusion Facility, the Paducah Gaseous Diffusion Plant, and facilities in the Formerly Utilized Site Remedial Action Program (FUSRAP). The second group of waste generators are national and university research laboratories. Major contributors include Argonne National Laboratory and Brookhaven National Laboratory. Other facilities disposing small quantities of waste at the Hanford Site include Battelle Columbus Operations, Ames Laboratory, Bettis Atomic Power Laboratory, Knolls Atomic Power Laboratory, Fermi Laboratory, University of California at Davis, University of Utah, Stanford University, and Princeton Plasma Physics Laboratory.

The volume forecast projections indicate that the largest contributors of waste will be Portsmouth (about 27,800 m^3), FUSRAP (about 16,700 m^3), Argonne (about 11,800 m^3), Brookhaven (about 11,700 m^3), Paducah (about 11,400 m^3), and Battelle Columbus Operations (about 2,700 m^3). The other offsite facilities combined are estimated to provide about 39,100 m^3 of waste during a 30-yr period. These estimates include LLMW as well as LLW.

Detailed radionuclide inventory records are listed in Appendix Table B-4 for waste disposed by offsite waste generators in the 200 Areas' burial grounds from 1989 to 1992. Frequently listed radionuclides include cobalt, plutonium, radium, thorium, and uranium. Less frequently listed radionuclides included ^{99}Tc (about 0.02 Ci), ^{14}C (about 30 Ci), and ^{63}Ni (about 5 E+04 Ci). Relatively small quantities of waste have been received from several offsite generators. The laboratories are expected to send a variety of wastes because their waste-generating processes are research projects. The Portsmouth and Paducah facilities will send waste whose dominant radionuclides are uranium isotopes and ^{99}Tc. The FUSRAP facilities are uranium processing facilities whose inventories include uranium isotopes and daughter products (e.g., thorium and radium).

The total volume of offsite generator waste deposited during the last 4 yr is about 3,000 m^3. This volume of generated waste is consistent with the waste volume forecast provided in Valero et al. (1993). However, substantial uncertainties in actual volumes of waste that will be received are derived from the possibility that some of the projected waste could be sent to other disposal facilities and some of the waste will be derived from decontamination and decommissioning activities that have not commenced.

2.4 TREATMENT OF WASTE CHARACTERISTICS IN THE PERFORMANCE ASSESSMENT ANALYSIS

A standard approach in PA analyses is to assume a specific waste inventory where particular waste isotopes are assumed to be present in the disposal facility at specific concentrations or total quantities. The analysis is completed to estimate potential dose from the entire inventory (i.e., the summation of doses from each isotope present in the disposal facility) and compared with the performance dose objectives (i.e., intruder scenario and all-pathway scenario). If the estimated dose is less than the performance objective dose, then the facility performance is considered adequate. If the inventory assumption is changed and all other parameters remain constant, a different potential dose will be calculated. If there is sufficient uncertainty in the actual inventory characteristics, a calculation of less than or greater than the dose limit could be made.

The discussion in Section 2.3 indicates that a general understanding of the types of waste which may be received is known with some confidence. Also, the set of commonly occurring radionuclides that are likely to be in the waste inventory are also known with some confidence. On the other hand, there are large uncertainties in a number of areas that severely restrict our ability to predict a finite LLW inventory. First, the eventual volumes of specific types of waste, particularly cleanup waste, are very difficult to predict. Second, the occurrence of less common radionuclides and the likely range of radionuclide concentrations in general are very difficult to predict because of the diversity of potential waste streams. Given this level of uncertainty, an additional primary approach has been taken in this analysis.

In the analyses discussed in Section 3.0, unit concentrations or quantities of radionuclides are assumed, depending on the type of analysis. Groups of radionuclides are also categorized into sets of different chemical properties (e.g., a set of radionuclides will be assumed to have the same sorption coefficient value). The analyses are then completed for a limited number of characteristic properties (e.g., four different Kd values). The predicted dose under these conditions are then determined and compared with the appropriate performance objective dose limit. Because a unique dose corresponds to a unit concentration or quantity of a radionuclide if all other parameters are held constant (depending on the radionuclides release scenario), the concentration or quantity of a radionuclide can be calculated which corresponds to the dose limit.

This approach has two advantages which are considered necessary and useful for this analysis. First, inventory limits can be calculated for any set of radionuclides. Thus, for a waste stream containing a radionuclide that is infrequently encountered, an estimate of the acceptability of that waste

stream for disposal can be determined by comparing the acceptable inventory with the actual inventory. Second, different sets of inventory limits can be calculated for a variety of combinations of environmental and disposal conditions, some of which provide greater isolation capability than others. Thus, a means of disposing of a range of waste inventory concentrations and/or quantities is provided.

A large group of waste streams are not being considered for disposal in the 200 West Area. These include wastes generated from remediation of CERCLA sites. These sites are primarily reactor sites in the 100 Areas and fuel processing waste sites in the 300 Areas. These wastes are to be disposed in the Environmental Restoration Disposal Facility. This facility is the subject of an ongoing PA analysis.

Another potential waste stream that is known at the Hanford Site and is not considered in this PA analysis is a group of graphite cores from the defunct 100 Area production reactors. The cores contain high levels of ^{14}C and are potential candidates for disposal in the 200 West Area burial grounds. Evaluation of this waste is not considered now for the following reasons:

- The method of remediation and timing of remediation is not well developed. It is expected that remediation will not be completed in the next decade.
- This waste material is unique in its physical, chemical, and radiological characteristics. Consequently, a separate waste release analysis is required. When it becomes clear that this waste will in fact be disposed in the 200 West Area burial grounds, the PA will be updated to determine the acceptable method of disposal.

Other special waste materials may be candidates for disposal in the future that are not known currently or are insufficiently characterized at present. For example, it is known that there are potential significant ^{99}Tc concentrations in the waste from Paducah and Portsmouth, but quantitative analyses of ^{99}Tc activity are not yet available. These kinds of wastes may contain high quantities of mobile radionuclides requiring waste form performance. If such wastes exist and are to be disposed in the future, additional analyses will be required to update the PA analysis.

Despite the uncertainties described above, an estimate of total inventory is provided for LLW during the 30-year period (Appendix B and Chapter 4). From this estimate, a total dose is calculated to compare with performance objectives.

2.5 WASTE TREATMENT, CERTIFICATION, AND DISPOSAL

In this section, a brief review of waste management practices at the Hanford Site is provided. Current practices and proposed modifications to current practice are discussed. The iterative interaction between PA analysis recommendations and disposal practice modifications are also provided.

2.5.1 Waste Treatment and Certification

Currently, there are no waste treatment facilities on site for LLW. The WRAP Facility is in the development stage and is scheduled for operation by 1997. The facility is split into several modules (WRAP 1 and WRAP 2A) and will provide treatment for some LLW streams in addition to handling TRU waste. The current plan is to provide a grouting or polymer cement encapsulation or solidification capability for appropriate wastes. The need for further types of treatment are dependent partly on the decisions about necessary treatment based on PA analysis and the types of wastes that are ultimately accepted for disposal. One alternative, for example, is in situ grouting at the disposal facility rather than treatment in a facility.

Waste certification is based on the waste acceptance criteria document, *Hanford Site Solid Waste Acceptance Criteria* (WHC 1993). This document requires the generator to provide characterization information about the waste stream (e.g., radionuclide inventory, chemical and physical property descriptions). They are also required to write a waste certification plan that describes their procedures for characterizing waste and packaging it for shipment to the burial ground. An auditing function in the solid waste management division must approve certification plans before the acceptance of waste at the Solid Waste Operations Complex (SWOC). The SWOC is located adjacent to the 200 West Area LLBG and contains storage and office facilities. Waste treatment facilities are being planned and constructed as well.

2.5.2 Low-Level Waste Disposal Practices and Facility Description

Shallow land disposal of solid waste has occurred at the Hanford Site since the late 1940's. Initially, numerous areas near processing facilities were chosen as disposal sites. Before 1970, no distinction was made between TRU and low-level waste. At that time, the Atomic Energy Commission (AEC) required that TRU waste be retrievable stored. Types of underground retrievable storage included shallow trenches, concrete lined "V" trenches, and asphalt pads. The segregated LLW continued to be disposed.

In the early 1980's, low-level liquid organic waste was segregated from LLW and stored retrievable underground. A further categorization of LLW was made in 1987 when the concept of MW was established with MW being defined as waste containing both radioactive and hazardous chemicals as identified by RCRA. Mixed waste disposal was largely discontinued except on a case-by-case basis where a significant reason for disposal (e.g., high- surface radiation of >200 mrem/h) could be justified. Storage of nonremote handled mixed waste in above-ground buildings in the SWOC is the current practice.

The 200 West Area LLBG are shown in Figure 2-10. As described above, disposal has occurred for several decades and as one burial ground became filled other burial grounds were begun. Active disposal trenches are found in 218-W-3A, 218-W-3AE, 218-W-4C, and 218-W-5 (Figures 2-11 through 2-14). The results of this analysis are applicable to all of these burial grounds, regardless of their present state of use. Several burial grounds (218-W-1, 218-W-2, 218-W-4A, 218-W-4B, and 218-W-11) are retired or inactive. Burial Ground 218-W-6 has been identified but never used. These burial grounds are

Figure 2-10. Low-level Waste Burial Ground Locations in the 200 West Area.

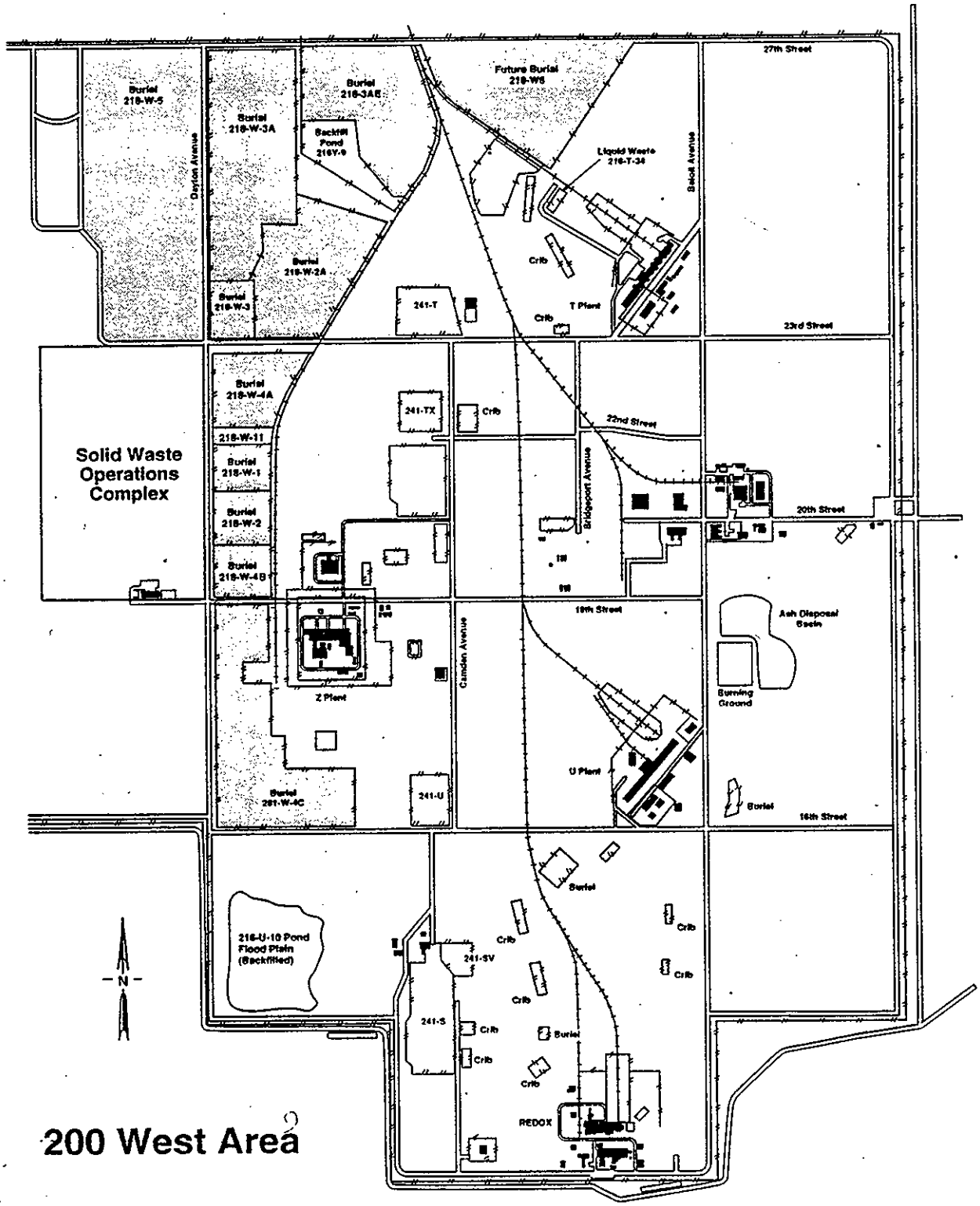

Figure 2-11. Topographic Map of Burial Ground 218-W-5.

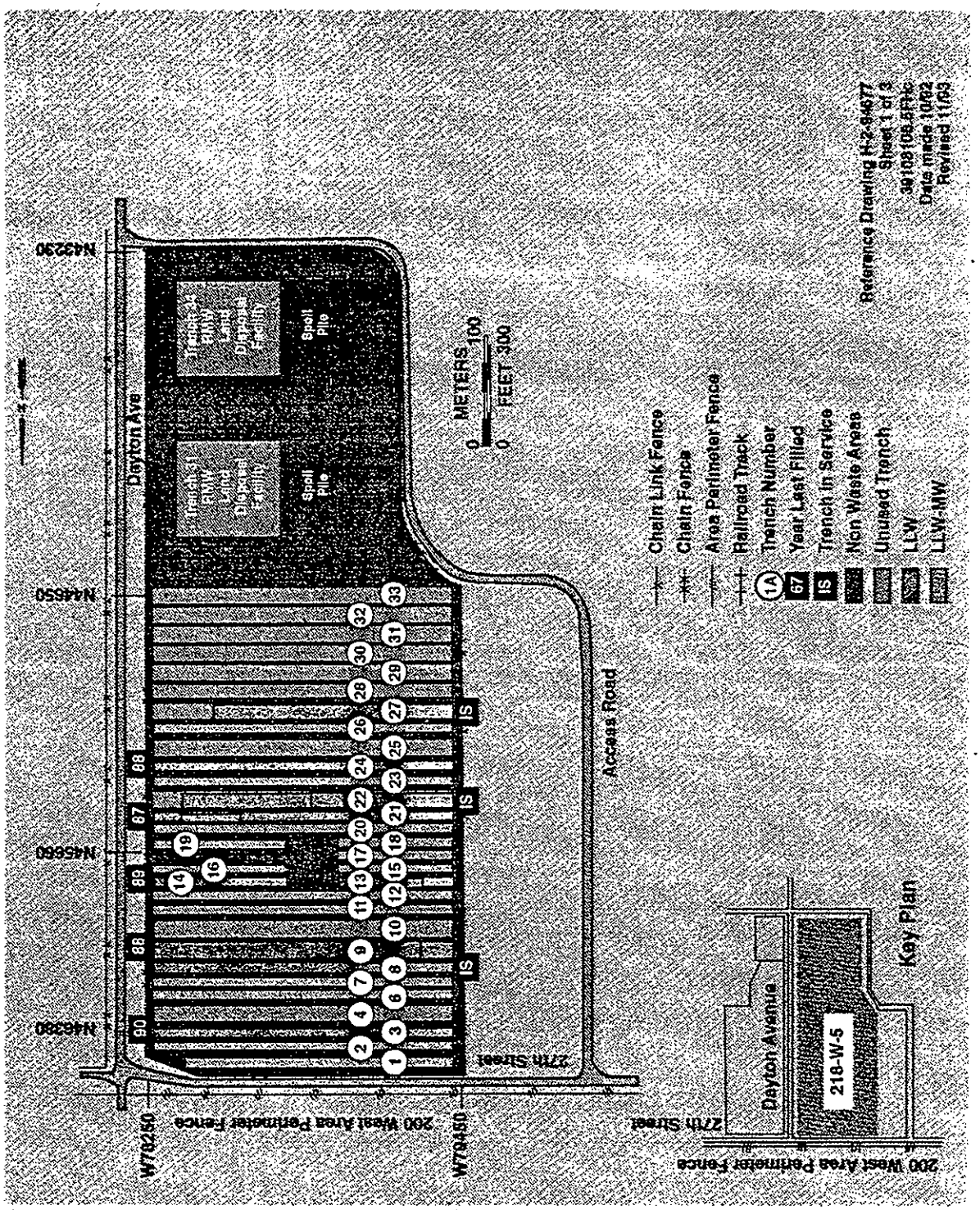

Figure 2-12. Topographic Map of Burial Ground 218-W-3A.

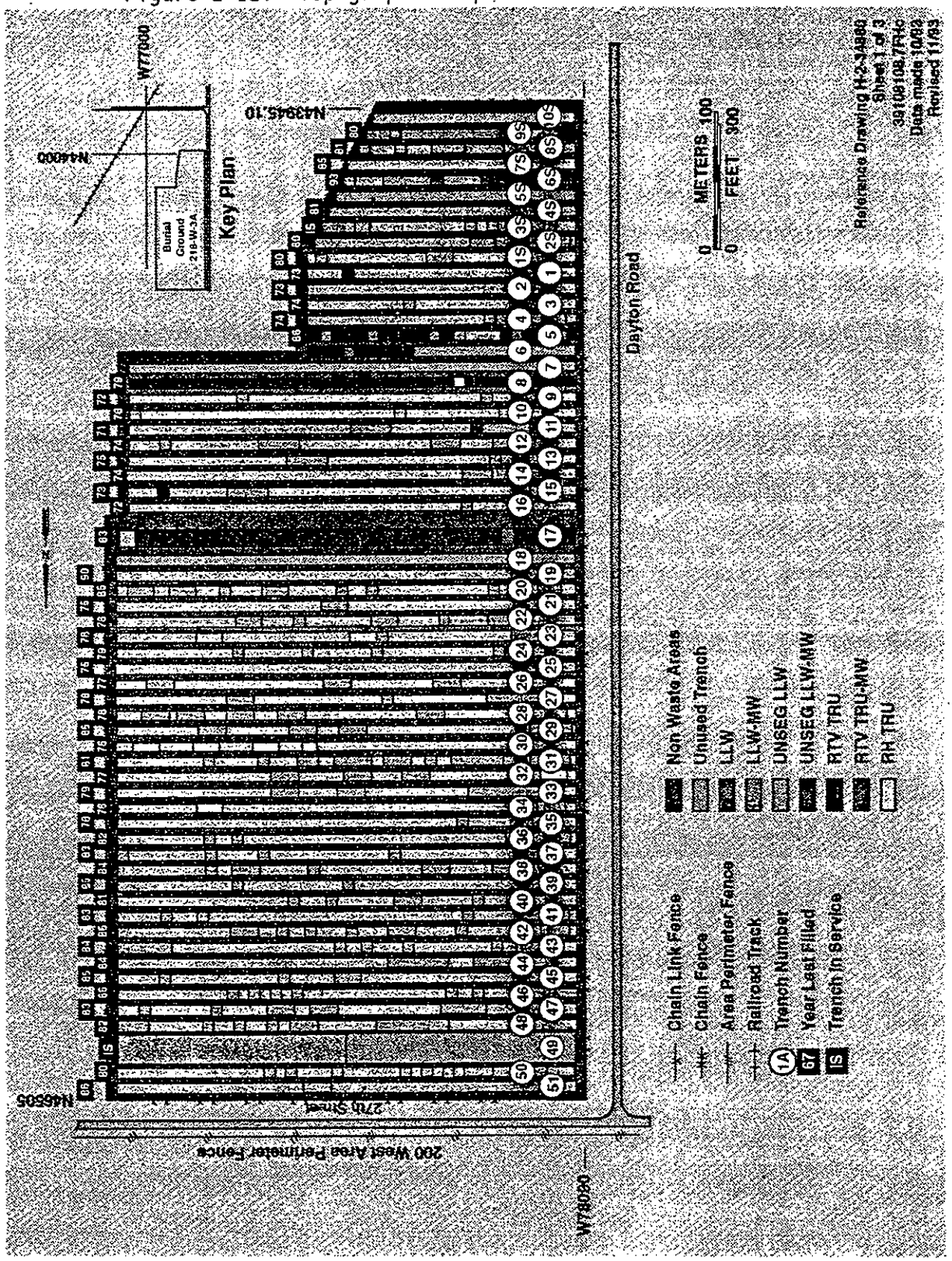

not specifically evaluated in this analysis because waste has not been disposed in them since September 1988, nor is any future waste disposal planned for these burial grounds.

The figures show several features that complicate the PA analysis. A variety of waste types have been disposed in these facilities including TRU, mixed TRU, mixed LLW, and LLW. TRU waste has not been disposed in the burial grounds since 1972. The waste is not segregated spatially by type and intermittent open space is potentially available for use.

The current method of disposal for LLW is to place waste in an unlined trench which is about 6 to 7 m deep and of variable length up to about 500 m. The slopes of the trenches are angled at about 45°. They are typically either wide-bottomed (about 8 m wide) or V-shaped (about 3 m wide). Waste is usually packaged in carbon-steel, 55-gallon drums or wooden boxes and placed in the trench. Packages may be stacked up to within about 2.5 m of the surface. Soil is then placed over the packages up to grade. Some retired trenches have been planted with cheatgrass to stabilize the soil cover. Active trench covers are kept free of vegetation through the use of herbicides to prevent root penetration into the waste and subsequent contamination.

In response to ongoing PA analytical results and past precedents set by the NRC in 10 CFR 61 for disposal of commercial LLW, an interim disposal practice has been established to dispose of higher inventory LLW in high-integrity containers (HIC) or in a stabilized (e.g., grouted) waste form/waste package. The higher inventory waste is labeled as Category 3 waste and has inventory limits established by the intruder scenario analyses completed for this analysis. A RCRA-compliant mixed waste disposal facility is being constructed in Burial Ground 218-W-5.

2.5.3 Planned Modifications to Current Low-Level Waste Disposal Practices

The approval of RCRA legislation and the DOE Order 5820.2A are both impacting the current disposal practice for LLW. Burial Ground 218-W-5 is part of the disposal area that will ultimately reach a state of closure that is consistent with RCRA regulations. The use of a protective cover over the burial trenches is the most likely change in disposal practices that will be adopted to satisfy the regulations. Typically, a cover is a multilayer cover that restricts the flow of precipitation through the waste volume. A secondary requirement may be to stabilize underlying waste in situ to prevent subsidence of the cover. The mixed waste facility also includes a liner and leachate collection system to satisfy RCRA requirements.

Additional modifications to disposal practices may be required to satisfy performance objectives in DOE Order 5820.2A. Specific disposal methods are not provided in the order. Rather, it must be shown that whatever method is used to dispose of LLW can satisfy the performance objectives with reasonable assurance. Necessary changes in disposal practices are identified by the PA analysis, which is structured to examine the performance of a given facility design and determine the relative effectiveness of the chief components of the system. If the performance is predicted to be inadequate for a given facility, design changes are recommended and an additional

Figure 2-13. Topographic Map of Burial Ground 218-W-3AE.

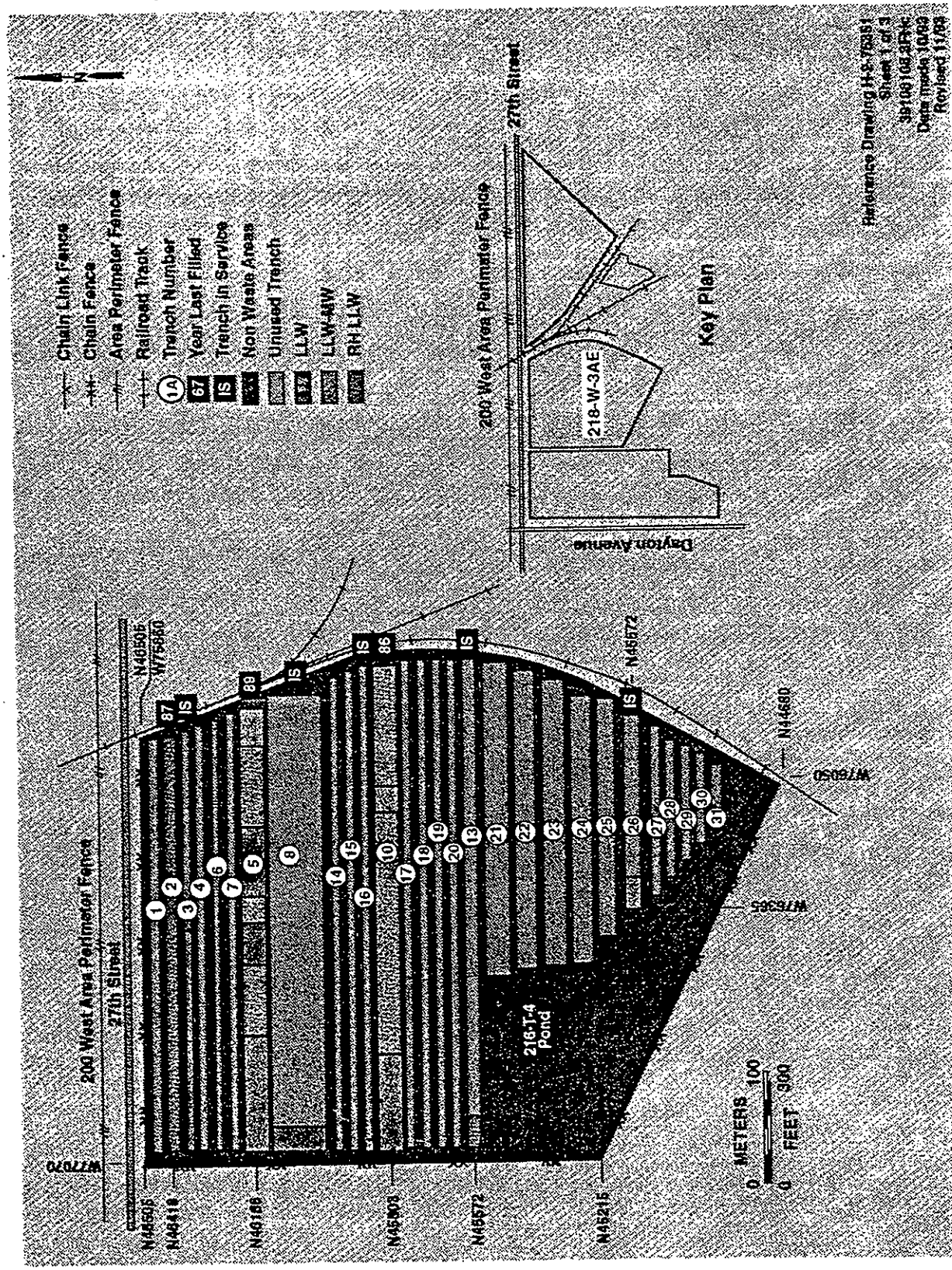

analysis is completed for the new conditions. This process is continued until a particular facility design is predicted to be adequate. In the following section, the initial base case conditions for LLW disposal facilities evaluated in this preliminary analysis are described.

2.6 TREATMENT OF DISPOSAL FACILITY FEATURES IN THE PERFORMANCE ASSESSMENT ANALYSIS

The aspects of the disposal facility that must be considered in the PA analysis include the physical dimensions of the facility and the characteristics of the facility that influence contaminant release and subsequent dose to man. Treatment of these characteristics are discussed in Chapter 3. Relevant characteristics differ depending on the consideration of intruder versus groundwater pathway scenarios. Parameter values for a given characteristic may also differ, depending on the type of facility being considered.

Figures 2-11 through 2-14 indicate that the burial grounds consist of multiple trenches and potential trenches that are usually oriented in parallel fashion with the long axis in the east-west direction and the short axis in the north-south direction. All trenches that have been constructed and partially or completely filled are aligned in this manner. The trenches are not identical in length or width. To deal with this variability and to facilitate modeling of radionuclide releases into the soil column from the 200 West Area LLBG, a representative section was assumed that consists of a part of a real trench. Both a topographic and a cross-sectional view of the representative trench are provided in Figure 2-15. The topographic view illustrates the relative difference in size between the representative section and a typical trench. The cross section is oriented east-west. In the following analyses, the trench is usually considered to be 20 m long in the east-west direction, 1 m wide in the north-south direction and 7 m deep. Waste is contained in the bottom 4.5 m (approximately a stack of three drums or two large boxes) and covered by a soil layer. Differences in soil layer properties are modeled as the assumption of different infiltration rates as described below for the Category 1 and 3 facilities. A groundwater well is assumed to exist 100 m downstream from the nearest waste boundary (the eastern boundary in this case).

In most cases considered in this analysis, the estimate of dose and inventory limit for a given radionuclide for the representative section can be extrapolated to a single real trench up to the entire LLBG regardless of dimensions because of (1) the parallel orientation of the trenches and the general direction of hydrologic flow and (2) the insensitivity of the dose estimates to the length of the trench parallel to the general hydrologic flow direction (east-west) for a given inventory. This occurs for two reasons. First, the parallel relationships between trench orientation and hydrologic flow directions define an identical volume of diluting unconfined aquifer water for any segment of trench in the 200 West Area LLBG that is aligned in the same fashion as the representative trench and is of the same width perpendicular to flow. Second, if the radionuclide mass is the same for that trench section and is transported vertically downward to the unconfined aquifer, thereby mixing with the same volume of diluting aquifer water, the peak groundwater concentration and, therefore, the dose estimate will be the

Figure 2-14. Topographic Map of Burial Ground 218-W-4C.

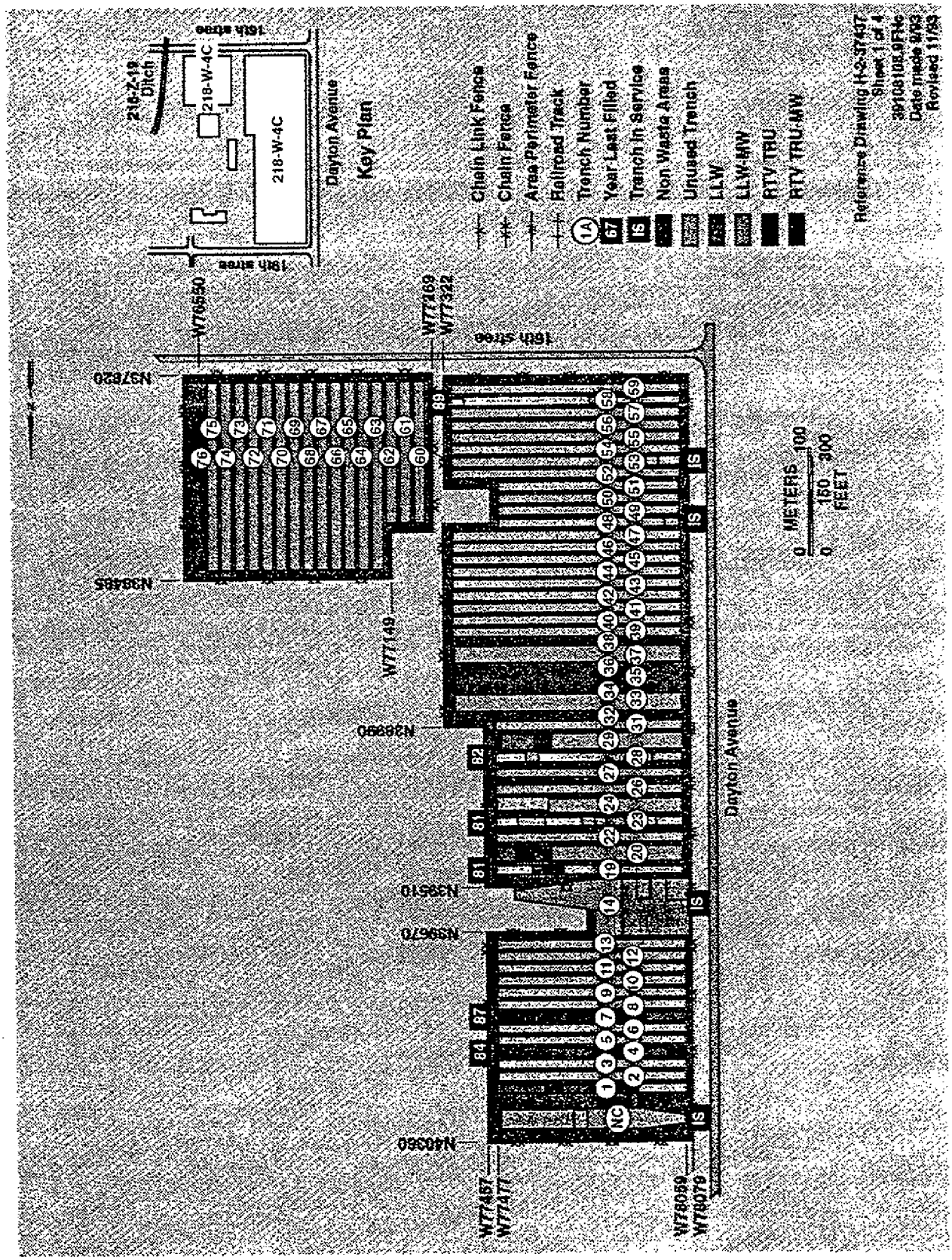

Figure 2-15. Schematic Comparison of Analyzed Trench Section Used in Groundwater Flow and Transport Analyses versus Actual Trench Dimensions.

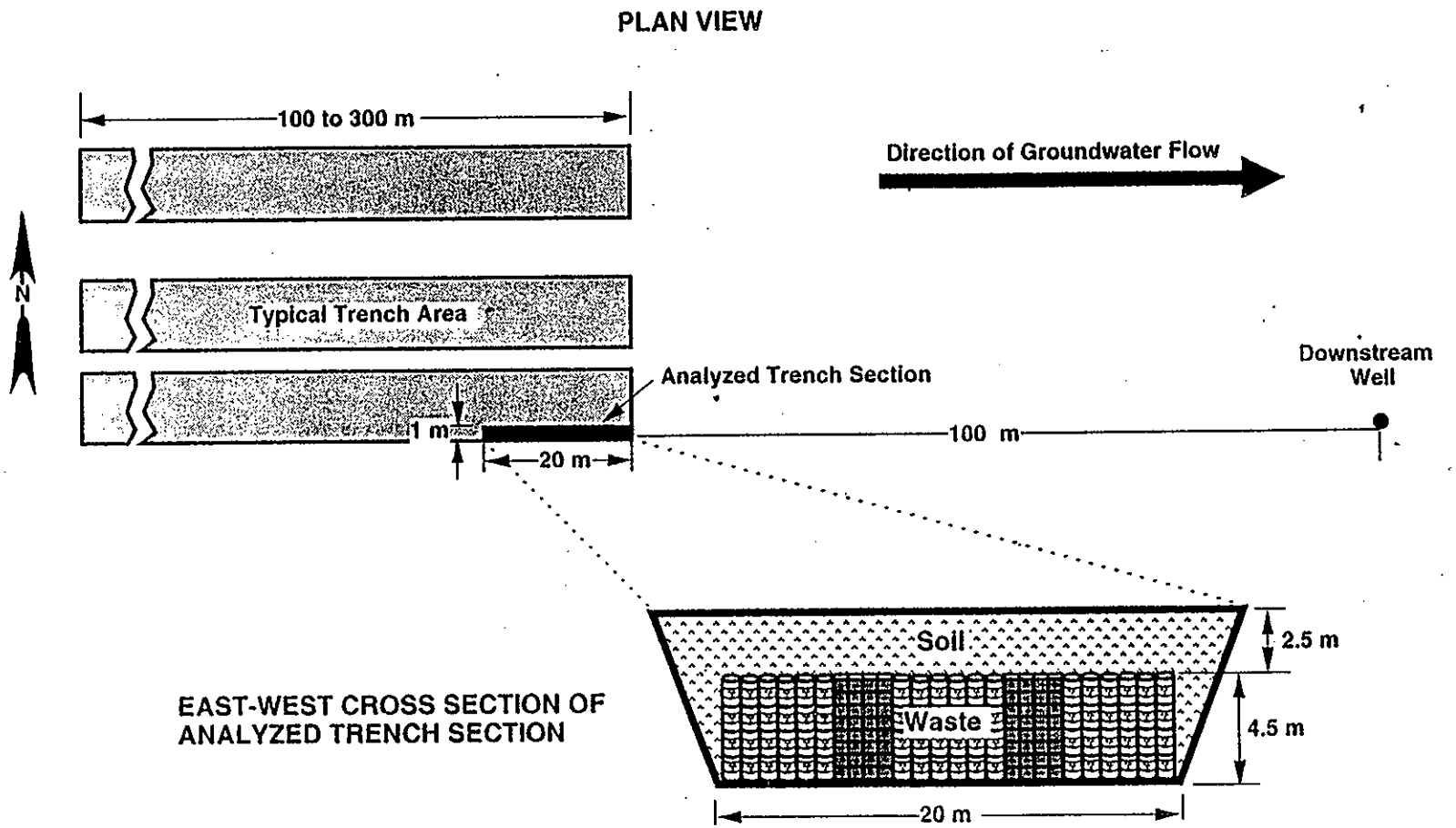

same as that estimated for the representative trench. Under these circumstances, the volume over which the radionuclide mass is spread is immaterial because the same radionuclide mass enters the same volume of water. There is one condition considered in this analysis where the east-west length of the trench has an impact to these relationships. This occurs when a solubility control is the assumed method of radionuclide release. Dose extrapolation to larger trenches can be accomplished as long as the effects of trench length are taken into account.

The following is an example of the extrapolation process. An inventory limit for a given radionuclide in a typical trench such as the one in Figure 2-15 is calculated by taking the product of the inventory limit calculated for the representative trench and the ratio of the north-south dimensions of the typical trench and the representative trench. This is demonstrated by the analyses and analytical results provided in Chapters 3 and 4.

In this PA analysis, two types of facilities have been evaluated, one that contains very low inventory waste and one that contains higher inventory wastes up to Class C limits as defined by the NRC in 10 CFR 61 or Category 3 limits as quantified in Chapter 4. The facilities are labeled Category 1 and Category 3 facilities. The wastes in Category 1 and Category 3 facilities are similar, although not identical, in radionuclide content to the NRC defined Class A and Class C wastes. The distinguishing features of the facilities as they relate to the analysis include the following:

1. The Category 1 waste facility is covered by a sand-gravel cover with no vegetation or sparse shallow-rooted vegetation such as cheat grass, thereby allowing maximum infiltration through the waste. The Category 3 facility is covered by a soil that supports a natural vegetation ecosystem that includes a mixture of shallow- and deep-rooted vegetation. Some fine soil additives may be required to support the vegetation. This cover is meant to be equivalent to natural conditions in limiting infiltration through the waste.

2. Waste is covered by a minimal thickness of cover (about 3 m) in the Category 1 facility, thus allowing the exhumation of waste by the inadvertent intruder who digs a basement or drills a well. The Category 3 facility contains a minimum 5-m cover to limit the exhumation of waste to drilling. A cover will be designed to limit or prevent erosion unless disturbed by man. Thus, ever if a basement is excavated over Category 3 waste, the waste will not be exhumed.

3. No waste form stabilization requirements are used for waste disposal in the Category 1 facility. For the Category 3 facility, stabilization is required to support the soil cover overburden.

4. Radionuclide immobilization is not required of the waste form/waste material disposed in the Category 1 waste facility. Radionuclide immobilization may be required for some wastes in the Category 3 waste facility depending on the concentration of long-lived radionuclides that are mobile in the soil column.

Specific locations have not been decided for Category 1 versus Category 3 disposal facilities nor has a specific decision been made to utilize a Category 1 facility. In all likelihood, when the existing burial grounds are finally closed, the facility will be a Category 3 facility. However, consideration of the Category 1 facility allows the option of using some part of the facility in this fashion. The other advantage to this approach has been the use of Category 1 conditions as an aid to sensitivity analyses.

The RCRA-compliant mixed waste facility is treated as if it were a LLW facility. This is justified because no credit is taken for the long-term behavior of the liner leachate system. Part of the liner consists of manmade materials whose long-term capability to contain waste cannot be determined (e.g., prediction of the type of failure and rate of failure is not feasible or necessary to demonstrate adequate performance). The cover for the facility will function in essentially the same manner as that over a LLW trench; thus, the assumed barrier function for the mixed waste facility and the facility are the same. Finally, the hazardous constituents of the waste have no significant influence on the geochemical behavior of radionuclides.

3.0 PERFORMANCE ASSESSMENT ANALYSIS METHODOLOGY

In this chapter, the methodology for estimating potential dose to man resulting from the release of radionuclides from the disposal facility is described. The chapter is organized by types of scenarios: (1) inadvertent intruder scenarios, (2) groundwater contamination scenarios, and (3) additional scenarios. The inadvertent intruder analysis is based on the assumption that knowledge of the disposal facility is lost and an intruder comes in contact with the waste. The groundwater contamination analysis is based on the assumption that groundwater is contaminated by leaching of radionuclides from the disposal facility and transported through the soil column to the water table. Additional scenarios include radionuclide transport by vapor diffusion and liquid diffusion to the surface from an undisturbed facility.

In each section, the discussion is initiated with a description of the conceptual model of the pathways considered. A brief description of the mathematical approach used to represent the model is then provided. Finally, a description of the primary parameters and parameter values used in the analysis to quantify dose estimates is provided.

3.1 INTRUDER SCENARIO ANALYSIS

Intruder scenarios must be selected and quantified to estimate potential dose from a disposal facility and to compare dose estimates with dose limit performance objectives (Section 1.4). In this section, the process of scenario selection and the scenarios used in the analysis are described.

3.1.1 Conceptual Model of the Inadvertent Intruder Scenarios

A large number of scenarios can be considered as plausible means of inadvertent intrusion. To complete an analysis, it is necessary to reduce the large number of possible scenarios to a few that are representative and will provide a maximum projected dose relative to other potential scenarios for an equivalent set of initial conditions. Using these criteria, it is possible to propose a disposal facility design that can be reasonably expected to satisfy the performance objectives defined in DOE Order 5820.2A to protect the inadvertent intruder.

In this analysis, inadvertent intrusion is defined as an activity that results in direct contact with the waste in the disposal facility. Three types of intrusion are considered including: (1) excavating a basement for dwelling, (2) drilling a well for water to be consumed or used in irrigation, and (3) crop roots penetrating into waste material. In each case, the waste must be extracted directly from the disposal facility. Exhumed waste is assumed to be indistinguishable from soil with the exception of activated metal. We have assumed (as has the NRC in 10 CFR 61) that radionuclides entrained in activated metals are less likely to be dispersed into the environment even when exhumed and mixed with soil, thus reducing the potential dose from this source relative to other waste materials.

The pathways by which the intruder may be exposed to radiation from the exhumed waste are listed below:

- Ingestion of vegetables grown in the contaminated soil
- Ingestion of soil
- Inhalation of radionuclides on dust suspended in the air by gardening activities and wind
- External exposure to contaminated soil while working in the garden or residing in the house built on top of the waste site.

Two methods of completing dose calculations were completed. The first and primary method was a set of hand calculations done on a spreadsheet. Radionuclide concentration inventory limits described in Chapter 4 are derived from these calculations. The second method was to use the computer code GENII, Version 1.485 (Napier et al. 1988) for benchmarking purposes. This code was developed at the Hanford Site. Use of the code has the advantage of rapid calculation, particularly when considering the effects of daughter contributions to the calculated dose for the parent. By developing a spreadsheet and doing a comparison with the GENII code, several goals were accomplished: (1) A spreadsheet was carefully constructed using GENII formulas to duplicate results accurately. The authors gained a detailed knowledge of the factors affecting dose calculations in GENII. These formulas are discussed in Appendix C. (2) The parameter value assumptions were evaluated. In some cases (see Section 3.1.2), different parameter values were chosen from the default values given in GENII. (3) A few radionuclides considered were not provided in the GENII database; these radionuclides were more easily considered with the spreadsheet.

The environmental dose estimation methods and assumptions used in the current document are very similar to those found in the double-shelled tank LLW PA (Kincaid et al. 1993). The differences are almost entirely simplifications that will not materially affect the computed doses. For example, the double-shelled tank LLW PA used the EPA values for local food production of 25 percent for vegetables and 20 percent for fruit. In the current document, these were simplified to 25 percent for all garden produce.

3.1.2 Mathematical Simulation of Dose Estimates to the Inadvertent Intruder

For each of the scenarios described above, dose to the intruder is calculated as a function of the pathway and the individual radionuclide. The three pathways through which dose is received in both the postexcavation and the postdrilling scenarios are ingestion, inhalation, and external exposure. The relative importance of each pathway is largely dependent on the type of radiation emitted by the specific radionuclide. To estimate dose, algebraic equations are used in a spreadsheet format. In this section, the basic equations are summarized for each pathway. Additional details of the analysis are provided in Appendix C.

Dose by ingestion is calculated by the following basic equation:

$$H = C \ Q \ D \tag{3.1}$$

where:

- H = annual dose received (mrem/yr)
- C = concentration in substance consumed (Ci/kg, Ci/L)
- Q = quantity of substance consumed (kg/yr, L/yr)
- D = dose conversion factor (mrem/Ci) from DOE/EH-0071 (DOE 1988c).

The soil concentration is quantified as a function of initial inventory, the dilution factor assumed as a result of mixing waste with uncontaminated soil, and the decay factor. In these analyses, a unit concentration is assumed to exist in the initial inventory at time zero.

Dose by inhalation is calculated by the following basic equation:

$$H = W \ V \ T \ M \ D \tag{3.2}$$

where:

- W = concentration in the dirt suspended in air (Ci/kg)
- V = breathing rate (m^3/h)
- T = time of inhalation (h/yr)
- M = concentration of dirt in the air (kg/m)
- D = dose conversion factor (mrem/Ci) from DOE/EH-0071 (DOE 1988c).

The soil concentration is equal to that defined in the ingestion pathway; therefore, it is dependent on the same factors. The time of inhalation is dependent on the assumptions of living conditions such as time spent indoors versus outdoors, time spent at the home versus away from home, and time spent awake versus time spent asleep.

Dose by external exposure is calculated from the following basic equation:

$$H = \rho \ d \ W \ T \ D \tag{3.3}$$

where:

- W = concentration in surface layer of soil (Ci/kg)
- ρ = soil density (1,500 kg/m^3)
- d = thickness of soil in which radionuclides are mixed (0.15 m)
- T = time of exposure (h/yr)
- D = dose conversion factor (mrem/h per Ci/m^2) for contaminated thickness d.

As described above, the soil concentrations are the same as for the other pathways. The time of exposure is calculated somewhat differently than for the inhalation pathway to account for shielding provided by the dwelling floors and walls.

3.1.3 Postexcavation and Postdrilling Base Case Parameter Selection

As shown in the previous discussion, the fundamental parameters governing intruder dose estimates are the inventory, the soil dilution factors, the time of exposure to external radiation, the quantity of contaminated air that is inhaled, the quantity of contaminated food that is ingested, and the dose conversion factors. These are briefly described below.

The postexcavation and postdrilling scenarios assume that the intruder has exhumed some of the waste and has relocated it to a garden. The scenarios differ only in the assumed initial soil concentration in the garden. All doses are proportional to this concentration. GENII assumes the added waste is uniformly distributed through the top 15 cm of soil in the garden (the tilling depth). This contaminated surface soil becomes the source of dose for the resident gardener. The size of the garden is assumed to be 2500m^2.

In the excavating operation, 100 m^3 is exhumed and spread over the garden. The large area exhumed is assumed to have 25% clean soil interspersed with the waste. Thus the actual volume of waste exhumed is 75 m^3. The resulting redistribution factor is (75 m^3)/(2,500 m^2) = 0.03 m. In effect, 3 cm of waste is added to the garden.

In the well-drilling operation, 0.35 m^3 of waste (0.3-m-diameter well through 5 m of waste) is brought to the surface and spread over a 2,500 m^2 garden. For input to GENII, the "manual redistribution factor" takes the value (0.35 m^3)/(2,500 m^2) = 1.4×10^{-4} m. In effect, 0.14 mm of waste is added to the garden.

The quantities of waste exhumed and the size of the garden were selected somewhat arbitrarily on the basis of common practice. The area of the garden (2,500 m^2) is a realistic size for supplying the residents' vegetable diet (Napier et al. 1984). The value has been used in other assessments (Kincaid et al. [1993] and Kennedy and Strenge [1992]). The 0.3-m diameter for the well is large and represents a well drilled to support irrigation rather than just drinking. The mixing depth of 15 cm is considered an average plowing depth for normal farming practices. An attempt has been made to be reasonably conservative in the selection of values such that dose estimates will be high. The reasonableness of these parameter value choices is best thought of in terms of the soil dilution factor (ratio of total activity to volume of mixing soil). For these scenarios, the soil dilution values are 2.0×10^{-1} and 9.3×10^{-4} for postexcavation and postdrilling. In essence, dilution of radionuclide concentration by factors of about 1 and 3 orders of magnitude are assumed as a result of excavation and drilling of waste, respectively.

The inhalation and external exposures are based on the following exposure times. The gardener is assumed to spend 1,800 h/yr outside in the garden and 4,380 h/yr inside. The remaining 2,580 h/yr are spent elsewhere.

For estimating external exposure from the soil contamination, the house is assumed to reduce the dose rate to one-third the direct dose rate (Kennedy and Strenge 1992). In effect, the average time exposed at the unshielded dose rate is

$$(1{,}800 \text{ h/yr})*1 + (4{,}380 \text{ h/yr})*(1/3) = 3{,}260 \text{ h/yr} \qquad (3.4)$$

For estimating inhalation exposure, the air concentrations shown on the table below are used to estimate the average time of exposure to an air concentration of 0.1 mg/m^3 (EPA 1992). The 4,380-h period has been divided into two equal periods of activity and sleep. The breathing rates shown below in Table 3-1 are from ICRP 23 (Reference Man). The time spent at each activity is based on common practice.

Table 3-1. Calculation of the Inhalation Time for the Intruders.

Activity	Air concentration (mg/m^3)*	Exposure time (h)	Breathing rate (m^3/h)	Soil inhaled (mg/yr)
Indoor (active)	0.05	2,190	1.2	131.4
Indoor (asleep)	0.05	2,190	0.45	49.3
Outdoor	0.1	1,700	1.2	204
Gardening	0.5	100	1.2	60
			Total Soil Inhaled:	445 mg/yr

*Representative averages are from Kennedy and Strenge (1992), Section 6.3.1.

For input to GENII, one must use a daily average breathing rate of 0.95 m^3/h. Thus, an inhalation exposure time of 4,680-h is needed to inhale the projected 445 mg at the average air concentration of 0.1 mg/m^3. This differs slightly from the previous PNL calculations (Aaberg and Kennedy 1990) of 4,390 h/yr because breathing rate changes are now included.

Human intakes of radioactivity from the ingestion of food grown in the garden uses transport models in GENII that were developed from NRC Regulatory Guide 1.109 (NRC 1977); however, the default consumption parameters in GENII were not used. In their place, values for the "West" region in a recent survey were used (Yang and Nelson 1986). These are listed in Table 3-2. Meat and milk consumption values are also given on this table, but are only assumed as a source of dose in the all-pathways irrigation scenario. The assumed intake is based on the individual obtaining 25% of vegetable diet and 50% of animal diet from his farm. In addition, it is assumed that the intruder unintentionally consumes 100 mg d^{-1} of contaminated soil (EPA 1989).

Internal dose conversion factors were compared from three sources, the GENII code, DOE (1988c), and EPA (1989). The values are shown in Appendix C and are very similar. In the dose calculations the DOE source was used. External dose conversion factors are taken from the GENII Version 1.485 software package. The values were recomputed using the EXTDF program that accompanies GENII. External dose factors are at 1 m above a 15 cm thick layer of contaminated soil.

Table 3-2. Human Food Consumption Parameters.

Type of Produce	Quantity* (g/d)	Calculated (kg/yr)	Assumed intake (kg/yr)
Leafy (leafy)	45.3	16.53	4.1
Other (protected)	152.5	55.66	13.9
Fruit (exposed and miscellaneous)	105.3	38.43	9.6
Cereal (grain)	202.6	73.95	18.5
Meat (beef and pork)	115.0	41.98	21
Milk	283.5	103.48	51.7

*Yang and Nelson (1986).

A large number of parameters are used in the estimates of dose in addition to those described above, particularly in the ingestion pathways where multiple transfers of radionuclides are assumed (e.g., soil-to-plant to animal-to-human). A listing of the significant parameters is found in Appendix C as part of the pathway formula discussion.

Two sets of transfer factors were considered in these analyses. Transfer factors define the distribution of a given radionuclide expected to occur along a food pathway which can include transfer of the radionuclide from soil-to-plant, plant-to-human, plant-to-animal, and animal-to-human. The first set has been recently compiled by Kennedy and Strenge (1992) and the second set (Baes et al. 1984b) was developed at Oak Ridge National Laboratory (ORNL) for dose calculations.

The selection of data sets in the literature are used because very little site-specific data are available on transfer factors and collection of such data would be time consuming and expensive. There is some potential that the generic values used in surveys identified above were selected from data derived under conditions unlike the dry and sandy conditions of the Hanford Site. However, the preparation of the soil for a garden changes the properties of the surface layer. The tilling, watering, and addition of fertilizers produces soil that resembles the generic garden soil of NUREG/CR-5512 and ORNL-5785. It is, therefore, assumed that the concentration ratios found in these documents are adequate to describe plant uptakes in possible future gardens on the Hanford Site.

3.2 GROUNDWATER CONTAMINATION ANALYSIS

The groundwater contamination analyses are developed to estimate the potential dose to man that may occur as a result of radionuclide leaching from the disposal facility by chemical interaction of waste material with

infiltrating rainwater and subsequent transport through the soil column to the water table. Use of the contaminated water by man is the mechanism by which man receives dose.

In this chapter, a general description of the analysis process is provided in Section 3.2.1. Following sections deal with the major components of the process in greater depth with source-term calculations (Section 3.2.2), flow and transport calculations (Section 3.2.3), and dose calculations (Section 3.2.4). In each section the conceptual model, the mathematical simulation of the model and the description of base case parameters is provided.

3.2.1 Overview of the Modeling Approach

A summary of the major components of the modeling approach is provided in Table 3-3. The relationship between the conceptual model, the mathematical models used to simulate the conceptual model, and the primary input parameters and data output are listed. The first two steps in the process provide the radionuclide flux at the disposal facility-soil column boundary. The third step in the process estimates flux through the soil column to the unconfined aquifer and is used to calculate flux at the water table or at any distance downstream in the unconfined aquifer. Groundwater concentrations are also calculated as a function of time. The fourth step is a calculation of dose assuming use of groundwater by man and the groundwater concentrations provided in step three as the source of dose.

For source term release, the mass transfer code VAM3D-CG is used to quantify the groundwater advective flux conditions and an analytical solution, and the mixing-cell cascade model (Kozak et al. 1990) is used to calculate the radionuclide release from the waste material or waste form. The VAM3D-CG code uses a finite element numerical approach to simulate the flow and transport processes. In this part of the model approach, it is used to quantify steady-state flow condition as determined by the input parameters that control groundwater movement such as assumed infiltration rate and hydrologic properties of the soil column, both vadose zone and unconfined aquifer.

The second part of the source term release analysis is the calculation of the radionuclide release rates from the waste or waste form. The mixing cell cascade model used in this analysis (Kozak et al. 1990) is an analytical approach that uses the flow field parameters, an assumed advective release mechanism, and a disposal facility configuration to produce a radionuclide flux history which is then input back into VAM3D-CG as a boundary condition to calculate radionuclide transport through the soil column.

If diffusion is the assumed release mechanism, a one-dimensional analytical model is used as the boundary condition input. For steady state or solubility controlled release, a constant concentration is the boundary condition input.

The third step of the process is the calculation of the radionuclide transport through the vadose zone to the water table. The conceptualization of the modeling approach is based on the hydrogeologic condition at the Hanford Site. The groundwater in the unconfined aquifer underneath the

Table 3-3. Summary of Performance Assessment Methodology.

Conceptual models steps	Primary input parameters	Mathematical model	Output
1. Establish steady-state groundwater flow field	* Infiltration rate * Surrounding soil * Cover * Hydrogeologic properties	VAM3D-CG RETC	Steady-state velocity field
2. Estimate source term release rate	* Steady-state velocity field * Release mechanism * Trench size * Waste volume	Mixing cell cascade model (Analytical)	Radionuclide flux history
3. Quantify soil column transport	* Radionuclide flux history * Infiltration rate * Cover * Surrounding area * Hydrogeologic properties * Well screen length * Trench size and orientation	VAM3D-CG RETC	Groundwater concentration versus time curves
4. Calculate dose	* Peak concentration * Peak time * Dose parameter * Edibles consumed * Exposure time * Air inhaled * Transfer factors * Dose conversion factors	Spreadsheet (Analytical)	Radionuclide specific dose estimates

200 West Area LLBG flows dominantly from west to east. The sources of natural recharge to the unconfined aquifer are the areas of high relief to the west of Hanford Site. From the recharge area, the groundwater flows downgradient to the discharge areas in the east, primarily the Columbia River. The general flow pattern is interrupted locally by groundwater mounds and basalt outcrops in the 200 West and East Areas. The mounds are dissipating and should have little effect on the flow pattern in the post-Hanford era. Therefore, the flow field can be characterized satisfactorily using a two-dimensional approach because the velocity in vadose zone is dominantly vertical and the velocity in the unconfined aquifer is dominantly from west to east.

The code VAM3D-CG is again used to quantify radionuclide flux using the source term flux history, infiltration rates, and the hydraulic gradient as boundary conditions. Additional primary inputs are the hydraulic conductivities of the geologic units in the vadose zone and the unconfined aquifer. An important consideration in the vadose zone is the variability of hydraulic conductivity as a function of moisture content. The primary output of the code is the groundwater concentration as a function of time which can be quantified at the vadose zone-unconfined aquifer boundary (the water table) or any location downstream.

Mass balance was used for every run to ensure that the modeling steps (first, second, and third steps) are well integrated. For instance, the total mass leaving the simulation domain at the right boundary (i.e., enter the drinking well) was checked to be approximately equal to the total mass of inventory which was released from the bottom of the trench.

Unlike the model used for double-shelled tank LLW PA (PORFLOW), VAM3D-CG code simulates the vadose zone and unconfined aquifer in a single

run. The concentration versus time at the drinking well is a direct output from the model run. In the grouted double-shelled tank LLW PA, the dose at the drinking well was calculated by multiplying the dose leaving the vadose zone by a dilution factor. For the vadose zone application, VAM3D-CG simulated results were benchmarked with the results simulated by PORFLOW (see Appendix G2). The solutions showed very good overall agreement when plotted, even though VAM3D-CG and PORFLOW employ significantly different solution techniques.

The fourth step of the modeling process is the dose calculation which takes the groundwater concentration in the unconfined aquifer calculated in the third step and calculates a dose to the offsite individual or individuals depending on water use. Three situations are considered in response to the performance requirements assumed in this analysis. These include the all-pathways scenario with a performance objective of 25 mrem/yr, the groundwater drinking scenario with a performance objective of 4 mrem/yr, and the Columbia River scenario with a performance objective of 500 person-rem/yr.

In the all-pathways scenario, water is drawn from a well 100 m downstream from the edge of the facility and used for drinking, watering crops, and watering livestock. The expected homogeneity of the regional hydrologic flow patterns (Figure 2-8) support the assumption that groundwater radionuclide concentrations and, therefore, potential dose will diminish as a function of distance down gradient of the disposal facility. The individual receives a dose from ingestion of contaminated water, crops, beef, and milk. Dose by inhalation and external exposure are also received. In the groundwater drinking scenario, the individual is exposed only by drinking well water. In the Columbia River scenario, groundwater discharges to the Columbia River and contaminated river water is used by an offsite population for swimming, drinking, and irrigation. The population receives dose through consumption of water, fish, meat, milk, and crops. Dose by inhalation and external exposure are also received.

3.2.2 Source Term Analysis

In this section, a discussion of the conceptual model of radionuclide release rates is provided with emphasis on the simplifying assumptions needed to complete a calculation (Section 3.2.2.1). A brief description of the mathematical treatment of the source term (Section 3.2.2.2) is followed by a discussion of base case parameter values (Section 3.2.2.3).

3.2.2.1 Conceptual Model of Source Term Release. The actual process of radionuclide release from LLW cannot be modeled precisely because of the variability of chemical and physical reactions that occur in the waste material. In the real system, radionuclides are distributed in a heterogeneous fashion among different waste materials, waste package containers fail at different rates, radionuclides are released into solution at different rates because of the variability in waste material, and variable types and quantities of radionuclides are dissolved into the infiltrating water over time depending on which waste material contacts a particular volume of water. Therefore, averaging concepts are used in modeling that simplify the mathematical representation of the real system. These concepts must be justified as being a conservative representation of the real system.

To introduce conservatism into the source term release estimates, the following assumptions were made:

1. It was assumed that containers were not present in the disposal facility and had no influence on the time at which waste would come in contact with infiltrating water. Obviously, some distribution of container release must occur over time because different container materials are used (carbon steel, galvanized steel, painted steel, wood, concrete) that degrade at different rates. Even like materials will corrode and fail at different rates over time because of variability in the chemical reaction rate and the variable thickness of the containers. Distributed failure will contribute to the reduction of the peak radionuclide flux value.

2. For waste materials disposed directly without treatment, it was assumed that the radionuclide inventory in those wastes was immediately available for release into the infiltrating solution. In fact, some waste materials will provide resistance to release and contribute to the reduction of the peak radionuclide flux. Some examples of these materials are concrete debris and activated metals. An exception to this assumption has been made for some specific waste materials with unusual radionuclide inventories and material characteristics (e.g., ^{14}C entrained in activated metal). These cases are discussed in Appendix F.

3. It is assumed that all infiltrating water receives the maximum amount of dissolved radionuclides prescribed by the release mechanism assumed in the modeling analysis. Because of the variability in water contact with waste, maximum possible concentrations will not occur in all the water passing through the facility. Consequently, some reduction in the peak flux is expected relative to the calculated value.

4. For those wastes that are incorporated into a waste form that controls radionuclide release by diffusion and sorption or solubility mechanisms (i.e., grout), it is assumed in the models that the diffusion coefficient values remain constant over time. Secondary chemical reactions first occur at surfaces of the material undergoing leaching and effectively reduce the diffusive coefficient characteristic of that material. If the peak flux rate from the facility has not been reached before the reduction in diffusive flux occurs, then a reduction in peak flux from the facility is expected relative to the calculated value. Given the relatively rapid nature of these secondary mineralization reactions in natural systems (frequently on the order of weeks) and the infrequency of actual advection of infiltrating water at the Hanford Site disposal facilities, it is likely that reduced flux will occur relative to the calculated value.

The conceptual model assumes additional conditions to facilitate modeling. These include the following:

1. Radionuclide inventories are assumed to be homogeneously distributed among the wastes.

2. For each modeling run, one type of release mechanism is assumed. In addition to instantaneous dissolution and diffusion, a steady-state concentration is assumed as a separate type of release to simulate solubility control of radionuclide release. Selection of the appropriate release mechanism in dose estimate calculations is dependent on the radionuclide of interest and the assumed conditions at disposal (Section 4.4.2)

3. Unit concentrations (for solubility runs) or unit quantities (for instantaneous release and diffusion control runs) of single radionuclides are assumed for the modeling runs. Because dose estimates are directly proportional to initial inventory, the modeling runs with unit concentrations or quantities can be ratioed to calculate dose for any initial inventory values.

3.2.2.2 Mathematical Simulation of Radionuclide Release Mechanisms. The source term is defined as the release of radionuclides from the low-level waste facility. The source terms were estimated by (1) an advection-dominated release model (a mixing-cell cascade model) (Kozak et al. 1990), (2) a diffusion-dominated release model (Kozak et al. 1990), and (3) a solubility-limited release model. The mathematical description and conditions under which the different mechanisms are assumed are provided in the following sections.

3.2.2.2.1 Advection-Dominated Release Model. The advection-dominated release model (mixing-cell cascade model) is used to simulate the processes of releases from unstabilized waste. For unstabilized waste, the radionuclides exit the facility at a rate determined by the flow of water and the amount of dispersion (mixing) in the disposal unit (i.e., by near-field transport processes). The mixing-cell cascade model (Kozak et al. 1990) is based on the dispersion analysis of chemical reactors and allows the analysis to incorporate the effects of dispersion in the trench in a simplified manner. In this model, the disposal unit is considered to be composed of a cascade of N equal-sized, well-stirred cells in series. The total volume of the N cells is equal to the volume of the disposal unit.

The mixing-cell cascade model for N equal-sized cells is described by the following equation:

$$Q(t) = vAC_0 e^{-\alpha Nt} \sum_{n=1}^{N} \frac{(\alpha Nt)^{n-1}}{(n-1)!} \qquad (3.5)$$

where:

- Q = release rate (Ci/yr)
- v = vertical Darcy velocity
- A = horizontal (planar) area of the disposal unit
- α = $v/\theta LR$
- θ = moisture content in the trench
- L = vertical depth of the disposal unit
- R = retardation factor in the disposal unit (in these analyses, R = 1).

The initial concentration of contaminant in the interstitial water can be determined from the following equation:

$$C_0 = \frac{m}{\theta VR} \tag{3.6}$$

where:

m = total facility inventory of the radionuclides in the disposal unit
V = total volume of the disposal unit.

The mixing-cell cascade model provides results equivalent to the one-dimensional, convective-dispersion equation with varying values of the dispersion coefficient (Kozak et al. 1990). In the limit, as N tends to infinity, the model represents flow through a system with zero dispersion, whereas for N equal to one, the model represents flow with an infinite dispersion coefficient(e.g., complete mixing). A value of 10 was used for N in these analyses.

3.2.2.2.2 Diffusion-Dominated Release Model. The diffusion-dominated release model is used to simulate the release of contaminants from stabilized wastes. In the absence of convection through the waste container, the release can be modeled as a diffusion-limited process. The diffusion from cylindrical containers leads to an expression for flux that contains infinite series (Kozak et al. 1990). The series converges slowly for small diffusion coefficients at short times and even for relatively long times. As a result, a 1-D diffusion solution was adopted (Crank 1975). The solution, for a semi-infinite medium with the concentration C_0 throughout, initially, and with zero surface concentration, is given by the following equation:

$$C = C_0 \operatorname{erf} \frac{x}{2\sqrt{(D_e t)}} \tag{3.7}$$

where:

erf = standard error function
D_e = effective diffusion coefficient of the radionuclides in the waste form
t = time.

The rate of loss of diffusing substance per unit area from the semi-infinite medium when the surface concentration is zero, is given by the following equation:

$$\left(D_e \frac{\partial C}{\partial x}\right)_{x=0} = C_0 \sqrt{\frac{D_e}{\pi t}} \tag{3.8}$$

Equation (3.8) has the form of diffusion mass transfer based on leaching theory. This simplified release model leads to the following form:

$$q = A\, C_0 \sqrt{\frac{D_e}{\pi t}} \tag{3.9}$$

where:

- q = release rate from a single waste container (Ci/yr)
- A = effective surface area of a single container
- C_0 = concentration in the container.

Because the LLW is likely contained in various sizes of drums and boxes, the diffusive release rate, Q, from all containers in the facility can be determined by the following equation:

$$\begin{aligned} Q &= C_0 \sqrt{\frac{D_e}{\pi t}} \sum_{i=1}^{n} A_i \\ &= C_0 A_t \sqrt{\frac{D_e}{\pi t}} \end{aligned} \tag{3.10}$$

where:

- n = the number of containers
- A_i = the surface area of i-th container
- A_t = total surface area of all containers.

Equation (3.10) was obtained by assuming that the concentration in all containers is constant, i.e.,

$$I = C_0 \sum_{i=1}^{n} V_i = C_0 V_t \tag{3.11}$$

where:

I = total inventory
V_i = the volume of i-th container
V_t = total volume of all containers.

Substituting equation (3.11) into equation (3.10), we obtain the following equation:

$$Q = I \frac{A_t}{V_t} \sqrt{\frac{D_e}{\pi t}} \tag{3.12}$$

For the case where all containers are same size and shape, the ratio A_t/V_t can be replaced by a ratio of a surface area over volume of a single container. The ratio A_t/V_t (or A/V of a single container) used throughout the model calculation is 5.33.

The model calculation is conservative in two respects: (1) the surface area of each container might not be completely exposed to a moving stream of water, and (2) the radionuclides reaching the surface of the container are assumed to be released into the water stream instantaneously.

3.2.2.2.3 Solubility-Limited Release Model. In addition to the diffusion-dominated release of the radionuclides from the burial trench, an alternative approach is to specify a solubility limit in the waste form. One way to go about this is to model the solubility-limited release by replacing C_0 in Equation 3.5 with the solubility-limited concentration. The other way is to use a constant boundary source model with $C/C_0=1$, where C_0 is the solubility-limited concentration. For a parametric study and with a lack of information on the inventory of particular radionuclides, the second approach appears appropriate.

3.2.2.3 Base Case Parameter Selection. The major parameters that determine source term release rate include those describing the release rate and the infiltration rate. With regard to the instantaneous dissolution assumption, the concentration in solution is arbitrarily set because there is no assumption of waste form controlled release. As discussed in Section 3.2.2.1, the peak groundwater concentration that is calculated in the modeling run (and, therefore, the dose estimate) is directly proportional to the initial inventory quantity in the disposal facility, allowing the calculation of dose for any initial inventory. The same argument holds for the assumption of steady-state concentrations. The actual value picked is dependent on the solubility of the radionuclide of interest, which is derived from the thermodynamic database and associated data. It turns out that the use of the solubility argument is significant for uranium isotopes and ^{10}Be. The

solubility values selected for uranium are 10^{-4} and 10^{-8} mol/L in a soil-dominated and Portland cement-dominated environment, respectively (Appendix E).

In the case of diffusion control, selection of the appropriate diffusion coefficient has been based on a range of values available in the literature for diffusion of different elements in different kinds of materials. A worst-case diffusion coefficient value of 10^{-5} cm^2/s can be chosen which is the measured value for diffusion of species through water. A low range of values is based on standard leach tests (ANS 16.1) for various nuclides in a Portland cement matrix where effective diffusion coefficients of about 10^{-8} to 10^{-12} cm^2/s have been measured (Kincaid et al. 1993). The difference in value reflects variable tendencies of different nuclides to react chemically with the matrix. The high value is representative of the nonreactive species such as iodine and the diffusion values decrease as the element becomes more reactive with the matrix either through precipitation or sorption reactions. The three orders of magnitude reduction in diffusion values in cement versus water reflects the effects of the solid matrix on the diffusion pathway. Diffusion occurs through a pore system which increases the path length to the surface (tortuosity). In addition, not all pores are connected and some are too small to allow diffusion. A typical diffusion value for soil is about 10^{-6} cm^2/s as a result of these solid matrix factors. This is the value chosen in this analysis as representative of the typical mixture of waste and soil in a landfill type facility. For a cement-type waste form the lower value of 10^{-8} cm^2/s has been used in these analyses to represent diffusion of an inert isotope in grout, reflecting a reduced porosity and increased tortuosity. For sorbing radionuclides, an effective diffusion coefficient is based on available data or by dividing the inert isotope diffusivity value by the sorption coefficient of the sorbing radionuclide. The analysis ultimately indicates that waste form performance is important for only a few mobile long-lived radionuclides and that some experimental data are available to use in the analysis (e.g., the diffusion of ^{14}C has been estimated as about 10^{-11} cm^2/s from sorption data [Bayliss, et al 1988] and cement diffusion data [Kincaid et al 1993]).

The other significant parameter affecting radionuclide flux in the source term release analysis is the assumed infiltration rate. Lysimeter data from various experiments conducted at the Hanford Site indicate that the fraction of recharge resulting from precipitation is highly dependent on the soil and vegetation conditions. These data are summarized by Gee et al. (1992) and are most conveniently considered in terms of three levels of infiltration. First, maximum recharge occurs in unvegetated coarse-grained soils with values ranging from about 5 to 10 cm/yr. Second, minimum recharge (no measurable infiltration or <0.1 cm/yr) occurs in bare silt loam soil or silt loam soil with shallow- and deep-rooted vegetation. There is also evidence from a long-term deep lysimeter test (Routson and Johnson 1990) that minimum recharge occurs in sandy soil with a mixture of shallow- and deep-rooted vegetation, a condition typical of undisturbed Hanford Site soils. Seasonal variability in the moisture content of the top 3 m of soil was measured but no measurable recharge occurred during a 13-yr period. Third, intermediate recharge (<0.1 to about 5 cm/yr) occurs in sandy soil vegetated with shallow-rooted vegetation (e.g., grasses).

Given this breakdown of plausible ranges of recharge rates, the boundary value between high and intermediate recharge rates (5 cm/yr) was chosen for the Category 1 facility, for which a minimal thickness of bare or sparsely vegetated soil cover is provided. For the Category 3 facility, a recharge rate of 0.5 cm/yr is assumed. In this case, it is assumed that care is taken to provide a thick cover that will support a typical suite of native vegetation for which infiltration rates are generally unmeasurable. The choice of 0.5 cm/yr is considered a reasonably conservative value averaged over a long time period.

3.2.3 Contaminant Flux in the Vadose Zone and the Unconfined Aquifer

Once radionuclides are released into the partially saturated vadose zone, transport down through the vadose zone is assumed, ultimately leading to contamination of the unconfined aquifer. In this section, a description of the methodology used to model this process is described beginning with the conceptual model. A brief description of the mathematical basis for the code VAM3D-CG and a description of the primary input parameters is also provided.

3.2.3.1 Conceptual Model of Mass Transport in the Hydrogeologic Environment. The primary factors controlling mass transport in the soil column are the infiltration rate of rainwater through the soil column, the features of the disposal facility affecting infiltration rate (in this analysis, the cover permeability), the permeability of the soils, and the hydraulic gradient. Given the variability of these conditions or processes as a function of time and space, certain simplifications must be made to complete a mathematical calculation. This is done by assuming steady-state conditions that approximate natural variability. The following assumptions are made in the conceptual model:

1. Recharge from infiltration of rainwater into the soil column occurs in nature on a sporadic basis. Recharge estimates are further complicated by the occurrence of other processes affecting actual infiltration such as seasonal storage in the soil cover or surface soil and evapotranspiration. In this model an averaged steady state annual infiltration rate is assumed for soil and disposal facility cover. The approach is sound because total mass transport over a fixed boundary and any given time is additive. As long as the average equals or exceeds the sum of the separate recharge events over a given time period, estimates of total mass or activity of nuclides that contaminate the unconfined aquifer will be equivalent or conservatively high. Similarly, as long as the averaged recharge rate equals or exceeds the net infiltration through soil or the cover, a sophisticated model of each individual process affecting recharge is not necessary. It is assumed that the available empirical database is sufficient to select a reasonably conservative parameter value.

2. The spatial variability in soil properties, even within the same formation, indicates that variability in hydraulic properties occurs in three dimensions. To limit the number of modeling analyses, a unique set of hydraulic conductivity values were assigned to each major stratigraphic unit in the vadose zone and unconfined aquifer

beneath the 200 West Area burial grounds as a function of moisture content and depth. It is assumed that variability in the permeability-moisture content relationships is sufficiently bounded by the available data base. It is also assumed that variability in these parameters has a minimal impact on the radionuclide concentration estimates in the unconfined aquifer and, therefore, potential dose to man. Sensitivity analyses were conducted to justify this assumption (Section 4.2.2.3).

3. The major stratigraphic units underlying the 200 West Area burial ground vary in thickness spatially. The conceptual model assumes a layer cake stratigraphy with constant thickness. This assumption is justified by the observation that variability in thicknesses are minor coupled with the sensitivity analysis that shows relative insensitivity of groundwater conditions to hydrologic conductivity values within the bounds of the existing soil properties (Section 4.2.2.3).

4. The actual disposal facility consists of a large number of trenches with varying widths and lengths, thus making up an irregularly shaped total facility. Currently, all trench borders are oriented north-south and east-west with the long axes of individual trenches running east-west. Within the total set of burial grounds in the 200 West Area, LLW is disposed of in a relatively random fashion and soil volumes that have not been excavated are subject to change in dimension relative to the current practice of long, narrow trench construction. In addition, space adjacent to the western edge of Burial Ground 218-W-5 is being considered as a future LLW disposal area.

   To treat the variability in trench types and the uncertainty of future disposal conditions, the analysis considers a representative segment of trench that is oriented orthogonally to the general direction of groundwater flow. The direction of flow is assumed to be east-west corresponding to the expected hydrologic patterns after the influence of Hanford Site activities on groundwater hydrology have disappeared. Fortuitously, the current and planned trenches are oriented parallel to the expected direction of flow. By assuming a trench width of unit length in the direction perpendicular to groundwater flux (north-south), the groundwater concentration estimates provided by the analysis can represent a similarly oriented trench of any width as long as the same inventory is present in a real trench for each meter of width in the north-south direction. This correlation is possible because estimated groundwater concentrations are proportional to the flux of uncontaminated groundwater into which radionuclides are discharged from the vadose zone and the relative orientation of the groundwater flow and contaminant plume. The length of the trench parallel to flow has very little influence on the outcome (see Section 4.2.2.1) because the same volume of water picks up contaminants in the direction parallel to flow, assuming no significant lateral dispersion.

The results of the analysis can be applied to either individual trenches or the entire disposal facility area as long as the north-south distance of the facility is known. In other words, the facility can be considered as a mixture of many trenches or as one large trench. Also, the irregularity of the disposal facility can be accommodated as long as the north-south dimension of the facility is known because the east-west dimensions are largely irrelevant to the groundwater concentration estimates. To clarify discussion of different lengths and orientations, the term "width" is used to describe the north-south dimension and the term "length" is used to describe the east-west dimension.

3.2.3.2 Mathematical Simulation of Contaminant Flux. The finite element computer code VAM3D-CG (Huyakorn and Panday 1992) was used to estimate the transfer of radionuclides that are released from the disposal facility and are transported through the vadose zone into the unconfined aquifer, and eventually into the biosphere. VAM3D-CG is a proprietary product of HydroGeologic, Inc., of Herndon, Virginia.

The code uses a finite element numerical approach to simulate the flow and transport process. It assumes a porous media that can be either partially or completely saturated. The code is three-dimensional but is used in a two-dimensional mode that considers a cross-sectional slice through the disposal facility (Figure 3-1). A geometric grid is set up that represents a waste trench at the upper boundary of the grid, the hydrogeologic units of the vadose zone, the unconfined aquifer and a well 100 m away from the trench, which makes up the right-hand boundary of the grid.

To perform a variably saturated flow analysis, the VAM3D-CG code uses the pressure head or hydraulic head as the dependent variable if a rectangular grid is used. For an orthogonal curvilinear grid, the dependent variable is the hydraulic head. The governing equation for water flow in a variably saturated soil is written as:

$$\frac{\partial}{\partial x_i}[\rho_w K_{ij} k_{rw}(\frac{\partial \psi}{\partial x_j} + e_j)] = \frac{\partial}{\partial t}(\rho_w \phi S_w) - \rho_w q \qquad (3.13)$$

where:

- ρ_w = density of water
- Ψ = pressure head
- K_{ij} = saturated hydraulic conductivity tensor
- k_{rw} = relative permeability with respect to the water phase
- x_i = (i=1,2,3) a set of orthogonal spatial coordinates
- t = time
- e_j = unit vector assumed to be vertically upward
- S_w = water phase saturation
- Φ = effective porosity
- q = volumetric flow rate via sources (or sinks) per unit volume.

The pressure head, Ψ, and hydraulic head, h, are related by $h=\Psi+z$ where z is in the vertical upward direction.

For a slightly compressible fluid, equation (3.13) can be written in the form:

$$\frac{\partial}{\partial x_i}[K_{ij}k_{rw}(\frac{\partial \psi}{\partial x_j} + e_j)] = (S_w S_s + \phi\frac{dS_w}{d\psi})\frac{\partial \psi}{\partial t} - q \qquad (3.14)$$

The specific storage coefficient, S_s, is defined as

$$S_s = \rho_w g(\phi\beta + \alpha) \qquad (3.15)$$

where:

g = the gravitational constant

α and β = coefficients of compressibility of the porous medium and water, respectively.

In order to solve the variably saturated flow problem, two supplementary equations must be specified: (1) the relationships of relative permeability versus water saturation and (2) pressure head versus water saturation. These functions are given by (Brooks and Corey 1966):

$$k_{rw} = S_e^n \qquad (3.16)$$

and (van Genuchten 1980):

$$k_{rw} = S_e^{1/2}[1 - (1 - S_e^{1/\gamma})^\gamma]^2 \qquad (3.17)$$

where:

n and γ = empirical parameters

S_e = the effective water saturation defined as $S_e=(S_w-S_{wr})/(1-S_{wr})$ with S_{wr} as the residual water saturation.

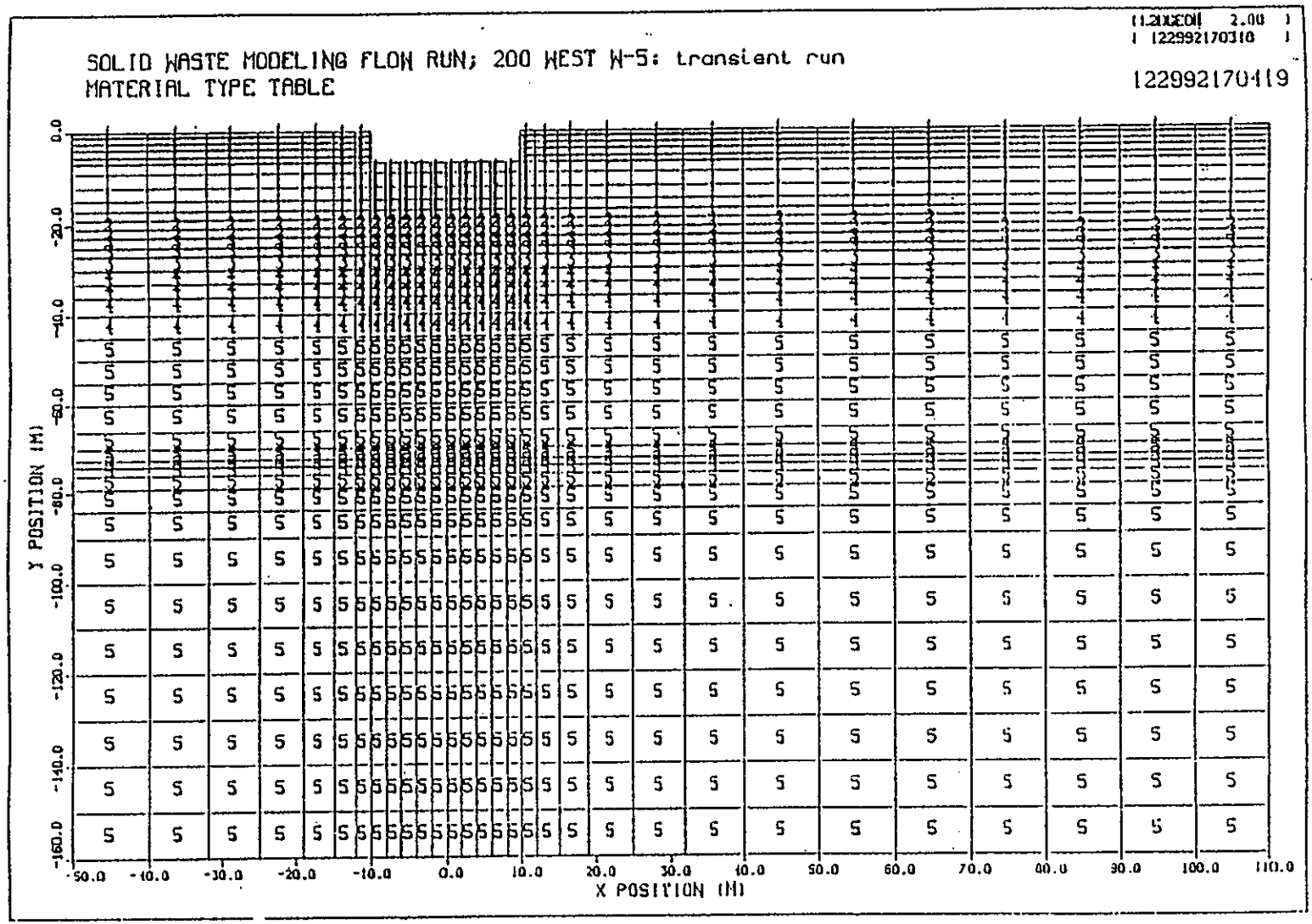

Figure 3-1. Finite Element Mesh With Material Type Table.

The relationship of pressure head versus water saturation is described by the following function (van Genuchten 1980; Mualem 1976):

$$\frac{S_w - S_{wr}}{1 - S_{wr}} = \frac{1}{[1 + (\alpha|\psi - \psi_a|)^{\beta}]^{\gamma}} \qquad \text{for } \psi < \psi_a \tag{3.18}$$

$$= 1 \qquad \text{for } \psi \geq \psi_a$$

where:

α = empirical parameters
β = empirical parameters
Ψ_a = the air entry pressure head.

The parameters β and γ are usually related $\gamma = 1 - 1/\beta$. The Brooks-Corey and van Genuchten functions for the moisture retention and relative permeability characteristics can be measured in the laboratory for a given soil.

The governing equation for three-dimensional transport of a nonconservative component in a variably saturated soil takes the form

$$\frac{\partial}{\partial x_i}\left(D_{ij}\frac{\partial c}{\partial x_j}\right) - \frac{\partial}{\partial x_i}(v_i c) = \frac{\partial}{\partial t}[\phi S_w c + \rho_s(1 - \phi)c_s] - qc^* \tag{3.19}$$

$$+ \lambda[\phi S_w c + \rho_s(1 - \phi)c_s] \qquad i,j = 1,2,3$$

where:

D_{ij} = hydrodynamic dispersion tensor
c = solute concentration in the fluid
v_i = Darcy velocity
ρ_s = density of solid grains
c_s = adsorbed concentration
λ = first-order decay coefficient
c^* = solute concentration in the injected fluid.

Assuming the relation between adsorbed and solution concentration is described by a linear equilibrium, equation (3.19) can be expressed as:

$$\frac{\partial}{\partial x_i}(D_{ij}\frac{\partial c}{\partial x_j}) - \frac{\partial}{\partial x_i}(v_i c) = \frac{\partial}{\partial t}(\phi S_w R c) + \lambda \phi S_w R c - q c^* \qquad (3.20)$$

where R is the retardation defined as:

$$R = 1 + \frac{\rho_s(1 - \phi)kd}{\phi S_w} = 1 + \frac{\rho_B kd}{\phi S_w} \qquad (3.21)$$

with the distribution coefficient kd and the bulk density, ρ_B, being defined as $\rho_B=(1-\phi)\rho_s$.

The hydrodynamic dispersion tensor components are computer derived using the following constitutive relations for homogeneous systems (Scheidegger 1961):

$$D_{ij} = \alpha_T|V|\delta_{ij} + (\alpha_L - \alpha_T)\frac{v_i v_j}{|V|} + \tau D^{\circ}\delta_{ij} \qquad (3.22)$$

where:

- α_L and α_T = longitudinal and transverse dispersivities, respectively
- δ_{ij} = the Kronecker delta
- D° = the bulk molecular diffusion coefficient
- τ = the tortuosity.

The Galerkin and upstream weighted residual procedures are employed for solving the flow and transport equations (equations 3.13 or 3.14 and 3.19 or 3.20, respectively). Preconditioned Conjugate Gradient (PCG) and ORTHOMIN techniques are used to solve the large symmetric and asymmetric matrix equations. Element matrices are generated using influence coefficient formulas, thus avoiding costly numerical integration. The code can easily be adapted for one-, two-, or three-dimensional applications, including axisymmetric configurations. The detailed description of the numerical methods implemented in the code are given in the users' manual.

3.2.3.3 Base Case Parameter Selection. In this section, the basic input parameters to the flow and transport analysis are described. These include (1) a description of stratigraphic parameters and hydrologic parameters used to control mass transport, (2) geochemical parameters used to represent radionuclide sorption in the soil column, (3) dimensions of the disposal trench used, (4) additional boundary conditions, and (5) the element grid used to simulate the disposal facility and hydrogeologic zones of the underlying soil column.

3.2.3.3.1 Representation of the Soil Column Stratigraphy. Construction of a geometric model to represent the vadose zone and unconfined aquifer zones beneath the 200 West Area burial grounds is limited by the scale of geologic heterogeneity and the amount of geohydrologic data available to distinguish the stratigraphic units and subunits from each other. The selected model uses four hydrologically distinct units that correspond to the major geologic units representing the vadose zone and the unconfined aquifer beneath the 200 West burial ground. Unit thicknesses are based on a detailed study of the stratigraphy underlying Burial Ground 218-W-5 (Bjornstad 1990).

For the vadose zone, units and thicknesses from the top down are Hanford formation (about 19 m), early Palouse soil (about 4 m), Plio-Pleistocene unit (about 7 m), and the upper part of the Ringold Formation (about 45 m) which includes the upper Ringold and the upper part of the middle Ringold. The unconfined aquifer comprises the lower part of the middle Ringold unit and the lower Ringold unit (>50 m). For modeling purposes, hydraulic properties assigned to each unit are based on the data available from a continuous core, as described in the next section. It is recognized, however, that all the units, with the possible exception of the early Palouse, are variable perhaps to the extent of containing lenses with distinctly different particle size distributions, porosities, phase mineralogy volumes, and hydrologic characteristics. Also, the portion of the unconfined aquifer that is >5 m below the water table is of no consequence in the analysis because plume depths are minimized by assuming very little vertical dispersion.

The use of layer cake stratigraphy is justified by the observation that variation in thickness is not extreme for any of the units considered in the analysis. In addition, a sensitivity analysis has been completed to evaluate the significance of variability in vadose zone permeabilties and thicknesses by doing a comparative analysis in which the most permeable unit was assumed to exist throughout the vadose zone (Section 4.2.2.2). The analysis supports the contention that radionuclide concentration estimates are not highly sensitive to these kinds of parameter variability.

It is assumed that preferential vertical pathways are not present in the soil column underneath the 200 West Area burial grounds and were not incorporated into the base case analyses. To justify this assumption, two main observations require consideration. First, the apparent occurrence of a secondary north-south channel in the Hanford formation on the east side of the burial grounds could result in a preferential path due to the scouring effect of the process. In the Hanford formation, soil characterization date show that the only manifestation of this event is a horizontal facies change from high concentrations of coarse-grained particles in the middle of the channel to diminished concentrations of coarse-grained particles underlying the western portion of the burial grounds. In addition, thinning and perhaps complete erosion in small areas of the Palouse layer is observed in the channel area. By completing the analysis described above where the most permeable coarse-grained gravel facies is assumed for the entire soil column, the potential effect of this channel has been evaluated.

Second, vertical features referred to as clastic dikes occur sporadically in the Hanford formation, although they have not been observed inside the 200 West Area boundary. The dikes are quite variable in the type of materials with which they are filled and their length. Typically the cross-sectional

area is small (<1 m^2). No permeability information is available. Because of the small volume of these dikes and low frequency of occurrence, it is expected that they will have little impact on the flux of contaminants. A sensitivity analysis has been completed to evaluate the impact of dikes (Section 4.2.2.2). The problem geometry includes a clastic dike directly beneath a trench that has the properties of highly conductive gravel.

3.2.3.3.2 Moisture Retention and Unsaturated Hydraulic Conductivity Curves. A number of parameters are needed to model the vadose zone hydrology and transport from a solid waste disposal site. The rate at which water can travel through the vadose zone is extremely sensitive to the moisture content of the sediment. Important parameters that characterize the vadose zone hydrology are the moisture characteristics and unsaturated hydraulic conductivities of the soils and sediments within the vadose zone. These parameters, along with hydraulic properties of the unconfined aquifer, are needed to model the flow and transport from a solid waste burial site.

A total of 13 samples from a continuous core of Borehole 299-W7-9 was analyzed to generate the moisture retention and unsaturated hydraulic conductivity curves for 218-W-5 soils. A total of four moisture characteristic curves (Table 3-4) representing four upper units (Hanford, Early Palouse, Plio-Pleistocene, and Upper-Ringold) were selected for the simulations (the completed data set is provided in Appendix A). The laboratory-measured moisture retention data and unsaturated hydraulic conductivity were fitted simultaneously with the van Genuchten-Mualem equation using the computer code RETC. Unsaturated hydraulic conductivity data were measured in the laboratory using the centrifuge technique. Appendix A documents the available data on laboratory measurements of moisture retention and unsaturated hydraulic conductivity for 218-W-5 soils. The four formation types, Hanford, Early Palouse, Plio-Pleistocene, and Upper-Ringold are referred to as material types 1, 2, 3, and 4, respectively (Table 3-4). Since no samples were available in the middle Ringold unit, the material type 5 is the same as the material type 4.

Table 3-4. Hydraulic Property Input Data to the Release and Transport Model.

Sample	Formation Type	Material	Depth (m)	Θ_s	Θ_r	α (1/m)	n	K_s (m/yr)	ρ_b (g/cm^3)
0-069	Hanford	(1)	3.05	0.301	0.000	9.45	1.2515	6,496.4	2.29
0-072	E.P	(2)	19.82	0.391	0.056	0.90	2.0877	517.12	1.81
0-082	Plio	(3)	24.70	0.455	0.127	4.86	1.3520	1,892.2	1.43
0-107	U.R.	(4)	40.40	0.317	0.025	9.16	1.807	5,203.4	1.59

Each of the major units, the Hanford and Ringold formations, are marked by heterogeneities in particle size distribution and mineralogy which will contribute to local heterogeneities in the hydrologic properties of each unit. By considering the available measurements across the site of hydrologic properties for these units, as well as detailed hydrologic property measurements of well core samples in Burial Ground 218-W-5, an "average" set

of hydrologic properties are used as input to the modeling analysis. A detailed discussion of hydrologic properties is provided in Appendix A.

Use of a single set of values for the base case analysis is justified on the basis that the best available database has been used and that the sensitivity of groundwater radionuclide concentration estimates to these parameters is not great. Two sensitivity analyses were completed to address this issue. In the first analysis, the saturated hydraulic conductivity values used to define the moisture content-permeability relationships for these vadose zone units were increased to compare groundwater contaminant concentration estimates with the base case. In the second analysis, a one-soil-type soil column was assumed with the most conservative hydrologic properties as a comparison with the base case of four representative layers.

3.2.3.3.3 Saturated Media and Transport Properties. The saturated hydraulic conductivity and storativity are of primary interest insofar as modeling of flow and transport within the unconfined aquifer is concerned. A value of 0.2 was used as the storativity for the unconfined aquifer material (Freeze and Cherry, 1979). The assumed hydraulic conductivity is the same as that shown in Table 3-4 for the upper Ringold (5,200 m/yr).

3.2.3.3.4 Geochemical Parameters. Sorption and desorption reactions that control the distribution of radionuclides between water and solid can have a significant impact on release rates of the radionuclides from waste solids, on retardation of mass transport rates relative to groundwater transport rates, and on the peak concentrations in groundwater. Typically, the distribution is quantified by a sorption coefficient or kd (mL/g) whose value increases as the relative fraction of radionuclide increases on the solid phases. In these analyses, Kd values of 0, 01,10, and 100 have been selected to represent a variety of radionuclides being considered as part of a waste inventory (Table 3-5). The values represent radionuclides that are nonsorbing, slightly sorbing, moderately sorbing, and strongly sorbing, respectively. Sorption data is available for numerous radionuclides from batch experiments conducted under site-specific conditions. For those radionuclides for which data is not available, the similar chemical behavior of the element to an element for which data exists was used as a guide.

Table 3-5. Radionuclide Sorption Coefficients in the Soil Column.

Kd (mL/g)	Radioelement
0	C, I, Mo, Re, Se, Tc, U, H
1	Ba, Cd, Co, Cs, Pa, Sr
10	Ac, Eu, K, Np, Pd, Ra
100	Am, Cm, Gd, Nb, Ni, Pu, Sm, Sn, Th, Zr

The four values used in the analysis allow the selection of reasonably conservative estimate of retardation for all radionuclides considered (Table 3-5). The sorption or desorption process (in the case of the waste) is used as an input parameter in the mass transport process through the vadose zone and unconfined aquifer. A Kd for sorbing radionuclides can also be used as an input parameter in the waste release process and has the effect of reducing predicted release rates.

In some cases, the sorption characteristic of an element in a waste form will differ from that assumed in the soil column. In this analysis, this situation occurs for one waste stream that contains ^{14}C that is encapsulated by a Portland cement-based grout cylinder. Empirical measurements of ^{14}C sorption in grout (Bayliss et al. 1988) (Appendix F) yield values of 600 to 10,000 mL/g. In this analysis, a sorption coefficient of 1,000 mL/g is assumed. Similarly, an effective Kd of about 1,000 mL/g is assumed for uranium encapsulated in grout.

3.2.3.3.5 Disposal Facility Parameters. The disposal trench dimensions used in the model are 7 m deep, 20 m long, and 1 m wide. About 2.5 m of space is left from the top of the waste to the surface for emplacement of a cover. In the base cases, the cover is assumed to have the same permeability as the surrounding soil and permits an annual infiltration of 5 and 0.5 cm/yr for Category 1 and 3 waste facilities, respectively. Two sensitivity cases are run with a cover that reduces the infiltration rate through the waste relative to the assumed surrounding infiltration. A sensitivity case is run with a RCRA-equivalent cover (infiltration rate of 3 cm/yr) over the Category 1 facility. Also, a case is run with the 0.05 cm/yr cover and larger area infiltration rates of 0.5 and 5 cm/yr.

3.2.3.3.6 Additional Modeling Parameters. As shown in Figure 3-1, a rectangular soil slab with open trench on the top is selected for simulation of all the cases. Boundary conditions were used to simulate the various release scenarios and the effect of the presence of the low-permeability cover material on the top of the trench. Grid spacings used in the problem geometry are also shown in Figure 3-1. The numbers in the grids show the material type of soil unit considered and correlate to those shown in Table 3-4. Smaller grid spacings are used beneath the trench and in the vicinity of the trench where the concentration gradients are expected to be steep. The grid spacings are gradually decreased in regions where abrupt changes in hydraulic conductivities occur or the head and/or concentration gradients are relatively sharp. Similarly, the grid spacings are gradually increased in regions where abrupt changes in hydraulic conductivities are not expected to occur or the head and/or concentration gradients are expected to be relatively mild.

The two-dimensional network geometry consists of 1,133 nodes and 1,060 rectangular elements. The lateral dimension and vertical dimension of the domain are both 160 m. The LLW trench is centered at 0 m and extends 10 m in both directions; the trench is 7 m deep. The near-field transport within the trench is performed by analytical models (discussed in Section 3.2.4) and incorporated into the finite element model as release boundary conditions. The right model boundary represents an intercepted well located at a distance of 100 m from the right edge of the trench.

It is assumed that larger concentrations of contaminants will not occur beyond 100 m. This assumption is supported by the estimated future water table elevation contours in the vicinity of the 200 West Area LLBG (Figure 2-8) and the observed concentration contours of radionuclide plumes currently present in the unconfined aquifer. The elevation contours indicate no convergence in the general hydrologic flow pattern that could lead to an increase in contaminant concentrations in the groundwater. Similarly, concentration isopleths in the current plumes decrease as a function of distance from the source, particularly in the present general direction of groundwater flow to the east-northeast. This behavior is most clearly shown by the tritium plume isopleths (Figure A-11).

Several boundary conditions must be defined to complete the analyses. A prescribed recharge (infiltration) value is assigned across the top boundary nodes of a two-dimensional, vertical-flow domain (see Section 3.2.2.3 for discussion of values used). The left and right boundary nodes within the vadose zone are assigned zero fluid and concentration fluxes. Based on the field data (Bjornstad 1990), a hydraulic gradient of 0.00438 (0.7/160) is established across the model flow domain from left to right. A hydrostatic pressure head distribution (i.e., a total hydraulic head of 86.7 m) is maintained for the lowermost 18 nodes at the left boundary within the unconfined aquifer. Similarly, a hydrostatic pressure head distribution (i.e., a total hydraulic head of 86 m) is maintained for the lowermost 17 nodes at the right boundary within the unconfined aquifer. The lower boundary nodes of the flow domain are assigned zero fluid and concentration fluxes.

Three contaminant flux boundary segments must be specified: (1) top boundary, (2) left-side boundary in the unconfined aquifer, and (3) trench bottom. The contribution to the total contaminant flux from the side boundary of the trench can be safely neglected. The total contaminant influx is specified to be zero at the (1) and (2) boundary locations to ensure that no additional contaminant enters the simulation area. The boundary condition at the trench bottom is varied for different release mechanisms and will be discussed later. The other nonspecified boundary (default) is treated by code as a zero-gradient boundary condition.

Initial conditions must also be defined to complete the analysis. VAM3D-CG requires input data on initial (t=0) pressures and concentrations. The initial pressure heads within the unsaturated (vadose) zone are assigned using a unit gradient model. This, in turn, assigns the infiltration rate as being equal to unsaturated hydraulic conductivity. Using the moisture characteristic curves, the pressure head value for the given unsaturated hydraulic conductivity (and, therefore, for the corresponding moisture content) is then obtained. Within the saturated unconfined region of the flow domain, the initial pressure head values are assigned using a hydrostatic pressure head distribution. A concentration value of C=0 is used as the initial concentration values for the radionuclides. Within the burial trench, however, an initial concentration value, based on the initial inventory, is assigned for all radionuclides.

3.2.4 Quality Control/Quality Assurance Practices for VAM3D-CG

In this section, practices being used for quality control and quality assurance in the use of VAM3D-CG are described. VAM3D-CG was placed under configuration management in mid-1993. This ensures the source and executable codes are carefully controlled, and the results are traceable to the code that created them. The current effort examines Version 2.4b of the source code, dated August 13, 1993 (the vender has released multiple revisions of Version 2.4b).

The bulk of the tests were run on an Silicon Graphics Inc. (SGI) workstation, under the operating system IRIX Release 4.0.5C, System V. Additional runs were made on a Cray XMP12-32 computer, operating under UNICOS 6.0, in an effort to verify the installation of VAM3D-CG as it was moved to the SGI.

When VAM3D-CG was moved to the SGI environment, two changes were made to the code. First, a traceability record was added to the top of the output files. File traceability is often a necessary feature, when the results must be archived for many years or when multiple versions of the modeling code are released. Second, the system-dependent routines were separated from the numeric modeling software. This allows the code to be moved between operating systems without making modifications to the source code files that do the actual computation.

Testing of the VAM3D-CG computer code, Version 2.4b, was conducted to establish confidence that the code is ready for use in performance assessment applications at the Hanford Site.

Three sets of testing problems were performed:

1. Reproduction of the verification and benchmark testing problems published by the vendor (HydroGeologic, Inc.) in the user's manual

2. Two benchmark testing problems relevant to performance assessment applications at Hanford

3. Verification of the VAM3D-CG source code as installed on the SGI workstation. The selected tests were performed to show that the VAM3D-CG code on the SGI produces the same results as those previously on the Cray computer, which is no longer in service.

The test results showed excellent agreement with the first and third sets of problems. Both maximum difference and the relative root mean square (RRMS) values are negligible. The differences can be explained by rounding errors between the two computers.

For the second set of problems, the solutions showed very good overall agreement when plotted, even though VAM3D-CG and the benchmark code employ significantly different solution techniques. Although minor discrepancies exist, the two codes should perform equally well in terms of performance assessment applications at the Hanford Site. The detail results of verification and benchmarking are presented in Appendixes G1 and G2.

3.2.5 Groundwater Pathway Dose Calculations

Dose calculations for the groundwater pathway analysis are completed in the same fashion as dose by intruder scenarios with the exception that slightly different sources of dose occur depending on the scenario being considered. Also, radioactivity originates from the contaminated groundwater rather than the waste itself as assumed in the intruder scenarios. Thus, the groundwater concentrations calculated from the flow and transport analyses are used to calculate dose. The pathways and parameter values for each of the three scenarios (all-pathways, groundwater drinking and Columbia River) are considered in this section.

3.2.5.1 All-Pathways Scenario. The farmer derives contaminated groundwater from a well 100 m down gradient from the disposal facility and uses the water to drink, irrigate crops, and water livestock. The farmer receives dose by the following:

- Ingestion of water, crops, beef, and milk
- Inhalation of contaminated dust in the air
- External exposure to radiation.

In this analysis, the same parameter and parameter values were used as in the intruder scenarios except that consumption of beef, milk, and water was added as additional sources of dose. The maximum exposed individual consumes 730 L/yr of water. The quantities of beef and milk consumption are shown in Table 3-2.

3.2.5.2 Groundwater Drinking. The individual derives contaminated groundwater from a well 100 m downgradient from the disposal facility and uses the water only for drinking. Thus, dose is received only through the ingestion of water. It is assumed that the annual consumption of contaminated water is 730 L/yr.

3.2.5.3 Columbia River Scenario. Contaminated groundwater discharges into the Columbia River and the downstream population receives dose through use of the contaminated water. The dose calculation was constructed somewhat differently from the previous scenarios in that a dose to a population rather than an individual is calculated. A population of 5 million people was assumed to live downstream.

As with the All-Pathways scenario, dose is received by ingestion, inhalation, and external exposure. In addition to the ingestion of water (some of which occurs while swimming), soil, crops, beef and milk, ingestion occurs through the consumption of contaminated fish. Assuming that a total of 15 metric tons of fish are harvested annually from the Columbia River, the average consumption per person is 3 g/yr. Inhalation and external exposure calculations are computed identically to the other exposure scenarios.

The assumptions used in this scenario will overestimate the population dose. First, the Columbia River is diluted by inflows of water from tributaries immediately below the Tri-Cities, and all along its length to the Pacific Ocean, resulting in lower radionuclide concentrations. Second, most drinking water passes through community water treatment systems. Such systems reduce the radionuclide concentrations reaching the affected people. Third,

the population estimate of 5 million is a significant increase over the present conditions. In addition, the production of nearly all food consumed by the downriver population with contaminated river water would require a very large increase in crop production below the site.

3.3 ADDITIONAL ANALYSES

To complete the discussion of potential exposure pathways, two other means of release must be considered: vapor release and upward diffusion. Vapor release is of concern only for three radionuclides: ^{14}C, ^{3}H, and ^{222}Rn. Upward liquid diffusion from the waste facility is a possible means of transport for all radionuclides because of the expected low recharge rates.

3.3.1 Vapor Diffusion Pathway Analysis

Three radionuclides, ^{14}C, ^{3}H, and ^{222}Rn, have the potential to migrate upward into the atmosphere in gaseous form, thereby potentially exposing man to radiation. Of these three radionuclides, ^{222}Rn releases and inventory limits are considered relative to the performance objective of 20 $pCi/m^2/s$ surface flux for the undisturbed facility (Chapter 4). To evaluate the most reasonable waste acceptance criteria for ^{14}C and ^{3}H, it is necessary to compare relative dose by inhalation from these radionuclides present in vapor-versus-dust for the intruder and exposure by the groundwater pathway for the offsite individual. A simple analytical steady state diffusion calculation was used to estimate dose for ^{14}C and ^{3}H. The details of the calculation are provided in Section 4.3.1.

Two cases were considered for ^{14}C and ^{3}H. The first was a postexcavation scenario as described previously for the intruder. The second case assumes a resident above the undisturbed facility. For each case the resident spends part of his time in a room of the house through which contaminated gas fluxes, thereby receiving a dose. The primary parameters in these calculations are the initial concentration of radionuclide in the soil column, the diffusivity of the gas containing the radionuclide, the air change rate in the room, and the annual volume of air consumed in the room. The initial concentration in the waste is assumed to be 1 Ci/m^3 for the purposes of calculation and the volume of air inhaled is the same as that used in the intruder scenarios for the inhalation pathway (Section 3.1.3). The diffusivity value of 0.01 cm^2/s (31.5 m^2/yr) was selected by considering the measured diffusion of gases in air (about 0.1 cm^2/s) and reducing the value because of the moisture content in the soil and the tortuosity factor provided by the solid materials.

The flux estimates are also used to evaluate dose from ^{14}C and ^{3}H to a maximally exposed offsite individual. An atmospheric dispersion model (ISC2) from the EPA was used to estimate dose as a function of activity release from the disposal facility. Wind data taken from the HMS between 1983 and 1991 were used as input to determine the direction and quantity of maximum exposure.

3.3.2 Upward Diffusion

The relatively low recharge expected at the Hanford Site gives rise to the possibility that mass transport upwards from an undisturbed disposal facility could bring radionuclides to the surface or into the plant root zone. A simple analytical model is used to compare the relative rates of upward movement driven by diffusion versus downward movement driven by infiltration. Consideration is given to nonsorbing radionuclides as being the most conservative and rapidly moving isotopes in the upward direction. Diffusion coefficient values were selected using a database of experimentally measured diffusion coefficients under site-specific conditions.

4.0 ANALYTICAL RESULTS

In this chapter, the results of the inadvertent intrusion scenarios (Section 4.1) and groundwater pathways scenarios (Section 4.2) analyses are presented. Each of these sections is organized to first present the base case analytical results. Subsequent sections are provided to discuss (1) the sensitivity of the results to variations in parameter values and (2) estimates of uncertainties in dose estimates based on ranges of plausible parameter variability.

The significance of other pathways and activities that may affect potential dose are also considered (Section 4.3). These include the vapor pathway, upward liquid diffusion from an undisturbed facility, the effects of mixing of contaminant plumes from the 200 West Area LLBG and other sources of waste on the Hanford Plateau, and the potential for enhanced dose resulting from increased recharge on the Hanford Plateau. This is postulated to occur if the Hanford Site is used in the future for large-scale agricultural purposes requiring irrigation.

In Section 4.4, the total set of results are integrated to define the most significant influences on potential dose to man for the Hanford Site conditions. Waste acceptance criteria for the disposal of LLW in the 200 West Area burial grounds are provided on the basis of this integration effort. Finally, an estimate of potential dose from the filled and closed facility is made and compared with the performance objectives.

4.1 ANALYTICAL RESULTS FOR INADVERTENT INTRUDER SCENARIOS

Dose estimates are provided for a large number of radionuclides for two types of intruder scenarios: the postexcavation scenario and the postdrilling scenario. A discussion of the sensitivities of dose estimates to changes in various parameter values and the estimated uncertainties in dose estimates is also provided.

4.1.1 Dose Estimate Results

Many uncertainties are involved in the prediction of which isotopes will be present in the LLW streams and in what quantities. Therefore, dose estimates have been provided for a large number of radionuclides. A list of these radionuclides is provided in Table 4-1. Some of the radionuclides on the list will frequently exist in the waste while others may rarely be present in actual waste or not at all. The consideration of this large list has been provided for completeness. Most, but not all radionuclides with half-lives >5 yr, are included. Those omitted have not been reported in Hanford Site waste inventories. Radionuclides with half-lives of 5 yr or less were not included in this list because it is assumed that intrusion does not occur until 100 yr after closure. For a radionuclide of 5-yr half-life, this corresponds to 20 half-lives or a reduction in concentration by a factor of about 10^6. It is not considered plausible that a radionuclide in this category could exist in any potential waste stream such that it could cause a

Table 4-1. Radionuclides Considered to be in Secular Equilibrium in the Dose Analysis. (sheet 1 of 2)

Radionuclide	Half-life (yr)	Progeny lumped with parent in the spreadsheet
^{3}H	12.28	
^{10}Be	1.60 E+06	
^{14}C	5,730	
^{36}Cl	301,000	
^{40}K	1.277 E+09	
^{60}Co	5.271	
^{59}Ni	75,000	
^{63}Ni	100.1	
^{79}Se	65,000	
^{90}Sr	28.6	^{90}Y
^{93}Zr	1.53 E+06	
^{93m}Nb	14.6	
^{94}Nb	20,300	
^{93}Mo	3,500	
^{99}Tc	213,000	
^{107}Pd	6.50 E+06	
^{113m}Cd	13.7	
^{121m}Sn	55	^{121}Sn (0.778)
^{126}Sn	100,000	^{126m}Sb, ^{126}Sb (0.14)
^{129}I	1.57 E+07	
^{135}Cs	2.30 E+06	
^{137}Cs	30.17	^{137m}Ba (0.946)
^{133}Ba*	10.5	
^{147}Sm	1.06 E+11	
^{151}Sm	90	
^{150}Eu*	36	
^{152}Eu	13.6	
^{154}Eu	8.8	
^{152}Gd*	1.10 E+14	
^{187}Re	4.7 E+10	
^{210}Pb	22.26	^{210}Bi, ^{210}Po
^{209}Po*	102	
^{226}Ra	1,600	^{222}Rn, ^{218}Po, ^{214}Pb, ^{214}Bi, ^{214}Po
^{228}Ra	5.75	^{228}Ac
^{227}Ac	21.773	^{227}Th (0.9862), ^{223}Fr (0.0138), ^{223}Ra, ^{219}Rn, ^{215}Po, ^{211}Pb, ^{211}Bi, ^{207}Tl (0.99727), ^{211}Po (0.00273)
^{228}Th	1.9132	^{224}Ra, ^{220}Rn, ^{216}Po, ^{212}Pb, ^{212}Bi, ^{212}Po (0.6407), ^{208}Tl (0.3593)
^{229}Th	7,340	^{225}Ra, ^{225}Ac, ^{221}Fr, ^{217}At, ^{213}Bi, ^{213}Po, ^{209}Tl
^{230}Th	77,000	
^{232}Th	1.405 E+10	
^{131}Pa	32,764	
^{232}U	72	
^{233}U	159,200	
^{234}U	244,500	
^{235}U	7.038 E+08	^{231}Th
^{236}U	2.34 E+07	

Table 4-1. Radionuclides Considered to be in Secular Equilibrium in the Dose Analysis. (sheet 2 of 2)

Radionuclide	Half-life (yr)	Progeny lumped with parent in the spreadsheet
^{238}U	4.468 E+09	^{234}Th, ^{234m}Pa, ^{234}Pa (0.0016)
^{237}Np	2.14 E+06	^{233}Pa
^{238}Pu	86.75	
^{239}Pu	24,131	
^{240}Pu	6,569	
^{241}Pu	14.4	^{237}U (2.45 E-05)
^{242}Pu	375,800	
^{244}Pu	8.26 E+07	^{240}U
^{241}Am	432.2	
^{242m}Am	152	^{242}Am (0.99524), ^{242}Cm (0.827), ^{238}Np (0.00476)
^{243}Am	7,380	^{239}Np
^{243}Cm	28.5	
^{244}Cm	18.11	
^{245}Cm	8,500	
^{246}Cm	4,750	
^{247}Cm	1.56 E+07	^{243}Pu
^{248}Cm	339,000	

*These are not present in the current GENII library (Version 1.485).
NOTE: The numbers in parentheses are the branching ratios for the progeny radionuclide shown. The half-lives of all progeny radionuclides are less than 1 yr.

significant dose after 100 yr. The one radionuclide with a <5-yr half-life that appears on the list of radionuclides is ^{242}Cm, which has a half-life of 163 d. This isotope is specifically identified in 10 CFR 61 and has been given a waste concentration limit for Class C waste. Consequently, if a waste stream contains ^{242}Cm, its concentration in that waste stream must be considered in the disposal of that waste because of the requirement in DOE Order 5820.2A forbidding the disposal of greater than Class C waste.

The estimate of dose for some radionuclides is complicated by the fact that daughter products resulting from decay are in secular equilibrium or near-secular equilibrium. Consequently, the activity of the daughter is equal to the parent or nearly equal and can provide a significant contribution to dose if they are not separated by the exposure pathway. To deal with this complication, the analysis was completed to incorporate daughter contributions into dose estimates of the parents. Those decay chains considered in the analysis are listed in Tables 4-1 and 4-2. In Table 4-1, radionuclides are listed with daughters assumed to be in secular equilibrium with the parent. For radionuclides in Table 4-2, radionuclide decay is assumed to be ongoing while dose is being received. For these radionuclides, the activity value of the daughter is different, depending on the time at which dose is assumed to occur.

Table 4-2. Radioactive Decay Chains Used in the Dose Analysis.

Parent radionuclide	Progeny radionuclides
^{93}Zr	^{93m}Nb
^{93}Mo	^{93m}Nb
^{226}Ra	^{210}Pb
^{228}Ra	^{228}Th
^{230}Th	^{226}Ra and ^{210}Pb
^{232}Th	^{228}Ra and ^{228}Th
^{232}U	^{228}Th
^{233}U	^{229}Th
^{241}Pu	^{241}Am and ^{237}Np
^{244}Pu	^{240}Pu
^{241}Am	^{237}Np
^{242m}Am	^{242}Pu, ^{238}Pu, ^{234}U
^{243}Am	^{239}Pu
^{243}Cm	^{239}Pu and ^{243}Am
^{244}Cm	^{240}Pu
^{245}Cm	^{241}Pu, ^{241}Am, ^{237}Np
^{247}Cm	^{243}Am

Dose estimates resulting from the postexcavation and postdrilling scenarios are listed in Tables 4-3 and 4-4. Unit concentrations (1 Ci/m^3) of all radionuclides in Tables 4-3 and 4-4 are assumed to be present in the waste stream initially. These results are easily adjusted for whatever initial concentration or quantity of radionuclide of interest because of direct proportionality between initial conditions and final results. This process is used in the final part of this chapter (Section 4.4) to calculate concentrations that result in dose estimates matching performance objectives (i.e., waste acceptance criteria). The dose numbers listed in these tables were calculated using the spreadsheet. For a given radionuclide, doses were calculated as a function of (1) time, and (2) the assumption of leaching or not leaching of radionuclides from the soil during crop growth. Note also that the soil-plant transfer coefficients for this table were taken from Kennedy and Strenge (1992). As part of the sensitivity analysis, an additional set of soil-plant transfer coefficients were also considered (Baes et al. 1984). For each radionuclide, the exposure pathway providing the greatest dose for a given radionuclide is also shown.

Table 4-3. Total Doses (mrem/yr per Ci/m³) for the Post-Excavation Scenario Using (Kennedy and Strenge 1990) Concentration Ratios.

Nuclide	With Soil Leaching			Without Soil Leaching			Dominant Pathway
	100 yr	300 yr	500 yr	100 yr	300 yr	500 yr	
H-3	4.09 E-04	5.11 E-09	6.39 E-14	1.09 E-03	1.37 E-08	1.71 E-13	Soil Ing
Be-10	9.08 E+01	9.08 E+01	9.08 E+01	9.09 E+01	9.09 E+01	9.09 E+01	Extern
C-14	1.07 E+03	1.05 E+03	1.02 E+03	1.10 E+03	1.07 E+03	1.05 E+03	Veggie
Cl-36	1.43 E+05	1.43 E+05	1.43 E+05	1.57 E+05	1.57 E+05	1.57 E+05	Veggie
K-40	5.51 E+04	5.51 E+04	5.51 E+04	5.60 E+04	5.60 E+04	5.60 E+04	Extern
Co-60	1.33 E+00	5.05 E-12	1.91 E-23	1.34 E+00	5.07 E-12	1.92 E-23	Extern
Ni-59	2.54 E+01	2.53 E+01	2.53 E+01	2.54 E+01	2.53 E+01	2.53 E+01	Extern
Ni-63	1.68 E+01	4.21 E+00	1.05 E+00	1.68 E+01	4.21 E+00	1.05 E+00	Veggie
Se-79	1.97 E+02	1.97 E+02	1.96 E+02	1.98 E+02	1.97 E+02	1.97 E+02	Veggie
Sr-90	6.35 E+03	4.99 E+01	3.91 E-01	6.43 E+03	5.05 E+01	3.96 E-01	Veggie
Zr-93	3.96 E+01	3.97 E+01	3.97 E+01	3.96 E+01	3.97 E+01	3.97 E+01	Inhale
Nb-93m	1.01 E-01	7.58 E-06	5.70 E-10	1.01 E-01	7.59 E-06	5.71 E-10	Extern
Nb-94	4.54 E+05	4.50 E+05	4.47 E+05	4.54 E+05	4.51 E+05	4.48 E+05	Extern
Mo-93	1.12 E+02	1.08 E+02	1.04 E+02	1.15 E+02	1.10 E+02	1.06 E+02	Veggie
Tc-99	2.60 E+03	2.60 E+03	2.59 E+03	4.28 E+03	4.27 E+03	4.27 E+03	Veggie
Pd-107	6.49 E+00	6.49 E+00	6.49 E+00	6.52 E+00	6.52 E+00	6.52 E+00	Veggie
Cd-113m	1.31 E+02	5.28 E-03	2.13 E-07	1.32 E+02	5.31 E-03	2.14 E-07	Veggie
Sn-121m	1.48 E+02	1.19 E+01	9.58 E-01	1.48 E+02	1.19 E+01	9.60 E-01	Extern
Sn-126	6.40 E+05	6.39 E+05	6.38 E+05	6.41 E+05	6.40 E+05	6.40 E+05	Extern
I-129	9.98 E+03	9.98 E+03	9.98 E+03	1.17 E+04	1.17 E+04	1.17 E+04	Veggie
Cs-135	6.09 E+02	6.09 E+02	6.09 E+02	6.09 E+02	6.09 E+02	6.09 E+02	Veggie
Cs-137	1.81 E+04	1.83 E+02	1.85 E+00	1.81 E+04	1.83 E+02	1.85 E+00	Extern
Ba-133	1.41 E+02	2.60 E-04	4.79 E-10	1.42 E+02	2.61 E-04	4.82 E-10	Extern
Sm-147	5.73 E+03	5.73 E+03	5.73 E+03	5.74 E+03	5.74 E+03	5.74 E+03	Inhale
Sm-151	2.19 E+00	4.69 E-01	1.00 E-01	2.19 E+00	4.69 E-01	1.01 E-01	Inhale
Eu-150	7.10 E+04	1.51 E+03	3.21 E+01	7.11 E+04	1.51 E+03	3.21 E+01	Extern
Eu-152	2.09 E+03	7.82 E-02	2.93 E-06	2.09 E+03	7.83 E-02	2.93 E-06	Extern
Eu-154	1.33 E+02	1.92 E-05	2.76 E-12	1.33 E+02	1.92 E-05	2.76 E-12	Extern
Gd-152	1.56 E+04	1.56 E+04	1.56 E+04	1.56 E+04	1.56 E+04	1.56 E+04	Inhale
Re-187	2.71 E+00	2.71 E+00	2.71 E+00	2.75 E+00	2.75 E+00	2.75 E+00	Veggie
Pb-210	2.68 E+03	5.29 E+00	1.05 E-02	2.69 E+03	5.30 E+00	1.05 E-02	Soil Ing
Bi-207	5.98 E+04	9.42 E+02	1.48 E+01	5.99 E+04	9.44 E+02	1.49 E+01	Extern
Po-209	1.02 E+04	2.62 E+03	6.73 E+02	1.02 E+04	2.62 E+03	6.74 E+02	Soil Ing
Ra-226	5.94 E+05	5.47 E+05	5.02 E+05	5.94 E+05	5.48 E+05	5.02 E+05	Extern
Ra-228	5.84 E+00	1.98 E-10	6.68 E-21	5.84 E+00	1.98 E-10	6.69 E-21	Extern
Ac-227	2.39 E+04	4.10 E+01	7.04 E-02	2.39 E+04	4.11 E+01	7.05 E-02	Inhale
Th-228	7.77 E-11	2.64 E-42	8.98 E-74	7.77 E-11	2.64 E-42	8.98 E-74	Extern
Th-229	2.28 E+05	2.24 E+05	2.19 E+05	2.28 E+05	2.24 E+05	2.19 E+05	Inhale
Th-230	4.77 E+04	9.71 E+04	1.42 E+05	4.78 E+04	9.71 E+04	1.42 E+05	Extern
Th-232	9.22 E+05	9.22 E+05	9.22 E+05	9.22 E+05	9.22 E+05	9.22 E+05	Extern
Pa-231	7.05 E+05	7.26 E+05	7.23 E+05	7.06 E+05	7.26 E+05	7.23 E+05	Inhale
U-232	2.17 E+05	3.17 E+04	4.62 E+03	2.18 E+05	3.18 E+04	4.64 E+03	Extern
U-233	1.34 E+04	1.76 E+04	2.18 E+04	1.36 E+04	1.78 E+04	2.20 E+04	Inhale
U-234	1.10 E+04	1.10 E+04	1.10 E+04	1.13 E+04	1.12 E+04	1.12 E+04	Inhale
U-235	3.56 E+04	3.87 E+04	4.17 E+04	3.63 E+04	3.94 E+04	4.25 E+04	Extern
U-236	1.03 E+04	1.03 E+04	1.03 E+04	1.05 E+04	1.05 E+04	1.05 E+04	Inhale
U-238	1.72 E+04	1.72 E+04	1.72 E+04	1.75 E+04	1.75 E+04	1.75 E+04	Inhale
Np-237	1.39 E+05	1.39 E+05	1.39 E+05	1.47 E+05	1.47 E+05	1.47 E+05	Extern
Pu-238	2.12 E+04	4.37 E+03	9.02 E+02	2.12 E+04	4.37 E+03	9.03 E+02	Inhale
Pu-239	5.22 E+04	5.19 E+04	5.16 E+04	5.22 E+04	5.19 E+04	5.16 E+04	Inhale
Pu-240	5.18 E+04	5.07 E+04	4.97 E+04	5.18 E+04	5.08 E+04	4.97 E+04	Inhale
Pu-241	1.64 E+03	1.19 E+03	8.67 E+02	1.64 E+03	1.19 E+03	8.67 E+02	Inhale
Pu-242	4.95 E+04	4.95 E+04	4.95 E+04	4.96 E+04	4.96 E+04	4.95 E+04	Inhale
Pu-244	1.64 E+05	1.65 E+05	1.66 E+05	1.64 E+05	1.65 E+05	1.66 E+05	Extern
Am-241	4.77 E+04	3.47 E+04	2.52 E+04	4.78 E+04	3.47 E+04	2.52 E+04	Inhale
Am-242m	5.32 E+04	2.95 E+04	1.35 E+04	5.32 E+04	2.95 E+04	1.35 E+04	Inhale
Am-243	9.79 E+04	9.63 E+04	9.48 E+04	9.79 E+04	9.64 E+04	9.49 E+04	Extern
Cm-243	5.62 E+03	1.05 E+02	6.22 E+01	5.62 E+03	1.05 E+02	6.23 E+01	Extern*
Cm-244	7.35 E+02	1.41 E+02	1.37 E+02	7.36 E+02	1.41 E+02	1.37 E+02	Inhale
Cm-245	7.53 E+04	8.75 E+04	9.59 E+04	7.53 E+04	8.75 E+04	9.59 E+04	Inhale
Cm-246	5.44 E+04	5.29 E+04	5.13 E+04	5.44 E+04	5.29 E+04	5.13 E+04	Inhale
Cm-247	1.78 E+05	1.79 E+05	1.80 E+05	1.78 E+05	1.79 E+05	1.80 E+05	Extern
Cm-248	1.95 E+05	1.95 E+05	1.95 E+05	1.95 E+05	1.95 E+05	1.95 E+05	Inhale

*The dominant pathway for ^{243}Cm changes to "Inhale" at times greater than 100 yr because of the ingrowth of ^{239}Pu.

Table 4-4. Total Doses (mrem/yr per Ci/m³) for the Post-Drilling Scenario Using NUREG/CR-5512 Concentration Ratios.

Nuclide	With Soil Leaching			Without Soil Leaching			Dominant Pathway
	100 yr	300 yr	500 yr	100 yr	300 yr	500 yr	
H-3	1.91 E-06	2.38 E-11	2.98 E-16	5.11 E-06	6.39 E-11	7.99 E-16	Soil Ing
Be-10	4.24 E-01	4.24 E-01	4.24 E-01	4.24 E-01	4.24 E-01	4.24 E-01	Extern
C-14	5.00 E+00	4.88 E+00	4.76 E+00	5.13 E+00	5.01 E+00	4.89 E+00	Veggie
Cl-36	6.70 E+02	6.69 E+02	6.69 E+02	7.35 E+02	7.34 E+02	7.34 E+02	Veggie
K-40	2.57 E+02	2.57 E+02	2.57 E+02	2.61 E+02	2.61 E+02	2.61 E+02	Extern
Co-60	6.22 E-03	2.35 E-14	8.91 E-26	6.26 E-03	2.37 E-14	8.96 E-26	Extern
Ni-59	1.18 E-01	1.18 E-01	1.18 E-01	1.19 E-01	1.18 E-01	1.18 E-01	Extern
Ni-63	7.85 E-02	1.97 E-02	4.92 E-03	7.85 E-02	1.97 E-02	4.92 E-03	Veggie
Se-79	9.20 E-01	9.19 E-01	9.17 E-01	9.22 E-01	9.20 E-01	9.18 E-01	Veggie
Sr-90	2.96 E+01	2.33 E-01	1.83 E-03	3.00 E+01	2.36 E-01	1.85 E-03	Veggie
Zr-93	1.85 E-01	1.85 E-01	1.85 E-01	1.85 E-01	1.85 E-01	1.85 E-01	Inhale
Nb-93m	4.70 E-04	3.54 E-08	2.66 E-12	4.71 E-04	3.54 E-08	2.66 E-12	Extern
Nb-94	2.12 E+03	2.10 E+03	2.09 E+03	2.12 E+03	2.11 E+03	2.09 E+03	Extern
Mo-93	5.24 E-01	5.04 E-01	4.85 E-01	5.35 E-01	5.14 E-01	4.95 E-01	Veggie
Tc-99	1.21 E+01	1.21 E+01	1.21 E+01	2.00 E+01	1.99 E+01	1.99 E+01	Veggie
Pd-107	3.03 E-02	3.03 E-02	3.03 E-02	3.04 E-02	3.04 E-02	3.04 E-02	Veggie
Cd-113m	6.12 E-01	2.47 E-05	9.94 E-10	6.15 E-01	2.48 E-05	9.98 E-10	Veggie
Sn-121m	6.91 E-01	5.56 E-02	4.47 E-03	6.93 E-01	5.57 E-02	4.48 E-03	Extern
Sn-126	2.99 E+03	2.98 E+03	2.98 E+03	2.99 E+03	2.99 E+03	2.98 E+03	Extern
I-129	4.66 E+01	4.66 E+01	4.66 E+01	5.47 E+01	5.47 E+01	5.47 E+01	Veggie
Cs-135	2.84 E+00	2.84 E+00	2.84 E+00	2.84 E+00	2.84 E+00	2.84 E+00	Veggie
Cs-137	8.44 E+01	8.53 E-01	8.62 E-03	8.45 E+01	8.54 E-01	8.63 E-03	Extern
Ba-133	6.56 E-01	1.21 E-06	2.24 E-12	6.60 E-01	1.22 E-06	2.25 E-12	Extern
Sm-147	2.68 E+01	2.68 E+01	2.68 E+01	2.68 E+01	2.68 E+01	2.68 E+01	Inhale
Sm-151	1.02 E-02	2.19 E-03	4.69 E-04	1.02 E-02	2.19 E-03	4.69 E-04	Inhale
Eu-150	3.31 E+02	7.05 E+00	1.50 E-01	3.32 E+02	7.06 E+00	1.50 E-01	Extern
Eu-152	9.75 E+00	3.65 E-04	1.37 E-08	9.76 E+00	3.65 E-04	1.37 E-08	Extern
Eu-154	6.21 E-01	8.94 E-08	1.29 E-14	6.22 E-01	8.96 E-08	1.29 E-14	Extern
Gd-152	7.27 E+01	7.27 E+01	7.27 E+01	7.28 E+01	7.28 E+01	7.28 E+01	Inhale
Re-187	1.27 E-02	1.27 E-02	1.27 E-02	1.28 E-02	1.28 E-02	1.28 E-02	Veggie
Pb-210	1.25 E+01	2.47 E-02	4.88 E-05	1.25 E+01	2.47 E-02	4.88 E-05	Soil Ing
Bi-207	2.79 E+02	4.39 E+00	6.92 E-02	2.80 E+02	4.41 E+00	6.94 E-02	Extern
Po-209	4.76 E+01	1.22 E+01	3.14 E+00	4.77 E+01	1.22 E+01	3.15 E+00	Soil Ing
Ra-226	2.77 E+03	2.55 E+03	2.34 E+03	2.77 E+03	2.56 E+03	2.34 E+03	Extern
Ra-228	2.72 E-02	9.22 E-13	3.12 E-23	2.73 E-02	9.22 E-13	3.12 E-23	Extern
Ac-227	1.11 E+02	1.91 E-01	3.29 E-04	1.12 E+02	1.92 E-01	3.29 E-04	Inhale
Th-228	3.63 E-13	1.23 E-44	4.19 E-76	3.63 E-13	1.23 E-44	4.19 E-76	Extern
Th-229	1.06 E+03	1.04 E+03	1.02 E+03	1.06 E+03	1.04 E+03	1.02 E+03	Inhale
Th-230	2.23 E+02	4.53 E+02	6.64 E+02	2.23 E+02	4.53 E+02	6.64 E+02	Extern
Th-232	4.30 E+03	4.30 E+03	4.30 E+03	4.30 E+03	4.30 E+03	4.30 E+03	Extern
Pa-231	3.29 E+03	3.39 E+03	3.37 E+03	3.29 E+03	3.39 E+03	3.38 E+03	Inhale
U-232	1.01 E+03	1.48 E+02	2.15 E+01	1.02 E+03	1.48 E+02	2.16 E+01	Extern
U-233	6.24 E+01	8.22 E+01	1.02 E+02	6.34 E+01	8.32 E+01	1.03 E+02	Inhale
U-234	5.15 E+01	5.15 E+01	5.14 E+01	5.25 E+01	5.25 E+01	5.25 E+01	Inhale
U-235	1.66 E+02	1.80 E+02	1.95 E+02	1.70 E+02	1.84 E+02	1.98 E+02	Extern
U-236	4.81 E+01	4.81 E+01	4.81 E+01	4.91 E+01	4.91 E+01	4.91 E+01	Inhale
U-238	8.01 E+01	8.01 E+01	8.01 E+01	8.18 E+01	8.18 E+01	8.18 E+01	Inhale
Np-237	6.49 E+02	6.49 E+02	6.49 E+02	6.87 E+02	6.87 E+02	6.87 E+02	Extern
Pu-238	9.88 E+01	2.04 E+01	4.21 E+00	9.89 E+01	2.04 E+01	4.21 E+00	Inhale
Pu-239	2.44 E+02	2.42 E+02	2.41 E+02	2.44 E+02	2.42 E+02	2.41 E+02	Inhale
Pu-240	2.42 E+02	2.37 E+02	2.32 E+02	2.42 E+02	2.37 E+02	2.32 E+02	Inhale
Pu-241	7.65 E+00	5.57 E+00	4.05 E+00	7.65 E+00	5.57 E+00	4.05 E+00	Inhale
Pu-242	2.31 E+02	2.31 E+02	2.31 E+02	2.31 E+02	2.31 E+02	2.31 E+02	Inhale
Pu-244	7.64 E+02	7.69 E+02	7.73 E+02	7.64 E+02	7.69 E+02	7.74 E+02	Extern
Am-241	2.23 E+02	1.62 E+02	1.17 E+02	2.23 E+02	1.62 E+02	1.17 E+02	Inhale
Am-242m	2.48 E+02	1.38 E+02	6.31 E+01	2.48 E+02	1.38 E+02	6.31 E+01	Inhale
Am-243	4.57 E+02	4.50 E+02	4.43 E+02	4.57 E+02	4.50 E+02	4.43 E+02	Extern
Cm-243	2.62 E+01	4.91 E-01	2.90 E-01	2.62 E+01	4.91 E-01	2.91 E-01	Extern*
Cm-244	3.43 E+00	6.56 E-01	6.41 E-01	3.43 E+00	6.56 E-01	6.41 E-01	Inhale
Cm-245	3.51 E+02	4.08 E+02	4.47 E+02	3.51 E+02	4.08 E+02	4.47 E+02	Inhale
Cm-246	2.54 E+02	2.47 E+02	2.40 E+02	2.54 E+02	2.47 E+02	2.40 E+02	Inhale
Cm-247	8.31 E+02	8.37 E+02	8.42 E+02	8.31 E+02	8.37 E+02	8.42 E+02	Extern
Cm-248	9.11 E+02	9.10 E+02	9.10 E+02	9.11 E+02	9.10 E+02	9.10 E+02	Inhale

*The dominant pathway for ^{243}Cm changes to "Inhale" at times greater than 100 yr because of the ingrowth of ^{239}Pu.

Doses estimates are provided for 100, 300, and 500 yr after emplacement in the disposal facility. This time frame was picked because of the assumptions that excavation occurs 100 yr after disposal and postdrilling occurs 500 yr after disposal. The comparative changes in dose are strictly related to half-life. For radionuclides with a half-life of 30 yr or less, the dose for the same initial concentration decreases by greater than 1 to greater than 10 orders of magnitude during this time period. For radionuclides with half-lives greater than 100 yr, little or no decrease in dose is estimated because of decay. For a given radionuclide, the differences between dose estimates in the postdrilling versus the postexcavation scenario are strictly related to the relative amounts of waste exhumed (basement excavation versus well drilling) and the subsequent soil dilution factor.

4.1.2 Intruder Dose Sensitivity Analysis

Each dose estimate value provided in Tables 4-3 and 4-4 assumes single values for each input parameter used to quantify the dose for a given exposure pathway. In most cases, only one value for a given parameter was considered. It is obvious with the number of parameters involved that many different dose estimates can be calculated by assuming a range of plausible values. It is necessary to consider the potential effects that changes in key parameter values have on dose estimates, particularly because of the direct correlation between dose estimates and waste classification concentration limits developed in Section 4.4.

The sensitivity analysis is approached deterministically by evaluating the change in dose estimate as a function of systematic changes in parameter value. In the case of the intruder dose estimates, the dose response to parameter value change is easily understood because simple algebraic relationships are used to estimate dose. The following discussion is organized by major parameter types and exposure pathways (e.g., soil dilution, ingestion, and inhalation parameters).

4.1.2.1 General Observations. Sensitivity of dose estimates to parameter value variability is radionuclide specific. This observation is noted in Tables 4-3 and 4-4 and further quantified in Table 4-5. In Table 4-5 the dose by pathway is provided for a unit quantity of radionuclide exhumed as a function of pathway. The column labeled "Root Up" refers to the ingestion of contaminated crops. Note that the dose by the primary exposure pathway frequently exceeds dose provided by the other pathways by a large factor. This is an important observation when considering sensitivity of dose estimates to specific parameters in that many parameters are pathway specific. If the pathway is not a significant means of dose for a radionuclide, then the parameter variability associated with that pathway is inconsequential. For example, dose by ingestion of ^{99}Tc in contaminated crops exceeds dose from other pathways by more than two orders of magnitude. Thus, variability in a parameter that affects dose by inhalation or external exposure has no effect on the dose estimate for ^{99}Tc.

Table 4-5. Comparison of Dose to the Intruder by Exposure Pathway at 100 Years Postclosure.

Nuclide	Inhale	Extern	Soil Ing	Root Up	Rain Sp	Case Totals	Maximum Pathway
H-3	1.0E-17	9.1E-21	8.2E-16	0.0E+00	2.0E-17	8.47E-16	Soil Ing
Be-10	2.8E-01	5.7E-01	2.7E-01	8.9E-02	5.1E-03	1.21E+00	Extern
C-14	1.5E-03	8.8E-03	1.2E-01	1.3E+01	2.3E-03	1.36E+01	Veggie
Cl-36	1.4E-02	9.5E-01	1.7E-01	1.9E+03	3.3E-03	1.91E+03	Veggie
K-40	9.4E-03	6.2E+02	1.2E+00	1.1E+02	2.3E-02	7.34E+02	Extern
Co-60	3.1E-30	2.5E-25	4.4E-29	2.3E-28	8.5E-31	2.55E-25	Extern
Ni-59	1.0E-03	1.7E-01	1.3E-02	1.5E-01	2.4E-04	3.37E-01	Extern
Ni-63	7.5E-05	7.8E-06	1.1E-03	1.3E-02	2.1E-05	1.41E-02	Veggie
Se-79	7.0E-03	6.9E-03	5.3E-01	2.1E+00	1.0E-02	2.62E+00	Veggie
Sr-90	1.0E-06	1.4E-04	4.8E-05	5.0E-03	9.1E-07	5.22E-03	Veggie
Zr-93	2.8E-01	6.9E-02	1.4E-01	4.2E-02	2.6E-03	5.29E-01	Inhale
Nb-93m	1.1E-12	3.3E-12	1.6E-12	1.6E-12	3.1E-14	7.60E-12	Extern
Nb-94	2.6E-01	6.0E+03	3.2E-01	3.1E-01	6.1E-03	5.96E+03	Extern
Mo-93	4.0E-02	3.5E-01	1.1E-01	8.8E-01	2.0E-03	1.38E+00	Veggie
Tc-99	2.8E-03	3.0E-02	3.9E-02	3.5E+01	9.6E-04	3.46E+01	Veggie
Pd-107	1.0E-02	5.4E-06	9.0E-03	6.7E-02	1.7E-04	8.66E-02	Veggie
Cd-113m	1.1E-11	5.6E-12	9.7E-11	2.7E-09	1.8E-12	2.84E-09	Veggie
Sn-121m	1.3E-05	1.2E-02	2.3E-04	2.8E-04	4.4E-06	1.28E-02	Extern
Sn-126	6.0E-02	8.5E+03	1.2E+00	1.4E+00	2.2E-02	8.51E+03	Extern
I-129	1.1E-01	5.7E+00	1.4E+01	1.1E+02	3.0E-01	1.33E+02	Veggie
Cs-135	3.6E-03	1.9E-02	4.6E-01	7.6E+00	8.6E-03	8.12E+00	Veggie
Cs-137	2.6E-07	2.4E-02	3.3E-05	5.5E-04	6.2E-07	2.46E-02	Extern
Ba-133	2.4E-17	6.4E-12	9.2E-16	3.6E-15	1.8E-17	6.39E-12	Extern
Sm-147	5.7E+01	0.0E+00	1.2E+01	8.0E+00	2.2E-01	7.64E+01	Inhale
Sm-151	4.9E-04	5.4E-05	4.7E-04	3.2E-04	8.8E-06	1.34E-03	Inhale
Eu-150	1.4E-05	4.3E-01	2.6E-05	1.8E-05	4.9E-07	4.28E-01	Extern
Eu-152	1.5E-12	3.9E-08	3.2E-12	2.2E-12	6.2E-14	3.90E-08	Extern
Eu-154	1.6E-18	3.7E-14	4.5E-18	3.1E-18	8.5E-20	3.68E-14	Extern
Gd-152	1.9E+02	0.0E+00	9.7E+00	6.7E+00	1.8E-01	2.08E+02	Inhale
Re-187	3.8E-05	0.0E+00	5.3E-04	3.6E-02	1.0E-05	3.62E-02	Veggie
Pb-210	2.9E-06	8.6E-07	7.4E-05	6.0E-05	1.4E-06	1.39E-04	Soil Ing
Bi-207	3.4E-07	2.0E-01	9.8E-06	1.1E-05	1.8E-07	1.98E-01	Extern
Po-209	2.7E-01	3.9E-01	4.3E+00	3.9E+00	8.1E-02	8.97E+00	Soil Ing
Ra-226	1.9E+01	5.9E+03	4.1E+02	3.7E+02	7.8E+00	6.69E+03	Extern
Ra-228	2.4E-24	8.5E-23	9.5E-25	7.7E-25	1.8E-26	8.91E-23	Extern
Ac-227	6.4E-04	1.7E-04	1.1E-04	1.0E-05	2.2E-06	9.39E-04	Inhale
Th-228	4.5E-77	1.1E-75	8.7E-78	8.5E-79	1.8E-79	1.20E-75	Extern
Th-229	1.5E+03	1.1E+03	2.4E+02	2.2E+01	4.5E+00	2.92E+03	Inhale
Th-230	2.6E+02	1.4E+03	1.3E+02	8.7E+01	2.4E+00	1.90E+03	Extern
Th-232	1.5E+03	1.0E+04	3.1E+02	1.3E+02	5.8E+00	1.23E+04	Extern
Pa-231	6.3E+03	1.5E+03	1.6E+03	1.3E+02	3.1E+01	9.64E+03	Inhale
U-232	6.3E+00	5.3E+01	1.1E+00	1.2E+00	2.0E-02	6.16E+01	Extern
U-233	1.8E+02	5.5E+01	2.9E+01	3.1E+01	5.4E-01	2.90E+02	Inhale
U-234	1.0E+02	2.4E-01	1.6E+01	2.9E+01	3.1E-01	1.47E+02	Inhale
U-235	1.6E+02	3.4E+02	3.3E+01	2.9E+01	6.2E-01	5.56E+02	Extern
U-236	9.4E+01	1.3E-01	1.6E+01	2.8E+01	3.0E-01	1.37E+02	Inhale
U-238	9.4E+01	9.3E+01	1.5E+01	2.7E+01	2.9E-01	2.29E+02	Inhale
Np-237	3.7E+02	8.7E+02	2.4E+02	3.7E+02	4.6E+00	1.85E+03	Extern
Pu-238	7.1E+00	1.7E-03	4.7E+00	1.3E-01	8.9E-02	1.20E+01	Inhale
Pu-239	4.0E+02	1.4E-01	2.8E+02	7.0E+00	5.2E+00	6.88E+02	Inhale
Pu-240	3.9E+02	9.0E-02	2.6E+02	6.8E+00	5.0E+00	6.62E+02	Inhale
Pu-241	6.4E+00	2.9E-01	4.5E+00	2.6E-01	8.5E-02	1.16E+01	Inhale
Pu-242	3.8E+02	6.8E-02	2.7E+02	6.8E+00	5.0E+00	6.60E+02	Inhale
Pu-244	4.0E+02	1.5E+03	2.7E+02	7.0E+00	5.1E+00	2.21E+03	Extern
Am-241	1.9E+02	8.5E+00	1.3E+02	7.6E+00	2.5E+00	3.35E+02	Inhale
Am-242m	1.0E+02	4.9E+00	6.8E+01	2.7E+00	1.3E+00	1.80E+02	Inhale
Am-243	4.0E+02	5.6E+02	2.8E+02	1.6E+01	5.3E+00	1.26E+03	Extern
Cm-243	4.8E-01	7.3E-03	3.3E-01	8.5E-03	6.2E-03	8.30E-01	Inhale
Cm-244	1.1E+00	2.5E-04	7.3E-01	1.9E-02	1.4E-02	1.83E+00	Inhale
Cm-245	6.4E+02	1.8E+02	4.4E+02	1.7E+01	8.2E+00	1.28E+03	Inhale
Cm-246	4.0E+02	5.1E-02	2.7E+02	7.3E+00	5.1E+00	6.85E+02	Inhale
Cm-247	4.0E+02	1.7E+03	2.7E+02	7.4E+00	5.2E+00	2.41E+03	Extern
Cm-248	1.5E+03	5.0E-02	1.0E+03	2.8E+01	1.9E+01	2.60E+03	Inhale

Note: The above values must be multiplied by the volume of waste exhumed.

The other general observation is that dose is rarely directly proportional to changes in the value of any given parameter. This occurs because numerous parameters invariably contribute to dose in conjunction with other parameters. At the same time, contributing parameters are in themselves not usually interrelated. Thus, a potential increase in one parameter value does not cause an expected increase in another parameter, even though both contribute to dose from the same pathway. In most cases, if a parameter value is doubled (i.e., increased by 100%) and all other parameters are kept constant, the dose increase is usually less than 50%. In the following sections, the parameters are discussed that have the largest effect on dose relative to other parameters.

4.1.2.2 Sensitivity Analysis of Parameters Affecting All-Intruder Pathways. The parameters considered in the analysis that affect all of the exposure pathways include (1) the initial concentration of radionuclides in the waste, (2) the soil dilution factor, and (3) the leachability of radionuclides in the soil after mixing. All three parameters are related to the concentration of radionuclides in the soil that are available for contribution to dose.

Estimated doses are directly proportional to the initial radionuclide concentration in the waste and inversely proportional to the soil dilution factor (the ratio of material volume containing waste to the volume of soil in which the waste is mixed). Also, the potential for leaching of radionuclides from the soil after mixing can reduce the available inventory. Thus, if the initial concentration is doubled and all other parameters kept constant, the dose estimate will be doubled. For the soil dilution factor, if it is assumed that the amount of waste exhumed is doubled and all other parameters are kept constant, then the dose estimate doubles. If the amount of soil in which waste is mixed is doubled and all other parameters are kept constant, the dose estimate is halved.

Once radionuclides are mixed into the soil, they can be leached by precipitation or irrigation during the time period that crops are growing in the soil. The available concentration for plant uptake is reduced by leaching. The extent of concentration reduction is assumed to be dependent on the reactivity of the isotope with the soil (i.e., the sorption coefficient or Kd) and the flux of water through the soil column. The assumed values for these parameters are provided in Appendix C. A comparison of doses for leaching versus nonleaching is shown to be relatively insignificant in Tables 4-6 and 4-7. These tables show the dose ratio for those radionuclides most affected by leaching. Typically, a decrease in dose up to a factor of 3 occurs for the nonsorbing radionuclides ^{14}C, ^{36}Cl, ^{3}H, and ^{99}Tc when leaching is assumed. For those radionuclides that are moderately or strongly sorbing, the effect of the leaching process is nil.

4.1.2.3 Sensitivity Analysis of Ingestion Parameters. For the ingestion pathway, dose is directly proportional to (1) the dose conversion factors and (2) the quantity of radionuclides ingested. For the dose conversion factors, the sensitivity is straightforward because only the dose conversion factor parameter is used. However, the quantity of radionuclides consumed must be considered in terms of the secondary parameters that are used to calculate the total quantity. These parameters include (1) types and quantities of food consumed (e.g., leafy vegetables, other vegetables, fruit and grain),

Table 4-6. Ratio of Total Doses: NUREG/CR-5512/ORNL-5785.

Nuclide	With Soil Leaching				Without Soil Leaching			
	100 yr	300 yr	500 yr	All Path	100 yr	300 yr	500 yr	All Path
Cl-36	1.30	1.30	1.30	1.24				
Ni-63	1.24	1.24	1.24		1.24	1.24	1.24	
Sr-90	1.57	1.57	1.57		1.58	1.58	1.58	
Tc-99	1.41	1.41	1.41	1.28	2.09	2.09	2.09	1.52
I-129	0.72	0.72	0.72		0.84	0.84	0.84	
Cs-135	2.82	2.82	2.82		2.82	2.82	2.82	
Pb-210	0.65	0.65	0.65		0.65	0.65	0.65	
Po-209	1.65	1.65	1.65		1.65	1.65	1.65	
U-233					1.11			
U-234	1.11	1.11	1.11		1.13	1.13	1.13	
U-236	1.12	1.12	1.12		1.14	1.14	1.14	
Np-237	0.84	0.84	0.84		0.88	0.88	0.88	

Notes: Differences <10% are not shown.
Postdrilling and postexcavation have the same ratios.

Table 4-7. Ratio of Total Doses: NonLeaching and Leaching.

Nuclide	NUREG/CR-5512 transfer factors				ORNL-5785 transfer factors			
	100 yr	300 yr	500 yr	All path	100 yr	300 yr	500 yr	All path
H-3	2.68	2.68	2.68		2.68	2.68	2.68	
Cl-36					1.42	1.42	1.42	1.35
Tc-99	1.65	1.65	1.65	1.22				
I-129	1.17	1.17	1.17					

Notes: Differences <10% are not shown.
Postdrilling and postexcavation have the same ratios.

(2) quantity of soil consumed, (3) relative efficiency of radionuclide transfer from soil to plant (soil-to-plant transfer coefficients), and (4) dry-to-wet ratios of different crops. Therefore, sensitivity is dependent on the relative values assumed for each of the food types and the behavior of each radionuclide in the biosphere.

To consider sensitivity, ingestion of soil can be separated from ingestion of crops because transfer of radionuclides to man is independent of the soil-to-plant transfer. Also, as shown in Table 4-5, soil ingestion is not significant for all radionuclides except ^{3}H, ^{210}Pb, and ^{209}Po. For ^{3}H, the dose estimates are directly proportional to the quantity of dirt consumed. For ^{210}Pb and ^{209}Po, the effect is not one for one because the contribution to

dose from the ingestion of crops is nearly equivalent to soil ingestion. For these radionuclides, doubling the annual quantity of soil consumed results in approximately a 50% increase in dose.

The sensitivity of potential dose to ingested food can be evaluated by considering the relative contributions to dose provided by each of the food groups that are consumed in the base case. It is also assumed that relative value of each parameter used in the ingestion calculation remains the same. The relative contribution to dose is provided in Table 4-8 for each of the radionuclides whose primary pathway is ingestion. The concentration is assumed to be 1 Ci/m^3 and the values are determined by the product of the quantity of each food group consumed (Table 3-2), the dry-to-wet ratio for each food type (Appendix C) and the soil-to-plant ratio for each food type (Appendix C).

Table 4-8. Relative Contributions (%) to Ingestion Dose by Food Type.

Radionuclide	Leafy	Root	Fruit	Grain
C-14	4.5	39.8	19.1	36.6
Cl-36	32.0	28.0	13.7	26.4
Ni	21.2	40.4	19.2	19.2
Se-79	4.5	40.9	18.2	36.4
Sr-90	15.4	67.3	7.0	10.3
Mo-93	16.4	34.4	16.4	32.8
Tc-99	16.8	36.4	24.3	22.4
Pd-107	15.0	35.0	17.5	32.5
Cd-113m	14.6	35.1	17.2	33.1
I-129	0.2	40.8	20.4	38.5
Cs-135	7.4	25.0	54.4	13.2
Re-187	16.7	33.3	16.7	33.3
Pb-210	3.8	19.2	38.5	38.5
Po-209	17.5	52.6	12.3	17.5

Relative contributions from each of the food groups vary somewhat depending on the radionuclide. Usually, the contributions from roots and grains are the largest. However, in no case does one factor completely dominate the total activity consumed. Doubling of any of the parameter values that make up this calculation results in up to a factor of 1.6 increase in the calculated total activity.

4.1.2.4 Inhalation Parameter Sensitivity Analysis. For the inhalation pathway, estimated dose is directly proportional to (1) the mass of contaminated dust inhaled, (2) the soil concentrations of radionuclides, and the (3) dose conversion factors. Dose estimates are directly proportional to radionuclide soil concentrations and dose conversion factor values (e.g., if either factor is doubled, the dose estimate will be doubled).

The sensitivity to mass of contaminated dust that is consumed is somewhat more complicated because several activities are included in the calculation. To evaluate sensitivity, changes in the parameters used to calculate the activity that provides the largest fraction of dose is considered, that being the time spent indoors and awake (Table 3-1). If any one of the factors contributing to the calculated amount of inhaled dust from this activity is doubled (i.e., air concentration of dust, exposure time, or breathing rate), the total mass of dust consumed is increased by a factor of about 1.3. Doubling of other parameters from the other activities will result in less increase in total dust consumed.

4.1.2.5 External Exposure Parameter Sensitivity Analysis. For the external exposure pathway, estimated dose is directly proportional to the effective time of exposure, radionuclide concentrations in soil, and dose conversion factors. Calculation of the effective time of exposure requires consideration of shielding provided by the floor and walls of the house for time spent indoors. Given the equation for calculating effective exposure time (Section 3.1.3) and the assumption that more time is spent indoors than outdoors, a maximum increase in dose would come from an assumed increase in the value of the shielding factor. If the base case shielding factor (0.33) is doubled (halving the effectiveness of the shielding), the effective exposure time increases by a factor of about 1.5.

4.1.3 Intruder Scenario Uncertainty Analysis

Uncertainty in dose estimates is evaluated deterministically in this analysis by considering likely ranges of values for parameters used to calculate dose estimates for each exposure pathway. By examining lower and upper value estimates (bounding values), changes in dose can be determined relative to the base case provided above. A range of parameter values can be considered for most parameters. The one exception for the intruder scenarios is the dose conversion factors for external exposure for which one set of values is calculated from the GENII Version 1.485 software package using the EXTDF program which uses ISOSHLD as the basis for dose conversion factor calculation.

4.1.3.1 Uncertainty Analysis of Parameters Affecting All-Intruder Pathways. Uncertainty in the initial concentration of radionuclides in the waste is not a factor when considering the development of waste acceptance criteria. By defining waste acceptance criteria, concentration limits are set and disposal of waste is administratively controlled to ensure that limits are not violated. The concentration limits are meant to be averaged over some volume (typically a trench volume or a partial trench volume) and occasional packages in excess of the limits could be permitted. When calculating a dose for waste that is actually disposed, the dose will fall below the limit but the range of potential dose below the limit is difficult to quantify because of uncertainty in the actual waste inventory.

In the excavation scenario, the waste volume is computed on the basis of some average size basement for a single dwelling (100 m^3), an average digging depth (3 m), and a nominal depth of burial (2 m). It is also assumed that the waste volume is not completely waste. A waste fraction of 75% is assumed. To vary the waste volume we assume a variation in the size of a basement that

corresponds to a range of common single-family dwelling sizes. Bounding values of 81 m^3 and 144 m^3 were chosen. The soil volume is based on the area of mixing and the depth of tilling. The base case area is a little over half an acre. The base case tilling depth is 15 cm (about 6 in.). Both parameters were varied. Bounding values for the mixing area of 1,500 and 4,000 m^2 (roughly 1/3 and 1 acre, respectively) were chosen. The tilling depth bounding values were estimated as ±30%. By adding the waste volume that was not waste to the soil volume a total mixing volume was calculated. The lower bounding dilution factor was then calculated by dividing the low waste volume by the high mixing volume, and the high bounding dilution factor by dividing the high waste volume by the low mixing volume. Relative to the base case, the bounding values increase or decrease the dilution factor by less than a factor of 2. Thus, the change in dose due to the variability in the dilution factor is estimated to change by the same factor.

For the drilling scenario, the same soil mixing volume is considered except that no appreciable contribution to the mixing volume from waste excavation occurs (e.g., the volume of well waste that is not waste is insignificant relative to the soil mixing volume). The waste volume is varied as a function of well radius and depth of waste. The well radius range is based on the approximate drinking water well radius (0.075 m) and the approximate irrigation well radius (0.15 m). Waste depth is varied from 5 to 10 m. Using these values, the maximum and minimum dilution factors calculated are about 2 times higher and about 17 times lower, respectively, than the base case value.

4.1.3.2 Uncertainty Analysis of Ingestion Parameters. Uncertainty is discussed in terms of the three major groups of parameters, dose conversion factors, soil dilution factors (see Section 4.2.3.1) and food consumption parameters. To evaluate uncertainty in dose conversion factors, three sources of factors were compared (Table 4-9): the GENII data base, DOE/EH-0071 (DOE 1988), and the EPA Federal Guidance Report Number 11 (EPA 1988). Comparison of ingestion values shows a difference of no more than ~40% for any radionuclide except ^{99}Tc and ^{187}Re where the GENII values are ~75% higher.

In the base case, the average quantities consumed by the individual were taken from a survey conducted by Yang and Nelson (1990). Then, an average percentage of the diet that came from these food types grown in contaminated soil was assumed in the base case (25%). To estimate uncertainty, the percentage was varied with bounding values of 15% and 40%. The dry-to-wet ratio variability was taken as ±10% of the base case value. Using this approach, the maximum and minimum variability due to these parameters is a factor of about 2.

Uncertainty in the value of the soil-to-plant transfer factors is determined by comparing the variability of radionuclide values from two data sets (Kennedy and Strenge 1992 [NUREG/CR-5512] and Baes et al. 1984 [ORNL]). Tables are provided in Appendix C. These databases are used because they are cohesive sets of data and because truly site-specific data does not exist for the most part. The variability in these values between the two data sets is radionuclide specific. A comparison of the effects of variability in selected soil-to-plant transfer factors between the two data sets is shown in Table 4-10. With the exception of ^{209}Po and ^{60}Co, the uncertainty in estimated

Table 4-9. Ratios of GENII and EPA Internal Dose Factors to DOE Internal Dose Factors.

Nuclide	Inhalation		Ingestion	
	GENII	EPA	GENII	EPA
Be-10			1.11	1.11
Co-60	1.34	1.46		
Se-79		1.11		
Sr-90	0.89			
Nb-94	1.18	1.26	1.42	1.40
Tc-99	1.20	1.11	1.72	1.12
Sn-121m	1.27	1.28	1.12	1.13
Sn-126	1.33	1.34	1.15	1.15
I-129	0.84		0.89	
Ba-133		1.13		
Sm-151			1.14	1.14
Re-187	1.20	1.11	1.75	1.15
Pb-210	1.11			
Bi-207	1.21	1.43		1.12
Po-209	1.20	1.16	1.20	1.19
Ra-226			0.87	1.20
Ra-228		1.13	0.70	1.20
Th-228	1.11		0.77	
U-238			1.12	
Np-237	1.30		1.35	1.14
Pu-238	0.85	0.85	0.84	0.84
Pu-239	0.85	0.84	0.83	0.82
Pu-240	0.85	0.84	0.83	0.82
Pu-241	0.82	0.83	0.79	0.80
Pu-242	0.84	0.86	0.81	0.82
Pu-244	0.84	0.84	0.83	0.83
Am-241	0.85	0.85	0.81	0.81
Am-242m	0.81	0.82	0.83	0.84
Am-243	0.85	0.85	0.81	0.80
Cm-243	0.88	0.88	0.87	0.87
Cm-244			0.87	0.88
Cm-245	0.84	0.84	0.82	0.83
Cm-246	0.84	0.84	0.83	0.82
Cm-247	0.86	0.85	0.84	0.83
Cm-248	0.86	0.87	0.84	0.85

Note: Differences <10% are not shown.

Table 4-10. Ratio of Pathway Doses for NUREG/CR-5512 and ORNL-5786 Parameters.

Nuclide	Soil Ing	Root Up	Rain Sp	Totals
Cl-36	1.51	1.30	1.30	1.30
Co-60		4.13		
Ni-59		1.27		
Ni-63		1.27		1.24
Sr-90		1.60		1.57
Tc-99	0.55	1.41	0.67	1.41
I-129	0.78	0.71	0.87	0.72
Cs-135		3.19		2.82
Cs-137		3.19		
Pb-210		0.44		0.65
Po-209		10.59		1.65
Ra-226		0.55		
Ra-228		3.78		
Th-228		4.15		
Th-229		4.15		
Th-230		0.60		
Th-232		3.82		
U-232		2.57		
U-233		2.56		
U-234		2.54		1.11
U-235		2.44		
U-236		2.54		1.12
U-238		2.54		
Np-237		0.58		0.84
Pu-238		2.23		
Pu-239		2.22		
Pu-240		2.22		
Pu-241		0.59		
Pu-242		2.22		
Pu-244		2.22		
Am-241		0.59		
Am-242m		0.77		
Am-243		0.59		
Cm-243		2.17		
Cm-244		2.22		
Cm-246		2.30		
Cm-247		2.30		
Cm-248		2.30		

Note: Values less than 10% are not shown. Ratios are obtained by dividing NUREG/CR-5512 doses by the ORNL-5786 doses. Intruder Garden scenario doses at 300 yr are used. Soil leaching is included.

dose due to differences in soil-to-plant transfer parameter values is a factor of 3 or less. Since we are considering uncertainty to the base case where the NUREG/CR-5512 values are assumed, the maximum increase resulting from the ORNL values in the dose estimates is a factor of about 2 for ^{210}Pb. A maximum decrease in dose estimate would be a factor of about 10 for ^{209}Po.

The overall potential changes in dose resulting from parameter variability can be estimated by taking the product of the factors for each of the major parameters (soil dilution factor, dry-to-wet ratio, quantity of food consumed, soil-to-plant transfer value). Thus, depending on the radionuclide, a potential relative increase or decrease in dose in the postexcavation scenario is estimated to be up to a factor of 18 and 90, respectively. Similarly, a potential relative increase in dose in the postdrilling scenario is calculated to be up to a factor of 18 or a potential relative decrease in dose by a factor of up to 3,400.

4.1.3.3 Inhalation Parameter Uncertainty Analysis. The mass of consumed dust is calculated on the basis of time spent in the presence of dust, the concentrations of dust in the air, and the breathing rate (see Section 3.1.2). The base case calculation assumes that the exposed individual is at the home site about 70% of the time. To make an estimate of bounding values, it is assumed that the individual is at the site 60% and 80% of the time and that relative times at different activities, air concentrations, and breathing rates are the same in each case. It is assumed that the breathing rates vary by 10% and dust concentration in the air varies by a factor of 2. Given these assumptions, the relative change in dust mass consumed is calculated to be a factor of about 2.6 increase or decrease relative to the base case.

To evaluate uncertainty in dose conversion factors, three sources of factors were compared (Table 4-9). These include the GENII data base, DOE/EH-0071 (DOE 1988) and the EPA Federal Guidance Report Number 11 (EPA 1988). Comparison of inhalation values shows a difference of no more than a factor of 1.46 higher (for ^{60}Co) or a factor of 1.24 lower (for ^{242m}Am) for all the radionuclides considered.

The overall estimated potential change or uncertainty in dose from all factors combined (soil dilution factor, mass of dust consumed, dose conversion factor) is an increase or decrease by a factor of up to about 8 for the postexcavation scenario. For the postdrilling scenario, the overall calculated change in dose from all factors combined is an increase by a factor of up to about 8 and a decrease by a factor of up to about 750.

4.1.3.4 External Exposure Parameter Uncertainty Analysis. As with the inhalation pathway, it is assumed in the base case that the individual is exposed about 70% of the time with two-thirds of the time spent outdoors and one-third of the time indoors. A shielding factor is applied to time indoors because of the structural barriers to radiation provided by the dwelling.

To estimate bounding values, both percentage of time and the value of the shielding factor can be varied. For this pathway, no variability in the dose conversion factor is assumed. For exposure time, it is assumed that the individual is exposed 60% or 80% of the time. A range of shielding values is referenced by Aaberg and Kennedy (1990) from 0.02 to 0.6. A lower effective exposure time is, therefore, calculated by assuming the 60% exposure time at

the same indoor/outdoor proportion as the base case and the lower shielding factor. The higher effective exposure time was calculated using the higher values. At 60% and 80% exposure time, the relative change in dose resulting from the changes in effective exposure time is a factor of 2 decrease and a factor of 1.5 increase, relative to the base case. The overall estimated potential change in dose from all factors combined is an increase by a factor of about 3 or decrease by a factor of about 4 for the postexcavation scenario. For the postdrilling scenario, the overall calculated change in dose from all factors combined is an increase by a factor of about 3 or a decrease by a factor of about 34.

4.1.3.5 Summary of Uncertainty Analysis. The uncertainty factors are directly proportioned to the dose calculations. Thus, the relative range of dose estimates around the base case estimates can be quantified using the uncertainty factors. Overall, this analysis indicates that doses will not exceed the base case assumptions by more than a factor of 20 and could be less than a factor at 3000, depending on the radionuclide and the dominant pathway.

4.2 ANALYTICAL RESULTS FOR THE GROUNDWATER PATHWAYS SCENARIOS

In this section, the results of the modeling calculations to quantify radionuclide release and transport processes are described. In the first major section (4.2.1), the groundwater radionuclide concentration versus time relationships are described for Category 1 and 3 waste facility conditions. The results (radionuclide groundwater concentrations as a function of time) are presented at the key boundaries along the pathway from the disposal facility to the unconfined aquifer. The second major section (4.2.2) describes the results of sensitivity analyses used to determine the influence of various key parameters on groundwater concentrations. As it turns out, the results of the sensitivity analyses allow us to eliminate the majority of radionuclides as potential contributors to dose by the groundwater pathway. Therefore, in Section 4.2.3, the screening process to eliminate radionuclides of concern is described and those remaining radionuclides of concern are identified. In Section 4.2.4, dose estimates are then presented for the remainder of the radionuclides for Category 1 and Category 3 waste disposal facilities. In Section 4.2.5, uncertainties associated with the groundwater concentration estimates for the remaining radionuclides are described.

4.2.1 Peak Time and Concentration Results from the Release and Transport Analyses

In this section, the results of the radionuclide release and transport calculations are presented for the base case conditions described previously for the Category 1 and Category 3 waste disposal facilities. The results are broken into the major aspects of release and transport, beginning with radionuclide flux from the disposal facility or source term (Section 4.2.1.1), followed by radionuclide flux to the unconfined aquifer and down to the 100-m downstream well (Section 4.2.1.2). Specific radionuclides are not considered in these sections. Instead, typical characteristics of radionuclide behavior are simulated to which individual radionuclides can be assigned. The relationship of the results to specific radionuclides is provided in

Section 4.2.3 where the potential contribution of individual radionuclides to dose by the groundwater pathway is evaluated.

4.2.1.1 Source Term Analysis for Base Case Conditions. To calculate radionuclide flux from the disposal facility, it is necessary to consider the flux of infiltrating water through the disposal facility and the mechanism of release from the waste material or the waste form. For the Category 1 facility, an average steady state flux of 5.0 cm/yr is assumed which establishes a steady-state flow field.

Figures 4-1 and 4-2 illustrate this steady-state condition in two ways. Figure 4-1 shows the steady-state saturation conditions in the soil column beneath the trench. Figures 4-2 and 4-3 show the distribution of groundwater velocity vectors in the vadose zone and the unconfined aquifer for the soil column that surrounds and underlies the disposal trench. These vector plots show the direction and magnitude of the water flow at every node in the model. The spacing of the arrows reflects the spacing of the mesh in the model and the magnitude is indicated by the size of the arrow (note the reference arrow at the top of the figure). In some cases the magnitude of the velocity is large enough that neighboring arrows overlap. There is no special significance to this.

For the Category 1 waste facility, only one mechanism of release was considered. It was assumed that the entire inventory is immediately available for release with the initial inventory of 1.0 Ci of any given radionuclide evenly distributed in the disposal facility. A simple mixing-cell calculation (using a recharge of 5.0 cm/yr) was then performed to establish a release rate from the facility to the underlying soil. This release rate is shown in Figure 4-4 where it is expressed as both flux and concentration (flux is equal to the recharge rate times the area times the concentration). Neither sorption effects nor decay are factored into these calculations. These effects are considered in the groundwater concentration versus time results. The release curve shows a maximum flux of about 0.086 Ci/yr at 0.0 yr, followed by a decrease in flux as the inventory is depleted. The area under the curve is the total initial inventory of 1.0 Ci and the entire inventory has been released from the facility within 25.0 yr. The time required to deplete the inventory completely is dependent on the rate of infiltration.

Calculation of radionuclide flux from the Category 3 facility is completed in a similar fashion except that a lower infiltration rate is assumed (0.5 cm/yr) and additional radionuclide release mechanisms are considered to account for the assumption that waste form performance may be utilized for certain waste streams.

Figure 4-5 depicts the steady-state saturation conditions for this infiltration rate and the steady-state groundwater velocity distribution of steady-state groundwater velocities in the vadose zone is shown in Figure 4-6. The velocities in the unconfined aquifer are essentially unaffected by the change in infiltration rate.

Three release mechanisms are considered for the Category 3 waste. The first is the same as above and assumes instantaneous release. The radionuclide flux curve assuming the infiltration rate of 0.5 cm/yr is shown in Figure 4-7. The influence of the decreased infiltration rate relative to

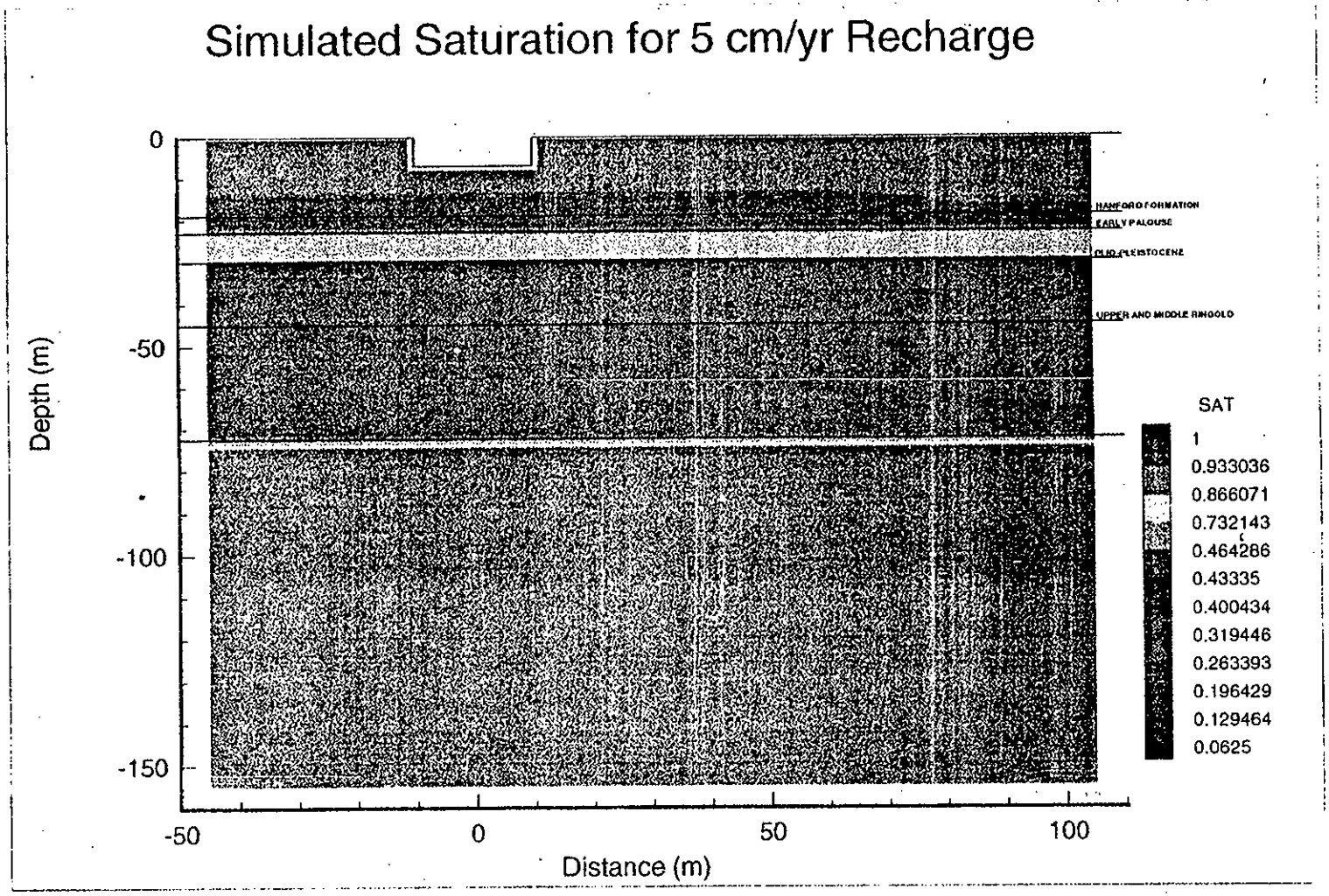

Figure 4-1. Saturation Contours for 5 cm/yr Recharge.

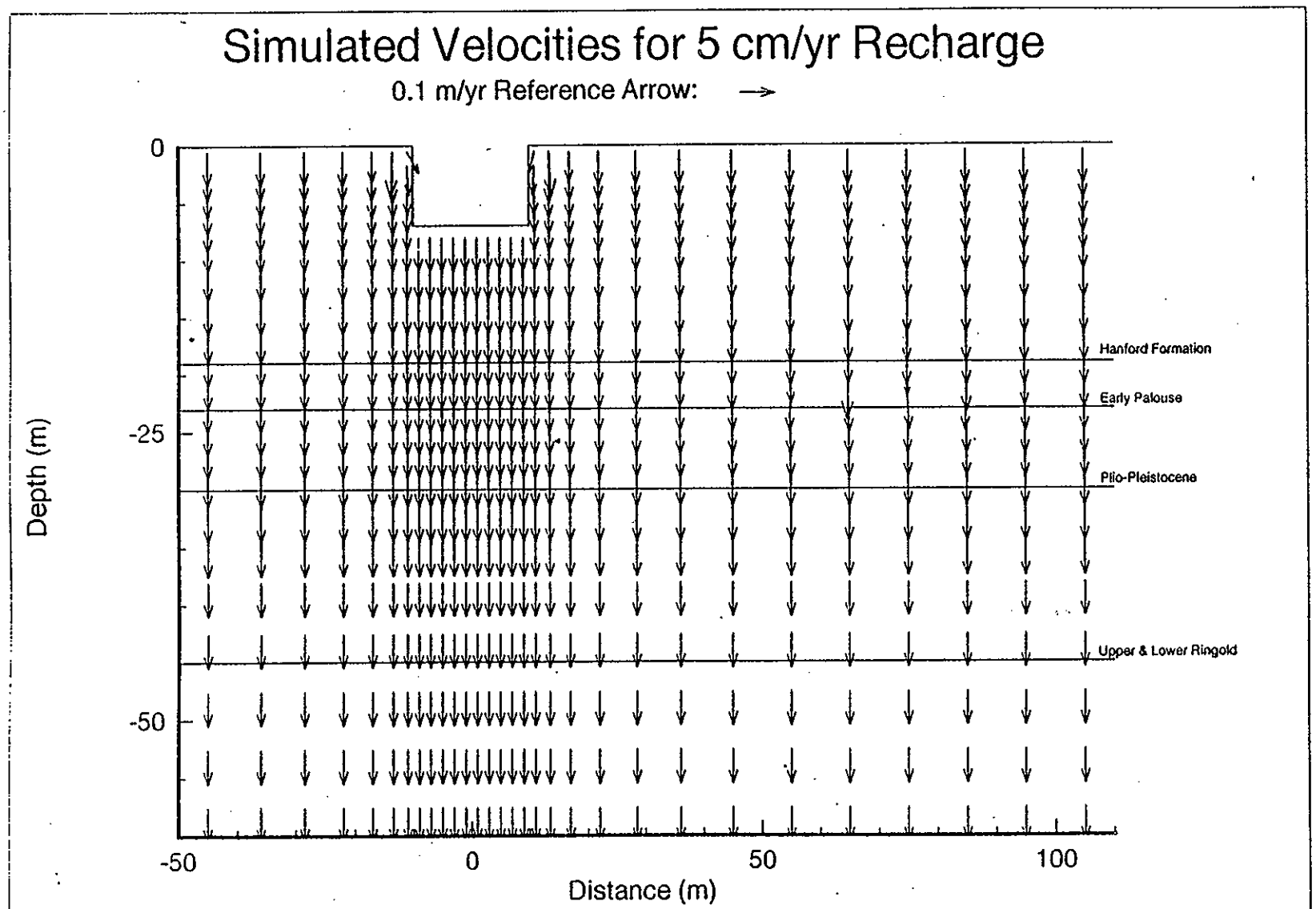

Figure 4-2. Velocity Plots for 5 cm/yr Recharge (Vadose Zone Blow-Up).

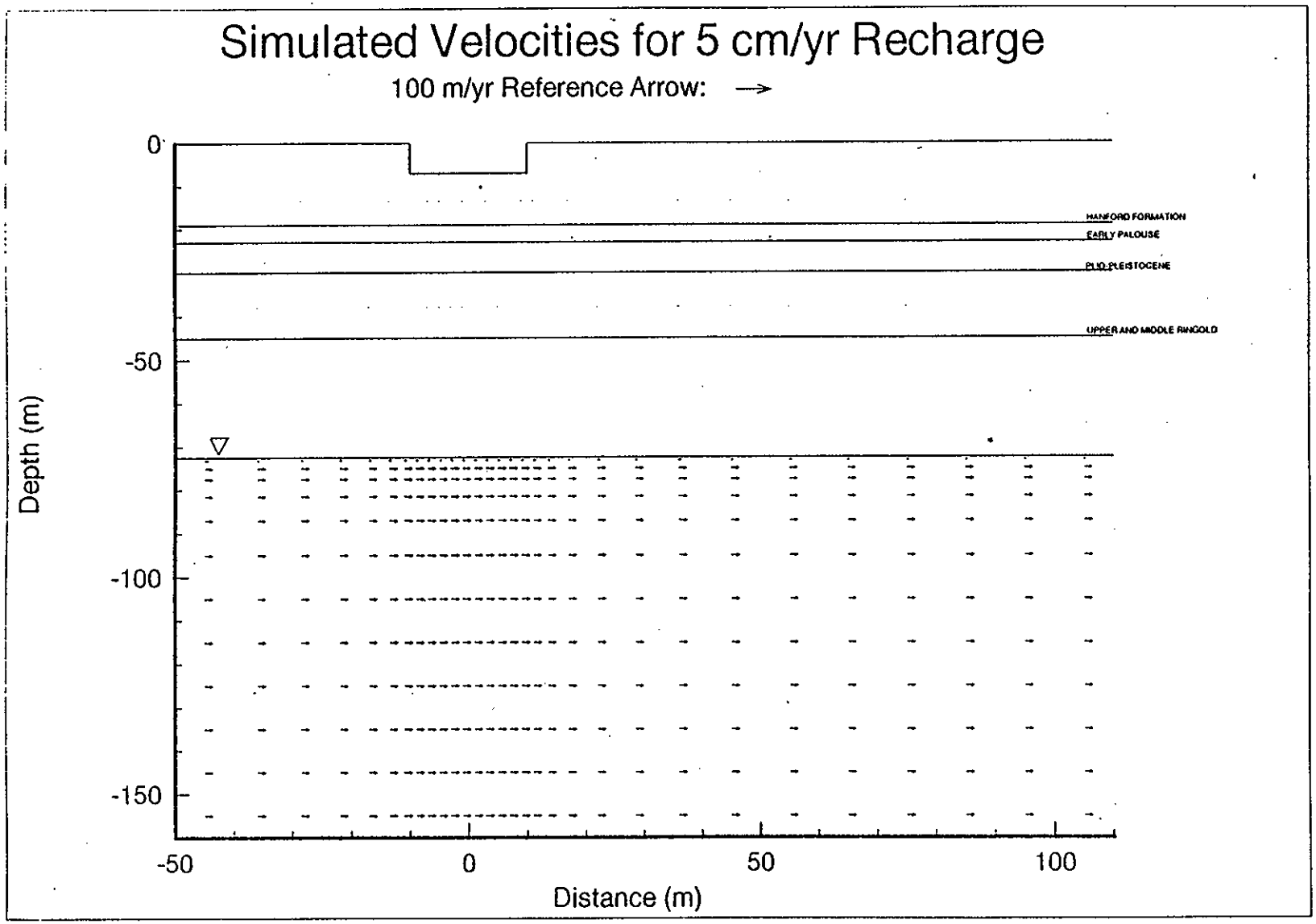

Figure 4-3. Velocity Plots for 5 cm/yr Recharge (Full Simulation Field).

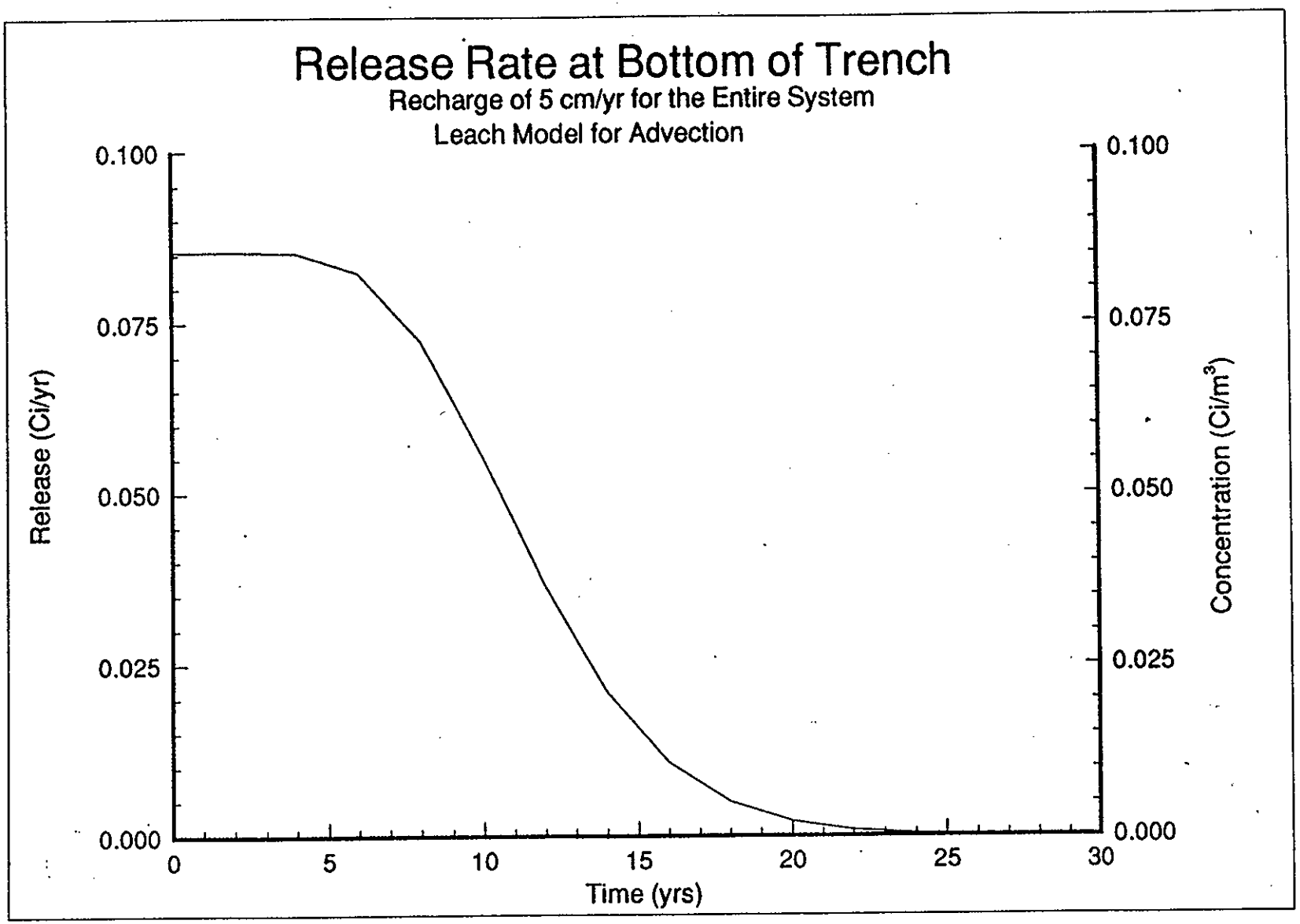

Figure 4-4. Release History for 5 cm/yr Recharge, Advection Dominated.

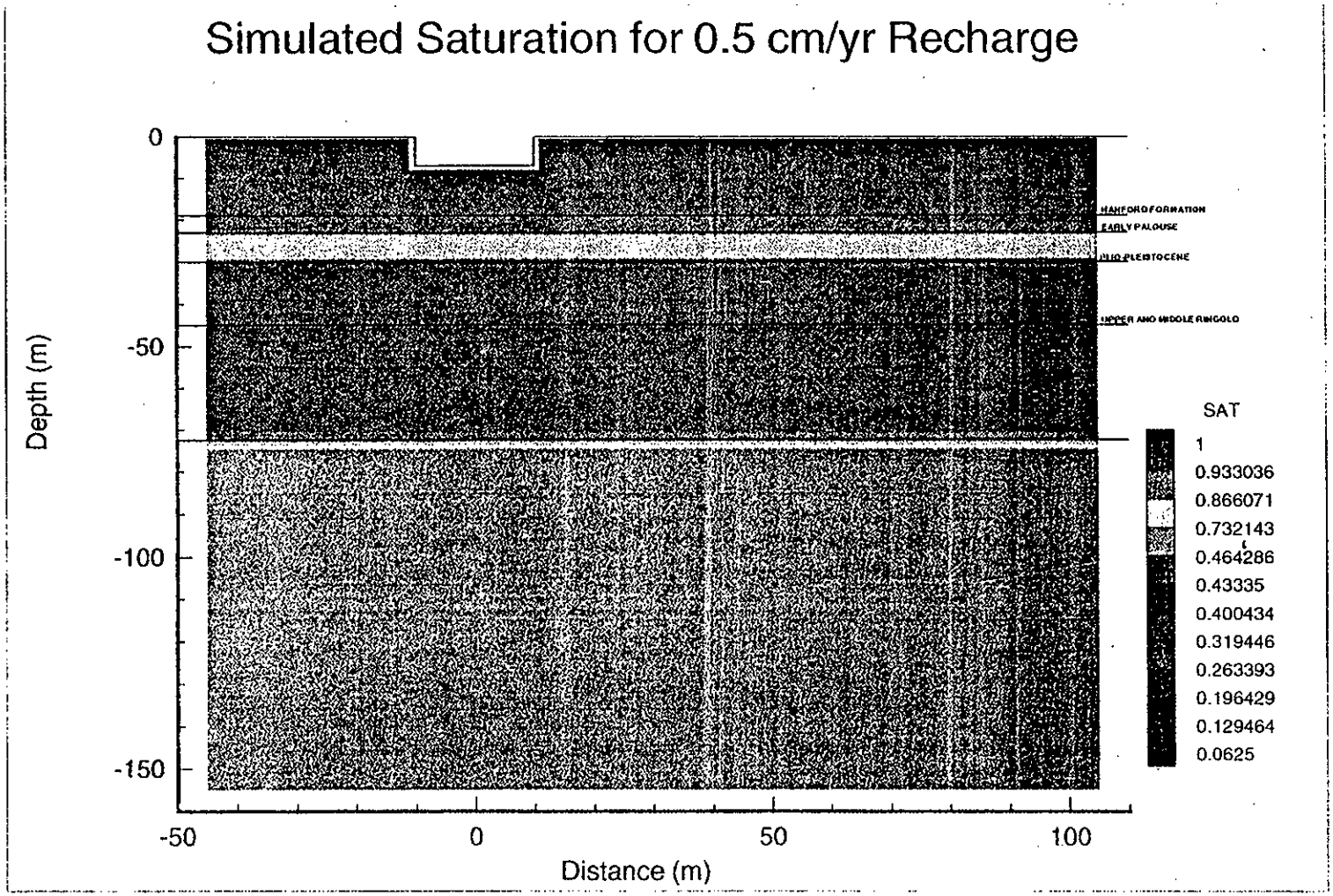

Figure 4-5. Saturation Contours for 0.5 cm/yr Recharge.

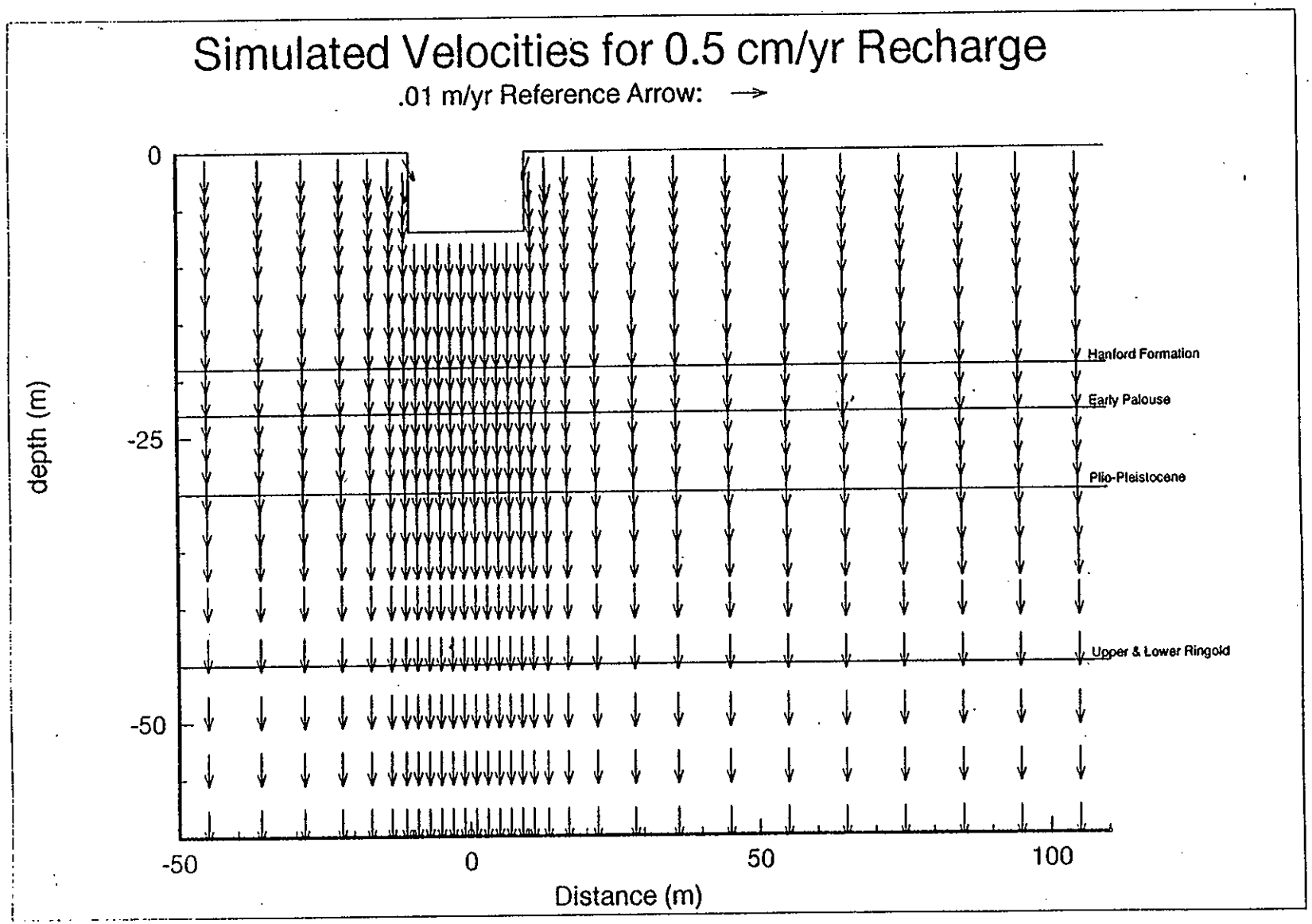

Figure 4-6. Velocity Plots for 0.5 cm/yr Recharge (Vadose Zone Blow-Up).

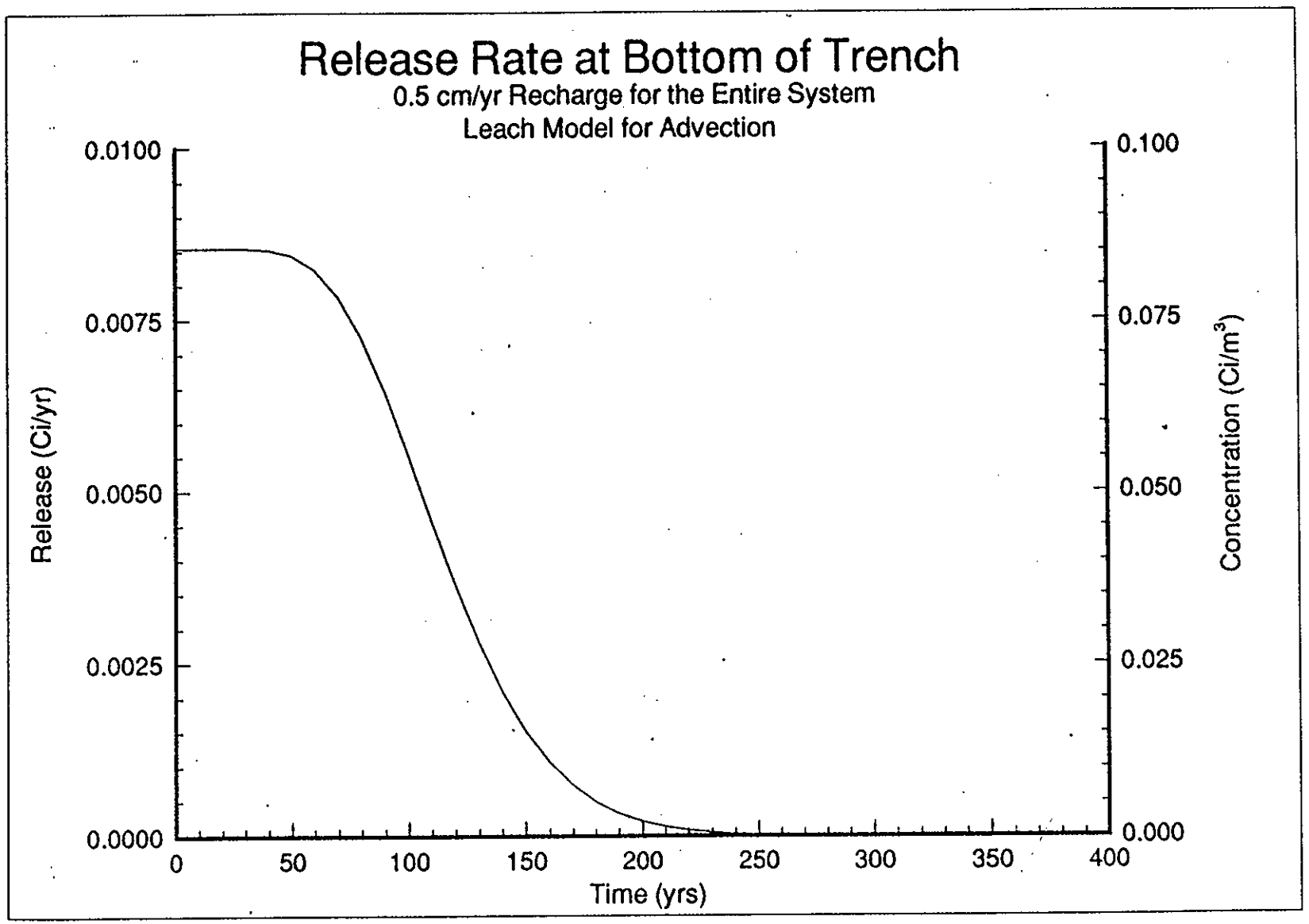

Figure 4-7. Release History for 0.5 cm/yr Recharge, Advection Dominated.

the Category 1 condition (Figure 4-4) is apparent. The shape of the release curve remains the same, but the maximum release rate is about 8.5 x 10^{-3} Ci/yr and release is not completed until about 250 yr have elapsed.

The additional release mechanisms are invoked when waste form performance is assumed. The first mechanism is diffusional control of radionuclide release by the waste form. A grout waste form is being considered primarily, but the analysis can be applied to any waste matrix by assuming the appropriate diffusion value. The release rate history assuming a diffusion coefficient of 10^{-8} cm^2/s is shown in Figure 4-8. This value is typically generated for an inert element encapsulated in an average permeability grout. As with the previous case, a total inventory of 1 Ci is assumed. Comparison of this release curve with the advection controlled release shown in Figures 4-4 and 4-7 show that the maximum flux is about 0.05 Ci/yr and about 900 yr are required to exhaust the 1 Ci inventory.

The final mechanism is a constant concentration release model that is used to simulate solubility control. In this case, an unlimited initial inventory is assumed but the concentration in solution is constant and controlled by the solubility reaction. In this analysis, a steady-state concentration of 1 Ci/m^3 is assumed. Thus, a constant flux occurs indefinitely.

4.2.1.2 Release And Transport Analysis for Base Case Conditions. Once the radionuclides are released into the soil column, transport to the unconfined aquifer is estimated. An additional parameter, the sorption coefficient, must be included in the analysis to evaluate the variability in reactivity of radionuclides under consideration with the soil phases. The Kd values considered in these base case analyses are 0, 1, 10, and 100 mL/g, representing radionuclides that are nonsorbing, weakly sorbing, moderately sorbing and strongly sorbing elements, respectively.

The contaminant behavior in the soil column is represented in two ways. First, cross-sections of the contaminant plumes in the soil column underlying the trench are presented for the given conditions at one point in time subsequent to release from the trench. Times are picked where the radionuclide concentrations in the unconfined aquifer are near peak value. Second, radionuclide concentration versus time graphs are presented for groundwater that intercepts a well penetrating the unconfined aquifer 100 m downstream from the edge of the trench. The estimated peak concentration and times at which peak concentration occur are used to identify radionuclides that cannot provide significant dose and to quantify inventory limits for radionuclides that can provide significant dose.

A few concentration values were also evaluated at the vadose zone adjacent to the unconfined aquifer as a point of comparison with concentrations at the trench-soil column interface and the downstream well. As a point of comparison for the final release values, a few intermediate values were also analyzed. Figures 4-4 and 4-7 show the release curves for the contaminants leaving the facility, for the 5 cm/yr and 0.5 cm/yr base cases. In both cases the peak concentration is about 0.085 Ci/m^3.

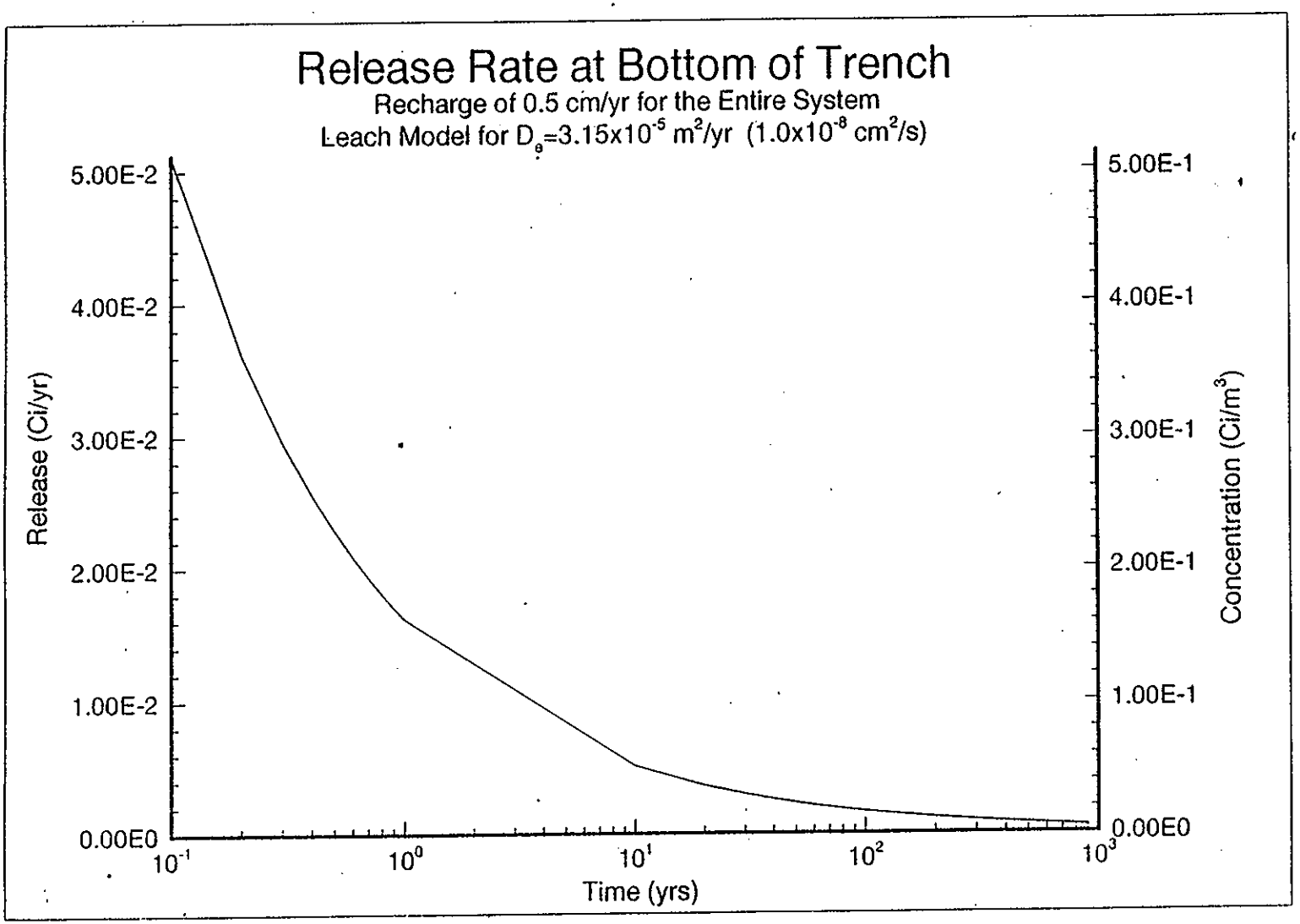

Figure 4-8. Release History for 0.5 cm/yr Recharge, Diffusion with D_e = 3.15 x 10^{-5} m^2/yr (1 x 10^{-8} cm^2/s).

Immediately above the aquifer, on a vertical line through the center of the trench, the 5 cm/yr case had a peak concentration of 7.94×10^{-3} Ci/m^3 while the 0.5 cm/yr case had a value of 9.18×10^{-3} Ci/m^3. In the aquifer the peak value for the high recharge case was 7.37×10^{-4} Ci/m^3 and for the low recharge case it was 9.16×10^{-5} Ci/m^3.

4.2.1.2.1 Peak Concentration Estimates for a Category 1 Waste Disposal Facility. The release and transport results for the Category 1 disposal facility conditions are shown in Figures 4-9 and 4-10. Some significant aspects of the soil column hydrologic characteristics are shown in Figure 4-9. First, little dispersion is assumed in the analysis as shown by the minimal spreading of the plume beyond the vertical boundaries of the trench until the plume reaches the aquifer and the minimal spreading of the plume in the aquifer. Second, the right-angle shape of the plume clearly demonstrates the change in direction of flow from vertical to horizontal in the vadose zone and the unconfined aquifer. Third, the concentration contour lines show a significant increase in dilution of radionuclide concentration brought about by mixing vadose bearing water with fresh water in the unconfined aquifer. These characteristics are present for all sets of conditions considered in this analysis. Additional figures of plume cross-sections are shown in Appendix D for other sets of analytical conditions. In the remainder of the modeling runs discussed in this chapter, results will be presented in terms of well water concentrations versus time (e.g., Figure 4-10).

In Figure 4-10, groundwater radionuclide concentrations rise to a peak and then decrease to zero as the inventory plume passes the interception point with the well. The conditions in the four subfigures are identical with the exception that a different Kd value is assumed in each one. Although the shape of the concentration curves are identical, the time over which the plume occurs shifts farther into the future with increasing Kd value, reflecting the increasing retardation of transport relative to groundwater flux with increasing reactivity between the radionuclide and the soil. Similarly, as the time of transport is increased and larger quantities of water interact with the radionuclide over time, a reduction in groundwater concentration occurs as shown by the reduced peak concentration with increased Kd. It is important to note that both peak times and concentrations are essentially proportional to the change in Kd value (more precisely, the proportionality is related to the retardation coefficient which is unity when Kd = 0, about 16 at Kd = 1, about 150 at Kd = 10, and about 1500 at Kd = 100).

4.2.1.2.2 Peak Concentration Estimates for a Category 3 Waste Disposal Facility. Groundwater versus time concentrations at the 100 m well for Category 3 disposal conditions (infiltration rate = 0.5 cm/yr) are shown for the three release mechanisms, advection control, diffusion control, and solubility control. A comparison of results among the different release mechanisms and with the Category 1 advection control result brings up some key points that are discussed in more detail in the sensitivity section (4.2.2.2), for example:

1. The shape of the groundwater concentration curves are the same for the advection control and diffusion control release mechanisms (see Figures 4-11 and 4-12). They begin and end over a finite period of time. The shape of the solubility control curve approaches a steady-state condition and levels off. This difference reflects the initial assumption of a finite inventory in the advection and diffusion cases and an infinite inventory in the solubility case.

Figure 4-9a. Plume Cross-Section for Cases 1a and 1b.

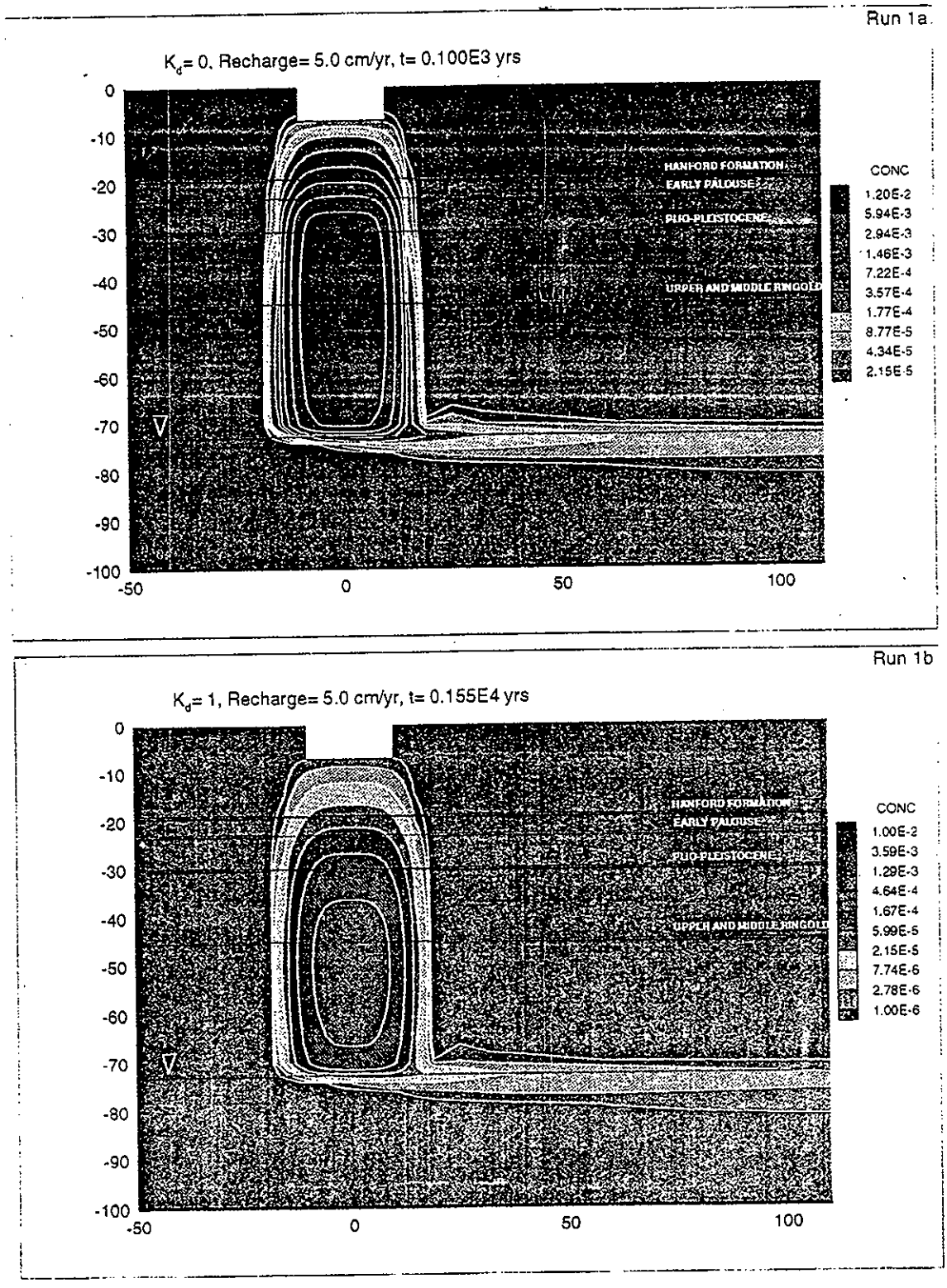

2. When solubility control with an unlimited source is assumed, the sorption of the element in the soil column has no influence on the peak steady-state concentration (Figure 4-13). However, the time required to reach the maximum steady-state concentration is almost linearly proportional to Kd values assumed.

3. In most cases, the infiltration rate and sorption values appear to be the dominant parameters controlling groundwater concentration versus time relationships when either advection control or diffusion control release mechanisms are assumed. Peak concentrations are inversely proportional to Kd and proportional to infiltration rate. Times of peak concentrations are nearly linearly proportional to changes in Kd values and inversely proportional to infiltration rates. For example, the 2b (Figure 4-11) and the 2h (Figure 4-12) curves are essentially identical. This indicates that the assumption of advection or diffusion control of release is immaterial to the outcome.

4. An exception to the previous observation occurs when diffusion is low (less than or equal to 10^{-8} cm^2/s) and no sorption is assumed in the soil column under the facility (Kd = 0 mL/g). In this case, diffusion control versus advection control is significant. Comparison of Runs 2a (Figure 4-11) and 2g (Figure 4-12) show that the diffusion control reduces the peak concentration by one-third even though the infiltration rate is identical. Another way of stating this observation is that the release rate controls groundwater concentrations rather than the infiltration rate. Once diffusion control of the release rate is established, the peak concentration decreases by a factor of the $\sqrt{10}$ (about 3.1) for every order of magnitude decrease in the assumed diffusion coefficient.

To further clarify these observations, additional sensitivity cases have been run. These are discussed in the next section.

4.2.2 Sensitivity Analyses for the Groundwater Pathway

The sensitivity analyses in this section have been developed for two purposes. First, it is necessary to understand more clearly which parameters have the dominant effect on the contaminant transport for a given set of conditions. Second, it is necessary to understand the sensitivity of the results to parameter variability. The following discussion is organized according to those parameters affecting the source term, followed by those affecting the transport through the soil column. The sensitivity analyses are conducted exactly as the base case calculations except for changes in the parameter values of interest. Interpretation of sensitivity analysis results is based on a comparison of peak concentrations and occasionally the time at which peak concentrations occur.

Figure 4-9b. Plume Cross-Section for Cases 1c and 1k.

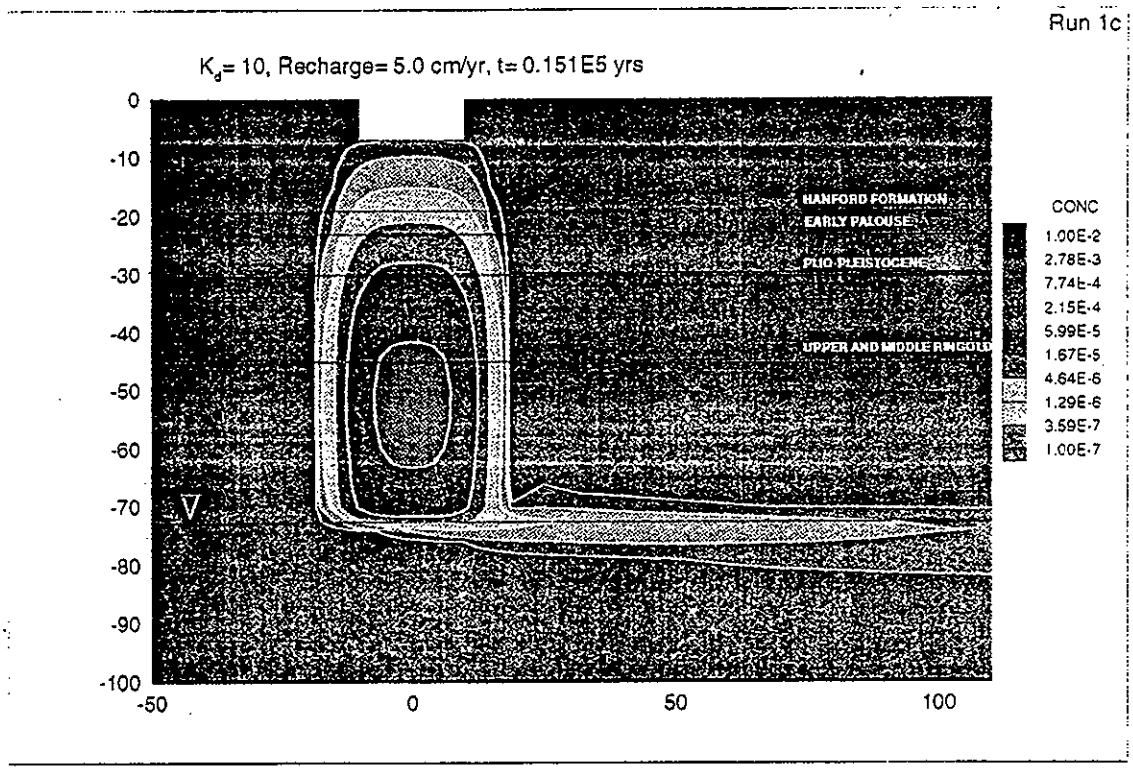

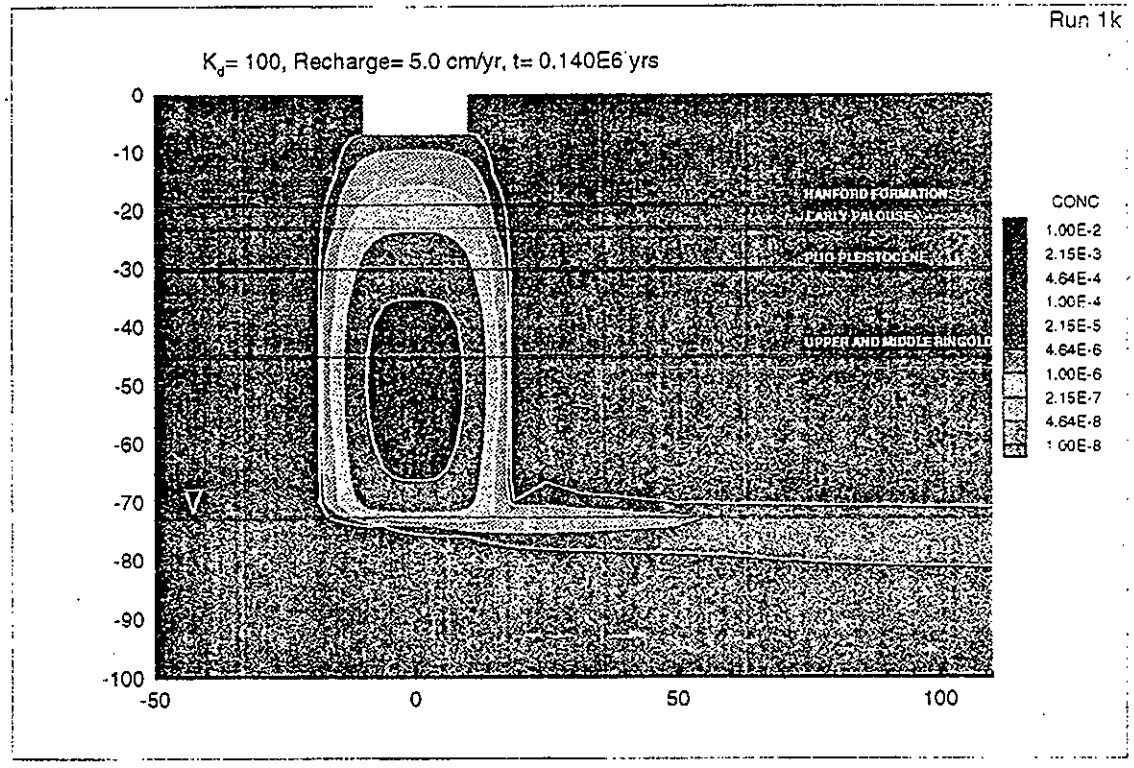

Peak Concentration At The 100m Downstream Well

Recharge Of 5 cm/yr For The Entire System

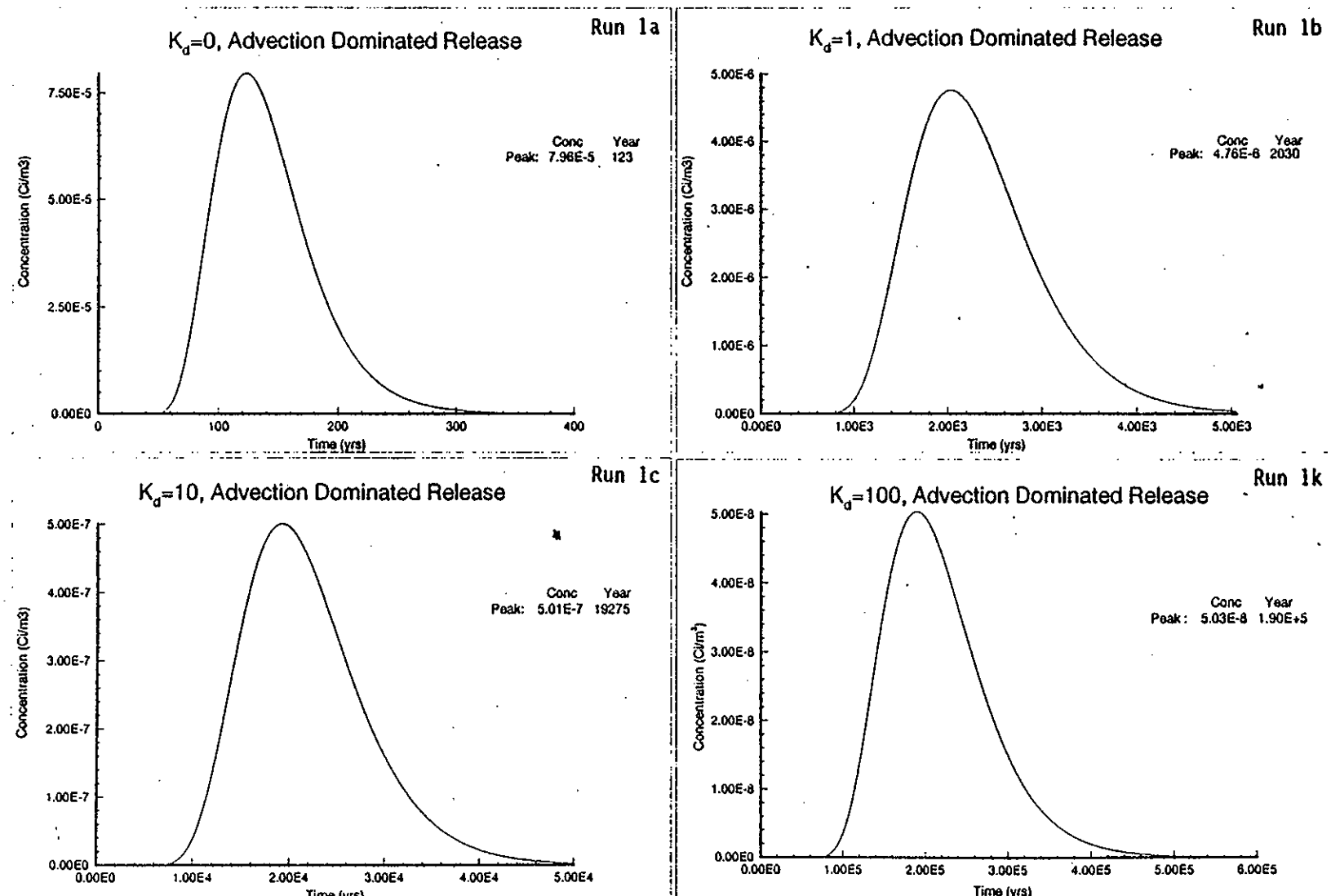

Figure 4-10. Radionuclide Concentrations at the 100-m Well Assuming Advective Release for Category 1 Conditions.

Peak Concentration At The 100m Downstream Well

Recharge Of 0.5 cm/yr For The Entire System

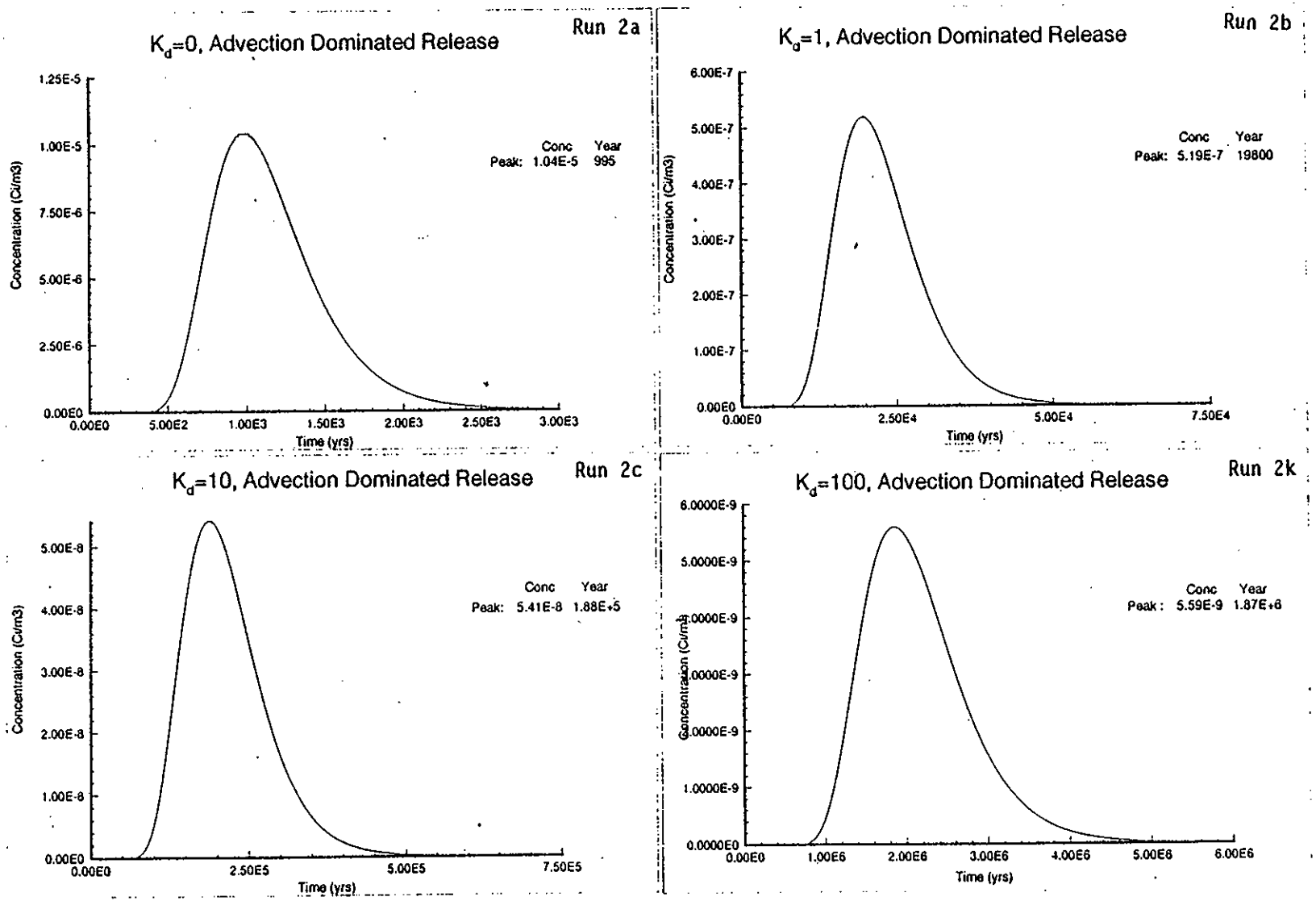

Figure 4-11. Radionuclide Concentrations at the 100-m Well Assuming Advective Release for Category 3 Conditions.

Figure 4-12. Radionuclide Concentrations at the 100-m Well Assuming Diffusional Release for Category 3 Conditions.

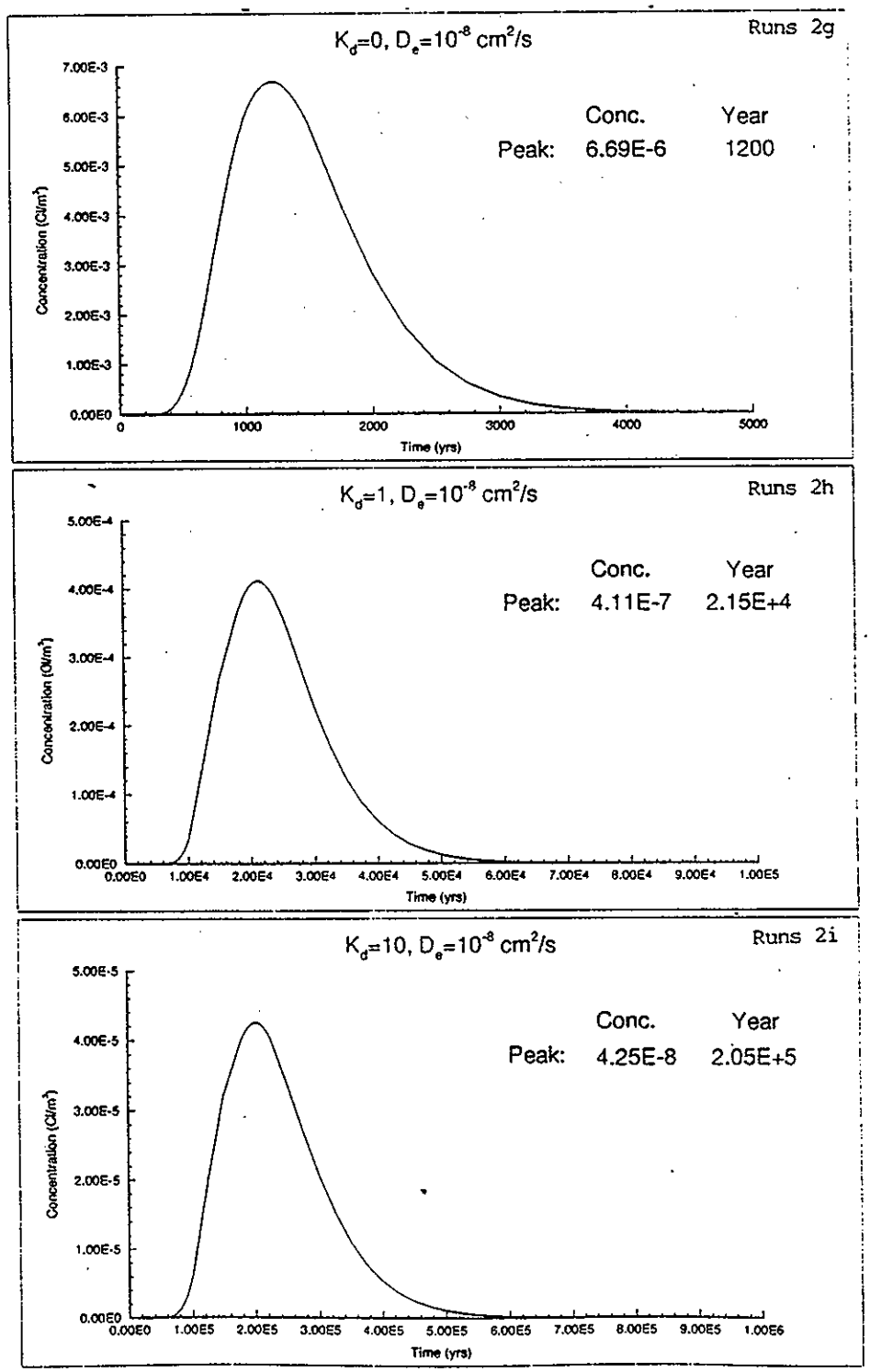

Figure 4-13. Radionuclide Concentrations at the 100-m Well Assuming Solubility Controlled Release for Category 3 Conditions.

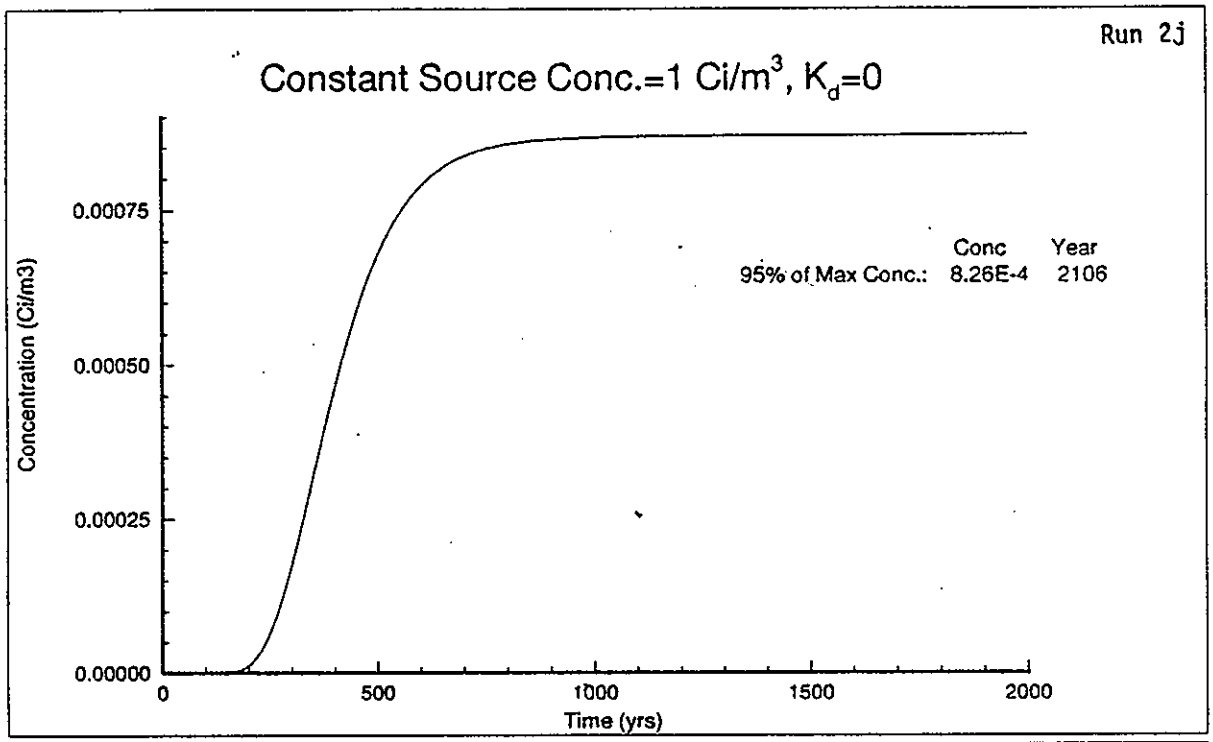

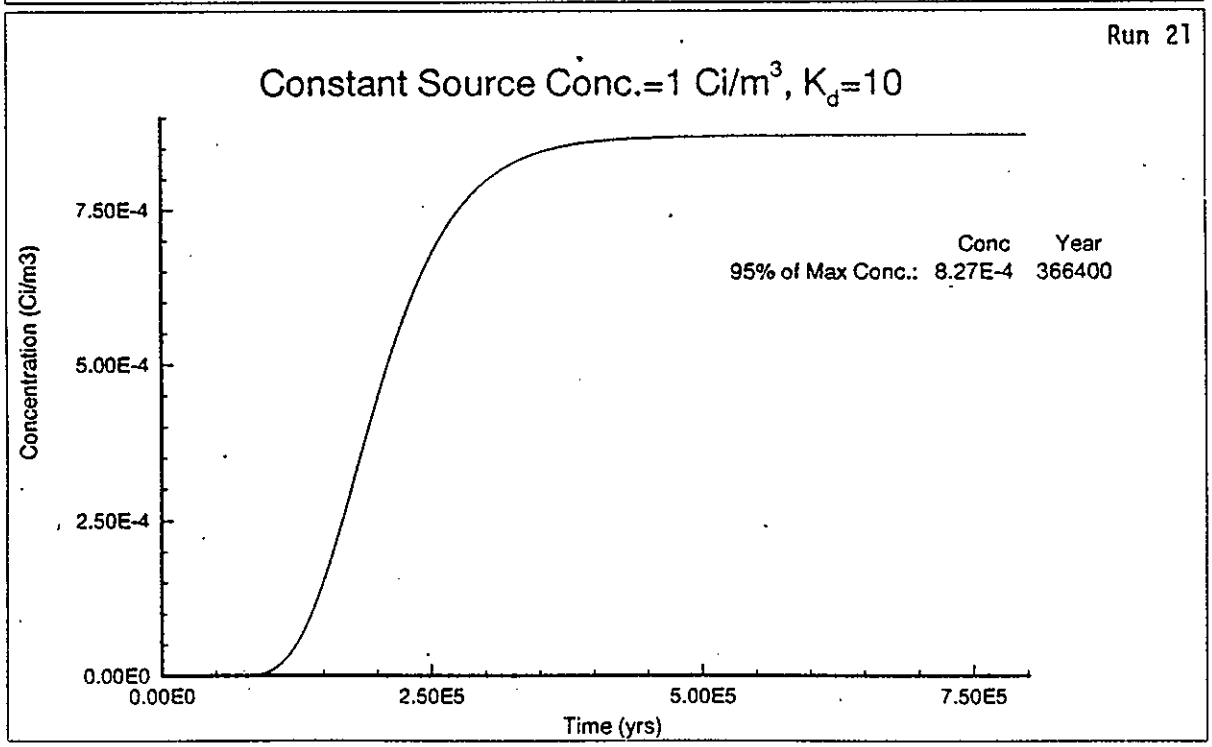

4.2.2.1 Sensitivity of Peak Concentration to Release Mechanism Versus Infiltration Rate. In this section, the relative influence of release rate assumptions (diffusional control and solubility control) versus infiltration rate assumptions are evaluated. To consider diffusion control versus infiltration, diffusion coefficients in the range of 1×10^{-6} to 1×10^{-12} cm^2/s and infiltration rates of 5 to 0.5 cm/yr were assumed for different modeling runs. As we noted in Section 4.2.1.3, the diffusion coefficient was only shown to be of significance at Kd = 0. Therefore, the cases being compared here assume no sorption in the soil column.

In Table 4-11, cases labeled 1 and 2 denote infiltration rates of 5 and 0.5 cm/r, respectively. Comparison of peak concentrations between the advection release cases (1a and 2a) and the case with $D = 10^{-6}$ cm^2/s (1d and 2d) shows that the results are essentially identical and a seven-fold decrease in peak concentration occurs as a result of the 10-fold decrease in infiltration rate. By contrast, at diffusion coefficients of $\leq 10^{-8} cm^2/s$, the peak concentration decreases by a factor of about 2.5 for a 10-fold decrease in infiltration rate. These results indicate that once the diffusion rate falls below a threshold value, the flux away from the disposal facility and the groundwater concentrations are controlled by a combination of the diffusion rate and the infiltration rate. Under these conditions, the peak concentrations are directly proportional to the diffusional coefficient value. For every order of magnitude decrease in the diffusion rate at a given infiltration rate, the peak concentration decreases by the square root of 10 (about 3X). Also, because the peak release flux from the trench is directly proportional to the area-to-volume ratio at the container (Eq. 3.9 in Section 3.2.2.2), the peak concentration is directly proportional to the area-to-volume ratio.

A comparison of the changes in peak concentrations for the constant concentration or solubility controlled release assumption as a function of changes in infiltration rates is shown in Table 4-12. As expected, the peak concentrations are controlled by the diluting effects of the soil column and the infiltration rate as demonstrated by the change in peak concentration between cases 1j and 2j or 1l and 2l. The peak concentration drops by a factor of about 9 which is consistent with the relative change in the advection control cases where a drop in peak concentration is a factor of about 8 (Cases 1a and 1b in Table 4-11). These factors are comparable to the assumed 10-fold differential change in infiltration rate in the paired cases.

4.2.2.2 Sensitivity Analysis of Differential Infiltration Rates of the Disposal Facility Cover and Surrounding Area. The assumption of minimal dispersion in the flow and transport calculations results in very little spreading of the contaminant plumes beyond the borders of the trench facility. This observation suggests that the infiltration rate allowed by the cover should have a greater influence over the peak concentration than the infiltration rate assumed in the surrounding area. This is an important hypothesis when considering the potential for increased infiltration resulting from large-scale irrigation and the need for a low permeability cover.

Table 4-11. Comparison of Advection and Diffusion Dominated Release Model, with De=10^{-6}, 10^{-8}, 10^{-9}, 10^{-10}, 10^{-12} cm^2/s.

Run number	Inventory depletion period (yr)	Peak concentration (Ci/m^3)	Time to peak concentration (yr)
Advection			
1a	25	7.96 E-5	123
2a	250	1.01 E-5	995
$D_e=10^{-6}$ cm^2/s			
1d	8.5	6.56 E-5	135
2d	8.5	9.42 E-6	1,024
$D_e=10^{-8}$ cm^2/s			
1g	900	1.7 E-5	150
2g	900	6.69 E-6	1,250
$D_e=10^{-9}$ cm^2/s			
1m	1.0 E+4	5.1 E-6	150
2m	1.0 E+4	2.0 E-6	1,250
$D_e=10^{-10}$ cm^2/s			
1n	1.0 E+5	1.6 E-6	150
2n	1.0 E+5	6.43 E-7	1,250
$D_e=10^{-12}$ cm^2/s			
1p	9.0 E+6	1.6 E-7	150
2p	9.0 E+6	6.4 E-8	1,250

Table 4-12. Comparison of Steady-State (Solubility Control) Release Rate and Infiltration Rate Effects on Peak Concentrations.

Run number	Recharge (cm/yr)	K_d	95% of maximum concentration year	Concentration (Ci/m^3)
1j	5.0	0	207	0.0076
1l	5.0	10	3.28 E+4	0.0076
2j	0.5	0	2,110	8.26 E-4
2l	0.5	10	3.66 E+5	8.27 E-4
3j	5.0 and 3.0	0	273	0.005
3l	5.0 and 3.0	10	4.38 E+4	0.005

To investigate these relationships, several cases were run using differential infiltration rates where the dominant parameter was concluded to be infiltration rates rather than diffusional release rate as discussed in the previous section. For the solubility case (Table 4-12), a cover and surrounding soil infiltration rates of 3 and 5 cm/yr were assumed. The same infiltration conditions were also assumed for a case in which the release rate was assumed to be a diffusion rate of 10^{-6} cm^2/s, a rate too large to influence peak concentrations. Two other cases were run for the advection dominated release in which the cover infiltration rate was kept constant at 0.05 cm/yr and the surrounding soil infiltration rate was varied at 0.5 and 5 cm/yr (Table 4-13).

Table 4-13. Effect of Differential Cover and Soil Infiltration Rates on Peak Concentrations.

Run number conc.	Recharge rate (cm/yr)	Cover infiltration (cm/yr)	Inventory depletion period (cm/yr)	Peak conc. (Ci/m^3)	Time to peak (yr)
1a	5	5	25	7.96 E-5	123
2a	0.5	0.5	250	1.04 E-5	995
5a	5	0.05	2,400	6.58 E-6	376
6a	0.5	0.05	2,400	6.09 E-6	1,405

These cases were broken into two sets, one where the source term was solubility controlled and one where the source term was advection controlled. The peak concentrations of these cases were compared with peak concentrations of cases with the same source term assumptions and undifferentiated infiltration rates between facility cover and surrounding soil. The infiltration rate of the surrounding soil has minimal influence on the peak concentration. This conclusion is supported by the data in Table 4-13 where the surrounding soil infiltration rate changes by a factor of 10 but the peak concentration changes by less than 10%. It should be noted that the time of the peak concentration is heavily dependent on the soil infiltration rate.

4.2.2.3 Sensitivity Analyses of Other Natural Parameters Affecting Radionuclide Transport. In the base case analysis, a very simple geometric model was used to simulate the natural environment. In this section, sensitivity analyses are described to evaluate the affects of presumed variability in the hydrogeologic system or parameter values on radionuclide concentrations in groundwater. These include (1) increased permeability of saturated soils, (2) decreased hydraulic gradient, (3) variability in the moisture content-permeability relationships in vadose zone soils, and (4) the presence of small vertical high permeability zones (e.g., clastic dikes).

4.2.2.3.1 Peak Concentration Response to Increased Permeability. The saturated permeability values used in the base case analysis for the vadose zone soils and the unconfined aquifer were taken from laboratory measurements. However, hydraulic conductivity field measurements are typically one or two

orders of magnitude higher than laboratory measurements. Therefore, the sensitivity study cases were conducted in which saturated hydraulic conductivity values for all stratigraphic units were increased by a factor of 10.

Four cases (7a, 7c, 8a, 8c) were run with two different recharge values, 5.0 cm/yr and 0.5 cm/yr, and two Kd values, 0 and 10 mL/g. The peak concentrations and times of peak concentration are shown in Table 4-14. Comparison of these results with the base case results (1a, 1c, 2a, 2c) shows a significant decrease in peak concentration has occurred. In fact, the factor of 10 increase in hydraulic conductivity generates peak concentration values that are essentially equivalent to a reduction in the infiltration rate by a factor of 10 (compare the results of Runs 2a with 7a and 2c with 7c).

Table 4-14. Advection-Dominated release, K_{sat} = 10X.

Run number	Recharge rate (cm/yr)	Kd (mL/g)	Inventory depletion period (yr)	Peak concentration (Ci/m^3)	Time to peak concentration (yr)
1a	5.0	0	25	7.96 E-5	123
7a	5.0	0	25	1.04 E-5	100
7c	5.0	10	25	5.46 E-8	1.89 E+4
1c	5.0	10	25	5.11 E-7	1.94 E+4
2a	0.5	0	250	1.04 E-5	995
8a	0.5	0	250	1.21 E-6	850
8c	0.5	10	250	5.48 E-9	1.89 E+5
2c	0.5	10	250	5.41 E-8	1.90 E+5

These results are best explained by the fact that the increased volumetric flow of water in the unconfined aquifer occurs with an increase in saturated hydraulic conductivity. This increases the volume of fresh water which is mixed with the contaminant plume and causes increased dilution. The results also indicate that changes in the unconfined aquifer properties will override variability in saturated conductivity values in the vadose zone soils.

4.2.2.3.2 Radionuclide Groundwater Concentration Response to Decreased Hydraulic Gradient. The hydraulic gradient used in the previous models was estimated from the water table measurements in the vicinity of Burial Ground 218-W-5 dated at 1988 (Bjornstad 1990). Most of the liquid discharges were stopped by that time at the Hanford site but the water mounds under liquid discharge facilities (such as U Pond) are still dissipating. The hydraulic gradient at 200 West Area is expected to be lower in the post-Hanford era.

For this study the gradient was lowered by decreasing the fixed pressure head difference from the left to the right sides of the aquifer from 0.7 m to 0.5 m. This reduced hydraulic gradient was estimated based on the pre-Hanford regional hydrogeology. The results are presented in Table 4-15.

Table 4-15. 30% Decrease in Hydraulic Gradient, Advection-Dominated Release.

Run number	Recharge rate (cm/yr)	Kd (mL/g)	Inventory depletion period (yr)	Peak conc. (Ci/m^3)	Time to peak concentration (yr)
1a	5.0	0	25	7.96 E-5	123
9a	5.0	0	25	1.08 E-4	125
2a	0.5	0	250	1.04 E-5	995
10a	0.5	0	250	1.46 E-5	990

Compared to the standard cases 1a and 2a, the result shows that the 0.2-m drop increased the peak concentration by approximately 30% but had essentially no effect on the travel time. With the 0.7-m pressure head difference across the study area, the aquifer had a velocity of about 22 m/yr, but lowered to 0.5 m produces a velocity of 15.4 m/yr. This 30% decrease in velocity is translated to a 30% increase in peak concentrations but essentially no charge in travel time because a large fraction of travel time was spent in the vadose zone, which remained unchanged. The most significant observation is that peak concentrations are inversely proportional to hydraulic gradient.

4.2.2.3.3 Radionuclide Groundwater Concentration Response to Variability in Vadose Layer Hydrologic Properties. Variability in soil moisture content-permeability relationships is expected and comes from two sources in this analysis. The first is the natural spatial heterogeneities in the physical makeup of soils which cause some variation in hydrologic characteristics. The second is the facies change that occurs in the Hanford formation between Burial Ground 218-W-5 and Burial Grounds 218-W-3A and 218-W-3AE to the east. As discussed in Chapter 2, a high-energy sediment deposition zone is evident in the eastern burial grounds in which the fraction of large gravel components increases and the fraction of smaller sand components decreases. The base case model assumed the hydrologic characteristics of the lower energy facies underlying 218-W-5. It is known that the higher energy gravel-rich soil deposits are more permeable and could result in shorter travel time and possibly higher peak concentrations if used as a parameter in the modeling runs.

To determine the sensitivity of groundwater concentration results to this variability, the Hanford formation soil was replaced with a 79% gravel mixture soil and the appropriate moisture content-permeability relationships used as input parameters. Two cases were analyzed with recharge values of 5 cm/yr and 0.5 cm/yr. Both cases are advection-dominated release having K_d=0. The results are presented in Table 4-16.

Table 4-16. Effects of Vadose Soil Hydrologic Property Variability on Estimated Peak Concentrations.

Run number	Recharge rate (cm/yr)	Kd (mL/g)	Inventory depletion period (yr)	Peak conc. (Ci/m^3)	Time to peak concentration (yr)
.1a	5.0	0	25	7.96 E-5	123
13a	5.0	0	25	8.99 E-5	103
2a	0.5	0	250	1.04 E-5	995
14a	0.5	0	250	1.16 E-5	830

For the case with 5 cm/yr recharge, the results show a 12% decrease in travel time and 15% increase in peak concentration in comparison with case 1a. For the case with 0.5 cm/yr recharge, the results show a 20% decrease in travel time and 10% increase in peak concentration in comparison with case 2a. The increase in peak concentration is due to the short travel time resulting in a less dispersed plume. The results indicate that the effect of hydrologic properties variability in sediments on dose estimates is likely to be small relative to variability in other parameters such as infiltration rates.

4.2.2.3.4 Radionuclide Groundwater Concentration Response to Presence of a Clastic Dike. The one hydrogeologic feature observed in the Hanford Plateau vadose zone sediments that could provide some degree of preferential vertical transport of a contaminant plume is the clastic dike. No clastic dikes have been reported in the 200 West Area burial grounds. However, they have been reported in the U.S. Ecology commercial waste disposal facility, which is southeast of the burial grounds (Bergeron et al. 1987). Consequently, even though these structures have not been observed in the burial grounds, their presence cannot be completely ruled out and their influence on contaminant transport must be addressed.

Clastic dikes are generally near-vertical planar structures composed of several small "dikelets" of well-sorted sands separated by clay skins. Typical dikes do not extend the total distance of the Hanford formation. Particle size distributions are also not uniform in dikes suggesting that hydraulic properties of these dikes are also not uniform. No information on dike hydraulic properties is available.

It is expected that truncated nature and limited volume of the dikes will prevent them from being major conduits for enhanced contaminant transfer to the unconfined aquifer. To test this hypothesis, a conservative analysis was conducted in which a dike is placed directly underneath a trench and given high permeability properties. The contaminant plume behavior is then compared to the standard case. A 2-meter-wide dike with the 79% gravel placed directly underneath the trench was modeled. Two cases were analyzed with recharge values of 5 cm/yr and 0.5 cm/yr, respectively. Both cases are advection-dominated release having K_d=0. The results are presented in Table 4-17.

Table 4-17. Effect of Clastic Dike Underlying Disposal Facility on Peak Concentrations.

Run number	Recharge rate (cm/yr)	Kd (mL/g)	Inventory depletion period (yr)	Peak conc. (Ci/m^3)	Time to peak concentration (yr)
1a	5.0	0	25	7.96 E-5	123
15a	5.0	0	25	8.87 E-5	1,000
2a	0.5	0	250	1.04 E-5	995
16a	0.5	0	250	1.08 E-5	880

For the case with 5-cm/yr recharge, the results show a 12% decrease in travel time and 11% increase in peak concentration in comparison with case 1a. For the case with 0.5 cm/yr recharge, the results show a 8% decrease in travel time and no significant impact on the peak concentration in comparison with base case 2a.

4.2.2.4 Sensitivity Analyses of Other Manmade Parameters Affecting Radionuclide Transport. Three processes relating to man's activities are discussed in this section that potentially impact radionuclide release and transport: (1) disposal of heterogenous waste with variable inventory, (2) disposal of wastes in variable length trenches parallel to the direction of flow, and (3) pumping of groundwater for irrigation and drinking.

4.2.2.4.1 Radionuclide Groundwater Concentration Response to Presence of High-Concentration Waste Packages. The base case studies assume that waste inventories are homogeneously distributed throughout the disposal facility. In fact, specific radionuclides are heterogeneously distributed because of the variety of waste streams with differing inventories being disposed. Therefore, the potential for increased groundwater concentrations resulting from releases from high-concentration packages are evaluated.

For this study, the total quantity of radionuclides (assumed 1 Ci) was distributed over a trench length of 1 m and evaluated with two different recharge values, 5 cm/yr and 0.05 cm/yr (Table 4-18). The results were compared to the standard analysis (Runs 1a and 2a) in which a homogeneous distribution of the radionuclide over of a trench length of 20 m was assumed. For the case 4a with recharge rate of 5 cm/yr the peak concentration occurred at 127 yr and had a value of 7.76×10^{-5} Ci/m^3. For the case 4a-1 with recharge rate of 0.5 cm/yr the peak concentration occurred at 1,030 yr and had a value of 1.01×10^{-5} Ci/m^3. These results show no significant increase in the peak concentration or travel time with respect to the base cases 1a and 2a.

Table 4-18. Effect of High Concentration Waste Package on Peak Concentration.

Run number	Recharge rate (cm/yr)	Kd (mL/g)	Inventory depletion period (yr)	Peak conc. (Ci/m^3)	Time to peak concentration (yr)
1a	5.0	0	25	7.96 E-5	123
4a	5.0	0	25	7.76 E-5	127
2a	0.5	0	250	1.04 E-5	995
4a-1	0.5	0	250	1.01 E-5	103

This result is consistent with our understanding of dilution effects from the mixing of fresh water in the unconfined water with the contaminant plume. The trench orientation in this analysis is the same as the base case and the total inventory was kept at the same level as the base case. Because the same total volume of water mixes with the same total concentration, the peak concentrations should not change. If the trench were oriented in the north-south direction, which is perpendicular to the flow, the concentration would be significantly higher if a down stream well were aligned with the hot spot. Similarly, if a well were to be drilled at precisely the location underneath the trench where the high-concentration part of the plume entered the unconfined aquifer and the contaminated water were used, a higher dose could be calculated. However, since the nearest well is assumed to be 100 m downstream from the edge of the facility and complete mixing with fresh water occurs rapidly, an increased dose by this pathway is not plausible.

4.2.2.4.2 Radionuclide Groundwater Concentration Response to Variable Length Trenches. The base case assumed a relatively short trench in the direction parallel to flow (east-west) based on the understanding that groundwater concentrations should not be greatly affected by variable trench length as long as the inventory in that trench remained constant. However, some dispersion effect should occur, and result in reduced peak concentrations as the trench lengthens.

To estimate the sensitivity of the results to this effect, analyses were completed assuming trench lengths of 40 and 60 m instead of the original 20 m. These cases have a recharge of 5 cm/yr and have the same release duration as the 20-m long trench model, 25 yr. The results are summarized in Table 4-19.

Table 4-19. Effect of Varying Trench Size on Peak Concentrations.

Run number	Recharge rate (cm/yr)	Kd (mL/g)	Inventory depletion period (yr)	Peak conc. (Ci/m^3)	Time to peak concentration (yr)
1a	5.0	0	25	7.96 E-5	123
1a-1 (40 m)	5.0	0	25	7.54 E-5	124
1a-2 (60 m)	5.0	0	25	7.25 E-5	124
1b	5.0	1	25	4.76 E-6	2030
1b-1 (40 m)	5.0	1	25	4.59 E-6	2040
1b-2 (60 m)	5.0	1	25	4.35 E-6	2030

When compared to the earlier study (Runs 1a and 1b), with a 20-m trench, a slight decrease in the peak concentration is seen as the trench length increases. These results are consistent with the conceptual model. When the trench length increased, the waste concentration in the trench decreased accordingly (total inventory remained unchanged). As a result, the total contaminant release rate remained unchanged. And since the trench length increased in the direction parallel to the flow, the amount of fresh water in the aquifer mixed with the contaminated water remained unchanged. This sensitivity study indicated further that if the trench length increased and the waste concentration remained the same (i.e., the inventory increased accordingly), an additive effect on the peak concentration in the downstream well would be realized.

The sensitivity analyses described above for the effects of trench length assume advective control of radionuclide release. As shown by Table 4-19, the trench length has little influence on the peak concentration. This is not the case if a steady-state concentration ($C/C_o = 1$) is the assumed mechanism of release. In this case, the peak groundwater concentration is approximately linearly proportional to the trench length. In the base case analyses, a 20-m trench was assumed and a peak groundwater concentration was calculated for that condition. If the trench length is doubled to 40 m and the other conditions are held constant, the peak groundwater concentration will be approximately double.

4.2.2.4.3 Radionuclide Groundwater Concentration Response to Pumping. To receive a dose in the all-pathways irrigation scenario, contaminated groundwater must be pumped to the surface. In the base case, no pumping is assumed. To complete a comparison with the base case, it was assumed that a pumping well is operating at the right-hand boundary of the cross-section at a rate of 6,500 m^3/yr (Table 4-20, runs 11a and 12a).

Table 4-20. Effect of Pumping on Peak Concentrations.

Run number	Recharge rate (cm/yr)	Kd (mL/g)	Inventory depletion period (yr)	Peak conc. (Ci/m^3)	Time to peak concentration (yr)
1a	5.0	0	25	7.96 E-5	123
11a	5.0	0	25	1.02 E-5	122
2a	0.5	0	250	1.04 E-5	995
12a	0.5	0	250	1.25 E-6	990

In comparison with Case 2a without pumping, the concentration is reduced by a factor of 8.3. With other conditions identical, a reduction of the peak concentration with pumping versus without pumping can be generalized to other cases. Although a high pumping rate was used in the analysis, the water fluxes in the unconfined aquifer would be generally increased under pumping. Thus, more fresh water is available to mix with same amount of contaminated water which would result in a reduction of the peak concentration.

4.2.3 Determination of Inconsequential Radionuclides in the Groundwater Pathway

The analytical results in Section 4.2 for the base case conditions and the sensitivity analyses are sufficient to eliminate a large number of radionuclides from further evaluation in the quantification of potential dose to man by the groundwater pathway. The first group of radionuclides considered here are those which have short half-lives relative to travel time and will decay to insignificant quantities during transport through the vadose zone.

The radionuclides that are expected to decay to insignificant quantities during transport from the disposal facility are listed in Table 4-21. The relative reduction in activity relative to an initial concentration has been calculated by assuming the extremely conservative recharge rate of 5 cm/yr and the assumption of complete availability of the inventory for release that are the conditions assumed for the Category 1 type of disposal facility. Also, sorption values that are zero or conservative relative to known behavior are assumed, and the dilution effects resulting from pumping are not assumed.

Table 4-21. Radionuclides that Decay to Insignificant Quantities During Transport from the Disposal Facility to the Unconfined Aquifer.

Radionuclide	Kd (mL/g)	Half-life (yr)	Peak or arrival time (yr)	Activity reduction factor
≤5-yr half life	*	≤5	123	2 E+07
^{60}Co, ^{133}Ba, ^{154}Eu, ^{228}Ra	>1	<10	>2,030	>1 E+61
^{93m}Nb	>1	13.6	>2,030	>8 E+44
^{113m}Cd	>1	14.6	>2,030	>7 E+41
^{121}Sn	>1	50	>2,030	>1 E+12
^{152}Eu	>10	13.4	~7,000	>1 E+99
^{242}Cm, ^{243}Cm, ^{244}Cm	>10	<29	~7,000	>1 E+99
^{241}Pu	>10	14.7	~7,000	>1 E+99
^{90}Sr, ^{137}Cs, and ^{243}Cm	>1	≤30	>2,030	>1 E+21
^{63}Ni	>10	100	~7,000	>1 E+21
^{151}Sm	>1	93	>2,030	>4 E+22
^{238}Pu	>10	87.7	~7,000	>1 E+22
^{241}Am	>100	432	~80,000	>5 E+55
^{227}Ac	>1	22	>2030	>1 E+29

*Shortness of half-life makes absorption characteristics irrelevant.

In this situation, it is only necessary to consider the time at which peak concentrations of a radionuclide occur or the time at which the radionuclide is first predicted to arrive at the unconfined aquifer. The time that provides the maximum dose is used in Table 4-21. The activity reduction factor in the right-hand column is the ratio of initial concentration to the maximum concentration in groundwater because of decay during transport. Based on these calculations it is concluded that these isotopes will have no impact on dose-to-man by the groundwater pathway and require no further consideration.

A second set of radionuclides can be eliminated on the basis of long travel time due to sorption. Again, assuming the most conservative condition of an infiltration rate of 5 cm/yr, a radionuclide with a Kd of 100 mL/g is calculated not to arrive at the unconfined aquifer until about 80,000 yr postclosure. Peak concentrations are predicted to occur about 190,000 yr postclosure. The time of compliance for disposal has been assumed in this analysis as 10,000 yr. Also, the geologic record indicates that the current geohydrologic environment at the Hanford Site is likely to undergo substantial changes due to glaciation in the 50,000- to 100,000-yr time frame. Although land usage cannot be predicted under such conditions, it seems implausible that dose to man is likely through retrieval of contaminated groundwater. We conclude, therefore, that highly sorbing radionuclides are essentially immobile and do not require inventory limits to satisfy groundwater pathway dose limits. Radioelements identified as highly sorbing include niobium, potassium, samarium, radium, plutonium, americium, curium, tin, zirconium, cesium, and thorium.

The remaining radionuclides of concern are typically nonsorbing long-lived radionuclides for which travel times are rapid relative to a 10,000-yr compliance time and decay provides no reduction in inventory during transport through the vadose zone. Radionuclides in this category include, ^{14}C, ^{36}Cl, ^{3}H, ^{129}I, ^{93}Mo, ^{187}Re, ^{79}Se, ^{99}Tc, and uranium. Of these, ^{3}H is anomalous because of its much shorter half life. If the expected conservative infiltration rate occurs (0.5 cm/yr), ^{3}H is calculated to reach the aquifer about 400 yr postclosure. The activity reduction factor is calculated to be 1×10^{10}. Consequently, no inventory limit for ^{3}H is required for a Category 3 facility which is assumed to control infiltration rates to $\leq$0.5cm/yr or better.

Three other radionuclides must be considered. The first, ^{237}Np, is moderately sorbing. Under Category 3 conditions, the Kd value of 10 mL/g is sufficient to delay the arrival of neptunium at the unconfined aquifer until about 80,000 yr postclosure. Thus, in a Category 3 facility, neptunium is considered to be essentially immobile and requires no inventory limit. Of course, the actual inventory of neptunium is controlled by the intruder limits and the TRU limit of 100 nCi/g. The other two radionuclides, ^{231}Pa and ^{209}Po, are assumed to be at least weakly sorbing because of their typically positive oxidation states. However, no information is available on their sorption characteristics. To assign inventory limits, a Kd value of 1 mL/g is assumed for these radionuclides. For ^{209}Po, its short half-life (about 102 yr) will result in essentially complete decay in the vadose zone at the Category 3 infiltration rate. Thus, an estimated inventory limit is only necessary for the Category 1 facility. In any event, the expected inventory of ^{231}Pa and ^{209}Po is expected to be very low and will provide an insignificant contribution to dose.

4.2.4 Dose Estimates for Dose-Producing Radionuclides in Groundwater

In this section, dose estimates are provided for those radionuclides identified in the previous section that are predicted to reach the unconfined aquifer in significant quantities. In response to three different performance objectives, two scenarios are assumed to provide dose to the maximum exposed individual and one scenario provides dose to the surrounding population. The individual dose scenarios are the all-pathways irrigator scenario and the groundwater drinking scenario with annual dose limits of 25 and 4 mrem/yr, respectively. For each scenario, contaminated water is drawn from a well 100 m downstream from the waste disposal facility. The population dose scenario is the Columbia River scenario with an annual dose limit of 500 person-rem/yr. In this scenario contaminated groundwater empties into the Columbia River. The contaminated river water is subsequently used by the downstream population.

Radionuclide-specific dose estimates are provided in Table 4-22 for each of the scenarios. To generate these doses it is assumed that (1) unit quantities of each radionuclide are present initially in the disposal facility and (2) Category 1 waste disposal facility conditions are used; the infiltration rate is 5 cm/yr and there is no waste form performance. The doses are calculated by multiplying the peak concentration by the appropriate dose conversion factors. The drinking water dose also requires multiplication by the quantity of water consumed (730 L/yr) and the population dose requires multiplication by a dilution factor to account for mixing of groundwater with Columbia River water. Dilution by 10^5 is assumed. This value is more than an order of magnitude more conservative than that used in the double-shell tank LLW analysis (Kincaid et al. 1993). Similar calculations can be completed for any of the other conditions considered in this analysis (e.g., Category 3 conditions and waste form performance) by substituting the appropriate peak groundwater concentration into the dose calculation.

Table 4-22. Radionuclide Dose Estimates for Groundwater Pathways.

Radionuclide	All-pathways dose (mrem/yr)	Groundwater dose (mrem/yr)	Population dose (person-rem/yr)	Dose ratios	
				All path/GW	Pop./GW
^{3}H	4.1 E-03	3.6 E-03	NA	1.1	NA
^{14}C	2.7 E+02	1.2 E+02	20	2.2	0.17
^{36}Cl	3.0 E+03	1.7 E+02	360	17	2.1
^{79}Se	8.5 E+02	4.8 E+02	78	1.8	0.16
^{99}Tc	2.5 E+02	7.6 E+01	20	3.3	0.26
^{129}I	2.9 E+04	1.6 E+04	2100	1.8	0.13
^{187}Re	7.0 E-01	4.8 E-01	0.051	1.5	0.11
^{237}Np	1.6 E+03	1.4 E+03	110	1.1	0.076
^{209}Po	3.3 E+01	2.9 E+01	2.3	1.1	0.078
^{231}Pa	4.2 E+04	3.9 E+04	2900	1.1	0.076
U	1.6 E+04	1.4 E+04	1100	1.1	0.080

A comparison of the all-pathways and groundwater dose estimates for every radionuclide except ^{36}Cl shows very little difference in value. ^{36}Cl is an exception because consumption of beef and crops rather the drinking water are the dominant contributors to dose for this isotope. Thus, relative dose is much higher in the all pathways scenario. Otherwise, the primary source of dose in each case is consumption of groundwater. Some additional dose due to other ingestion pathways plus inhalation and external exposure contribute to the slightly larger dose in the all-pathways analysis.

This observation is significant when considering the quantification of waste acceptance criteria. A larger dose relative to the dose limit is provided by the groundwater drinking scenario relative to the all-pathways scenario. If the relative dose to dose limit ratios were identical, the all-pathways dose to drinking water dose would be equal to the ratio of the limits (6.25). The dose ratios are 2 to 5 times less than this value (Table 4-22) except for ^{36}Cl. A similar argument also applies to the comparison of the

groundwater dose to the population dose. Equivalent dose-to-dose limit ratios would result in a population to groundwater dose ratio of 125. The dose ratios are more than 100 times lower in all cases. These comparisons show that only the groundwater pathway must be considered when developing waste acceptance criteria except for ^{36}Cl. The primary waste acceptance criteria are radionuclide-specific inventory limits that are calculated to provide the maximum allowable dose. Thus, if a radionuclide limit satisfies the groundwater drinking dose, it automatically satisfies the all-pathways limit and the population dose limit.

In Section 4.2.5, attention is focused on uncertainties related to the estimate of peak radionuclide groundwater concentrations. Additional uncertainties exist for the all-pathways and population dose estimates that are essentially the same as those discussed for the intruder scenario. However, these are irrelevant to the development of waste acceptance criteria and are not discussed further. With regard to ^{36}Cl, it is argued that the all pathways scenario is not the dominant dose-producing scenario because the all pathway dose estimates in Table 4-22 do not account for the diluting effect of pumping that would be assumed in this scenario if it were used to develop waste acceptance criteria. The all pathways doses would be about a factor of 8 less than that shown (Section 4.2.2.4.3). The all pathway-to-groundwater dose ratio is, therefore, about 2, indicating that the groundwater drinking scenario is also dominant for ^{36}Cl.

4.2.5 Groundwater Concentration Uncertainty Analysis

In this section, the results of the sensitivity analyses and the screening process are used to focus the potential uncertainties in the groundwater concentration estimates on critical radionuclides and system parameters that can contribute to dose by the groundwater pathway. The discussion of uncertainty is organized to first consider radionuclide concentrations that do not depend on waste form performance. The uncertainties introduced by assumptions of waste form performance are then addressed.

Outside of the waste form performance, the system parameters identified that could influence radionuclide groundwater concentrations are (1) the infiltration rate, particularly that allowed by the disposal facility cover, (2) permeability of saturated soils, (3) moisture content-permeability relationships in vadose zone soils, (4) the presence of vertical, high-permeability zones (clastic dikes), (5) the regional hydraulic gradient, (6) high radionuclide concentration zones in the disposal facility, (7) sorption distribution coefficients (Kds), and (8) solubility values. Of these, the results of the sensitivity analyses show that for a disposal facility configuration identical to the base case conditions, local high permeability zones in the soil column and high-concentration packages had essentially no effect on predicted groundwater concentrations.

The infiltration rates assumed for the Category 1 and Category 3 facilities are considered to be maximum average rates for the cover conditions assumed. For the purposes of estimating uncertainty in peak groundwater concentrations, a reduction in the base case values by a factor of 5 to 1 and 0.1 cm/yr is considered a reasonable estimate of a lower bound based on the

lysimeter study data summarized previously. The base case data indicate that the peak groundwater concentration decreases by a factor of about 8 with a decrease in infiltration rate from 5 to 0.5 cm/yr. Thus, it is assumed that the relative potential decrease in peak concentration is a factor of 4 because of uncertainty in the average infiltration rate.

When considering the permeability (hydraulic conductivity) of the various soils in the soil column, it was shown that the overriding control is the hydraulic conductivity of the unconfined aquifer and that groundwater concentrations are inversely proportional to change in the hydraulic conductivity value. The most recent compilation of field data (Connelly et al. 1992) shows a range of hydraulic conductivity values in the 200 West Area burial grounds of 10 to 5,100 ft/d, with the majority of the area contoured in excess of 50 ft/d. The assumed average conductivity in the analysis is 46 ft/d. To quantify the potential uncertainty in groundwater concentration, an averaged range of values is a factor of 5 lower and a factor of 100 higher than the base case value. This corresponds to a factor of five increase and a factor of 100 decrease in groundwater concentration.

To bracket uncertainty due to the permeabilities in the vadose zone, the example used in the sensitivity analysis is assumed to represent an upper bound for increasing the groundwater concentration. The increased permeability of the gravel dominated sands in the Hanford formation resulted in a predicted increase in groundwater concentration of about 17%. Similarly, to bracket uncertainty due to changes in the hydraulic gradient, the estimated pre-Hanford gradient is used to bound the increase in groundwater concentration. The sensitivity analyses indicate that the peak concentrations are inversely proportional to the change in gradient. Therefore, assuming that the estimated pre-Hanford gradient value is 30% of the measured value today, it is estimated that the peak concentration could increase by 30%.

The base case analyses show that the Kd value is inversely proportional to the peak concentration. Of the remaining radionuclides in Table 4-22, only ^{237}Np, ^{209}Po, and ^{231}Pa are expected to sorb onto the soil column during transport. Of these, data is available only for ^{237}Np. No assumption concerning uncertainty due to ^{209}Po or ^{231}Pa Kd values is made nor is any required unless a significant inventory source becomes available for disposal. For ^{237}Np, the assumed Kd value of 10 is low compared to the site-specific measured value of about 20 mL/g. To calculate uncertainty, it is estimated that the peak concentration of ^{237}Np could be halved due to sorption.

The total range of potential peak groundwater concentrations due to uncertainty in the parameter values discussed above is determined by calculating the product of the uncertainty factors. For nonsorbing radionuclides with no waste form performance, the peak concentrations relative to the base case potentially increase by a factor of 7.6 and potentially decrease by a factor of 400. For ^{237}Np, the additional of the Kd uncertainty does not affect the potential increase. However, the potential decrease is calculated to be a factor of about 800.

Uncertainty about solubility values is significant for those radionuclides whose peak groundwater concentrations are controlled by a precipitation reaction. In this analysis, this condition is relevant to uranium only. The uncertainty in peak groundwater concentrations is directly

proportional to the solubility. Uncertainty in solubility values are dependent on the accuracy of the thermodynamic data base which is, in turn, dependent on the reliability of the data base developed to quantify thermodynamic properties. The solubility estimates can also be checked with empirical data to evaluate the accuracy of the estimates. Data for uranium indicate that solubility values could be double the value chosen under natural soil conditions. In a grout-dominated environment solubility may vary by 2 orders of magnitude. The other parameters affecting uranium peak concentrations are infiltration rate, the trench length parallel to flow, the vadose zone hydrologic properties, the hydraulic gradient, and the aquifer hydraulic conductivity. Combined with the other parameter uncertainty factors, the bounding changes in groundwater concentration for uranium are estimated to be an increase by a factor of about 18 and a decrease by a factor of about 2,000 relative to base case conditions.

The need for and use of waste forms to control radionuclide release is dependent on the specific radionuclides of concern and the total activities of the radionuclides in the expected waste streams. The results of the base case analysis indicate that waste form performance in the 200 West Area burial grounds is only needed for long-lived nonsorbing radionuclides. None of the waste streams listed in Appendix B (wastes received from 1988-1992) require waste form development. The majority of uranium wastes are fine materials that are encapsulated in a grout waste matrix. The grout properties that reduce uranium mobility by controlling solubility are assumed in the dose estimate analysis. Given our understanding of future waste streams, some may contain sufficient quantities of ^{14}C and ^{99}Tc to require waste form performance. A Portland cement-based grout material is the waste form being considered in this analysis because it combines chemical and physical properties that are useful for controlling the release of ^{14}C and ^{99}Tc.

The solubility concept is also used to evaluate the release of two waste streams of activated metal containing large inventories of ^{14}C (Appendix F). In this case, a steady-state solution concentration is estimated determining the yearly quantity of ^{14}C released by corrosion and the yearly volume of infiltration water. The potential dose is then calculated from the solubility peak concentration analysis.

Empirical measurements have been completed (Serne et al. 1987) to quantify effective diffusion coefficients that combine both chemical and physical mechanisms to control release. The value reported in Kincaid et al. (1993) for ^{14}C and uranium in grout is about 1×10^{-11} cm^2/s and is assumed in this analysis. This value is consistent with a frequently used calculation to estimate the effective diffusion coefficient where the diffusion coefficient measured for an inert substance in the waste matrix is divided by the retardation factor of a reactive element to estimate the actual diffusion coefficient value. For example, the diffusion of nitrate from grout has been measured at about 1×10^{-8} cm^2/s (Kincaid et al. 1993). Distribution coefficients for carbon and uranium have been reported in the range of 1,000 to 10,000 mL/g in grout. Thus, the effective diffusion coefficient would be estimated at about 1×10^{-11} to 1×10^{-12} cm^2/s.

The same approach can be taken for the immobilization of ^{99}Tc in grout. Immobilization of ^{99}Tc by the addition of sulfide-rich slag as a reducing agent to grout has been shown to be successful (WSRC 1994). An estimated

sorption distribution coefficient of about 800 mL/g is reported that can be used to estimate an effective diffusion coefficient of about 1×10^{-11} cm^2/s.

Several areas of uncertainty are inherent in the use of diffusion as the release rate mechanism from grout or any other waste matrix in a hydrogeologic environment. First, the mathematical representation of release by diffusion is not straightforward because of the simplistic analytical solutions required to facilitate modeling of radionuclide release compared to the complex release patterns observed experimentally. The limited empirical data base (see Appendix F) shows that contaminant release from grout is strongly affected by the formation of secondary mineralization in a reaction rind at the grout-soil interface. The net effects are that diffusion coefficient values are reduced over time, contaminants are not released at a maximum rate and complete release of the entire inventory is unlikely to occur. Because empirical diffusion coefficients are measured on fresh materials, a maximum value should be obtained that is subsequently used and held constant in the analysis. The consequence is a conservatively high release rate and dose estimate.

Second, the conceptual model of the mechanics of contaminant release represented by the use of an empirical diffusion coefficient is a general mechanism that may not be an accurate approximation of some contaminant/waste matrix interactions. When using the empirical diffusion concept it is assumed that all of the contaminant is available for release and that physical characteristics of the waste matrix (e.g., constrictivity and tortuosity) impose diffusional control of release. The initial concentration is then defined as the mass of the contaminant divided by the volume of the waste matrix. This concentration also determines the concentration gradient and therefore, the release rate estimate. The diffusional characteristic of the waste matrix is quantified as a diffusion coefficient for an inert contaminant being released from the waste matrix that is measured or estimated. If a contaminant sorbs onto the waste matrix during transport out to the surrounding environment, then the release rate is reduced and quantified by dividing the inert diffusion coefficient by a retardation factor that is proportional to the sorption coefficient.

If it is expected that the contaminant-waste matrix reactions are primarily precipitation reactions or a combination of precipitation and sorption reactions, care must be taken in the use of the approximating diffusion coefficient because the conceptual model is no longer correct. The initial concentration is controlled by the solubility constraint rather than the mass of contaminant in the waste matrix. Consequently, use of the initial mass in the waste to calculate the initial concentration is incorrect and must be countered by the use of an appropriate retardation factor whose reliability is dependent on the accuracy and repeatability of the experimental database. When assuming the grout waste matrix, solubility reactions are expected for uranium and ^{14}C. In these cases, it is necessary to also consider the peak groundwater concentrations predicted from solubility controlled release. Maximum groundwater concentrations cannot exceed those determined by solubility controlled release. Diffusion controlled release estimates that result in larger groundwater concentration estimates than the solubility controlled estimates are an indication that the assumption of an empirical diffusion release rate is inappropriate for such conditions.

Finally, a third area of uncertainty associated with the use of these diffusion coefficient values is the effect of long-term physical and chemical processes that can degrade the performance of the waste form such that waste form release rates are increased. Qualitative evaluation of potential degrading mechanisms suggests that a credible means of significantly degrading grout matrix material in the Hanford Site environment is unlikely, thus minimizing the potential for effectively increasing the diffusion coefficient. The following arguments are made:

1. One way to reduce the integrity of the waste form is to physically crack the material. This may occur through seismic motion or shrinkage cracking as the grout sets up. The potential for seismic disruption is assumed to be very small because of the lack of evidence in the soil column of seismic disturbance, the typical record of seismic events (small clusters of low-intensity activity), and the stability of the Columbia River Basalt Group, particularly over a 10,000-yr period. The potential for both types of degradation to occur decreases with decreased size of the waste form. Neither vaults nor large monoliths are planned for the disposal of burial ground LLW. The largest waste container is likely to be a 4 by 4 by 8 ft box. Small shrinkage cracks may form but these can be minimized with proper grout formulation.

2. Given that small shrinkage cracks will form, two conditions tend to alleviate their importance in terms of radionuclide release. First, the normal burial ground environment will be partially saturated material with no advection of infiltrating water through the waste material. Thus, mass transport will generally occur by diffusion. Under these conditions, the cracks do not serve as dominant conduits for transport. Second, secondary mineralization, particularly the formation of calcite in the void spaces of the cracks, will occur under normal conditions. A discussion of experimental work to date is provided in Appendix F.

3. Chemical dissolution of the grout material is another potential source of increased release of contaminants. Typical agents of dissolution include sulfate attack, chloride attack, and rebar corrosion. Neither sulfate nor chloride are present in significant quantities in Hanford groundwater or soil. Also, rebar is not required to make waste forms for LLW disposal. A third mechanism frequently cited is carbonation. However, as the experimental data indicate (Appendix F), carbonation acts to reduce the permeability of grout and essentially stop the release of radionuclides from the waste form. Thus, it is concluded that there is at least as good a probability that enhanced performance will occur as degraded performance due to chemical interaction with the soil environment under expected Hanford Site conditions.

If diffusion controlled release can be considered a reasonable release controlling mechanism, the significant parameters affecting the radionuclide groundwater concentration are variability in the diffusion coefficient, the vadose zone hydrologic properties, the hydraulic gradient and the aquifer hydraulic conductivity. The sensitivity analyses indicate at these low diffusion rates that infiltration rates in the range expected have no

significant impact on groundwater concentrations. Because of the small amount of data supporting the hypothesis that a grout matrix becomes less permeable with a decreasing diffusivity over time, to calculate uncertainty, a potential increase in diffusivity by a factor of 5 is assumed and a decrease by a factor of 10 is assumed. Combined with the other parameter uncertainty factors, the bounding changes in groundwater concentration are estimated to increase by a factor of about 8 and decrease by a factor of about 15.

4.3 ADDITIONAL ANALYSES

In this section, a number of additional radionuclide transport pathways and site conditions are evaluated for their potential impact on dose-to-man. The additional pathways include vapor diffusion for those radionuclides that are known to partition into the vapor phase under ambient conditions and upward diffusion in liquid. Dose due to transport by vapor are considered for the inadvertent intruder and the offsite individual. The liquid diffusion process requires consideration because of the expected low infiltration rates. Site conditions that may impact dose to man include (1) the potential for mixing of a contaminant plume from the 200 West Area burial grounds with current contaminant plumes in the unconfined aquifer or potential plumes from other LLW disposal facilities, and (2) large-scale commercial agriculture irrigation that might occur onsite in the future.

4.3.1 Analytical Result for Vapor Transport of Carbon-14, Tritium, and Radon-222

In this section, dose calculated for vapor diffusion of ^{14}C and ^{3}H are estimated for the intruder and the offsite individual. Doses are compared to those for the standard postexcavation scenario and the significance relative to waste acceptance criteria are discussed. Flux of ^{222}Rn gas is compared with the flux performance objective of 20 $pCi/m^2/s$.

4.3.1.1 Tritium Analysis. Exposure to the intruder is assumed to occur in two ways. First, exposure occurs under conditions similar to the postexcavation scenario in which waste is exhumed as a result of basement excavation and mixed with uncontaminated soil in a garden plot. The intruder builds a house on top of the soil and is exposed during residence in the house. Second, the intruder does not exhume the waste but resides on the ground above the undisturbed waste. As for comparison of the vapor pathway with the postdrilling case, there is no need because decay still dominates the dose calculation based on the assumption of intrusion at 500 yr.

To estimate flux to the atmosphere in both cases, a simple Fickian diffusion process is assumed to calculate flux and a steady-state condition is assumed. In this case, flux is described by the equation:

$$J = C_o \exp(-x\sqrt{\lambda/D})\sqrt{\lambda D} \tag{4.1}$$

where:

- J = flux ($Ci/m^2/yr$)
- D = diffusion coefficient in soil, 31.5 m^2/yr (1×10^{-2} cm^2/s)
- λ = decay constant, $5.6 \times 10^{-2}/yr$
- C_o = concentration in water vapor (Ci/m^3)
- x = soil thickness (m).

In the first case, the soil thickness is 0.15 m. To calculate the concentration, it is assumed that the initial ^3H concentration is 1 Ci/m^3 and 100 m^3 of material is exhumed, of which 75 m^3 is waste. Excavation occurs 100 yr after disposal leaving a total quantity of ^3H of 0.27 Ci (75 exp ($-\lambda$ t)) assuming no diffusion nor other migration mechanism occurs. This waste is spread over a garden plot of 2,500 m^2 and 0.15 m deep (375 m^3). Typical water contents are about 7 vol%, leading to a total water volume of 26.3 m^3. Thus, the final water concentration is estimated as 0.01 Ci/m^3.

To estimate the concentration of ^3H in water vapor, it is assumed that ^3H is evenly distributed in water mass, whether liquid or vapor. The mass relationship is defined by Henry's Law:

$$C(\text{vapor}) = \frac{Avp \times MW}{RT} \tag{4.2}$$

where:

- Avp = actual vapor pressure (0.012 bars)
- R = gas constant (8.314 E-5 bar $m^3/mol/^0K$)
- T = temperature (283 ^0K)
- MW = molecular weight of water (18 g/mol).

This results in a water vapor concentration of 9.2 g/m^3 for every 1×10^6 g/m^3 of liquid water. Therefore, the concentration of ^3H in vapor in this case is 9.2×10^{-8} Ci/m^3. Using this value for C_o, the flux is estimated as 1.2×10^{-7} $Ci/m^2/yr$.

Given the flux estimates, it is necessary to determine the annual inhalation of ^3H. This is determined by taking the product of the steady-state concentration of ^3H in the house and the volume of air consumed. Dose

is then calculated by taking the product of the activity inhaled and the dose conversion factor. A steady-state concentration is calculated by the following relationship:

$$C_{ss} = \frac{J\ A}{K\ V} = \frac{J}{Kh} \qquad (4.3)$$

where:

J = radionuclide flux ($Ci/m^2/yr$)
A = area of the room (m^2)
K = the ventilation constant (yr^{-1})
V = volume of the room (m^3)
h = height of the room (m).

Taking the flux value from the previous calculation, the height of the room as 2.4 m, and the ventilation constant of one air change/h (8,760/yr), the steady-state concentration is calculated to be 5.7×10^{-12} Ci/m^3.

In the second case, the intruder lives on top of the undisturbed waste. Steady-state concentration is calculated by the same method. The parameter differences are that the soil thickness is assumed to be 3 m. The initial ^3H water concentration is larger in this case because there is no soil dilution. To determine the ^3H vapor concentration, it is assumed that the waste moisture content is similar to soil (7% vol%). Thus, the water concentration of ^3H is estimated to be 14.3 Ci/m^3. Then, accounting for decay and partitioning between vapor and liquid, the vapor concentration is estimated at 4.9×10^{-7} Ci/m^3 at 100 yr. From this concentration, a flux of 5.6×10^{-7} $Ci/m^2/yr$ and a steady-state concentration in the house of 2.7×10^{-11} Ci/m^3 is estimated.

Having calculated the steady-state concentration, the dose is calculated by multiplying the concentration (Ci/m^3) by the annual volume of air inhaled (m^3/yr) and the dose conversion factor (mrem/pCi). Of the two cases, the undisturbed soil case provides a larger steady-state concentration and is used in the dose calculation. To derive the annual inhalation of air, it is assumed that the resident of the house spends half his time inside, equally divided between sleep and daily activity. The total annual volume of air consumed is 3,614 m^3 (Table 3-1). Multiplying these values by the dose conversion factor of 9.5×10^4 mrem/Ci (DOE 1988c) leads to an estimated dose of 9.2×10^{-3} mrem/yr. By comparison, the dose estimated for the intruder in the postexcavation scenario for the same initial inventory is 1.09×10^{-3} mrem/yr. Thus, an increased dose is estimated from this pathway relative to the postexcavation scenario. This pathway is considered in the concentration limit calculations (Section 4.4).

To evaluate the flux to the offsite individual, the following equation is used to calculate dose:

$$\text{Annual Inhalation Dose} = J^* A^* (X/Q)^* BR^* DCF \qquad (4.4)$$

where:

J = radionuclide flux ($Ci/m^2/yr$)
A = area of the facility (m^2)
X/Q = normalized integrated exposure (1.0×10^{-4} s/m^3)
BR = inhalation rate (2.67×10^{-4} m^3/s)
DCF = 9.5×10^4 mrem/Ci (DOE 1988c).

By assuming the larger flux calculated (5.6×10^{-7} Ci/m^2/yr for the undisturbed soil case) and an area of 1.0×10^5 m^2, a dose of 1.4×10^{-4} mrem/yr is calculated for the initial inventory of 1 Ci/m^3.

This dose is more than a factor of 10 less than the dose to the intruder by inhalation of tritiated vapor and nearly a factor of 10 lower than the base case postexcavation scenario. Given that the performance objectives differ by a factor of exactly 10 (an annual dose limit of 100 mrem versus 10 mrem for intruder versus offsite atmospheric dose) it is concluded that the offsite dose by atmospheric dispersion will not be exceeded if the concentration limits are based on the base case postexcavation scenario dose estimates.

4.3.1.2 ^{14}C Analysis. Evaluation of ^{14}C vapor transport is treated similarly to ^{3}H with some differences. First, ^{14}C can be immobilized if it is in activated metal or encapsulated by grout. Consequently, the quantity that is available for release from these kinds of wastes is restricted and this analysis does not apply to such wastes. In this analysis, it is assumed that ^{14}C is completely mobile and all the inventory is present in the vapor. As with ^{3}H, two intruder cases are considered: the postexcavation scenario where a limited quantity of waste is exhumed and mixed with garden soil and an undisturbed waste case where the intruder builds a home on top of the soil. In each case, it is assumed that intrusion occurs 100 yr after closure. If ^{14}C is mobile, release is rapid and it is assumed that freely available ^{14}C is no longer present in the disposal facility after 100 yr, thus making this transport pathway implausible beyond that time.

In the postexcavation scenario, an initial concentration 1 Ci/m^3 is assumed and 100 m^3 of waste, which is 75% contaminated (75 Ci of ^{14}C), are mixed with a volume of garden soil (2,500 m^2 and 0.15 m depth). If a porosity of 40% is assumed, the volumetric concentration of ^{14}C is 0.5 Ci/m^3. Assuming a cover depth of 0.15 m and a diffusion coefficient of 0.01 cm^2/s (31.5 m^2/yr), a flux of 3.1×10^{-2} Ci/m^2/yr is calculated. Given the dose conversion factor of 2.1×10^6 mrem/Ci, an annual dose of 1.1×10^4 mrem is calculated for the 1 Ci/m^3 initial concentration.

In the undisturbed waste case, the same type of analysis is completed except that the vapor concentration and cover thickness are different. In this case, the initial waste loading is assumed to be 1.0 Ci/m^3 and the waste thickness is 3 m. Assuming that all ^{14}C is in vapor and void space is 50%, the volumetric concentration is 2.0 Ci/m^3. Assuming a cover thickness of 3 m and a diffusion coefficient of 0.01 cm^2/s (31.5 m^2/yr), a flux of 1.2×10^{-1} Ci/m^2/yr is calculated. Given the dose conversion factor of 2.1×10^6 mrem/Ci (DOE 1988c), an annual dose of 4.3×10^4 mrem is calculated for the 1 Ci/m^3 initial concentration. This dose exceeds the postexcavation intruder dose (1.07×10^3 mrem/yr) and must be considered in the concentration limit discussion.

The estimate of offsite atmospheric dispersion is completed using the same approach as for ^{3}H. By assuming the larger flux calculated (1.2×10^{-1} Ci/m^2/yr for the undisturbed facility case), a dose of 6.7×10^2 mrem/yr is calculated for the initial inventory of 1 Ci/m^3. This dose estimate is more than 10 times smaller than the undisturbed soil dose for the same initial concentration but only a factor of 2 smaller than the base

case postexcavation scenario dose estimate. Therefore, the offsite atmospheric dispersion scenario dose estimate is considered in the concentration limit discussion (Section 4.4).

4.3.1.3 Radon-222 Analysis Results. To evaluate the flux of ^{222}Rn and compare with the standard of 20 $pCi/m^2/s$, the steady state flux equation (Equation 4.1) is applied. Two cover situations were considered, the minimal 3-m cover assumed for Category 1 waste and the 5-m cover for Category 3 waste. Assuming 1 Ci/m^3 as the initial composition in the waste, the estimated fluxes are 1.9×10^4 and 1000 $pCi/m^2/s$ for 3- and 5-m cover depth, respectively. Given that the dose is proportional to the initial concentration in the inventory, the initial concentrations that are calculated to provide the maximum allowable flux are 0.001 and 0.02 Ci/m^3 for Category 1 and 3 waste, respectively.

The significance of these limits is determined by considering the sources of ^{222}Rn, (^{226}Ra and the uraniam isotopes ^{238}U and ^{234}U), and the limits provided for these parent isotopes in the intruder scenarios. The impact of radon release on uranium and ^{226}Ra limits is discussed in Section 4.4.

4.3.2 Upward Transport of Radionuclides by Liquid Diffusion

The anticipated low recharge for the 200 West Area LLBG provides potential for upward migration of contaminants. The potential for upward diffusion was investigated by comparing the computed upward diffusive front with the downward advective front of contaminants. Fick's second law is used to compute the concentration (C) of a diffusive, nonreactive contaminant:

$$D\frac{\partial^2 C}{\partial Z^2} = \frac{\partial C}{\partial t} \tag{4.5}$$

where:
- z = distance
- t = time
- D = the diffusion coefficient.

The solution for concentration C in equation (4.5) in the z direction over time t is given by:

$$\frac{C}{C_o} = \mathrm{erfc}\left[\frac{z}{2\sqrt{Dt}}\right] \tag{4.6}$$

where:
- erfc = complimentary error function
- C/C_o = the relative concentration.

From (4.6), the mean penetration distance (L) by diffusion (i.e., for $C/C_o = 0.5$) is given by:

$$L = \sqrt{Dt}\,. \tag{4.7}$$

To determine the distance (L) traveled by advection, a steady, one-dimensional (vertical), unit gradient model was used:

$$L = Vt = \left(\frac{q}{\theta}\right)t \tag{4.8}$$

where:

- V = fluid velocity through the Hanford formation sediments under conditions of unit gradient
- t = travel time
- q = recharge rate
- θ = moisture content for Hanford formation sediments under unit gradient condition (derived from $K(\theta)$ versus θ curve).

Natural Hanford sediments below the near-surface zone affected by seasonal, diurnal, and plant evapotranspiration cycles generally are found to have a moisture content between 4 to 7 vol%. Laboratory measurements (Serne et al. 1993) of diffusion coefficients indicate that for volumetric moisture contents of 4% to 7%, the diffusion coefficients for a nonreacting tracer would be in the range of $<5 \times 10^{-8}$ to 2.2×10^{-7} cm^2/s. Using estimates of moisture content based on K(q) versus q relationship for Hanford sediments (Serne et al. 1993), Table 4-23 shows the diffusive distances traveled by upward migration and the advective distances traveled by downward migration for the anticipated low recharge of 0.005 and 0.05 cm/yr.

Table 4-23. Upward Versus Downward Transport in the Soil Cover Resulting from Diffusion and Advection.

Time, yrs	Advective distance traveled (m) for q= 0.005 cm/yr	Diffusive distance (m) for q= 0.005 cm/yr	Advective distance traveled (m) for q= 0.05 cm/yr	Diffusive distance (m) for q= 0.05 cm/yr
1	0.00071	0.019	0.00625	0.024
10	0.0071	0.062	0.0625	0.077
100	0.071	0.195	0.625	0.245
1000	0.71	0.615	6.25	0.774
2000	1.42	0.870	12.5	1.095

Using a very low recharge estimate of 0.005 cm/yr (less than base case values) to enhance upward movement by diffusion, the advective travel distances expected for movement under unit gradient conditions in unsaturated Hanford sediments beneath 218-W-5 are 0.071 m, 0.71 m, and 1.42 m at 100, 1,000 and 2,000 yr, respectively. The computed diffusive distances are 0.195 m, 0.615 m, and 0.87 m at 100, 1,000, and 2,000 yr, respectively. Therefore, under very low recharge (and, therefore, very dry conditions) around buried waste in the unsaturated sediments beneath 218-W-5, the diffusive transport could be of equal or greater magnitude compared to the advective transport up to a time period of slightly more than 1,000 yr; however, at a time scale beyond 2,000 yr, the advective transport exceeds the diffusive transport. For a recharge estimate of about 0.05 cm/yr, the diffusive distance traveled is almost same as the advective transport distance up to a time period of about 10 yr. Beyond 10 yr, the computed advective transport distances are greater than the diffusive transport distances. In either case, the maximum upward distance that can be traveled is computed to be less than 0.2 m.

The fact that precipitation occurs episodically and at much higher rates than the proposed average rate in the calculation for short periods of time may effectively prevent any real upward movement by diffusion over a long period of time. It is expected that covers will be designed also to prevent erosion by simulating natural desert armoring (e.g., use of pea gravel as a surface layer [Ligotke and Klopfer 1990]) and/or planting natural vegetation on the cover. Thus, with a minimum soil cover of about 3 m for disposed waste, the upward radionuclide transport by diffusion does not appear to be a significant process for the conditions analyzed and is not considered a viable means of providing any significant dose.

4.3.3 Dose Effects from the Mixing of Contaminant Plumes

Two types of plumes must be considered that can potentially mix with a contaminant plume emanating from the 200 West Area burial grounds. The first type are existing plumes that developed from the discharge of large volumes of contaminated processing liquids directly into the soil column. The second type are long-term plumes which may result from leaching of other solid waste disposal facilities on the Hanford Site.

A systematic estimate of the fate of current plumes in the unconfined aquifer has not been completed. Thus, a quantitative evaluation of the potential interaction of contaminant plumes from the 200 West Area LLBG with the existing plumes cannot be provided. However, some qualitative arguments can be provided that suggest that such interaction is unlikely. For Category 3 waste, a minimum travel time of about 1,000 yr is estimated. For the Category 1 facility, a minimum travel time of about 125 yr is estimated. These times are compared to a rough estimate of plume migration.

Two factors suggest that the existing plumes will dissipate in a matter of decades. First, the average particle velocity in the unconfined aquifer is on the order of 10 m/yr. Thus, over a few decades, the plume can be expected to migrate a few hundred meters. Second, the relatively rapid infiltration rate at which the initial plumes were generated of about 5×10^{-4} cm/s (WHC 1990) approximates a travel time in months. This observation coupled with the

environmentally mobile characteristics of the radionuclides that make up the plumes indicates that very small quantities of these radionuclides are still present in the soil column. Because liquid discharge of water with any appreciable amounts of activity has essentially been discontinued in the 200 West Area, additional plume generation is unlikely. Other sorbing radionuclides are present in the soil column, but they are dominantly short-lived (e.g., ^{60}Co, ^{137}Cs, ^{90}Sr) and are predicted to decay to insignificant quantities before reaching the unconfined aquifer. It is concluded, therefore that even for a very short travel time of a solid waste plume from a Category 1 facility, that plume mixing is unlikely.

In addition, in the 200 Area plateau, current or planned low-level disposal projects include the following (Figure 4-14).

- U.S. Ecology site southwest of the 200 East Area on land leased by the state
- The ERDF west of the U.S Ecology Site
- Active solid waste burial grounds present in the northeast and northwest corners of the 200 East Area
- Disposal site for vitrified waste from liquid tank waste remediation in or near the 200 East Area.

Figure 4-14 also shows an approximation of the configuration of the Hanford Site water table in January 1944 with the location of solid LLW disposal facilities and potential facilities shown.

Figure 4-14 illustrates that leachate from the 200 Waste Area LLBG is unlikely to intercept contaminant plumes from the other LLW disposal sites in any significant way. To get an additive effect in terms of radionuclide concentrations contributed by the interaction of the two plumes, they must be directly in line with the groundwater with the groundwater flow path as must the well from which contaminated water is drawn. Some mixing of plumes from the 200 West and 200 East LLBG could occur. Three factors suggest that the contribution from the 200 West Area LLBG will be small. First, the estimates of potential dose (Section 4.4.3) from the 200 West Area LLBG are within the performance objectives. Second, these groundwater concentrations will be further reduced by transverse and lateral dispersion during travel through the aquifer. Third, the source of waste for disposal in the 200 East LLBG is essentially the same as for the 200 West Area LLBG. Thus, it is anticipated that a similar estimate of potential dose will be predicted. If so, the total dose from both sites will still fall below the performance objectives. This topic will be considered in the 200 East Area LLBG PA analysis.

The positions of the ERDF facility and the U.S. Ecology site suggests that contaminant plume interaction with the 200 West Area LLBG is unlikely. An estimate of the potential dose from the ERDF site will be provided in a separate PA analysis. It is anticipated that the potential dose form this site will also be very small relative to the performance objectives. LLW from the double-shelled tanks was initially planned for the east side of the 200 East Area. However, current plans for a disposal site are not firm.

Figure 4-14. Relative Location of Existing and Potential Low-Level Waste Disposal Sites in the Vicinity of the 200 West Area Low-Level Burial Ground.

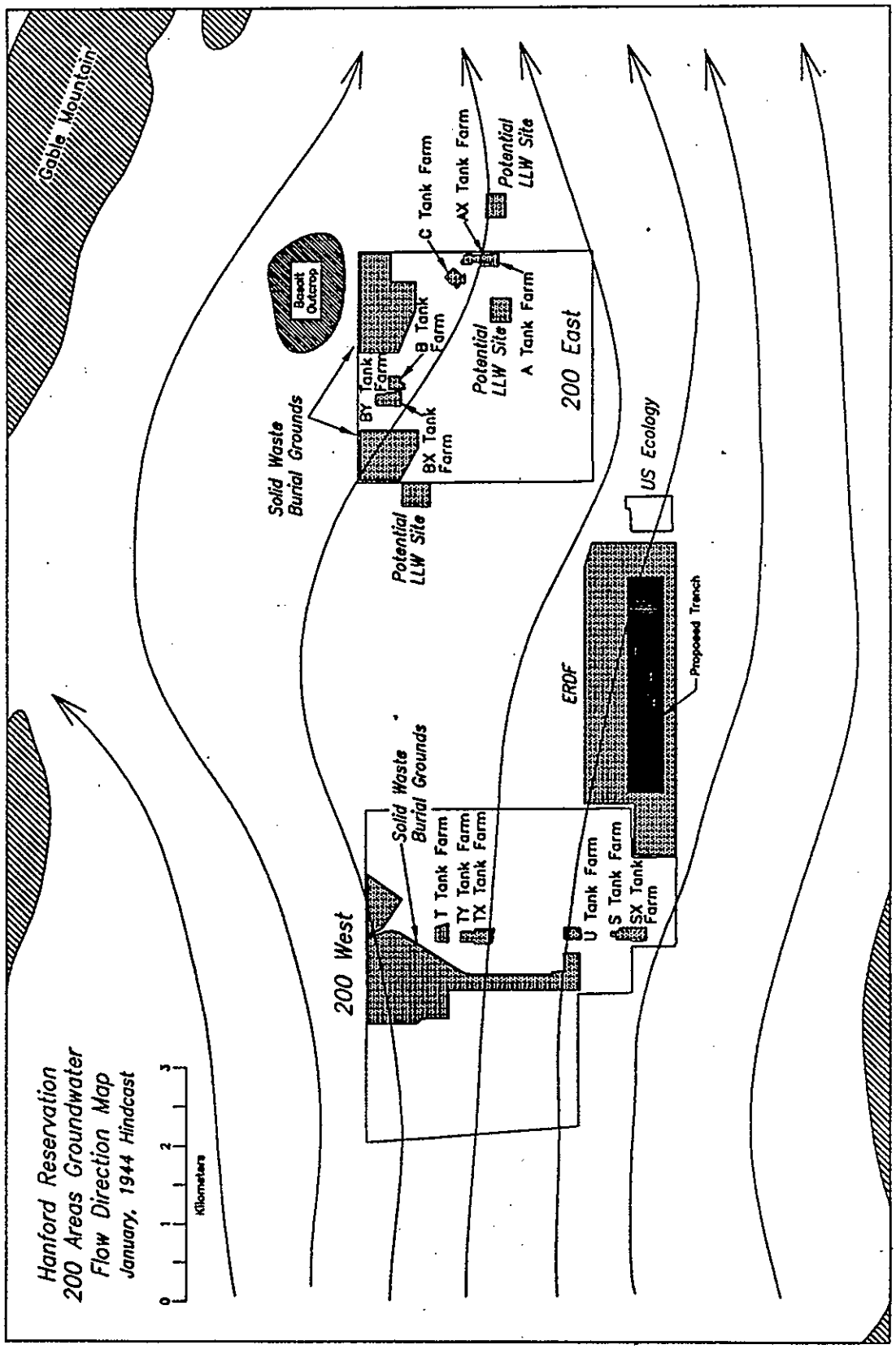

Three potential sites are shown on the map. The locations may line up with the 200 West Area LLBG. However, it is not expected that plume interaction will occur if a facility similar to the one proposed previously is constructed. Significant delays in release from such a facility relative to the 200 West Area LLBG should occur because of the extensive use of isolation barriers.

In summary, a relative increase in groundwater contamination due to the interaction of plumes form the 200 West Area Burial Grounds and other plumes on site is not expected.

4.3.4 Large-Scale Commercial Irrigation Effects on Dose Estimates

Land surrounding the Hanford Site is heavily irrigated to support the growth of crops in commercial agricultural businesses. Because the land is similar to that of the Hanford Site and water from the Columbia River is readily available to support large-scale irrigation, it is conceivable that usage of land for commercial agriculture on the 200 Areas Plateau could occur. If this situation occurred, an increase in the regional infiltration rate near the disposal facilities could result from increased irrigation, thus providing a larger driving force for contaminant transport and increased dose to the offsite individual. Estimates of infiltration increases from 10 to 30 cm/yr have been proposed. To address this possibility, the results of the sensitivity analyses that assumed variable infiltration rates between the soil cover and the surrounding soil can be used to evaluate the potential effects of this activity on dose to man (Section 4.2.2.2).

It is assumed in this case that the 100-m buffer zone remains intact around the facility and the cover over the disposal facility maintains its expected control of infiltration. As described in Section 4.2.2.2, two variable infiltration conditions were considered, one with 0.05 cm/yr cover infiltration rate and 0.5- and 5-cm/yr soil infiltration rates. When the peak groundwater concentrations were compared with cases of uniform infiltration rates, the nearly linear relationship shown when cover infiltration rates were plotted versus peak groundwater concentrations indicates that the cover infiltration rate dominates radionuclide flux.

Based on this analysis, it is concluded that increased infiltration due to irrigation will have only a slight affect on peak concentrations as long as the disposal facility cover is not degraded. An indication of the relative change in groundwater concentration that may occur is shown in the first case where the cover infiltration rate was kept constant at 0.05 cm/yr and the surrounding soil infiltration rates were increased by a factor of 10 from 0.5 to 5 cm/yr. In comparison, the peak groundwater concentration increased by 8% or a factor of 1.08. Thus, if the soil infiltration rate were increased by a factor of about 60 due to irrigation (from 0.5 to 30 cm/yr), an estimated increase of less than 50% would be predicted. Given the uncertainty of other parameters in the calculation, it is concluded that the impact of large-scale irrigation is of no concern.

4.4 INTEGRATION OF RESULTS

In this section, the results from the base case analyses, the sensitivity analyses and the uncertainty analyses are used to develop waste acceptance criteria and to estimate total dose up to 10,000 yr as a result of the disposal of LLW in the 200 West Area burial grounds. The first two sections (4.4.1 and 4.4.2) deal with the development of intruder and groundwater scenario limits. Each section reviews the major parameters influencing dose estimates and, therefore, concentration and inventory limits. Limits are quantified and the conditions to which they apply are specified. In Section 4.4.3, the intruder and groundwater doses for the total projected inventory are compared with the performance objectives. The estimate of total dose involves the use of the waste acceptance criteria to project Category 1 and Category 3 waste streams.

4.4.1 Determination of Inadvertent Intruder Concentration Limits

In this section, the derivation of base case concentration limits is described (Section 4.4.1.1). In Section 4.4.1.2, special case conditions are discussed that have influenced a few specific radionuclide concentration limit calculations. In Section 4.4.1.3, the method for classifying wastes containing multiple radionuclides is summarized.

4.4.1.1 Summary of Parameters Affecting Dose Calculations and Quantification of Concentration Limits. Concentration limits based on intruder scenarios are derived from the dose estimates described in Section 4.2 in which unit concentrations of specific radionuclide were assumed to exist in the disposal facility. Because dose estimates for a given radionuclide are directly proportional to the concentration at the time of intrusion, concentration limits are calculated by taking the ratio of the performance objective (100 mrem/yr) to the dose estimate. A base case set of parameter values was selected to calculate the dose estimates. Realizing that the base case dose estimates consisted of a unique set of parameter values and that other values could be selected, sensitivity analyses and uncertainty analyses were conducted to identify those parameters to which dose was most sensitive and to calculate bounding dose estimates as a function of expected parameter value ranges.

The following key observations were made:

1. Dose estimate changes were not directly proportional to changes in any parameter value except the radionuclide concentration at the time of intrusion. Typically, increasing any one parameter value by 100% results in dose changes of 10% to 60%.

2. When computing potential uncertainties in dose estimates, cumulative factors were computed to combine the effects of all the parameters. Thus, the potential increase or decrease in dose estimates is larger than that of any one parameter and a bounding value could be calculated. Not unexpectedly, the calculated changes in dose by the ingestion pathway are relatively larger than either inhalation or

external exposure because of the larger number of steps and parameters involved in the radionuclide transfer from soil to man through the food chain.

3. Dose resulting from a given radionuclide tends to be dominated by one major pathway (e.g., ingestion versus inhalation or external exposure). Therefore, parameter variability affecting the other pathways have no impact on the dose estimate from that radionuclide.

4. Quantitative changes in dose relative to the base case conditions were calculated as no greater than a factor of 10 and potentially lower by a factor of 100 or more.

These observations support the hypothesis that reasonably conservative doses are being estimated in the base case analysis because the potential for decreased dose appears to be greater than potential for increased dose. The calculations also show that the variability in parameter values and, therefore, the range of dose estimates is not extremely large which improves confidence that an acceptable estimate of dose and, therefore, concentration limits can be generated.

The potential increased dose of up to a factor of 10 means that recommended concentration limits could be estimated at too high a value by the same factor. However, it is argued that such concern is unfounded primarily because the majority of waste to be disposed at the Hanford Site burial grounds contains radionuclide specific concentrations that are well below (e.g., more than a factor of 10) the limits. The purpose of the dose limits is to ensure that an averaged inventory does not allow excessive dose. Thus, an occasional high inventory package that approaches the concentration limit or even exceeds it by as much as a factor of 10 should not lead to an expected excessive dose. Again, the observed distribution of specific radionuclide concentrations for individual containers in the data base sample suggests that the average dose will fall well below the dose limit. This hypothesis is tested in the total inventory dose calculation (Section 4.4.3) by assuming that the Category 1 projected waste includes wastes with radionuclide concentrations up to a factor of 10 greater than the Category 1 limits (Table 4-24).

Concentration limits are quantified for the two types of waste facilities (Category 1 and Category 3) in Table 4-24. The following assumptions are associated with the formulation of the table for most of the radionuclides:

- Concentration limits for Category 1 waste have been calculated from the dose estimates of the postexcavating scenario occurring 100 yr after disposal. It is assumed that disposal facility features allow all reasonable intrusion scenarios to occur.

- Concentration limits for Category 3 waste have been calculated from the dose estimates of the postdrilling scenario occurring 500 yr after disposal. It is assumed that disposal facility features prevent excavation from being a likely event. At a minimum, a $\geq$5-m depth of burial condition is assumed. It is also assumed that a combination of disposal features and institutional memory delay intrusion until 500 yr postclosure.

Table 4-24. Category 1 and 3 Concentration Limits Based on Intruder Scenarios.

Nuclide	Concentration Limits (Ci/m3)		Nuclide	Concentration Limits (Ci/m3)	
	Category 1	Category 3		Category 1	Category 3
H-3	9.9E+04	NL	Pa-231	1.4E-04	3.0E-02
Be-10	1.1E+00	2.4E+02	U-232	4.6E-04	4.6E+00
C-14	9.1E-02	2.1E+01	U-233*	7.4E-03	9.7E-01
C-14°	9.1E-01	2.1E+02	U-234	8.9E-03	1.9E+00
Cl-36	6.4E-05	1.4E-01	U-235	2.8E-03	5.0E-01
K-40	1.8E-03	3.8E-01	U-236	9.5E-03	2.0E+00
Co-60	7.5E+01	NL	U-238	5.7E-03	1.2E+00
Co-60°	7.5E+02	NL	Np-237*	6.8E-04	1.5E-01
Ni-59	3.9E+00	8.5E+02	Pu-238*	4.7E-03	2.4E+01
Ni-59°	3.9E+01	8.5E+03	Pu-239*	1.9E-03	4.2E-01
Ni-63	5.9E+00	2.0E+04	Pu-240*	1.9E-03	4.3E-01
Ni-63°	5.9E+01	2.0E+05	Pu-241	6.1E-02	2.5E+01
Se-79	5.1E-01	1.1E+02	Pu-242*	2.0E-03	4.3E-01
Sr-90	1.6E-02	5.4E+04	Pu-244*	6.1E-04	1.3E-01
Zr-93	2.5E+00	5.4E+02	Am-241*	2.1E-03	8.5E-01
Nb-94	2.2E-04	4.8E-02	Am-242m*	1.9E-03	1.6E+00
Nb-94°	2.2E-03	4.8E-01	Am-243*	1.0E-03	2.3E-01
Mo-93	8.7E-01	2.0E+02	Cm-243*	1.8E-02	3.4E+02
Tc-99	2.3E-02	5.0E+00	Cm-244*	1.4E-01	1.6E+02
Pd-107	1.5E+01	3.3E+03	Cm-245*	1.3E-03	2.2E-01
Cd-113m	7.6E-01	NL	Cm-246*	1.8E-03	4.2E-01
Sn-121m	6.7E-01	2.2E+04	Cm-247*	5.6E-04	1.2E-01
Sn-126	1.6E-04	3.4E-02	Cm-248*	5.1E-04	1.1E-01
I-129	8.5E-03	1.8E+00			
Ba-133	7.1E-01	NL			
Cs-135	1.6E-01	3.5E+01			
Cs-137	5.5E-03	1.2E+04	° Isotope is in activated metal		
Sm-147	1.7E-02	3.7E+00	Category 1and 3 limits are 10 times that		
Sm-151	4.6E+01	2.1E+05	for isotope not in activated metal		
Eu-150	1.4E-03	6.7E+02			
Eu-152	4.8E-02	NL	*Category 3 limit is the lower of this		
Eu-154	7.5E-01	NL	value and 100 nCi/g		
Gd-152	6.4E-03	1.4E+00			
Re-187	3.6E+01	7.8E+03	NL = no limit		
Pb-210	3.7E-02	2.1E+06			
Po-209	9.8E-03	3.2E+01			
Ra-226	1.7E-04	4.3E-02			
Ra-228	1.7E+01	NL			
Ac-227	4.2E-03	3.0E+05			
Th-229	4.4E-04	9.8E-02			
Th-230	2.1E-03	1.5E-01		Edited April 1994	
Th-232	1.1E-04	2.3E-02			

- The selection of radionuclides on the list is not predicated on a particular waste stream or set of waste streams. The set of radionuclides includes all isotopes with half lives greater than 5 yr. It is assumed that radionuclides with half-lives ≤5yr will have decayed to insignificant activities during the assumed minimum 100-yr interval between disposal and intrusion.

For TRU isotopes, the TRU limit (100 nCi/g) is likely to be more restrictive than the intruder concentration limit calculated in this analysis depending on the density of the waste assumed. If this is the case, the TRU limit takes precedence.

4.4.1.2 Additional Considerations for Establishing Concentration Limits. Some additional conditions require additional consideration for a few specific radionuclides to ensure that a reasonably conservative concentration limit is provided. These conditions or circumstances arise because they have the potential to increase dose-to-man and therefore necessitate the reduction of concentration limits.

For most radionuclides with daughter products in secular equilibrium at the times of intrusion, the contribution of the daughter is factored into the calculation of dose estimate and concentration limit. The primary exception is ^{238}U which is assumed not to be in equilibrium with its daughter products. The uranium waste that is disposed is not natural uranium but processed uranium that has been separated from its daughters. Extremely long time periods relative to the 10,000-yr performance objective time of compliance period are required to achieve secular equilibrium or generate daughters that have a significant effect on dose, primarily ^{222}Rn. A separate performance objective defining maximum allowable flux from a disposal facility (20 $pCi/m^2/s$) is applied to the ^{222}Rn inventory limit. To evaluate the relative importance of ^{222}Rn in this context and to determine what effect, if any, the ^{222}Rn contribution to dose should have on the ^{238}U concentration limit, the potential flux of ^{222}Rn based on the ^{238}U concentration limit was calculated using the results of the analysis in Section 4.3.1.3 that relate flux to concentration.

To evaluate ^{222}Rn release, the actual amounts of the isotope in the disposal facility are dependent on the decay process. A decay chain calculation shows that the fraction of ^{222}Rn relative to a unit activity of ^{238}U is 1.65×10^{-6}, 7.94×10^{-4}, 0.024 and 0.084 at 1,000, 10,000, 50,000, and 100,000 yr, respectively. The ^{238}U limits have been established previously as 0.006 and 1.22 Ci/m^3 for Category 1 and 3 waste. If it is assumed that the entire facility is filled with uranium at the concentration limits, the flux of ^{222}Rn at 10,000 yr is estimated as 8.6 and 97 $pCi/m^2/s$ for Category 1 and 3 waste, respectively. At 50,000 yr, the estimated fluxes are about 30 times higher.

Assuming that the time of compliance is 10,000 yr, to satisfy the ^{222}Rn flux criteria, this analysis indicates that the ^{234}U concentration limits are acceptable for Category 1 waste, but should be reduced by approximately a factor of 6.5 for Category 3 waste. Similarly Category 3 ^{226}Ra limits should be decreased by a factor of about 2. However, for the purposes of establishing concentration limits, it is important to remember that the radon flux performance objective is applied to an average flux over the entire

facility. It is known that the facility will not be completely filled with uranium nor will the disposed uranium waste be at the concentration limit. Using the last 4 yr of data as a qualitative indicator, average ^{234}U concentrations is Category 1 and 3 wastes are 8.7×10^{-9} and 4.6×10^{-4} Ci/m^3 contained in <10% by volume of the waste disposed. Similarly the ^{222}Rn average concentrations are more than an order of magnitude less than the concentration limits and occur in <10% of the waste disposed. Given these low values, a large increase in the average uranium and ^{226}Ra concentrations in waste disposed would be needed to equal the radon flux limit at 10,000 yr. If the Category 3 limit were lowered by a factor of 4, some small quantities of uranium waste could be prevented from being disposed that have an inconsequential impact on the average radon flux. Thus, it is concluded that the Category 3 limit should not be reduced to accommodate radon flux requirements.

For radionuclides present in activated metal it is assumed that the isotopes are more tightly bound to the waste matrix and, therefore, less available for providing dose. Thus, a factor of 10 increase in the concentration limit has been allowed for these isotopes. The same practice has been applied by the NRC in 10 CFR 61. The NRC (NRC 1981) applies simple corrosion estimate arguments to compare mobility of radionuclides attached to the surface of trash waste versus imbedded in activated metal.

Both ^3H and ^{14}C can partition into the vapor phase and, therefore, present a potential for providing dose to an intruder who excavates waste or resides on top of the disposal facility. These cases were considered in Section 4.3.1 and larger doses by about a factor of 10 and 40 (for ^3H and ^{14}C, respectively) were calculated from the vapor pathway relative to the base case scenario where it was assumed that the two radionuclides provided dose through the ingestion of dirt and crops. Thus, it could be argued that the intruder dose limits should be correspondingly lower than those proposed.

However, this is not considered a reasonable approach given the extremely conservative assumptions that were used to facilitate the vapor pathway analysis. It was assumed that the two radionuclides remained in the waste for 100 yr postclosure. This is an unlikely event for these radionuclides and was assumed to allow a comparative calculation. For ^{14}C, the estimated flux of 0.12 Ci/m^2/yr would result in the complete release of ^{14}C in less than 10 yr. In addition, the potential for transport away from the facility by the groundwater pathway was not considered. Thus, for ^{14}C, the estimated dose by these pathways is probably fictitious. For ^3H, the estimated flux by vapor is small enough to leave ^3H in the facility at 100 yr, but again, the potential for transport away from the facility by the groundwater pathway is not considered. A factor of 10 increase in the estimated dose should be more than countered by the loss of inventory from all pathways during the 100-yr postclosure period. Therefore, it is concluded that the vapor pathway dose should not be used to estimate intruder-based concentration limits.

4.4.1.3 Use of the Concentration Limits Table. The purpose of the table is to designate the category of any given LLW stream. Once categorization has

Category 1 limit is used in the calculation and the ratio is greater than 1 then the waste is classified as Category 3 or Greater than Category 3 (GTC3) waste. A second ratio calculation must be done with the Category 3 limit to determine if the waste is Category 3 or GTC3.

- When a waste stream is categorized which has a number of radionuclides present, a sum of fractions calculation must be made to define the category of the waste. This is accomplished by dividing the actual concentration of each radionuclide in the waste stream by its concentration limit and then summing the fractions. If the sum exceeds 1.0, then the waste category is greater than the category concentration limits (either Category 1 or 3) used to calculate the sum of fractions.

- If a radionuclide with a half life ≤ 5 yr has a longer lived daughter product which is assumed to be present at the time of intrusion, the presence of that daughter must be considered in the designation process.

- For Category 3 or GTC3 designated waste, a designation per 10 CFR 61 must also be made to determine whether the waste is Class C or Greater than Class C (GTCC). This calculation is required by DOE Order 5820.2A which specifies that GTCC waste cannot be disposed in a near surface LLW disposal facility without a specific performance assessment analysis to justify the disposal method. The Category 3 and Class C wastes are intended to be generally equivalent as the methodology used to develop concentration limits is similar. However, changes in scenario assumptions, performance objectives and dose estimate methodologies have resulted in some changes in concentration limits. Also, the NRC approach to the sum of fractions is different in that either short lived or long lived radionuclides are summed rather than the entire inventory.

4.4.2 Determination of Groundwater Pathway Inventory Limits

In this section, the derivation of base case inventory limits is described (Section 4.4.2.1). In Section 4.4.2.2, the method for classifying wastes containing multiple radionuclides is summarized.

4.4.2.1 Summary of Parameters Affecting Dose Calculations and Quantification of Groundwater Pathway Inventory Limits. In Section 4.2.3, a screening process was developed to eliminate the majority of radionuclides under consideration as potential contributors to dose by the groundwater pathway. The radionuclides that remained after the screening process were mostly long-lived radionuclides that traveled through the soil column unretarded by sorption processes. These included: ^{14}C, ^{36}Cl, ^{3}H, ^{129}I, ^{187}Re, ^{79}Se, and ^{99}Tc and uranium. Three sorbing radionuclides, ^{237}Np, ^{231}Pa, and ^{209}Po, were also left as requiring inventory limits if disposed in a Category 1 facility.

The results of the sensitivity analyses showed that the most important parameters affecting maximum groundwater concentration are the infiltration rate through the waste and the waste form properties limiting the release of

radionuclides. For the Category 1 waste facility where no waste form performance is assumed, the infiltration rate is the most important parameter. For the Category 3 waste facility, if diffusion is the release controlling mechanism for non sorbing radionuclides, the value of the diffusion coefficient is the overriding parameter. For uranium, if solubility is the release controlling mechanism, the solubility controlled concentration and the infiltration rate dominate the maximum groundwater concentration estimates.

The effects of pumping can also have a significant dilution effect for scenarios that assume irrigation as a use for groundwater. In those scenarios, radionuclide concentrations in the water that is used are reduced, thereby reducing the dose estimates. Pumping is not assumed to occur in the groundwater drinking scenario and is, therefore, not a contributing factor when calculating dose or inventory limits for this scenario.

The results of the uncertainty analysis indicated that groundwater concentrations could exceed the base case estimates by up to a factor of 10. This is relevant to the calculation of inventory limits because limits are inversely proportional to maximum concentrations. For all of the factors discussed in Section 4.3, it is most likely that the decrease in infiltration rate is a real expectation because of the data base that supports the uncertainty evaluation. Thus, the potential for decreased groundwater concentration relative to the base case is considered more likely than increased concentrations. In particular, it is expected for Category 3 waste facilities that the actual infiltration rate will be much less than the 0.5 cm/yr assumed (i.e., 5 to 10 times lower). This factor would increase the Ci limits by a factor of about 4 to 8. It is concluded that the base case peak concentration values are reasonably conservative and can be used to estimate inventory limits.

Inventory limits for the groundwater pathway radionuclides are provided in Table 4-25. Comparison of dose from the same groundwater concentration for these radionuclides show that maximum dose relative to a performance objective occurred with the drinking water standard of 4 mrem/yr. Consequently, inventory limits are determined that satisfy the drinking water standard.

The limits are calculated by taking the ratio of the groundwater limiting concentration that corresponds to the 4 mrem/yr dose to the maximum groundwater concentration estimated to result from the initial inventory of 1 Ci in the disposal facility for a given radionuclide. The inventory limits are quantified in Table 4-25 for two conditions. In the first case, the limit applies to any slice of trench whose north-south width is 1 m. To determine a limit for a trench that is 10-m wide in the north south direction, the limits for any radionuclide are ten times the value listed in the table. In the second case, the whole facility curie limits in Table 4-25 are calculated by assuming that the north-south length of the active LLBG in the 200 West Area is about 1,720 m.

Table 4-25. Inventory Limits (Ci) for Groundwater Pathway Performance Objectives.

Radionuclide	Category 1*		Category 3*		Category 3**	
	1 m trench	Whole facility	1 m trench	Whole facility	1 m trench	Whole facility
H-3	1.1 E+03	1.9 E+06	NL	NL	NL	NL
C-14	3.3 E-02	5.7 E+01	2.5 E-01	4.3 E+02	1.8	3040
Cl-36	2.3 E-02	4.0 E+01	1.8 E-01	3.1 E+02	1.3	2160
Se-79	8.5 E-03	1.5 E+01	6.3 E-02	1.1 E+02	0.5	784
Tc-99	5.3 E-02	9.1 E+01	4.0 E-01	6.9 E+02	2.9	4960
I-129	2.5 E-04	4.3 E-01	1.9 E-03	3.3 E+00	0.01	23
Re-187	8.3 E+00	1.4 E+04	6.3 E+01	1.1 E+05	464	8.0 E+0.5
Np-237	2.8 E-03	4.8 E+00	NL	NL	NL	NL
Po-209	1.4 E-01	2.4 E+02	NL	NL	NL	NL
Pa-231	1.0 E-04	1.7 E-01	9.6 E-04	1.7 E+00	4.3 E-03	7.6 E+00
U	2.8 E-04	4.8 E-01	NA	NA	NA	NA

NA = not applicable. The uranium limit is related to solubility control at radionuclide release.
NL = no limit.
*No waste form performance is assumed.
**Diffusional control of radionuclide release is assumed ($D = 1 \times 10^{-8}$ cm^2/s).

The limits listed for conditions of diffusion control assume the minimum diffusion coefficient of 10^{-8} cm^2/s. The limits will increase by a factor of the square root of 10 as the assumed diffusion coefficient decreases by an order of magnitude. The limit is also sensitive to the assumed container area-to-volume ratio. As the ratio decreases (smaller container), the limit increases. In this case, an area to volume ratio between that of a 55 gallon drum (0.09) and a 4 x 4 x 8 box (1.25) was used (0.67), because a mixture of these sizes is most common.

An alternative limit based on solubility control is used for uranium. In this case, the limit is a steady-state concentration in the facility that results in a peak groundwater concentration that corresponds to the 4-mrem/yr limit if 730 L of groundwater are consumed by an individual. The other condition attached to the limit is that a length of trench parallel to groundwater flow is specified to which the limit is applied because the limit is proportional to trench length. For a 20-m trench, the steady-state concentration is calculated to be 2.8×10^4 pCi/L. The assumption of solubility control allows the disposal of unlimited Ci of uranium within that

20 m of trench because steady-state concentrations due to solubility controls are dependent on geochemical conditions rather than the mass of uranium present.

4.4.3 Dose Estimate for the Total Projected Inventory and Comparison with Performance Objectives

To evaluate compliance of a filled and closed 200 West Area LLBG with the performance objectives, a dose estimate was prepared for the entire LLBG using the available data base. To address the intruder performance objectives a list of averaged radionuclide specific concentrations was determined using the four year record of radionuclide and generator specific waste disposed in the LLBG from 1989 through 1993. This record is provided in Appendix B. To address the groundwater contamination performance objectives, a total projected inventory for the long-lived environmentally mobile radionuclides was estimated by extrapolating the 4-yr inventory to 30 yr. This was done by taking the 30 yr volume forecast (Valero et al. 1993) and multiplying the 4 yr inventory by the ratio of the 30 yr volume to the 4 yr volume.

Having estimated the appropriate concentration or inventory projections, the dose estimate from the appropriate base case analysis was used to estimate radionuclide specific doses for the projected inventory for each performance objective. By summing the dose estimate for each radionuclide, a total dose estimate for each performance objective was provided and compared with that performance objective. Parallel calculations were completed for Category 1 and Category 3 waste by dividing the existing waste streams (Appendix B) into the appropriate category.

To divide the wastes into Category 1 and Category 3 wastes, the waste acceptance criteria described in Sections 4.4.1 and 4.4.2 were used. Two assumptions were made when determining whether a given waste stream was a Category 1 or Category 3 waste. First, a factor of ten increase in the Category 1 limit was allowed for each radionuclide in a waste stream. This was deemed reasonable because of the distribution of observed radionuclide concentrations. A comparison of the Category 1 intruder limits with the actual concentrations for specific radionuclides showed that the majority of wastes by volume contain radionuclide concentrations more than an order of magnitude below the Category 1 limits. Because the total intruder dose estimate is based on an averaged value over the facility it was postulated that the estimated dose for the facility would satisfy the performance objectives. Second, for the groundwater mobile radionuclides in any given waste stream, if the total activity was greater than 1% of the Category 1 limit for a 1 m slice of the facility, the waste was assumed to be a Category 3 waste. This was done because the inventory limits for these radionuclides can easily be exceeded by a small volume of waste as limited by the Category 1 concentration limits.

4.4.3.1 Estimate of Intruder Doses. A total volume of about 26, 700 m^3 of waste are listed in Appendix B. Using the assumptions described above, the volume of Category 1 waste was about 15,900 m^3 and the volume of Category 3 waste was about 10,800 m^3. Of the large number of radionuclides listed in the waste streams, very few occur in sufficient concentration to provide

significant dose. A summary list of average radionuclide concentrations is provided in Table B-5, Appendix B. Of the radionuclides present in the waste, only Category 1 concentrations of ^{90}Sr and ^{137}Cs are sufficient to provide a potential dose in excess of 1 mrem/yr (Table 4-26). Three other radionuclides, ^{238}Pu, ^{241}Am, and ^{152}Eu provide a combined potential dose of about 2 mrem/yr. For Category 3, no radionuclide is projected to provide a dose greater than 1 mrem/yr. The largest dose of about 0.7 mrem/yr is provided by ^{226}Ra.

Table 4-26. Radionuclide Specific Intruder Dose Estimates for Category 1 Waste.

Radionuclide	Total activity (Ci)	Concentration (Ci/m^3)	Dose (mrem/yr)
^{60}Co	4.6 E+04	2.4 E+00	3.0 E-01
^{90}Sr	6.3 E+01	4.0 E-03	2.5 E+01
^{137}Cs	1.1 E+01	1.0 E-03	1.9 E+01

4.4.3.2 Estimate of Groundwater Contamination Doses. Maximum dose by the groundwater pathway can only be provided by the radionuclides listed in Table 4-25. Of these radionuclides only those that sorb with the same Kd in the soil column are projected to occur at peak dose at the same time. Thus, when calculating the contribution from each radionuclide to the summed dose estimate, only those radionuclides with the same assumed Kd are counted in the same summation. As it turns out, the only radionuclides in the projected inventory that are estimated to contribute more than 1% of the dose limit by groundwater contamination all have assumed Kd values of 0 ml/g. This also means that peak dose is predicted to occur well before the 10,000 yr compliance time for all Category 1 and Category 3 radionuclide release cases. The relative concentration versus time curves (e.g., Figures 4-10 and 4-11) provide a graphic illustration of the predicted changes in potential dose to man because doses are directly proportional to groundwater concentrations. The peak concentrations are those used to calculate dose for comparison with performance objectives.

The total projected inventory (Table 4-27) estimates indicate that only ^{14}C, ^{129}I, ^{99}Tc, and U are present in sufficient quantities to provide sufficient dose for comparison with the performance objectives. The general approach to estimating the future inventory is to (1) take the ratio of the radionuclide activity disposed in the 4 yr period to the total volume of waste disposed in that same time frame (~25,000 m^3) and (2) to take the product of the ratio and the total projected volume of waste up to the year 2022. The projected volume of waste is about 450,000 m^3. It is here assumed that the environmental restoration waste will not be disposed in the 200 West Area burial grounds. This method of calculation is used for ^{14}C and ^{99}Tc. In the case of U it is assumed that ^{238}U and ^{234}U are in secular equilibrium, each isotope providing half of the dose. For ^{14}C, the inventory calculation does not include two large sources of ^{14}C that occur in activated metal. The potential doses from these sources are treated separately because of their relative immobility (Appendix F).

Table 4-27. Current and Projected Inventories of Groundwater Contaminating Radionuclides.

Radionuclide	Current Inventory (Ci)		Projected Inventory (Ci)	
	Category 1	Category 3	Category 1	Category 3
U	2.0 E-05	11	3.6 E-04	20
I-129	8.3 E-04	0.05	0.014	0.17
Tc-99	1.4 E-04	0.089	0.0025	1.6
C-14	7.0 E-06	0.029	1.3 E-04	5.2

Estimate of the ^{129}I future inventory is complicated because of the skewed distribution of the present inventory. Of the 0.05 Ci presently disposed, 0.046 Ci come from one source, the PUREX facility, in a volume of 350 m^3. Thus, to get a representative estimate of future ^{129}I content it is necessary to consider the projected inventory from this facility. The current waste forecast (Valero, et al, 1993) calls for an additional 370 m^3 of LLW to be provided by PUREX. Using this number, we estimate an additional 0.049 Ci to be provided from this source. For the remainder of the ^{129}I inventory, the ratio of the additional ^{129}I currently disposed (0.004 Ci) to the disposed volume (~25,000 m^3) is used to calculate an additional inventory of 0.07 Ci of ^{129}I to be disposed. Thus, the total ^{129}I disposed is estimated to be 0.017 Ci.

Estimates of the uranium future inventory are also influenced by a skewed distribution of inventory among generators. Of the 11.1 Ci of inventory currently listed in Category 3 waste, 10.6 Ci are from wastes generated by single projects. The primary contributor is PNL. Thus, to derive a 30-yr projected inventory, the remaining 0.5 Ci is multiplied by the ratio of 30-yr volume to the available 4-yr volume. Thus, the total uranium inventory estimate, including the presently disposed waste, is about 20 Ci.

The dose estimates (Table 4-28) from the individual radionuclides contributing to dose in the various groundwater scenarios are shown in Table 4-28. For the Category I facility, ^{129}I is the dominant dose contributing radionuclide for all scenarios. For the Category 3 facility, uranium dominates the population dose in the Columbia River scenario. In the all-pathways scenario, uranium, ^{129}I, and ^{14}C provides similar doses. In the drinking water scenario, uranium and ^{129}I provide similar doses. A comparison of total doses with the performance objectives shows that the doses are more than an order of magnitude below their respective performance objective dose limits.

Table 4-28. Radionuclide Specific Groundwater Dose Estimates for Category 1 and 3 Waste.

Radionuclide	U	^{129}I	^{99}T	^{14}C	Total
Category 1					
Drinking water (mrem/yr)	0.0033	0.13	1.1 E-04	9.1 E-06	0.13
All pathways (mrem/yr)	0.0036	0.23	3.6 E-04	2.0 E-05	0.23
Population (person-rem/yr)	2.6 E-04	0.017	2.9 E-05	1.5 E-05	0.017
Category 3					
Drinking water (mrem/yr)	0.10	0.20	0.009	0.047	0.35
All pathways (mrem/yr)	0.14	0.23	3.6 E-04	0.1	0.47
Population (person-rem/yr)	1.6	0.026	0.002	0.008	1.6

The estimate of the potential dose provided by uranium is dependent on the physical nature of the waste material and the assumed method of radionuclide release. Several conditions were considered to provide an estimate of uranium dose. The majority of uranium waste activity accepted at the burial grounds consists of uranium metal shavings that are grouted in containers (about 90% grout by volume). The grout is required to negate the pyrophoric nature of uranium metal in this physical form. At the same time, grout serves the purpose of reducing the release rate of uranium into the soil column. An estimated dose is, therefore, projected by using the diffusional control analysis and the solubility control analysis to estimate potential dose.

It is assumed that the projected inventory of 20 Ci of uranium in the Category 3 facility is evenly distributed across the 200 West Area LLBG, resulting in an average inventory of 0.012 Ci/m width of trench in the north-south direction. If we select a diffusion coefficient of 1×10^{-11} cm^2/s (about the value identified in Kincaid et al. [1993] for uranium in grout at ambient conditions), the peak concentration is estimated as 2.0×10^{-7} Ci/m^3 for an initial inventory of 1 Ci. For an initial inventory of 0.012 Ci, the peak concentration is calculated as 2.4×10^{-9} Ci/m^3 (2.4 pCi/L). Taking the product of the concentration, the amount of water consumed (730 L/yr) and the ingestion dose conversion factor (2.4×10^{-4} mrem/pCi), a dose of 0.42 mrem/yr is calculated.

To estimate of dose from uranium assuming solubility control of release, a solubility controlling concentration is selected. A theoretical estimate of solubility under a grout controlled regime is about 10^{-8} M. Some experimental data (Serne et al. 1989) indicate that steady-state concentrations could be as high as 10^{-6} M. Dose estimates using the solubility argument are proportional to the infiltration rate, the solubility value and the length of the trench parallel to flow. The analytical results showed that, for the Category 3 infiltration rate of 0.5 cm/yr over a trench length of 20 m and an initial steady-state concentration of 1 Ci/m^3, a peak concentration of 8.3×10^{-4} Ci/m^3 was estimated. Assuming the larger concentration value of 10^{-6} M (7.9×10^{-11} Ci/L), a peak concentration of 6.5×10^{-14} Ci/L (6.5×10^{-2} pCi/L).

Taking the product of the concentration, the amount of water consumed (730 L/yr) and the ingestion dose conversion factor (2.4×10^{-4} mrem/pCi), a dose of 0.01 mrem/yr is calculated. If the trench is 400 m long (the approximate length of a trench in 218-W-5), then the estimated dose is 0.2 mrem/yr. In this case, there is no limit on the Ci of uranium present in the facility because the steady-state concentration is controlled by the chemical environment rather than the inventory of uranium.

A higher dose using the solubility control of uranium release can potentially occur when the buffering capacity of the grout is exhausted in the waste volume and the solubility imposed by the natural environment takes over. At this point, the solubility value is increased by about 2 orders of magnitude (solubility in soil is estimated at 2.7×10^{-4} M) and a corresponding increase in dose is estimated (e.g., in a 20-m section of trench, a potential dose of about 3 mrem/yr is calculated). Two observations suggest that these concentrations and associated doses cannot be achieved or maintained when uranium is initially encapsulated in concrete. These include the following:

1. The buffering capacity of grout is lost slowly because of the low flux of water through the disposal facility. At the same time, secondary mineralization processes are occurring rapidly that reduce the diffusion rate of uranium from the grout into the surrounding soil. Thus, by the time buffering capacity is lost, the diffusional characteristics of the waste matrix should be sufficiently reduced to essentially prevent a rate of uranium release capable of maintaining the higher solubility value.

2. The volume of soil water that might become saturated with uranium at soil-water solubility values would be limited because of the small quantity of uranium projected for disposal in the facility. Consequently, the uranium activity released into any given volume of aquifer water that is subsequently consumed would be reduced by mixing with uncontaminated water or water contaminated with uranium at lower concentrations.

A comparison of the predicted dose discussed above due to solubility control versus diffusion control of uranium release predicts that the diffusion controlled dose is considerably greater. Because this is not a chemically reasonable result (Section 4.2.5), the estimated dose is based on the solubility controlled release analysis and the diffusional release rate analysis for uranium is rejected. To evaluate a maximum dose using the solubility control analysis, it is useful to consider the largest area of the 200 West Area LLBG currently containing a sufficient inventory of uranium to sustain solubility concentrations in solution.

Currently, two trenches contain the bulk of the uranium disposed in the 4-yr inventory. Trench 22 in Burial Ground 218-W-5 contains 4.39 Ci of uranium, and Trench 24 in Burial Ground 218-W-4C contains 6.25 Ci of uranium. Of these, the potential dose from Trench 22 is probably greater because it is spread over a larger volume (about 1,100 versus 50 m^3). This large relative inventory consists of uranium shavings encapsulated in grout. It is unlikely that a greater inventory will occur in any other trench, based on our current knowledge of other waste streams. To estimate dose from the waste in

Trench 22 using the solubility controlled release rate, it is assumed that the 1,100 m^3 is evenly distributed across the north south width of the trench (about 13 m) with a waste depth of 3 m. In this configuration the east-west length of the uranium waste is about 30 m. Given the solubility of uranium in grout (10^{-6} M), an estimated dose of 0.015 mrem/yr is predicted.

In summary, the potential dose-to-man from uranium contamination of groundwater is based on solubility control of uranium release from a grout waste matrix. An estimated dose of 0.1 mrem/yr is proposed. This dose is a factor of 10 greater than that predicted above and has been selected to provide a reasonably conservative estimate. Variability in the actual dose may be less or greater depending on the values selected for several parameters. On the one hand, the predicted value may be smaller than the actual value because of the relatively high infiltration rate assumed (0.5 versus 0.05 to 0.1 cm/yr) and the high solubility value chosen (10^{-6} versus 10^{-8} mol/L). These two factors would reduce the dose estimate by almost 3 orders of magnitude. On the other hand, increased dose (up to 2 orders of magnitude) is possible if uranium is released from ungrouted waste streams or from grouted waste that have lost their buffering capacity. Based on these considerations, the selection of a uranium dose estimate of 0.1 mrem/yr is considered to be a reasonably conservative value.

4.4.3.3 Estimates of Air Contamination Doses. The final performance objectives to consider are potential dose from atmospheric dispersion of ^{14}C and ^{3}H released from the 200 West Area LLBG in the vapor state and the flux of ^{222}Rn. The estimates of atmospheric dispersion dose are based on the analytical results developed in Section 4.3.1. in which the relationship between average concentration and potential dose were quantified. To estimate dose for the total projected inventory of ^{14}C and ^{3}H, the activities (5.2 and 4.7 x 10^3 Ci) were first divided by the volume of waste associated with the area of release assumed in the dispersion calculation (1 x 10^5 m^2). Assuming an average depth of waste of 3 m, the representative volume is 3 x 10^5 m^3. The average concentrations, therefore are 1.7 x 10^{-5} and 0.16 Ci/m^3 for ^{14}C and ^{3}H, respectively. Using the concentration to dose relationships (Section 4.3.1), doses of 0.012 and 2.2 x 10^{-6} mrem/yr for ^{14}C and ^{3}H, respectively were calculated. Relative to the performance objective of 10 mrem/yr, it is concluded that the performance objective is easily satisfied.

The potential ^{222}Rn flux performance objective of 20 pCi/m^2/s for the total inventory is addressed by fisrt estimating the average concentrations of the parents ^{234}U, ^{238}U, and ^{226}Ra that are expected to be present in the wastes. Using the inventory estimates from the four yr data base in Appendix B the average concentrations of these radionuclides was estimated (Table B-5). To complete this calculation, the average values for these radionuclides listed were reduced by a factor of 10 because the values in Table B-5 are based on the volumes of waste containing those radionuclides (< 2000 m^3) instead of the entire volume of waste disposed (> 25000 m^3). Because the flux limit is meant to be applied over the entire facility, it is reasonable to assume that the radionuclides are homogeneously distributed over the entire disposed volume of waste. On this basis, the intial concentrations of ^{234}U, ^{238}U, and ^{226}Ra are 8.7 x 10^{-10}, 8.7 x 10^{-10}, and 6.2 x 10^{-8} Ci/m^3 for Category 1 waste and 4.6 x 10^{-5}, 4.6 x 10^{-5}, and 1.5 x 10^{-4} Ci/m^3 for Category 3 waste.

The impact of these parents on ^{222}Rn flux is variable depending on the decay characteristics. If ^{226}Ra is the parent, immediate secular equilibrium is assumed and flux is maximized at time zero and will decrease in the future. The maximum estimated fluxes are 0.0012 and 0.15 pCi/m^2/s for Category 1 and Category 3 waste respectively. If the uranium isotopes are the parents, it is assumed that the majority of uranium received for disposal has been processed and no daughters are present in the waste beyond ^{234}U in the decay chain. Consequently, ingrowth of ^{222}Rn occurs over time leading to ever increasing flux estimates until secular equilibrium is achieved. Of the two uranium parents present, the flux contribution from ^{234}U exceeds that from ^{238}U by about 2 orders of magnitude in the 10,000 to 100, 000 year time period following disposal of wastes containing these radionuclides. Therefore, flux estimates assuming ^{234}U are provided here to represent the contribution to ^{222}Rn flux from uranium. At 10,000 years, the estimated fluxes are 1.1×10^{-6} and 0.003 pCi/m^2/s for Category 1 and Category 3 wastes respectively. At 100,000 years, the estimated fluxes are 8.9×10^{-4} and 0.24 pCi/m2/s for Category 1 and Category 3 wastes respectively.

These estimates indicate that the ^{222}Rn flux performance objective is easily satisfied at the time of compliance and at times well beyond the time of the compliance period.

5.0 PERFORMANCE EVALUATION

The purpose of this PA analysis has been to evaluate the radiological hazard posed by the disposal of low-level radioactive waste in the 200 West Area LLBG located in the 200 West Area on the Hanford Site. Potential dose has been estimated for a number of scenarios and disposal conditions and compared to dose limit performance objectives. In addition, waste acceptance criteria (primarily radionuclide specific inventory limits), have been quantified to limit the potential dose from the disposal of future waste in the burial grounds. In Section 5.1, the estimated doses are compared to the dose limit objectives assumed for this disposal facility. In Section 5.2, design changes required to satisfy the performance objectives are identified. In Section 5.3, the expected effects of the PA results on other aspects of waste management at the burial grounds are discussed. These include characterization, treatment, closure and monitoring. Finally, in Section 5.4 future data and analysis needs are addressed.

5.1 COMPARISON OF ESTIMATED DOSES WITH PERFORMANCE OBJECTIVES

A summary of dose estimates is provided in Table 5-1 along with the performance objectives assumed as design goals in this analysis. The estimates are based on the projected inventories of the primary dose producing radionuclides in the LLW inventory. Doses for Category 1 and Category 3 waste facility conditions are provided and no waste form performance is assumed.

Table 5-1. Comparison of Dose Estimates with Performance Objectives.

Performance objectives	Exposure pathway	Estimated dose or flux*	
		Category 1	Category 3
25 mrem/yr	Groundwater, irrigated farm	0.23	0.47
4 mrem/yr	Groundwater, drinking	0.13	0.35
100 mrem/yr (100 yr)	Postexcavation	44	NA
100 mrem/yr (500 yr)	Postdrilling	NA	0.7
20 pCi m^2/s at $\leq$10,000 yr	Radon emission	0.012	0.15
10 mrem/yr	Atmospheric dispersion	1.1 E-06	0.012
500 person-rem/yr	Columbia River	0.017	1.6

NA = not applicable.
*The estimated values are in the same units as the performance objectives.

All of the doses shown in Table 5-1, except for the radon flux, are predicted to occur before 10,000 yr and are based on the peak groundwater

concentration. The radon flux will increase beyond 10,000 yr as it approaches secular equilibrium with ^{238}U. Increases by a factor of about 30 and 100 in flux are predicted at 50,000 and 100,000 yr. Based on the projected inventory, the performance objectives are satisfied by the proposed disposal methods in the 200 West Area LLBG.

As stated in the previous chapter, it is difficult to project a LLW inventory and the uncertainty in the range of radionuclide concentrations that could occur in the future. This uncertainty affects the dose estimates provided in Table 5-1. On the other hand, the conservatism used in development of inventory limit waste acceptance criteria, the ability to administratively control wastes that are accepted, and the options to use waste form performance to immobilize wastes containing the groundwater mobile radionuclides in larger quantities are expected to prevent potential dose in excess of the performance objectives.

5.2 DESIGN CHANGES REQUIRED TO MEET PERFORMANCE OBJECTIVES

The current method of LLW disposal requires no significant change relative to current operations. At the time of burial ground closure or partial burial ground closure, however, for those parts of the burial ground containing Category 3 waste, a cover must be constructed that satisfies the infiltration rate control assumption of 0.5 cm/yr. Given the present state of knowledge this is viewed as a design objective that can be easily accomplished with a simple one- or two-layer cover whose primary means of controlling infiltration is the use of a mixture of naturally occurring shallow- and deep-rooted vegetation. The thickness of cover over the waste must also be $\geq$5m. This is also easily achievable since the current operational covers are between 2 and 3 m.

Given the uncertainty of radionuclide inventories of future waste, it is possible that waste form performance may be required for waste streams that contain large quantities of the groundwater mobile radionuclides. At present, none of the wastes received have contained sufficiently large quantities of these radionuclides to require waste form performance. In the two cases of high ^{14}C content (Appendix F), the nature of the waste material (corrosion-resistant steel and a grout sleeve) provides sufficient immobilization such that the potential dose is negligible.

5.3 ADDITIONAL APPLICATIONS OF PERFORMANCE ASSESSMENT RESULTS IN WASTE MANAGEMENT

The PA function is part of the Solid Waste Disposal Division at the Hanford Site. A routine interface is maintained with other aspects of the waste management organization to ensure that disposed waste is in compliance with the performance objectives. Some activities are ongoing and some are planned that are affected by the results of the PA analysis. Currently, the primary interface occurs with the waste acceptance criteria document (WHC 1993). This document identifies waste packaging requirements and waste characterization information that are required of the generator before waste can be accepted for disposal. Stabilization requirements for Category 3 waste

and Category 1 and 3 radionuclide concentration limits are provided in this document. The document is revised as needed and accepts evolving requirements from the PA analysis.

An interface is also maintained with generators who have characterization issues to resolve and with potential waste treatment facilities. Issues revolving around the level of effort required to characterize waste and decisions concerning the need to segregate and treat waste are issues requiring PA input on a regular basis. Another area that is expected to require PA input will be utilization of existing burial ground space and the impacts of adding contiguous disposal sites in the 200 West Area.

Numerous groundwater monitoring wells are in operation around the burial grounds and will continue to operate as long as the burial grounds are operational and for some time postclosure. This analyses indicate that groundwater monitoring wells are not likely to be an effective means of monitoring performance of solid waste disposal facilities because of the very slow releases predicted for these disposal conditions. Even if a contaminant plume from a LLW disposal facility were to reach the unconfined aquifer, the analytical results predict low levels of contamination that would be difficult to detect.

It is expected that the most effective form of monitoring will be to track the amount of precipitation that penetrates the disposal facility cover. The PA analysis results indicate that recharge rates are one of the dominant drivers for the release of radionuclides that can be monitored on a real time basis. The most likely method for monitoring recharge will likely be a combination of neutron probe measurements and lysimeters, placed either in the disposal facility cover or near the facility. If the lysimeter is placed near the facility, the cover materials can be duplicated in the lysimeter. Another possible area of monitoring may be in the vadose zone. Such techniques are not well developed but should receive some consideration.

5.4 ADDITIONAL DATA AND ANALYSIS NEEDS

A number of assumptions used in the PA analysis would benefit from the collection of further data to bolster confidence in their assumed degree of conservatism. One area is the expectation that a grout waste form will become less permeable over time in the disposal facility as secondary mineralization fills pore space. Tests to measure the release of contaminants from waste matrices under site-specific conditions are ongoing. Numerous testing methods are being used to derive a database that supports the analytical assumptions of release rates. Currently, data from scoping tests (see Appendix F) have been generated to quantify iodine release rates from a grout waste form. Similarly, methods for measuring transport of radionuclides in soil under site-specific conditions (primarily partial saturation) have been evaluated and tests are being conducted to provide a database that supports the assumptions used in groundwater modeling analysis to quantify radionuclide transport in the vadose zone. These methods include the unsaturated flow apparatus and the hanging column system. These data collection activities will be continued as funding permits.

Additional waste release analyses may be required on a case-by-case basis for future waste streams if they contain large quantities of groundwater mobile radionuclides. The immobilization properties of the waste materials may be sufficient to dispose of a given waste or waste form development work may be required to dispose of this waste.

As closure covers are developed, it is expected that infiltration monitoring in the covers will be used to support the assumption that infiltration rates are below acceptable levels. Standard techniques exist for monitoring infiltration (e.g., lysimeters and moisture content sensors). As closure plans are developed and covers are placed over the facility, a program will be established to collect infiltration data in the cover. The exact methods used and the length of time over which data are collected have not been determined to date. As part of a PA maintenance program these data should be collected and evaluated periodically to determine their effects on dose estimates.

6.0 LIST OF PREPARERS

Bruce N. Bjornstad, Research Scientist, Geosciences Department, Earth and Environmental Science Center, Pacific Northwest Laboratory.

M.S. Geology, Eastern Washington University 1980

Mr. Bjornstad has been involved in numerous studies to characterize the geohydrologic properties of the Hanford Site. His primary contribution to this document was the collection and summarization of geohydrologic features of the 218-W-5 Burial Ground and surrounding area.

Kirk J. Cantrell, Research Scientist, Geosciences Department, Earth and Environmental Science Center, Pacific Northwest Laboratory.

B.S. Chemical Engineering, University of North Dakota 1982
M.S. Marine Chemistry, University of South Florida 1986
Ph.D. Geochemistry, Georgia Institute of Technology 1989

Dr. Cantrell performs experimental and modeling studies of transport parameters of radionuclides and hazardous materials including metals and organic chemicals. This work includes determination of sorption parameters, solubility data, complexation and colloid formation, and interaction properties. He summarized thermodynamic and sorption data for key radionuclides in support of this PA analysis. He is also involved in the application of these types of geochemical principles for development, design, and evaluation of groundwater remediation techniques.

Truc H. DeLorenzo, Scientist, Water Resources Engineering and Modeling, Westinghouse Hanford Company.

B.S. Physical Science, Washington State University 1990

Ms. DeLorenzo has 2 years of groundwater modeling experience with Westinghouse Hanford Company. She has been a key contributor in performing computer runs with VAM3D-CG for radionuclide release scenarios in the hydrogeologic system. She has provided graphic representations and tabular summaries of the results.

Scott H. Finfrock, Staff Scientist, Water Resources Engineering and Modeling, Westinghouse Hanford Company.

M.S. Nuclear Engineering 1987
M.S. Computer Science 1993

Mr. Finfrock has over 8 years of experience developing and applying finite difference computer codes. He has been a key contributor in performing computer runs with VAM3D-CG for radionuclide release scenarios in the hydrogeologic system. He has provided graphic representations of the results and written discussions on the results for the document.

Raziuddin Khaleel, Fellow Engineer, Water Resources Engineering and Modeling, Westinghouse Hanford Company.

B.S.	Civil Engineering, Bangladesh University of Engineering and Technology	1966
M.S.	Water Science and Engineering, Asian Institute of Technology	1970
Ph.D.	Soil and Water Engineering, Texas A&M University	1977

Dr. Khaleel has over 25 years of experience in groundwater hydrology and numerical simulations of subsurface flow and transport. He is a key contributor to the Solid Waste PA analysis in the areas of conceptual model development of the hydrogeologic environment, technical direction of modeling runs, and writing of analytical results in various sections of the document.

Allen H. Lu, Fellow Engineer, Water Resources Engineering and Modeling, Westinghouse Hanford Company.

B.S.	Naval Navigation and Engineering, Chinese Naval Academy	1958
M.S.	Nuclear Physics, Tsin-Hua University, Taiwan	1964
Ph.D.	Nuclear Physics, Rensselaer Polytechnic Institute	1969

Dr. Lu has been employed at the Hanford Site since 1979. He has been responsible for selecting the source term model and integrating the model with the flow and transport code for the analyses in this document. He also provided technical direction of modeling runs and the writing of sections describing the analytical results. Previously, Dr. Lu has worked in various nuclear engineering projects. He developed a novel technique to measure gas permeability and estimate gas-production in the late 1970's at a low-level radioactive waste burial site in West Valley, NY. He performed benchmark calculations of ^{236}Pu content of ^{238}Pu production at the Fast Flux Test Facility (FFTF) using a general Monte Carlo code for neutron/photon transport. He is an expert in shielding and criticality studies. Dr. Lu has recently been in charge of various modeling studies using the VAM3D-CG flow and transport code.

Paul D. Rittmann, Principal Engineer, Water Resources Engineering and Modeling, Westinghouse Hanford Company.

B.A.	Physics, University of Wisconsin	1971
M.S.	Physics, Purdue University	1973
Ph.D.	Physics, Purdue University	1976

Dr. Rittmann has been employed at the Hanford Site since 1980. He has been using environmental transport and dose models since 1983. He has been responsible for the development and calculation of radionuclide-specific dose estimates for radionuclide release scenarios in this analysis. Dr. Rittmann's current responsibilities include application of mathematical models for estimating environmental doses from long-term waste disposal, from normal operations, and from accidental releases. He is currently a member of the Hanford Environmental Dose Overview Panel, the Health Physics Society, the American Nuclear Society, and the American Academy of Health Physics.

R. Jeff Serne, Staff Scientist, Geosciences Department, Earth and Environmental Science Center, Pacific Northwest Laboratory.

B.S.	Chemistry, University of Washington	1969
B.S.	Oceanography, University of Washington	1969

For the past 23 years, Mr. Serne has worked primarily in the areas of solidified waste-groundwater reactions, soil-waste interaction, sediment-heavy metal sorption-desorption phenomena, and radioactive waste disposal processes. He has developed test techniques and gathered data for measuring radionuclide behavior under site-specific conditions in support of this effort. He has also collaborated on the summary of thermodynamic data for quantifying solubilities of key radionuclides. Previously, his work has involved developing mathematical predictor equations to evaluate the migration potential of contaminants and investigating, through laboratory experiments and field studies, the mechanisms of waste form leaching, sediment and soil-water ion exchange, and precipitation and sequestration of trace contaminants, with emphasis on radionuclides and regulated trace metals.

Marcus I. Wood, Principal Scientist, Solid Waste Disposal, Westinghouse Hanford Company.

B.S.	Geology, University of North Carolina	1973
Ph.D.	Geology, Brown University	1980

Dr. Wood is currently responsible for the development of the PA analyses for the disposal of solid low-level waste at the Hanford Site. He is the coordinating author of this document and has been largely responsible for the integration and interpretation of the analytical results in this document. He is currently preparing a similar analysis for the Environmental Restoration Disposal Facility (ERDF) which is planned for disposing of wastes generated in the remediation of Hanford CERCLA sites. In the past, he has directed numerous projects to quantify the geochemical properties of radionuclides in the Hanford geohydrologic environment.

This page intentionally left blank.

7.0 REFERENCES

56(138) FR 33050, 1991, U.S. Environmental Protection Agency, "National Primary Drinking Water Regulations: Radionuclides," Notice of Proposed Rulemaking, *Federal Register*.

58 FR 7924, 1992, U.S. Environmental Protection Agency, "Environmental Radiation Protection Standards for the Management and Disposal of Spent Nuclear Fuel, High-Level and Transuranic Radioactive Wastes," Proposed Amendment to 40 CFR 191, *Federal Register*.

Aaberg, R. L., and Kennedy, W. E. Jr., 1990, *Definition of Intrusion Scenarios and Example Concentration Ranges for the Disposal of Near-Surface Waste at the Hanford Site*, PNL-6312, Pacific Northwest Laboratories, Richland, Washington.

ANS, 1986, *Measurement of the Leachability of Solidified Low-Level Radioactive Wastes*, ANS-16.1, American Nuclear Society Standards Committee Working Group.

Baes III, C. F., R. D. Sharp, A. L. Sjoreen, and O. W. Hermann, 1984a, *TERRA: A Computer Code for Simulating the Transport of Environmentally Released Radionuclides through Agriculture*, ORNL-5785, Oak Ridge National Laboratory, Oak Ridge, Tennessee (November).

Baes III, C. F., R. D. Sharp, A. L. Sjoreen, and R. W. Shor, 1984b, *A Review and Analysis of Parameters for Assessing Transport of Environmentally Released Radionuclides through Agriculture*, ORNL-5786, Oak Ridge National Laboratory, Oak Ridge, Tennessee (September).

Bayliss, S., F. T. Ewart, R. M. Howse, J. L. Smith-Briggs, H. P. Thomason, and H. A. Wilmott, 1988, *The Solubility and Sorption of Lead-210 and Carbon-14 in a Near-Field Environment*, Material Research Society Symposium Proceedings, Vol. 112. pp. 33-42, Materials Research Society, New York, New York.

Bjornstad, B., 1990, *Geohydrology of the 218-W-5 Burial Ground, 200 West Area, Hanford Site*, Pacific Northwest Laboratories, Richland, Washington.

Brooks, R. H., and A. T. Corey, 1966, *Properties of Porous Media Affecting Fluid Flow*, *ASCE J.* Irrig. drain. Div., 92(IR2):61-88.

Caggiano, J. A., and D. W. Duncan, 1983, *Preliminary Interpretation of the Tectonic Stability of the Reference Repository Location, Cold Creek Syncline*, Hanford Site, RHO-BW-ST-19P, Rockwell Hanford Operations, Richland, Washington.

Case, M. J., R. L. Dodge, T. G. Frangos, W. R. Hansen, W. E. Kennedy, Jr., D. W. Layton, D. W. Lee, E. L. Wilhite, 1989, *Recommended Format and Content for DOE Low-Level Waste Disposal Facility Radiological Performance Assessment Report*, DOE/LLW-81, U.S. Department of Energy, Washington D.C.

Conca, J. L., and J. Wright, 1990, *Diffusion Coefficients in Gravel Under Unsaturated Conditions*, *Water Resour. Res.*, v. 26, pp. 1055-1066.

Connelly, M. P., B. H. Ford, and J. V. Borghese, 1992, *Hydrogeologic Model for the 200 West Groundwater Aggregate Area*, WHC-SD-EN-TI-014, Westinghouse Hanford Company, Richland, Washington.

Crank, J., 1975, *The Mathematics of Diffusion, 2nd Ed.*, Oxford University Press, Oxford, England.

Delaney, C. N., K. A. Lindsey, and S. P. Reidel, 1991, *Geology and Hydrology of the Hanford Site; A Standardized Text for Use in WHC Documents and Reports*, WHC-SD-ER-TI-003, Rev. 0, Westinghouse Hanford Company, Richland, Washington.

Dodge, R. L., W. R. Hansen, W. E. Kennedy, Jr., D. W. Layton, D. W. Lee, S. T. Maheras, S. M. Neuder, E. L. Wilhite, R. C. Curl, K. F. Grahn, B. A. Heath, and K. H. Turner, 1991, *Performance Assessment Review Guide for DOE Low-Level Radioactive Waste Disposal Facilities*, DOE/LLW-93, Idaho National Engineering Laboratory, Idaho Falls, Idaho.

DOE, 1994, *Remedial Investigation and Feasibility Study Report for the Environmental Restoration Disposal Facility*, DOE/RL-93-99 U.S. Department of Energy, Richland, Washington.

DOE, 1993, *Radiation Protection of the Public and the Environment*, Proposed Rule, 10 CFR Part 834, U.S. Department of Energy, Washington D.C.

DOE, 1988a, *Radioactive Waste Management*, DOE Order 5820.2A.

DOE, 1988b, *Site Characterization Plan, Reference Repository Location, Hanford Site, Richland, Washington*, Consultation Draft, DOE/RW-0164, U.S. Department of Energy, Office of Civilian Radioactive Waste Management, Washington, D.C.

DOE, 1988c, *Internal Dose Conversion Factors for Calculation of Dose to the Public*, DOE/EH-0071 (DE88-014297), U.S. Department of Energy, Washington, D.C.

DOE, 1987, *Final Environmental Impact Statement: Disposal of Hanford Defense High-Level, Transuranic and Tank Wastes*, DOE/EIS-0113, Vol. 1-5, U.S. Department of Energy, Washington, D.C.

DOE-RLID, 1990, *Radioactive Waste Management*, Richland Operations Supplement to DOE Order 5820.2A.

Duncan, D. R., C. L. Blackburn, P. S. Kaae, K. J. Beverlin, S. M. K. Garrett, and D. L. Stiles, 1992, *1992 Solid Waste Reference Forecast Summary*, Westinghouse Hanford Company, Richland, Washington.

EPA, 1992, *Total Suspended Particulate Information for Kennewick, Washington (1985-1988)*, U.S. Environmental Protection Agency, National Air Data Branch, Aerometric Information Retrieval System, Washington, D.C.

EPA, 1989, *Exposure Factors Handbook*, EPA/600/8-89/043, U.S. Environmental Protection Agency, Washington, D.C.

Fayer, M. J., M. L. Rockhold, and G. W. Gee, 1991, *Recharge Potential of a Sandy Soil*, EOS (*Transactions of the American Geophysical Union*), Vol. 72, p. 1074.

Ford, B. H., 1993, *Groundwater Field Characterization Report for the 200 Aggregate Area Management Study*, WHC-SD-EN-TI-020, Rev. 0, Westinghouse Hanford Company, Richland, Washington.

Freeze, R. A. and J. A. Cherry, 1979, *Groundwater*, Prentice-Hall, Inc. Englewood Cliffs, New Jersey.

Gee, G. W., 1987, *Recharge at the Hanford Site: Status Report*, PNL-6403, Pacific Northwest Laboratory, Richland, Washington.

Gee, G. W., M. J. Fayer, M. L. Rockhold, and M. D. Campbell, 1992, "Variations in Recharge at the Hanford Site," in *Northwest Science*, Vol. 66, No. 4, pp. 237-250.

Graham, M. J., M. D. Hall, S. R. Strait, and W. R. Brown, 1981, *Hydrology of the Separations Area*, RHO-ST-42, Rockwell Hanford Operations, Richland, Washington.

Hajek, B. F., 1968, *Waste Disposal to the Ground at 100-N*, BNWL-CC-1670, Battelle Northwest Laboratory, Richland, Washington.

Huyakorn, P. S., and Sorab Panday, 1992, *VAM3DCG: A Variably Saturated Analysis Model in Three-Dimensions with Preconditioned Conjugate Gradient Matrix Solvers - Documentation and User's Guide, Version 2.4*, HydroGeologic, Inc., Herndon, Virginia.

Huyakorn, P. S., and G. F. Pinder, 1983, *Computational Methods in Subsurface Flow*, Academic Press, New York, New York.

ICRP, 1975, *Report of the Task Group on Reference Man*, Publication 23, Pergamon Press, New York, New York.

Kennedy, W. E., and D. L. Strenge, 1990, *Residual Radioactive Contamination from Decommissioning*, Vol. 1, NUREG/CR-5512, Pacific Northwest Laboratory, Richland, Washington.

Khaleel, R., and M. I. Wood, 1990, *Performance Assessment Modeling of Flow Transport from a Low-Level Solid Waste Burial Ground: Conceptual Model and Data Requirements*, Letter Report to J. L. Scott from J. W. Cammann, Westinghouse Hanford Company, Richland, Washington.

Kincaid, C. T., J. W. Shade, G. A. Whyattt, M. G. Piepho, K. Rhoads, J. A. Voogd, J. H. Westsik, Jr., M. D. Freshley, K. A. Blanchard, B. G. Lauzon, 1993, *Performance Assessment of Grouted Double-Shell Tank Waste Disposal at Hanford*, WHC-SD-WM-EE-004, Rev 0., Westinghouse Hanford Company, Richland, Washington.

Kozak, M. W., M. S. Chu, T. A. Mattingly, J. D. Johnson, and J. T. McCord, 1990, *Background Information for the Development of a Low-Level Waste Performance Assessment Methodology*, NUREG/CR-5453, SAND90-0375, Vol. 5.

Ligotke, M. W., 1988, *Soil Erosion Rates from Mixed Soil and Gravel Surfaces in a Wind Tunnel: A Preliminary Report*, PNL-6677, Pacific Northwest Laboratory, Richland, Washington.

Ligotke, M. W., and D. C. Klopfer, 1990, *Soil Erosion Rates from Mixed Soil and Gravel Surfaces in a Wind Tunnel*, PNL-7435, Pacific Northwest Laboratory, Richland, Washington.

Mualem, Y., 1976, "A New Model for Predicting the Hydraulic Conductivity of Unsaturated Porous Media," in *Water Resour. Res.*, vol. 12, no. 3, pp. 513-522.

Napier, B. A., R. A. Peloquin, W. E. Kennedy, Jr., and S. M. Neuder, 1984, *Intruder Dose Pathway Analysis for the Onsite Disposal of Radioactive Wastes: The ONSITE/MAXII Computer Program*, NUREG/CR-3620, U.S. Nuclear Regulatory Commission, Washington, D.C.

Napier, B. A., D. L. Strenge, R. A. Teloquin, and J. V. Ramsdell, 1988, *GENII - The Hanford Environmental Radiation Dosimetry Software System*, PNL-6584, Pacific Northwest Laboratory, Richland, Washington.

NRC, 1977, *Calculation of Annual Doses to Man from Routine Releases of Reactor Effluents for the Purpose of Evaluating Compliance with 10 CFR 50, Appendix I*, Regulatory Guide 1.109, Revision 1, U.S. Nuclear Regulatory Commission.

Rockhold, M. L., M. J. Fayer, G. W. Gee, and M. J. Kanyid, 1990, *Natural Groundwater Recharge and Water Balance at the Hanford Site*, PNL-7215, Pacific Northwest Laboratory, Richland, Washington.

Routson, R. C., and V. G. Johnson, 1990, *Recharge Estimates for the Hanford Site 200 Areas Plateau*, Northwest Science, Vol. 64, No. 3, pp. 150-158.

Scheidegger, A. E., 1961, *General Theory of Dispersion in Porous Media*, J. Geophys, Res., v. 66, pp. 3273-3278.

Serne, R. J., W. J. Martin, S. B. McLaurine, S. P. Airhart, V. L. LeGore, and R. L. Treat, 1987, *Laboratory Leach Tests of Phosphate/Sulphate Waste Grout and Leachate Adsorption Tests Using Hanford Sediment*, PNL-6019, Pacific Northwest Laboratory, Richland, Washington.

Serne, R. J., J. L. Conca, V. L. LeGore, K. J. Cantrell, C. W. Lindenmeier, J. A. Campbell, J. E. Amonette, and M. I. Wood, 1993, *Solid-Waste Leach Characteristics and Contaminant-Sediment Interactions Volume 1: Batch Leach and Adsorption Tests and Sediment Characterization*, PNL-8889 Vol. 1, Pacific Northwest Laboratory, Richland, Washington.

Sheppard, M. I., S. C. Sheppard, and B. D. Amiro, 1991, "Mobility and Plant Uptake of Inorganic ^{14}C and ^{14}C-Labelled PCB in Soils of High and Low Retention," in *Health Physics*, Volume 61, Number 4, pp. 481-492.

Valero, O. J., C. L. Blackburn, P. S. Kaae, L. L. Armacost, and S. M. K. Garrett, 1993, *1993 Solid Waste Reference Forecast Summary*, WHC-EP-0567-1, Westinghouse Hanford Company, Richland, Washington.

van Genuchten, M. Th., 1980, "A Closed-Form Solution for Predicting the Conductivity of Unsaturated Soils," in *Soil Science Society of America J.*, 44, 892-898.

WHC, 1993, *Hanford Site Solid Waste Acceptance Criteria*, WHC-EP-0063-4, Westinghouse Hanford Company, Richland, Washington.

Wilhite, E. L. to J. A. Coleman, Letter, October 12, 1993, "Preliminary Review of the Hanford LLW PA."

WSRC, 1994, *Radiological Performance Assessment for the E-Area Vaults Disposal Facility (U)*, WSRC-RP-94-218, Westinghouse Savannah River Company, Aiken, South Carolina.

Yang, Y., and C. B. Nelson, 1986, "An Estimation of Daily Food Usage Factors for Assessing Radionuclide Intakes in the U.S. Population," in *Health Physics*, Volume 50, Number 2, pp. 245-257.

This page intentionally left blank.

APPENDIX A

STRATIGRAPHIC AND VADOSE ZONE HYDROLOGIC PROPERTIES

This page intentionally left blank.

STRATIGRAPHIC AND VADOSE ZONE HYDROLOGIC PROPERTIES

A.1 GEOLOGIC FEATURES AND CONTAMINANT PLUMES IN THE 200 WEST AREA

Three cross-sections are provided in Figures A-1 through A-3 that represent the stratigraphy underneath Burial Ground 218-W-5. These stratigraphic relationships were used as the basis for defining the base case stratigraphic column. In Figures A-4 through A-10, isopach maps are shown that define the thicknesses for each of the stratigraphic units in the vadose zone. Figure A-4 shows the location of the burial grounds with respect to the isopach contours shown in Figures A-5 through A-10. Two facies of the uppermost unit, the Hanford formation, are shown in Figures A-5 and A-6. These include the gravel-rich layer (HC) and the sand-rich layer (HSZ). The water table occurs in the middle of the Ringold E unit (Figure A-10).

The north-south flood channel that is postulated to have existed during the deposition of the Hanford formation is indicated by the thickness of the gravel rich unit (HC) that extends through Burial Grounds 218-W-3A to 218-W-4C (Figure A-5). The channel clearly had some localized eroding effects on the underlying early Palouse layer (Figure A-7) but not in subsequent underlying layers (e.g., the Plio-Pleistocene [Figure A-8]).

Existing radionuclide contaminant plumes in the unconfined aquifer underlying the 200 West Area are shown in Figures A-11 through A-15. The primary sources of contamination were U-Pond and a group of cribs covering the southern part of the 200 West Area. The plumes, particularly the tritium plume, show the general direction of groundwater flow to the east and northeast. The data were taken from 1988 to 1992.

A.2 VADOSE ZONE SOIL PROPERTIES

A number of parameters are needed to model the vadose zone hydrology and transport from a solid waste disposal site. The hydrologic data that are critical in quantifying the water storage and transport properties for unsaturated soils include a characterization of heterogeneities of various soil layers and the moisture characteristics for various layers. The following section describes the laboratory-measured data on moisture retention (capillary pressure head as a function of moisture content) and unsaturated hydraulic conductivity as a function of moisture content. A simultaneous curve fitting approach, based on van Genuchten-Mualem relationships, is used to obtain the best-fit moisture retention and unsaturated hydraulic conductivity curves.

A.2.1 Van Genuchten-Mualem Relationships

A computer program, called RETC (van Genuchten et al. 1991), uses a nonlinear, least squares curve fitting routine to match the measured soil water retention data to the following equation:

$$\theta = \theta_r + \frac{(\theta_s - \theta_r)}{[1+(\alpha\varphi)^n]^m} \qquad \text{(A.1)}$$

where:

- θ = volumetric moisture content
- θ_s = saturated moisture content
- θ_r = residual moisture content
- α = van Genuchten Curve Fitting Parameter (1/cm)
- φ = Matric Potential (suction head (-cm))
- n = van Genuchten Curve Fitting Parameter
- m = 1 - 1/n.

Using Mualem's (1976) general model (equation 2) to predict the hydraulic conductivity from moisture retention data,

$$K(S_e) = K_s S_e^{\ell}\left[\frac{f(S_e)}{f(1)}\right]^2 \qquad \text{(A.2)}$$

$$\text{where} \qquad f(S_e) = \int_0^{S_e} \frac{1}{\varphi(x)}\,dx$$

where:

- $S_e = (\theta - \theta_r)/(\theta_s - \theta_r)$,
- ℓ = A pore-connectivity parameter estimated by Mualem (1976) to be about 0.5 as an average for many soils.

Equations A.2 and A.3 are from van Genuchten et al. (1991, p. 13).

Van Genuchten (1980) derived a closed form analytic solution to equation 1 to predict the relative hydraulic conductivity (K_r) by assuming m = 1 - 1/n at a specified volumetric moisture content. This solution is given in equation 3.

$$K_r = \left[\frac{(\theta-\theta_r)}{(\theta_s-\theta_r)}\right]^{1/2}\left\{1-\left[1-\left(\frac{(\theta-\theta_r)}{(\theta_s-\theta_r)}\right)^{1/m}\right]^m\right\}^2 \qquad \text{(A.3)}$$

Figure A-1. Cross Section A-A'.

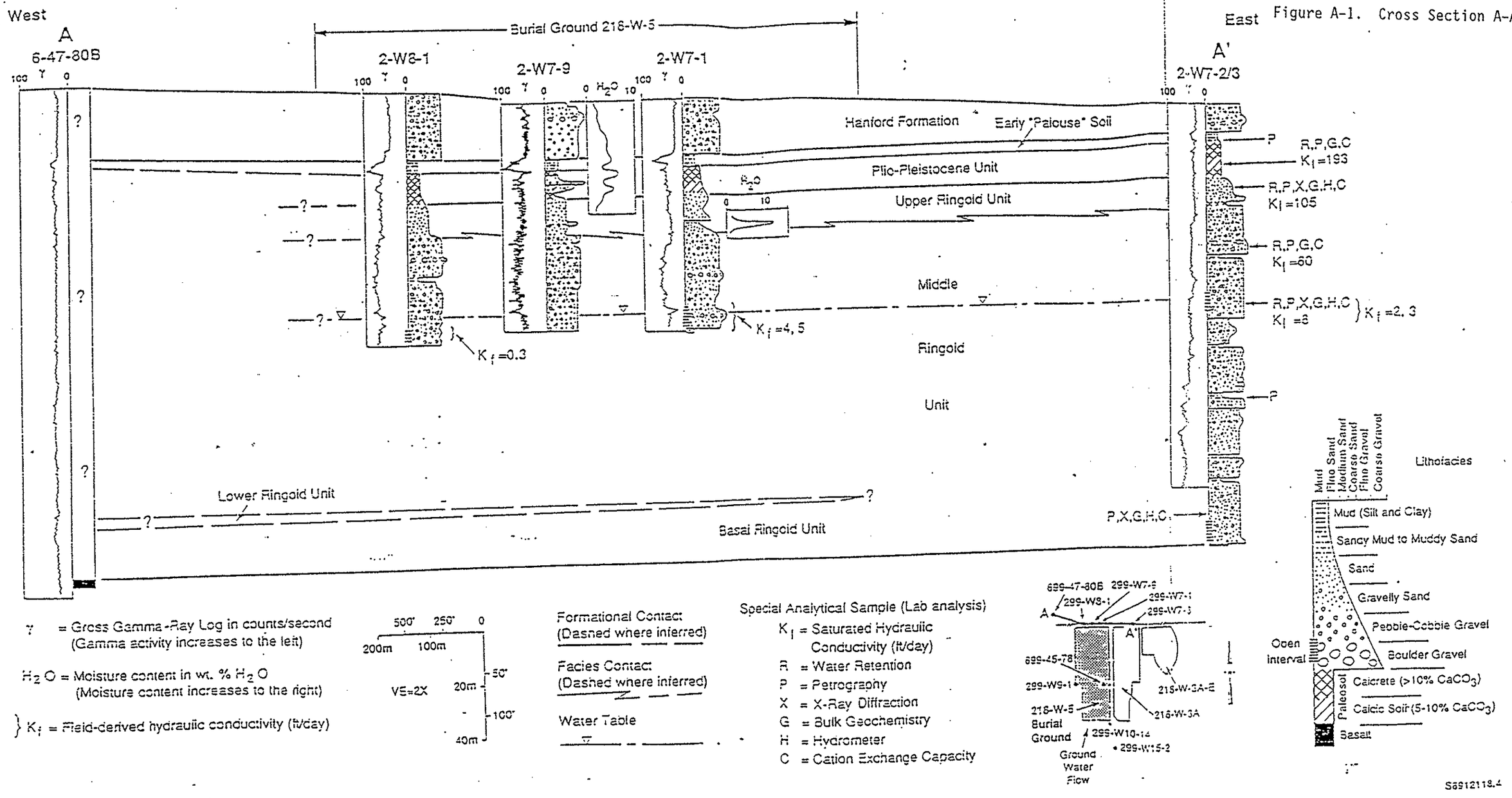

Figure A-2. Cross Section B-B'.

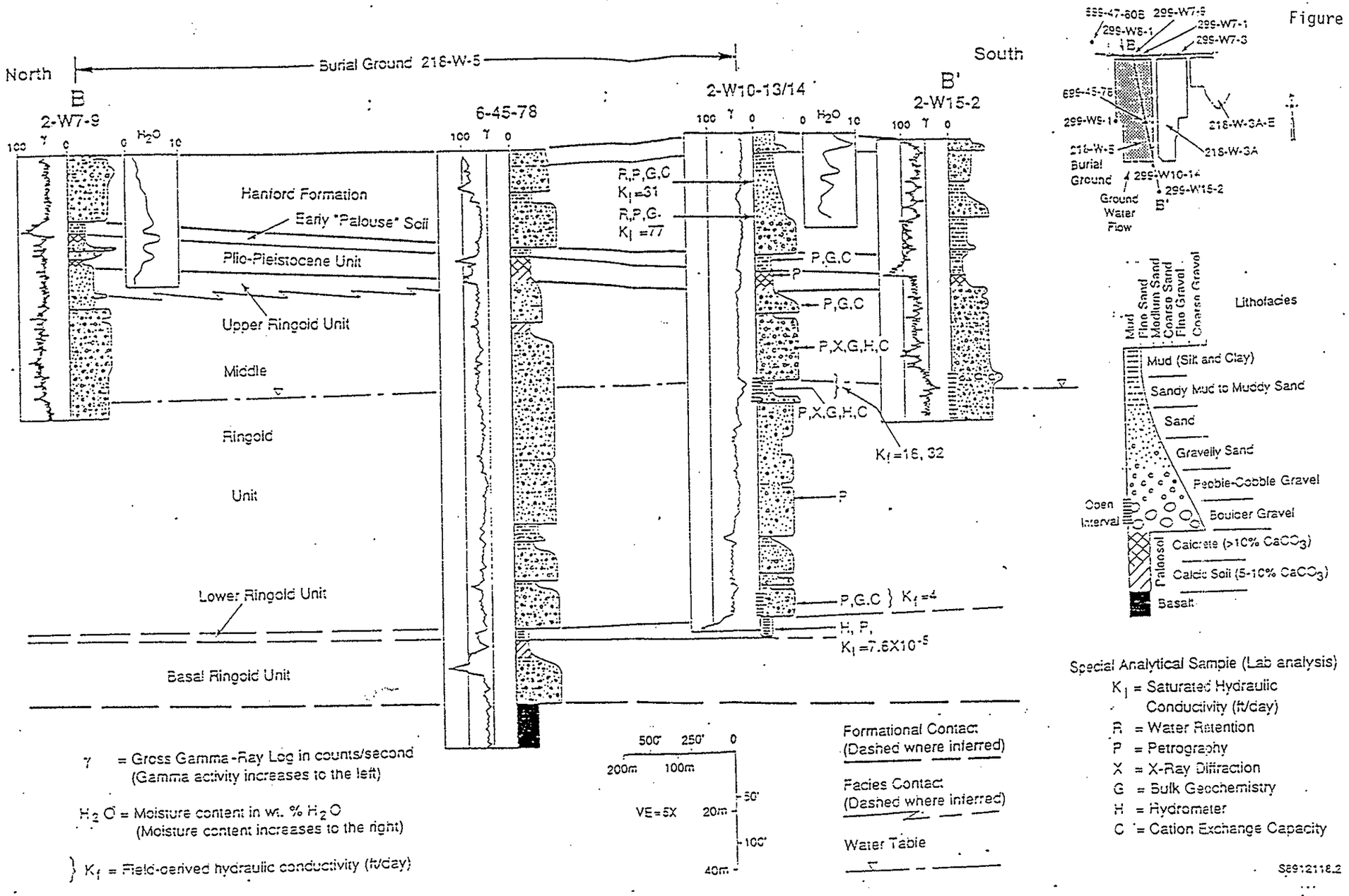

Figure A-3. Cross Section C-C'.

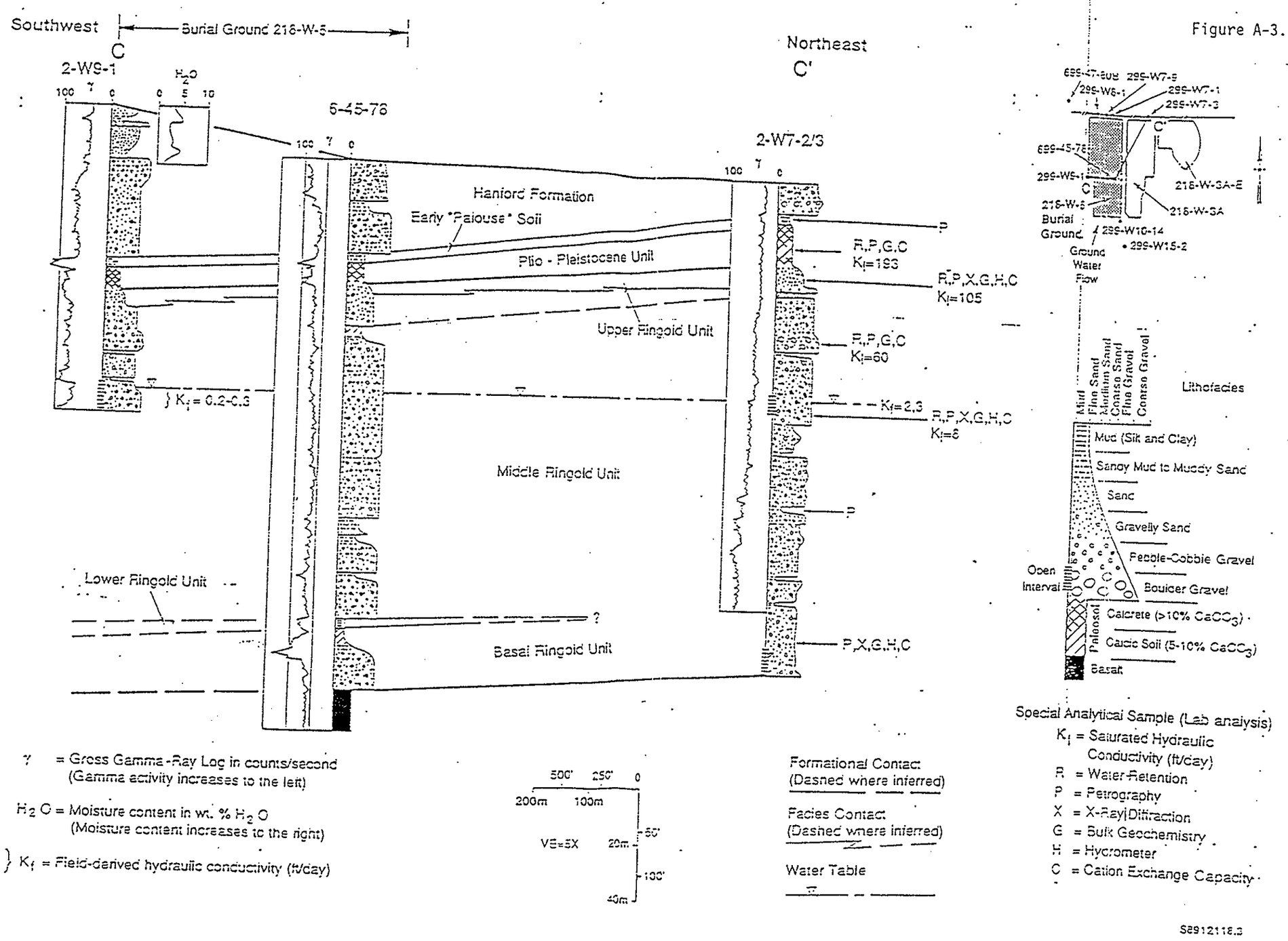

2.13

Figure A-4. Location of the 200 West Area Low-Level Waste Burial Grounds on the Isopach Maps (Modified from Connelly et al. 1992).

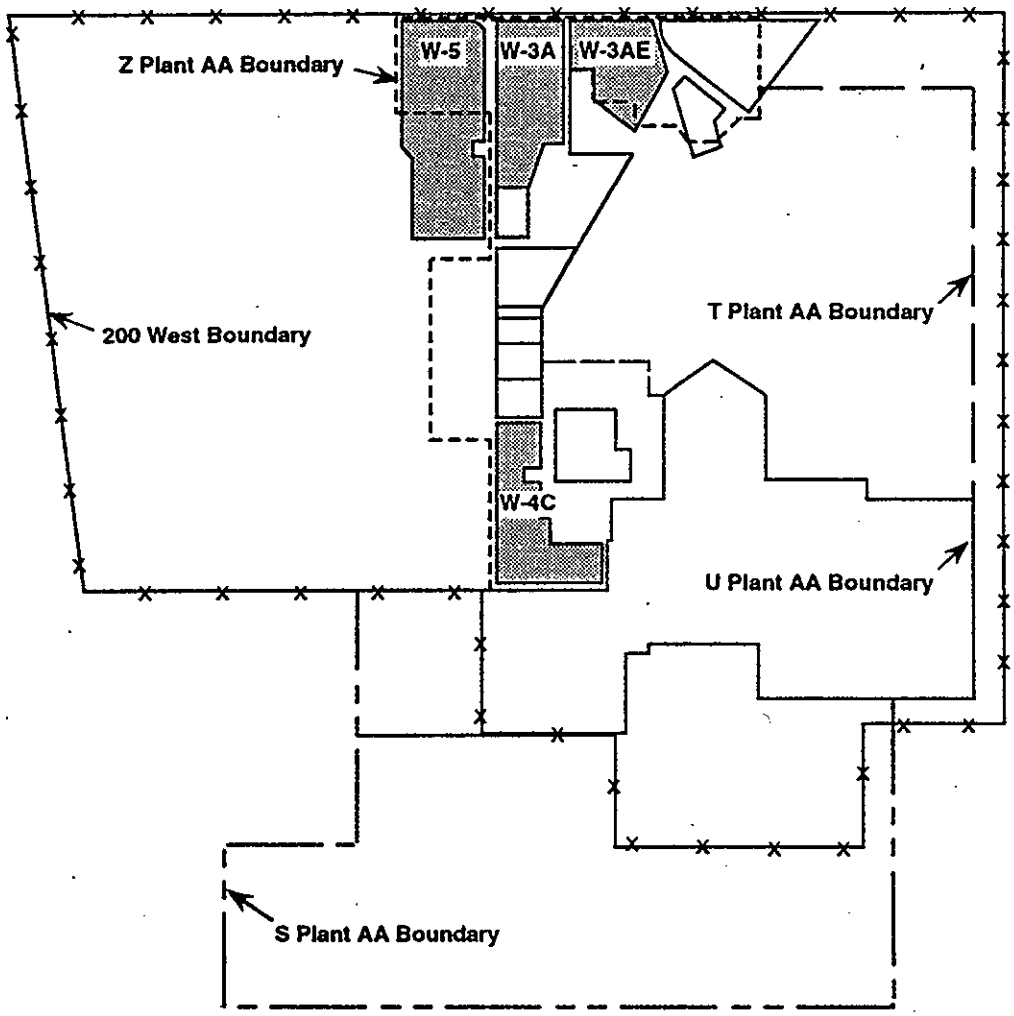

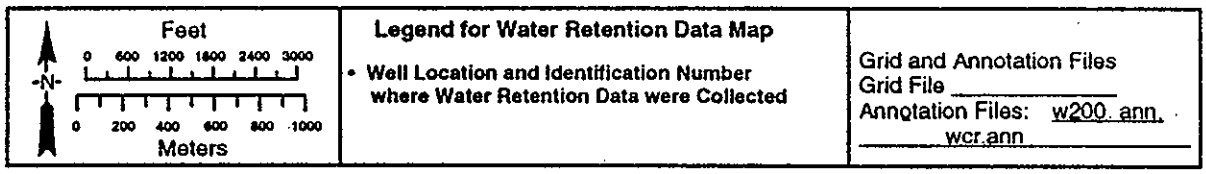

875-MLH-00200.1/94

Figure A-5. Isopach Map of the Hanford Formation (HC) (Connelly et al. 1992).

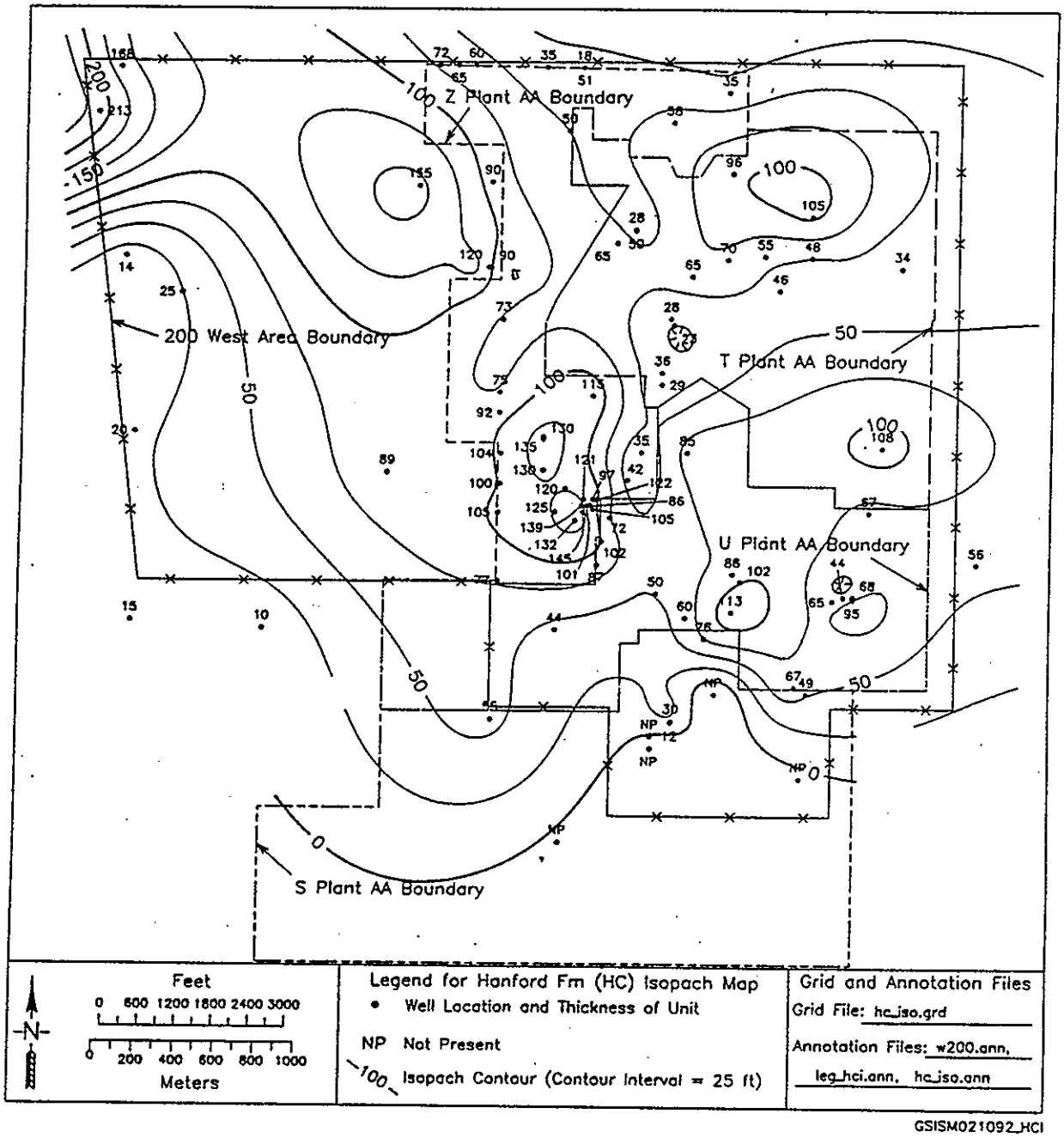

Figure A-6. Isopach Map of the Hanford Formation (HSZ) (Connelly et al. 1992).

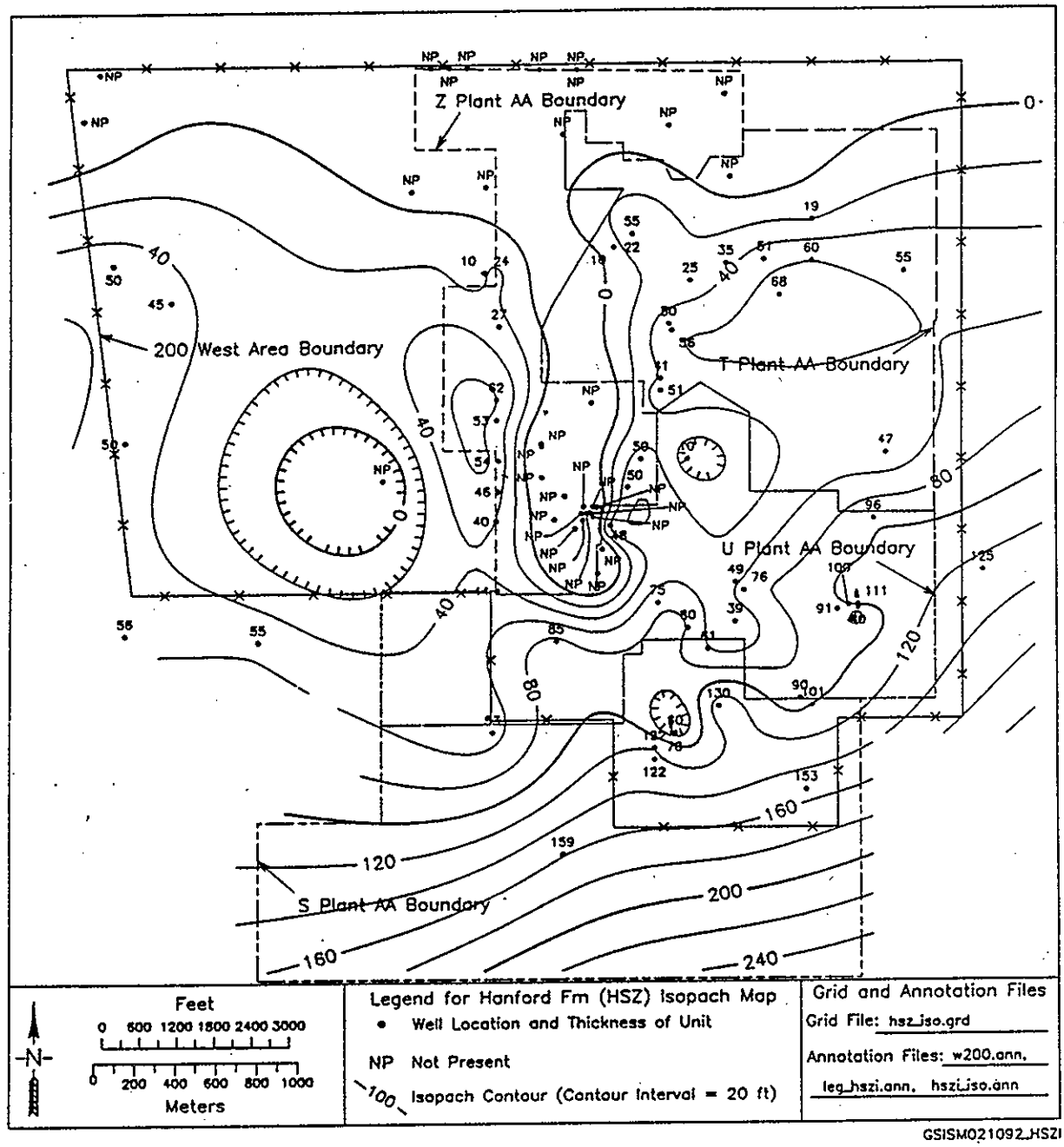

Figure A-7. Isopach Map of the Early "Palouse" Soils (Connelly et al. 1992).

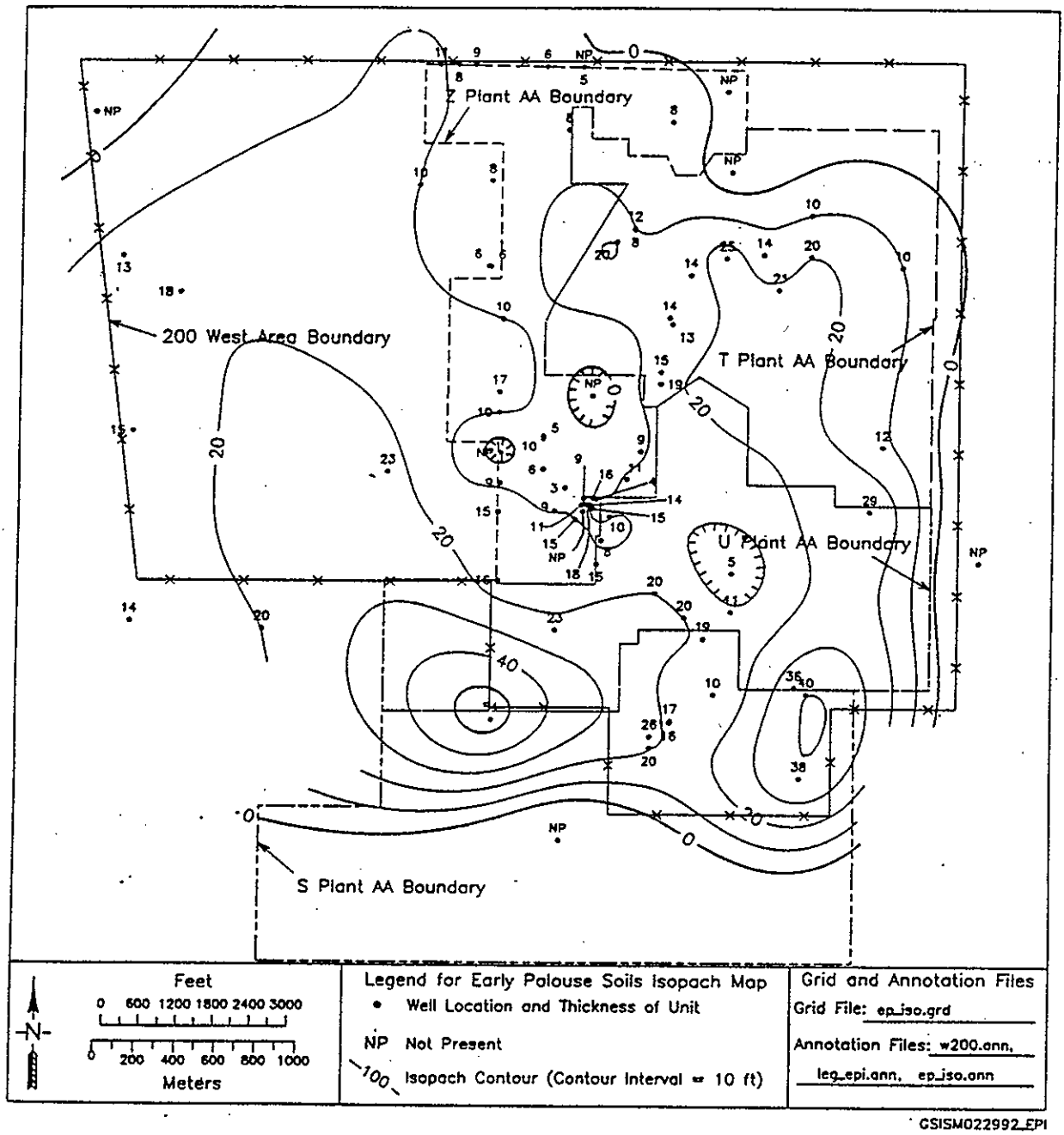

Figure A-8. Isopach Map of the Plio-Pleistocene Unit (Connelly et al. 1992).

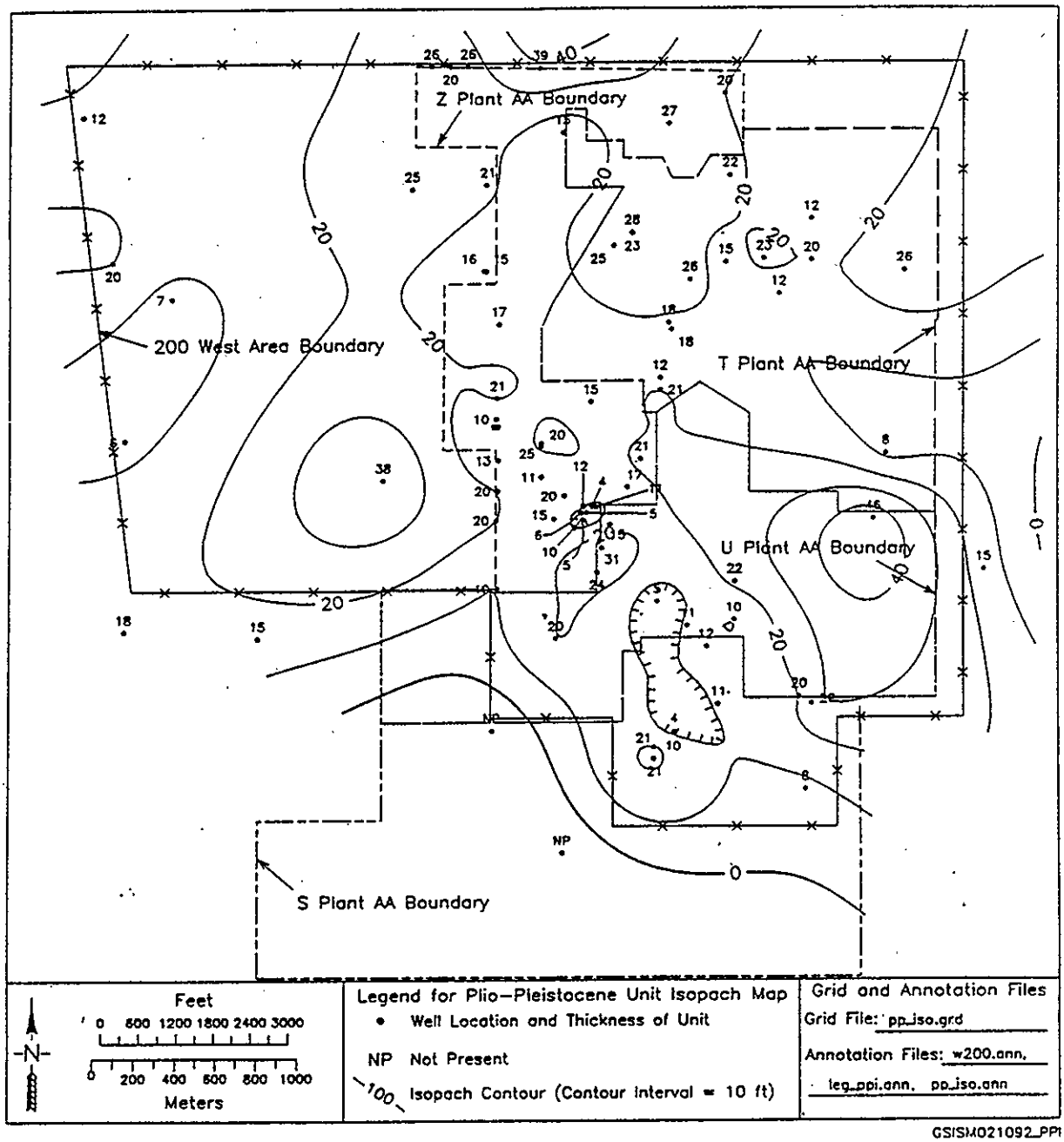

Figure A-9. Isopach Map of the Upper Ringold (Connelly et al. 1992).

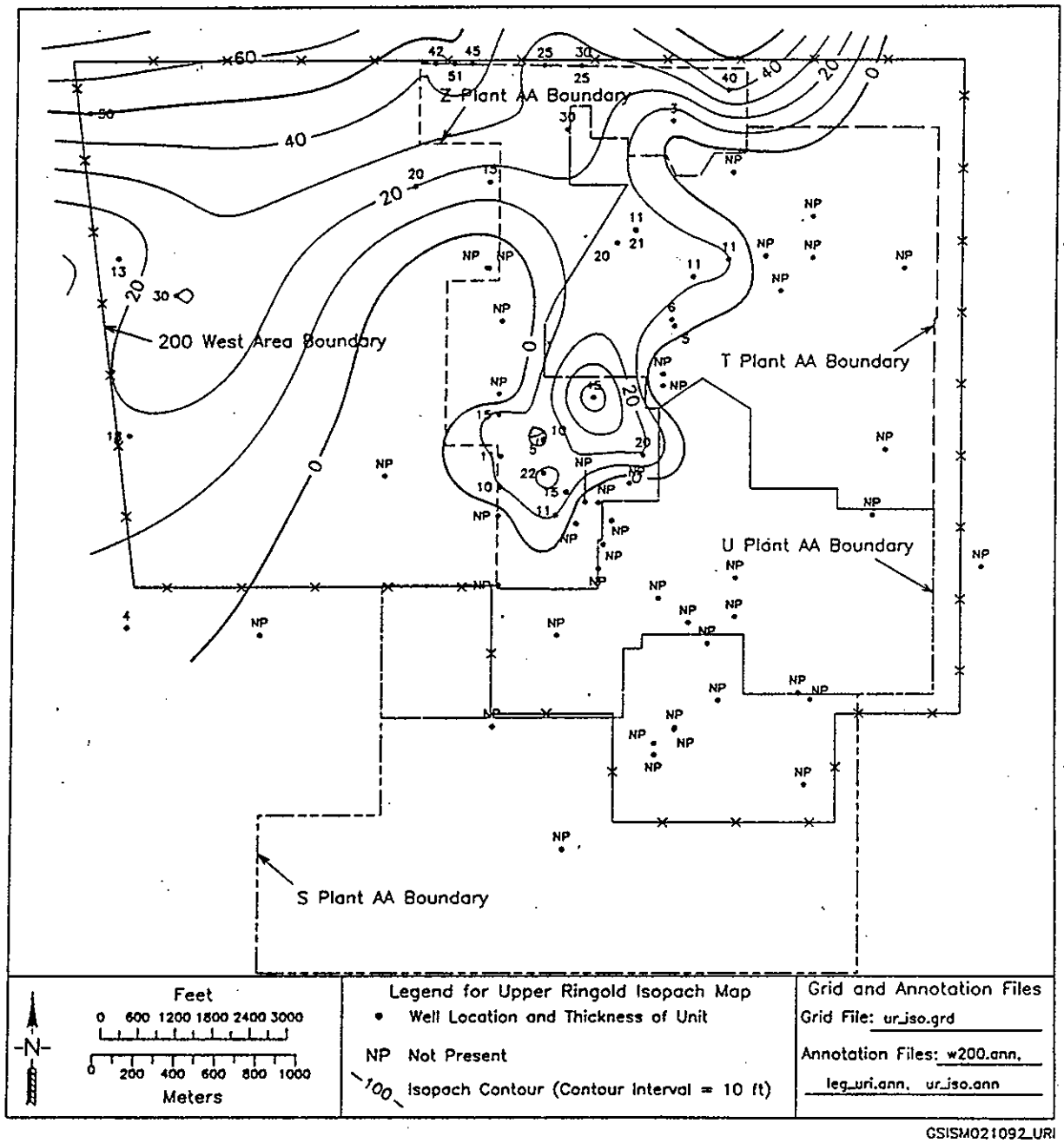

Figure A-10. Isopach Map of Ringold Unit E (Connelly et al. 1992).

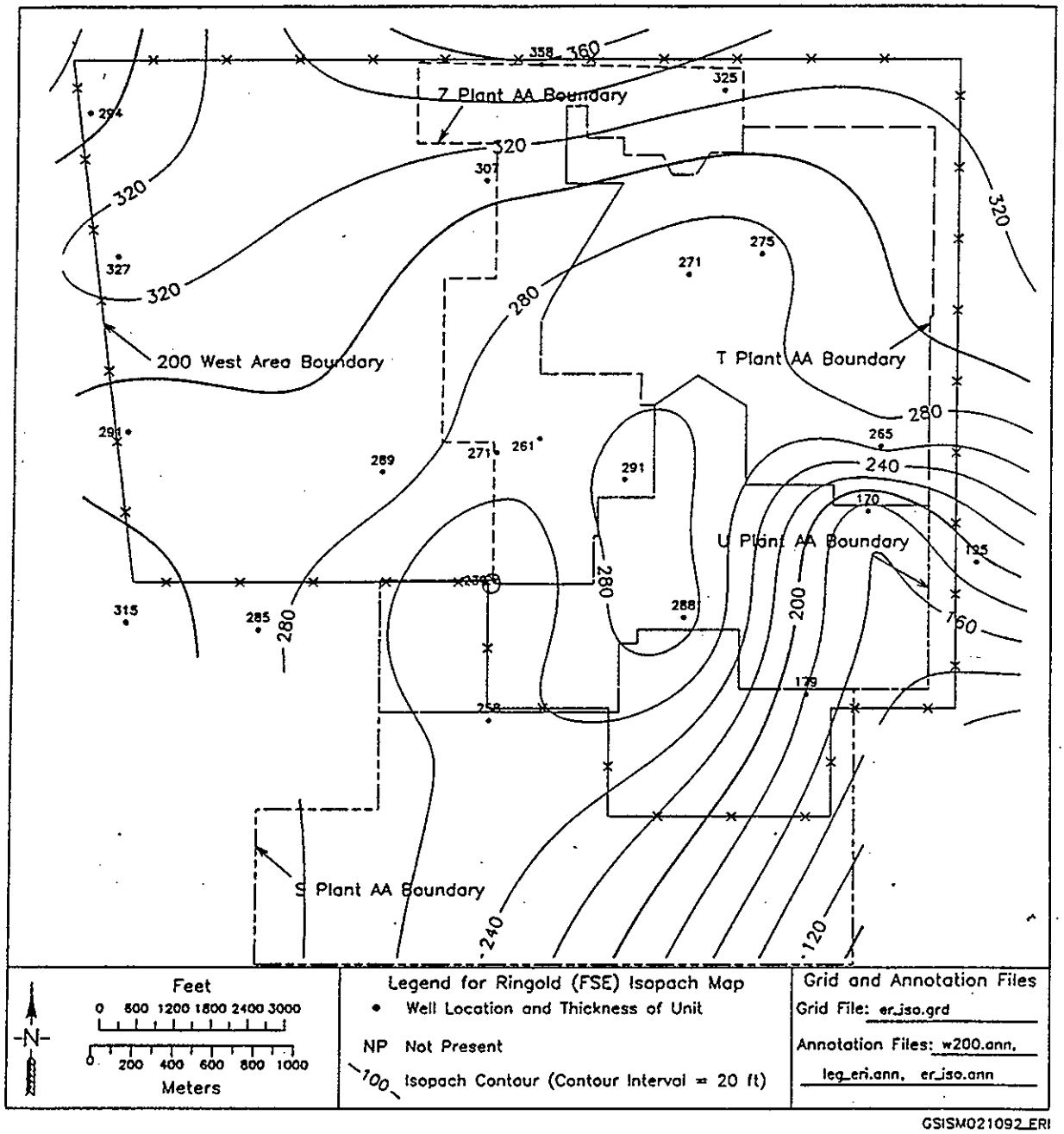

Figure A-11. Tritium Plume In the Unconfined Aquifer Underlying the 200 West Area (Connelly et al. 1992).

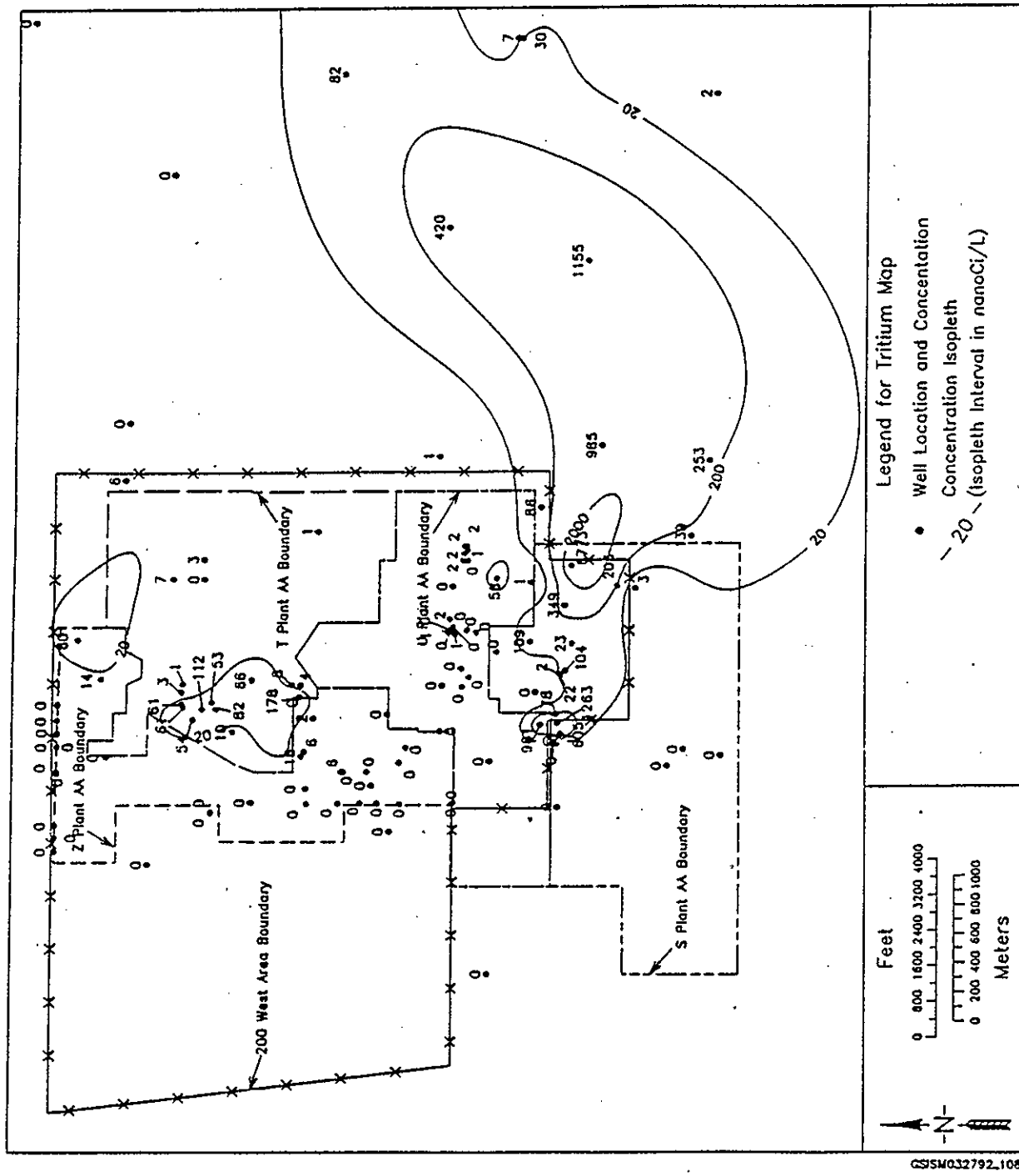

Figure A-12. Technetium-99 Plume In the Unconfined Aquifer Underlying the 200 West Area (Connelly et al. 1992).

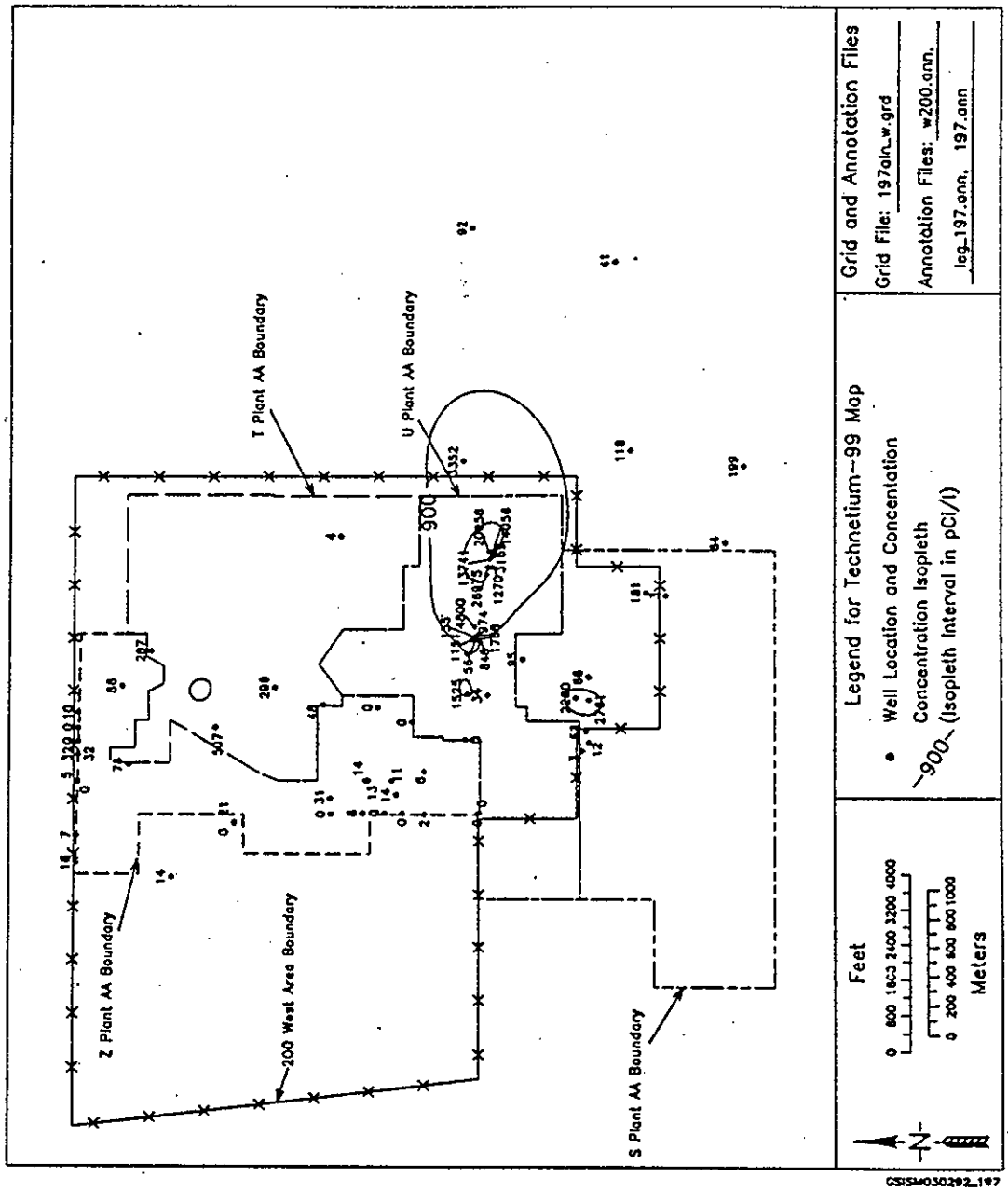

Figure A-13. Uranium Plume In the Unconfined Aquifer Underlying the 200 West Area (Connelly et al. 1992).

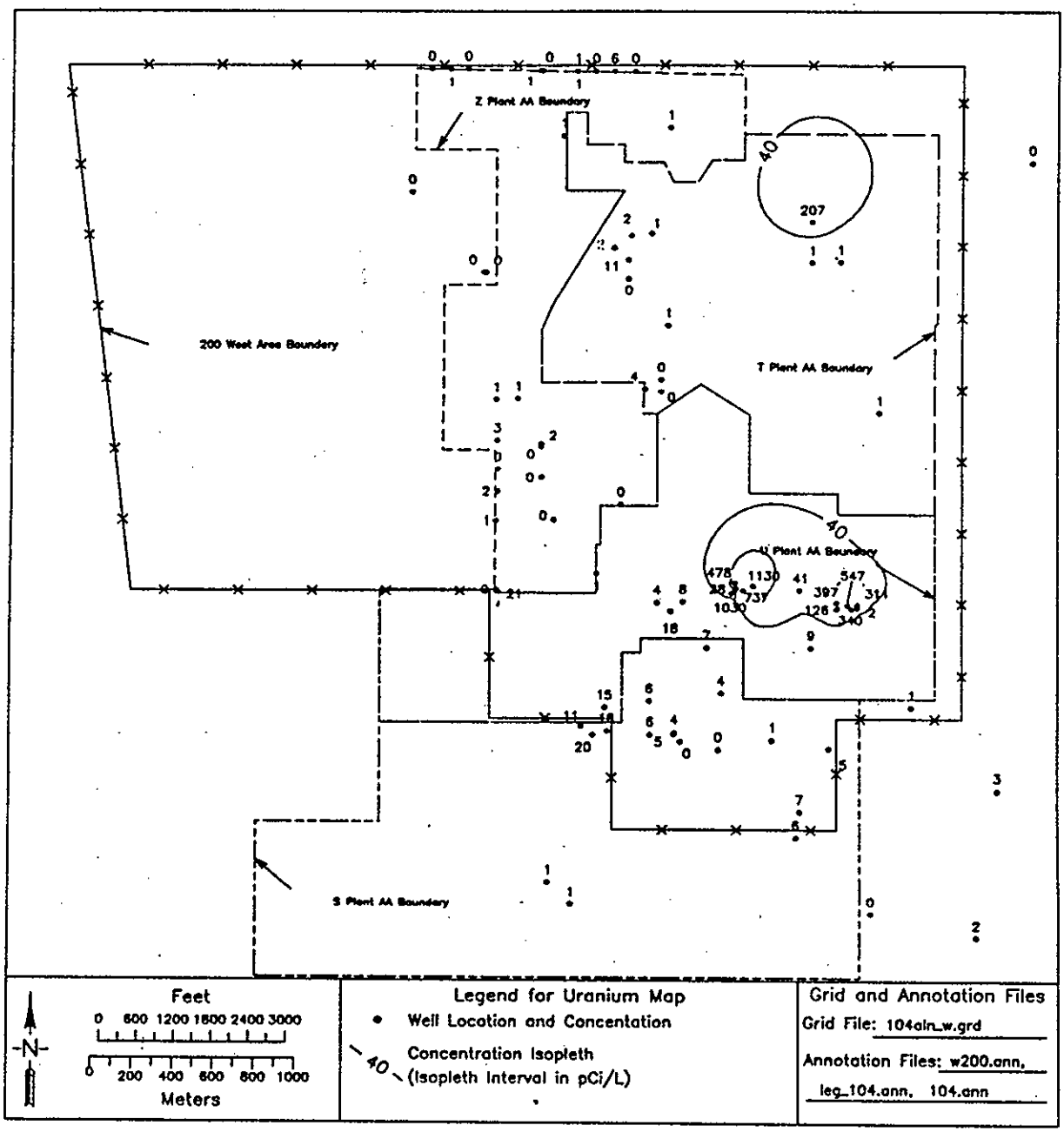

Figure A-14. Plutonium Plume In the Unconfined Aquifer Underlying the 200 West Area (Connelly et al. 1992).

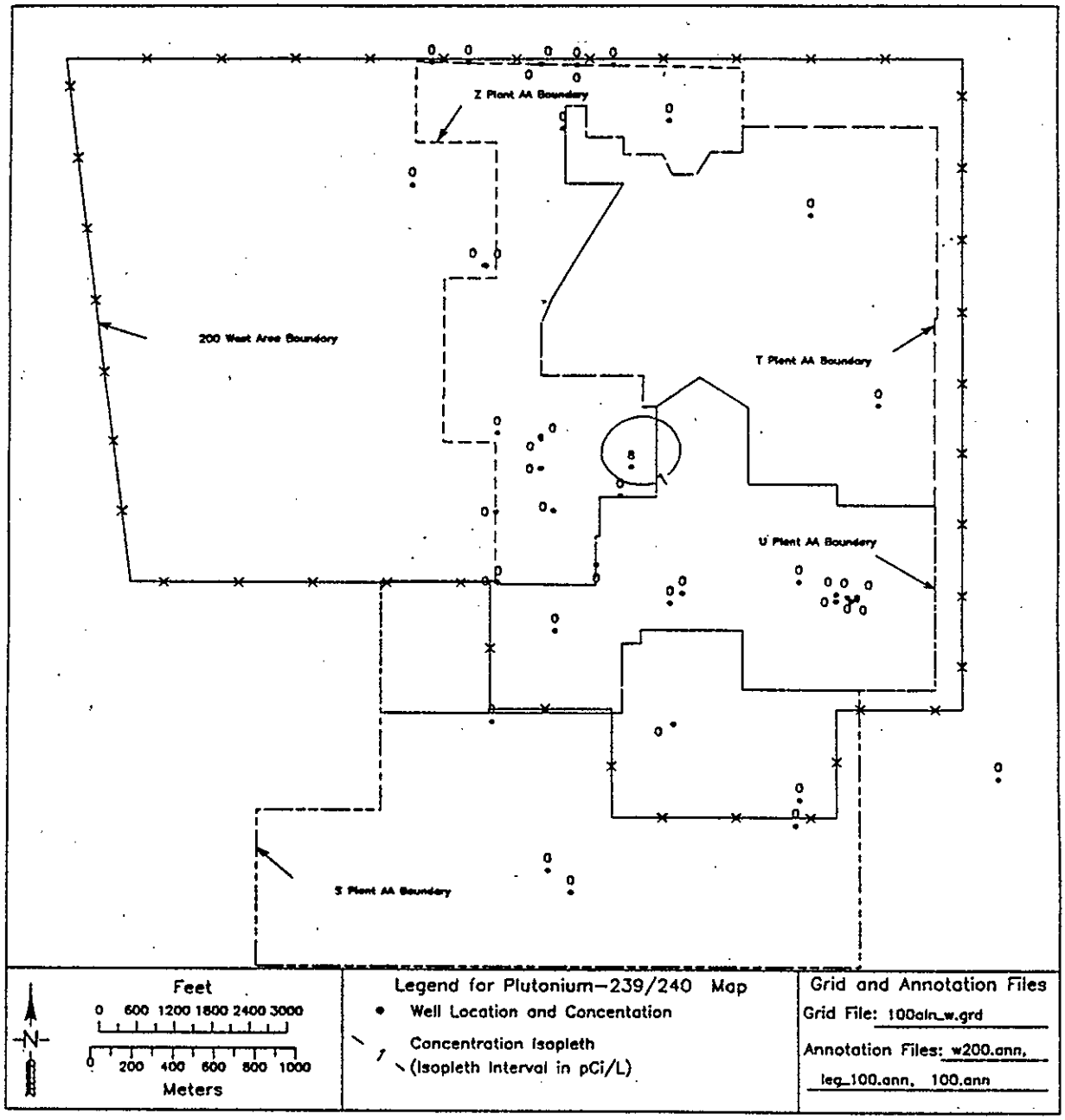

Figure A-15. Iodine-129 Plume In the Unconfined Aquifer Underlying the 200 West Area (Connelly et al. 1992).

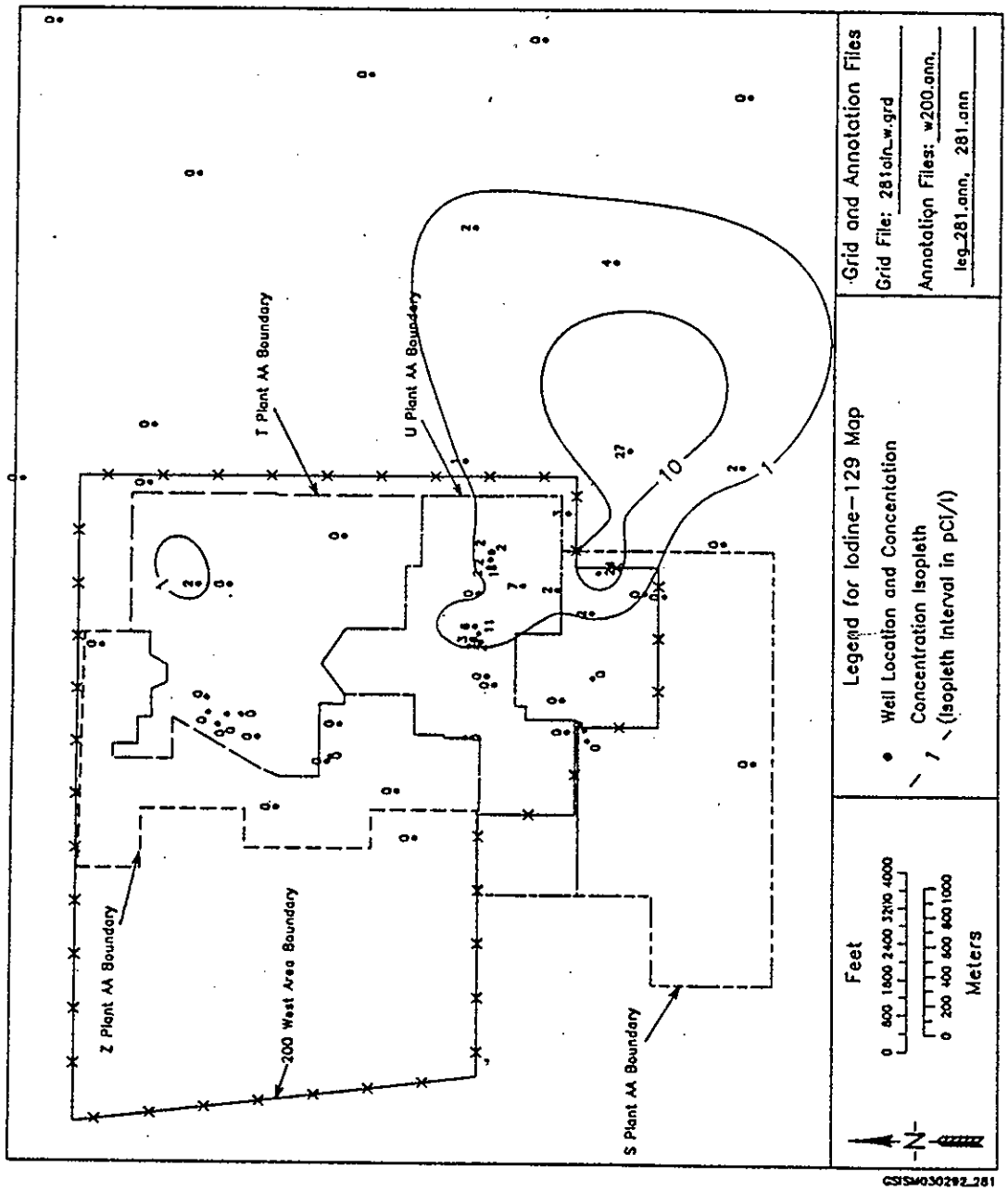

The unsaturated hydraulic conductivity at a specified moisture content is:

$$K(\theta) = K_{(sat)} * K_r \qquad \text{(A.4)}$$

Saturated hydraulic conductivities for each of the samples were measured in the laboratory using a permeameter.

A number of samples from a continuous core of borehole 299-W7-9 within the Burial Trench 218-W-5 was analyzed to generate the moisture characteristic curves for W-5 soils. The moisture retention data were obtained in February and March of 1990 and again in April and May of 1992. The drying curves were measured in tempe cells to one bar in 1990. The rest of the drying curve was measured in 1992 using pressure kettles. The detailed laboratory methods of measurements of moisture retention data are described in WHC-IP-0635, *Geological Engineering Laboratory Procedures Manual* (WHC 1990).

A.2.2 Unsaturated Hydraulic Conductivity Measurements

When measuring unsaturated hydraulic conductivity, conventional methods of investigation require very long times to attain homogeneous distributions of water contents, because normal gravity does not provide a large enough driving force relative to the low hydraulic conductivities that characterize unsaturated conditions. An unsaturated flow apparatus (UFA™), based on the centrifuge technique, was used to measure the unsaturated hydraulic conductivities (Conca and Wright 1990).

The unsaturated flow apparatus used consists of an ultracentrifuge with an ultralow constant-rate flow pump that provides liquid to the sample surface through a rotating seal assembly and microdispersal system (see Figure 1; Conca and Wright 1990). Accelerations up to 20,000 g are attainable at temperatures from 0 to 150 °C and flow rates as low as 0.1 mL/h. The effluent is collected in a transparent, volumetrically calibrated container at the bottom of the sample assembly which can be observed during centrifugation using a strobe light. The maximum sample volume allowed is 40 cm^3.

Under a centripetal acceleration in which the water is driven by both the matric potential and the centrifugal force per unit volume, $\rho\omega^2 r$, Darcy's Law is given by:

$$q = -K(\psi)\ [d\psi/dr - \rho\omega^2 r] \qquad \text{(A.5)}$$

where:

- q = The flux density into the sample
- K = The hydraulic conductivity, which is a function of the matric suction (ψ) and therefore of water content (θ)
- r = The radius from the axis of rotation
- ρ = The fluid density
- ω = The rotation speed.

Appropriate values of rotation speed and flow rate into the sample are chosen to obtain desired values of flux density, water content, and hydraulic conductivity within the sample. At speeds above about 300 rpm, provided that sufficient flux density exists, $d\psi/dr << \rho\omega^2 r$ and equation 1a reduces to $q = K(\psi)\ [\rho\omega^2 r]$, or

$$K(\psi) = q/\rho\omega^2 r \tag{A.6}$$

A.2.3 Results

Two methods of parameter estimation were used to analyze the laboratory-measured data on moisture retention and unsaturated hydraulic conductivity: (1) predictive method and (2) simultaneous fitting with five parameters. For the predictive method, the laboratory-measured saturated conductivity, K_s, was fixed at its measured value and the pore parameter ℓ was fixed at 0.5; θ_r, θ_s, α, n, with m = 1-1/n, were fitted to the moisture retention data. For simultaneous fitting with five parameters, all five unknown parameters θ_r, θ_s, α, n, and K_s, with m = 1-1/n, were fitted to the data.

As expected, for the predictive method, excellent agreement was obtained between the observed and fitted moisture retention curves. Although not shown here, to the contrary, the predicted unsaturated hydraulic conductivities, based on the fitted moisture retention curves and measured K_s, deviated considerably from the measured K data. Since excellent agreement was observed between the measured and fitted van Genuchten moisture retention curves, disagreement between the measured and predicted K's cannot be ascribed to the inability to match the experimental moisture retention data.

Figures A-16 through A-28 show a comparison of measured and fitted data for moisture retention and unsaturated K's, using the simultaneous fitting (five parameters). Although saturated conductivity values were obtained in the laboratory for the samples analyzed in this study, the value for K_s is frequently ill-defined and difficult to measure accurately (van Genuchten et al. 1991). Therefore, it is appropriate to use the laboratory-measured K_s as an empirical, curve-fitting parameter. The same is true for the saturated water content, θ_s, which is best regarded as an empirical parameter to be used in the context of a specific moisture retention curve, and hence was fitted to observed data (van Genuchten et al. 1991). The solid squares on the figures represent the laboratory measurements and the solid lines represent the fitted curves. A measure of the agreement between the laboratory data and van Genuchten-Mualem fitted curves is provided by the coefficient of determination or r^2 value; an r^2 value of close to unity suggesting an excellent agreement between the measured and fitted data. As indicated in Figures A-16 through A-28, the r^2 values, for all samples, are close to 0.99 or higher. The measured data on hydraulic conductivities are within one-half of an order of magnitude of the fitted curve for nearly all data. An exception is sample 0-104 where one measured point near saturation is off from the fitted curve by about two orders of magnitude.

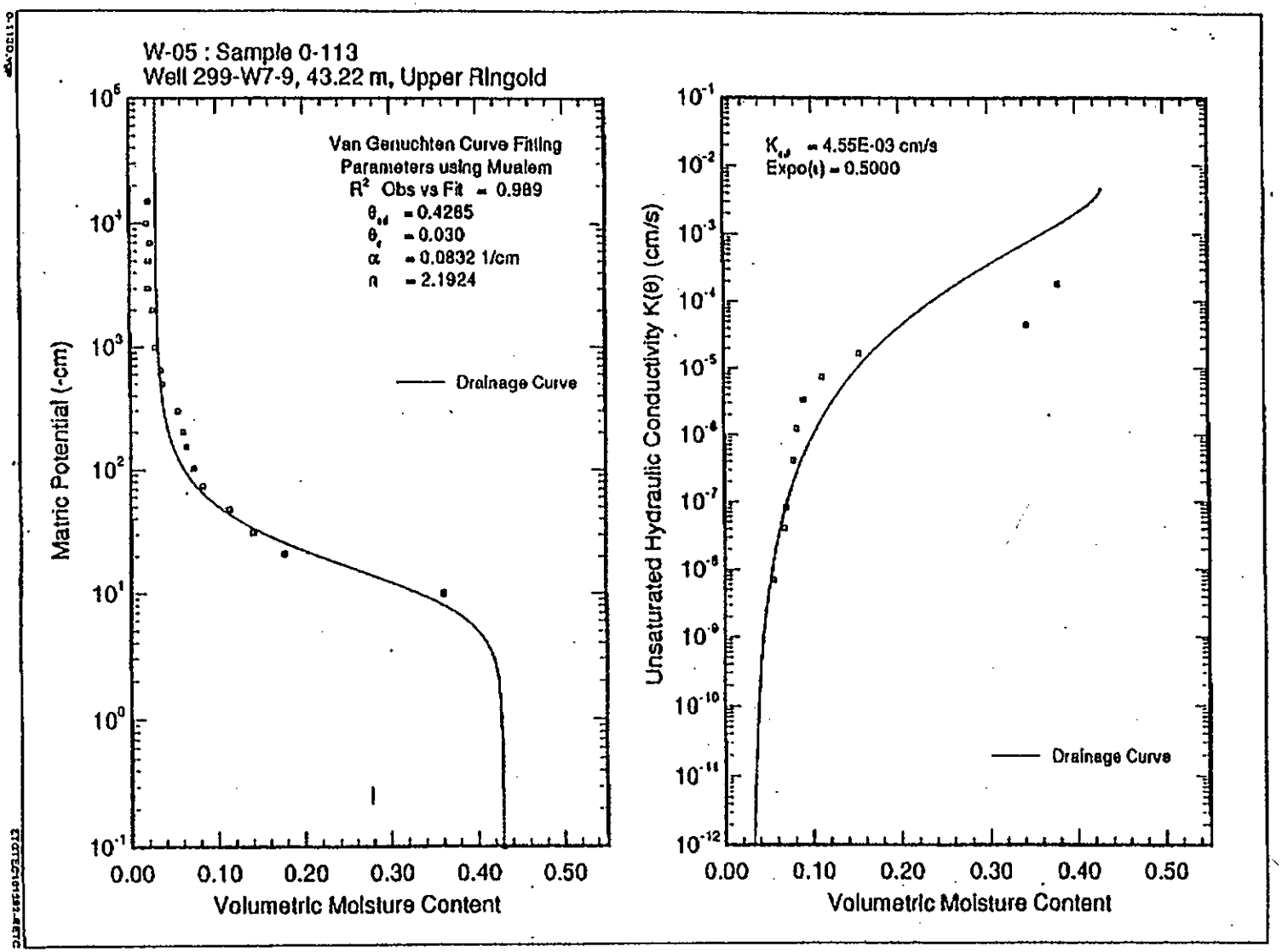

Figure A-16. Moisture Retention Curve and Calculated Hydraulic Conductivity Values for Sample 0-113.

Figure A-17. Moisture Retention Curve and Calculated Hydraulic Conductivity Values for Sample 0-107.

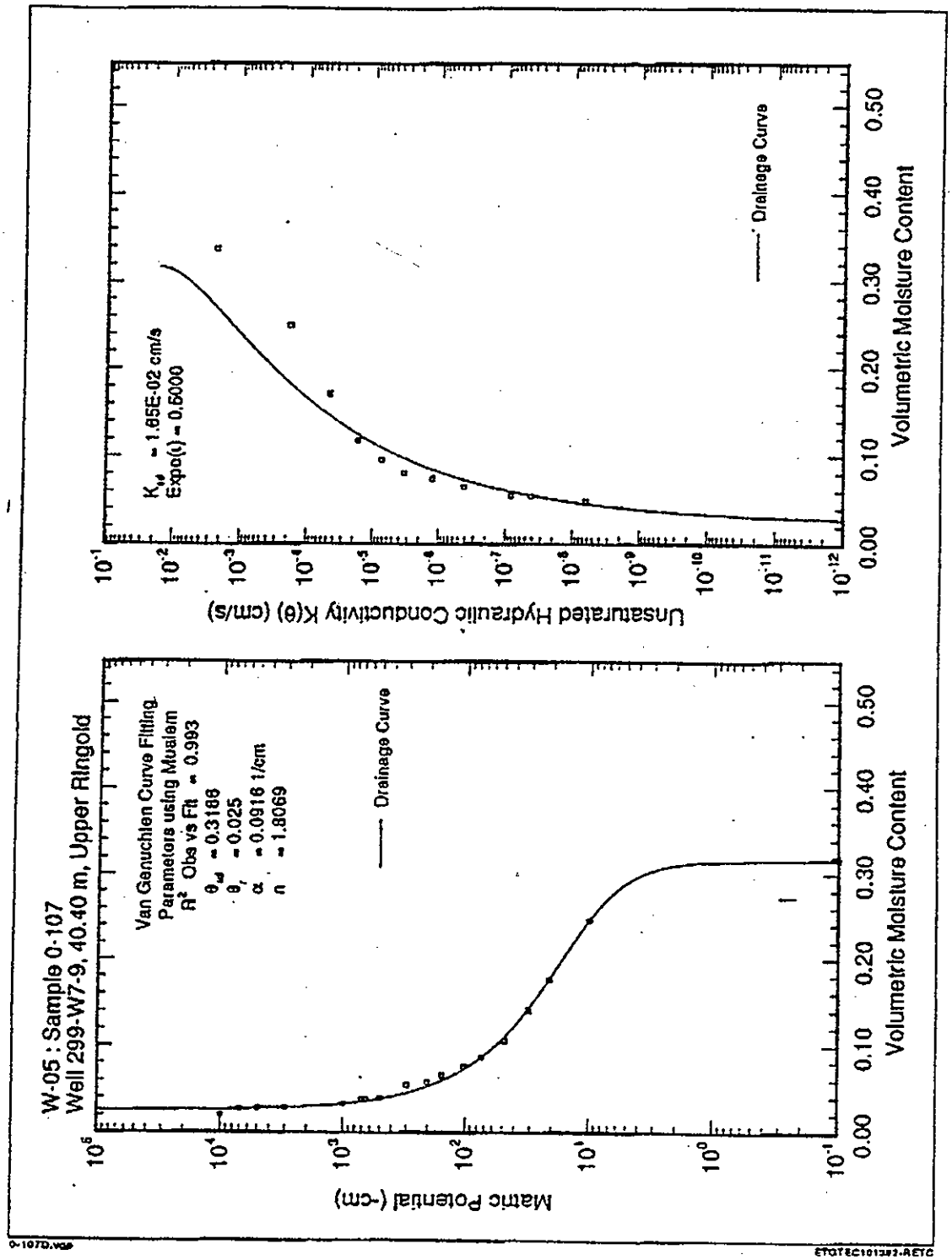

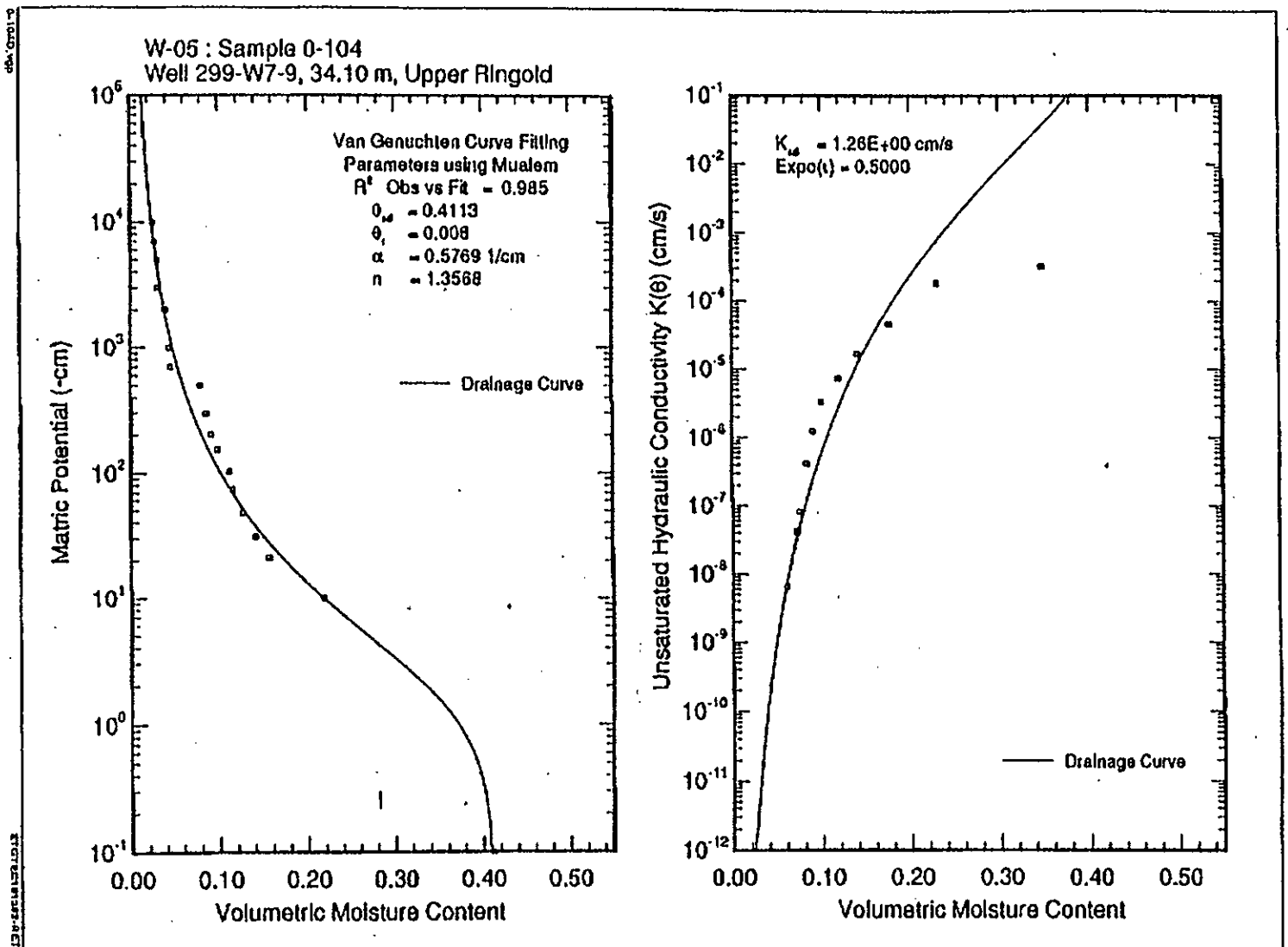

Figure A-18. Moisture Retention Curve and Calculated Hydraulic Conductivity Values for Sample 0-104.

Figure A-19. Moisture Retention Curve and Calculated Hydraulic Conductivity Values for Sample 0-101.

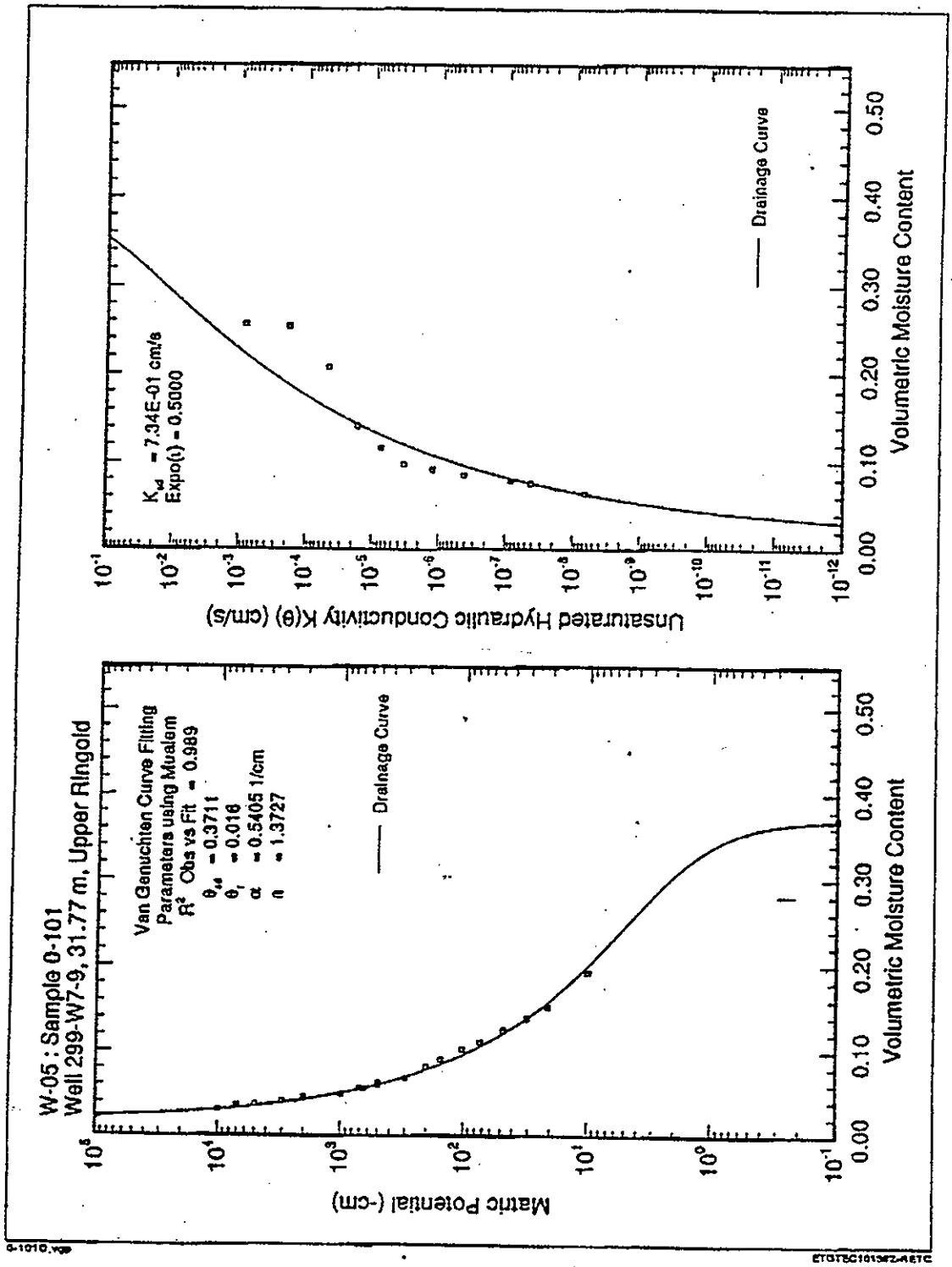

Figure A-20. Moisture Retention Curve and Calculated Hydraulic Conductivity Values for Sample 0-099.

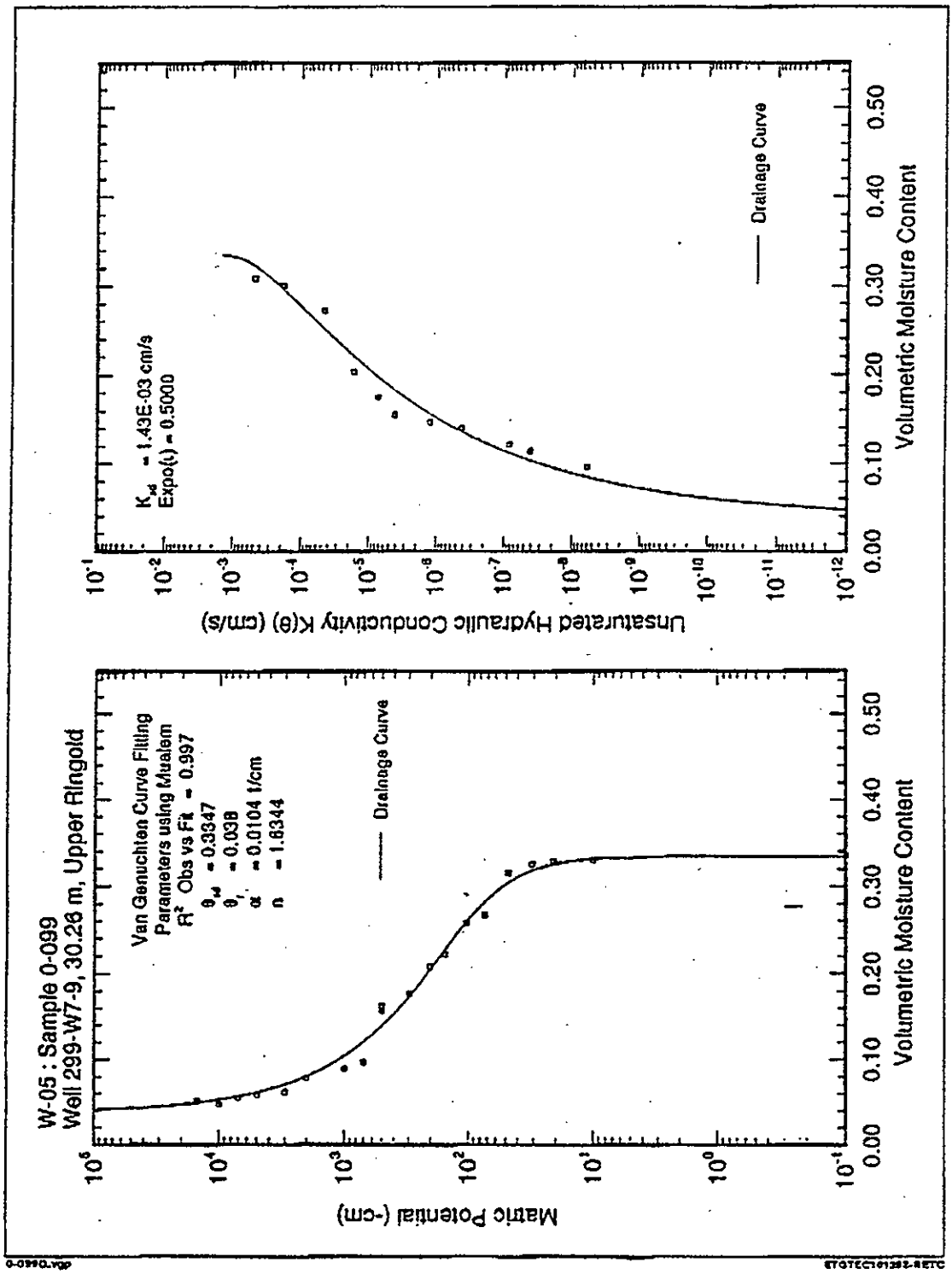

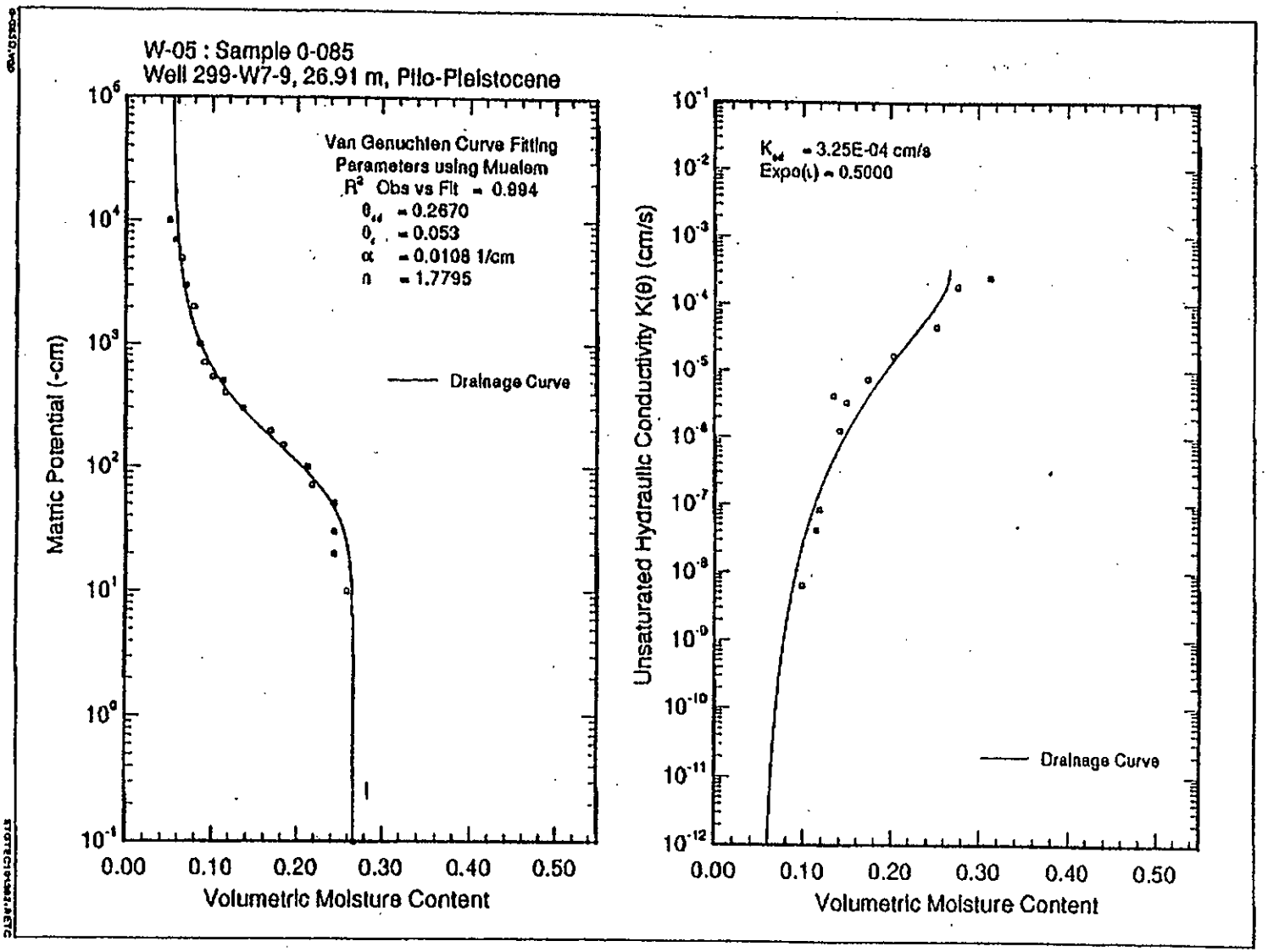

Figure A-21. Moisture Retention Curve and Calculated Hydraulic Conductivity Values for Sample 0-085.

Figure A-22. Moisture Retention Curve and Calculated Hydraulic Conductivity Values for Sample 0-083.

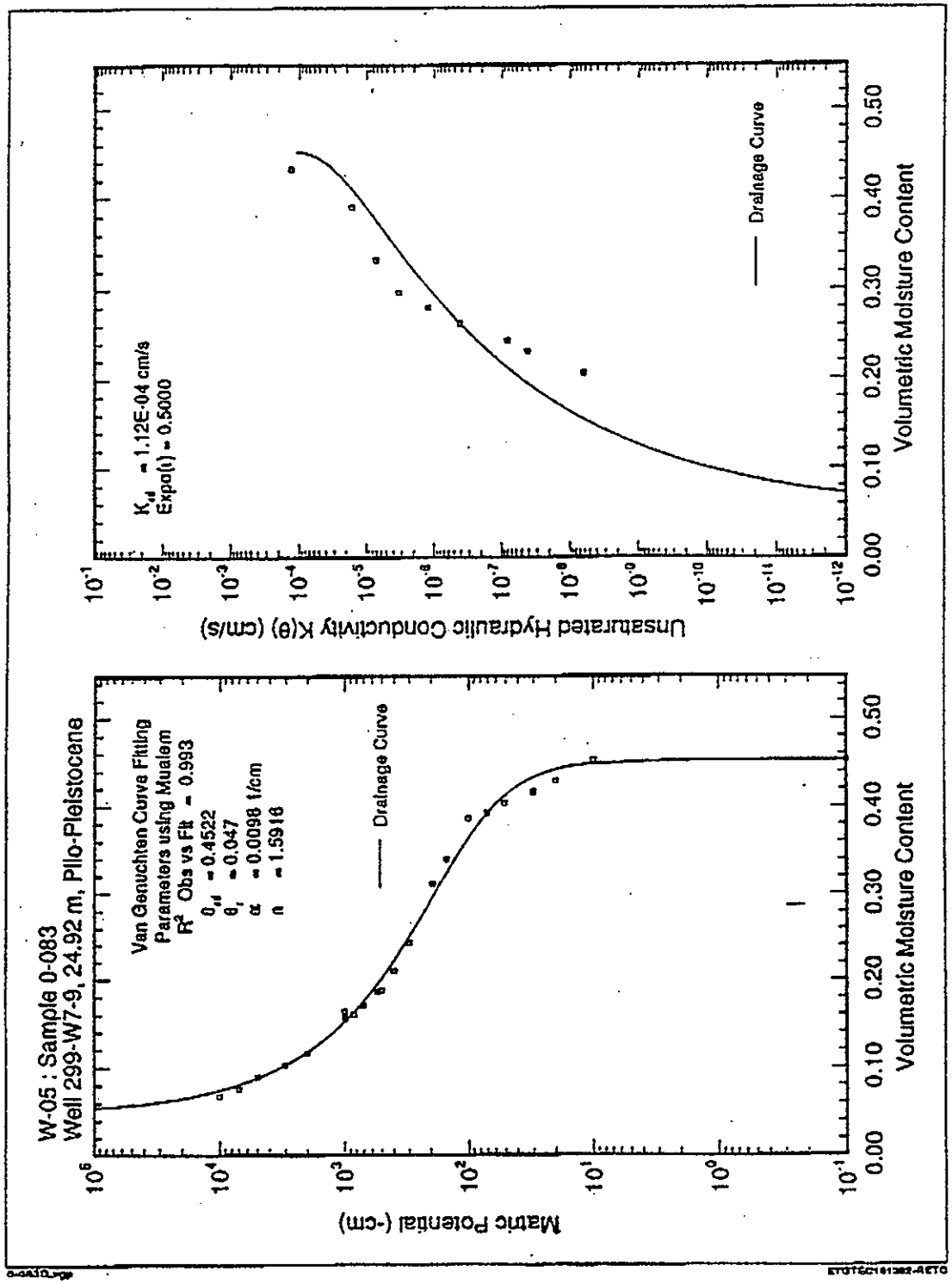

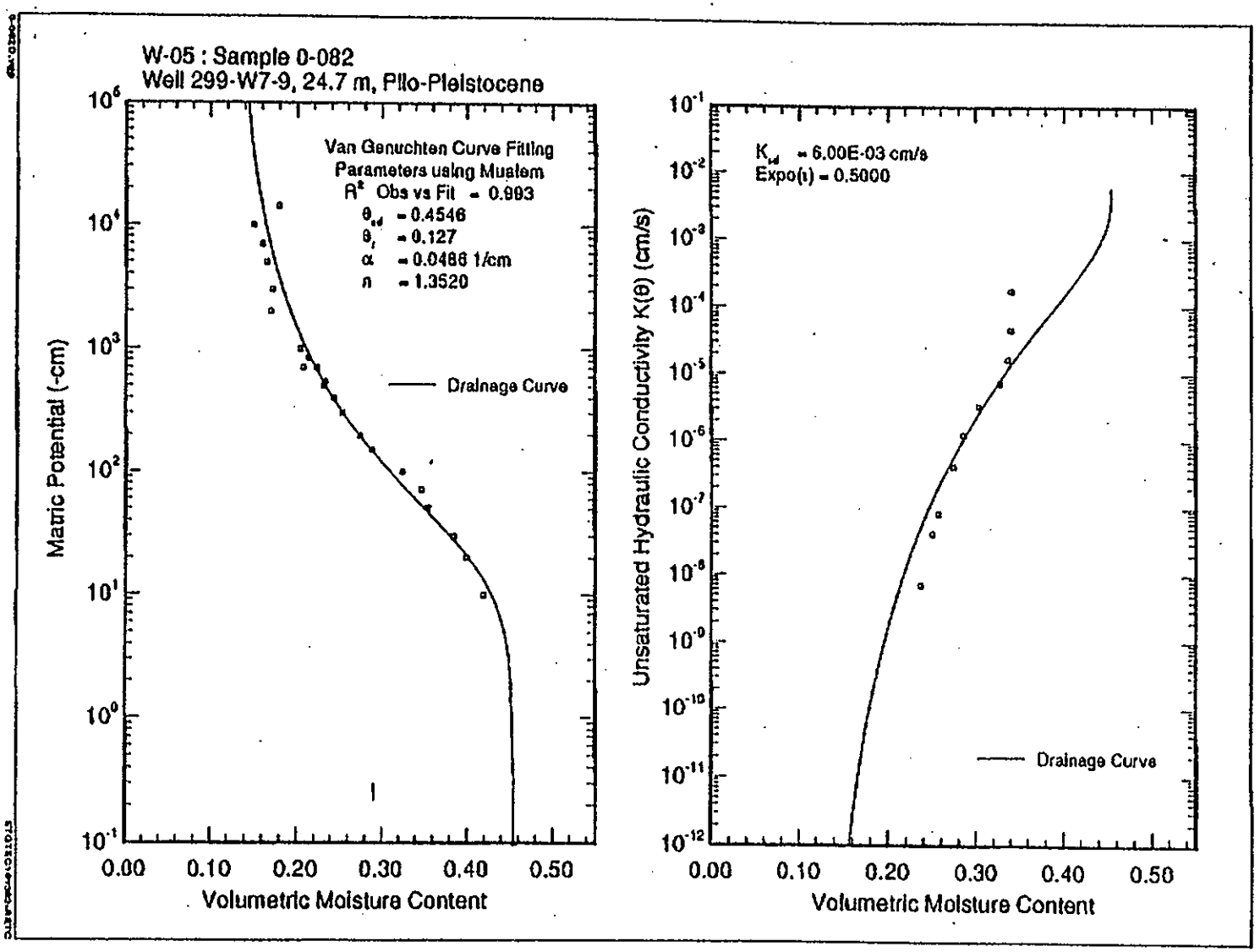

Figure A-23. Moisture Retention Curve and Calculated Hydraulic Conductivity Values for Sample 0-082.

Figure A-24. Moisture Retention Curve and Calculated Hydraulic Conductivity Values for Sample 0-080.

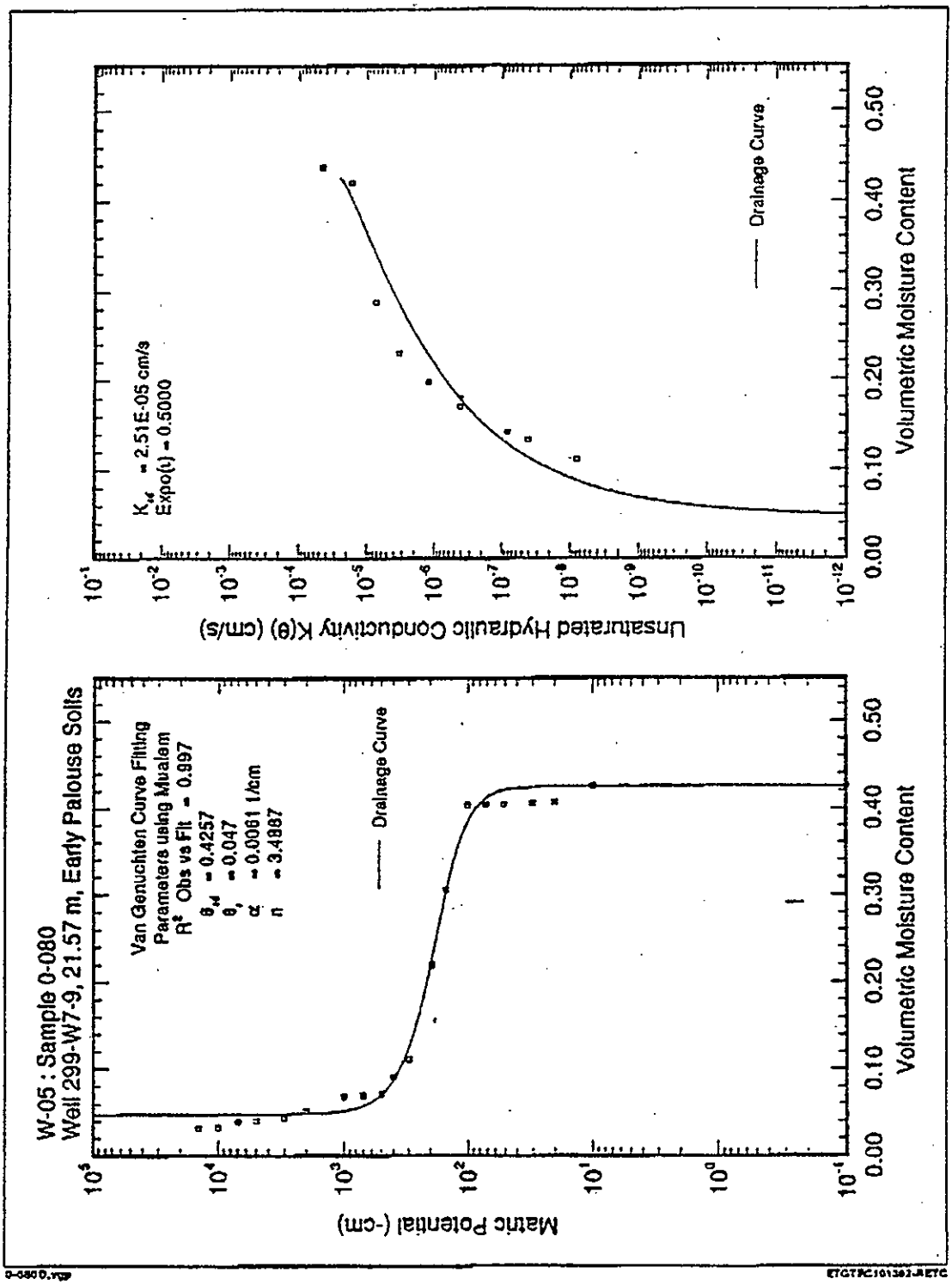

Figure A-25. Moisture Retention Curve and Calculated Hydraulic Conductivity Values for Sample 0-079.

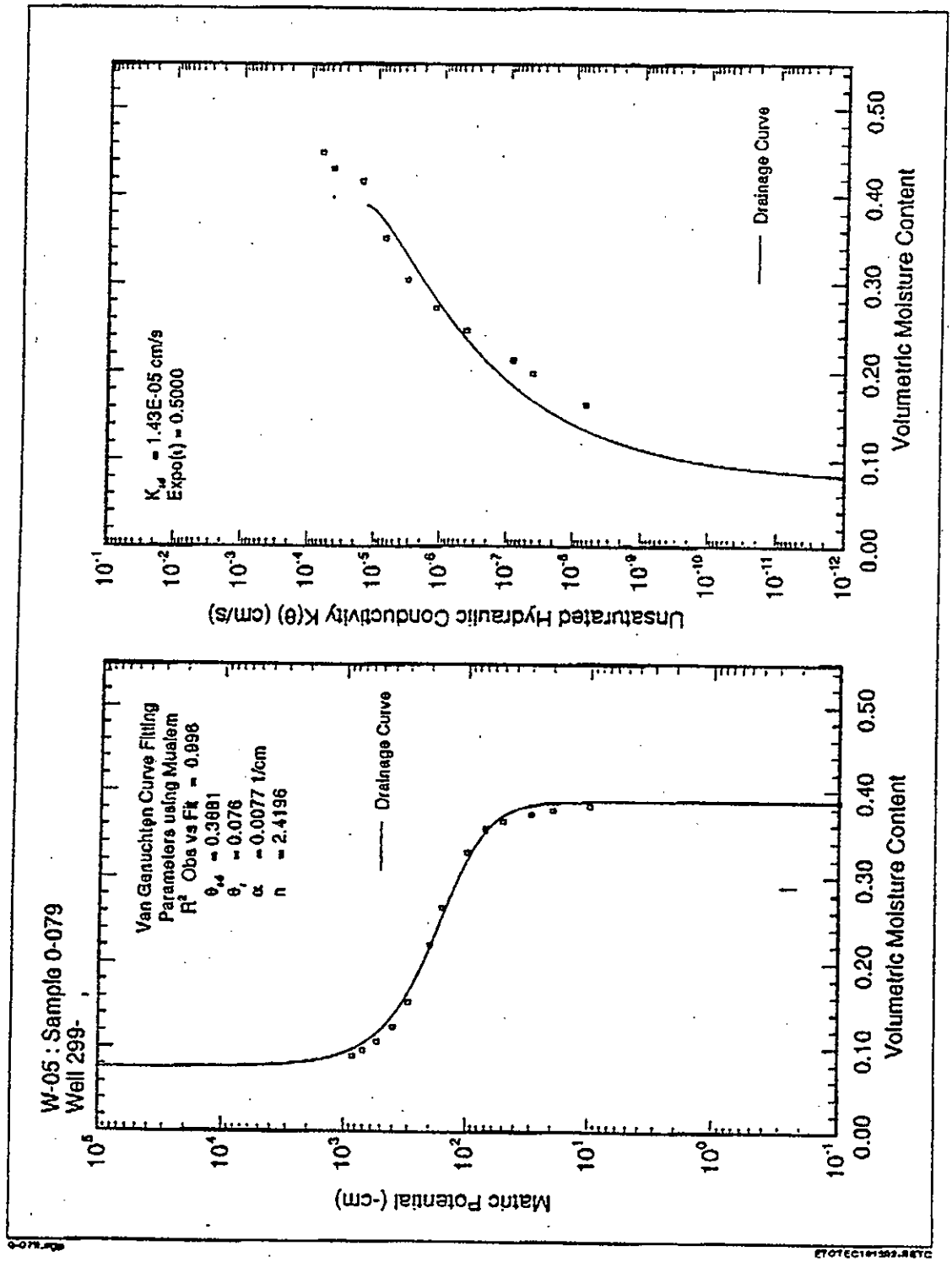

Figure A-26. Moisture Retention Curve and Calculated Hydraulic Conductivity Values for Sample 0-073.

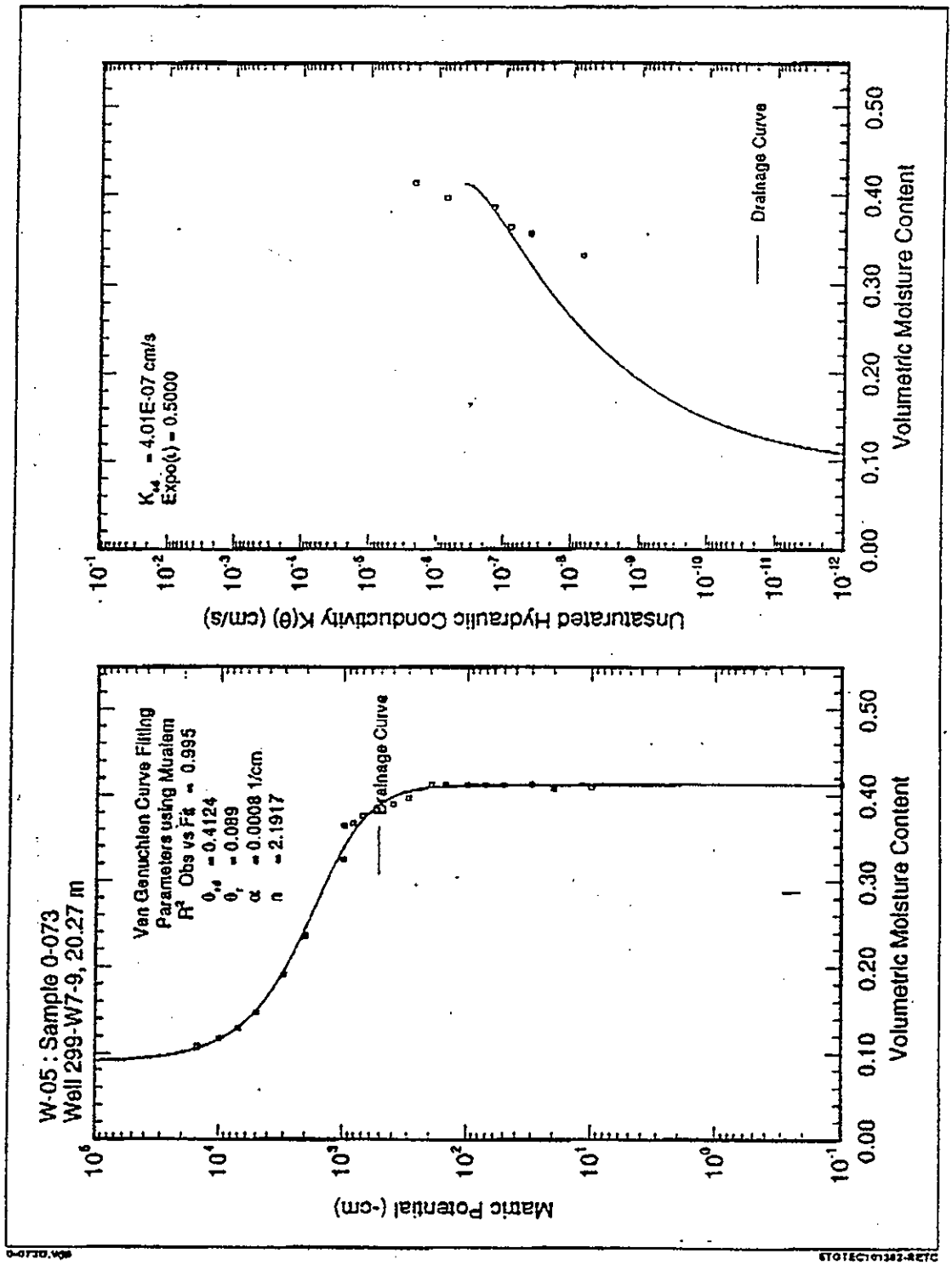

Figure A-27. Moisture Retention Curve and Calculated Hydraulic Conductivity Values for Sample 0-069.

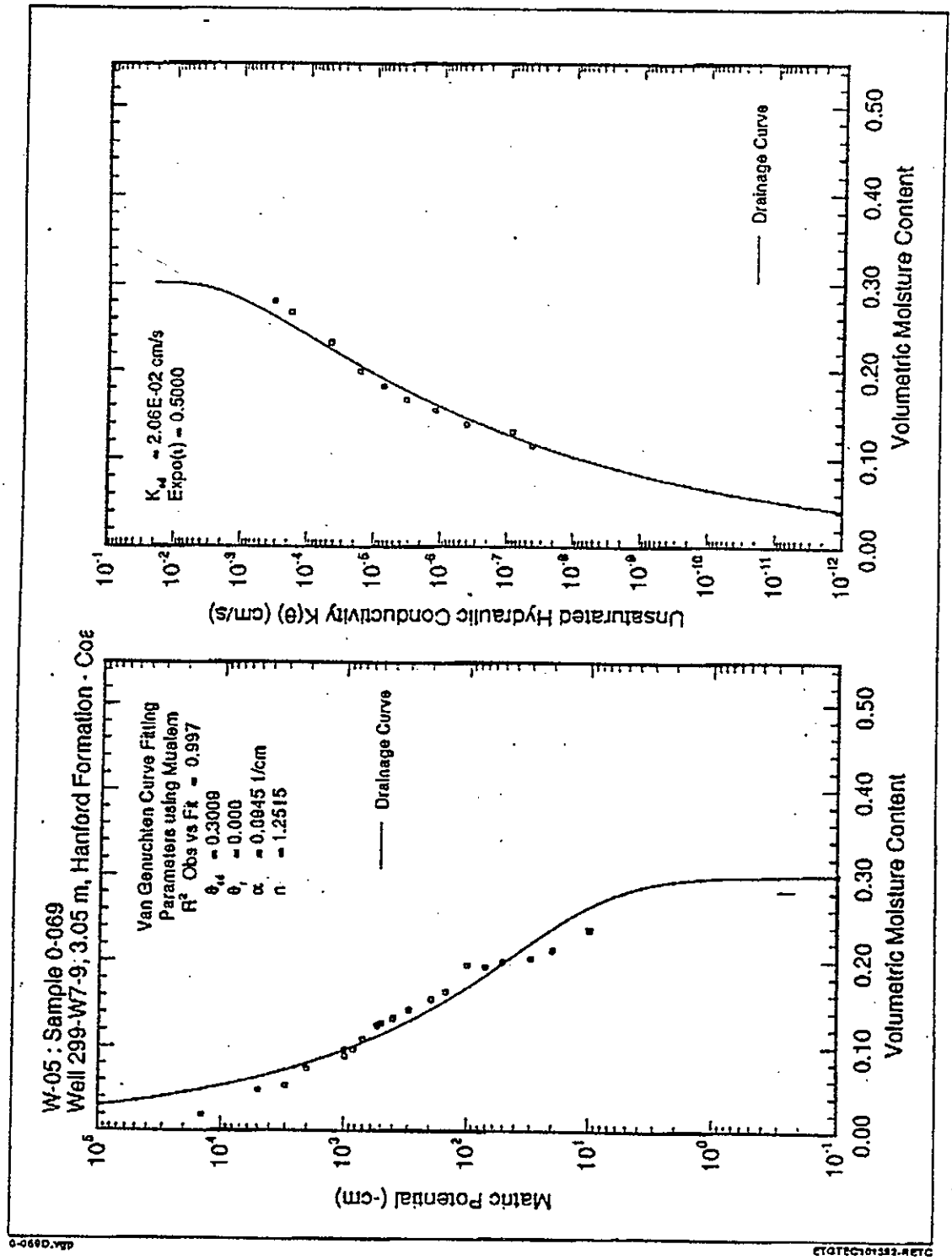

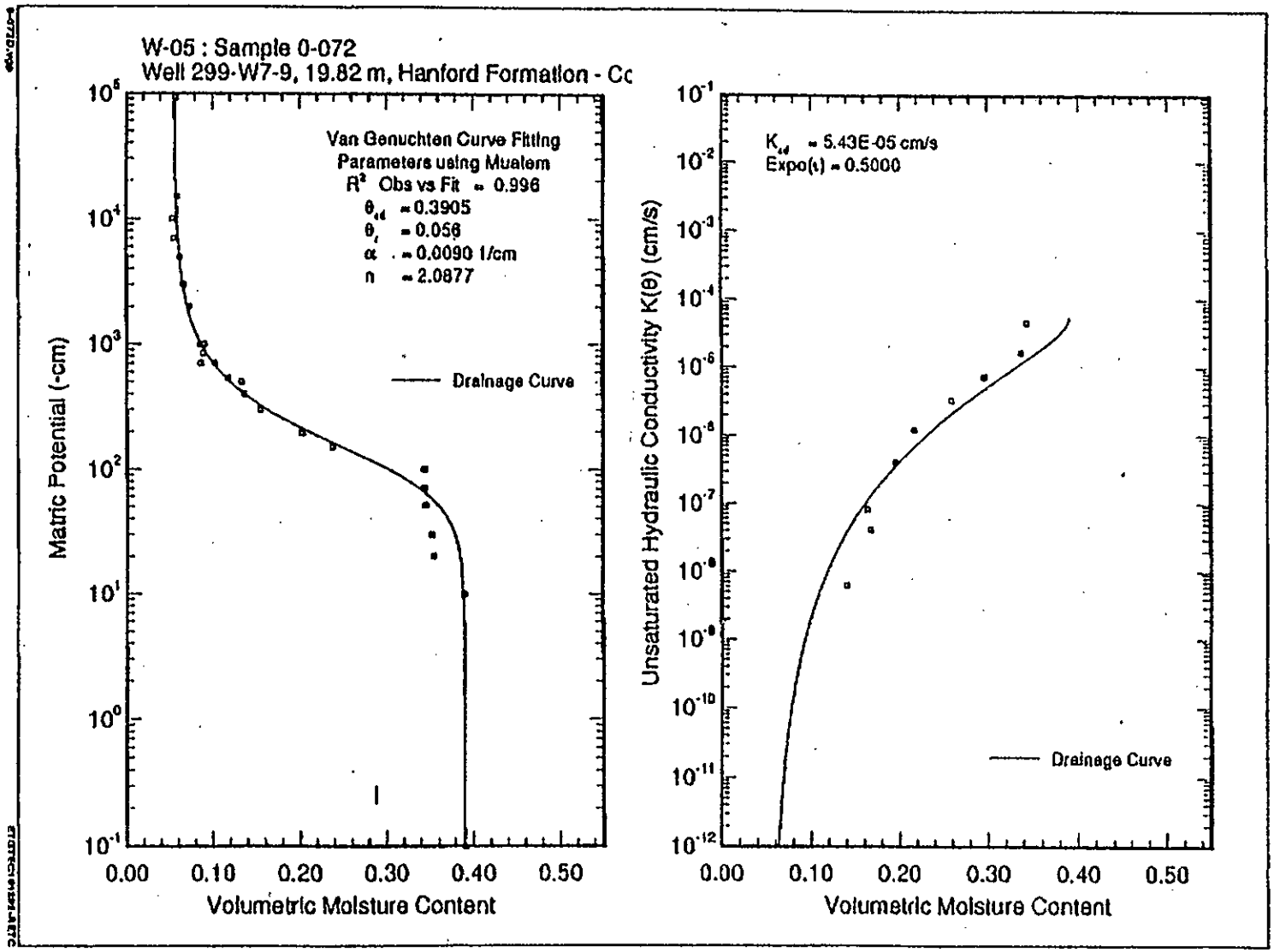

Figure A-28. Moisture Retention Curve and Calculated Hydraulic Conductivity Values for Sample 0-072.

The parameter ℓ was kept fixed at 0.5 during the simultaneous fitting procedure. It is possible that a further improvement on the curve-fitting procedure might be provided by letting the parameter ℓ to vary, in addition to the other five parameters. Mualem (1976) estimated the parameter ℓ to be 0.5 as an average for 45 relatively coarse-textured, repacked soils. However, while the average was 0.5, fitted ℓ values for different soils ranged from -5 to +5. Wosten and van Genuchten (1988), in an analysis of some 200 soil hydraulic data sets, found ℓ to vary between -16 and more than 2. This suggests that, provided enough measured data are available, keeping parameter ℓ variable in the parameter estimation process may further improve the analysis of data. However, one limitation of the approach is that a computer code such as VAM3D-CG does not allow for a variable ℓ. The parameter ℓ was, therefore, kept fixed at 0.5 for this study. Table A-1 summarizes the fitted, van Genuchten-Mualem parameters from a simultaneous fitting of laboratory-measured moisture retention and unsaturated conductivity data.

Table A-1. Results of Simultaneous Fitting of Moisture Retention and Unsaturated Hydraulic Conductivity Data.

Well	Sample	Depth (ft)	Depth (m)	θs	θr	α (1/cm)	α (1/m)	n	m=1-1/n	l	K_s (cm/s)	K_s (m/yr)
299-W7-9	0-069	10.00	3.05	0.3005	0.000	0.0945	9.45	1.2515	0.2010	0.5	2.06E-2	6496.416
299-W7-9	0-072	65.01	19.82	0.3905	0.056	0.0090	0.90	2.0877	0.5210	0.5	5.43E-5	517.124
299-W7-9	0-073	66.48	20.27	0.4124	0.089	0.0008	0.08	2.1917	0.5437	0.5	4.01E-7	0.1264
299-W7-9	0-079	69.24	21.11	0.3881	0.076	0.0077	0.77	2.4196	0.5867	0.5	1.43E-5	4.510
299-W7-9	0-080	70.75	21.57	0.4257	0.047	0.0061	0.61	3.4887	0.7133	0.5	2.51E-5	7.916
299-W7-9	0-082	81.02	24.70	0.4546	0.127	0.0486	4.86	1.3520	0.2603	0.5	6.00E-3	1892.16
299-W7-9	0-083	81.74	24.92	0.4522	0.047	0.0096	0.96	1.5916	0.3717	0.5	1.12E-4	35.320
299-W7-9	0-085	88.26	26.91	0.2670	0.053	0.0108	1.08	1.7795	0.4380	0.5	3.25E-4	102.492
299-W7-9	0-099	99.25	30.26	0.3347	0.038	0.0104	1.04	1.6344	0.3882	0.5	1.43E-3	450.964
299-W7-9	0-101	104.21	31.77	0.3711	0.016	0.5405	5.405	1.3727	0.2715	0.5	7.34E-1	231474
299-W7-9	0-104	111.85	34.10	0.4113	0.006	0.5769	57.69	1.3560	0.2630	0.5	1.26E-0	397353.6
299-W7-9	0-107	132.51	40.40	0.3166	0.025	0.0916	9.16	1.8069	0.4466	0.5	1.65E-2	5203.44
299-W7-9	0-113	141.76	43.22	0.4285	0.030	0.0832	8.32	2.1924	0.5439	0.5	4.55E-3	1434.89

A.3 REFERENCES

Mualem, Y., 1976, "A New Model for Predicting the Hydraulic Conductivity of Unsaturated Porous Media," in *Water Resour. Res.*, vol. 12, no. 3, pp. 513-522.

van Genuchten, M. Th., F. J. Leij, and S. R. Yates, 1991, *The RETC Code for Quantifying the Hydraulic Functions of Unsaturated Soils*, U.S. Environmental Protection Agency, EPA/000/0-91/000.

van Genuchten, M. Th., 1980, "A Closed-Form Solution for Predicting the Conductivity of Unsaturated Soils," in *Soil Science Society of America J.*, 44, 892-898.

WHC, 1990, *Geological Engineering Laboratory Procedures Manual*, WHC-IP-0635, Westinghouse Hanford Company, Richland, Washington.

Wosten, J. H. M., and M. Th. van Genuchten, 1988, "Using Texture and Other Soil Properties to Predict the Unsaturated Soil Hydraulic Functions," in *Soil Science Society of America J.*, 52, 1762-1770.

APPENDIX B

DETAILED LISTING OF RADIONUCLIDE INVENTORIES OF WASTE DISPOSED AT THE HANFORD BURIAL GROUNDS (1989 to 1992)

This page intentionally left blank.

DETAILED LISTING OF RADIONUCLIDE INVENTORIES OF WASTE DISPOSED AT THE HANFORD BURIAL GROUNDS (1989 to 1992)

Radionuclide specific inventories of LLW disposed at the Hanford Burial Grounds from 1989 to 1992 are provided in this appendix. The information is collected in the Solid Waste Information Tracking System (SWITS). The tables are organized in terms of primary groups of generators provided in Valero et al. (1993). Both total Ci and isotope concentrations (Ci/m^3) are provided. In some cases, the total beta-gamma values exceeds the sum of the specific beta-gamma-emitting radionuclides listed. This is due to deliberate omission of beta-gamma-emitting radionuclides with half lives <5 yr.

Table B-5 summarizes the average concentrations of radionuclides in the 4 yr inventory data base that were used to compare against Category 1 and 3 concentration limits. Figure B-1 is a copy of the questionnaire used to elicit descriptions of waste streams from generators.

This page intentionally left blank.

Table B-1. Isotope and Volume Summary of Disposed Waste (1989-1992) from Defense Waste Management Facilities. (6 sheets)

Generator	Volume (m3)	No. Containers	Isotope	Activity (Ci)	Concentration (Ci/m3)
200W	1.5E+01	1	Cs-137	2.3E-06	1.5E-07
	1.5E+01		Sr-90	8.2E-06	5.4E-07
201C	4.1E+03	623	Cs-137	6.9E-01	1.7E-04
	4.1E+03		Eu-154	1.1E-06	2.7E-10
	4.1E+03		Sr-90	1.2E+01	3.0E-03
211S	2.4E+01	7	Cs-137	6.3E-03	2.6E-04
	2.4E+01		Sr-90	8.3E-03	3.5E-04
211U	2.7E+01	5	U-Enriched	1.0E-01 gm	
213W	6.4E+01	22	Am-241	5.6E-05	8.8E-07
	6.4E+01		Co-60	2.4E-03	3.8E-05
	6.4E+01		Cs-137	3.3E-02	5.2E-04
	6.4E+01		H-3	6.7E-04	1.1E-05
	6.4E+01		I-129	5.0E-04	7.8E-06
	6.4E+01		Pm-147	1.2E-03	1.9E-05
	6.4E+01		Pu-238	1.7E-05	2.7E-07
	6.4E+01		Pu-239	5.2E-06	8.2E-08
	6.4E+01		Sr-90	1.4E-02	2.2E-04
	6.4E+01		Tc-99	6.1E-06	9.5E-08
	6.4E+01		U-238	4.6E-08	7.2E-10
	6.4E+01		U-234	4.6E-08	7.2E-10
	6.4E+01		U-235	2.2E-09	3.4E-11
216-U-12	1.2E+01	3	Co-60	3.1E-06	2.6E-07
	1.2E+01		Cs-137	9.5E-05	7.9E-06
	1.2E+01		H-3	1.1E-04	9.2E-06
	1.2E+01		I-129	6.0E-07	5.0E-08
	1.2E+01		Pu-238	1.4E-09	1.2E-10
	1.2E+01		Pu-239	6.0E-11	5.0E-12
	1.2E+01		Pu-240	9.0E-10	7.5E-11
	1.2E+01		Sr-90	1.1E-04	9.0E-06
	1.2E+01		Tc-99	1.6E-06	1.3E-07
216A	4.7E+02	28	Co-60	5.0E-03	1.1E-05
	4.7E+02		CS-134	7.5E-03	1.6E-05
	4.7E+02		Cs-137	1.3E-02	2.7E-05
	4.7E+02		Sr-90	1.0E-04	2.2E-07
216B	3.9E-01	14	Cs-137	2.2E-05	5.7E-05
	3.9E-01		K-40	9.0E-08	2.3E-07
	3.9E-01		Sr-90	3.4E-03	8.7E-03
	3.9E-01		Tc-99	1.0E-06	2.6E-06

Table B-1. Isotope and Volume Summary of Disposed Waste (1989-1992) from Defense Waste Management Facilities. (6 sheets)

Generator	Volume (m3)	No. Containers	Isotope	Activity (Ci)	Concentration (Ci/m3)
216C	2.8E-02	1	Cs-137	4.5E-06	1.6E-04
	2.8E-02		Sr-90	8.5E-04	3.0E-02
216E	1.3E+00	6	Cs-137	9.0E-06	7.1E-06
	1.3E+00		Sr-90	2.6E-05	2.0E-05
216S	2.0E+01	30	Cs-137	3.7E-05	1.8E-06
	2.0E+01		Sr-90	7.7E-05	3.8E-06
216U1	1.9E+01	2	Cs-137	3.3E-06	1.7E-07
	1.9E+01		Sr-90	3.0E-06	1.6E-07
218E12B	2.6E+01	2	Cs-137	4.5E-10	1.7E-11
	2.6E+01		Sr-90	4.5E-10	1.7E-11
218W4B	1.2E+01	12	Am-241	1.4E-09	1.2E-10
	1.2E+01		Co-60	1.0E-11	8.3E-13
	1.2E+01		Cs-137	3.0E-06	2.4E-07
	1.2E+01		Np-237	2.8E-08	2.3E-09
	1.2E+01		Pm-147	5.9E-09	4.9E-10
	1.2E+01		Pu-241	1.9E-08	1.6E-09
	1.2E+01		Sr-90	2.7E-06	2.3E-07
	1.2E+01		Th-232	5.0E-09	4.1E-10
	1.2E+01		U-Enriched	6.1E-06 gm	
218W4C	6.3E+00	2	Tc-99	3.4E-05	5.4E-06
	6.3E+00		U-238	2.2E-08	3.5E-09
	6.3E+00		U-234	2.2E-08	3.5E-09
	6.3E+00		U-235	1.0E-09	1.6E-10
221B	8.1E+02	658	Cs-137	5.6E-01	6.9E-04
	8.1E+02		Sr-90	3.3E+01	4.0E-02
224T	3.0E+01	71	Co-60	1.0E-05	3.4E-07
	3.0E+01		Cs-137	8.7E-05	2.8E-06
	3.0E+01		Eu-154	7.8E-07	2.6E-08
	3.0E+01		Pu	2.4E-05 gm	
	3.0E+01		Sr-90	1.1E-04	3.6E-06
	3.0E+01		U-238	7.2E-16	2.4E-17
	3.0E+01		U-234	7.2E-16	2.4E-17
	3.0E+01		U-235	3.4E-17	1.1E-18
225B	1.3E+02	340	Cs-137	1.3E-01	9.7E-04
	1.3E+02		Sr-90	1.3E-01	1.0E-03

Table B-1. Isotope and Volume Summary of Disposed Waste (1989-1992) from Defense Waste Management Facilities. (6 sheets)

Generator	Volume (m3)	No. Containers	Isotope	Activity (Ci)	Concentration (Ci/m3)
241A	2.0E+01	1	Co-60	2.0E-04	9.8E-06
	2.0E+01		Cs-137	5.0E-04	2.5E-05
241AY	1.5E+02	11	Co-60	6.3E-04	4.3E-06
	1.5E+02		Cs-137	2.3E-03	1.6E-05
241B	6.1E+01	3	Co-60	6.0E-04	9.9E-06
	6.1E+01		Cs-137	1.5E-03	2.5E-05
241C	4.1E+01	2	Co-60	4.0E-04	9.9E-06
	4.1E+01		Cs-137	1.0E-03	2.5E-05
241SX	6.3E-01	3	Cs-137	3.0E-04	4.8E-04
	6.3E-01		Sr-90	3.0E-04	4.8E-04
241TX	3.0E+02	3	Co-60	2.0E-04	6.6E-07
	3.0E+02		Cs-137	3.0E-04	1.0E-06
	3.0E+02		Sr-90	3.0E-04	1.0E-06
242B	2.5E+01	9	U-238	2.0E-06	8.1E-08
	2.5E+01		U-234	2.0E-06	8.1E-08
	2.5E+01		U-235	9.7E-08	3.9E-09
242S	4.0E+01	2	Cs-137	2.0E-04	5.0E-06
	4.0E+01		Sr-90	2.0E-04	5.0E-06
271B	6.2E+02	576	Cs-137	1.8E+00	2.8E-03
	6.2E+02		Sr-90	1.1E+00	1.8E-03
271T	2.3E+02	210	Co-60	3.0E-01	1.3E-03
	2.3E+02		Cs-137	3.7E-01	1.6E-03
	2.3E+02		Sr-90	9.3E-01	4.0E-03
271U	4.1E+00	23	Cs-137	4.5E-03	1.1E-03
	4.1E+00		Sr-90	4.7E-03	1.1E-03
2727W	5.0E+00	10	Pu	1.0E-05 gm	
272AW	7.1E+00	2	Co-60	2.2E-04	3.1E-05
	7.1E+00		Cs-137	1.1E-03	1.5E-04

Table B-1. Isotope and Volume Summary of Disposed Waste (1989-1992) from Defense Waste Management Facilities. (6 sheets)

Generator	Volume (m3)	No. Containers	Isotope	Activity (Ci)	Concentration (Ci/m3)
272WA	2.5E+01	6	Am-241	2.2E-05	8.9E-07
	2.5E+01		Co-60	2.6E-03	1.1E-04
	2.5E+01		Cs-137	9.3E-03	3.8E-04
	2.5E+01		H-3	3.4E-04	1.4E-05
	2.5E+01		I-129	2.9E-04	1.2E-05
	2.5E+01		Pm-147	6.6E-04	2.7E-05
	2.5E+01		Pu-238	8.6E-08	3.5E-09
	2.5E+01		Pu-239	2.9E-06	1.2E-07
	2.5E+01		Sr-90	3.2E-03	1.3E-04
	2.5E+01		Tc-99	3.4E-06	1.4E-07
	2.5E+01		U-238	2.4E-08	9.8E-10
	2.5E+01		U-234	2.4E-08	9.8E-10
	2.5E+01		U-235	1.2E-09	4.9E-11
276U	1.7E+01	4	Cs-137	7.3E-05	4.4E-06
291S	1.9E+00	9	Cs-137	7.3E-06	3.9E-06
	1.9E+00		Sr-90	6.0E-05	3.2E-05
2EBG	1.6E+00	1	Cs-137	1.0E-05	6.1E-06
2ETF	5.8E+02	1412	Co-60	6.3E+00	1.1E-02
	5.8E+02		Cs-137	8.7E+00	1.5E-02
	5.8E+02		Pm-147	7.0E-04	1.2E-06
	5.8E+02		Sm-151	9.0E-06	1.6E-08
	5.8E+02		Sr-90	1.4E+01	2.5E-02
	5.8E+02		Th-232	2.2E-11	3.8E-14
2WBG	6.1E+00	3	Co-60	1.0E-05	1.6E-06
	6.1E+00		Cs-137	1.8E+01	3.0E+00
2WTF	4.4E+02	699	Co-60	2.1E-04	4.7E-07
	4.4E+02		Cs-137	4.9E-01	1.1E-03
	4.4E+02		Eu-154	1.5E-05	3.3E-08
	4.4E+02		K-40	1.8E-04	4.0E-07
	4.4E+02		Sr-90	4.9E-01	1.1E-03
	4.4E+02		U-238	1.9E-10	4.4E-13
	4.4E+02		U-234	1.9E-10	4.4E-13
	4.4E+02		U-235	9.4E-12	2.2E-14
306	2.7E+01	133	Cs-137	1.0E-03	3.8E-05
	2.7E+01		U-238	1.9E-06	7.2E-08
	2.7E+01		U-234	1.9E-06	7.2E-08
	2.7E+01		U-235	9.2E-08	3.5E-09
	2.7E+01		U-Enriched	2.0E+02 gm	

Table B-1. Isotope and Volume Summary of Disposed Waste (1989-1992) from Defense Waste Management Facilities. (6 sheets)

Generator	Volume (m3)	No. Containers	Isotope	Activity (Ci)	Concentration (Ci/m3)
333	2.6E+02	87	Co-60	9.7E-03	3.8E-05
	2.6E+02		Eu-154	1.6E-03	6.4E-06
	2.6E+02		U-238	3.4E-06	1.3E-08
	2.6E+02		U-234	3.4E-06	1.3E-08
	2.6E+02		U-235	1.6E-07	6.2E-10
	2.6E+02		U-Enriched	4.8E+00 gm	
340	4.0E+01	130	Am-241	1.0E-04	2.5E-06
	4.0E+01		Cs-137	1.1E-01	2.8E-03
	4.0E+01		Eu-152	1.1E-03	2.7E-05
	4.0E+01		Eu-154	2.3E-03	5.6E-05
	4.0E+01		Pu-238	9.7E-04	2.4E-05
	4.0E+01		Pu-239	4.0E-09	9.9E-11
	4.0E+01		Pu-241	1.0E-04	2.5E-06
	4.0E+01		Sr-90	1.7E-03	4.3E-05
	4.0E+01		U-Enriched	3.2E+01 gm	
377	9.2E+00	3	Co-60	3.5E-01	3.8E-02
3902A	1.0E+00	5	Co-60	2.5E-07	2.5E-07
	1.0E+00		Cs-137	5.1E-07	5.1E-07
	1.0E+00		Eu-154	2.6E-06	2.6E-06
	1.0E+00		Pu-238	2.2E-03	2.2E-03
	1.0E+00		Sr-90	5.3E-09	5.3E-09
	1.0E+00		U-238	1.1E-07	1.1E-07
	1.0E+00		U-234	1.1E-07	1.1E-07
	1.0E+00		U-235	5.3E-09	5.3E-09
600	4.5E+00	1	Cs-137	7.6E-07	1.7E-07
	4.5E+00		Sr-90	2.7E-06	5.9E-07
618	7.5E+01	18	Cs-137	2.8E-05	3.7E-07
	7.5E+01		U-238	1.1E-05	1.5E-07
	7.5E+01		U-234	1.1E-05	1.5E-07
	7.5E+01		U-235	5.3E-07	7.1E-09
BG002	1.4E-01	5	Cs-137	9.0E-07	6.4E-06
	1.4E-01		K-40	1.6E-06	1.1E-05
			Sr-90	4.7E-08	
BG005	4.0E+00	2	Co-60	4.0E-04	9.9E-05
	4.0E+00		Cs-137	2.0E-04	5.0E-05
	4.0E+00		Sr-90	2.0E-04	5.0E-05

Table B-1. Isotope and Volume Summary of Disposed Waste (1989-1992) from Defense Waste Management Facilities. (6 sheets)

Generator	Volume (m3)	No. Containers	Isotope	Activity (Ci)	Concentration (Ci/m3)
BG02A	1.4E+01	53	Cs-137	2.0E-04	1.4E-05
	1.4E+01		Sr-90	3.9E-03	2.7E-04
BG03A	1.1E+02	19	Cs-137	1.4E+01	1.3E-01
	1.1E+02		Sr-90	7.7E-03	7.3E-05
	1.1E+02		Tc-99	1.1E-04	1.0E-06
BG04B	1.5E+02	14	Co-60	4.0E-04	2.8E-06
	1.5E+02		Cs-137	4.0E-04	2.8E-06
	1.5E+02		Sr-90	2.0E-04	1.4E-06
BG12A	2.8E-01	10	Cs-137	9.2E-07	3.3E-06
	2.8E-01		K-40	3.4E-06	1.2E-05
	2.8E-01		Nb-95	1.7E-08	6.1E-08
	2.8E-01		Sr-90	7.0E-07	2.5E-06
BG12B	2.0E+03	217	Cs-137	9.8E-03	4.9E-06
	2.0E+03		K-40	9.1E-03	4.5E-06
	2.0E+03		Sr-90	3.3E-01	1.6E-04
BG3AE	1.8E+02	2	Sr-90	8.0E-04	4.4E-06
CRB57	4.1E-01	2	Cs-137	2.0E-08	4.8E-08
	4.1E-01		Sr-90	2.0E-08	4.8E-08
CWC	1.3E+02	8	Co-60	7.6E-04	5.9E-06
	1.3E+02		Cs-137	3.0E-04	2.3E-06
	1.3E+02		Sr-90	3.4E-04	2.6E-06
U216E	5.1E-01	4	Cs-137	1.4E-05	2.6E-05
	5.1E-01		Sr-90	2.6E-03	5.0E-03
U216W	2.5E-01	9	Cs-137	9.9E-07	3.9E-06
	2.5E-01		Sr-90	3.1E-07	1.2E-06

Table B-2. Isotope and Volume Summary of Disposed Waste (1989-1992) from Chemical Processing Facilities. (3 sheets)

Generator	Volume (m3)	No. Containers	Isotope	Activity (Ci)	Concentration (Ci/m3)
202A	3.5E+03	2.6E+03	Am-241	1.4E-10	4.0E-14
	3.5E+03		C-14	3.0E-04	8.6E-08
	3.5E+03		Cm-242	4.6E-02	1.3E-05
	3.5E+03		Co-60	3.0E-11	8.5E-15
	3.5E+03		Cs-137	1.6E+00	4.7E-04
	3.5E+03		Eu-154	1.6E-10	4.6E-14
	3.5E+03		H-3	6.9E-03	2.0E-06
	3.5E+03		I-129	4.6E-02	1.3E-05
	3.5E+03		Pm-147	4.5E+00	1.3E-03
	3.5E+03		Pu-238	6.8E-02	1.9E-05
	3.5E+03		Pu-241	4.9E-04	1.4E-07
	3.5E+03		Se-79	1.0E-08	2.9E-12
	3.5E+03		Sm-151	9.5E-01	2.7E-04
	3.5E+03		Sr-90	1.4E+00	3.9E-04
	3.5E+03		Tc-99	4.1E-07	1.2E-10
	3.5E+03		U-238	2.4E-07	6.8E-11
	3.5E+03		U-234	2.4E-07	6.8E-11
	3.5E+03		U-235	1.1E-08	3.1E-12
202AL	1.7E+02	1.1E+03	C-14	4.2E-10	2.5E-12
	1.7E+02		Cs-137	4.6E-01	2.7E-03
	1.7E+02		H-3	1.7E-03	9.9E-06
	1.7E+02		I-129	1.0E-10	5.9E-13
	1.7E+02		Nb-94	0.0E+00	0.0E+00
	1.7E+02		Pm-147	1.7E+00	1.0E-02
	1.7E+02		Pu-238	1.0E-07	5.9E-10
	1.7E+02		Pu-241	6.5E-05	3.8E-07
	1.7E+02		Se-79	1.1E-08	6.6E-11
	1.7E+02		Sm-151	2.7E-01	1.6E-03
	1.7E+02		Sr-90	4.0E-01	2.3E-03
	1.7E+02		Tc-99	5.5E-08	3.2E-10
	1.7E+02		U-238	3.2E-08	1.9E-10
	1.7E+02		U-234	3.2E-08	1.9E-10
	1.7E+02		U-235	1.5E-09	9.1E-12
202S	6.2E+01	9.0E+01	Cs-137	8.8E-04	1.4E-05
	6.2E+01		Sr-90	1.2E-03	1.9E-05
204T	4.5E+00	1.0E+00	Am-241	1.1E+00	2.5E-01
	4.5E+00		Co-60	5.0E-04	1.1E-04
	4.5E+00		Cs-137	6.0E-04	1.3E-04
	4.5E+00		Eu-154	5.0E-05	1.1E-05

Table B-2. Isotope and Volume Summary of Disposed Waste (1989-1992) from Chemical Processing Facilities. (3 sheets)

Generator	Volume (m3)	No. Containers	Isotope	Activity (Ci)	Concentration (Ci/m3)
209E	9.3E+00	7.0E+00	Pu-239	7.9E-07	8.5E-08
	9.3E+00		Th-232	1.7E-05	1.8E-06
	9.3E+00		U-238	6.6E-10	7.1E-11
	9.3E+00		U-234	6.6E-10	7.1E-11
	9.3E+00		U-235	3.1E-11	3.3E-12
	9.3E+00		U-Enriched	8.2E+01 gm	
211S	2.4E+01	7.0E+00	Cs-137	6.3E-03	2.6E-04
	2.4E+01		Sr-90	8.3E-03	3.5E-04
221T	4.5E+02	1.5E+02	Co-60	3.0E-05	6.7E-08
	4.5E+02		Cs-137	6.5E-05	1.4E-07
	4.5E+02		Sr-90	1.3E-04	2.9E-07
221TS	4.0E+02	4.0E+02	Co-60	2.7E-04	6.8E-07
	4.0E+02		Cs-137	5.4E-02	1.4E-04
	4.0E+02		Sr-90	5.4E-02	1.4E-04
221U	7.1E+01	3.6E+02	Co-60	1.1E-06	1.5E-08
	7.1E+01		Cs-137	1.6E-04	2.3E-06
	7.1E+01		Pu	1.6E-08 gm	
	7.1E+01		Sr-90	6.7E-04	9.4E-06
	7.1E+01		U-233	1.7E-02	2.4E-04
	7.1E+01		U-238	1.3E-06	1.8E-08
	7.1E+01		U-234	1.3E-06	1.8E-08
	7.1E+01		U-235	6.1E-08	8.6E-10
222S	9.9E+02	3.2E+03	Am-241	8.8E-03	8.9E-06
	9.9E+02		Co-60	1.7E+00	1.8E-03
	9.9E+02		Cs-137	2.1E-01	2.1E-04
	9.9E+02		H-3	3.2E-03	3.3E-06
	9.9E+02		I-129	3.9E-05	4.0E-08
	9.9E+02		Pm-147	6.2E-03	6.3E-06
	9.9E+02		Pu-238	1.3E-06	1.3E-09
	9.9E+02		Pu-239	5.7E-05	5.8E-08
	9.9E+02		Pu-242	1.6E-10	1.6E-13
	9.9E+02		Se-79	1.7E-07	1.7E-10
	9.9E+02		Sr-90	2.6E-01	2.7E-04
	9.9E+02		Tc-99	3.0E-05	3.1E-08
	9.9E+02		U-238	2.4E-07	2.4E-10
	9.9E+02		U-234	2.4E-07	2.4E-10
	9.9E+02		U-235	1.1E-08	1.1E-11

Table B-2. Isotope and Volume Summary of Disposed Waste (1989-1992) from Chemical Processing Facilities. (3 sheets)

Generator	Volume (m3)	No. Containers	Isotope	Activity (Ci)	Concentration (Ci/m3)
224U	3.8E+02	3.5E+02	Cs-137	2.0E-03	5.3E-06
	3.8E+02		Sr-90	2.0E-03	5.3E-06
	3.8E+02		Tc-99	5.8E-04	1.6E-06
	3.8E+02		U-238	9.0E-06	2.4E-08
	3.8E+02		U-234	9.0E-06	2.4E-08
	3.8E+02		U-235	4.3E-07	1.1E-09
	3.8E+02		U-Enriched	3.9E+03 gm	
233S	1.8E+00	1.4E+01	Cs-137	2.0E-08	1.1E-08
	1.8E+00		Sr-90	2.0E-08	1.1E-08
2345Z	1.4E+03	3.6E+03	Am-241	5.7E-03	4.0E-06
	1.4E+03		Cs-137	2.3E-06	1.6E-09
	1.4E+03		Pu-238	4.0E-01	2.8E-04
	1.4E+03		Pu-239	5.0E-02	3.5E-05
	1.4E+03		Pu-240	1.2E-02	8.5E-06
	1.4E+03		Pu-241	5.6E-01	4.0E-04
	1.4E+03		Pu-242	1.5E-05	1.1E-08
	1.4E+03		Sr-90	8.2E-06	5.8E-09

Table B-3. Isotope and Volume Summary of Disposed Waste (1989-1992) from Other Onsite Generator Facilities. (11 sheets)

Generator	Volume (m3)	No. Containers	Isotope	Activity (Ci)	Concentration (Ci/m3)
N-Reactor					
100B	4.4E+01	1.8E+01	Co-60	4.7E-04	1.1E-05
	4.4E+01		Cs-137	1.4E-09	3.1E-11
	4.4E+01		Eu-152	5.8E-03	1.3E-04
	4.4E+01		Eu-154	9.9E-04	2.3E-05
	4.4E+01		Sr-90	7.0E-11	1.6E-12
100C	1.7E+00	8.0E+00	Co-60	1.7E-04	1.0E-04
	1.7E+00		Cs-137	3.7E-04	2.2E-04
	1.7E+00		Eu-152	9.3E-04	5.5E-04
	1.7E+00		Eu-154	1.3E-04	7.8E-05
100D	1.3E+01	4.0E+01	Co-60	7.3E-07	5.8E-08
	1.3E+01		Cs-137	3.0E-10	2.4E-11
	1.3E+01		Sr-90	3.0E-10	2.4E-11
100F	3.2E+00	1.5E+01	Cs-137	1.5E-01	4.8E-02
100H	3.9E+01	1.0E+02	Co-60	4.9E-02	1.2E-03
	3.9E+01		Cs-137	3.8E-10	9.6E-12
	3.9E+01		Sr-90	3.8E-10	9.6E-12
	3.9E+01		Tc-99	3.3E-07	8.4E-09
			U-Enriched	4.3E-01 gm	
100K	3.1E+00	2.0E+01	Co-60	4.9E-05	1.6E-05
	3.1E+00		Cs-137	7.3E-05	2.4E-05
100N	8.6E+02	8.4E+01	C-14	4.5E-02	5.2E-05
	8.6E+02		Co-60	1.7E+00	2.0E-03
	8.6E+02		Cs-137	2.0E-02	2.3E-05
	8.6E+02		Eu-154	4.8E-08	5.6E-11
	8.6E+02		Ni-63	6.8E-09	7.9E-12
	8.6E+02		Sr-90	7.0E-04	8.2E-07
	8.6E+02		U-Enriched	1.2E+05 gm	
	8.6E+02		U-238	2.5E-02	3.0E-05
	8.6E+02		U-234	2.5E-02	3.0E-05
	8.6E+02		U-235	1.2E-03	1.4E-06
105B	2.0E+01	4.0E+00	Co-60	4.6E-05	2.4E-06
	2.0E+01		Eu-152	3.6E-03	1.9E-04
	2.0E+01		Eu-154	6.3E-04	3.2E-05
105C	4.1E+01	2.0E+00	U-Enriched	3.1E-03 gm	

Table B-3. Isotope and Volume Summary of Disposed Waste (1989-1992) from Other Onsite Generator Facilities. (11 sheets)

Generator	Volume (m3)	No. Containers	Isotope	Activity (Ci)	Concentration (Ci/m3)
N-Reactor					
105D	2.5E-01	2.0E+00	Co-60	3.8E-08	1.5E-07
105F	8.0E-01	4.0E+00	Cs-137	1.4E-05	1.8E-05
	8.0E-01		Eu-152	1.4E-05	1.8E-05
	8.0E-01		Sr-90	2.2E-05	2.8E-05
105H	4.0E+00	1.0E+00	Cs-137	1.7E-05	4.3E-06
105K	2.9E+01	7.0E+00	Co-60	5.0E-08	1.8E-09
	2.9E+01		Cs-137	3.6E-07	1.3E-08
	2.9E+01		Sr-90	2.2E-07	7.6E-09
	2.9E+01		Th-232	4.8E-10	1.7E-11
105KE	3.3E+01	1.0E+01	Co-60	1.0E-02	3.0E-04
	3.3E+01		Cs-137	9.5E+02	2.9E+01
	3.3E+01		Pu	1.1E+01 gm	
	3.3E+01		Pu-238	1.2E-01	3.6E-03
	3.3E+01		Sr-90	3.0E+02	9.0E+00
105KW	2.4E+01	3.0E+00	Co-60	2.0E-03	8.5E-05
	2.4E+01		Cs-137	1.9E+01	8.2E-01
	2.4E+01		Pu	3.2E-01 gm	
	2.4E+01		Pu-238	8.6E+00	3.7E-01
	2.4E+01		Sr-90	2.7E+00	1.2E-01
105N	3.0E+02	2.4E+02	Co-60	7.6E-01	2.6E-03
	3.0E+02		Cs-137	1.5E-02	5.1E-05
	3.0E+02		Eu-154	8.0E-07	2.7E-09
	3.0E+02		Ni-63	8.8E-08	3.0E-10
	3.0E+02		Sr-90	1.5E-02	5.1E-05
	3.0E+02		Tc-99	4.2E-09	1.4E-11
109H	2.1E+01	2.0E+00	Co-60	5.0E-03	2.4E-04
	2.1E+01		Eu-154	5.3E-02	2.5E-03
1120N	1.2E+01	1.0E+00	Co-60	1.0E-03	8.7E-05
116B	2.5E+00	1.2E+01	Co-60	2.5E-04	1.0E-04
	2.5E+00		Cs-137	7.0E-03	2.8E-03
	2.5E+00		Sr-90	3.4E-04	1.3E-04
1310P	4.0E+01	8.0E+00	Co-60	1.5E-02	3.7E-04
	4.0E+01		Sr-90	1.0E-11	2.5E-13

Table B-3. Isotope and Volume Summary of Disposed Waste (1989-1992) from Other Onsite Generator Facilities. (11 sheets)

Generator	Volume (m3)	No. Containers	Isotope	Activity (Ci)	Concentration (Ci/m3)
N-Reactor					
163N	5.3E+01	1.3E+01	Co-60	1.4E-02	2.5E-04
	5.3E+01		Cs-137	7.0E-11	1.3E-12
	5.3E+01		Eu-154	1.4E-09	2.5E-11
	5.3E+01		Ni-63	7.2E-10	1.4E-11
163PA	5.2E+01	6.4E+01	Co-60	2.6E-01	5.0E-03
	5.2E+01		Cs-137	4.0E-03	7.7E-05
	5.2E+01		Sr-90	5.0E-03	9.6E-05
1706KE	8.2E+00	3.0E+00	Co-60	1.1E-08	1.3E-09
	8.2E+00		Cs-137	9.4E-09	1.1E-09
	8.2E+00		Eu-154	1.2E-09	1.5E-10
	8.2E+00		Ni-63	1.4E-10	1.7E-11
170KE	8.2E+00		Sr-90	1.4E-10	1.7E-11
183KE	2.5E+00	1.5E+01	Co-60	6.8E-05	2.7E-05
	2.5E+00		Cs-137	5.8E-03	2.3E-03
	2.5E+00		Sr-90	1.8E-05	7.2E-06
Pacific Northwest Laboratory (PNL)					
1234	8.4E-01	4.0E+00	K-40	4.0E-03	4.8E-03
209E	9.3E+00	7.0E+00	Pu-239	7.9E-07	8.5E-08
	9.3E+00		Th-232	1.7E-05	1.8E-06
	9.3E+00		U-238	6.6E-05	7.1E-06
	9.3E+00		U-234	6.6E-05	7.1E-06
	9.3E+00		U-235	3.1E-06	3.3E-07
	9.3E+00		U-Enriched	8.2E+01 gm	
2718E	4.2E-01	2.0E+00	Pu	1.5E-02 gm	
			Tot. Beta/Gamma	1.0E-03	
300	1.3E+01	1.9E+01	Co-60	1.6E-06	1.3E-07
	1.3E+01		Cs-137	5.8E-02	4.7E-03
	1.3E+01		K-40	2.8E-04	2.3E-05
	1.3E+01		Ra-226	9.6E-06	7.7E-07
	1.3E+01		Sr-90	1.7E-03	1.3E-04
	1.3E+01		U-238	1.5E-12	1.2E-13
	1.3E+01		U-234	1.5E-12	1.2E-13
	1.3E+01		U-235	7.3E-14	5.8E-15

Table B-3. Isotope and Volume Summary of Disposed Waste (1989-1992) from Other Onsite Generator Facilities. (11 sheets)

Generator	Volume (m3)	No. Containers	Isotope	Activity (Ci)	Concentration (Ci/m3)
Pacific Northwest Laboratory (PNL)					
3000	1.8E+00	9.0E+00	Tot. Beta/Gamma	4.6E-03	2.6E-03
	1.8E+00		U-238	5.0E-03	2.8E-03
	1.8E+00		U-234	5.0E-03	2.8E-03
	1.8E+00		U-235	2.4E-04	1.3E-04
306W	9.9E+01	1.8E+02	Co-60	5.0E-06	5.1E-08
	9.9E+01		Cs-137	6.0E-08	6.1E-10
	9.9E+01		Sr-90	3.5E-08	3.5E-10
	9.9E+01		U-238	4.7E+00	4.7E-02
	9.9E+01		U-234	4.7E+00	4.7E-02
	9.9E+01		U-235	2.2E-01	2.3E-03
	9.9E+01		U-Enriched	9.0E-03 gm	
314	1.4E+01	1.3E+01	Co-60	5.0E-06	3.6E-07
	1.4E+01		Cs-137	4.0E-04	2.9E-05
	1.4E+01		U-238	1.0E-06	7.2E-08
	1.4E+01		U-234	1.0E-06	7.2E-08
	1.4E+01		U-235	4.8E-08	3.5E-09
318	1.5E+00	7.0E+00	Am-241	8.8E-10	6.0E-10
	1.5E+00		Am-243	8.1E-10	5.5E-10
	1.5E+00		Ba-133	1.4E-08	9.2E-09
	1.5E+00		C-14	1.4E-08	9.2E-09
	1.5E+00		Cl-36	1.4E-08	9.2E-09
	1.5E+00		Co-60	4.5E-06	3.1E-06
	1.5E+00		Cs-137	4.5E-06	3.1E-06
	1.5E+00		Eu-152	1.4E-08	9.2E-09
	1.5E+00		Eu-154	1.4E-08	9.2E-09
	1.5E+00		H-3	1.4E-08	9.2E-09
	1.5E+00		I-129	8.1E-10	5.5E-10
	1.5E+00		Kr-85	1.4E-08	9.2E-09
	1.5E+00		Nb-94	1.4E-08	9.2E-09
	1.5E+00		Ni-63	1.1E-08	7.7E-09
	1.5E+00		Pu-238	8.5E-10	5.8E-10
	1.5E+00		Pu-239	8.1E-10	5.5E-10
	1.5E+00		Pu-240	8.2E-10	5.6E-10
	1.5E+00		Pu-242	8.3E-10	5.6E-10
	1.5E+00		Se-79	1.4E-08	9.2E-09
	1.5E+00		Sr-90	2.7E-09	1.8E-09
	1.5E+00		Tc-99	1.4E-08	9.2E-09
	1.5E+00		Th-232	2.7E-09	1.8E-09
	1.5E+00		U-232	2.7E-09	1.8E-09
	1.5E+00		U-238	1.3E-08	8.8E-09

Table B-3. Isotope and Volume Summary of Disposed Waste (1989-1992) from Other Onsite Generator Facilities. (11 sheets)

Generator	Volume (m3)	No. Containers	Isotope	Activity (Ci)	Concentration (Ci/m3)
Pacific Northwest Laboratory (PNL)					
318	1.5E+00		U-234	1.3E-08	8.8E-09
	1.5E+00		U-235	6.1E-10	4.1E-10
320	1.1E+00	6.0E+00	Co-60	5.0E-04	4.6E-04
	1.1E+00		Cs-137	5.0E-04	4.6E-04
	1.1E+00		Sr-90	2.0E-06	1.8E-06
	1.1E+00		Th-232	5.1E-08	4.7E-08
	1.1E+00		U-238	3.3E-10	3.0E-10
	1.1E+00		U-234	3.3E-10	3.0E-10
	1.1E+00		U-235	1.6E-11	1.5E-11
323	4.8E+00	5.0E+00	Co-60	4.5E-03	9.2E-04
	4.8E+00		Cs-137	5.0E-04	1.0E-04
	4.8E+00		Sr-90	5.0E-04	1.0E-04
324	1.0E+03	3.3E+02	Co-60	1.9E+01	1.9E-02
	1.0E+03		Cs-137	6.1E+03	6.1E+00
	1.0E+03		Eu-152	1.3E+03	1.3E+00
	1.0E+03		Eu-154	1.9E+03	1.9E+00
	1.0E+03		I-129	5.0E-11	5.0E-14
	1.0E+03		Ra-226	3.3E-04	3.3E-07
	1.0E+03		Sr-90	4.6E+03	4.6E+00
	1.0E+03		Tc-99	1.0E-03	1.0E-06
	1.0E+03		U-238	1.2E-02	1.2E-05
	1.0E+03		U-234	1.2E-02	1.2E-05
	1.0E+03		U-235	5.8E-04	5.8E-07
	1.0E+03		U-Enriched	1.7E+02 gm	
325	7.2E+02	4.1E+02	Am-241	2.4E-02	3.3E-05
	7.2E+02		Cm-243	3.2E-05	4.5E-08
	7.2E+02		Cm-244	1.5E-06	2.1E-09
	7.2E+02		Co-60	9.2E-01	1.3E-03
	7.2E+02		Cs-137	4.2E+00	5.8E-03
	7.2E+02		Eu-154	6.5E-03	9.1E-06
	7.2E+02		H-3	1.8E+01	2.5E-02
	7.2E+02		Np-237	1.8E-05	2.5E-08
	7.2E+02		Pm-147	1.0E-01	1.4E-04
	7.2E+02		Pu	1.2E-01 gm	
	7.2E+02		Pu-238	6.3E-06	8.8E-09
	7.2E+02		Pu-239	9.9E-11	1.4E-13
	7.2E+02		Sm-151	2.5E-04	3.5E-07
	7.2E+02		Sr-90	3.0E+00	4.2E-03
	7.2E+02		Tc-99	1.0E-02	1.4E-05

Table B-3. Isotope and Volume Summary of Disposed Waste (1989-1992) from Other Onsite Generator Facilities. (11 sheets)

Generator	Volume (m3)	No. Containers	Isotope	Activity (Ci)	Concentration (Ci/m3)
Pacific Northwest Laboratory (PNL)					
325	7.2E+02		Th-232	4.8E-04	6.7E-07
	7.2E+02		U-238	2.2E-02	3.1E-05
	7.2E+02		U-234	2.2E-02	3.1E-05
	7.2E+02		U-235	1.1E-03	1.5E-06
	7.2E+02		U-Enriched	1.8E+03 gm	
325A	3.6E+01	9.0E+00	Cs-137	6.8E-07	1.9E-08
	3.6E+01		Eu-154	1.8E-06	5.1E-08
	3.6E+01		Sr-90	4.5E-08	1.3E-09
326	1.5E+01	4.2E+01	C-14	6.0E-06	4.2E-07
	1.5E+01		Co-60	1.4E-01	9.9E-03
	1.5E+01		H-3	4.0E-03	2.8E-04
	1.5E+01		Ni-59	1.0E-03	6.9E-05
	1.5E+01		Ni-63	9.6E-03	6.6E-04
	1.5E+01		Pu-238	1.7E-03	1.2E-04
	1.5E+01		U-238	4.0E-08	2.8E-09
	1.5E+01		U-234	4.0E-08	2.8E-09
	1.5E+01		U-235	1.9E-09	1.3E-10
327	9.7E+01	3.6E+02	Am-241	8.1E-05	8.3E-07
	9.7E+01		Am-243	1.0E-03	1.0E-05
	9.7E+01		Ba-133	2.5E-06	2.6E-08
	9.7E+01		C-14	6.3E-03	6.4E-05
	9.7E+01		Cl-36	1.0E-06	1.0E-08
	9.7E+01		Co-60	1.0E+03	1.1E+01
	9.7E+01		Cs-137	9.4E+01	9.6E-01
	9.7E+01		Eu-154	1.6E-01	1.6E-03
	9.7E+01		Eu-155	3.9E-04	4.0E-06
	9.7E+01		H-3	7.1E-03	7.3E-05
	9.7E+01		I-129	1.2E-06	1.3E-08
	9.7E+01		Mo-93	1.0E-05	1.0E-07
	9.7E+01		Nb-91	2.8E-02	2.9E-04
	9.7E+01		Ni-59	6.0E-04	6.2E-06
	9.7E+01		Ni-63	8.5E-04	8.8E-06
	9.7E+01		Np-237	4.1E-07	4.2E-09
	9.7E+01		Pu-239	3.7E-04	3.8E-06
	9.7E+01		Pu-241	8.0E-01	8.2E-03
	9.7E+01		Ra-226	4.1E-05	4.2E-07
	9.7E+01		Re-187	2.0E-04	2.1E-06
	9.7E+01		Sm-147	2.0E-04	2.1E-06
	9.7E+01		Sr-90	1.2E+00	1.2E-02
	9.7E+01		Tc-99	4.9E-03	5.0E-05

Table B-3. Isotope and Volume Summary of Disposed Waste (1989-1992) from Other Onsite Generator Facilities. (11 sheets)

Generator	Volume (m3)	No. Containers	Isotope	Activity (Ci)	Concentration (Ci/m3)
Pacific Northwest Laboratory (PNL)					
327	9.7E+01		U-232	1.0E-09	1.0E-11
	9.7E+01		U-238	1.6E-04	1.6E-06
	9.7E+01		U-234	1.6E-04	1.6E-06
	9.7E+01		U-235	7.5E-06	7.7E-08
	9.7E+01		U-Enriched	4.91E+02 gm	
327C	7.8E+01	2.7E+02	C-14	8.7E-03	1.1E-04
	7.8E+01		Cm-244	8.1E-04	1.0E-05
	7.8E+01		Cm-245	1.7E-06	2.2E-08
	7.8E+01		Co-60	1.5E+04	2.0E+02
	7.8E+01		Cs-137	6.8E+01	8.8E-01
	7.8E+01		Eu-154	2.4E-01	3.1E-03
	7.8E+01		H-3	1.1E-02	1.5E-04
	7.8E+01		I-129	2.5E-03	3.2E-05
	7.8E+01		Kr-85	2.0E-03	2.6E-05
	7.8E+01		Ni-59	6.5E-03	8.4E-05
	7.8E+01		Ni-63	1.0E-04	1.3E-06
	7.8E+01		Np-237	1.0E-05	1.3E-07
	7.8E+01		Pu	2.0E-03 gm	
	7.8E+01		Ra-226	2.0E-06	2.6E-08
	7.8E+01		Se-79	1.0E-04	1.3E-06
	7.8E+01		Sr-90	3.9E-01	5.1E-03
	7.8E+01		Tc-99	3.3E-03	4.3E-05
	7.8E+01		Th-232	2.2E-13	2.8E-15
	7.8E+01		U-238	4.1E-04	5.3E-06
	7.8E+01		U-234	4.1E-04	5.3E-06
	7.8E+01		U-235	1.9E-05	2.4E-07
	7.8E+01		U-Enriched	6.7E-02 gm	
329	3.8E+01	9.0E+01	Am-241	3.5E-08	9.2E-10
	3.8E+01		Am-243	1.1E-07	2.9E-09
	3.8E+01		C-14	1.1E-07	2.9E-09
	3.8E+01		Co-60	4.5E-02	1.2E-03
	3.8E+01		Cs-137	3.0E-02	7.9E-04
	3.8E+01		Eu-152	2.8E-04	7.5E-06
	3.8E+01		Eu-154	3.3E-04	8.7E-06
	3.8E+01		H-3	1.0E-04	2.6E-06
	3.8E+01		Ni-63	5.8E-04	1.5E-05
	3.8E+01		Po-210	5.0E-08	1.3E-09
	3.8E+01		Pu	2.7E-05 gm	
	3.8E+01		Pu-241	1.6E-08	4.2E-10
	3.8E+01		Sr-90	9.6E-03	2.5E-04
	3.8E+01		Tc-99	6.0E-05	1.6E-06

Table B-3. Isotope and Volume Summary of Disposed Waste (1989-1992) from Other Onsite Generator Facilities. (11 sheets)

Generator	Volume (m3)	No. Containers	Isotope	Activity (Ci)	Concentration (Ci/m3)
Pacific Northwest Laboratory (PNL)					
329	3.8E+01		U-238	6.6E-08	1.7E-09
	3.8E+01		U-234	6.6E-08	1.7E-09
	3.8E+01		U-235	3.1E-09	8.2E-11
	3.8E+01		U-Enriched	2.0E+01 gm	
331	4.5E+01	2.1E+02	C-14	5.7E-03	1.3E-04
	4.5E+01		Co-60	3.5E-03	7.9E-05
	4.5E+01		Cs-137	2.1E-02	4.7E-04
	4.5E+01		H-3	5.9E-03	1.3E-04
	4.5E+01		Pm-147	1.0E-09	2.2E-11
	4.5E+01		Pu	1.3E-03 gm	
	4.5E+01		Pu-238	1.9E-05	4.3E-07
	4.5E+01		Pu-239	7.8E-07	1.8E-08
	4.5E+01		Pu-240	9.0E-08	2.0E-09
	4.5E+01		Sr-90	4.0E-04	9.0E-06
	4.5E+01		Th-232	1.0E-13	2.2E-15
	4.5E+01		U-238	3.6E-13	8.1E-15
	4.5E+01		U-234	3.6E-13	8.1E-15
	4.5E+01		U-235	1.7E-14	3.8E-16
3708	1.2E+00	7.0E+00	Am-241	3.5E-06	2.8E-06
	1.2E+00		C-14	1.0E-06	8.1E-07
	1.2E+00		Cm-243	5.2E-05	4.2E-05
	1.2E+00		Co-60	1.1E-08	8.9E-09
	1.2E+00		Cs-137	1.7E-04	1.4E-04
	1.2E+00		I-129	1.0E-09	8.1E-10
	1.2E+00		Pa-231	5.0E-11	4.1E-11
	1.2E+00		Pu	1.0E-05 gm	
	1.2E+00		Ra-226	9.9E-07	8.0E-07
	1.2E+00		Sr-90	3.0E-08	2.4E-08
	1.2E+00		Tc-99	1.0E-09	8.1E-10
	1.2E+00		Th-232	1.0E-09	8.1E-10
	1.2E+00		U-238	4.3E-09	3.5E-09
	1.2E+00		U-234	4.3E-09	3.5E-09
	1.2E+00		U-235	2.0E-10	1.6E-10
	1.2E+00		U-Enriched	5.0E-01 gm	

Table B-3. Isotope and Volume Summary of Disposed Waste (1989-1992) from Other Onsite Generator Facilities. (11 sheets)

Generator	Volume (m3)	No. Containers	Isotope	Activity (Ci)	Concentration (Ci/m3)
Pacific Northwest Laboratory (PNL)					
3720	4.0E+01	9.9E+01	Am-241	3.5E-04	8.7E-06
	4.0E+01		Am-243	4.0E-05	1.0E-06
	4.0E+01		C-14	2.4E-03	5.9E-05
	4.0E+01		Co-60	3.8E-01	9.5E-03
	4.0E+01		Cs-137	1.1E-01	2.7E-03
	4.0E+01		Eu-154	2.0E-06	5.0E-08
	4.0E+01		H-3	7.3E-03	1.8E-04
	4.0E+01		Ra-226	9.9E-07	2.5E-08
	4.0E+01		Tc-99	4.9E-02	1.2E-03
	4.0E+01		U-238	5.2E-06	1.3E-07
	4.0E+01		U-234	5.2E-06	1.3E-07
	4.0E+01		U-235	2.5E-07	6.2E-09
	4.0E+01		U-Enriched	3.2E-01 gm	
3730	1.4E+00	6.0E+00	Co-60	1.5E-01	1.1E-01
	1.4E+00		Ni-63	6.0E-04	4.4E-04
3745	1.9E-01	3.0E+00	Co-60	6.0E-05	3.2E-04
	1.9E-01		Cs-137	1.2E-03	6.5E-03
3746	1.3E+00	7.0E+00	C-14	5.0E-03	4.0E-03
	1.3E+00		H-3	1.0E+01	7.9E+00
6652	1.4E+00	9.0E+00	Co-60	9.0E-04	6.5E-04
	1.4E+00		Cs-137	2.8E-03	2.0E-03
	1.4E+00		Sr-90	1.0E-03	7.2E-04
6652H	2.1E-01	1.0E+00	Co-60	1.0E-06	4.8E-06
	2.1E-01		Pu	1.6E-05 gm	
6652I	2.0E+01	5.0E+00	Am-241	2.4E-02	1.2E-03
	2.0E+01		C-14	1.0E-03	5.0E-05
	2.0E+01		Cm-244	2.5E-01	1.2E-02
	2.0E+01		I-129	3.0E-05	1.5E-06
	2.0E+01		Np-237	1.0E-02	5.0E-04
	2.0E+01		Pu	5.2E-01 gm	
	2.0E+01		U-232	3.1E-03	1.5E-04
ISV	9.8E+00	7.0E+00	Co-60	9.9E-04	1.0E-04
	9.8E+00		Cs-137	1.1E-03	1.1E-04
	9.8E+00		Sr-90	1.0E-03	1.1E-04

Table B-3. Isotope and Volume Summary of Disposed Waste (1989-1992) from Other Onsite Generator Facilities. (11 sheets)

Generator	Volume (m3)	No. Containers	Isotope	Activity (Ci)	Concentration (Ci/m3)
Pacific Northwest Laboratory (PNL)					
LSLII	1.2E+01	7.2E+01	C-14	2.5E-02	2.1E-03
	1.2E+01		Cl-36	1.0E-04	8.4E-06
	1.2E+01		Co-60	1.3E-03	1.1E-04
	1.2E+01		Cs-137	1.6E-03	1.3E-04
	1.2E+01		H-3	5.6E-03	4.7E-04
	1.2E+01		Ni-63	2.2E-03	1.9E-04
	1.2E+01		Ra-228	6.0E-04	5.1E-05
	1.2E+01		Tc-99	1.8E-03	1.5E-04
	1.2E+01		U-238	6.6E-07	5.6E-08
	1.2E+01		U-234	6.6E-07	5.6E-08
	1.2E+01		U-235	3.1E-08	2.6E-09
RTL	2.1E+00	1.1E+01	C-14	5.5E-03	2.7E-03
	2.1E+00		Cs-137 --Ba-137m	7.2E-04	3.5E-04
	2.1E+00		Total Beta/Gamma	9.1E-03	4.4E-03
	2.1E+00		U-Depleted	0.018 gm	
Support Services					
1171	1.5E+01	2.0E+00	Tot. Beta/Gamma	2.0E-04	1.3E-05
2713W	6.5E+02	1.6E+01	Co-60	3.0E-03	4.6E-06
	6.5E+02		Cs-137	1.5E-03	2.3E-06
	6.5E+02		Sr-90	1.5E-03	2.3E-06
	6.5E+02		Tc-99	5.6E-06	8.6E-09
	6.5E+02		U-238	3.5E-07	5.4E-10
	6.5E+02		U-234	3.5E-07	5.4E-10
	6.5E+02		U-235	1.7E-08	2.6E-11
2724W	6.9E+02	5.4E+02	Am-241	2.7E-03	3.9E-06
	6.9E+02		Co-60	2.9E-02	4.3E-05
	6.9E+02		Cs-137	1.3E-03	1.9E-06
	6.9E+02		Eu-154	3.0E-04	4.3E-07
	6.9E+02		K-40	8.3E-05	1.2E-07
	6.9E+02		Pm-147	3.6E-07	5.2E-10
	6.9E+02		Sr-90	1.1E-02	1.6E-05
	6.9E+02		U-238	5.2E-06	7.6E-09
	6.9E+02		U-234	5.2E-06	7.6E-09
	6.9E+02		U-235	2.5E-07	3.6E-10
	6.9E+02		U-Enriched	3.7E-05 gm	

Table B-3. Isotope and Volume Summary of Disposed Waste (1989-1992) from Other Onsite Generator Facilities. (11 sheets)

Generator	Volume (m3)	No. Containers	Isotope	Activity (Ci)	Concentration (Ci/m3)
Support Services					
2727S	2.2E+01	5.0E+00	Co-60	5.0E-06	2.3E-07
	2.2E+01		Cs-137	5.0E-06	2.3E-07
	2.2E+01		Sr-90	5.0E-06	2.3E-07
277W	3.4E-01	1.0E+00	Co-60	1.0E-04	2.9E-04
	3.4E-01		Sr-90	1.0E-04	2.9E-04
300A	4.5E+01	1.4E+01	Co-60	6.6E-02	1.5E-03
	4.5E+01		Cs-137	4.8E-06	1.1E-07
	4.5E+01		Eu-152	2.6E-05	5.8E-07
	4.5E+01		Ni-63	4.3E-02	9.5E-04
	4.5E+01		U-Enriched	1.5E+02 gm	
309	1.6E+01	3.0E+00	Cs-137	1.4E-04	8.6E-06
	1.6E+01		Pu	6.4E-03 gm	
Fast Flux Test Facility					
437	5.8E+01	1.1E+02	Co-60	2.2E-03	3.8E-05
	5.8E+01		Cs-137	6.9E-03	1.2E-04
Hanford Environmental Health Foundation (HEHF)					
748	2.1E-01	1.0E+00	Cs-137	1.0E-06	4.8E-06
	2.1E-01		Eu-154	2.5E-07	1.2E-06
			Pu	1.4E-06 gm	

Table B-4. Isotope and Volume Summary of Disposed Waste (1989-1992) from Offsite Waste Facilities. (6 sheets)

Generator	Volume (m3)	No. Containers	Isotope	Activity (Ci)	Concentration (Ci/m3)
ALBNY	1.3E+02	61	Ra-226	8.1E-04	6.4E-06
	1.3E+02		Th-232	3.2E-02	2.5E-04
	1.3E+02		Tot. Beta/Gamma	5.8E-03	4.6E-05
	1.3E+02		U-238	1.8E-03	1.4E-05
	1.3E+02		U-234	1.8E-03	1.4E-05
	1.3E+02		U-235	8.3E-05	6.5E-07
ALQPA	1.0E+01	9	Tot. Beta/Gamma	7.6E-03	7.3E-04
	1.0E+01		U-238	2.9E-02	2.8E-03
	1.0E+01		U-234	2.9E-02	2.8E-03
	1.0E+01		U-235	1.3E-03	1.3E-04
AMES	3.5E+01	9	Co-60	7.5E-06	2.2E-07
	3.5E+01		Cs-137	9.4E-06	2.7E-07
	3.5E+01		Th-232	2.6E-04	7.5E-06
	3.5E+01		Tot. Beta/Gamma	4.1E-04	1.2E-05
	3.5E+01		U-238	1.1E-04	3.2E-06
	3.5E+01		U-234	1.1E-04	3.2E-06
	3.5E+01		U-235	5.2E-06	1.5E-07
ARGON	2.2E+02	376	Am-241	1.5E-02	6.8E-05
	2.2E+02		Am-243	9.8E-05	4.5E-07
	2.2E+02		Ba-133	1.1E-03	4.8E-06
	2.2E+02		C-14	2.3E-03	1.1E-05
	2.2E+02		Cm-244	8.1E-10	3.7E-12
	2.2E+02		Co-60	6.2E-02	2.8E-04
	2.2E+02		Cs-137	3.2E-01	1.4E-03
	2.2E+02		Eu-152	1.4E-04	6.3E-07
	2.2E+02		Eu-154	6.5E-05	3.0E-07
	2.2E+02		H-3	7.1E-03	3.2E-05
	2.2E+02		I-129	5.4E-05	2.5E-07
	2.2E+02		Mo-93	8.9E-02	4.1E-04
	2.2E+02		Np-237	2.9E-03	1.3E-05
	2.2E+02		Pa-231	1.8E-02	8.2E-05
	2.2E+02		Po-210	1.0E-06	4.6E-09
	2.2E+02		Pu-238	9.9E-01	4.5E-03
	2.2E+02		Pu-239	8.7E-03	4.0E-05
	2.2E+02		Pu-240	1.1E-06	5.0E-09
	2.2E+02		Pu-241	1.7E-03	7.7E-06
	2.2E+02		Pu-242	1.7E-06	7.7E-09
	2.2E+02		Ra-226	1.1E-06	5.0E-09
	2.2E+02		Sr-90	2.8E-05	1.3E-07
	2.2E+02		Tc-99	1.8E-02	8.2E-05
	2.2E+02		Th-232	2.0E-05	9.1E-08
	2.2E+02		U-233	2.3E-05	1.0E-07

Table B-4. Isotope and Volume Summary of Disposed Waste (1989-1992) from Offsite Waste Facilities. (6 sheets)

Generator	Volume (m3)	No. Containers	Isotope	Activity (Ci)	Concentration (Ci/m3)
ARGON	2.2E+02	376	U-238	8.1E-03	3.7E-05
	2.2E+02		U-234	8.1E-03	3.7E-05
	2.2E+02		U-235	3.9E-04	1.8E-06
BAPL	4.2E+01	20	Be-10	8.0E-10	1.9E-11
	4.2E+01		C-14	3.3E-04	7.9E-06
	4.2E+01		Cl-36	3.3E-07	7.9E-09
	4.2E+01		Cm-242	1.6E-03	3.8E-05
	4.2E+01		Co-60	8.7E-02	2.1E-03
	4.2E+01		Cs-135	2.0E-06	4.7E-08
	4.2E+01		Cs-137	4.8E+00	1.1E-01
	4.2E+01		Eu-152	5.3E-01	1.3E-02
	4.2E+01		Eu-154	4.0E-01	9.4E-03
	4.2E+01		H-3	1.4E-02	3.4E-04
	4.2E+01		I-129	7.1E-07	1.7E-08
	4.2E+01		Kr-85	4.8E-01	1.1E-02
	4.2E+01		Nb-94	1.4E-04	3.3E-06
	4.2E+01		Ni-59	4.4E-04	1.0E-05
	4.2E+01		Ni-63	6.8E-02	1.6E-03
	4.2E+01		Pm-147	2.9E+00	6.8E-02
	4.2E+01		Pu-238	5.3E-02	1.3E-03
	4.2E+01		Pu-241	1.6E-01	3.8E-03
	4.2E+01		Se-79	3.0E-06	7.2E-08
	4.2E+01		Sm-151	1.8E-03	4.2E-05
	4.2E+01		Sn-121M	5.1E-07	1.2E-08
	4.2E+01		Sn-126	2.6E-06	6.2E-08
	4.2E+01		Sr-90	4.9E+00	1.2E-01
	4.2E+01		Tc-99	3.3E-04	7.9E-06
	4.2E+01		Zr-93	3.3E-05	7.8E-07
BATCO	6.0E+01	103	Am-241	8.4E-04	1.4E-05
	6.0E+01		Am-243	2.2E-03	3.6E-05
	6.0E+01		C-14	7.4E-08	1.2E-09
	6.0E+01		CM-243	2.2E-06	3.6E-08
	6.0E+01		Cm-244	2.7E-03	4.5E-05
	6.0E+01		Cm-245	2.4E-08	4.0E-10
	6.0E+01		Co-60	3.8E-02	6.2E-04
	6.0E+01		Cs-137	1.1E-01	1.8E-03
	6.0E+01		Eu-154	5.8E-03	9.7E-05
	6.0E+01		H-3	5.7E-04	9.4E-06
	6.0E+01		I-129	6.2E-06	1.0E-07
	6.0E+01		Ni-59	2.9E-05	4.8E-07
	6.0E+01		Ni-63	3.7E-03	6.1E-05
	6.0E+01		Np-237	3.8E-05	6.3E-07
	6.0E+01		Pu	1.2E-02 gm	

Table B-4. Isotope and Volume Summary of Disposed Waste (1989-1992) from Offsite Waste Facilities. (6 sheets)

Generator	Volume (m3)	No. Containers	Isotope	Activity (Ci)	Concentration (Ci/m3)
BATCO	6.0E+01	103	Ra-226	1.1E-05	1.8E-07
	6.0E+01		Sr-90	8.5E-02	1.4E-03
	6.0E+01		Tc-99	1.5E-05	2.5E-07
	6.0E+01		Th-232	6.5E-14	1.1E-15
	6.0E+01		U-233	3.3E-12	5.5E-14
	6.0E+01		U-Enriched	3.6E+04 gm	
BETTS	1.1E+02	4	Am-241	3.5E-06	3.2E-08
	1.1E+02		C-14	2.0E+01	1.8E-01
	1.1E+02		Cm-244	3.3E-06	3.0E-08
	1.1E+02		Co-60	4.6E+04	4.1E+02
	1.1E+02		Cs-137	6.0E-04	5.4E-06
	1.1E+02		H-3	9.4E-01	8.5E-03
	1.1E+02		I-129	6.2E-08	5.6E-10
	1.1E+02		Nb-94	5.6E-01	5.1E-03
	1.1E+02		Ni-59	4.0E+02	3.6E+00
	1.1E+02		Ni-63	4.8E+04	4.3E+02
	1.1E+02		Pu	1.2E-04 gm	
	1.1E+02		Se-79	6.2E-08	5.6E-10
	1.1E+02		Sr-90	4.5E-02	4.0E-04
	1.1E+02		Tc-99	1.5E-05	1.4E-07
	1.1E+02		Zr-93	6.2E-07	5.6E-09
BNLAB	1.4E+03	221	Am-241	7.4E-05	5.3E-08
	1.4E+03		Ba-133	6.2E-02	4.4E-05
	1.4E+03		Bi-207	2.7E-03	1.9E-06
	1.4E+03		C-14	1.6E-04	1.1E-07
	1.4E+03		Cl-36	1.0E-04	7.2E-08
	1.4E+03		Co-60	3.9E+00	2.8E-03
	1.4E+03		Cs-137	7.0E+01	5.0E-02
	1.4E+03		Eu-152	6.9E-02	4.9E-05
	1.4E+03		Eu-154	2.8E-03	2.0E-06
	1.4E+03		H-3	2.5E+02	1.8E-01
	1.4E+03		K-40	5.4E-04	3.9E-07
	1.4E+03		Kr-85	8.0E-04	5.7E-07
	1.4E+03		Nb-94	7.5E-05	5.4E-08
	1.4E+03		Pu	1.4E+02 gm	
	1.4E+03		Pu-238	5.8E-05	4.1E-08
	1.4E+03		Pu-239	5.2E-07	3.7E-10
	1.4E+03		Pu-240	2.2E-07	1.6E-10
	1.4E+03		Ra-226	3.8E-04	2.7E-07
	1.4E+03		Sr-90	2.0E+02	1.5E-01
	1.4E+03		Tc-99	1.6E-05	1.1E-08
	1.4E+03		Th-232	4.3E-07	3.1E-10
	1.4E+03		U-238	1.1E-01	7.9E-05

Table B-4. Isotope and Volume Summary of Disposed Waste (1989-1992) from Offsite Waste Facilities. (6 sheets)

Generator	Volume (m3)	No. Containers	Isotope	Activity (Ci)	Concentration (Ci/m3)
BNLAB	1.4E+03	221	U-234	1.1E-01	7.9E-05
	1.4E+03		U-235	5.2E-03	3.7E-06
CENEL	2.9E-01	1	Co-60	1.6E+03	5.6E+03
CNGA	8.4E+00	40	Tot. Beta/Gamma	7.0E-03	8.3E-04
CRBBC	8.4E-02	3	Cs-137	5.5E-06	6.5E-05
	8.4E-02		Sr-90	6.9E-07	8.2E-06
	8.4E-02		Tc-99	2.7E-07	3.2E-06
	8.4E-02		Tot. Beta/Gamma	1.3E-05	1.5E-04
CUPRC	6.8E-01	1	Tot. Beta/Gamma	2.0E+00	2.9E+00
	6.8E-01		U-Enriched	1.4E+06 gm	
DAVIS	2.1E+02	867	Cm-243	6.8E-09	3.3E-11
	2.1E+02		Cm-244	5.7E-04	2.7E-06
	2.1E+02		H-3	3.0E-03	1.4E-05
	2.1E+02		Pu	1.6E+00 gm	
	2.1E+02		Pu-241	1.1E-04	5.3E-07
	2.1E+02		Ra-226	2.9E+00	1.4E-02
	2.1E+02		Sr-90	6.1E-02	2.9E-04
	2.1E+02		Th-232	3.1E-04	1.5E-06
	2.1E+02		Tot. Beta/Gamma	1.8E-01	8.8E-04
ESG	2.4E+02	111	Co-60	6.8E+00	2.9E-02
	2.4E+02		Cs-137	2.0E-03	8.4E-06
	2.4E+02		Eu-152	1.3E-01	5.5E-04
	2.4E+02		Eu-154	1.6E-02	6.8E-05
	2.4E+02		Ni-63	3.2E+00	1.3E-02
	2.4E+02		Tot. Beta/Gamma	4.7E+01	2.0E-01
	2.4E+02		U-238	5.8E-09	2.4E-11
	2.4E+02		U-234	5.8E-09	2.4E-11
	2.4E+02		U-235	2.7E-10	1.1E-12
LBLAB	1.5E+02	230	Am-241	9.9E-05	6.5E-07
	1.5E+02		Am-243	1.5E-06	9.9E-09
	1.5E+02		Ba-133	1.0E-06	6.6E-09
	1.5E+02		C-14	7.4E-02	4.9E-04
	1.5E+02		Cm-244	4.1E-04	2.7E-06
	1.5E+02		Co-60	4.4E-02	2.9E-04
	1.5E+02		Cs-137	1.2E-05	8.0E-08
	1.5E+02		Eu-152	3.4E-03	2.2E-05
	1.5E+02		FE-59	6.1E-04	4.0E-06
	1.5E+02		H-3	4.3E+04	2.8E+02

Table B-4. Isotope and Volume Summary of Disposed Waste (1989-1992) from Offsite Waste Facilities. (6 sheets)

Generator	Volume (m3)	No. Containers	Isotope	Activity (Ci)	Concentration (Ci/m3)
LBLAB	1.5E+02	230	I-129	1.0E-05	6.6E-08
	1.5E+02		K-40	1.0E-04	6.6E-07
	1.5E+02		Nb-91	2.0E-05	1.3E-07
	1.5E+02		Np-237	3.3E-05	2.2E-07
	1.5E+02		Pa-231	6.8E-03	4.5E-05
	1.5E+02		Pu	8.1E-05 gm	
	1.5E+02		Ra-226	5.8E-08	3.8E-10
	1.5E+02		Sr-90	2.7E-04	1.8E-06
	1.5E+02		Tc-99	2.5E-04	1.6E-06
	1.5E+02		Th-232	5.1E-03	3.4E-05
	1.5E+02		U-238	9.5E-02	6.3E-04
	1.5E+02		U-234	9.5E-02	6.3E-04
	1.5E+02		U-235	4.6E-03	3.0E-05
	1.5E+02		U-Enriched	9.7E+01 gm	
NALAB	7.3E+01	343	Am-241	1.8E-02	2.5E-04
	7.3E+01		Am-243	1.4E-06	1.9E-08
	7.3E+01		Bi-207	2.4E-05	3.2E-07
	7.3E+01		Co-60	5.2E-02	7.1E-04
	7.3E+01		Cs-137	1.1E-04	1.5E-06
	7.3E+01		H-3	2.9E-01	4.0E-03
	7.3E+01		Ra-226	9.7E-05	1.3E-06
	7.3E+01		Sr-90	5.0E-07	6.8E-09
	7.3E+01		Tc-99	3.0E-07	4.1E-09
	7.3E+01		U-238	5.0E-03	6.8E-05
	7.3E+01		U-234	5.0E-03	6.8E-05
	7.3E+01		U-235	2.4E-04	3.3E-06
NAVY	1.6E+02	18	C-14	1.2E-01	7.3E-04
	1.6E+02		Co-60	4.8E+00	2.9E-02
	1.6E+02		H-3	4.3E-04	2.6E-06
	1.6E+02		I-129	1.2E-06	7.3E-09
	1.6E+02		Ni-63	2.9E-01	1.8E-03
	1.6E+02		Tc-99	1.2E-06	7.3E-09
PGDF	1.6E+01	4	Tot. Beta/Gamma	1.0E-02	6.3E-04
	1.6E+01		U-238	1.9E-05	1.2E-06
	1.6E+01		U-234	1.9E-05	1.2E-06
	1.6E+01		U-235	9.1E-07	5.5E-08

Table B-4. Isotope and Volume Summary of Disposed Waste (1989-1992) from Offsite Waste Facilities. (6 sheets)

Generator	Volume (m3)	No. Containers	Isotope	Activity (Ci)	Concentration (Ci/m3)
PHNSY	1.9E+02	25	C-14	8.0E+00	4.3E-02
	1.9E+02		H-3	4.5E-02	2.4E-04
	1.9E+02		I-129	1.0E-03	5.4E-06
	1.9E+02		Ni-63	2.0E+01	1.1E-01
	1.9E+02		Tc-99	1.0E-03	5.4E-06
	1.9E+02		Tot. Beta/Gamma	9.1E+02	4.9E+00
PRINC	2.1E+00	10	H-3	1.0E-04	4.8E-05
RF	1.9E+01	89	Am-241	8.6E-04	4.6E-05
	1.9E+01		Pu-238	2.9E-06	1.6E-07
	1.9E+01		Pu-239	3.8E-05	2.0E-06
	1.9E+01		Pu-240	8.9E-06	4.8E-07
	1.9E+01		Pu-241	2.7E-04	1.5E-05
	1.9E+01		Pu-242	1.4E-09	7.5E-11
	1.9E+01		Tot. Beta/Gamma	1.0E-02	5.4E-04
SLACU	1.2E+01	58	Co-60	5.0E-03	4.1E-04
	1.2E+01		Cs-137	2.1E-05	1.7E-06
	1.2E+01		Tot. Beta/Gamma	1.7E-02	1.4E-03
SPAP	9.2E+01	30	Co-60	1.9E+01	2.0E-01
	9.2E+01		Ra-228	6.0E-04	6.5E-06
TRWSG	3.0E+01	138	Ni-63	5.0E-03	1.7E-04
	3.0E+01		Tot. Beta/Gamma	1.6E-02	5.4E-04
	3.0E+01		U-238	7.1E-03	2.4E-04
	3.0E+01		U-234	7.1E-03	2.4E-04
	3.0E+01		U-235	3.4E-04	1.2E-05
	3.0E+01		U-Enriched	8.9E+03 gm	
UURD	3.9E+00	3	Am-241	1.5E-04	3.8E-05
	3.9E+00		H-3	3.4E-03	8.8E-04
	3.9E+00		Pu	1.0E-02 gm	
	3.9E+00		Ra-226	5.2E-04	1.3E-04
	3.9E+00		Sr-90	1.5E-02	3.9E-03
	3.9E+00		Tot. Beta/Gamma	3.4E-01	8.6E-02
	3.9E+00		U-238	1.0E-06	2.6E-07
	3.9E+00		U-234	1.0E-06	2.6E-07
	3.9E+00		U-235	4.8E-08	1.2E-08
	3.9E+00		U-Enriched	1.2E-05 gm	

Table B-5. Average Radionuclide Concentrations in the 1989-1992 Data Base Waste Stream

Nuclide	Average Concentration		Nuclide	Average Concentration	
	Category 1	Category 3		Category 1	Category 3
H-3	3.3E-05	5.3E+00	Pa-231		6.7E-05
Be-10		1.9E-11	U-232	1.8E-09	2.6E-05
C-14	2.5E-08	4.5E-05	U-233		5.8E-05
C-14°		9.3E-02	U-234	8.7E-09	4.6E-04
Cl-36	9.2E-09	1.3E-07	U-235	4.2E-10	2.2E-05
K-40	5.5E-06	3.2E-07	U-236		
Co-60	5.8E-03	6.4E+00	U-238	8.7E-09	4.6E-04
Ni-59	1.0E-03	1.2E+00	Np-237	5.2E-07	1.0E-05
Ni-63	4.3E-03	3.0E+01	Pu-238	1.1E-05	1.4E-03
Se-79	9.3E-09	2.1E-08	Pu-239	9.4E-07	2.5E-06
Sr-90	4.5E-03	4.5E-01	Pu-240	1.6E-10	4.5E-09
Zr-93		2.2E-07	Pu-241	1.4E-06	2.3E-04
Nb-94	9.2E-09	1.5E-07	Pu-242	1.1E-10	1.4E-09
Nb-94°		5.1E-03	Pu-244		
Mo-93		4.1E-04	Am-241	1.5E-05	1.2E-04
Tc-99	9.6E-08	9.8E-06	Am-242m		
Pd-107			Am-243	2.8E-09	5.2E-06
Cd-113m			Cm-243	8.2E-09	8.2E-07
Sn-121m		1.2E-08	Cm-244	4.5E-05	1.7E-04
Sn-126		6.2E-08	Cm-245	4.0E-10	2.2E-08
I-129	2.8E-08	7.6E-06	Cm-246		
Ba-133	9.2E-09	3.4E-05	Cm-247		
Cs-135	4.7E-08		Cm-248		
Cs-137	9.4E-04	6.5E-01			
Sm-147	1.6E-08	2.1E-06			
Sm-151		2.9E-04	° Isotope is in activated metal		
Eu-150					
Eu-152	3.7E-04	4.6E-01			
Eu-154	1.4E-05	2.1E-01			
Gd-152					
Re-187		2.1E-06			
Pb-210	2.9E-09				
Po-209					
Ra-226	6.2E-07	1.5E-03			
Ra-228		5.1E-05			
Ac-227					
Th-229					
Th-230					
Th-232	2.5E-08	1.3E-05			

Figure B-1. 1994 Solid Waste Forecast Questionnaire (4 sheets)

1994 SOLID WASTE FORECAST QUESTIONNAIRE

A. Please answer all questions. This information will help determine Hanford's treatment, storage, and disposal requirements.

Question 4 (for all waste classes) and Question 5 (for mixed and hazardous waste only) provide a basis for determining how your waste will be grouped. Be sure to answer these questions or your forms will be returned.

B. Ensure that the contact name, Level 3 Manager, and budget personnel are identified in the sign-off area of the questionnaire. Names must be typed (or printed) as well as written.

1. Please circle the waste classes that will be generated.

CH_LLW_I	CH_LLW_III	CH_LLW_GTCIII
RH_LLW_I	RH_LLW_III	RH_LLW_GTC_III
CH_LLMW_I	CH_LLMW_III	CH_LLMW_GTCIII
RH_LLMW_I	RH_LLMW_III	RH_LLMW_GTCIII
CH_TRU	CH_TRUM	HAZ
RH_TRU	RH_TRUM	

2. Generally describe these wastes and how they will be generated.

_____

_____

_____

_____

3. Have your waste volumes changed from your previous forecast? Yes No

Explain:_____

_____

_____

_____

_____

Figure B-1. 1994 Solid Waste Forecast Questionnaire (4 sheets)

1994 SOLID WASTE FORECAST QUESTIONNAIRE

4. Will waste be separated into like waste forms prior to shipping? (If you generate contaminated soils, inorganic particulates and metal debris, will you ship these waste in separate containers or will the waste be combined and placed into one container?)

Please explain for each waste class:

5. If you generate hazardous or mixed waste please answer the following question.

Will you place several hazardous constituents in one container or will you segregate the constituents prior to shipping? (If you generate toxic metals and ignitables will you ship these constituents in separate containers or will they be combined and placed into one container?)

If the hazardous constituents are segregated, make sure each waste class by waste form (reference Table 4) has been explained using the method in Attachment B. Please provide further explanation if needed.

6. Describe your quarterly expected shipping schedule for each applicable waste class during FY-1995 (e.g., 40% of waste shipped during the first quarter, 20% in the second quarter, etc.).

Figure B-1. 1994 Solid Waste Forecast Questionnaire (4 sheets)

1994 SOLID WASTE FORECAST QUESTIONNAIRE

7. Discuss the assumptions that were used to prepare this forecast. (Identify known dates for facility closure, decontamination and decommissioning [D&D], or any new programs that drive the forecast data provided in this request.)

_____

_____

_____

_____

_____

_____

_____

8. What assumptions were used in estimating the minimum and maximum waste volumes identified in Table 1? (Minimum waste percentage is based upon the majority of the waste being sent to a commercial disposal site. Maximum waste percentage is based upon additional projects being initiated that will generate waste not accounted for in the best estimate volume.)

Minimum: _____

_____

_____

Maximum: _____

_____

_____

9. Indicate confidence level for the following waste characterization data: (The physical waste forms are based upon historical characterization information.)

Physical Waste Forms (Table 3): High Low Medium

Explain: _____

Hazardous Constituents (Table 4): High Low Medium

Explain: _____

Radiation Type (Table 5) High Low Medium

Explain: _____

Figure B-1. 1994 Solid Waste Forecast Questionnaire (4 sheets)

1994 SOLID WASTE FORECAST QUESTIONNAIRE

10. What percentage of the waste forecasted is existing waste? _____
Of your existing waste, how confident are you in the current shipping schedule? HIGH LOW MEDIUM

Explain: _____

What percentage of waste forecasted is future generated waste? _____

Of your future generated waste, how confident are you in the volumes and shipping schedule? HIGH LOW MEDIUM

Explain: _____

10a. Please indicate whether your forecasts include only operational waste, or if transitional waste, environmental restoration (ER) and/or D&D activities have also been included. If transitional waste, ER and D&D have been included, indicate when each of these activities will take place.

_____

_____

_____

10b. If you have not included transitional waste, ER, or D&D waste, will this waste potentially be managed at Hanford? Please provide an estimate of the expected volumes and years that the waste would be shipped.

_____

_____

_____

11. Please supply contact personnel information for data verification. Names must be typed (or printed) as well as written:

LLW: _____ Phone: _____

LLMW: _____ Phone: _____

TRU: _____ Phone: _____

TRUM: _____ Phone: _____

HAZ: _____ Phone: _____
(Waste Contact)

Approved by: _____ Date: _____
(Level 3 Manager Signature)

Approved by: _____ Date: _____
(Budget Concurrence)

APPENDIX C

MODELING EQUATIONS, PARAMETER SELECTION, AND PARAMETER VALUES USED FOR THE EXPOSURE PATHWAY ANALYSIS

This page intentionally left blank.

MODELING EQUATIONS, PARAMETER SELECTION, AND PARAMETER VALUES USED FOR THE EXPOSURE PATHWAY ANALYSIS

In this section, the details needed to quantify the internal and external doses for each exposure pathway are described. Exposure pathways that are assumed in the inadvertent intrusion scenarios, the groundwater pathway scenarios (irrigator and Columbia River) and the atmospheric dispersion scenario are discussed. Section C.1 follows the progression of contaminants from soil through plants and animals into the human. Section C.2 considers vapor transport from the soil to the atmosphere to man.

C.1 MODELS AND PARAMETER VALUES FOR EXPOSURE FROM CONTAMINATED SOIL AND WATER

In this section the details for each exposure pathway are described. It follows the progression from soil through plants and animals into the human.

C.1.1 Soil Concentration for the Intruder Garden Scenarios

In the intruder scenarios the initial waste concentration is given. The age of the waste may require additional nuclides (progeny) to be included. The initial soil concentration in the garden is calculated from the assumed volume exhumed and the surface area of the garden. No other calculations are required to determine the initial soil concentration.

The soil concentration decreases with time due to leaching and radioactive decay. Leaching is the process by which radioactive materials migrate from the surface layer of soil into deeper layers below. The driving force behind the leaching process is the application of water to the soil. Leaching is treated as a removal rate constant giving the fraction of the material in the surface layer which is removed per unit of time. It is calculated using the equation shown below.

$$\lambda_s = \frac{P + I - E}{\theta\ d\ (1 + \rho/\theta\ K_d)}$$

where:

λ_s = annual average soil leaching coefficient, fraction removed from a soil layer of thickness "d" per year
P = total precipitation, in centimeters per year
I = total irrigation, assumed to be 82.3 cm per year (32.4 inches/yr)
E = total evapo-transpiration, in centimeters per year
d = thickness of soil from which nuclides migrate, in centimeters. This is assumed to be 15 cm (5.9 inches).
ρ = bulk density of the surface soil, in grams per cubic centimeter. In GENII this is 1.5 g/cc.
θ = volumetric water content of the surface soil, milliliters of water per cubic centimeter of soil. A value of 0.4 ml/cc is assumed.

K_d= distribution coefficient in surface soil for an element, in milliliters per gram.

For input to GENII, the leaching parameters are placed in the data file named FTRANS.DAT. The values for the nuclides considered in the base case dose assessment are listed in Tables C-1 and C-2. The following assumptions were used to relate the λ_s and K_d values: ρ = 1.5 g/cc; θ = 0.4 ml/cc; d = 15 cm; and P+I-E = 15 cm/yr. Note that the amount of irrigation was the same for all plant types.

For the intruder scenarios, the initial soil concentration in the top layer of soil decreases exponentially with time until the plant type is harvested. This is shown in the equation below.

$$W^s = W_o \, Exp[-(\lambda_s + \lambda_r)T]$$

where:

W^s= soil concentration after time T, in curies per kilogram of soil
W_o= initial soil concentration at time of intrusion, in curies per kilogram of soil
λ_r= radioactive decay constant, namely, the natural logarithm of 2 divided by the radioactive decay half-life in years
T = soil leaching time, in years

The soil leaching times for the ingestion dose pathways differ from those for inhalation and external pathways. The ingestion doses are based on the soil concentration 100 days after intrusion. The inhalation and external dose accumulates during the year after intrusion. These assumptions differ from those coded into GENII, namely no decay or leaching for inhalation and external, and 10 to 30 days of radioactive decay only for ingestion pathways. This later time corresponds to the time between harvest and consumption of the produce.

C.1.2 Soil Concentration for the Groundwater Use Scenarios

During irrigation, the radioactivity in the irrigation water accumulates in plants and soil differently. For accumulation on plants by direct deposition, the rate of deposition determines the final concentration in the plants. For determining the soil concentration, which determines the root uptake, inhalation and external doses, the total activity remaining in the surface layer of soil at the end of the year is all that matters. These differences are included in the equations below.

The rate of addition of contamination to the soil is given by the equation shown below. The conversion factor from inches of water applied to the soil to units of liters applied per square meter is shown in the equation.

Table C-1. Transfer Factors in NUREG/CR-5512 (Kennedy & Strenge, 1992).

Name	Dry Plant/Soil Conc Ratio			(B_p) Grain	Beef day/kg (F_b)	Milk day/L (F_m)	Fish (B_f)	Leaching per yr (λ_s)	Distr ml/g (K_d)
	Leafy	Root	Fruit						
H	(special model)						1	2.5	0
BE	1.0E-2	1.5E-3	1.5E-3	1.5E-3	1.0E-3	9.0E-7	2	2.77E-3	240
C	7.0E-1	7.0E-1	7.0E-1	7.0E-1	4.9E-2	1.1E-2	4,600	9.57E-2	6.7
CL	70	70	70	70	8.0E-2	1.5E-2	50	3.39E-1	1.7
K	1.0	5.5E-1	5.5E-1	5.5E-1	2.0E-2	7.0E-3	1,000	3.65E-2	18
CO	8.1E-2	4.0E-2	7.0E-3	3.7E-3	2.0E-2	2.0E-3	330	1.11E-2	60
NI	2.8E-1	6.0E-2	6.0E-2	3.0E-2	6.0E-3	1.0E-3	100	1.67E-3	400
SE	2.5E-2	2.5E-2	2.5E-2	2.5E-2	1.5E-2	4.0E-3	170	4.75E-3	140
SR	1.6	8.1E-1	1.7E-1	1.3E-1	3.0E-4	1.5E-3	50	4.37E-2	15
Y	1.5E-2	6.0E-3	6.0E-3	6.0E-3	3.0E-4	2.0E-5	25	3.50E-3	190
ZR	2.0E-3	5.0E-4	5.0E-4	5.0E-4	5.5E-3	3.0E-5	200	1.15E-3	580
NB	2.0E-2	5.0E-3	5.0E-3	5.0E-3	2.5E-1	2.0E-2	200	4.16E-3	160
MO	2.5E-1	6.0E-2	6.0E-2	6.0E-2	6.0E-3	1.5E-3	10	6.49E-2	10
TC	44	1.1	1.5	7.3E-1	8.5E-3	1.0E-2	15	1.82	0.1
PD	1.5E-1	4.0E-2	4.0E-2	4.0E-2	4.0E-3	1.0E-2	10	1.28E-2	52
CD	5.5E-1	1.5E-1	1.5E-1	1.5E-1	5.5E-4	1.0E-3	200	1.66E-2	40
IN	4.0E-3	4.0E-4	4.0E-4	4.0E-4	8.0E-3	1.0E-4	100,000	1.71E-3	390
SN	3.0E-2	6.0E-3	6.0E-3	6.0E-3	8.0E-2	1.0E-3	3,000	5.12E-3	130
SB	1.3E-4	5.6E-4	8.0E-5	3.0E-2	1.0E-3	1.0E-4	200	1.47E-2	45
TE	2.5E-2	4.0E-3	4.0E-3	4.0E-3	1.5E-2	2.0E-4	400	4.75E-3	140
I	3.4E-3	5.0E-2	5.0E-2	5.0E-2	7.0E-3	1.0E-2	500	5.26E-1	1
CS	1.3E-1	4.9E-2	2.2E-1	2.6E-2	2.0E-2	7.0E-3	2,000	2.47E-3	270
BA	1.5E-1	1.5E-2	1.5E-2	1.5E-2	1.5E-4	3.5E-4	200	1.28E-2	52
SM	1.0E-2	4.0E-3	4.0E-3	4.0E-3	5.0E-3	2.0E-5	25	2.77E-3	240
EU	1.0E-2	4.0E-3	4.0E-3	4.0E-3	5.0E-3	2.0E-5	25	2.77E-3	240
GD	1.0E-2	4.0E-3	4.0E-3	4.0E-3	3.5E-3	2.0E-5	25	2.77E-3	240
RE	1.5	3.5E-1	3.5E-1	3.5E-1	8.0E-3	1.5E-3	120	4.67E-2	14
PB	5.8E-3	3.2E-3	9.0E-3	4.7E-3	3.0E-4	2.5E-4	100	2.47E-3	270
BI	3.5E-2	5.0E-3	5.0E-3	5.0E-3	4.0E-4	5.0E-4	15	5.54E-3	120
PO	2.5E-3	9.0E-3	4.0E-4	4.0E-4	3.0E-4	3.5E-4	500	4.44E-3	150
RN	0.0	0.0	0.0	0.0	0.0	0.0	1	2.5	0
FR	(none given)						2,000		
RA	7.5E-2	3.2E-3	6.1E-3	1.2E-3	2.5E-4	4.5E-4	70	1.33E-3	500
AC	3.5E-3	3.5E-4	3.5E-4	3.5E-4	2.5E-5	2.0E-5	25	1.59E-3	420
TH	6.6E-3	1.2E-4	8.5E-5	3.4E-5	6.0E-6	5.0E-6	100	2.08E-4	3,200
PA	2.5E-3	2.5E-4	2.5E-4	2.5E-4	1.0E-5	5.0E-6	11	1.31E-3	510
U	1.7E-2	1.4E-2	4.0E-3	1.3E-3	2.0E-4	6.0E-4	50	4.37E-2	15
NP	1.3E-2	9.4E-3	1.0E-2	2.7E-3	5.5E-5	5.0E-6	250	1.27E-1	5
PU	3.9E-4	2.0E-4	4.5E-5	2.6E-5	5.0E-7	1.0E-7	250	1.21E-3	550
AM	5.8E-4	4.1E-4	2.5E-4	5.9E-5	3.5E-6	4.0E-7	250	3.51E-4	1,900
CM	3.0E-4	2.4E-4	1.5E-5	2.1E-5	3.5E-6	2.0E-5	250	1.67E-4	4,000

Note: Animal fresh forage and stored hay are treated as leafy vegetables.

Table C-2. Transfer Factors from ORNL-5785 (Baes, 1984).

Nuc Name	Leafy Vegt. (B_p)	Grains* (B_p)	Beef day/kg (F_b)	Milk day/L (F_m)	Leaching per yr (λ_e)	Distr ml/g (K_d)	Atomic No. (Z)
BE	0.01	0.0015	0.001	9E-07	1.03E-3	650	4
CL	70	70	0.08	0.015	1.29	0.25	17
K	1	0.55	0.02	0.007	0.116	5.5	19
CO	0.02	0.007	0.02	0.002	1.47E-2	45	27
NI	0.06	0.06	0.006	0.001	4.44E-3	150	28
SE	0.025	0.025	0.015	0.004	2.22E-3	300	34
SR	2.5	0.25	0.0003	0.0015	1.89E-2	35	38
Y	0.015	0.006	0.0003	2E-05	1.33E-3	500	39
ZR	0.002	0.0005	0.0055	3E-05	2.22E-4	3,000	40
NB	0.02	0.005	0.25	0.02	1.90E-3	350	41
MO	0.25	0.06	0.006	0.0015	3.29E-2	20	42
TC	9.5	1.5	0.0085	0.01	0.377	1.5	43
PD	0.15	0.04	0.004	0.01	1.11E-2	60	46
CD	0.55	0.15	0.00055	0.001	9.85E-2	6.5	48
IN	0.004	0.0004	0.008	0.0001	4.44E-4	1,500	49
SN	0.03	0.006	0.08	0.001	2.66E-3	250	50
SB	0.2	0.03	0.001	0.0001	1.47E-2	45	51
TE	0.025	0.004	0.015	0.0002	2.22E-3	300	52
I	0.15	0.05	0.007	0.01	1.11E-2	60	53
CS	0.08	0.03	0.02	0.007	6.66E-4	1,000	55
BA	0.15	0.015	0.00015	0.00035	1.11E-2	60	56
SM	0.01	0.004	0.005	2E-05	1.03E-3	650	62
EU	0.01	0.004	0.005	2E-05	1.03E-3	650	63
GD	0.01	0.004	0.0035	2E-05	1.03E-3	650	64
RE	1.5	0.35	0.008	0.0015	8.58E-2	7.5	75
PB	0.045	0.009	0.0003	0.00025	7.41E-4	900	82
BI	0.035	0.005	0.0004	0.0005	3.33E-3	200	83
PO	0.0025	0.0004	0.0003	0.00035	1.33E-3	500	84
RN	0	0	0	0	2.50	0	86
FR	0.03	0.008	0.0025	0.02	2.66E-3	250	87
RA	0.015	0.0015	0.00025	0.00045	1.48E-3	450	88
AC	0.0035	0.00035	2.5E-05	2E-05	4.44E-4	1,500	89
TH	0.00085	8.5E-05	6E-06	5E-06	4.44E-6	150,000	90
PA	0.0025	0.00025	1E-05	5E-06	2.67E-4	2,500	91
U	0.0085	0.004	0.0002	0.0006	1.48E-3	450	92
NP	0.1	0.01	5.5E-05	5E-06	2.20E-2	30	93
PU	0.00045	4.5E-05	5E-07	1E-07	1.48E-4	4,500	94
AM	0.0055	0.00025	3.5E-06	4E-07	9.52E-4	700	95
CM	0.00085	1.5E-05	3.5E-06	2E-05	3.33E-3	200	96

*The ratios for Grains were also used on Root Vegetables and Fruit.

$$D_p = C_w\ I_p\ (25.4\ L/m^2/inch)\ /\ F_i$$

where:

D_p= activity deposition rate due to irrigation of soils growing plant type p, in curies per square meter per year ($Ci/yr/m^2$)
C_w= irrigation water concentration, in curies per liter (Ci/L) at the time irrigation pumping begins
I_p= inches of irrigation water applied each year to plant type p. For the maximum individual cases, this value is 32.4 inches per year. For the population dose, this value is 25 inches per year (Kincaid, 1993).
F_i= fraction of the year that irrigation water is applied. The value 0.5 is used since the irrigation is assumed to take place 6 months per year.

The soil concentration in the irrigation model increases due to the application of water, but the increase is offset by the removal of contaminants by leaching and radioactive decay. The function used to represent this is shown in the equation below. The soil concentration has units of Ci/kg. At the end of the irrigation period, the soil concentration is given by the equation below.

$$W_p^i = \frac{F_i\ D_p\ (1 - Exp[-(\lambda_s + \lambda_r)T])}{\rho\ d\ (\lambda_s + \lambda_r)}$$

where:

W_p^i= soil concentration due to irrigation, in curies per kilogram of soil
λ_r= radioactive decay constant, namely, the natural logarithm of 2 divided by the radioactive decay half-life in years
T = soil leaching time, in years. In the GENII program, this time is always one year for irrigation scenarios.

The GENII software also considers reduction in the soil concentration due to uptake in plants and their subsequent harvest. This is a smaller effect which was not included in the spreadsheet.

It was not necessary to include the effects of holdup due to the long half-lives of the important nuclides. However, for a few nuclides, the production of daughter activity leads to a small increase in certain doses. Since this effect is small, the calculation of holdup was not included in the spreadsheet.

C.1.3 Concentration in Vegetables

The calculation of radionuclide concentrations in living plants uses three main routes, (1) root uptake, (2) resuspension to leaves (also called "rain splash"), and (3) direct deposition of irrigation water on foliage. Each of these will be considered separately below. The three uptake routes are then combined to get the total concentration in the vegetables.

GENII includes the effects of radioactive decay between the time a plant type is harvested and when it is consumed. This time period is called the holdup time. It enters the equations for plant concentration as shown below.

$$C_p = (C_p^d + C_p^f + C_p^r)\ \mathrm{Exp}(-\lambda_r\ T_p^h)$$

where:

C_p= radionuclide concentration in plant type p at the time it is consumed, in curies per kilogram
C_p^d= concentration of a radionuclide in plant type p due to direct deposition of irrigation water. The units for C_p^d are Ci/kg.
C_p^r= concentration of a radionuclide in plant type p due to absorption from the soil through the roots. The units for C_p^r are Ci/kg.
C_p^f= concentration of a radionuclide in plant type p due to foliar deposition from soil resuspension. The units for C_p^f are Ci/kg.
T_p^h= holdup time, i.e., the time between harvest and consumption of plant type p, in days

It was not necessary to include the effects of holdup due to the long half-lives of the important nuclides. However, for a few nuclides, the production of daughter activity leads to a small increase in certain doses. Since this effect is small, the calculation of holdup was not included in the spreadsheet.

C.1.3.1 Root Uptake into Edible Portions. Root uptake is calculated through a concentration ratio. These ratios are listed in Tables C-1 and C-2. There are some major differences, therefore, both were used and compared.

Notes for Table C-1 and C-2 are the following. "Leafy" refers to vegetables whose leafy parts are normally eaten. "Root," "Fruit," and "Grains" refers to all other types of vegetables whose reproductive parts are eaten. In applying the ORNL ratios, the "Leafy Vegt." ratios were only applied to Leafy Vegetables. All other vegetable types use the ratios shown under "Grains."

The ratios under both "Leafy Vegt.," "Leafy," "Root," "Fruit" and "Grains" are the Ci/kg dry weight of vegetables to Ci/kg of soil. For this reason, a dry-to-wet ratio must be used when calculating the plant concentrations from root uptake. The dry-to-wet ratios are listed in Table C-3. The values shown are from GENII Version 1.485 (Napier, 1988).

The plant concentration due to root uptake into the various types of vegetation is described with the equation shown below. In GENII there are four plant types consumed by humans: leafy vegetables, other vegetables, fruit, and grain. There are also two plant types consumed by animals: grass (forage) and grain (stored feed). Forage is treated as a leafy vegetable.

$$C_p^r = R_p\ B_p\ W$$

where:

R_p= dry to wet ratio for plant type p. See Table C-3 for values.

B_p = soil to plant concentration ratio, as Ci/kg dry weight of vegetables to Ci/kg of soil. See Tables C-1 and C-2 for values.
W = soil concentration at the time of harvest, in Ci/kg (either W^s or W_p^i)

C.1.3.2 Resuspension of Surface Soil to Foliage (Rain Splash). The resuspension of dust by wind, or water drops splashing soil onto the foliage leads to some contamination of the edible portion of the plant. The concentration of the radionuclide in the plant is approximated by the equation shown below. This method is also used in the GENII program.

$$C_p^f = \frac{W\ R^a\ \rho\ d\ V_d\ T_v\ F_p^f\ \{\ 1 - \mathrm{Exp}[-(\lambda_w + \lambda_r)T_p^f]\ \}}{Y_p\ (\lambda_w + \lambda_r)\ (1\ \mathrm{day}/86400\ \mathrm{sec})}$$

where:

R^a = resuspension factor, i.e., the ratio of the air concentration to the surface contamination causing it. The GENII value of 1E-9 per meter is used to calculate the rain splash onto plants.
V_d = diffusion attachment speed, or ground deposition speed, in meters per second. The GENII value of 0.001 m/s is used for every nuclide.
T_v = translocation factor, i.e., the fraction of what deposits on the foliage that ends up in the edible portions of the plant. See Table C-3.
F_p^f = interception fraction for plant type p. The fraction of what falls to the earth that lands on the plant. See Table C-3.
Y_p = yield of crop type p, in kilograms per square meter (wet weight). Also called the standing biomass. See Table C-3.
λ_w = weathering removal coefficient, 0.0495105 per day, or 18.0713 per year, which corresponds to a 14 day half time.
λ_r = radioactive decay constant, namely, the natural logarithm of 2 divided by the radioactive decay half-life in days (1 year = 365.25 days)
T_p^f = exposure time of the plant type p to the airborne contamination depositing on the foliage, in days (also called growing period)

The weathering process removes contaminants from the outer surfaces of the plants due to the action of wind and water. The method used in GENII to compute interception fractions from the standing biomass uses the equation shown below.

$$F_p^f = 1 - \mathrm{Exp}(\ -K_p^f\ Y_p\ R_p\ )$$

where:

F_p^f = interception fraction for plant type p. The fraction of what falls to the earth that lands on the plant. See Table C-3.
K_p^f = constant used to relate the standing biomass (dry) and the interception fraction for plant type p, in square meters per kilogram
Y_p = yield of crop type p, in kilograms per square meter (wet weight). Also called the standing biomass.
R_p = dry to wet ratio for plant type p. See Table C-3 for values.

Table C-3. Dietary Parameters for the Maximum Individual[3].

Type, p	T_v	K_p^f	Y_p	R_p	F_p^{f1}	I_p	T_p^f	T_p^h
Plants Consumed by Humans								
Leafy	1.0	2.9	2.0	0.10	0.440	32.4	90	1
Other	0.1	3.6	2.0	0.25	0.835	32.4	90	5
Fruit	0.1	3.6	3.0	0.18	0.857	32.4	90	5
Grain	0.1	2.9	0.8	0.18	0.341	0.0	90	180
Plants Consumed by Beef Cattle								
Forage	1.0	2.9	1.0	0.20	0.440	32.4	45	100
Stored[2]	0.1	2.9	0.8	0.18	0.341	32.4	90	180
Plants Consumed by Milk Cows								
Forage	1.0	2.9	1.5	0.20	0.581	32.4	45	0
Stored[2]	0.1	2.9	1.0	0.18	0.407	32.4	90	100

[1]The values shown were calculated. For direct deposition of nuclides on plants by irrigation water, the interception fraction (F_p^f) is 0.25 for all plant types.

[2]In GENII, the stored feed model uses the translocation factor (T_v) and soil-to-plant concentration ratio (B_p) for grain.

[3]These were also used in the exposure scenarios in the double-shelled tank LLW Performance Assessment (Kincaid 1993; Rittmann 1993b).

C.1.3.3 Direct Deposition of Irrigation Water on Foliage. The previous two avenues by which contamination reaches the edible portions of the plants apply only to activity which is present in the soil. This section discusses direct deposition of contaminants in irrigation water onto the foliage. The concentration in the edible portion of the plants due to direct deposition on foliage is given in the equation below.

$$C_p^d = \frac{D_p\ T_v\ F_p^f\ \{\ 1 - \mathrm{Exp}[-(\lambda_w + \lambda_r)T_p^f]\ \}}{Y_p\ (\lambda_w + \lambda_r)\ (365\ \text{days}/1\ \text{year})}$$

where:

D_p= activity deposition rate due to irrigation of soils growing plant type p, in curies per square meter per year (Ci/yr/m²)

T_v= translocation factor, i.e., the fraction of what deposits on the foliage that ends up in the edible portions of the plant. See Table C-3.

F_p^f= interception fraction for plant type p. The fraction of what falls to the earth that lands on the plant. For direct deposition on plants by irrigating water, the interception fraction takes the value 0.25 for all plant types.
λ_w= weathering removal coefficient, 0.0495105 per day, or 18.0713 per year, which corresponds to a 14 day half time.
λ_r= radioactive decay constant, namely, the natural logarithm of 2 divided by the radioactive decay half-life in days (1 year = 365.25 days)
T_p^f= exposure time of the plant type p to the airborne contamination depositing on the foliage, in days (also called growing period)
Y_p= yield of crop type p, in kilograms per square meter (wet weight). Also called the standing biomass. See Table C-3.

The plant concentration due to direct deposition depends on the rate at which water is applied. In the previous two pathways, root uptake and rain splash, the determining factor is the total amount of water (and thus activity) applied to the soil.

C.1.4 Concentration in Animals and Fish

Radionuclide concentrations in animal products (meat and milk) are derived from two sources, drinking water and feed. In GENII, the cattle used for milk production and meat production are considered separately. Each has its own dietary parameters. These were listed on Table C-3. The nuclide concentrations in drinking water and feed determine the meat or milk concentration through a concentration ratio. These concentration ratios were listed in Tables C-1 and C-2. The equation relating feed and water concentrations to the eventual concentration in meat and milk is shown below.

$$C_q = F_q \left[Q_v^q \left(F_f^q C_l^q + F_s^q C_g^q\right) + Q_w^q C_w\right]$$

where:

C_q= radionuclide concentration in beef or milk (q), in curies per kilogram
F_q^q= ratio of the equilibrium concentration of a nuclide in the animal product (beef or milk) to the daily intake by cattle. For beef the units are Ci/kg(beef) per Ci/day, while for milk the units are Ci/L(milk) per Ci/day. See Tables C-1 and C-2 for values.
Q_v^q= amount of fresh forage consumed by beef or milk cattle on an average day, in kilograms per day. The assumed values for beef cattle and milk cows are 68 kg/day and 55 kg/day (Napier, 1988).
F_f^q= fraction of cattle diet which is forage. In GENII this is 0.75, and forage (grass & hay) is treated as a leafy vegetable for both types of cattle.
C_l^q= radionuclide concentration in forage (leafy vegetables) the cattle eat, in curies per kilogram. This includes the decay during holdup.
F_s^q= fraction of cattle diet which is stored feed. In GENII this is 0.25, and stored feed is treated as a grain.
C_g^q= radionuclide concentration in stored feed (grain) the cattle eat, in curies per kilogram. This includes the decay during holdup.
Q_w^q= amount of drinking water consumed by cattle, in liters per day. It is assumed (Napier, 1988) that the beef cattle drink 50 L/day, while the milk cows drink 60 L/day.
C_w= irrigation water concentration, in curies per liter (Ci/L)

Radionuclide concentrations in fish are assumed to be at equilibrium with the water in which they are raised. The fish concentration is therefore the product of the water concentration and the concentration ratio for that element as shown in the equation below. The fish concentration ratios are sometimes called bioaccumulation factors.

$$C_f = C_w B_f$$

where:

B_f= bioaccumulation factor for a given radionuclide in fish, in liters per kilogram. The values assumed are shown on Table C-1.
C_f= radionuclide concentration in fish, in curies per kilogram.

C.1.5 Special Models for Tritium

Tritium in the soil of the intruder's garden is assumed to be unavailable for absorption by the plants. The principal reason is that tritiated water will quickly diffuse or be washed from the garden soil. Tritium in the soil gives a small inhalation dose and even smaller external dose. The main dose pathway is the small amount of soil ingested each day. This is also how the GENII program deals with tritium in the surface layer.

For the scenario using contaminated irrigation water, the concentrations of tritium in food crops, beef and milk are calculated using a specific activity model based on the concentration of tritium in the irrigation water. This same concentration is assumed to exist in the water present in all food items, since the plants and animals obtain nearly all their water from the contaminated source.

The soil concentration of tritium due to irrigation is based on the assumption that all of the soil moisture is contaminated at the same level as the water. The concentration of tritium in the air is calculated from the soil contamination, just as it is for all the nuclides. The formula for soil concentration of tritium is shown below.

$$W = \theta_w C_w$$

where:

θ_w= moisture content of soil assumed for the tritium model, in liters per kilogram of soil. The value 0.1 L/kg (Kennedy and Strenge, 1992) is used for this parameter, but only in the tritium model.

The plants derive nearly all of their water from the irrigation applied, thus the tritium concentration in the plant water is the same as the ground water. Since the feed given the cattle as well as the water are contaminated with tritium, all of the water in the animal will have the same tritium concentration as the ground water. Using this simple assumption, the tritium concentration in plants, cows and milk is calculated from the equation shown below.

$$C_p = F_p^w C_w$$

where:

F_p^w= fraction of water in produce type p, where p refers to meat and milk as well as vegetables. The dry to wet ratio (R_p) can be calculated from this since $R_p = 1 - F_p^w$.

The tritium model considers the organically bound hydrogen in the produce to be contaminated as well as the water. The specific activity model actually requires that the concentration of tritium in the hydrogen in the water be reproduced throughout the food product. In GENII, an effective water fraction is added to the actual water fraction, and this is used to calculate results. The formula used to adjust the water fractions is shown below. Values for these parameters are shown in Table C-4. Values from ORNL-5785 (water only) are also shown for comparison.

$$F_p^{w2} = F_p^w + (1 - F_p^w)\ F_p^H\ 9$$

where:

F_p^{w2}= effective water fraction in produce type p, where p refers to meat and milk as well as vegetables. This water fraction includes hydrogen which is not in the form of water. It is used in place of F_p^w.

F_p^H= fraction of hydrogen in the dry produce. The scale factor of 9 converts this to an effective water fraction.

Table C-4. Dietary Parameters Used in the Tritium and Carbon-14 Models.

Type, p	Tritium Model Parameters			C-14	ORNL-5785	
	F_p^w	F_p^H	F_p^{w2}	B & F	F_p^w	C_p^c
Leafy	0.80	0.0625	0.9125	1.0	0.93	0.026
Other	0.80	0.0625	0.9125	1.0	0.77	0.116
Fruit	0.80	0.0625	0.9125	1.0	0.87	0.050
Grain	0.12	0.0625	0.6150	1.0	0.11	0.293
Beef	0.60	0.094	0.9384	0.031	0.61	0.228
Milk	0.88	0.083	0.9696	0.012	0.85	0.069

The water fractions shown above are only used in the tritium model. The water fractions taken from ORNL-5785 were used in the tritium results shown for ORNL-5785 assumptions.

C.1.6 Special Parameters for Carbon-14

In GENII, the concentrations of ^{14}C in food crops, beef and milk are calculated using a specific activity model based on the concentration of ^{14}C in the soil. In GENII, the plants are assumed to obtain 90 percent of their carbon from the air, and 10 percent from the soil. The ratio of the ^{14}C concentration in plants to the concentration of carbon in the soil is assumed to be the same in all plant types. This specific activity model is not used in the present calculations.

Based on recent data for ^{14}C uptake in plants (Sheppard, 1991), ^{14}C will be treated like the other nuclides described earlier. The specific activity model used by GENII on plants is not used here. Parameters found in NUREG/CR-5512 are applied. The soil leaching coefficient is 0.0957 per year based on a Kd of 6.7 ml/g, as well as the other soil parameters discussed earlier. The concentration ratio for all plant types is assumed to be 0.7, on a dry-weight basis.

Continuing with the NUREG/CR-5512 model for ^{14}C, the transfer of ^{14}C into beef and milk are computed using a specific activity model. The concentration of ^{14}C in animal products (beef and milk) is computed using the equation shown below. This equation gives the ratio of ^{14}C activity consumed by the cow, to total carbon consumed by the cow. In the specific activity model, this ratio also holds for the carbon in the cow.

$$\frac{C_q^{c14}}{C_q^c} = \frac{Q_f^q C_f^q + Q_h^q C_h^q + Q_g^q C_g^q + Q_w^q C_w}{Q_f^q C_f^c + Q_h^q C_h^c + Q_g^q C_g^c + Q_w^q C_w^c}$$

where:

C_q^{c14} = concentration of ^{14}C in animal product q (beef or milk) consumed by the human, in Ci/kg

C_q^c = concentration of carbon in animal product q consumed by the human, in kg carbon per kilogram (wet) of animal product q (beef or milk)

C_p^c = concentration of carbon in animal feed type p, in kg carbon per kilogram (wet) of plant. In this equation p refers to fresh forage, stored hay, stored grain, and drinking water. The carbon concentration of drinking water is small enough that it can be ignored.

Using the specific equation above, the effective transfer factor (F_q^{c14}) for the cattle can be computed from the parameters given. The diet-to-animal product transfer factor is the ratio of the equilibrium ^{14}C concentration in the cow to the daily intake of activity.

$$F_q^{c14} = \frac{C_q^c}{Q_f^q C_f^c + Q_h^q C_h^c + Q_g^q C_g^c + Q_w^q C_w^c}$$

The effective diet-to-animal transfer factors for ^{14}C was computed from pathway parameters already described. The computed F values for ^{14}C are shown in Table C-1.

C.1.7 Human Intakes and Effective Dose Factors

Human exposure to radiation is estimated for both internal and external sources. External sources are outside the body. The only source of external exposure in these scenarios is the contaminated soil. Internal sources of exposure are located inside the body, and get there by being inhaled or ingested. Each of these types of exposure will be discussed separately below. The total dose is the sum of the different types of exposure.

C.1.7.1 Internal and External Dose Factors. The internal dose factors applied to unit quantities of ingested or inhaled activity are shown in Table C-5. The GENII internal dose factors from the July 1993 revision are shown only for comparison with the other values. The EPA values are from Federal Guidance Report Number 11 (US EPA 1988) and are also only shown for comparison. The DOE internal dose factors (DOE 1988c) were actually used in the calculations. The three collections of internal dose factors are compared by means of ratios in Table C-6. All three collections are based on a dose commitment period of 50 yr.

External dose rate factors are also shown on Table C-5. These are from a large area of soil 15 centimeters thick. The assumed soil density is 1.5 grams per cubic centimeter. The values shown on Table C-5 come from the GENII GRDF.DAT file. The last column shows values from a recent recomputation using EXTDF, a program which is part of the GENII software package. The recalculation increased the dose rate factors by about 15 percent in all cases due to a difference in the assumed soil composition. The original GENII dose factors were based on a composition like that of air. The recalculated values used a composition like that of ordinary concrete.

Five of the nuclides shown in Table C-5 are not found in the GENII library. The GENII dose factors for ^{133}Ba, ^{150}Eu, ^{152}Gd, and ^{207}Bi were computed by averaging the values from the EPA and DOE. Dose factors for the fifth nuclide, ^{209}Po, are not found in any dose factor collection. Dose factors for ^{209}Po were computed by comparison with ^{210}Po. Corrections were made for the energy of the alpha particles emitted, and the decay half-life using the equation shown below.

$$\text{Dose Factor} \propto \frac{E\alpha}{\lambda_{eff}} \left[1 - e^{(-\lambda_{eff} * T_d)} \right]$$

where:

- $E\alpha$ = total alpha energy per decay. For ^{209}Po this is 4.882 Mev per decay, while for ^{210}Po this is 5.3045 Mev per decay.
- λ_{eff} = effective removal constant, which combines both the biological elimination and the radioactive decay of the nuclide.
- T_d = dose commitment period used in the dose factor collections shown in Table C-5, namely, 50 years.

The biological removal halftime for polonium is 50 days (ICRP 30). The decay half-life of ^{209}Po is 102 year, thus its λ_{eff} is 0.01388 per day. The decay half-life of ^{210}Po is 138 days, thus its λ_{eff} is 0.01889 per day. Since these are so large, the dose integration term in brackets is always 1. The

Table C-5. Internal Dose Factors (mrem/pCi) Used in the Spreadsheet.

		Ingestion (mrem/pCi)				Inhalation (mrem/pCi)			External ◆ mrem/hr per Ci/m²	
Nuclide	f1	GENII	DOE	EPA	Sol	GENII	DOE	EPA	GENII	Redone
H-3	(1.00)	6.1E-08	6.3E-08	6.40E-08	(V)	9.0E-08	9.5E-08	9.60E-08	2.93E-08	3.50E-08
Be-10	(5E-3)	4.7E-06	4.2E-06	4.66E-06	(Y)	3.5E-04	3.5E-04	3.54E-04	3.66E-01	4.34E-01
C-14	(1.00)	2.1E-06	2.1E-06	2.09E-06	(Org)	2.1E-06	2.1E-06	2.09E-06	6.28E-03	7.51E-03
Cl-36	(1.00)	3.0E-06	3.0E-06	3.03E-06	(W)	2.2E-05	2.0E-05	2.19E-05	7.23E-01	8.57E-01
K-40	(1.00)	1.8E-05	1.9E-05	1.86E-05	(D)	1.2E-05	1.2E-05	1.24E-05	4.31E+02	4.87E+02
Co-60	(0.30)	2.7E-05	2.6E-05	2.69E-05	(Y)	2.0E-04	1.5E-04	2.19E-04	6.61E+03	7.51E+03
Ni-59	(0.05)	2.1E-07	2.0E-07	2.10E-07	(D)	1.3E-06	1.3E-06	1.32E-06	1.10E-01	1.32E-01
Ni-63	(0.05)	5.6E-07	5.4E-07	5.77E-07	(D)	3.0E-06	3.0E-06	3.10E-06	1.59E-04	1.91E-04
Se-79	(0.80)	8.4E-06	8.3E-06	8.70E-06	(W)	9.5E-06	8.9E-06	9.84E-06	4.47E-03	5.36E-03
Sr-90	(0.30)	1.3E-04	1.4E-04	1.53E-04	(D)	2.1E-04	2.4E-04	2.47E-04	1.70E+01	1.97E+01
Zr-93	(2E-3)	1.6E-06	1.6E-06	1.66E-06	(D)	3.2E-04	3.2E-04	3.21E-04	1.12E-04	1.34E-04
Nb-93m	(0.01)	5.1E-07	5.3E-07	5.22E-07	(Y)	3.0E-05	2.8E-05	2.92E-05	4.39E-02	5.28E-02
Nb-94	(0.01)	7.3E-06	5.1E-06	7.14E-06	(Y)	3.9E-04	3.3E-04	4.14E-04	4.08E+03	4.66E+03
Mo-93	(0.80)	1.4E-06	1.3E-06	1.35E-06	(Y)	2.8E-05	2.8E-05	2.84E-05	2.12E-01	2.54E-01
Tc-99	(0.80)	2.2E-06	1.3E-06	1.46E-06	(W)	9.0E-06	7.5E-06	8.33E-06	4.22E-02	5.05E-02
Pd-107	(5E-3)	1.5E-07	1.4E-07	1.49E-07	(Y)	1.3E-05	1.3E-05	1.28E-05	3.49E-06	4.17E-06
Cd-113m	(0.05)	1.6E-04	1.5E-04	1.61E-04	(D)	1.5E-03	1.4E-03	1.53E-03	3.60E-01	4.28E-01
Sn-121m	(0.02)	2.2E-06	2.0E-06	2.25E-06	(W)	1.2E-05	9.3E-06	1.19E-05	0	5.16E+00
Sn-126	(0.02)	2.1E-05	1.8E-05	2.11E-05	(W)	1.0E-04	7.5E-05	1.01E-04	5.71E+03	6.56E+03
I-129	(1.00)	2.5E-04	2.8E-04	2.76E-04	(D)	1.5E-04	1.8E-04	1.74E-04	4.64E+00	5.59E+00
Cs-135	(1.00)	6.9E-06	7.1E-06	7.07E-06	(D)	4.5E-06	4.5E-06	4.55E-06	1.22E-02	1.45E-02
Cs-137	(1.00)	4.8E-05	5.0E-05	5.00E-05	(D)	3.0E-05	3.2E-05	3.19E-05	1.58E+03	1.82E+03
Ba-133◂	(0.10)	3.3E-06	3.2E-06	3.40E-06	(D)	7.4E-06	6.9E-06	7.81E-06	9.57E+02	1.10E+03
Sm-147	(3E-4)	1.9E-04	1.8E-04	1.85E-04	(W)	7.5E-02	7.1E-02	7.47E-02	0	0
Sm-151	(3E-4)	3.9E-07	3.4E-07	3.89E-07	(W)	3.0E-05	2.9E-05	3.00E-05	1.63E-03	1.95E-03
Eu-150◂	(1E-3)	6.3E-06	6.2E-06	6.36E-06	(W)	2.7E-04	2.7E-04	2.68E-04	4.38E+03	5.03E+03
Eu-152	(1E-3)	6.5E-06	6.0E-06	6.48E-06	(W)	2.1E-04	2.2E-04	2.21E-04	3.15E+03	3.59E+03
Eu-154	(1E-3)	9.6E-06	9.1E-06	9.55E-06	(W)	2.8E-04	2.6E-04	2.86E-04	3.26E+03	3.73E+03
Gd-152◂	(3E-4)	1.6E-04	1.5E-04	1.62E-04	(D)	2.4E-01	2.4E-01	2.43E-01	0	0
Re-187	(0.80)	1.5E-08	8.3E-09	9.51E-09	(W)	5.9E-08	4.9E-08	5.44E-08	0	0
Pb-210	(0.20)	7.4E-03	6.7E-03	7.31E-03	(D)	2.4E-02	2.1E-02	2.33E-02	3.29E+00	3.88E+00
Bi-207◂	(0.05)	5.2E-06	4.9E-06	5.48E-06	(D)	1.7E-05	1.4E-05	2.00E-05	4.29E+03	4.93E+03
Po-209✱	(0.10)	2.4E-03	2.0E-03	2.38E-03	(D)	1.2E-02	1.0E-02	1.18E-02	7.78E+00	8.93E+00
Ra-226	(0.20)	9.6E-04	1.1E-03	1.32E-03	(W)	8.2E-03	7.9E-03	8.58E-03	4.92E+03	5.60E+03
Ra-228	(0.20)	8.4E-04	1.2E-03	1.44E-03	(W)	4.4E-03	4.3E-03	4.86E-03	2.67E+03	3.04E+03
Ac-227	(1E-3)	1.4E-02	1.5E-02	1.48E-02	(D)	6.7E+00	6.7E+00	6.72E+00	9.26E+02	1.07E+03
Th-228	(2E-4)	5.8E-04	7.5E-04	8.09E-04	(Y)	3.5E-01	3.1E-01	3.45E-01	4.35E+03	4.91E+03
Th-229	(2E-4)	3.9E-03	3.9E-03	4.03E-03	(W)	2.2E+00	2.0E+00	2.16E+00	7.80E+02	9.03E+02
Th-230	(2E-4)	5.4E-04	5.3E-04	5.48E-04	(W)	3.2E-01	3.2E-01	3.26E-01	3.43E-01	4.10E-01
Th-232	(2E-4)	2.7E-03	2.8E-03	2.73E-03	(W)	1.7E+00	1.6E+00	1.64E+00	1.79E-01	2.13E-01
Pa-231	(1E-3)	1.1E-02	1.1E-02	1.06E-02	(W)	1.3E+00	1.3E+00	1.28E+00	7.82E+01	9.09E+01
U-232	(0.05)	1.3E-03	1.3E-03	1.31E-03	(Y)	6.7E-01	6.7E-01	6.59E-01	2.61E-01	3.11E-01
U-233	(0.05)	2.9E-04	2.7E-04	2.89E-04	(Y)	1.4E-01	1.3E-01	1.35E-01	4.05E-01	4.80E-01
U-234	(0.05)	2.9E-04	2.6E-04	2.83E-04	(Y)	1.3E-01	1.3E-01	1.32E-01	1.58E-01	1.89E-01
U-235	(0.05)	2.7E-04	2.5E-04	2.67E-04	(Y)	1.2E-01	1.2E-01	1.23E-01	2.13E+02	2.52E+02
U-236	(0.05)	2.7E-04	2.5E-04	2.69E-04	(Y)	1.3E-01	1.2E-01	1.25E-01	8.22E-02	9.83E-02
U-238	(0.05)	2.7E-04	2.4E-04	2.68E-04	(Y)	1.2E-01	1.2E-01	1.18E-01	6.32E+01	7.26E+01
Np-237	(1E-3)	5.3E-03	3.9E-03	4.44E-03	(W)	6.4E-01	4.9E-01	5.40E-01	6.16E+02	7.13E+02
Pu-238	(1E-3)	3.2E-03	3.8E-03	3.20E-03	(W)	3.9E-01	4.6E-01	3.92E-01	5.26E-02	6.30E-02
Pu-239	(1E-3)	3.6E-03	4.3E-03	3.54E-03	(W)	4.3E-01	5.1E-01	4.29E-01	1.16E-01	1.12E-01
Pu-240	(1E-3)	3.6E-03	4.3E-03	3.54E-03	(W)	4.3E-01	5.1E-01	4.29E-01	5.23E-02	7.29E-02
Pu-241	(1E-3)	6.8E-05	8.6E-05	6.85E-05	(W)	8.2E-03	1.0E-02	8.25E-03	6.26E-03	1.04E-02
Pu-242	(1E-3)	3.3E-03	4.1E-03	3.36E-03	(W)	4.1E-01	4.8E-01	4.11E-01	4.36E-02	5.24E-02
Pu-244	(1E-3)	3.3E-03	4.0E-03	3.32E-03	(W)	4.0E-01	4.8E-01	4.03E-01	1.02E+03	1.17E+03
Am-241	(1E-3)	3.6E-03	4.5E-03	3.64E-03	(W)	4.4E-01	5.2E-01	4.44E-01	1.19E+01	1.44E+01
Am-242m	(1E-3)	3.6E-03	4.3E-03	3.61E-03	(W)	4.4E-01	5.3E-01	4.40E-01	3.09E+01	3.64E+01
Am-243	(1E-3)	3.6E-03	4.5E-03	3.62E-03	(W)	4.4E-01	5.2E-01	4.40E-01	3.82E+02	4.49E+02
Cm-243	(1E-3)	2.5E-03	2.9E-03	2.51E-03	(W)	3.1E-01	3.5E-01	3.07E-01	2.46E+02	2.90E+02
Cm-244	(1E-3)	2.0E-03	2.3E-03	2.02E-03	(W)	2.5E-01	2.7E-01	2.48E-01	4.25E-02	5.08E-02
Cm-245	(1E-3)	3.7E-03	4.5E-03	3.74E-03	(W)	4.5E-01	5.4E-01	4.55E-01	1.11E+02	1.32E+02
Cm-246	(1E-3)	3.7E-03	4.5E-03	3.70E-03	(W)	4.6E-01	5.4E-01	4.51E-01	3.49E-02	4.19E-02
Cm-247	(1E-3)	3.4E-03	4.1E-03	3.42E-03	(W)	4.2E-01	4.9E-01	4.14E-01	1.13E+03	1.30E+03
Cm-248	(1E-3)	1.4E-02	1.6E-02	1.36E-02	(W)	1.6E+00	1.9E+00	1.65E+00	3.18E-02	3.82E-02

◂GENII values for these nuclides were obtained by averaging the DOE and EPA values.
✱All Po-209 internal dose factors are estimated from Po-210, as described in Section 3.7.1.
◆The External Dose Rate Factors are described in more detail in Section 3.7.1.

Table C-6. Ratios of GENII and EPA Internal Dose Factors to DOE Internal Dose Factors. (Differences less than 10 percent not shown)

Nuclide	Inhalation		Ingestion	
	GENII	EPA	GENII	EPA
Be-10			1.11	1.11
Co-60	1.34	1.46		
Se-79		1.11		
Sr-90	0.89			
Nb-94	1.18	1.26	1.42	1.40
Tc-99	1.20	1.11	1.72	1.12
Sn-121m	1.27	1.28	1.12	1.13
Sn-126	1.33	1.34	1.15	1.15
I-129	0.84		0.89	
Ba-133		1.13		
Sm-151			1.14	1.14
Re-187	1.20	1.11	1.75	1.15
Pb-210	1.11			
Bi-207	1.21	1.43		1.12
Po-209	1.20	1.16	1.20	1.19
Ra-226			0.87	1.20
Ra-228		1.13	0.70	1.20
Th-228	1.11		0.77	
U-238			1.12	
Np-237	1.30		1.35	1.14
Pu-238	0.85	0.85	0.84	0.84
Pu-239	0.85	0.84	0.83	0.82
Pu-240	0.85	0.84	0.83	0.82
Pu-241	0.82	0.83	0.79	0.80
Pu-242	0.84	0.86	0.81	0.82
Pu-244	0.84	0.84	0.83	0.83
Am-241	0.85	0.85	0.81	0.81
Am-242m	0.81	0.82	0.83	0.84
Am-243	0.85	0.85	0.81	0.80
Cm-243	0.88	0.88	0.87	0.87
Cm-244			0.87	0.88
Cm-245	0.84	0.84	0.82	0.83
Cm-246	0.84	0.84	0.83	0.82
Cm-247	0.86	0.85	0.84	0.83
Cm-248	0.86	0.87	0.84	0.85

ratio of ^{209}Po to ^{210}Po internal dose factors is shown below. This ratio was applied to the ^{210}Po inhalation and ingestion dose factors to arrive at the ^{209}Po internal dose factors.

$$\frac{\text{Po-209 Dose Factor}}{\text{Po-210 Dose Factor}} = \frac{4.882 \text{ Mev} * 0.01889 \text{ per day}}{5.3045 \text{ Mev} * 0.01388 \text{ per day}} = 1.252$$

C.1.7.2 Internal Exposure from Ingested Activity. The ingestion dose is calculated from the ingestion dose factor and the quantity of radioactivity consumed in food, soil and water. The ingestion dose is calculated using the general equation below.

$$H_{ing} = (Q_w^h C_w + Q_s^h W + \sum_p Q_p^h C_p) D_{ing} (1.0x10^{12} \text{ pCi/Ci})$$

where:

H_{ing}= the ingestion dose, in mrem

Q_w^h= amount of drinking water consumed annually by the human, in liters per year. The value 730 L/yr is used.

Q_s^h= amount of soil consumed annually by the human, in kilograms per year. The value 0.0365 kg/yr is used.

Q_p^h= amount of produce type p the human consumes each year, in kilograms (or liters for milk) per year. Values are listed in Table 2. Note that p refers to meat and milk as well as vegetables.

C_p= radionuclide concentration in plant or animal type p at the time it is consumed by the human, in curies per kilogram (or curies per liter for milk). Includes an insignificant amount of decay during holdup prior to consumption.

D_{ing}= internal dose factor for ingestion, in mrem per picocurie ingested. Values are shown on Table C-5.

C.1.7.3 Internal Exposure from Inhaled Activity. The activity inhaled in the course of a year depends on the volume of air inhaled during the year, as well as the average air concentration. The average air concentration is estimated from an average mass loading of particulate material in the air. The material in the air is assumed to have the same concentration as the soil. Thus the equation for inhaled activity is shown below.

$$H_{inh} = M_a V_a D_{inh} (1.0x10^{12} \text{ pCi/Ci}) W\{1 - Exp[-(\lambda_s+\lambda_r)T_h]\}/(\lambda_s+\lambda_r)$$

where:

H_{inh}= inhalation dose, in mrem

D_{inh}= internal dose factor for inhalation, in mrem per picocurie inhaled. Values are shown on Table C-5.

M_a= average mass concentration in the air during the year, in kilograms per cubic meter. The GENII value (1E-07 kg/m³) is used for the inhalation dose calculation.

V_a= daily average breathing rate, in cubic meters per hour. The value for Reference Man (0.95 m³/hr, in ICRP 23) is used.

T_h= inhalation time, in hours. This is the number of hours per year that the individual is breathing the average air concentration. The 4680 hour value for maximum individuals was derived using Table 3-1.

Note that the nuclide intake is accumulated over the time T_h. The equation shows how leaching from the surface layer is included. This portion of the calculation differs from GENII in that GENII does no decay or leaching when computing inhalation dose. GENII assumes the air concentration remains constant during the year.

In reality, the respirable dust loading of the air is lower than the assumed 100 $\mu g/m^3$. The EPA air quality standard is 50 $\mu g/m^3$, which is normally attainable. However, the soil contaminants are found with the small diameter fraction of the surface soil. Hence the concentration of nuclides in the airborne dust is higher than the concentration in the bulk soil. These two effects are assumed to offset one another, so that 100 $\mu g/m^3$ adequately represents the resuspended activity concentration.

For populations, the inhalation exposure time was increased from 4,680 hours per year to 8,766 hours per year. This increase is related to the broader distribution of radioactivity in the environment from widespread use of the Columbia River for irrigation.

C.1.7.4 External Exposure. The GENII program calculates external dose from surface contamination using unit dose factors computed by the EXTDF program. The EXTDF program uses parts of the ISOSHLD program to calculate dose equivalent rates from external sources for user entered geometry data. Values from the GENII library (GRDF.DAT) are shown in Table C-5. These values have been converted from the SI units to mrem/hr per Ci/m^2. The values for the added nuclides were calculated using EXTDF and the new values are shown on Table C-5. External dose to the intruder and the irrigator is calculated using the formula shown below.

$$H_{ext} = \rho \; d \; D_{ext} \; W \; \{1 - Exp[-(\lambda_s+\lambda_r)T_e]\}/(\lambda_s+\lambda_r)$$

where:

H_{ext}= total external dose, in mrem

D_{ext}= external dose rate factor for exposure to radiation from contaminated soil, in mrem/hr per Ci/m^2. Values are shown on Table C-5.

d = thickness of soil from which nuclides migrate, in centimeters. The GENII value for this is 15 centimeter.

ρ = bulk density of the surface soil, in grams per cubic centimeter. In GENII this is 1.5 g/cc.

T_e= time exposed to external radiation sources in the soil, in hours. The effective exposure time for maximum individuals is 3260 hours, from Section 1.1.

Note that the dose is accumulated over the time T_h. The equation shows how leaching from the surface layer is included. For the intruder scenario

this portion of the calculation differs from GENII in that GENII does no decay or leaching when computing inhalation dose. GENII assumes the soil concentration remains constant during the year.

For populations, the external exposure time was increased from 3,260 hours per year to 4,383 hours per year. This increase is related to the broader distribution of radioactivity in the environment from widespread use of the Columbia River for irrigation.

External dose to the Columbia River population from recreational activities was computed using GENII for several radionuclides. The average person spends 10 hours swimming and 17 hours on the river shoreline each year (Kincaid, 1993). These recreational activities increase the average external dose by approximately four percent. Therefore, the external dose from recreational activities is not explicitly included in the population dose estimates.

C.1.8 Comparison of Spreadsheet Versus GENII Dose Estimates

In this section, a comparison of results using the spreadsheet calculations and the GENII code is used.

C.1.8.1 Special Input Assumptions for the Comparisons. The comparisons were done using the NUREG/CR-5512 concentration ratios. In addition, since GENII does not allow input of internal dose factors, the spreadsheet used the values that are currently in GENII (Rittmann, 1993a). These were shown on Table C-5.

The comparisons were done for each nuclide in the spreadsheet. Three intrusion scenarios were used: 100 year decay with leaching, 100 year decay without leaching, and 500 year decay without leaching. Two irrigation scenarios were also used, with and without leaching. Only one population dose was computed, without leaching.

To compare the parts of the vegetation model (root uptake, rain splash, and direct deposition by irrigation water), special input files (DEFAULT.IN and FTRANS.DAT) were prepared for GENII. These are shown at then end of this appendix, along with the other GENII input files. Note that asterisks mark those lines which were changed from the GENII defaults. A special version of FTRANS.DAT was used to set the leaching coefficients to zero for the non-leaching runs. The two main input files used for the intruder and irrigator comparison tables are also attached. These show the inhalation and external exposure times, as well as the food and water consumption rates.

C.1.8.2 Comparison Results. The tables below (C-7 and C-8) summarize the observed differences. All spreadsheet results were divided by the corresponding GENII results. Nuclides with differences less than 10 percent are not shown. If one column for a nuclide has a difference greater than 10 percent, then the other differences are also shown. In some cases, entire columns were deleted. This was true for the irrigated farm inhalation, external, soil ingestion and drinking water. Table columns are described below.

Table C-7. Dose Ratios (Spreadsheet Divided by GENII) After Intrusion. Differences less than 10 percent are not shown.

Post-Intrusion Scenario -- 100 Years -- Leaching						
Nuclide	Inhale	Extern	Soil	Root	Rain	Total
H-3	4.24	4.43	4.23			4.41
C-14						108.26
Cl-36	1.15	1.14	1.16	1.25	1.31	1.25
Co-60	0.92	0.92	0.92	0.90	0.96	0.92
Tc-99	2.79	2.85	2.67	3.70	3.75	3.71
I-129	1.32	1.31	1.30	1.48	1.46	1.44
Ra-228	0.90	0.89	0.90	0.89	0.90	0.89
Ac-227	0.96	0.98	0.98	0.88		
Th-228	0.84	0.80	0.84	0.67	0.91	0.84
Th-229				0.60		
Np-237				1.11	1.10	
Post-Intrusion Scenario -- 100 Years -- NO Leaching						
C-14						103.22
Co-60	0.87	0.92	0.92	0.91	0.92	0.93
Ra-228	0.90	0.89	0.90	0.89	0.90	0.89
Ac-227				0.88		
Th-228	0.84	0.80	0.84	0.67	0.91	0.84
Th-229				0.60		
Post-Intrusion Scenario -- 500 Years -- NO Leaching						
C-14						98.35
Co-60	0.73	0.73	0.74	0.75	0.79	0.73
Cd-113m	0.89	0.93	0.89	0.96	0.96	0.94
Ra-228	0.68	0.68	0.72	0.72	0.75	0.72
Ac-227				0.84		
Th-229				0.61		
Cm-248		0.88				

Table C-8. Dose Ratios (Spreadsheet Divided by GENII) for Irrigation Scenarios. Differences less than 10 percent are not shown.

Irrigated Farm Scenario -- With or Without Leaching					
Nuclide	Root	Rain	Direct	Beef	Milk
C-14			0.31	1.12	0.81
Zr-93					1.25
Tc-99[1]				1.16	1.26
Ac-227	0.89				0.74
Th-228	0.77	1.11		0.85	0.044
Th-229	0.62			0.42	0.17
Th-232					1.15
Pu-244					0.28
Am-242m					0.44
[1]The Tc-99 difference only occurs if leaching is allowed.					

Columbia River Population Scenario -- NO Leaching				
Nuclide	Vege	Beef	Milk	Fish
C-14	0.16	1.13	0.75	
Zr-93			1.66	
Pb-210			0.84	0.36
Ac-227			0.71	
Th-228		1.16	0.065	1.27
Th-229		0.54	0.16	
Th-232			1.30	
Pu-244			0.85	
Am-242m			0.40	

Beef - dose from ingested beef
Direct - dose from vegetation, direct deposition by irrigation water only
Extern - external dose from what is in the surface soil
Fish - dose from ingested fish
Inhale - inhalation dose
Milk - dose from ingested milk
Rain - dose from vegetation, rain splash only
Root - dose from vegetation, root uptake only
Soil - dose from soil ingestion
Total - all pathways used in a given exposure scenario
Vege - dose from ingested garden produce (sum of root, rain and direct)

For the intruder's garden, the spreadsheet computes the effect of contaminant leaching differently than GENII. The spreadsheet computes the annual dose allowing for continuous exposure during the year that leaching occurs. GENII computes the soil concentration at the end of the year and assumes this existed throughout the entire year. GENII thus underestimates the inhalation, external, and soil ingestion doses for nuclides which are mobile in the soil (^{3}H, ^{36}Cl, ^{99}Tc, and ^{129}I). For these nuclides the dose ratios are greater than one. Note that the dose ratios increase for the vegetable pathways (Root and Rain). This difference is due to the assumed growing period. In the spreadsheet the vegetables grow for 100 days, and then are harvested. In GENII, however, the vegetables grow for the entire year, and then are harvested. For mobile nuclides, this leads GENII to further lower the amount used in the dose calculation, and increases the dose ratios.

For the intruder's garden, the spreadsheet gives lower doses than GENII for ^{60}Co, ^{228}Ra, and ^{228}Th. These dose ratios are different because GENII does not compute radioactive decay along with leaching during the year of exposure. Since these nuclides have comparatively short half-lives and are not mobile, the difference is noticeable.

For the intruder's garden, the spreadsheet gives noticeably lower doses via root uptake than GENII for ^{228}Ra, ^{227}Ac, ^{228}Th, and ^{229}Th. Note that the ^{228}Ra difference is due to the difference in its progeny nuclide ^{228}Th. The differences for ^{227}Ac, ^{228}Th and ^{229}Th are due to the spreadsheet assumption that the progeny nuclides (^{223}Ra, ^{224}Ra, and ^{225}Ra) are in radioactive equilibrium with the parents. However, GENII computes the actual amounts in the plants based on the different concentration ratios. Since the radium concentration ratios are roughly an order of magnitude larger than thorium or actinium, the amount of the progeny is much greater than is assumed by the spreadsheet. Thus the GENII doses are larger and the dose ratios are less than one for some pathways.

For ^{14}C, the vegetation doses are based on different models. GENII gives zero dose, while the spreadsheet gives quite a bit. The total doses are radically different.

At 500 years of prior decay, there begins to be noticeable departures from the spreadsheet decay calculation for nuclides with short half-lives. Evidently, a calculation is performed in GENII, that introduces differences in the decay calculation after 50 or so half-lives. The difference for ^{248}Cm external dose comes about because the spreadsheet ignores the ingrowth of ^{240}U. The other differences are as described before.

For the irrigated farm the leaching computations are similar in both GENII and the spreadsheet. The differences shown in Table C-8 are largely due to the different treatment of short-lived progeny nuclides. The following nuclides illustrate this: ^{210}Pb (^{210}Po), ^{227}Ac (^{223}Ra), ^{228}Th (^{224}Ra), ^{229}Th (^{225}Ra), ^{244}Pu (^{240}U), and ^{242m}Am (^{242}Cm). The principle progeny nuclide is shown in parentheses. In each case, the progeny nuclide is found in the cow (or fish) in higher than equilibrium amounts. Therefore, GENII gives larger doses than the spreadsheet, since the spreadsheet assumes the progeny nuclides are always present in equilibrium amounts.

The differences for ^{93}Zr, ^{99}Tc, and ^{232}Th for Beef and Milk follow from differences in the calculation of soil leaching and progeny ingrowth during the growing period.

C.2 CONCENTRATION IN VEGETABLES

In GENII, the calculation of radionuclide concentrations in living plants uses three main routes, (1) root uptake, (2) resuspension to leaves (also called "rain splash"), and (3) direct deposition of irrigation water on foliage. Each of these will be considered separately and then combined to get the total concentration in the vegetables.

GENII includes the effects of radioactive decay between the time a plant type is harvested and when it is consumed. This time period is called the holdup time. It enters the equations for plant concentration as shown below.

$$C_p = (C_p^d + C_p^f + C_p^r)\ \mathrm{Exp}(-\lambda_r\ T_p^h)$$

where:

- C_p = Radionuclide concentration in plant type p at the time it is consumed, in Ci/kg
- C_p^d = Concentration of a radionuclide in plant type p due to direct deposition of irrigation water. The units for C_p^d are Ci/kg
- C_p^r = Concentration of a radionuclide in plant type p due to absorption from the soil through the roots. The units for C_p^r are Ci/kg
- C_p^f = Concentration of a radionuclide in plant type p due to foliar deposition from soil resuspension. The units for C_p^f are Ci/kg
- T_p^h = Holdup time, i.e., the time between harvest and consumption of plant type p, in days.

It was not necessary to include the effects of holdup in the spreadsheet due to the long half-lives of the important nuclides. However, for a few nuclides, the production of daughter activity made a small increase in certain doses. Since the four nuclides missing from GENII decay to stable isotopes, the effects of holdup were not included.

C.2.1 Root Uptake into Edible Portions

Root uptake is calculated through a concentration ratio. These ratios are tabulated below in Tables C-1 and C-2. Two sources are used for the numbers. The first is GENII, which provides no references to the literature. The second is ORNL-5785, which is extensively documented in ORNL-5786. There are some major differences, therefore, both were used and compared.

C.3 AIR TRANSPORT OF BURIAL GROUND EMISSIONS USING ISC2

The atmospheric dispersion of chronic airborne emissions from the surface of a burial ground was estimated using the ISC2 programs from the U.S. Environmental Protection Agency. The ISC2 programs were used two ways, as a check. The first was to treat the air emissions source as a point. The second approach was the more realistic treatment as an extended source. The extended source was assumed to be a square 316 meters by 316 meters. Hanford Site wind data collected at the Hanford Meteorological Station for the years 1983 to 1991 was used. Note that the source was divided into 36 smaller squares to improve accuracy at small distances. All input files are provided in Tables C-10 through C-13.

Results for the chronic release case (ISCLT) are shown on the table below. The release occurs over the better part of one year. The wind direction ESE had the largest concentrations for most of the distances. The normalized integrated exposure (X/Q) is the final air concentration divided by the total release rate of the source.

Distance is measured from the center of the square. The distances from the outer edge of the square are found by subtracting 171 meters from the table distance. The 171 meters is the distance from the center of the square to the edge at an angle of 22.5° from perpendicular. As the distance from the burial site increases, the average air concentration decreases.

The largest annual average integrated exposure will not exceed 1.0E-04 seconds per cubic meter at the boundary in the ESE direction. The annual inhalation dose is the product shown below. The only nuclides considered are tritium and ^{14}C. The only other nuclide with volatile emissions is ^{222}Rn, which is limited by the surface emanation rate rather than the projected dose downwind.

Annual Inhalation Dose = Q•(X/Q)•BR•DF

where:

Q = annual curies released into the air from the burial ground
X/Q = normalized integrated exposure, in seconds per cubic meter, the value 1.0E-04 s/m^3 was used, based on Table C-9.
BR = inhalation rate for reference man, 3.33E-04 m^3/second for light activity, and 2.67E-04 m^3/second averaged over 24 hours.
DF = inhalation dose factor for the nuclide being released. Values for tritium and ^{14}C are 95 and 2100 rem/Ci inhaled.

Table C-9. Air Concentrations and Normalized Integrated Exposures (X/Q) from Chronic Releases. (Release rate is 1.0 gram/second)

Distance meters	Air Conc, $\mu g\ m^{-3}$		X/Q, sec m^{-3}	
	Point	Area	Point	Area
221	71.047	62.088	7.10E-05	6.21E-05
241	61.644	53.525	6.16E-05	5.35E-05
271	50.730	44.308	5.07E-05	4.43E-05
321	38.183	33.959	3.82E-05	3.40E-05
371	29.921	26.815	2.99E-05	2.68E-05
421	24.128	21.599	2.41E-05	2.16E-05
471	19.900	17.811	1.99E-05	1.78E-05
521	16.718	15.000	1.67E-05	1.50E-05
671	10.763	9.823	1.08E-05	9.82E-06
871	6.882	6.384	6.88E-06	6.38E-06
1,171	4.204	3.971	4.20E-06	3.97E-06
2,171	1.549	1.500	1.55E-06	1.50E-06
5,171	0.411	0.405	4.11E-07	4.05E-07
10,000	0.155	0.154	1.55E-07	1.54E-07

The combination of X/Q, BR and DF leads to the following scenario dose factors: for tritium, 2.5×10^{-6} rem Ci^{-1} released; for ^{14}C, 5.6×10^{-5} rem Ci^{-1} released. As an example of how these numbers are used, suppose a burial ground is projected to release 10 curies of ^{14}C over the course of a year. Then the largest inhalation dose from ^{14}C near the burial ground would be 5.6×10^{-4} rem.

Table C-10. ISCLT Input for the Area Source Calculations (sheet 1 of 3).

```
CO STARTING
   TITLEONE  Area Source Emissions from Burial Ground Sites
   TITLETWO  25 Acre Source (316 meter)²
   MODELOPT  DFAULT  CONC  RURAL
   AVERTIME  annual
   POLLUTID  Dust
   RUNORNOT  RUN
CO FINISHED

SO STARTING
   LOCATION  Burial1   AREA  -158.0   -158.0  0.0
**                      g/s/m²   ht,m   length,m
   SRCPARAM  Burial1   1.00E-5    1.0     52.67
   LOCATION  Burial2   AREA  -158.0   -105.33  0.0
**                      g/s/m²   ht,m   length,m
   SRCPARAM  Burial2   1.00E-5    1.0     52.67
   LOCATION  Burial3   AREA  -158.0    -52.66  0.0
**                      g/s/m²   ht,m   length,m
   SRCPARAM  Burial3   1.00E-5    1.0     52.67
   LOCATION  Burial4   AREA  -158.0      0.0   0.0
**                      g/s/m²   ht,m   length,m
   SRCPARAM  Burial4   1.00E-5    1.0     52.67
   LOCATION  Burial5   AREA  -158.0     52.66  0.0
**                      g/s/m²   ht,m   length,m
   SRCPARAM  Burial5   1.00E-5    1.0     52.67
   LOCATION  Burial6   AREA  -158.0    105.33  0.0
**                      g/s/m²   ht,m   length,m
   SRCPARAM  Burial6   1.00E-5    1.0     52.67
   LOCATION  Burial7   AREA  -105.33  -158.0  0.0
**                      g/s/m²   ht,m   length,m
   SRCPARAM  Burial7   1.00E-5    1.0     52.67
   LOCATION  Burial8   AREA  -105.33  -105.33  0.0
**                      g/s/m²   ht,m   length,m
   SRCPARAM  Burial8   1.00E-5    1.0     52.67
   LOCATION  Burial9   AREA  -105.33   -52.66  0.0
**                      g/s/m²   ht,m   length,m
   SRCPARAM  Burial9   1.00E-5    1.0     52.67
   LOCATION  Burial10  AREA  -105.33     0.0   0.0
**                      g/s/m²   ht,m   length,m
   SRCPARAM  Burial10  1.00E-5    1.0     52.67
   LOCATION  Burial11  AREA  -105.33    52.66  0.0
**                      g/s/m²   ht,m   length,m
   SRCPARAM  Burial11  1.00E-5    1.0     52.67
   LOCATION  Burial12  AREA  -105.33   105.33  0.0
**                      g/s/m²   ht,m   length,m
   SRCPARAM  Burial12  1.00E-5    1.0     52.67
   LOCATION  Burial13  AREA   -52.66  -158.0  0.0
**                      g/s/m²   ht,m   length,m
   SRCPARAM  Burial13  1.00E-5    1.0     52.67
   LOCATION  Burial14  AREA   -52.66  -105.33  0.0
**                      g/s/m²   ht,m   length,m
   SRCPARAM  Burial14  1.00E-5    1.0     52.67
```

Table C-10. ISCLT Input for the Area Source Calculations (sheet 2 of 3).

```
   LOCATION  Burial15  AREA   -52.66   -52.66  0.0
**                      g/s/m²   ht,m   length,m
   SRCPARAM  Burial15  1.00E-5    1.0     52.67
   LOCATION  Burial16  AREA   -52.66     0.0   0.0
**                      g/s/m²   ht,m   length,m
   SRCPARAM  Burial16  1.00E-5    1.0     52.67
   LOCATION  Burial17  AREA   -52.66    52.66  0.0
**                      g/s/m²   ht,m   length,m
   SRCPARAM  Burial17  1.00E-5    1.0     52.67
   LOCATION  Burial18  AREA   -52.66   105.33  0.0
**                      g/s/m²   ht,m   length,m
   SRCPARAM  Burial18  1.00E-5    1.0     52.67
   LOCATION  Burial19  AREA     0.0   -158.0  0.0
**                      g/s/m²   ht,m   length,m
   SRCPARAM  Burial19  1.00E-5    1.0     52.67
   LOCATION  Burial20  AREA     0.0   -105.33  0.0
**                      g/s/m²   ht,m   length,m
   SRCPARAM  Burial20  1.00E-5    1.0     52.67
   LOCATION  Burial21  AREA     0.0    -52.66  0.0
**                      g/s/m²   ht,m   length,m
   SRCPARAM  Burial21  1.00E-5    1.0     52.67
   LOCATION  Burial22  AREA     0.0      0.0   0.0
**                      g/s/m²   ht,m   length,m
   SRCPARAM  Burial22  1.00E-5    1.0     52.67
   LOCATION  Burial23  AREA     0.0     52.66  0.0
**                      g/s/m²   ht,m   length,m
   SRCPARAM  Burial23  1.00E-5    1.0     52.67
   LOCATION  Burial24  AREA     0.0    105.33  0.0
**                      g/s/m²   ht,m   length,m
   SRCPARAM  Burial24  1.00E-5    1.0     52.67
   LOCATION  Burial25  AREA    52.66  -158.0  0.0
**                      g/s/m²   ht,m   length,m
   SRCPARAM  Burial25  1.00E-5    1.0     52.67
   LOCATION  Burial26  AREA    52.66  -105.33  0.0
**                      g/s/m²   ht,m   length,m
   SRCPARAM  Burial26  1.00E-5    1.0     52.67
   LOCATION  Burial27  AREA    52.66   -52.66  0.0
**                      g/s/m²   ht,m   length,m
   SRCPARAM  Burial27  1.00E-5    1.0     52.67
   LOCATION  Burial28  AREA    52.66     0.0   0.0
**                      g/s/m²   ht,m   length,m
   SRCPARAM  Burial28  1.00E-5    1.0     52.67
   LOCATION  Burial29  AREA    52.66    52.66  0.0
**                      g/s/m²   ht,m   length,m
   SRCPARAM  Burial29  1.00E-5    1.0     52.67
   LOCATION  Burial30  AREA    52.66   105.33  0.0
**                      g/s/m²   ht,m   length,m
   SRCPARAM  Burial30  1.00E-5    1.0     52.67
   LOCATION  Burial31  AREA   105.33  -158.0  0.0
**                      g/s/m²   ht,m   length,m
   SRCPARAM  Burial31  1.00E-5    1.0     52.67
   LOCATION  Burial32  AREA   105.33  -105.33  0.0
```

Table C-10. ISCLT Input for the Area Source Calculations (sheet 3 of 3).

```
**                          g/s/m²   ht,m   length,m
   SRCPARAM  Burial32  1.00E-5    1.0     52.67
   LOCATION  Burial33  AREA   105.33   -52.66  0.0
**                          g/s/m²   ht,m   length,m
   SRCPARAM  Burial33  1.00E-5    1.0     52.67
   LOCATION  Burial34  AREA   105.33     0.0   0.0
**                          g/s/m²   ht,m   length,m
   SRCPARAM  Burial34  1.00E-5    1.0     52.67
   LOCATION  Burial35  AREA   105.33    52.66  0.0
**                          g/s/m²   ht,m   length,m
   SRCPARAM  Burial35  1.00E-5    1.0     52.67
   LOCATION  Burial36  AREA   105.33   105.33  0.0
**                          g/s/m²   ht,m   length,m
   SRCPARAM  Burial36  1.00E-5    1.0     52.67
   SRCGROUP ALL
SO FINISHED

RE STARTING
   GRIDPOLR Nearby STA
                    ORIG   0    0
**   distance from edge:   50   70  100  150  200  250  300  350  500  700
                    DIST  221  241  271  321  371  421  471  521  671  871
**   distance from edge: 1000 2000 5000  9829 m
                    DIST 1171 2171 5171 10000
                    GDIR   16   0   22.5
   GRIDPOLR Nearby END
RE FINISHED

ME STARTING
   INPUTFIL  JF20010.STA  FREE
   ANEMHGHT  10.0
   SURFDATA  67656  1991  HANFORD200
   UAIRDATA  67656  1991  HANFORD200
   STARDATA  ANNUAL
   AVESPEED  1.00   2.682  4.694  7.153  9.835  14.304
   AVETEMPS  ANNUAL   6*285.3
   AVEMIXHT  ANNUAL  A  6*1000.0
   AVEMIXHT  ANNUAL  B  6*1000.0
   AVEMIXHT  ANNUAL  C  6*1000.0
   AVEMIXHT  ANNUAL  D  6*1000.0
   AVEMIXHT  ANNUAL  E  6*1000.0
   AVEMIXHT  ANNUAL  F  6*1000.0
ME FINISHED

OU STARTING
   RECTABLE  SRCGRP
   MAXTABLE  10  INDSRC  SOCONT
OU FINISHED
```

Table C-11. Wind Data for ISCLT (file named JF20010.STA) (sheet 1 of 2).

0.003602	0.006904	0.002602	0.000700	0.000200	0.000300
0.002001	0.004403	0.002401	0.000700	0.000200	0.000400
0.002301	0.002902	0.001001	0.000500	0.000100	0.000000
0.002602	0.003202	0.000300	0.000100	0.000000	0.000000
0.004002	0.006004	0.000800	0.000000	0.000000	0.000000
0.002401	0.005103	0.001001	0.000000	0.000000	0.000000
0.001701	0.004503	0.001001	0.000100	0.000000	0.000000
0.001001	0.002902	0.001301	0.000300	0.000000	0.000000
0.001001	0.002401	0.001201	0.000400	0.000100	0.000000
0.000600	0.001201	0.000700	0.000400	0.000100	0.000000
0.000600	0.001701	0.001401	0.001101	0.000500	0.000200
0.000600	0.001901	0.003402	0.002502	0.001601	0.000700
0.001001	0.002502	0.003502	0.002502	0.001001	0.000200
0.001001	0.003002	0.003502	0.002502	0.001101	0.000200
0.001401	0.004203	0.004002	0.003302	0.002401	0.000400
0.002201	0.004803	0.001701	0.000500	0.000000	0.000000
0.001501	0.002101	0.000901	0.000200	0.000100	0.000100
0.001301	0.001501	0.000600	0.000300	0.000100	0.000200
0.001001	0.000600	0.000300	0.000100	0.000000	0.000000
0.001101	0.000800	0.000100	0.000100	0.000000	0.000000
0.001601	0.001601	0.000300	0.000000	0.000000	0.000000
0.000901	0.001301	0.000300	0.000000	0.000000	0.000000
0.000700	0.001301	0.000400	0.000000	0.000000	0.000000
0.000300	0.000901	0.000500	0.000100	0.000000	0.000000
0.000500	0.000800	0.000300	0.000200	0.000000	0.000000
0.000200	0.000400	0.000200	0.000100	0.000000	0.000000
0.000100	0.000300	0.000500	0.000400	0.000200	0.000100
0.000300	0.000500	0.000700	0.000800	0.000400	0.000200
0.000400	0.000700	0.001001	0.000600	0.000200	0.000100
0.000500	0.000901	0.001401	0.000700	0.000300	0.000000
0.000700	0.001601	0.001201	0.000901	0.000600	0.000100
0.001001	0.001601	0.000600	0.000100	0.000000	0.000000
0.001401	0.001901	0.000800	0.000200	0.000100	0.000200
0.001001	0.001201	0.000500	0.000300	0.000100	0.000400
0.000901	0.000600	0.000300	0.000100	0.000000	0.000000
0.001201	0.000901	0.000100	0.000000	0.000000	0.000000
0.001401	0.001301	0.000200	0.000000	0.000000	0.000000
0.001001	0.001301	0.000200	0.000000	0.000000	0.000000
0.000600	0.001901	0.000400	0.000000	0.000000	0.000000
0.000400	0.001001	0.000400	0.000100	0.000000	0.000000
0.000400	0.000600	0.000500	0.000200	0.000100	0.000000
0.000200	0.000200	0.000200	0.000100	0.000000	0.000000
0.000200	0.000300	0.000300	0.000200	0.000200	0.000200
0.000200	0.000500	0.000600	0.000700	0.000500	0.000200
0.000400	0.000800	0.000901	0.000600	0.000200	0.000000
0.000400	0.001001	0.001301	0.000700	0.000300	0.000100
0.001001	0.001901	0.001201	0.000600	0.000500	0.000100
0.001001	0.001501	0.000300	0.000100	0.000000	0.000000
0.008705	0.008405	0.003202	0.001001	0.000200	0.000700
0.005803	0.004803	0.002001	0.001001	0.000400	0.001201
0.005904	0.004002	0.000901	0.000300	0.000100	0.000000
0.005904	0.003302	0.000400	0.000100	0.000000	0.000000

Table C-11. Wind Data for ISCLT (file named JF20010.STA) (sheet 2 of 2).

0.007705	0.006604	0.001201	0.000000	0.000000	0.000000
0.005003	0.005703	0.001101	0.000100	0.000000	0.000000
0.004303	0.007505	0.002502	0.000300	0.000000	0.000000
0.003202	0.005303	0.002702	0.000700	0.000000	0.000000
0.002702	0.003502	0.002401	0.001001	0.000200	0.000000
0.001901	0.001801	0.001301	0.001101	0.000700	0.000200
0.002101	0.002401	0.002301	0.002502	0.001601	0.001201
0.001701	0.002802	0.003902	0.003802	0.002401	0.001201
0.004002	0.006904	0.008305	0.005803	0.001301	0.000500
0.004403	0.010907	0.014609	0.011407	0.005003	0.000700
0.005403	0.010506	0.008405	0.005003	0.002902	0.000800
0.005503	0.007705	0.002101	0.000500	0.000100	0.000000
0.003902	0.003202	0.001901	0.000700	0.000100	0.000901
0.002602	0.001701	0.000901	0.001201	0.000600	0.001501
0.002802	0.001101	0.000400	0.000100	0.000100	0.000100
0.002502	0.001301	0.000100	0.000000	0.000000	0.000000
0.004603	0.003102	0.000600	0.000000	0.000000	0.000000
0.003402	0.003402	0.000600	0.000000	0.000000	0.000000
0.003102	0.004703	0.001501	0.000100	0.000000	0.000000
0.003002	0.005203	0.002502	0.000500	0.000000	0.000000
0.003402	0.004603	0.002201	0.000700	0.000100	0.000000
0.002101	0.002101	0.001201	0.000800	0.000500	0.000100
0.002502	0.002902	0.001801	0.001701	0.001101	0.000500
0.002902	0.004803	0.003902	0.003002	0.001501	0.000200
0.004903	0.015809	0.019812	0.006504	0.000600	0.000100
0.004403	0.016810	0.025015	0.017511	0.003802	0.000500
0.004503	0.011107	0.007505	0.004102	0.001101	0.000300
0.003902	0.003902	0.001301	0.000200	0.000000	0.000000
0.003302	0.001701	0.000500	0.000300	0.000100	0.000400
0.001701	0.000700	0.000600	0.000200	0.000100	0.000700
0.002001	0.000700	0.000100	0.000000	0.000000	0.000000
0.002201	0.000800	0.000100	0.000000	0.000000	0.000000
0.004403	0.002502	0.000100	0.000000	0.000000	0.000000
0.003602	0.003102	0.000300	0.000000	0.000000	0.000000
0.004102	0.005904	0.000600	0.000000	0.000000	0.000000
0.004002	0.006704	0.002602	0.000200	0.000000	0.000000
0.005203	0.006504	0.002101	0.000200	0.000100	0.000000
0.003202	0.002902	0.000400	0.000000	0.000000	0.000000
0.003202	0.003702	0.000901	0.000100	0.000000	0.000000
0.003602	0.006604	0.002902	0.000200	0.000000	0.000000
0.007004	0.024215	0.017511	0.000700	0.000000	0.000000
0.005003	0.023814	0.024415	0.000901	0.000000	0.000000
0.004603	0.011207	0.004503	0.000300	0.000000	0.000000
0.003202	0.003302	0.000700	0.000000	0.000000	0.000000

200 AREA (HMS) - 10 M - Pasquill A - G (1983 - 1991 Average)
Created 8/26/92 KR, ***> ISCLT2 Format 3-15-93, PDR

Table C-12. ISCST Input for the Area Source Calculations (sheet 1 of 3).

```
CO STARTING
   TITLEONE  Area Source Emissions from Burial Ground Sites
   TITLETWO  25 Acre Source (316 meter)²
   MODELOPT  DFAULT  CONC  RURAL
   AVERTIME  1
   POLLUTID  Dust
   RUNORNOT  RUN
CO FINISHED

SO STARTING
   LOCATION  Burial1   AREA  -158.0   -158.0  0.0
**                      g/s/m²   ht,m   length,m
   SRCPARAM  Burial1   1.00E-5    1.0     52.67
   LOCATION  Burial2   AREA  -158.0   -105.33  0.0
**                      g/s/m²   ht,m   length,m
   SRCPARAM  Burial2   1.00E-5    1.0     52.67
   LOCATION  Burial3   AREA  -158.0    -52.66  0.0
**                      g/s/m²   ht,m   length,m
   SRCPARAM  Burial3   1.00E-5    1.0     52.67
   LOCATION  Burial4   AREA  -158.0      0.0   0.0
**                      g/s/m²   ht,m   length,m
   SRCPARAM  Burial4   1.00E-5    1.0     52.67
   LOCATION  Burial5   AREA  -158.0     52.66  0.0
**                      g/s/m²   ht,m   length,m
   SRCPARAM  Burial5   1.00E-5    1.0     52.67
   LOCATION  Burial6   AREA  -158.0    105.33  0.0
**                      g/s/m²   ht,m   length,m
   SRCPARAM  Burial6   1.00E-5    1.0     52.67
   LOCATION  Burial7   AREA  -105.33  -158.0  0.0
**                      g/s/m²   ht,m   length,m
   SRCPARAM  Burial7   1.00E-5    1.0     52.67
   LOCATION  Burial8   AREA  -105.33  -105.33  0.0
**                      g/s/m²   ht,m   length,m
   SRCPARAM  Burial8   1.00E-5    1.0     52.67
   LOCATION  Burial9   AREA  -105.33   -52.66  0.0
**                      g/s/m²   ht,m   length,m
   SRCPARAM  Burial9   1.00E-5    1.0     52.67
   LOCATION  Burial10  AREA  -105.33     0.0   0.0
**                      g/s/m²   ht,m   length,m
   SRCPARAM  Burial10  1.00E-5    1.0     52.67
   LOCATION  Burial11  AREA  -105.33    52.66  0.0
**                      g/s/m²   ht,m   length,m
   SRCPARAM  Burial11  1.00E-5    1.0     52.67
   LOCATION  Burial12  AREA  -105.33   105.33  0.0
**                      g/s/m²   ht,m   length,m
   SRCPARAM  Burial12  1.00E-5    1.0     52.67
   LOCATION  Burial13  AREA   -52.66  -158.0  0.0
**                      g/s/m²   ht,m   length,m
   SRCPARAM  Burial13  1.00E-5    1.0     52.67
   LOCATION  Burial14  AREA   -52.66  -105.33  0.0
**                      g/s/m²   ht,m   length,m
   SRCPARAM  Burial14  1.00E-5    1.0     52.67
```

Table C-12. ISCST Input for the Area Source Calculations (sheet 2 of 3).

```
   LOCATION  Burial15  AREA   -52.66   -52.66  0.0
**                      g/s/m²   ht,m   length,m
   SRCPARAM  Burial15  1.00E-5    1.0     52.67
   LOCATION  Burial16  AREA   -52.66     0.0   0.0
**                      g/s/m²   ht,m   length,m
   SRCPARAM  Burial16  1.00E-5    1.0     52.67
   LOCATION  Burial17  AREA   -52.66    52.66  0.0
**                      g/s/m²   ht,m   length,m
   SRCPARAM  Burial17  1.00E-5    1.0     52.67
   LOCATION  Burial18  AREA   -52.66   105.33  0.0
**                      g/s/m²   ht,m   length,m
   SRCPARAM  Burial18  1.00E-5    1.0     52.67
   LOCATION  Burial19  AREA     0.0   -158.0  0.0
**                      g/s/m²   ht,m   length,m
   SRCPARAM  Burial19  1.00E-5    1.0     52.67
   LOCATION  Burial20  AREA     0.0   -105.33  0.0
**                      g/s/m²   ht,m   length,m
   SRCPARAM  Burial20  1.00E-5    1.0     52.67
   LOCATION  Burial21  AREA     0.0    -52.66  0.0
**                      g/s/m²   ht,m   length,m
   SRCPARAM  Burial21  1.00E-5    1.0     52.67
   LOCATION  Burial22  AREA     0.0      0.0   0.0
**                      g/s/m²   ht,m   length,m
   SRCPARAM  Burial22  1.00E-5    1.0     52.67
   LOCATION  Burial23  AREA     0.0     52.66  0.0
**                      g/s/m²   ht,m   length,m
   SRCPARAM  Burial23  1.00E-5    1.0     52.67
   LOCATION  Burial24  AREA     0.0    105.33  0.0
**                      g/s/m²   ht,m   length,m
   SRCPARAM  Burial24  1.00E-5    1.0     52.67
   LOCATION  Burial25  AREA    52.66  -158.0  0.0
**                      g/s/m²   ht,m   length,m
   SRCPARAM  Burial25  1.00E-5    1.0     52.67
   LOCATION  Burial26  AREA    52.66  -105.33  0.0
**                      g/s/m²   ht,m   length,m
   SRCPARAM  Burial26  1.00E-5    1.0     52.67
   LOCATION  Burial27  AREA    52.66   -52.66  0.0
**                      g/s/m²   ht,m   length,m
   SRCPARAM  Burial27  1.00E-5    1.0     52.67
   LOCATION  Burial28  AREA    52.66     0.0   0.0
**                      g/s/m²   ht,m   length,m
   SRCPARAM  Burial28  1.00E-5    1.0     52.67
   LOCATION  Burial29  AREA    52.66    52.66  0.0
**                      g/s/m²   ht,m   length,m
   SRCPARAM  Burial29  1.00E-5    1.0     52.67
   LOCATION  Burial30  AREA    52.66   105.33  0.0
**                      g/s/m²   ht,m   length,m
   SRCPARAM  Burial30  1.00E-5    1.0     52.67
   LOCATION  Burial31  AREA   105.33  -158.0  0.0
**                      g/s/m²   ht,m   length,m
   SRCPARAM  Burial31  1.00E-5    1.0     52.67
   LOCATION  Burial32  AREA   105.33  -105.33  0.0
```

Table C-12. ISCST Input for the Area Source Calculations (sheet 3 of 3).

```
**                        g/s/m²   ht,m   length,m
   SRCPARAM  Burial32  1.00E-5    1.0     52.67
   LOCATION  Burial33  AREA   105.33   -52.66  0.0
**                        g/s/m²   ht,m   length,m
   SRCPARAM  Burial33  1.00E-5    1.0     52.67
   LOCATION  Burial34  AREA   105.33     0.0   0.0
**                        g/s/m²   ht,m   length,m
   SRCPARAM  Burial34  1.00E-5    1.0     52.67
   LOCATION  Burial35  AREA   105.33    52.66  0.0
**                        g/s/m²   ht,m   length,m
   SRCPARAM  Burial35  1.00E-5    1.0     52.67
   LOCATION  Burial36  AREA   105.33   105.33  0.0
**                        g/s/m²   ht,m   length,m
   SRCPARAM  Burial36  1.00E-5    1.0     52.67
   SRCGROUP ALL
SO FINISHED

RE STARTING
   GRIDPOLR Nearby STA
                    ORIG   0    0
**   distance from edge:   50   70  100  150  200  250  300  350  500  700
                    DIST   221  241  271  321  371  421  471  521  671  871
**   distance from edge: 1000 2000 5000  9829 m
                    DIST  1171 2171 5171 10000
                    GDIR   16   0   22.5
   GRIDPOLR Nearby END
RE FINISHED

ME STARTING
   INPUTFIL  JF-F.HR
   ANEMHGHT  10.0
   SURFDATA  67656  1987  HANFORD200
   UAIRDATA  67656  1987  HANFORD200
ME FINISHED

OU STARTING
   RECTABLE  ALLAVE  1st
OU FINISHED
```

Table C-13. Wind Data Used by ISCST (file named JF-F.HR).

```
 67656      87  67656      87   Class F
87 1 1 1 180.00      1.00   293.0 6 1000.0 1000.0
87 1 1 2 202.50      1.00   293.0 6 1000.0 1000.0
87 1 1 3 225.00      1.00   293.0 6 1000.0 1000.0
87 1 1 4 247.50      1.00   293.0 6 1000.0 1000.0
87 1 1 5 270.00      1.00   293.0 6 1000.0 1000.0
87 1 1 6 292.50      1.00   293.0 6 1000.0 1000.0
87 1 1 7 315.00      1.00   293.0 6 1000.0 1000.0
87 1 1 8 337.50      1.00   293.0 6 1000.0 1000.0
87 1 1 9   0.00      1.00   293.0 6 1000.0 1000.0
87 1 110  22.50      1.00   293.0 6 1000.0 1000.0
87 1 111  45.00      1.00   293.0 6 1000.0 1000.0
87 1 112  67.50      1.00   293.0 6 1000.0 1000.0
87 1 113  90.00      1.00   293.0 6 1000.0 1000.0
87 1 114 112.50      1.00   293.0 6 1000.0 1000.0
87 1 115 135.00      1.00   293.0 6 1000.0 1000.0
87 1 116 157.50      1.00   293.0 6 1000.0 1000.0
87 1 117 180.00      2.00   293.0 6 1000.0 1000.0
87 1 118 202.50      2.00   293.0 6 1000.0 1000.0
87 1 119 225.00      2.00   293.0 6 1000.0 1000.0
87 1 120 247.50      2.00   293.0 6 1000.0 1000.0
87 1 121 270.00      2.00   293.0 6 1000.0 1000.0
87 1 122 292.50      2.00   293.0 6 1000.0 1000.0
87 1 123 315.00      2.00   293.0 6 1000.0 1000.0
87 1 124 337.50      2.00   293.0 6 1000.0 1000.0
87 1 2 1   0.00      2.00   293.0 6 1000.0 1000.0
87 1 2 2  22.50      2.00   293.0 6 1000.0 1000.0
87 1 2 3  45.00      2.00   293.0 6 1000.0 1000.0
87 1 2 4  67.50      2.00   293.0 6 1000.0 1000.0
87 1 2 5  90.00      2.00   293.0 6 1000.0 1000.0
87 1 2 6 112.50      2.00   293.0 6 1000.0 1000.0
87 1 2 7 135.00      2.00   293.0 6 1000.0 1000.0
87 1 2 8 157.50      2.00   293.0 6 1000.0 1000.0
87 1 2 9 180.00      3.00   293.0 6 1000.0 1000.0
87 1 210 202.50      3.00   293.0 6 1000.0 1000.0
87 1 211 225.00      3.00   293.0 6 1000.0 1000.0
87 1 212 247.50      3.00   293.0 6 1000.0 1000.0
87 1 213 270.00      3.00   293.0 6 1000.0 1000.0
87 1 214 292.50      3.00   293.0 6 1000.0 1000.0
87 1 215 315.00      3.00   293.0 6 1000.0 1000.0
87 1 216 337.50      3.00   293.0 6 1000.0 1000.0
87 1 217   0.00      3.00   293.0 6 1000.0 1000.0
87 1 218  22.50      3.00   293.0 6 1000.0 1000.0
87 1 219  45.00      3.00   293.0 6 1000.0 1000.0
87 1 220  67.50      3.00   293.0 6 1000.0 1000.0
87 1 221  90.00      3.00   293.0 6 1000.0 1000.0
87 1 222 112.50      3.00   293.0 6 1000.0 1000.0
87 1 223 135.00      3.00   293.0 6 1000.0 1000.0
87 1 224 157.50      3.00   293.0 6 1000.0 1000.0
```

This page intentionally left blank.

APPENDIX D

RADIONUCLIDE GROUNDWATER CONCENTRATION VERSUS TIME RESULTS FROM THE NUMERICAL RELEASE AND TRANSPORT ANALYSES--SUMMARY FIGURES AND TABLES

This page intentionally left blank.

APPENDIX D

RADIONUCLIDE GROUNDWATER CONCENTRATION VERSUS TIME RESULTS FROM THE NUMERICAL RELEASE AND TRANSPORT ANALYSES--SUMMARY FIGURES AND TABLES

Tables and figures are presented in this appendix from all groundwater pathway modeling runs completed with the VAM3D-CG computer code. Some of the figures and tables were presented in Chapter 4. These are also shown in this appendix for comparison with other runs. The figures and tables are organized in the order of the pathway analyses, beginning with the flow field and source term release estimates and finishing with the radionuclide concentration versus time relationships in groundwater. They are as follows:

1. Figures D-1 through D-7 present the degrees of saturation and velocity flow fields in the vadose and unconfined aquifer sediments for three infiltration conditions, 5.0 cm/yr, 0.5 cm/yr, and a differential infiltration condition of 3 cm/yr for the waste cover and 5 cm/yr for the surrounding soil.

2. Figures D-8 through D-16 present flux of radionuclides from the disposal facility (e.g., the source term) for advection and diffusion control release estimates.

3. Tables D-1 through D-17 summarize the key parameters in each run and the peak concentration and peak time values. The results can be applied to any radionuclide by defining the K_d appropriate to that radionuclide. The results are also generic in the sense that a unit quantity of a radionuclide is assumed to exist in the trench at time zero.

4. Figures D-17 through D-24 present example figures of radionuclide concentrations in the soil column and unconfined aquifer. For each run, a cross-section of the contaminant plume in the soil column underneath the trench near the time of maximum groundwater concentration is provided. Also, a plot of radionuclide concentration versus time at the 100 m downstream well is provided for each run.

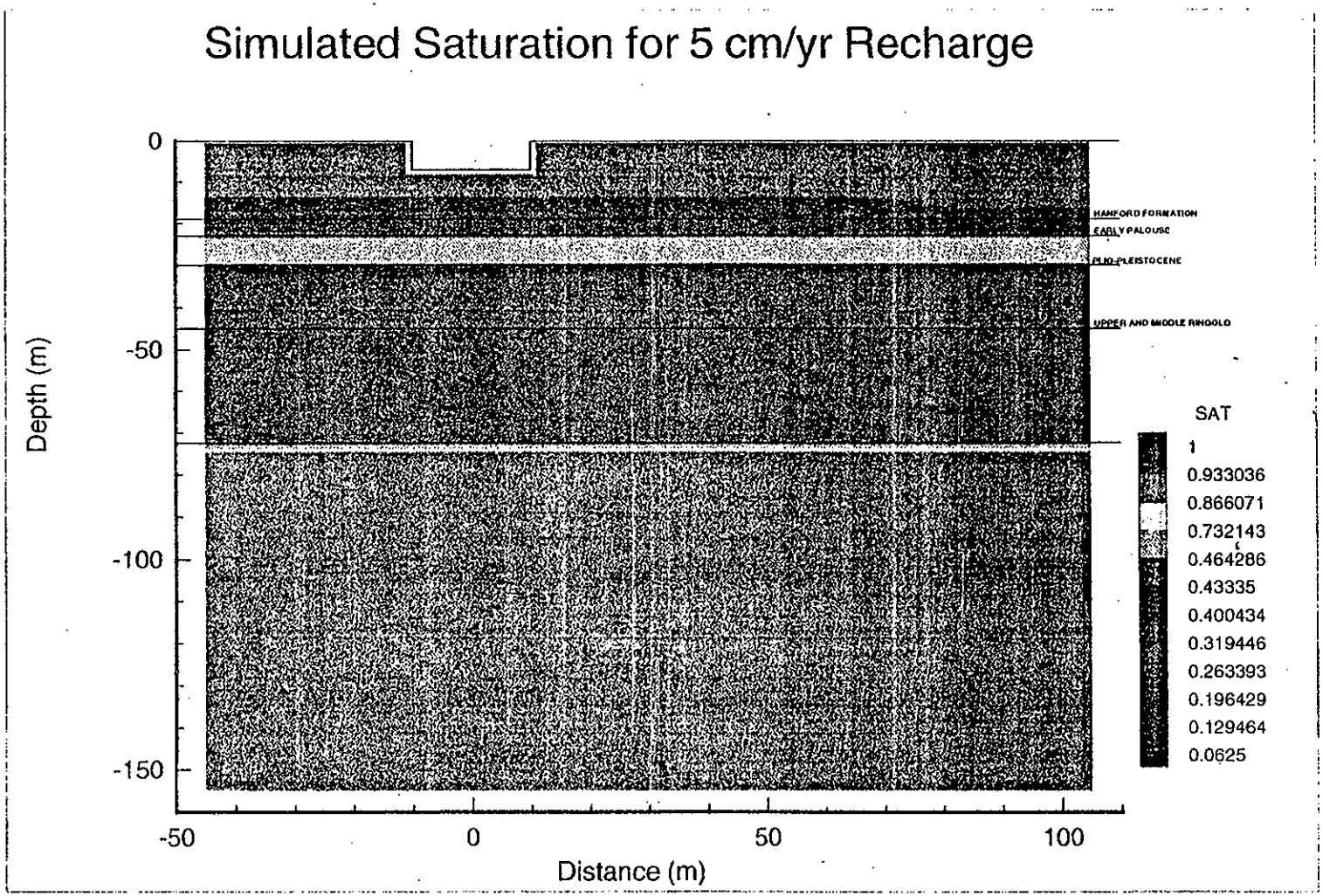

Figure D-1. Saturation Contours for 5-cm/yr Recharge.

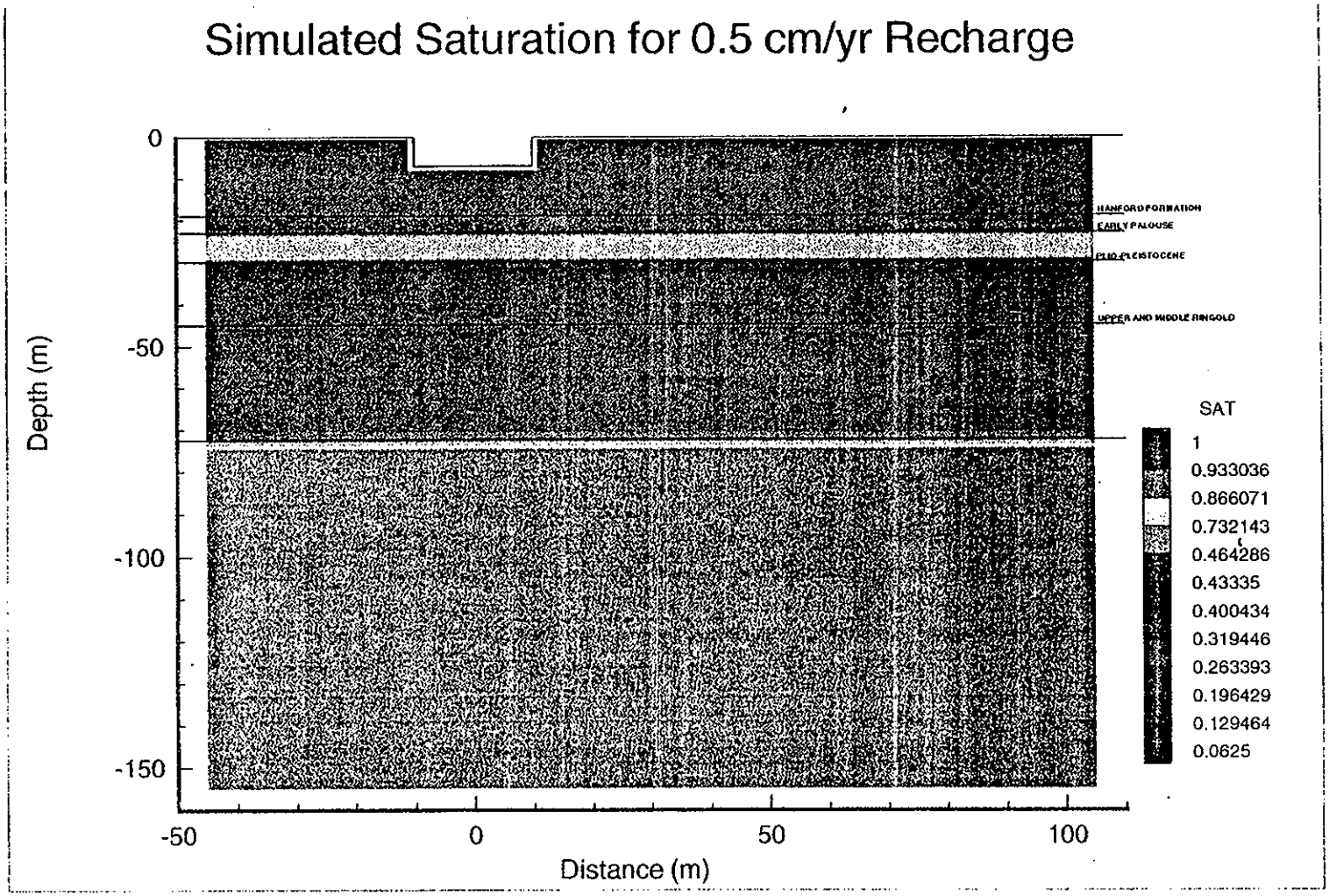

Figure D-2. Saturation Contours for 0.5-cm/yr Recharge.

Figure D-3. Velocity Plots for 5-cm/yr Recharge (Vadose Zone Blow-Up).

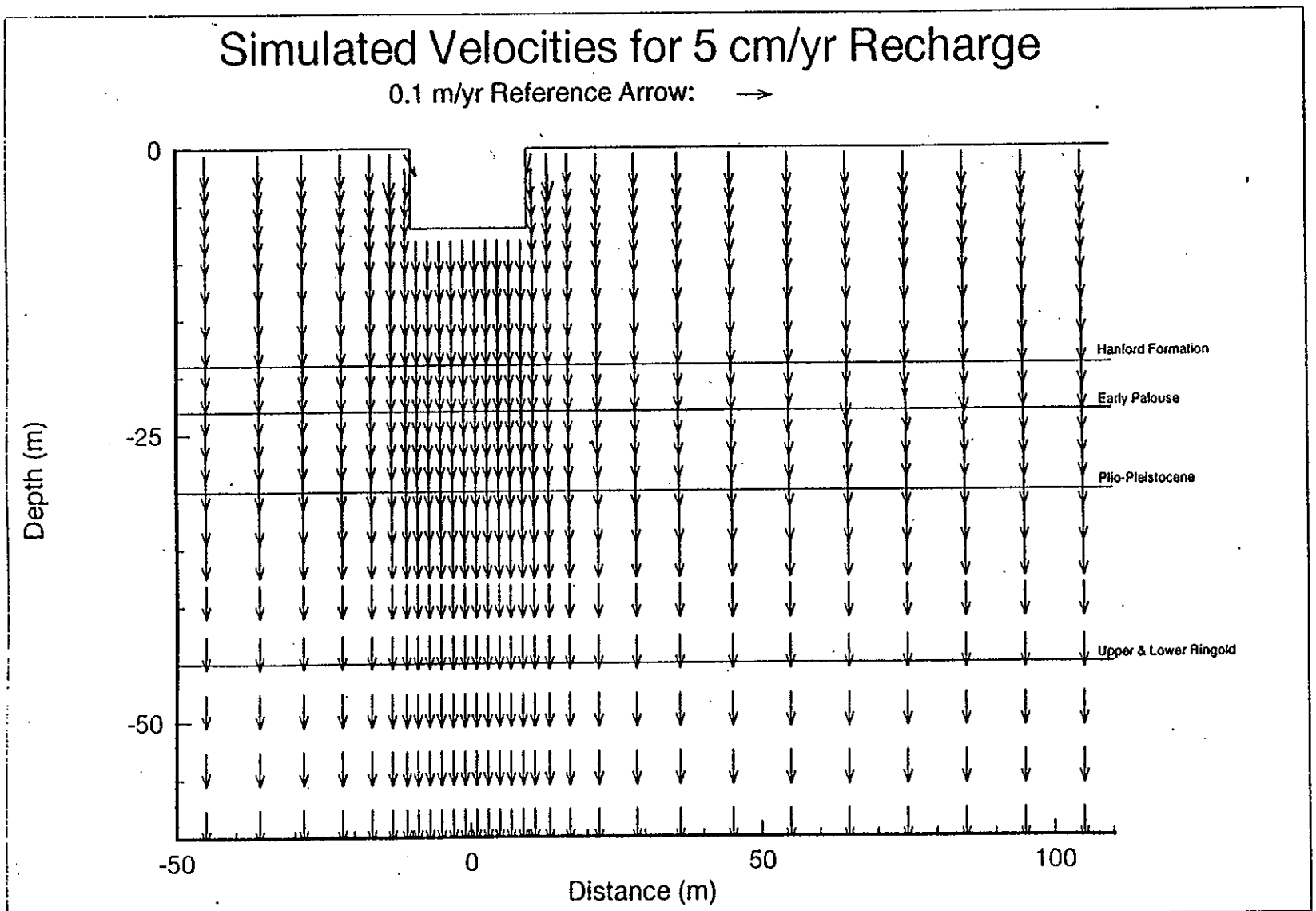

Figure D-4. Saturation Contours for 5- and 3-cm/yr Recharge.

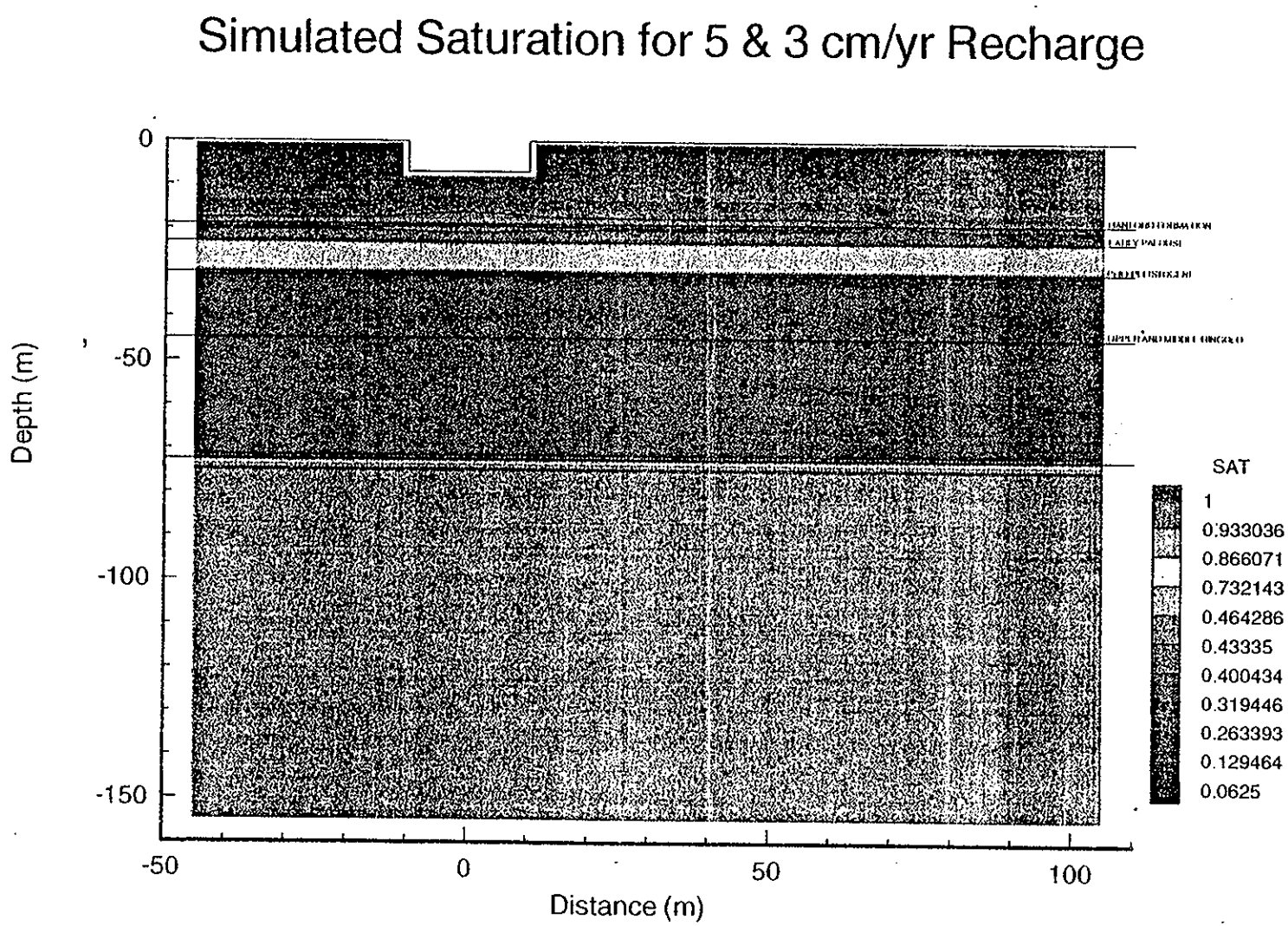

Figure D-5. Velocity Plots for 0.5-cm/yr Recharge (Vadose Zone Blow-Up).

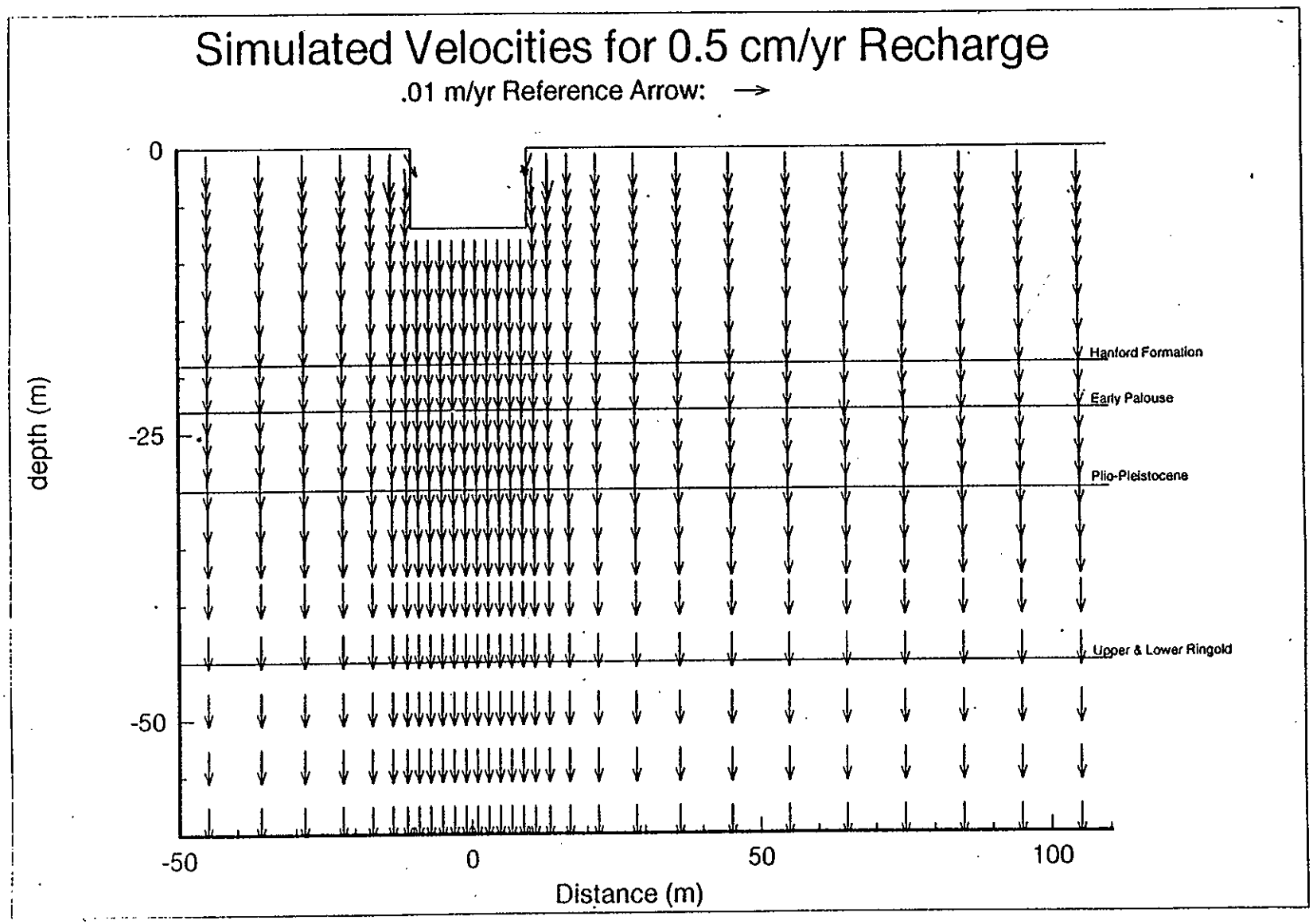

Figure D-6. Velocity Plots for 5- and 3-cm/yr Recharge (Vadose Zone Blow-Up).

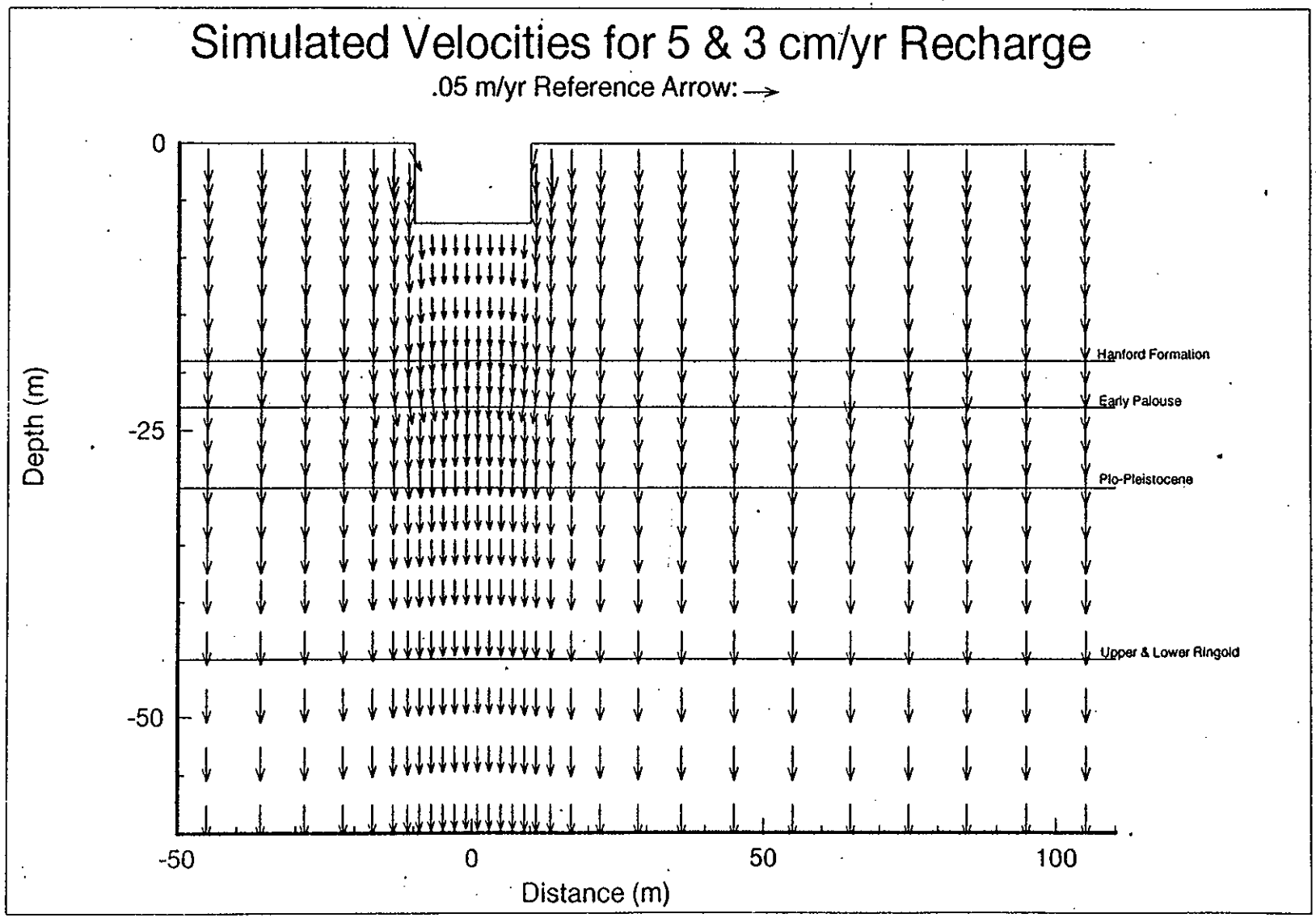

Figure D-7. Velocity Plots for 5-cm/yr Recharge (Full Simulation Field).

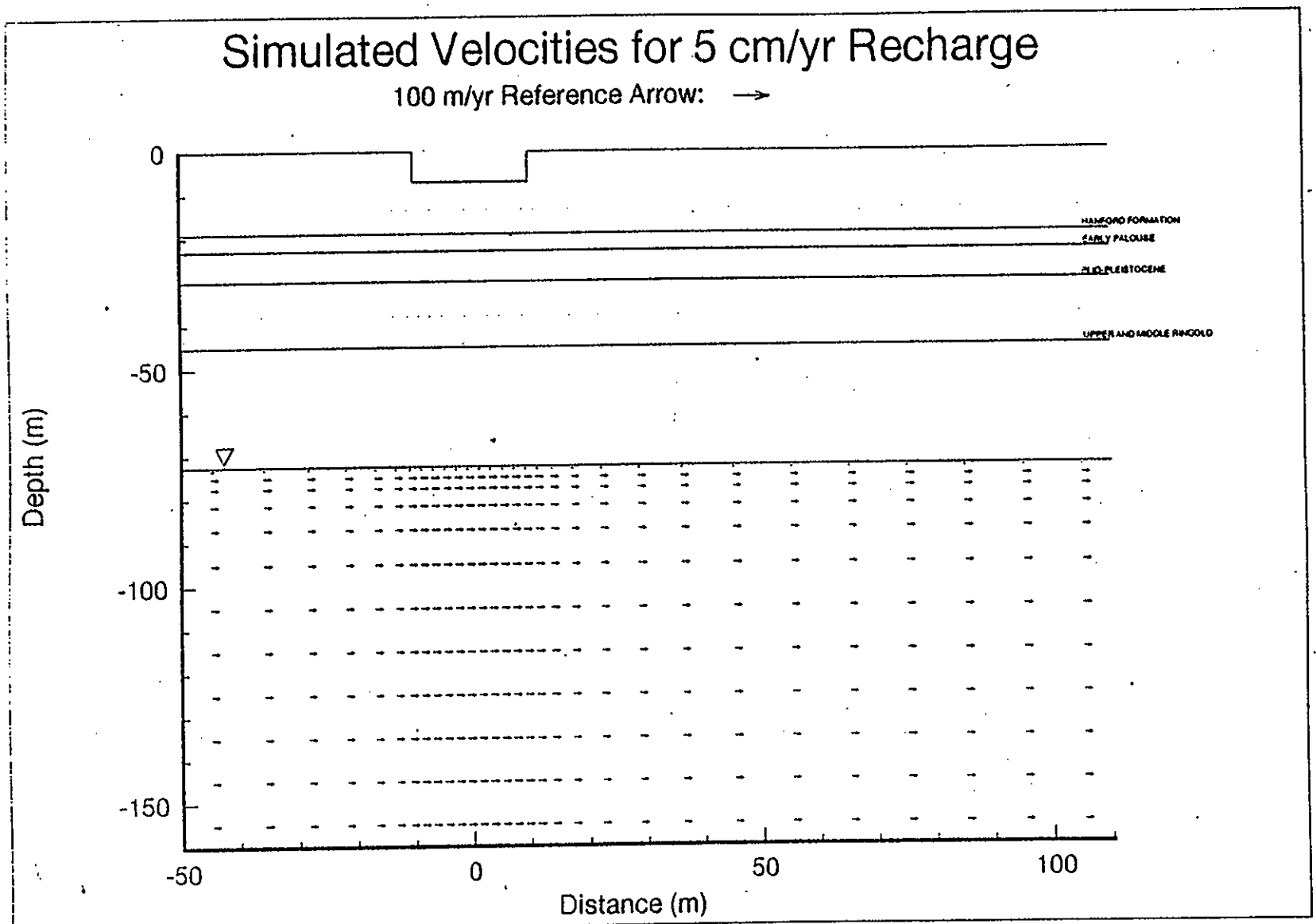

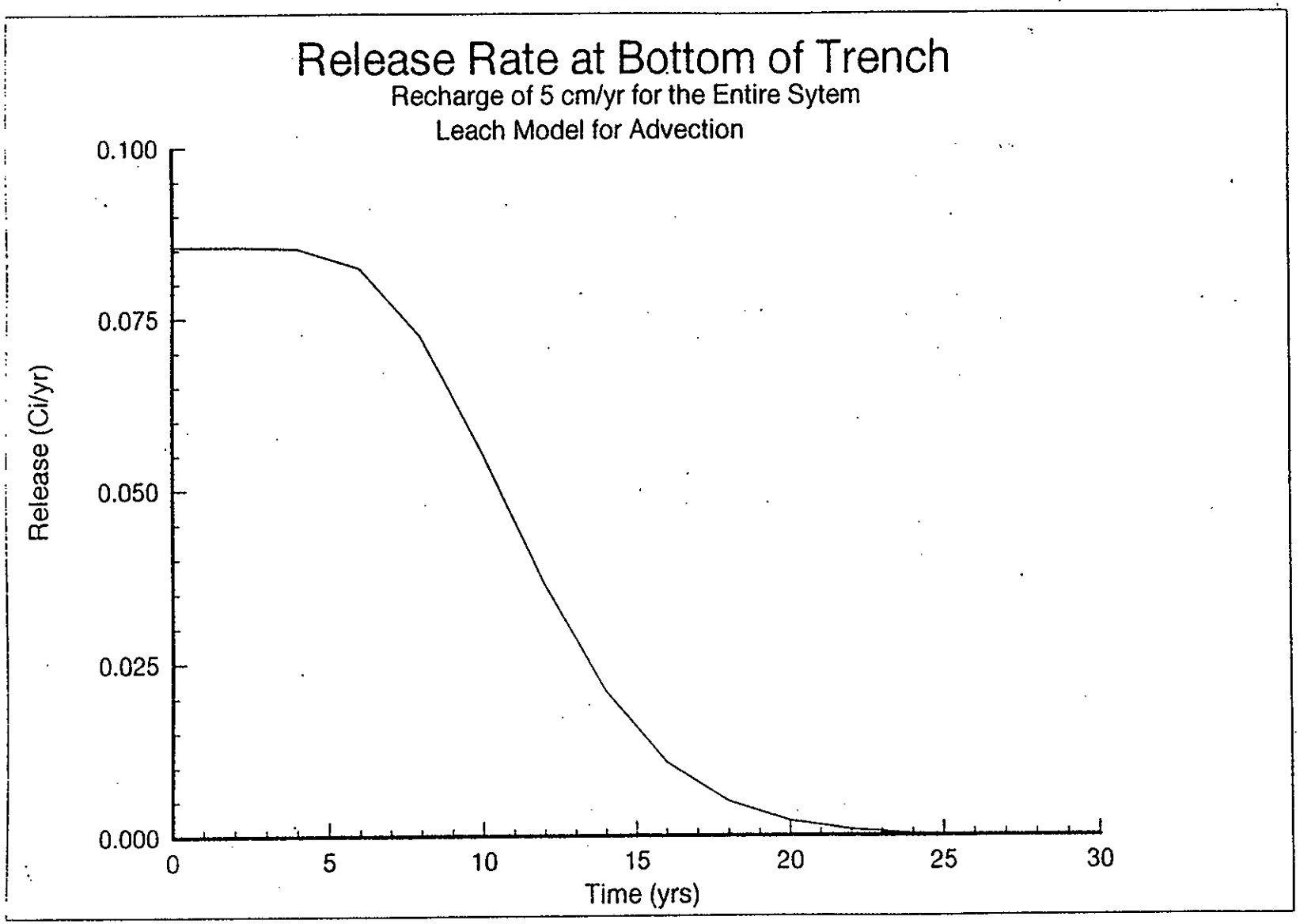

Figure D-8. Flux Release History, 5-cm/yr Recharge Advection Dominated.

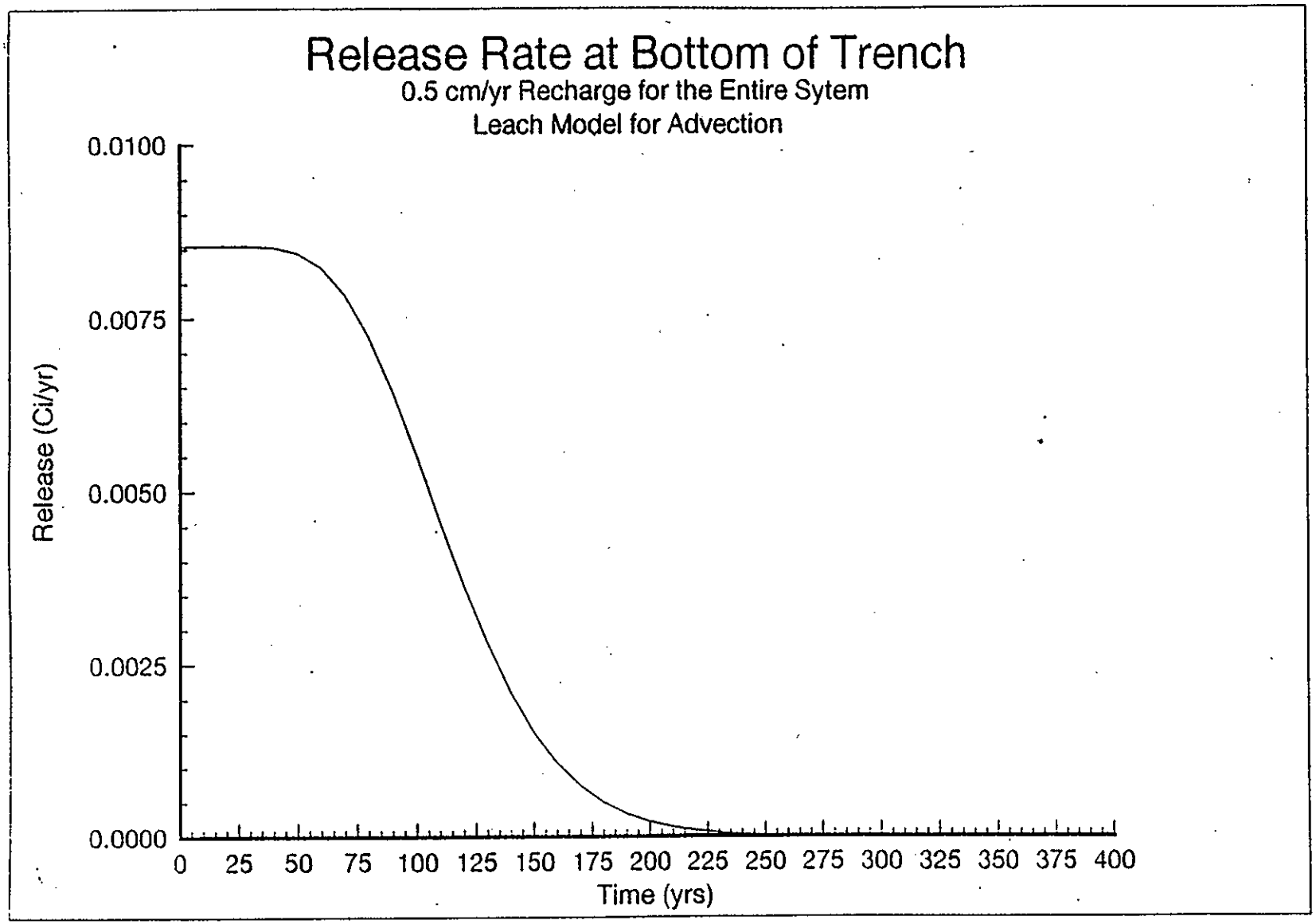

Figure D-9. Flux Release History, 0.5-cm/yr Recharge Advection Dominated.

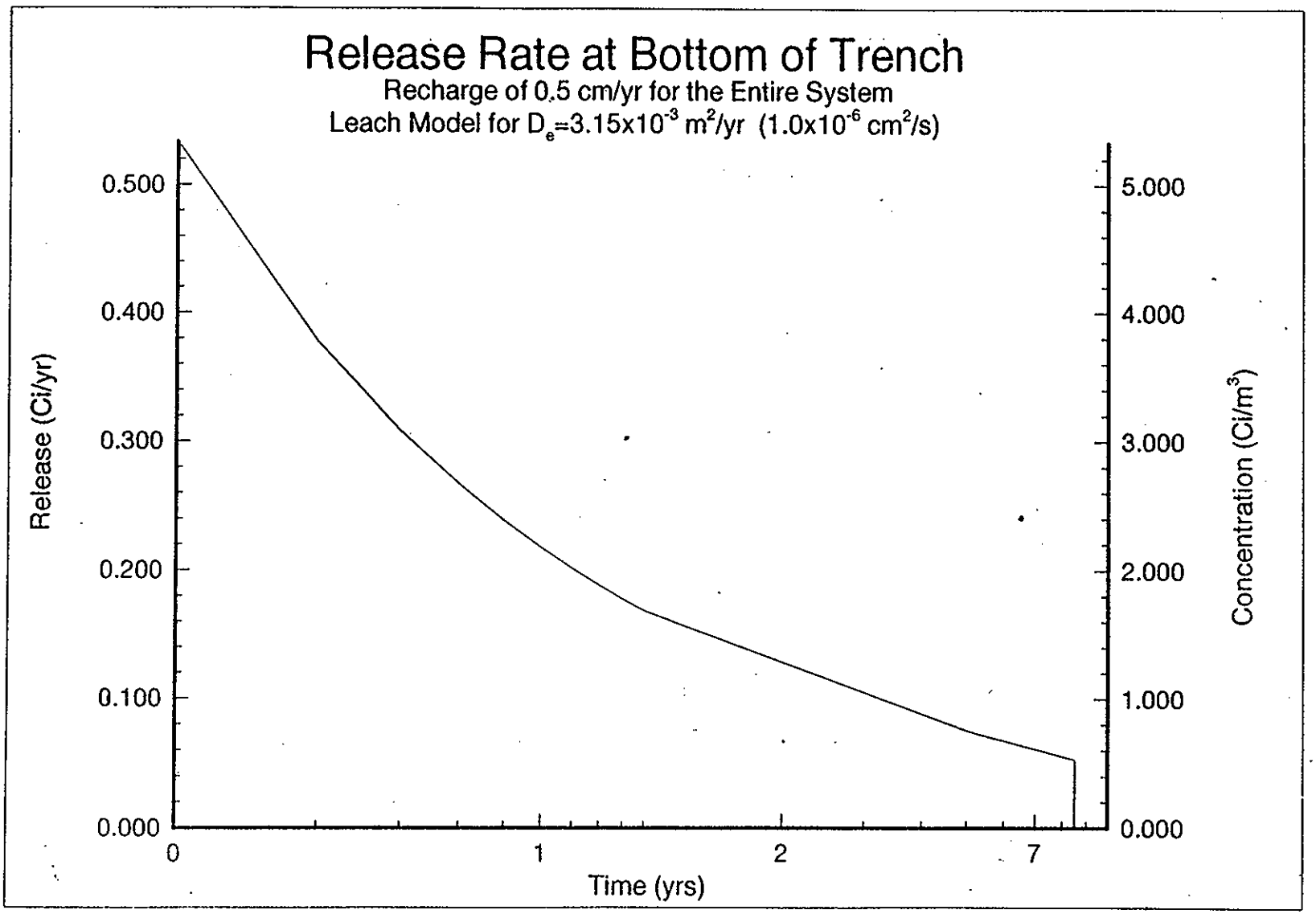

Figure D-10. Flux Release History, 0.5-cm/yr Recharge, Diffusion with D_e = 3.15 x 10^{-3} m^2/yr (1 x 10^{-6} cm^2/s).

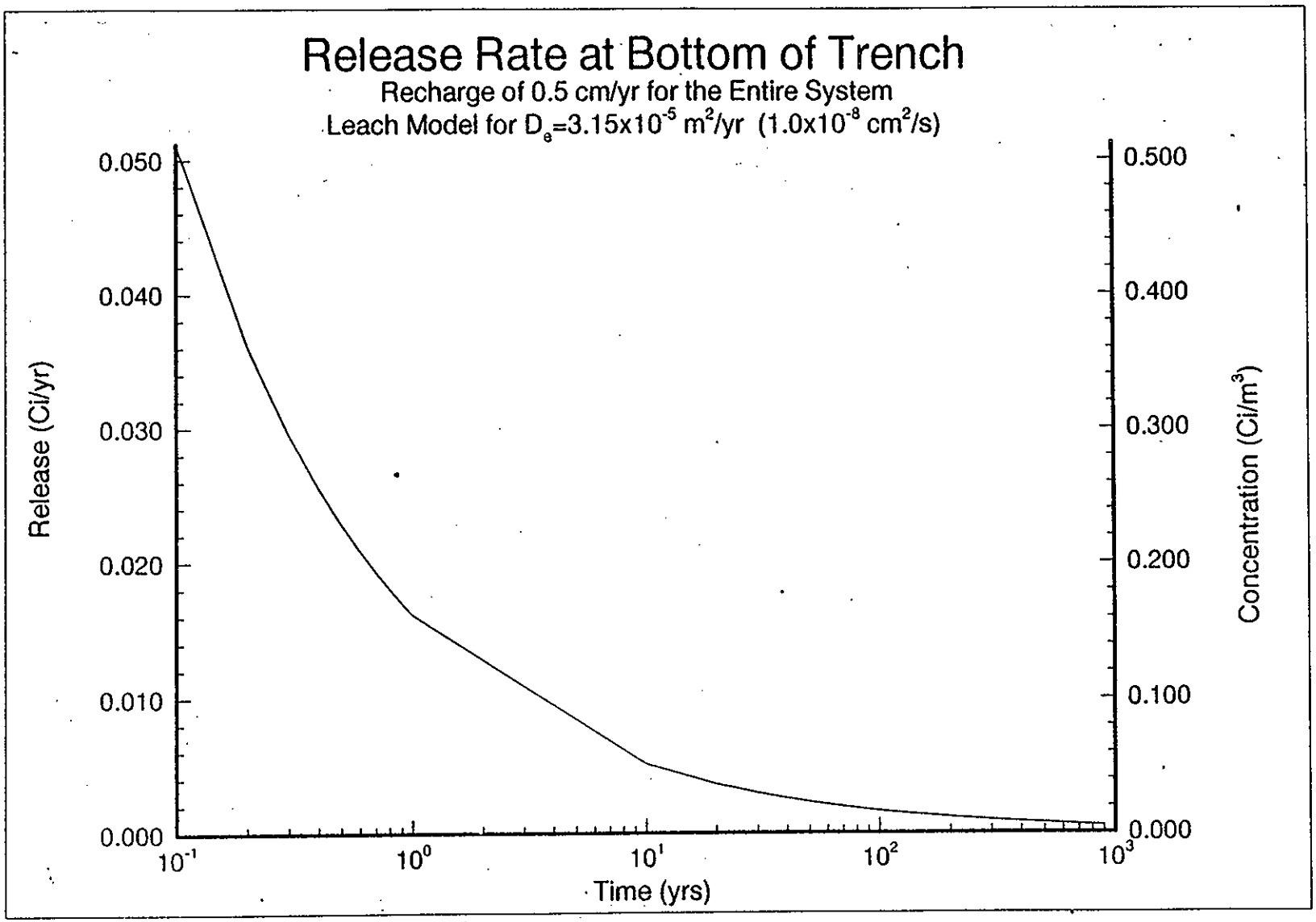

Figure D-11. Flux Release History, 0.5-cm/yr Recharge, Diffusion with D_e = 3.15 x 10^{-5} m^2/yr (1 x 10^{-8} cm^2/s).

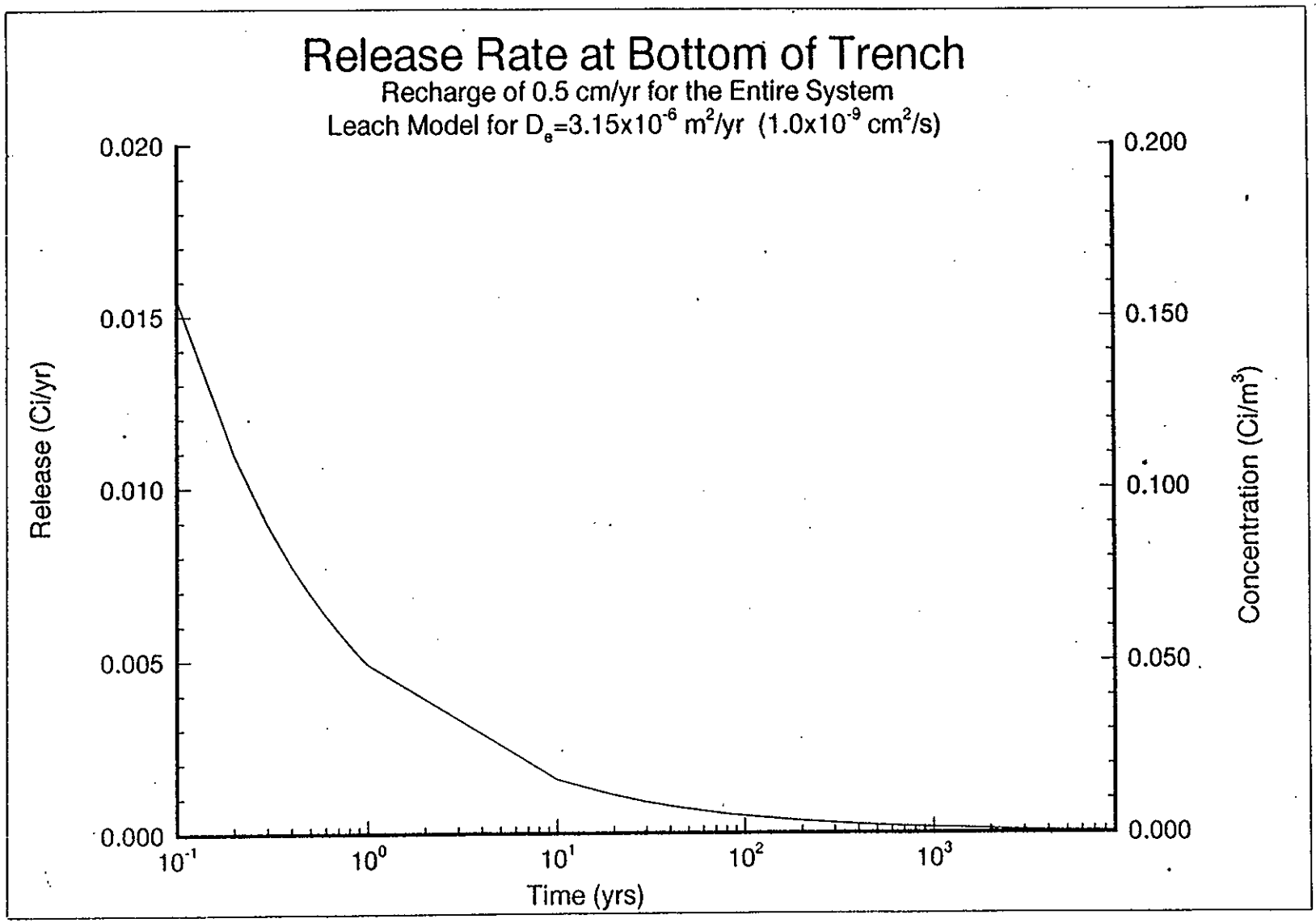

Figure D-12. Flux Release History, 0.5-cm/yr Recharge, Diffusion with D_e = 3.15 x 10^{-6} m^2/yr (1 x 10^{-9} cm^2/s).

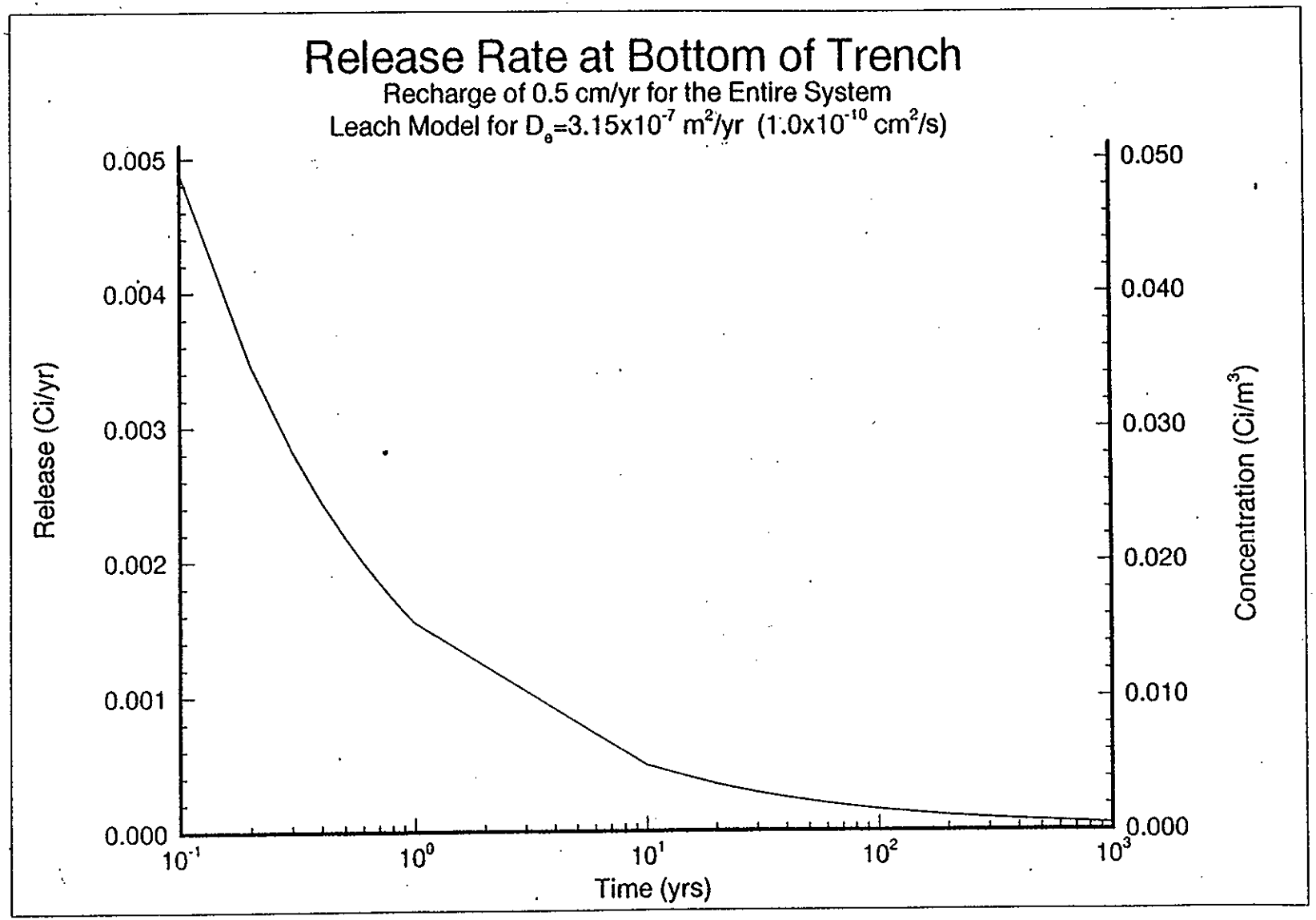

Figure D-13. Flux Release History, 0.5-cm/yr Recharge, Diffusion with D_e = 3.15 x 10^{-7} m^2/yr (1 x 10^{-10} cm^2/s).

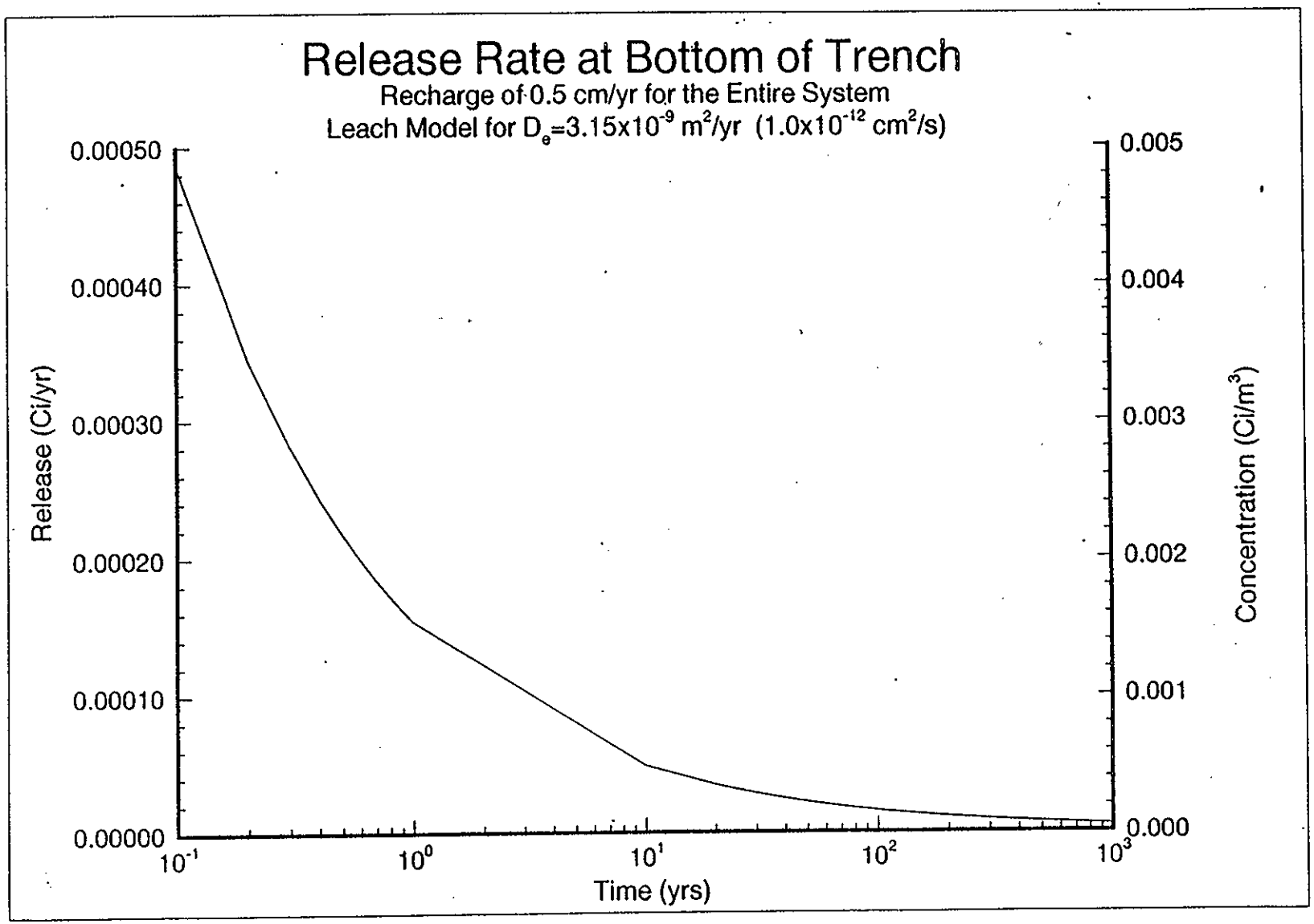

Figure D-14. Flux Release History, 0.5-cm/yr Recharge, Diffusion with D_e = 3.15 x 10^{-9} m^2/yr (1 x 10^{-12} cm^2/s).

Figure D-15. Plume Cross-Section for Cases 1a and 1b.

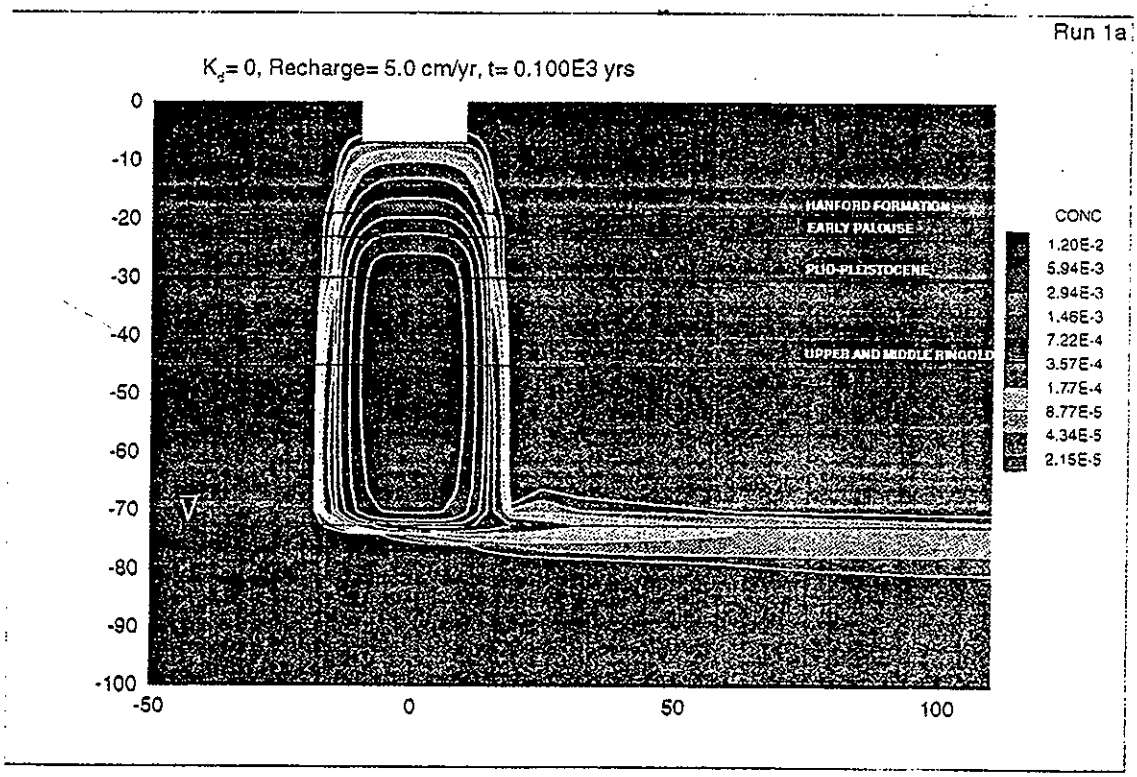

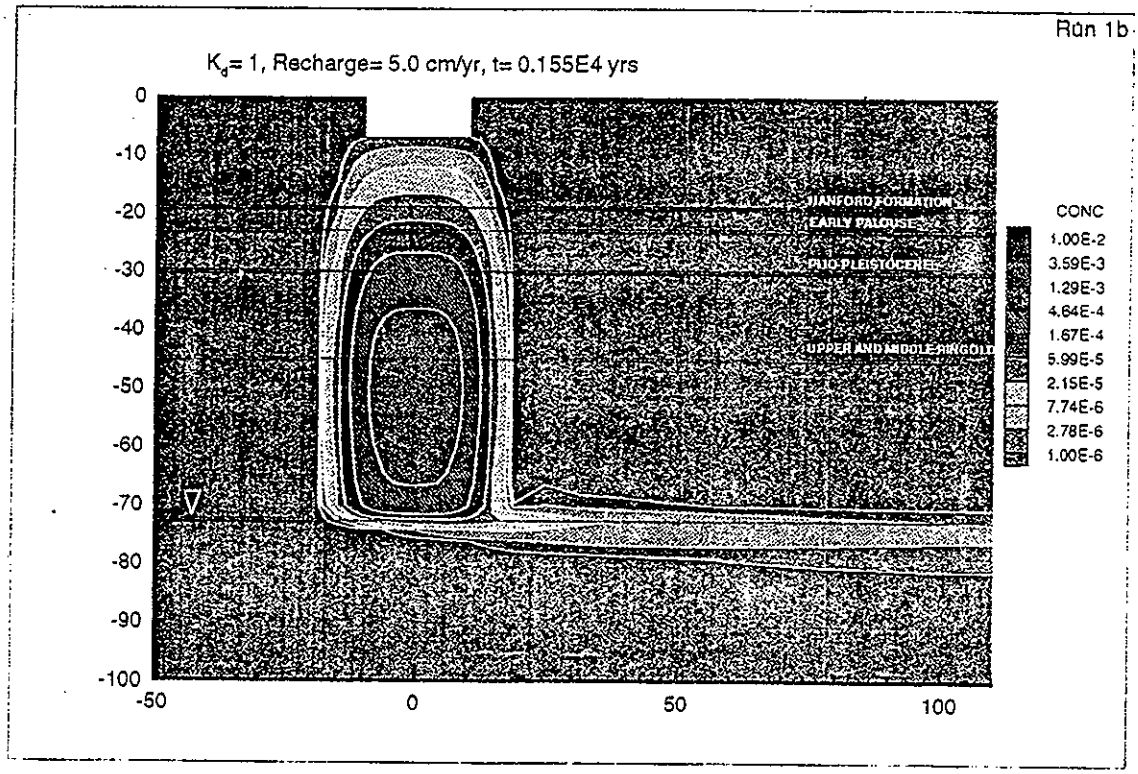

Figure D-16. Plume Cross-Section for Cases 1c and 1k.

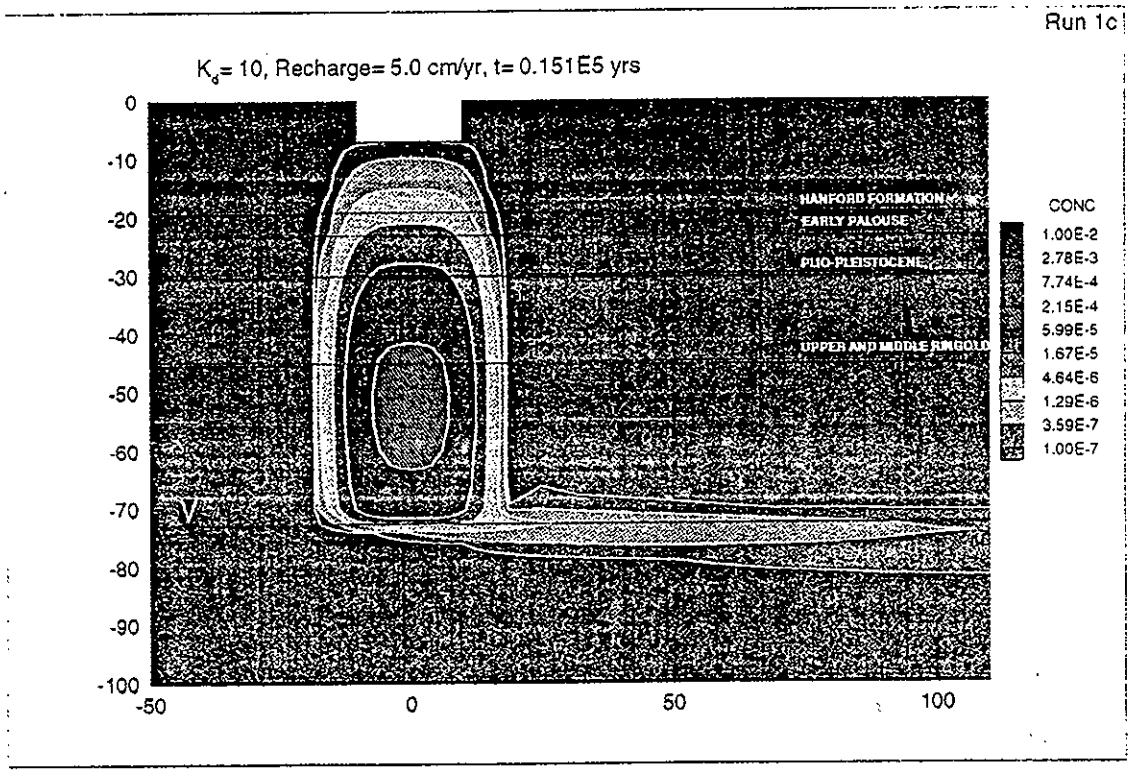

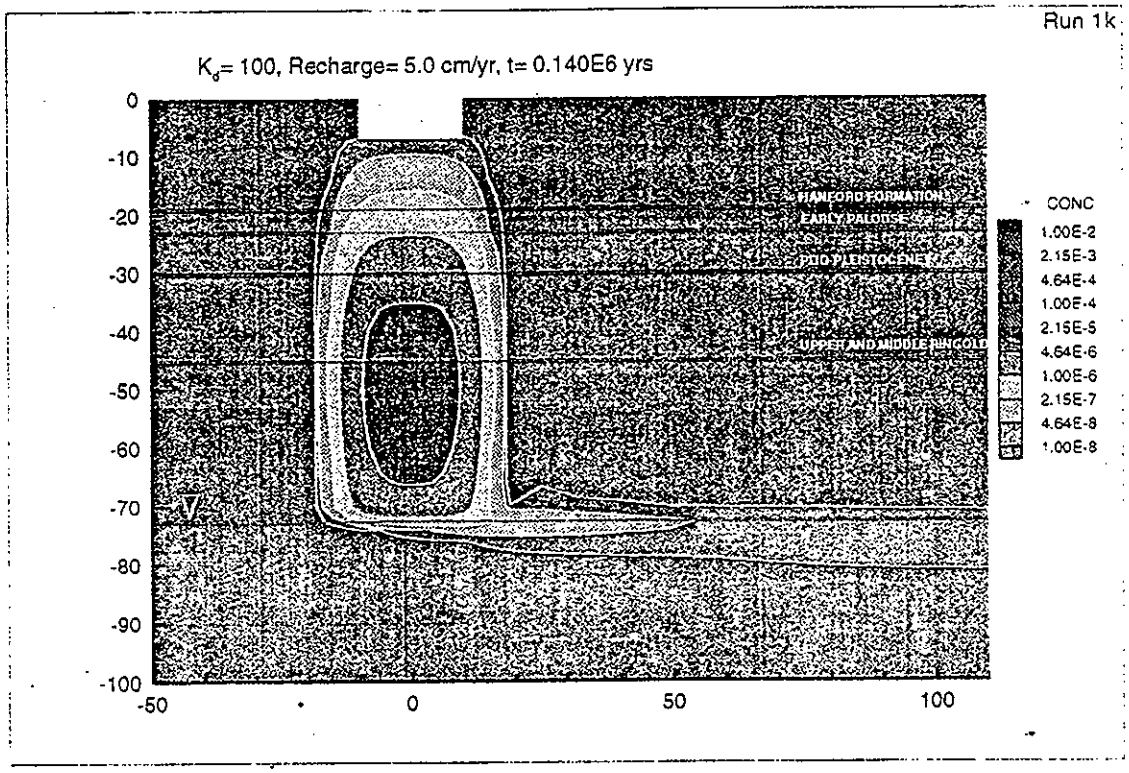

Table D-1. Case Parameter Listings. (2 sheets)

Run	Recharge	K_d	Type of release
1a	5.0 cm/yr	0	Advection
1b		1	
1c		10	
1k		100	
2a	0.5 cm/yr	0	
2b		1	
2c		10	
2k		100	
1d	5.0 cm/yr	0	Diffusion, De=1 x 10^{-6} cm^2/s
1e			
1f			
2d	0.5 cm/yr	0	
2e			
2f			
1g	5.0 cm/yr	0	Diffusion, De=1 x 10^{-8} cm^2/s
2g	0.5 cm/yr	0	
2h		1	
2i		10	

Table D-1. Case Parameter Listings. (2 sheets)

Run	Recharge	K_d	Type of release
1m	5.0 cm/yr	0	Diffusion, De=1 x 10^{-9} cm^2/s
1n	5.0 cm/yr	0	Diffusion, De=1 x 10^{-10} cm^2/s
1p	5.0 cm/yr	0	Diffusion, De=1 x 10^{-12} cm^2/s
1j	5.0 cm/yr	0	C/C_0 = 1
1l		10	
2j	0.5 cm/yr	0	
2l		10	
3j	5.0 and 3.0 cm/yr	0	
3l		10	

Table D-2. Results of the Advection-Dominated Release Model.

Run number	Inventory depletion period (yr)	Peak concentration (Ci/m^3)	Time to peak concentration (yr)
5.0 cm/yr recharge rate			
1a	25	7.96 E-5	123
1b	25	4.76 E-6	2,030
1c	25	5.01 E-7	19,350
1k	25	5.03 E-8	190,000
0.5 cm/yr recharge rate			
2a	250	1.04 E-5	995
2b	250	5.19 E-7	20,100
2c	250	5.41 E-8	190,300
2k	250	5.59 E-9	1,870,000

Table D-3. Results of The Diffusion-Dominated Release Model, with De = 3.15×10^{-3} m^2/yr (1×10^{-6} cm^2/s).

Run number	Inventory depletion period (yr)	Peak concentration (Ci/m^3)	Time to peak concentration (yr)
5.0 cm/yr recharge rate			
1d	8.5	6.56 E-5	125
0.5 cm/yr recharge rate			
2d	8.5	9.42 E-6	950

Table D-4. Results of The Diffusion-Dominated Release Model, with De = 3.15×10^{-5} m^2/yr (1×10^{-8} cm^2/s).

Run number	Inventory depletion period (yr)	Peak concentration (Ci/m^3)	Time to peak concentration (yr)
5.0 cm/yr recharge rate			
1g	1,560	5.18 E-6	1,476
0.5 cm/yr recharge rate			
2g	900	6.69 E-6	1,250
2h	900	4.1 E-7	21,500
2i	900	4.25 E-8	205,000

Table D-5. Results of The Diffusion Dominated Release Model, with $De=10^{-9}$, 10^{-10}, 10^{-12} cm^2/s.

Run number	Inventory depletion period (yr)	Peak concentration (Ci/m^3)	Time to peak concentration (yr)
$D_e=10^{-9}$ cm^2/s			
1m	1.0 E+4	5.1 E-6	150
2m	1.0 E+4	2.04 E-6	1,250
$D_e=10^{-10}$ cm^2/s			
1n	1.0 E+5	1.6 E-6	150
2n	1.0 E+5	6.43 E-7	1,250
$D_e=10^{-12}$ cm^2/s			
1p	1.0 E+5	1.6 E-7	150
2p	9.0 E+6	6.41 E-8	1,250

Table D-6. Results of $C/C_0 = 1$ Cases.

Run number	Recharge (cm/yr)	K_d	95% of maximum concentration	
			Year	Concentration (Ci/m^3)
1j	5.0	0	207	7.60 E-03
1l	5.0	10	32,795	7.59 E-03
2j	0.5	0	2106	8.26 E-04
2l	0.5	10	366,400	8.27 E-04
3j	5.0 and 3.0	0	273	4.95 E-03
3l	5.0 and 3.0	10	43,781	4.95 E-03

Table D-7. Estimate of Dilution Factors.

Run	Recharge (cm/yr)	K_d	Peak concentration (Ci/m^3) at vadose zone aquifer boundary	Peak concentration (Ci/m^3) at the downstream well	Dilution factor
1a	5.0	0	7.94 E-3	7.96 E-5	.01
2a	0.5	0	9.18 E-3	1.04 E-5	.001

Table D-8. Sensitivity Case Parameter Listings.

Run	Recharge (cm/yr)	K_d	Type of release	Remark
1a-1	5.0	0	Advection	Trench Width = 40m
1a-2				Trench Width = 60m
1b-1		1		Trench Width = 40m
1b-2				Trench width = 60m
4a	5	0	Advection	Hot spot release
4a-1	0.5			
5a	5 and 0.05	0	Advection	Low permeable cover
6a	0.5 and 0.05	0		
6j	0.5 and 0.05	0	Advection	$C/C_0 = 1$
7a	5	1	Advection	All $K_{sat} \times 10$
7c		10		
8a	0.5	0		
8c		10		
9a	5			Hydrau. grad. -30% pro-Hanford proj.
10a	0.5			
11a	5	0	Advection	Pumping
12a	0.5			
13a	5	0	Advection	Gravel for Hanford formation
14a	0.5			
15a			Advection	Clastic dikes
16a	0.5			

Table D-9. Varying Trench Size, Advection-Dominated Release.

Run number	Inventory depletion period (yr)	Peak concentration (Ci/m^3)	Time to peak concentration (yr)
5.0-cm/yr recharge, trench width = 40 m, 60 m; K_d = 0			
1a-1	25	7.54 E-5	124
1a-2	25	7.25 E-5	124
5.0-cm/yr recharge, trench width = 40 m, 60 m; K_d = 1			
1b-1	25	4.59 E-6	2,045
1b-2	25	4.35 E-6	2,025

Table D-10. Hot Spot, Advection-Dominated Release.

Run number	Inventory depletion period (yr)	Peak concentration (Ci/m^3)	Time to peak concentration (yr)
5.0-cm/yr recharge, K_d = 0			
4a	25	7.76 E-5	127
0.5-cm/yr recharge, K_d = 0			
4a-1	250	1.01 E-5	1,030

Table D-11. Low Cover Permeability = 0.05 cm/yr, Advection-Dominated Release.

Run number	Inventory depletion period (yr)	Peak concentration (Ci/m^3)	Time to peak concentration (yr)
5.0-cm/yr recharge, K_d = 0			
5a	2,400	6.58 E-6	376
0.5-cm/yr recharge, K_d = 0			
6a	2,400	6.09 E-6	1,405

Table D-12. Low Cover Permeability = 0.05 cm/yr, C/C_o = 1.

Run number	Inventory depletion period (yr)	Peak concentration (Ci/m^3)	Time to peak concentration (yr)
0.5-cm/yr recharge, K_d = 0			
6j	2,400	2.71 E-4	2,762

Table D-13. Advection-Dominated Release, K_{sat} = 10X.

Run number	Inventory depletion period (yr)	Peak concentration (Ci/m^3)	Time to peak concentration (yr)
5.0-cm/yr recharge, K_d = 0, 10			
7a	25	1.04 E-5	100
7c	25	5.46 E-8	18,850
0.5 cm/yr Recharge, K_d = 0, 10			
8a	250	1.21 E-6	850
8c	250	5.48 E-9	189,300

Table D-14. 30% Decrease in Hydraulic Gradient, Advection-Dominated Release.

Run number	Inventory depletion period (yr)	Peak concentration (Ci/m^3)	Time to peak concentration (yr)
5.0-cm/yr recharge, K_d = 0			
9a	25	1.08 E-4	125
0.5-cm/yr recharge, K_d = 0			
10a	250	1.46 E-5	990

Table D-15. Pumping, Advection-Dominated Release.

Run number	Inventory depletion period (yr)	Peak concentration (Ci/m^3)	Time to peak concentration (yr)
5.0-cm/yr recharge, K_d = 0			
11a	25	1.02 E-5	122
0.5-cm/yr recharge, K_d = 0			
12a	250	1.25 E-6	990

Table D-16. Saturated Hydraulic Conductivity Increase (10X), Advection-Dominated Release.

Run number	Inventory depletion period (yr)	Peak concentration (Ci/m^3)	Time to peak concentration (yr)
5.0-cm/yr recharge, K_d = 0			
13a	25	8.99 E-5	103
0.5-cm/yr recharge, K_d = 0			
14a	250	1.16 E-5	830

Table D-17. Clastic Dikes, High Permeability, Advection-Dominated.

Run number	Inventory depletion period (yr)	Peak concentration (Ci/m^3)	Time to peak concentration (yr)
5.0-cm/yr recharge, K_d = 0			
15a	25	8.87 E-5	103
0.5-cm/yr recharge, K_d = 0			
16a	250	1.08 E-5	880

Figure D-17. Plume Cross-Section for Cases 2a and 2b.

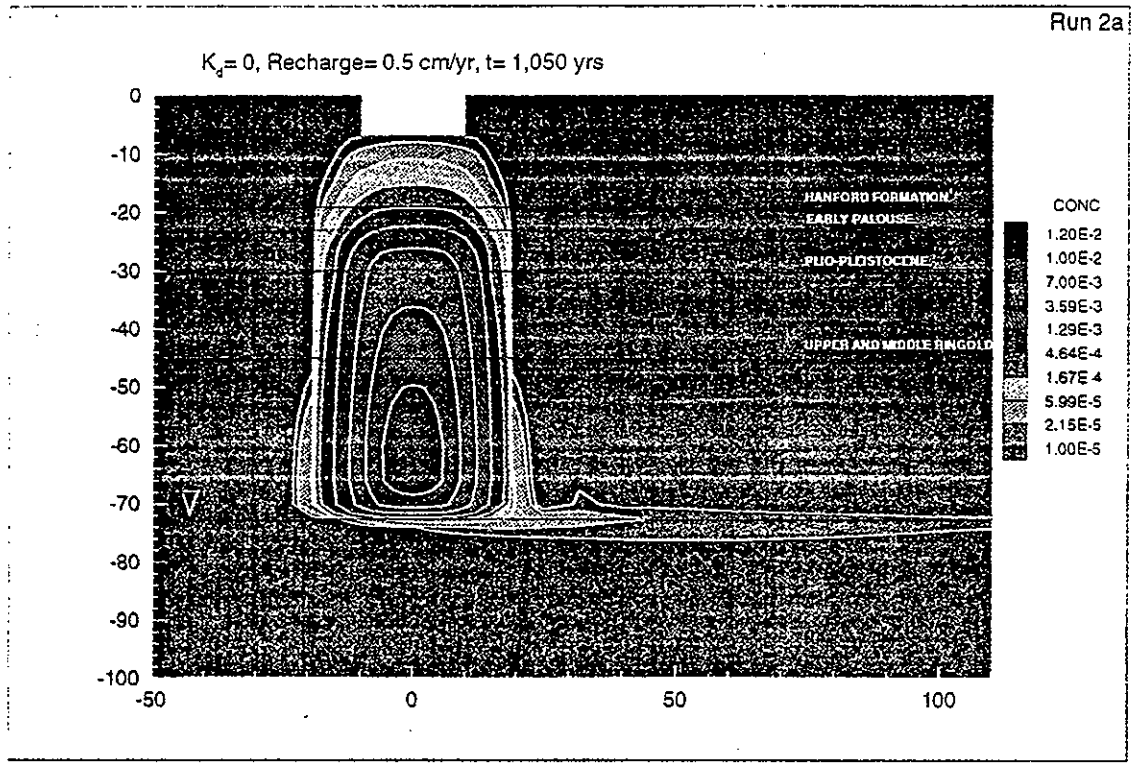

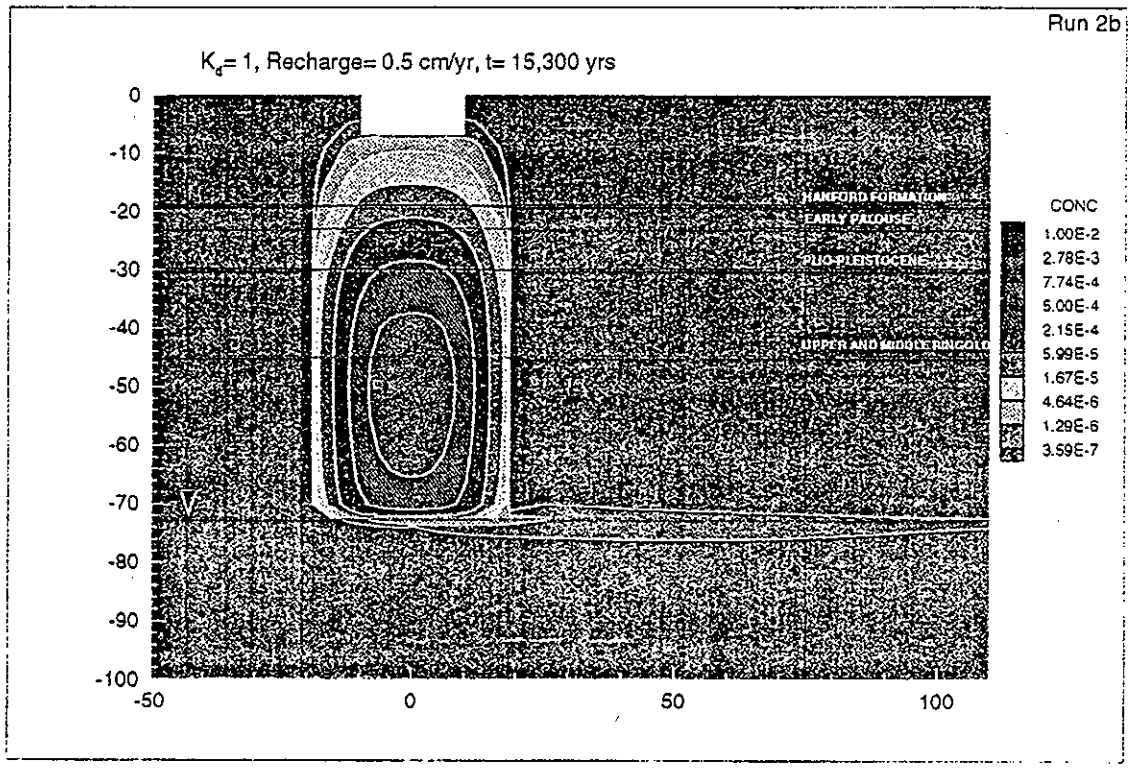

Figure D-18. Radionuclide Concentration Versus Time at the 100-m Downstream Well for Cases 1a, 1b, 1c, and 1k.

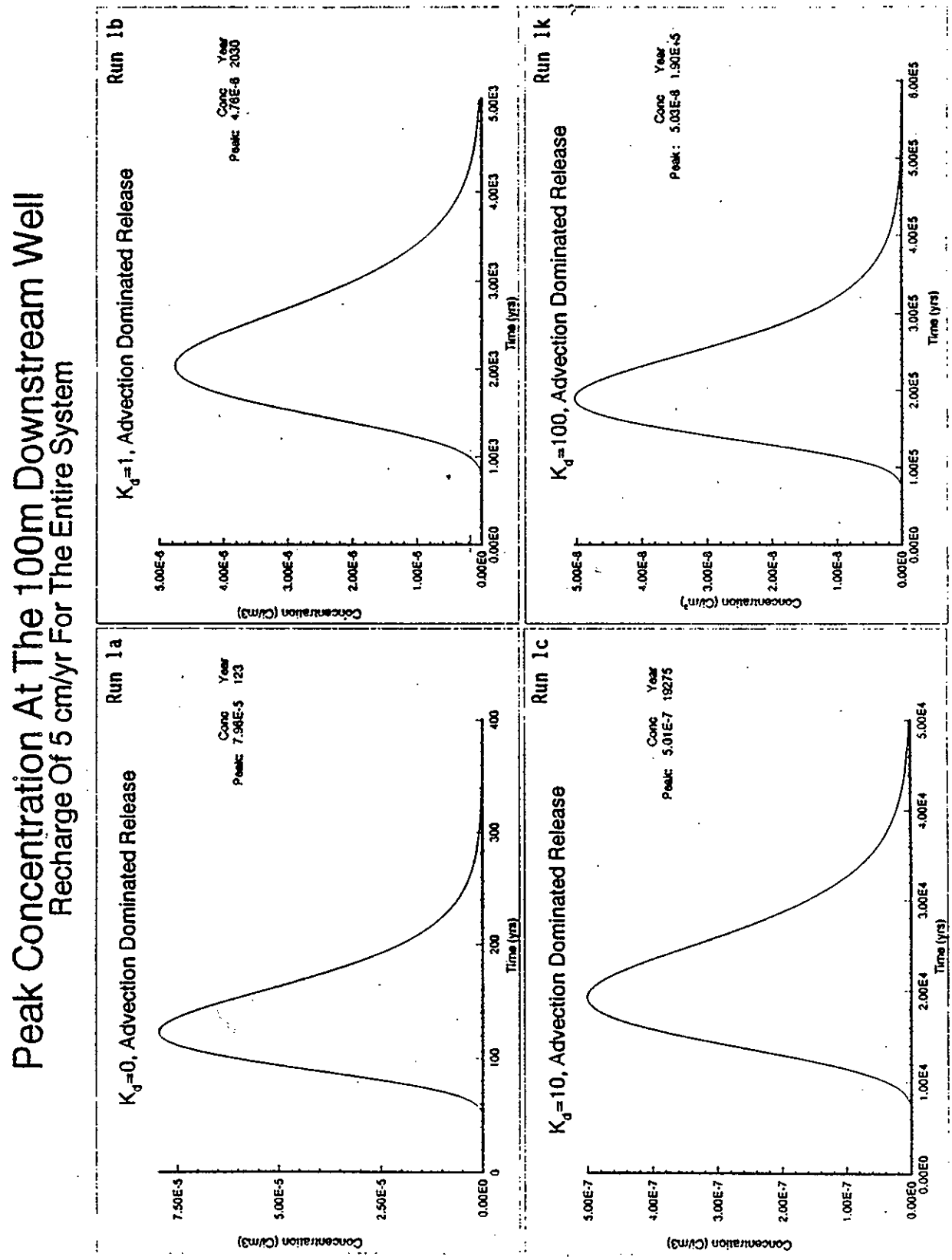

Figure D-19. Plume Cross-Section for Cases 2c and 2k.

Concentration Reaching Aquifer

0.5 cm/yr Recharge with varying K_d

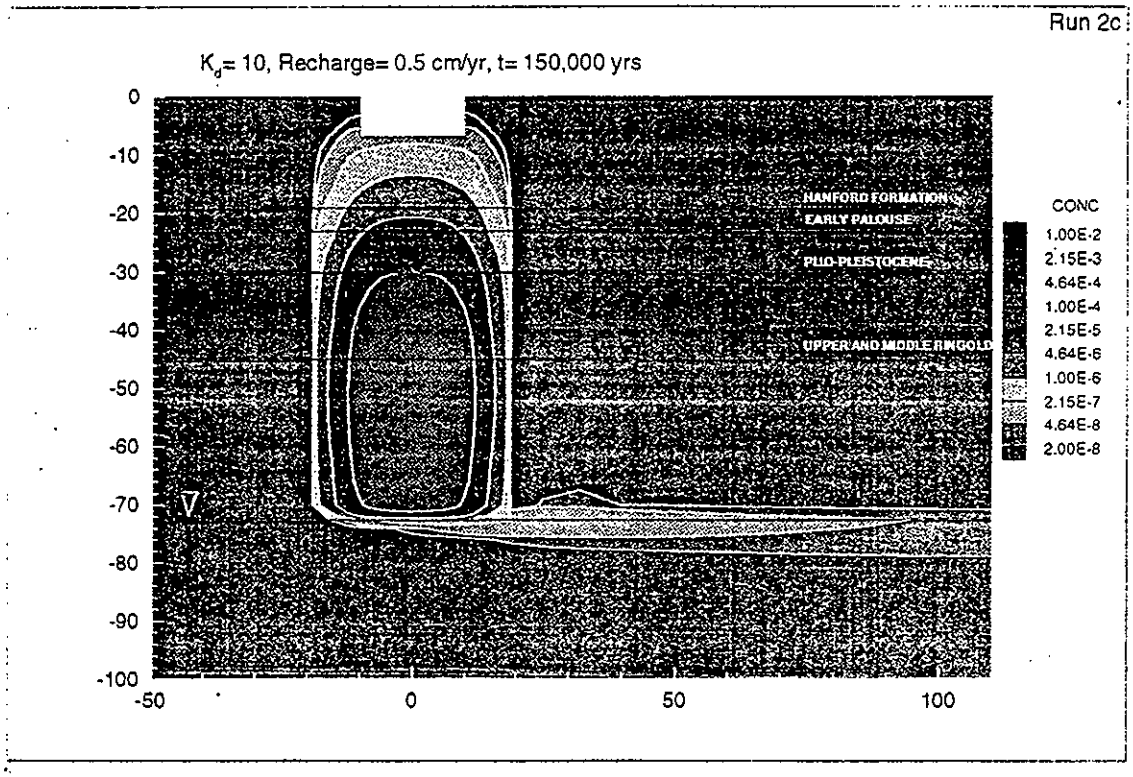

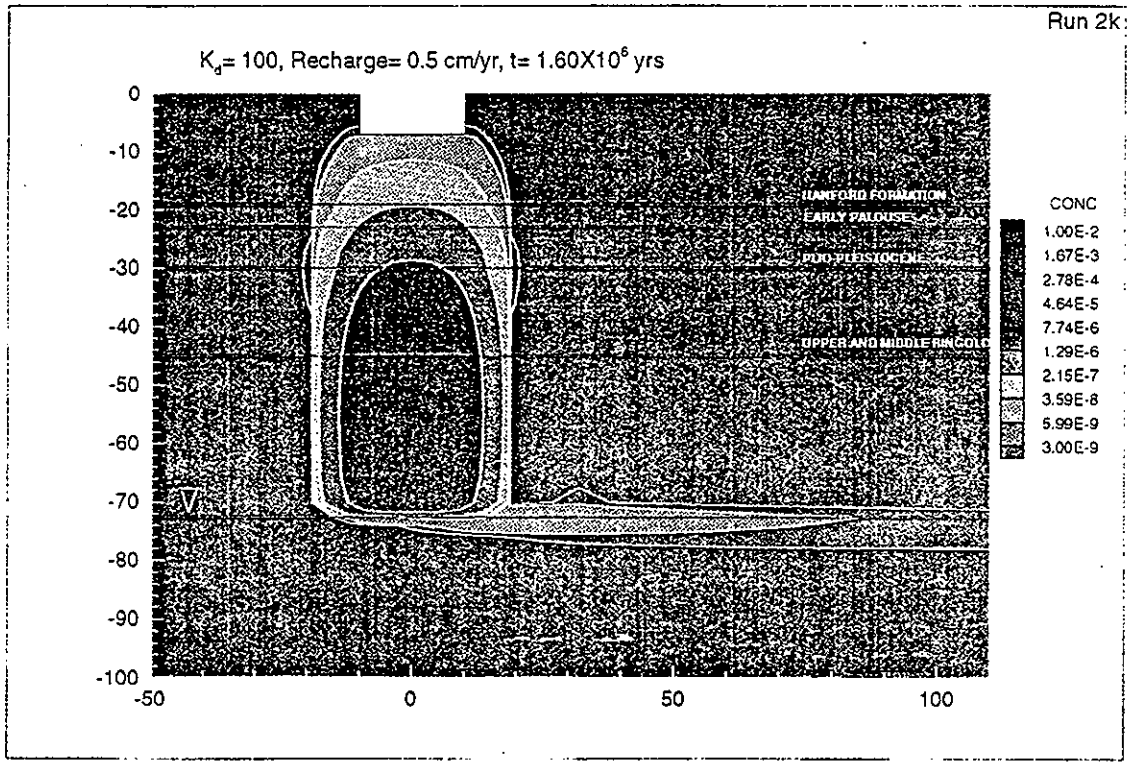

Peak Concentration At The 100m Downstream Well

Recharge Of 0.5 cm/yr For The Entire System

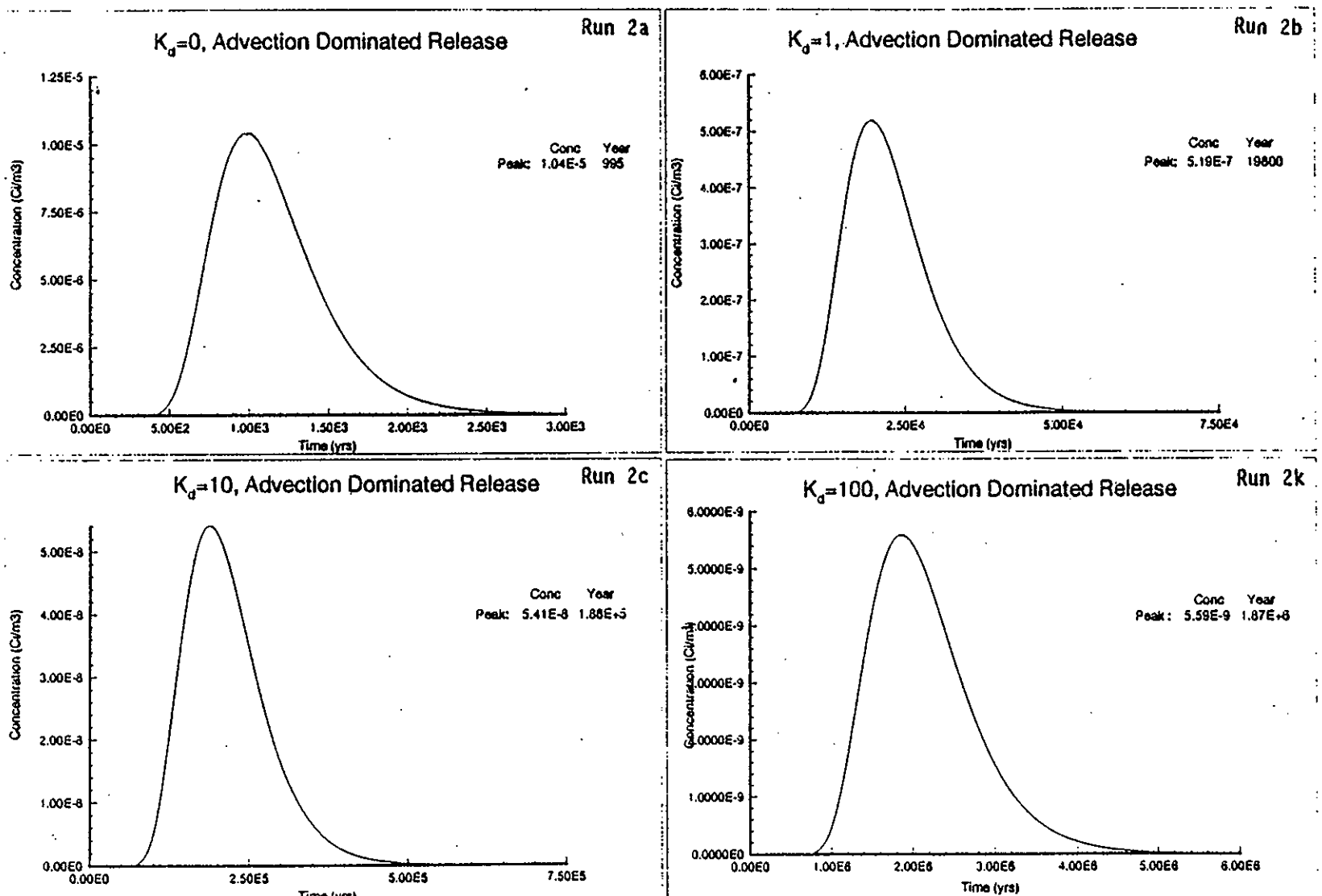

Figure D-20. Radionuclide Concentration Versus Time at the 100-m Downstream Well for Cases 2a, 2b, 2c, and 2k.

Figure D-21. Plume Cross-Section for Cases 1j and 1l.

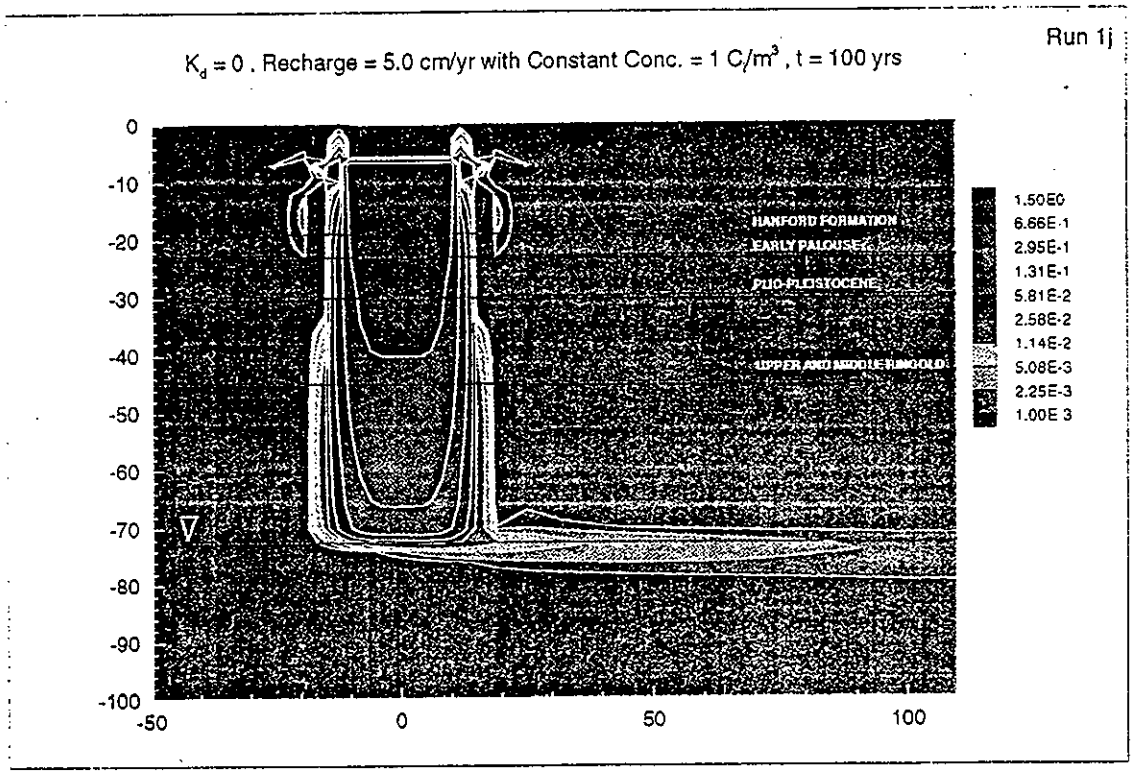

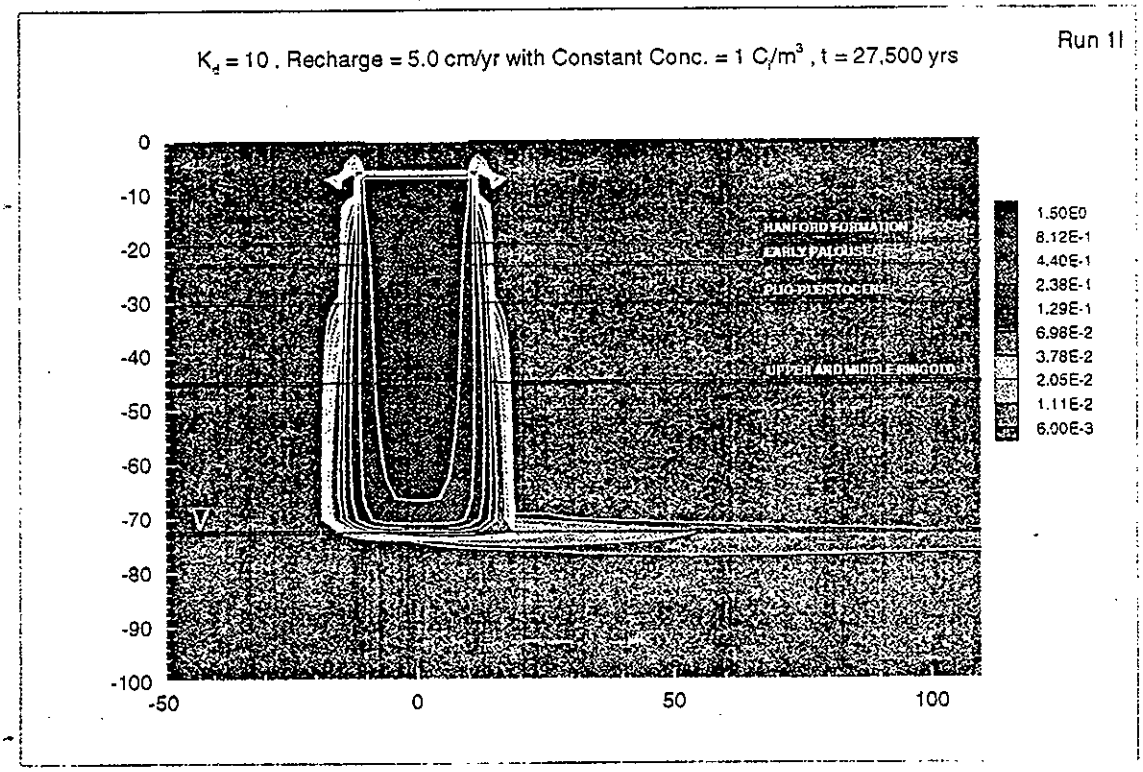

Figure D-22. Radionuclide Concentration Versus Time at the 100-m Downstream Well for Cases 1j and 1l.

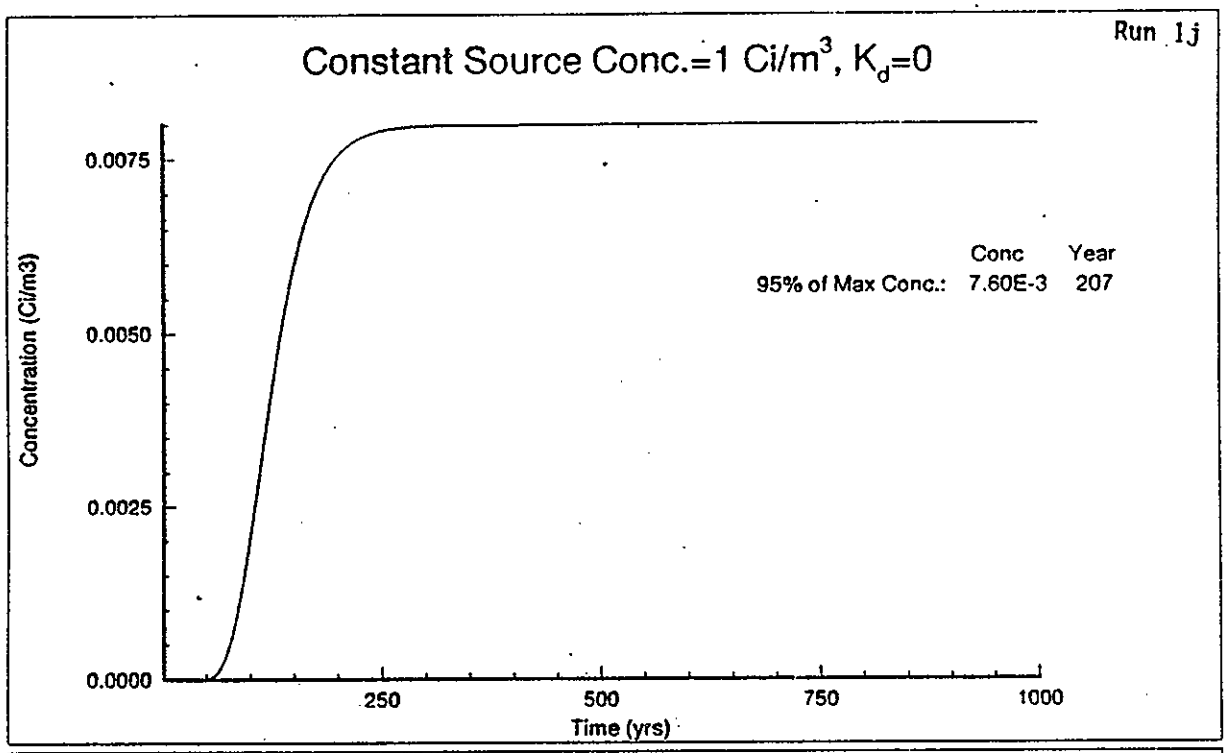

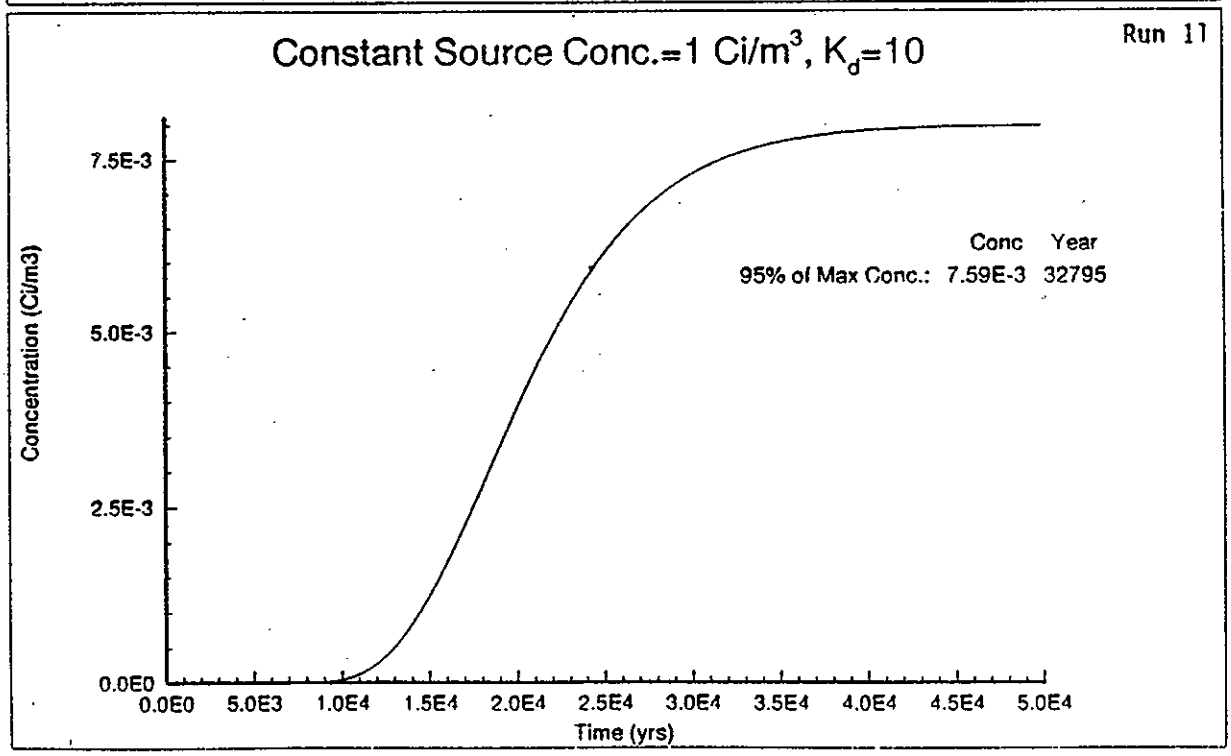

Figure D-23. Plume Cross-Section for Cases 2j and 2l.

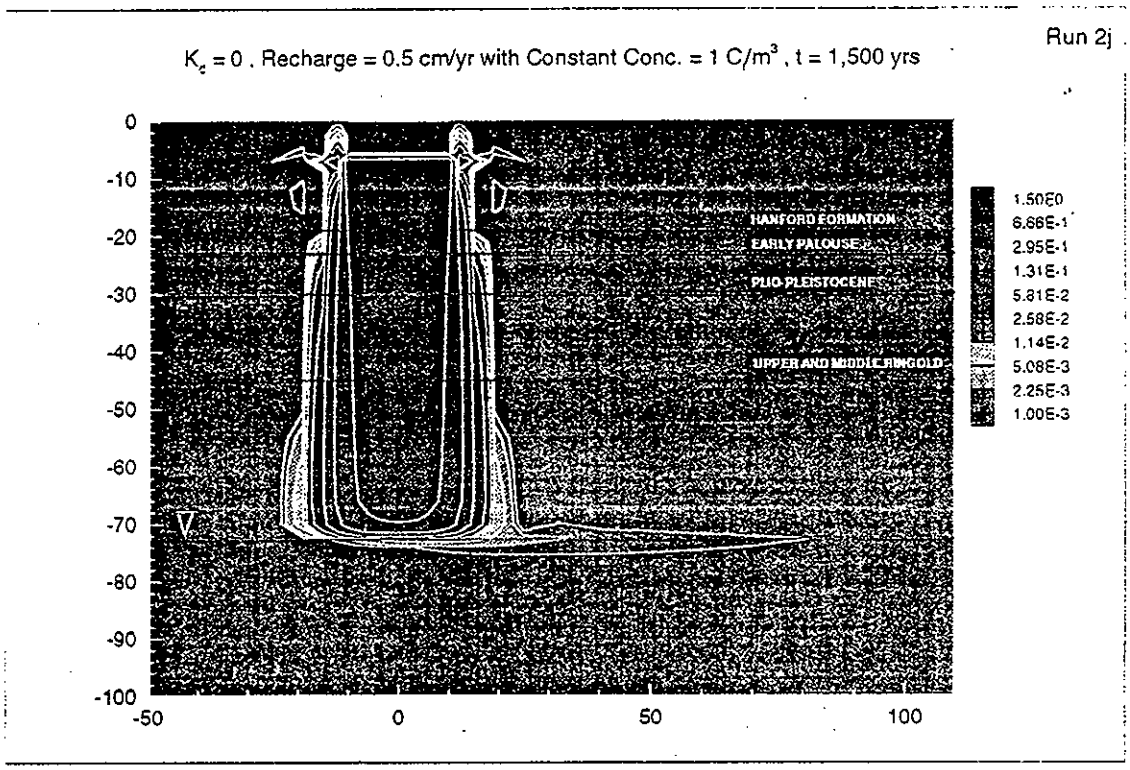

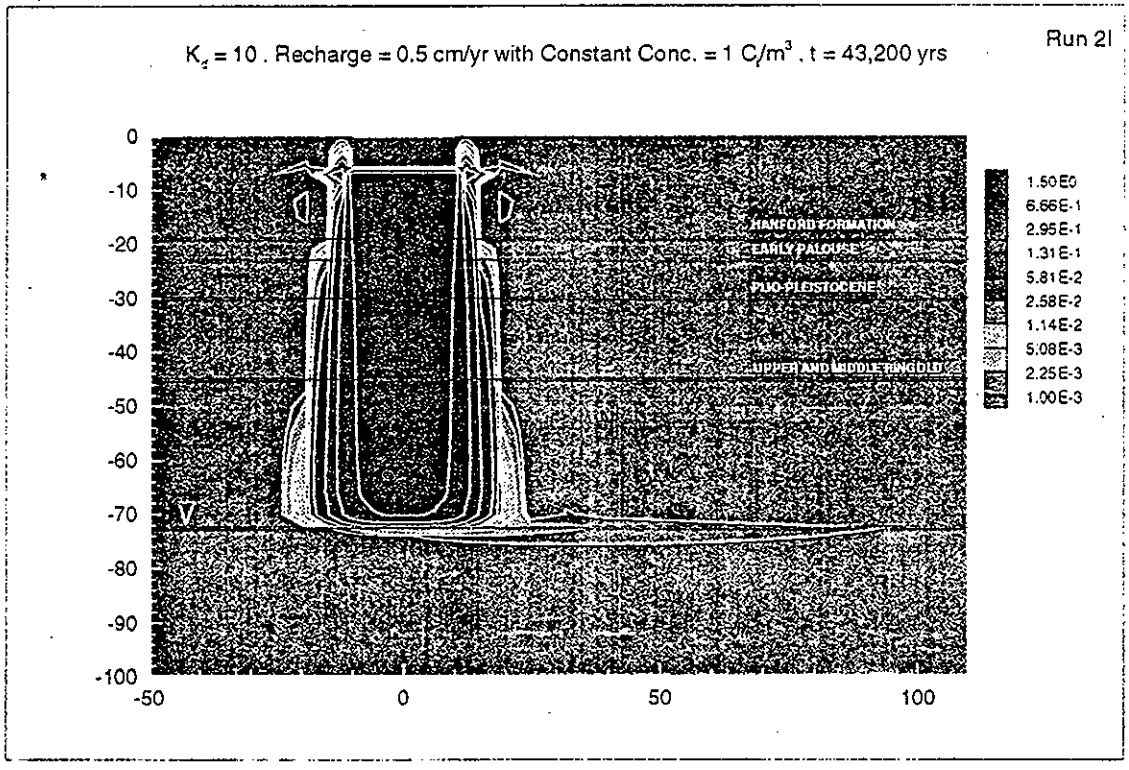

Figure D-24. Radionuclide Concentration Versus Time at the 100-m Downstream Well for Cases 2j and 2l.

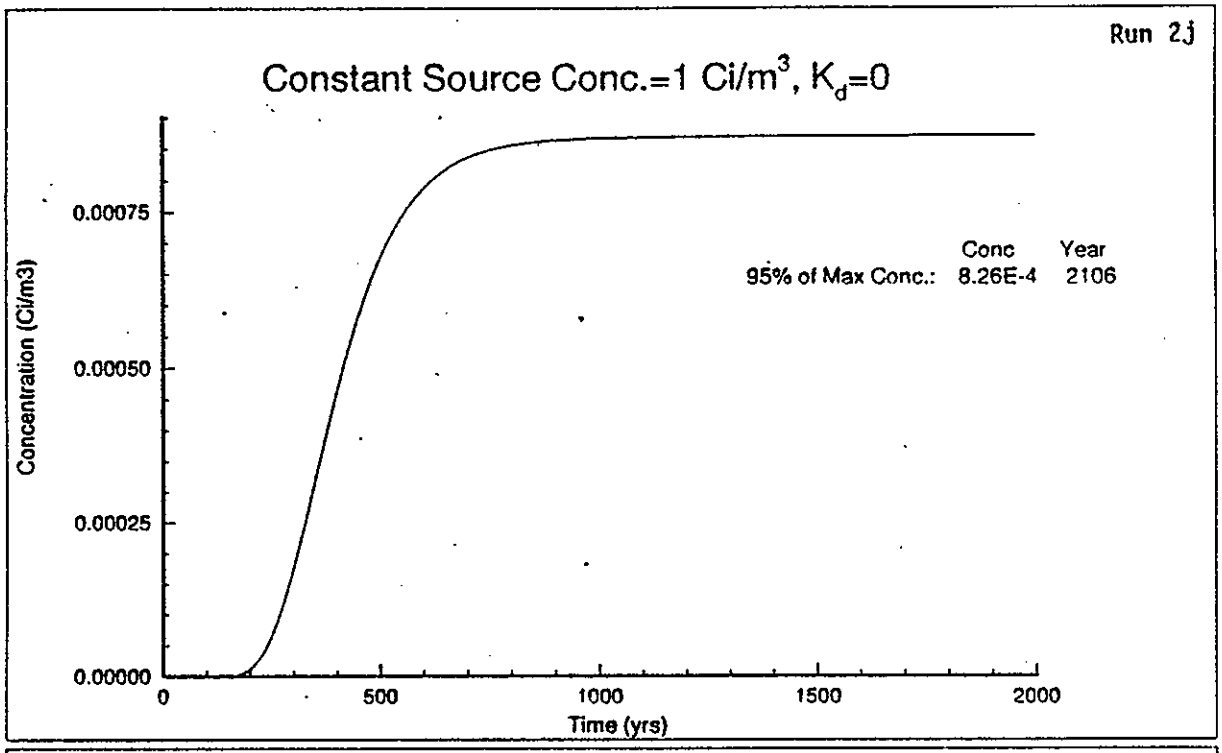

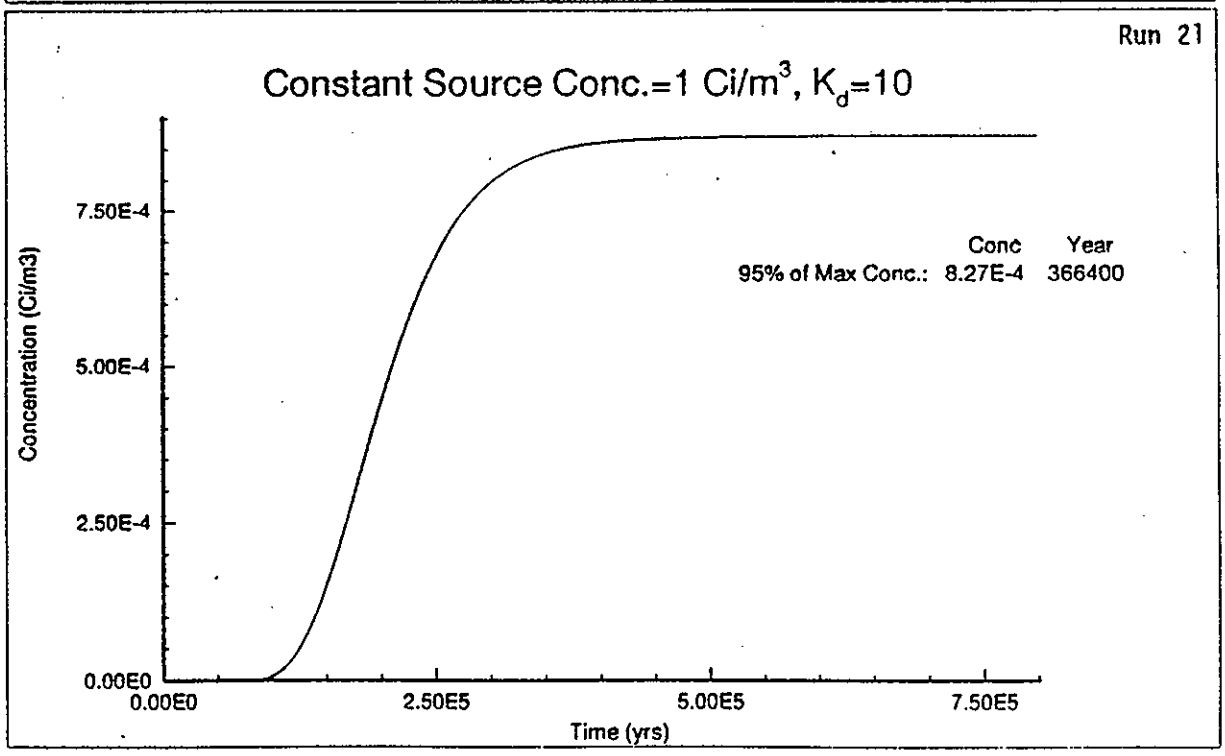

This page intentionally left blank.

APPENDIX E

SELECTED SOLUBILITY AND SORPTION DATA

This page intentionally left blank.

APPENDIX E

SELECTED SOLUBILITY AND SORPTION DATA

A literature search was completed to determine the solubility and adsorption properties of beryllium, nickel, tin, niobium, and samarium in the Hanford Site soil and grout porewaters and onto the Hanford Site soil, respectively. In addition, the solubility of neptunium, plutonium, radium, and uranium in the Hanford Site soil and cement leachate solutions was estimated. These nuclides were selected to determine if their solubility limits could control radionuclide groundwater concentration such that dose objectives would be satisfied. Consideration of geochemical control by cement was of interest to determine the relative benefit of a grout waste form, if any.

Recent work by Serne et al.[1] indicate that distilled water saturation extracts of the Hanford Site soil have practically the same composition as the Hanford Site groundwater. Solubility calculations for soil solutions in the Hanford Site vadose zone were, therefore, determined using the composition of the Hanford Site groundwater, which is listed in Attachment Table E.A-1. The chemical composition of the cement leachate used is listed in Attachment Table E.A-2. These data were taken from Serne et al. The cement leachate concentrations obtained after 12 wk of equilibration were used for the solubility calculations. The solubility calculations were generated with the MINTEQA2 geochemical code (Allison et al. 1991) using the solution compositions discussed above and the thermodynamic data reviewed below. Estimated solubility concentrations in both the Hanford Site groundwater and cement leachate, which were determined by review, are provided in Table E-1. A qualitative assessment of the expected reliability of this data is also provided in the text. The thermodynamic data that were used in these calculations, but were not part of the original MINTEQA2 (version 3.0) data base, are tabulated in Attachment Table E.A-3.

Of the five elements (beryllium, nickel, niobium, samarium, and tin) for which adsorption data were to be reviewed, the Hanford Site-specific data were available only for nickel.

E.1 BERYLLIUM SOLUBILITY

Beryllium solubility was determined using thermodynamic data available in Baes and Mesmer (1976) for the solubility of $Be(OH)_2(\alpha)$. These data were entered into the MINTEQ computer code data base. MINTEQ was then used to calculate the equilibrium solubility and speciation scheme. In natural Hanford Site groundwater the solubility of Be^{2+} was determined to be 2.5 x 10^{-7} M. In cement leachate the solubility of Be^{2+} is estimated to be 3.7 x 10^{-5} M.

---

[1]1991 unpublished results, Pacific Northwest Laboratory, Richland, Washington.

Table E-1. Estimated Solubility Concentrations (M) of Beryllium, Nickel, Tin, Niobium, Samarium, Uranium, Plutonium, Neptunium, and Radium, Oxidation State of the Dissolved Species is also Indicated.

Species	Hanford Site groundwater solubility	Cement leachate solubility
Beryllium (II)	2.5×10^{-7}	3.7×10^{-5}
Nickel (II)	2.8×10^{-4}	9.9×10^{-8}
Tin (IV)	5.5×10^{-10}	5.5×10^{-10}
Niobium (V)	4.9×10^{-5}	0.32
Samarium (III)	4.9×10^{-9}	3.3×10^{-8}
Uranium (VI)	2.7×10^{-4}	1.8×10^{-8}
Plutonium (IV) or plutonium (V)	$< 2 \times 10^{-8}$	$< 2 \times 10^{-8}$
Neptunium (V)	3.2×10^{-5}	1.1×10^{-4}
Radium (II)	1.6×10^{-7}	1.0×10^{-5}

Although the solubility data for $Be(OH)_2(\alpha)$ appear to be reliable, the effects of carbonate on the solubility of Be^{2+} are unknown. It is known that a $BeCO_3$ phase does form, but its solubility is not known and the importance of carbonate complexation with Be^{2+} to form soluble species is not known.

E.2 BERYLLIUM ADSORPTION

No data were found concerning the adsorption of beryllium onto the Hanford Site soils. Very little data are available for other soils as well. Data reviewed by Rai and Zachara (1984) indicate that beryllium adsorption onto 11 soils from 7 prominent soil orders was stronger than for cadmium, mercury, nickel, and zinc. It was also indicated that calcareous soils containing high concentrations of layer silicates were most effective at adsorbing beryllium. Kd values determined by Gerritse et al. (1982) at trace beryllium concentrations range from 50 to 700 mL/g for a sandy top soil in equilibrium with a 0.0035 M solution of ($CaCl_2$ + NaCl + kCl) in a 3:2:2 ratio; for a sandy loam top soil Kd values ranged from 8,000 to 12,000 mL/g in equilibrium with the same solution.

E.3 NICKEL SOLUBILITY

The solubility of nickel was determined using existing thermodynamic data contained within the MINTEQ database. Calculations indicate that the most stable solid phase of nickel in both the Hanford Site groundwater and cement leachate should be $Ni(OH)_2(c)$. The solubility of nickel in natural

Hanford Site groundwater was determined to be 2.8 x 10^{-4} M, assuming equilibrium with $Ni(OH)_2(c)$. In the cement leachate the solubility of nickel decreases to 9.9 x 10^{-8} M. The thermodynamic data for Ni^{2+} appears to be reliable.

E.4 NICKEL ADSORPTION

Nickel adsorption studies conducted for this project on Trench 8 sediment have been reported in Serne et al. (1993). The results of this work, which were determined at trace nickel concentrations, are as follows: for the Hanford Site groundwater the average Kd values were determined to be 440 mL/g after a 5-d equilibration period and 2,350 mL/g after 43-d; the average values determined in a cement waste leachate solution (which also contained significant concentrations of dissolved organic carbon) were 2.9 mL/g after 5-d and 6.0 after 43-d.

More recently adsorption work has been conducted on Trench 94 soil as a function of nickel concentration. Results for a 10-d equilibration period ranged from 48 mL/g at a final nickel concentration in solution of approximately 1,000 ppb to 337 mL/g at a final nickel concentration of approximately 2 ppb. Nickel adsorption onto Trench 94 soil from the Hanford Site groundwater was found to fit a Freundlich isotherm, $X = KC^N$, where X is the concentration of nickel adsorbed to soil (μg/Kg), C is the concentration of nickel in solution (μg/Kg), and K and N are constants. Linear regression of the nickel adsorption data onto Trench 94 soil from the Hanford Site groundwater yielded the following constants: log K = 2.38 and N = 0.845.

E.5 TIN SOLUBILITY

Few thermodynamic data are available for tin. The solubility of tin was determined by assuming that solubility was controlled by formation of $SnO_2(c)$. The solubility and hydrolysis data were obtained from Baes and Mesmer (1976). The solubility of tin in both the Hanford Site groundwater and cement leachate was calculated to be 5.5 x 10^{-10} M using MINTEQ. The data used to determine this value are considered as estimates only.

E.6 TIN ADSORPTION

No data were found for the adsorption of tin onto the Hanford Site soil. Gerritse et al. (1982) measured R_d values for tin adsorption onto a sandy top soil and a sandy loam top soil in equilibrium with a dilute inorganic solution. The Kd results ranged between approximately 1,000 and 3,000 mL/g for the sandy top soil and 4,400 and 11,000 mL/g in the sandy loam. Trace concentrations of $^{113}Sn^{4+}$ were used in these experiments to determine R_d values.

E.7 NIOBIUM SOLUBILITY

Thermodynamic data available in Baes and Mesmer (1976) for the solubility of Nb_2O_5 and the hydrolysis species of Nb^{5+} were input to the MINTEQ database and subsequently used to determine the solubility of Nb^{5+} in both the Hanford Site groundwater and cement leachate. These calculations indicate that the solubility of Nb^{5+} in the Hanford Site groundwater is 4.9×10^{-5} M and 0.32 M in cement leachate, assuming Nb_2O_5 is the solubility controlling solid. The data used in these calculations were considered by Baes and Mesmer (1976) to be "very approximate." These data were measured on freshly precipitated Nb_2O_5 (Babko et al. 1963) which was uncharacterized and likely to have been amorphous. Because well crystallized materials tend to have lower solubilities than amorphous precipitates, the solubility estimate provided above may overestimate the actual solubility of niobium in the environment.

E.8 NIOBIUM ADSORPTION

Rhodes (1957) reported Kd values for zirconium-niobium adsorption onto the Hanford Site subsoil which ranged from 90 mL/g at pH 6.0 to >1,980 mL/g at pH values of 2.7, 3.5, 4.4, 8.4, and 9.3. These data are not particularly useful since we cannot determine if they are most appropriate for describing the adsorption of zirconium or niobium.

E.9 SAMARIUM SOLUBILITY

A complete set of thermodynamic data necessary to calculate Sm^{3+} solubility in the Hanford Site groundwater is not available. Thermodynamic data are available for the solubility of $Sm(OH)_3(c)$ and the hydrolysis of SM^{3+} (Baes and Mesmer 1976), but not for the solubility of $SMOHCO_3$ or carbonate complexation of Sm^{3+}. Other phases and complexes are not likely to be important in natural Hanford Site groundwater.

Due to the similarity in electronic structure, ionic radius and chemical properties, the trivalent lanthanides have often been used as chemical analogs for the trivalent actinides (Cantrell 1988; Allard 1988; Krauskopf 1986). In this case, we will use solubility data determined for $AMOHCO_3(c)$ as an analog for $SMOHCO_3$. It has been shown that $AMOHCO_3(c)$ is the thermodynamically stable phase for Am under conditions which exist in the Hanford Site groundwater (Felmy et al. 1990). In addition, we will use carbonate stability constants for Sm^{3+} determined using an estimation technique which is based on data determined for several other lanthanide ions (Cantrell and Byrne 1987).

Using the thermodynamic data discussed above (i.e., assuming $SM(OH)CO_3$ is the solubility controlling phase), and the groundwater composition listed in Table E-1, the solubility of samarium was determined to be 4.9×10^{-9} M. In cement leachate samarium solubility increases to 3.3×10^{-8} M. Based on our knowledge of other lanthanides and actinides these estimates are likely to be reliable.

E.10 SAMARIUM ADSORPTION

No Hanford Site-specific data are available for samarium, however, as indicated above, analogous behavior is expected for other trivalent lanthanides and actinides. Sheppard et al. (1976) reported R_d values for americium between two Hanford soils and a solution (apparently distilled water) containing $^{241}Am^{3+}$ to be 125 mL/g and 833 mi/g, respectively. These values are likely to be larger than values appropriate for the Hanford Site groundwater because of the strong tendency of samarium to form carbonate complexes which will inhibit adsorption. The adsorption of samarium onto the Hanford Site soil in contact with cement leachate cannot be predicted from the available data.

E.11 URANIUM SOLUBILITY

Uranium solubility was determined using thermodynamic data available in MINTEQ. Uranium solubility was assumed to be controlled by schoepite ($UO_2(OH)2 \bullet H_2O$). In the Hanford Site groundwater, UO_2^{2+} solubility was determined to be 2.7×10^{-4} M. In cement leachate solution the solubility was determined to be 1.2×10^{-8} M. The reliability of these data are considered fair (Newton and Sullivan 1985).

E.12 PLUTONIUM SOLUBILITY

The aqueous chemistry of plutonium is complex and the thermodynamic data needed to describe plutonium chemistry in groundwaters are incomplete and sometimes unreliable. One of the main barriers to obtaining reliable thermodynamic data for plutonium is the difficulty in maintaining plutonium in solution in a single oxidation state. Plutonium can exist as Pu^{3+}, PU^{4+}, PuO_2^+ and PuO^{+2}.

Plutonium (IV) oxide and amorphous hydrous oxide are the plutonium compounds most likely to precipitate and be present in nuclear wastes (Rai and Ryan 1982). Although thermodynamic considerations dictate that the $PuO_2 \times H_2O(am)$ will eventually convert to $PuO_2(c)$, radiolytic effects oppose the crystallization process, causing the crystallinity of the equilibrium solid phase to be somewhere between $PuO_2 \times H_2O(am)$ and $PuO_2(c)$, depending on the radiation field (Rai and Ryan 1982). Because $PuO_2 \times H_2O(am)$ is the more soluble phase, its solubility can be used to set maximum limits on the plutonium concentration in solution. Data from Rai et al. (1980) and Rai (1984) indicate that the solubility of $PuO_2 \times H_2O(am)$ in CO_2 free solution at a pH of 8.2 is approximately 1×10^{-8} M. The data also indicate that practically all of the dissolved plutonium is oxidized to PuO_2^+.

Because carbonate is a good complexing agent for actinide ions and because carbonate is ubiquitous in groundwaters, it is possible that carbonate could significantly affect the solubility of plutonium in groundwater. If we assume the same as that determined for $NPO2(CO_3)$- that log p, = 4.5 for $Puo2(CO_3)$, at zero ionic strength (Bidoglio et al. 1987), then carbonate complexation should increase the solubility of PuO+ to approximately 2×10^{-8} M in the Hanford Site groundwater.

It has been demonstrated that high carbonate concentrations stabilize the PU(IV) oxidation state in solution (Eiswirth et al. 1985; Lierse and Kim 1984; Kim et al. 1983). It is not known, however, if this is also true for the lower carbonate concentrations existing in groundwater. In a solubility study of the NP(IV) hydrous oxide system in which dissolved neptunium was stabilized as Np(IV), it has been demonstrated that addition of 0.01 M total carbonate does not increase the solubility of $NpO_2 \times H_2O$ (am) (Rai and Ryan 1985). Because log K for the reaction: $PuO \times H_2O$ (am) = Pu4+ + 4OH+ + (x-2)H O is smaller than that for Np(IV), the data of Rai and Ryan (1985) should provide an upper bound to the solubility of $PuO_2 \times H_2O$(am), if plutonium is stabilized in the Pu(IV) oxidation state. The solubility of NP(IV) determined by Rai and Ryan (1985) in 0.01M total CO_2 was approximately 5×10^{-9} M both at pH = 8.2 (pH of groundwater) and at pH = 12.1 (pH of cement leachate). In addition to the plutonium oxides and hydrous oxides, it is possible that $Pu(OH)2CO_3$ forms; however, if this phase does form it will have a solubility which is less than that of $PuO_2 \times H_2O$(am) or PuO_2(c), whichever is present. We can, therefore, conclude that the maximum solubility of plutonium in the Hanford Site groundwater and cement leachate should be less than 2×10^{-8} M. Actual values, however, cannot be ascertained from the available data.

E.13 NEPTUNIUM SOLUBILITY

The MINTEQ database was modified by adding thermodynamic data for the solubility of NpO_2OH(c) and data for hydrolysis and carbonate complexation of NpO+ (Nakayama et al. 1988; Bidoglio et al. 1987). The solubility of NpO+ was calculated to be 3.2×10^{-5} M in the Hanford Site groundwater and 1.1×10^{-4} 2 in cement leachate solution. The reliability of these data is considered to be fair.

E.14 RADIUM SOLUBILITY

Radium salts of strong acids, such as HCl and HNO are quite soluble (Molinari and Snodgrass 1990). Radium salts of sulfate, carbonate and phosphate are less soluble. Thermodynamic solubility products for radium are available only for sulfate (Sillen and Martell 1964). The solubility product is $10^{-10.37}$ of $RaSO_4$ at 20 °C and zero ionic strength (Sillen and Martell 1964). Stability constants for radium complexation are available for both sulfate and carbonate. Log K_1, values for these constants are 2.43 and 2.48 at 25 °C and zero ionic strength, respectively (Benes et al. 1982).

MINTEQ calculations indicate that for a typical the Hanford Site groundwater (Table E.A-1, sulfate concentration of 75 mg/L or 7.8×10^{-4} M), the solubility of radium is controlled by $RaSO_4$. The solubility controlled maximum radium concentration was determined to be 1.6×10^{-7} M. The proposed EPA MCL for adjusted gross alpha emitters is 20 pCi/L for ^{226}Ra plus ^{228}Ra. This is equivalent to a concentration of 6×10^{-14} M, assuming all radium is ^{226}Ra. Solubility calculations in cement leachate, using the composition listed in Table E.A-2 for a 12-wk leaching period, indicate an equilibrium radium concentration of 1.0×10^{-5} M. These calculated solubility constraints are considered fairly reliable.

Radium is also known to coprecipitate with barite and a mixing model that describes the correlation between radium and barium concentrations during precipitation has been used with reasonable success (Beaucaire and Toulhoat 1987). The solubility product for BaSO4 is 10^{-9}, (Sillen and Martell 1964). The concentration of barium in the Hanford Site groundwater at equilibrium with barite was calculated to be 3.6 x 10^{-7} M (0.05 ppm) using the MINTEQ geochemical code. This value lies within the range of barium concentrations measured in the Hanford Site groundwater (Table E-1), suggesting that the Hanford Site groundwaters are in equilibrium with barite. Although coprecipitation could occur, it is unlikely because the saturation index of barite in groundwater will actually decrease as it mixes with cement leachate solution. If barite does not precipitate, radium will not coprecipitate.

E.15 REFERENCES

Allard B., 1982, *In Actinides in Perspective* (N. M. Edelstein, Ed.), pp. 553-580, Pergamon Press, Oxford.

Allison J. D., D. S. Brown, K. J. Novo-Gradac, 1991, MINTEQA2/PRODEFA2, *A Geochemical Assessment Model for Environmental Systems: Version 3.0 User's Manual*, EPA/600/3-91/021, U.S. Environmental Protection Agency, Athens, Georgia.

Babko A. K., V. V. Lukachina, and B. I. Nabivanets, 1963, "Solubility and Acid-Base Properties of Tantalum and Niobium Hydroxides," Russ. J. Inorg, *Chem.*, 8:957-961.

Baes C. F., and R. E. Mesmer, 1976, *The Hydrolysis of Cations*, Wiley, New York.

Beaucaire C., and P. Toulhoat, 1987, "Redox Chemistry of Uranium and Iron, Radium Geochemistry, and Uranium Isotopes in the Groundwaters of the Lodeve Basin, Massif Central, France," *Applied Geochemistry*, 2:417-426.

Benes P., M. Obdrzalek, and M. Cejchanova, 1982, "The Physicochemical Forms of Traces of Radium in Aqueous Solutions Containing Chlorides, Sulfates and Carbonates," *Radiochem, Radioanal*, Letter 50:277.

Bidoglio G., P. Offermann, and A. Saltelli, 1987, "Neptunium Migration in Oxidizing Clayey Sand," *Applied Geochemistry*, 2:275-284.

Cantrell K. J., and R. H. Byrne, 1987, "Rare Earth Element Complexation by Carbonate and Oxalate Ions," *Geochim, Cosmochim. Acta*, 51:597-605.

Eiswirth M., J. I. Kim, and Ch. Lierse, 1985, "Optical Absorption Spectra of Pu(IV) in Carbonate/Bicarbonate Media," *Radiochimica Acta*, 38:197-201.

Felmy A. R., D. Rai, and R. W. Fulton, 1990, "The Solubility of $AMOHCO_3$ and the Aqueous Thermodynamics of the System Na^+-Am^{3+} -HCO_3-CO_3^2 -OH^--H_2O," *Radiochimica Acta*, 50:193-204.

Gerritse R. G., R. Vriesema, J. W. Dalenberg, and H. P. De Roos, 1982, "Effect of Sewage Sludge on Trace Element Mobility in Soils," *J. Environmental* Quality 11:359-364.

Kim J. I., Ch. Lierse, and F. Baumgartner, 1983, In Plutonium Chemistry, (W. T. Carnall, G. R. Choppin, eds.), ACS symp. Ser. 216:317.

Krauskopf K. B., 1986, *Chemical Geology*, 55:323.

Lierse Ch., and J. I. Kim, 1984, Radioanalysis Nuclear Chemistry Letter 86:37.

Molinari, J., and W. J. Snodgrass, 1990, In The Environmental Behavior of Radium, Vol. 1. Technical Reports Series No. 310, International Atomic Energy Agency, Vienna, Austria.

Nakayama, S., H. Arimato, N. Yamada, H. Moriyama, and K. Higashi, 1988, "Column Experiments on Migration Behavior of Neptunium(V)," *Radiochimica Acta*, 44/45:179-182.

Newton, T. W., and J. C. Sullivan, 1985, "Actinide Carbonate Complexes in Aqueous Solution," In *Handbook on the Physics and Chemistry of the Actinides*, A. J. Freeman and C. Keller, eds., Elsevier Science Publishers, B.V.

Rai, D., 1984, "Solubility Product of PU(IV) Hydrous Oxide and Equilibrium Constants of Pu(IV)/Pu(V), Pu(IV)/Pu(VI), and Pu(V)/Pu(VI) Couples." Radiochimica Acta. 35:97-106.

Rai, D., and J. L. Ryan, 1985, "Neptunium(IV) Hydrous Oxide Solubility Under Reducing and Carbonate Conditions," *Inorganic Chemistry*, 24:247-251.

Rai, D., and J. L. Ryan, 1982, "Crystallinity and Solubility of PU(IV) Oxide and Hydrous Oxide in Aged Aqueous Suspensions," Radiochimica Acta. 30:213-216.

Rai, D., and J. M. Zachara, 1984, Chemical Attenuation Rates, Coefficients, and Constants in Leachate Migration, Vol. 1: A Critical Review, EPRI EA-3356, Vol 1, Research Project 2198-1, Battelle, Pacific Northwest Laboratory, Richland, Washington.

Sheppard, J. C., J. A. Kittrick, and T. L. Hart, 1976, "Determination of Distribution Ratios and Diffusion Coefficients of Neptunium, Americium and Curium in Soil-Aquatic Environments," RLO-221-T-12-2.

Sillen, L. G., and A. E. Martell, 1964, Stability Constants of Metal-Ion Complexes, Special Publication Number 17, The Chemical Society, London, England.

ATTACHMENT 1

Table E.A-1. Chemical Composition (mg/L) of Groundwater (Hanford Well 6-S3-25).

Constituents	Sample Used (4/90)	Range in Composition (1985-1990)
pH	8.14	7.82 - 8.47
Eh(mv)	309	283 - 385
Al	<0.03	<0.03 - 0.064
B	0.1	0.02 - 0.10
Ba	0.08	0.04 - 0.08
Ca	48.8	48.8 - 58.8
Cd	<0.004	<0.004
Cr	4.020	<0.02 - 0.034
Cu	4.004	<0.004
Fe	<0.005	<0.005 - 0.008
K	9.9	4.9 - 9.9
i	<0.004	<0.004
Mg	14.6	13.2 - 14.6
Mn	4.002	<0.002 - 0.13
Na	32.1	23.8 - 32.1
p	4.1	<0.1
Pb	<0.06	<0.06
Si	16.4	14.6 - 16.4
Sr	0.25	0.23 - 0.25
Zn	<0.02	<0.02 - 0.08
F-	0.5	<0.5 - 0.7
Cl-	27	21 - 27
$NO-_2$	<0.3	<0.3
$NO-_3$	<0.5	<0.5
PO^3_4	<0.4	<3
SO^2_4	75	63 - 92
T-Alk (as CO^2_3-)	67.5	67.5 - 92.4
TOC	1	0.3 - 1.7
Cations (meq/L)	5.29	4.9 - 5.4
Anions (meq/L)	4.60	4.6 - 6.1

Table E.A-2. Solid Waste Performance Leach Study.

		4 all waste types and cement			
		4-1 1 week	4-2 3 weeks	4-3 6 weeks	4-4 12 weeks
PH		11.77	12.04	12.03	12.12
Eh		266	95	117	149
Al	mg/L	17	55.5	57.3	43.5
B	mg/L	0.1	0.05	0.24	2.18
Ba	mg/L	0.37	1.18	1.7	<0.002
Ca	mg/L	177	311	360	296
Cd	mg/L	<0.004	4.004	<0.004	<0.004
Cr	mg/L	<0.020	4.020	4.020	<0.020
Cu	mg/L	<0.004	<0.004	<0.004	<0.004
Fe	mg/L	<0.005	4.005	<0.005	<0.005
K	mg/L	94	146	186	235
Li	mg/L	0.07	0.09	<0.004	0.17
Mg	mg/L	<0.06	4.06	<0.06	<0.06
Mn	mg/L	<0.002	<0.002	<0.002	<0.002
Na	mg/L	58	75.6	88	96
P	mg/L	<0.10	<0.10	<0.10	<0.10
Pb	mg/L	<0.060	<0.060	<0.060	<0.060
Si	mg/L	3.2	1.5	1.1	0.7
Sr	mg/L	0.66	1.29	1.6	1.96
Zn	mg/L	<0.020	<0.020	<0.020	<0.020
F-	mg/L	6.8	8.4	15	20
Cl-	mg/L	16.7	12.9	15	14
NO_2-	mg/L	<0.300	<0.300	<0.300	<0.300
NO3-	mg/L	0.6	0.6	1.7	3
PO4	mg/L	<0.400	<0.400	<0.400	3
SO4-	mg/L	35.1	13.2	1.1	1.5
TALK	mg/L	225	645	727.5	1050
TOC	mg/L	90	110	148	245
IC	mg/L	5	3	2	14
CATIONS	meq/L	13.77	22.57	26.58	25.00
ANIONS	meq/L	9.07	22.59	25.51	36.53

Table E.A-3. Thermodynamic data which were used but are not in the MINTEQA2 Database (data appropriate to zero ionic strength).

Reaction	Log K
$Be^{2+} + 2H_2O = Be(OH)_2(a) + 2H^+$	-6.69
$Be^{2+} + H_2O = BEOH^+ + H^+$	-5.40
$Be^{2+} + 2H_2O = Be(OH)_2^o(aq) + 2H^+$	-13.65
$Be^{2+} + 3H_2O = Be(OH)_3 + 3H^+$	-37.41
$Be^{2+} + 4H_2O = Be(OH)_4^2 + 4H^+$	-23.25
$Sn^{4+} + 2H_2O = SnO_2(c) + 4H^+$	8.40
$Sn^{4+} + H_2O = SnOH^{3+} + H^+$	0.57
$Sn^{4+} + 2H_2O = Sn(OH)_2^2 + 2H^+$	0.63
$Sn^{4+} + 3H_2O = Sn(OH)_3^+ + 3H^+$	0.36
$Sn^{4+} + 4H_2O = Sn(OH)_4^o(aq) + 4H^+$	-0.86
$2Nb(OH)_5(aq) + Nb_2O_5(am) + 5H_2O$	9.60
$Nb(OH)_5(aq) + H^+ = Nb(OH)_4^+ + H_2O$	-0.79
$Nb(OH)_5(aq) + H_2O = Nb(OH)_6 + H^+$	-7.82
$Sm^{3+}\ H_2O + CO_3^2 = SM(OH)CO_3(c) + H^+$	8.50
$SM^{3+} + 3H_2O = Sm(OH)_3(c) + 3H^+$	-16.50
$SM^{3+} + 3H_2O = SmOH^{2+} + H^+$	-7.719
$SM^{3+} + 2H_2O = Sm(OH)_2^+ + 2H^+$	-16.855
$SM^{3+} + 3H_2O = Sm(OH)_3^o(aq) + 3H^+$	-26.101
$SM^{3+} + 4H_2O = Sm(OH)_4 + 4H^+$	-36.115
$SM^{3+} + CO_3^2 = SMCO_3^+$	7.851
$SM^{3+} + 2CO_3^2 = SM(CO_3)_2$	12.985
$NpO_2^+ + H_2O = NpO_2OH(c) + H^+$	-3.30
$NpO_2^+ + H_2O = NpO_2OH(aq) + H^+$	-8.30
$NpO_2^+ + CO2_3^2 = NpO_2CO_3$	4.51
$NpO_2^+ + 2CO_2 = NpO_2(CO_3)_2^3$	6.86

This page intentionally left blank.

APPENDIX F

WASTE FORM RELEASE ANALYSIS AND DATA COLLECTION

This page intentionally left blank.

APPENDIX F

WASTE FORM RELEASE ANALYSIS AND DATA COLLECTION

F.1 DESCRIPTION OF RELEASE RATE FOR ^{14}C IN ACTIVATED METAL

A common type of waste material disposed in the Hanford Site burial grounds is activated metal. Occasional wastes contain high quantities of ^{14}C which exceed normal inventory limits for this isotope if no credit is taken form waste material or container properties that limit release. Two individual cases are discussed below for wastes that have been placed in the 200 West Area LLBG. Estimates of potential dose resulting from the release of ^{14}C by corrosion of the activated metal waste material are discussed.

The first waste consists of core basket and thermal shield metal hardware material. The ^{14}C content of this material is 13.5 Ci. The weight of the waste is 29.459 kg. This material is placed inside a cylinder that is 115 in. (about 290 cm) in diameter and 198 in. (about 500 cm) long. The container is a three-layer system that includes a 9-in. inner steel wall surrounded by a 9-in. concrete sleeve surrounded by a 0.5-in. steel shell. This extremely thick container system provides shielding from the intense radiation provided by the short-lived activation products (primarily ^{60}Co). Both the thick outer metal shell and the concrete shell provide immobilization of the ^{14}C isotope and are expected to contain the inventory for thousands of years. However, in this analysis it is assumed that the outer container materials are not present and release is occurring as a result of activated metal corrosion.

To estimate dose the annual Ci of ^{14}C released from the corrosion of activated metal are calculated and divided by the annual flux of water passing through the waste to determine an average steady state concentration. The solubility analytical results assume steady state concentrations as the release rate mechanism are then used to calculate the peak groundwater concentration and the corresponding peak dose. The solubility approach is appropriate because a steady state concentration is assumed to be the release rate.

The average concentration of ^{14}C (4.1×10^{-10} Ci/mg) is determined by taking the ratio of total CI (13.5 Ci) to the weight of the waste (2.9×10^{9} mg). The pump is an irregularly shaped material. To determine the amount of metal corroded annually, it is assumed to be a rectangular slab with dimensions large enough to just fit into the interior of the container (290 by 500 cm). The slab area is about 1.45×10^{5} cm^2. It is assumed that release occurs by corrosion at a steady rate. General corrosion rates in Hanford soil have not been extensively measured. However, by looking at corrosion rate measurements in soil conditions similar to Hanford Site soil, (alkaline, low moisture content, and low chloride content), a reasonably conservative average corrosion rate can be selected this type of steel. Jenkins (1993) recommends value of 0.01 to 0.02 mg/dm^2-yr for corrosion resistant steels. If a corrosion rate of 0.1 mg / dm^2-yr is assumed, 14.5 mg of metal will corrode releasing 5.9×10^{-8} Ci into solution. Assuming an infiltration rate of 0.5 cm/yr through the area of the container, an annual volume of water receiving the ^{14}C is 0.073 m^3. The estimated steady state concentration is, therefore, 8.2×10^{-7} Ci/m^3. Using this concentration, a peak groundwater

concentration of 0.68 pCi/L is calculated that corresponds to a dose of 0.001 mrem/yr. It is concluded that this waste package is an insignificant source of dose and acceptable for disposal.

The second case consists of a steel pump encased in a thin steel-walled container. The steel is a high nickel alloy that is corrosion resistant. In this case, no credit can be taken for delay of release due to corrosion of the container. The waste package contains 7.9 Ci of ^{14}C in 5.1×10^9 mg of steel. The container measures 42 in. in diameter (107 cm) and 107 in. long (272 cm). Because the pump is an irregularly shaped material, it is assumed to a rectangular slab with dimensions large enough to just fit into the interior of the container (100 by 250 cm). It is assumed that release occurs by corrosion at a steady rate. Using the same set of calculations as described for the first case, a dose estimate of 0.004 mrem/yr is calculated. It is concluded that this waste package is also an insignificant source of dose and acceptable for disposal.

F.2 IODINE RELEASE CHARACTERISTICS FROM GROUT WASTE FORMS UNDER PARTIALLY SATURATED CONDITIONS

Standard leaching studies are completed under conditions that are not representative of those expected in a low-level waste (LLW) disposal facility at the Hanford Site. Typically a waste form containing a contaminant is immersed in a water bath for a specified period of time and then removed. The concentration of the contaminant is then measured. The waste form is then placed in a fresh water bath and the process is repeated. By measuring the change in contaminant concentration with each batch of fresh water, a release curve can be fitted to the data that can be described as a leach index or a diffusion coefficient. This value can then be input to a computer code as the release rate or source term in flow and transport analyses.

It is expected that this approach is conservative, because the use of fresh water repeatedly maximizes the concentration gradient of the contaminant that drives the mass transport. On the other hand, when computer models are used for long-term predictions, there is a difficulty in expecting the waste form to maintain its initial characteristics over time. Consequently, increased release rates are frequently assumed to offset uncertainty about the actual behavior of the waste form.

To get a better understanding of actual waste form behavior in a Hanford Site LLW disposal facility, a series of scoping experiments were completed to measure contaminant release from a waste form under site-specific conditions. The contaminant and waste form selected were iodine and Portland cement-based grout. The experimental work described here is of a scoping nature and therefore preliminary. A fundamental hypothesis being tested in these experiments is the theory that secondary mineralization in grout (primarily the formation of calcium carbonate) readily occurs in a reactive outer rind and reduces the permeability of the waste form such that contaminant release rates are reduced over time rather than increased as is conservatively assumed in typical performance assessment analyses.

F.2.1 Experimental Procedure

To simulate the disposal of grout waste under a commonly occurring set of Hanford environmental conditions, an iodine-spiked grout cylinder was placed in contact with a partially saturated column of Hanford Site soil. One large batch of grout was made up for the entire suite of experiments. The initial mixture consisted of 14,224 g of cement, 42,794 g of sand, and 8,508 g of water containing about 5% sodium iodide by weight. This corresponds to fraction of iodine by weight in the grout of 0.0055. Two moisture contents (about 4 and 7 vol%) were set up in a closed system to cover a range of commonly observed moisture content conditions in Hanford soil. The interface between grout and soil occurred at the end cap of the cylinder and the column of soil. The column of soil interfaced with a large reservoir of like soil at the same moisture content at the other end of the soil column. The entire system was sealed during the course of the experiment. Other parameters investigated were the length of the grout cylinder, and treatment of the grout (air-dried versus oven-dried). Finally, numerous duplicates for each set of conditions were provided so that samples could be collected and analyzed over time.

Moisture probes were set in the soil and grout at regular intervals to measure moisture content as a function of distance away from the soil grout interface during the experiment. When a sample was pulled, iodine concentrations were measured at regular intervals in the soil column to quantify the iodine content as a function of distance away from the soil/grout interface. One grout sample has been sectioned length wise and measured for relative changes in iodine concentration and carbon concentration as a function of distance from the soil grout interface.

F.2.2 Experimental Results

Three types of data were gathered. First, moisture contents were measured in the grout sample and the soil column at regular intervals away from the soil-grout interface in both materials. Second, each time an experiment was sacrificed (at 4, 9, 19, and 75 wk), consecutive 1/8-in. slices of soil were sectioned from the soil column beginning at the soil grout interface. The soil was placed in 100 mL of distilled water to dissolve the iodine from the sample. An iodine probe was then used to measure the iodine concentration. Eventually, iodine concentrations were measured as a function of time and distance from the grout interface. Third, for two grout samples, the cylinders were split lengthwise, perpendicular to the soil-grout interface. Using a scanning electron microscope energy dispersive system (SEM/EDS), relative concentrations of iodine and carbon were determined as a function of distance away from the grout-soil interface.

As an example of the data collected, iodine concentrations in the soil wash solution as a function of time and distance from the soil-grout interface are shown in Table F-1 for an 8-in. grout sample placed in contact with a initial 4% moisture content soil. The grout was cured in air for 28 d before the start of the experiment. A direct measurement of the iodine quantity in the initial grout sample was not made. However, by taking the product of the

approximate fraction of iodine in the grout (0.0055), the volume of the grout cylinder (about 412 cm^3), and the approximate density (about 2 g/cm^3), a total iodine inventory in the initial grout sample of about 4.5 g is estimated.

Table F-1. Iodine Soil Moisture Concentrations (mg/L) As a Function of Time and Distance Away From the Soil-Grout Interface.

Distance	Time (wk)			
	4	9	16	75
0.125	147	268	211.5	48.36
0.375	30.87	132	161.3	35.33
0.625	5.59	52.3	105.9	21.91
0.875	3.88	16.4	73.8	17.27
1.125	2.78	4.57	42.2	12.04
1.375	2.12	1.75	23.1	8.49
1.625	2.12	0.82	12.92	7.02
1.875	2.31	0.86	6.29	4.94
2.125	1.72	0.79	4.29	3.65
2.375	1.84	1.91	2.92	3.36
2.625	2.05	1.87	2.29	2.40
2.875	2.30	1.57	1.77	2.00

In Figure F-1, iodine quantity per soil sample as a function of time is illustrated. During the 75-wk period, a maximum occurs for each soil segment and the maximum occurs at later times as the distance from the grout interface increases. Also, the iodine quantities are largest near the interface. This pattern is also observed in Table F-1 with the iodine concentrations.

The most important aspect of these observations is the fact that only a small fraction of the iodine initially present in the grout sample has been released. In the soil columns, the maximum amount of iodine measured is less than 5 mg. This compares to the approximately 4,500 mg of iodine estimated to be in the grout at the beginning of the experiment. The presence of significant quantities of iodine in grout is illustrated by the SEM/EDS data shown in Figure F-2. An iodine deficient zone exists at the soil-grout interface and then appears to level off in the interior of the grout sample. At the same time, a carbon scan shows a maximum relative concentration at the soil-grout interface that decreases rapidly away from the interface (Figure F-3).

F.2.3 Interpretation of Results

Each experiment exhibits a two-stage process in which the iodine tracer first diffuses out of the grout cylinder and then stops diffusing or the flux is greatly reduced. This is indicated by changes in concentration of iodine near the soil-grout interface. The change is always an increase in iodine concentration followed by a decrease in iodine concentration. This behavior is expected to occur as the source of the iodine becomes depleted through the diffusion process. However, in these experiments, the source of iodine only

Figure F-1. Iodine Concentrations in the Soil Column As a Function of Time.

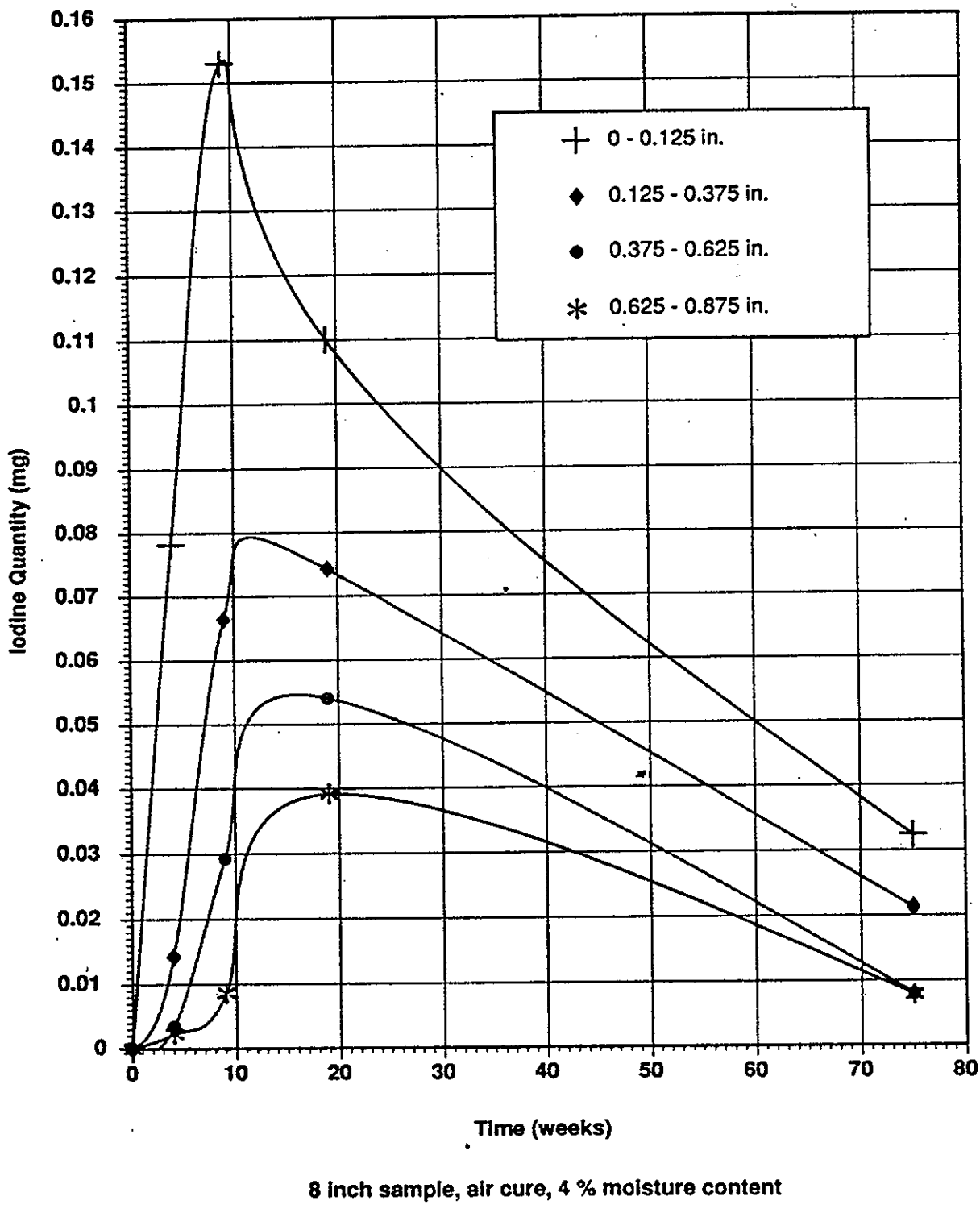

Figure F-2. Total Iodine Counts in the Grout Sample As a Function of Distance From the Soil-Grout Interface.

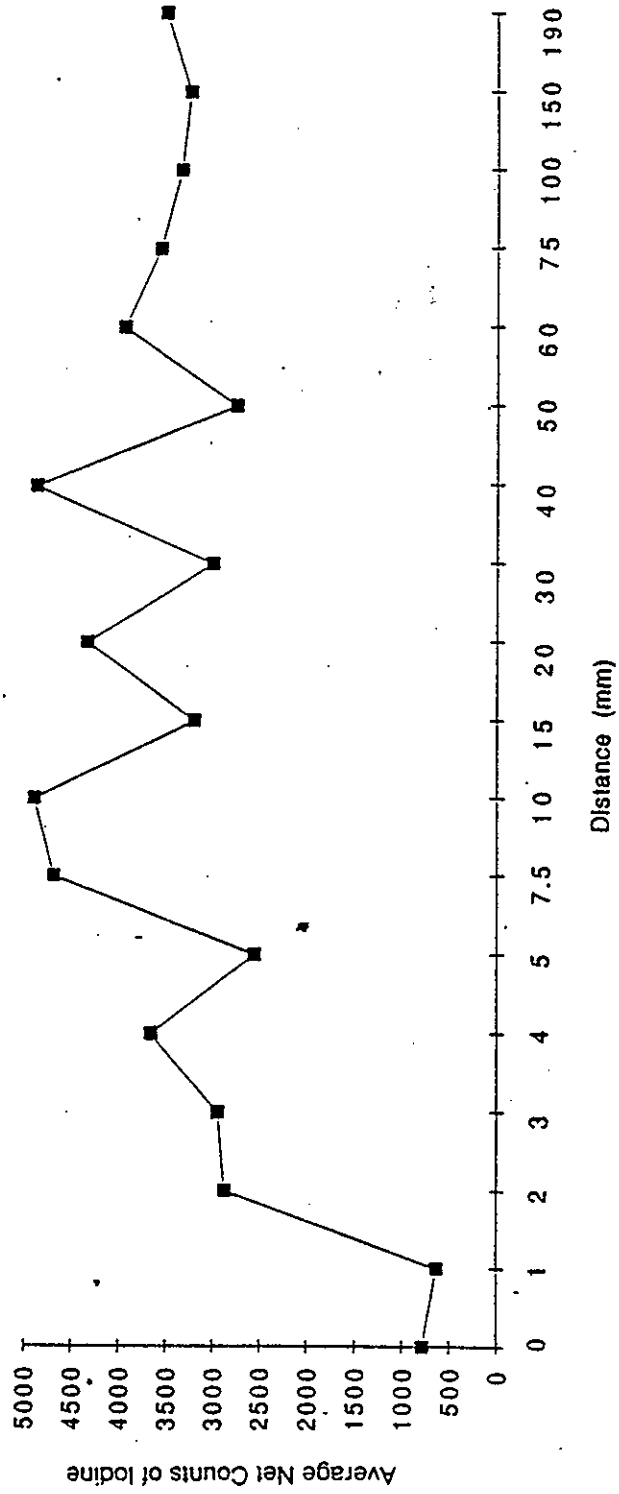

Figure F-3. Total Carbon Counts in the Grout Sample As a Function of Distance From the Soil-Grout Interface.

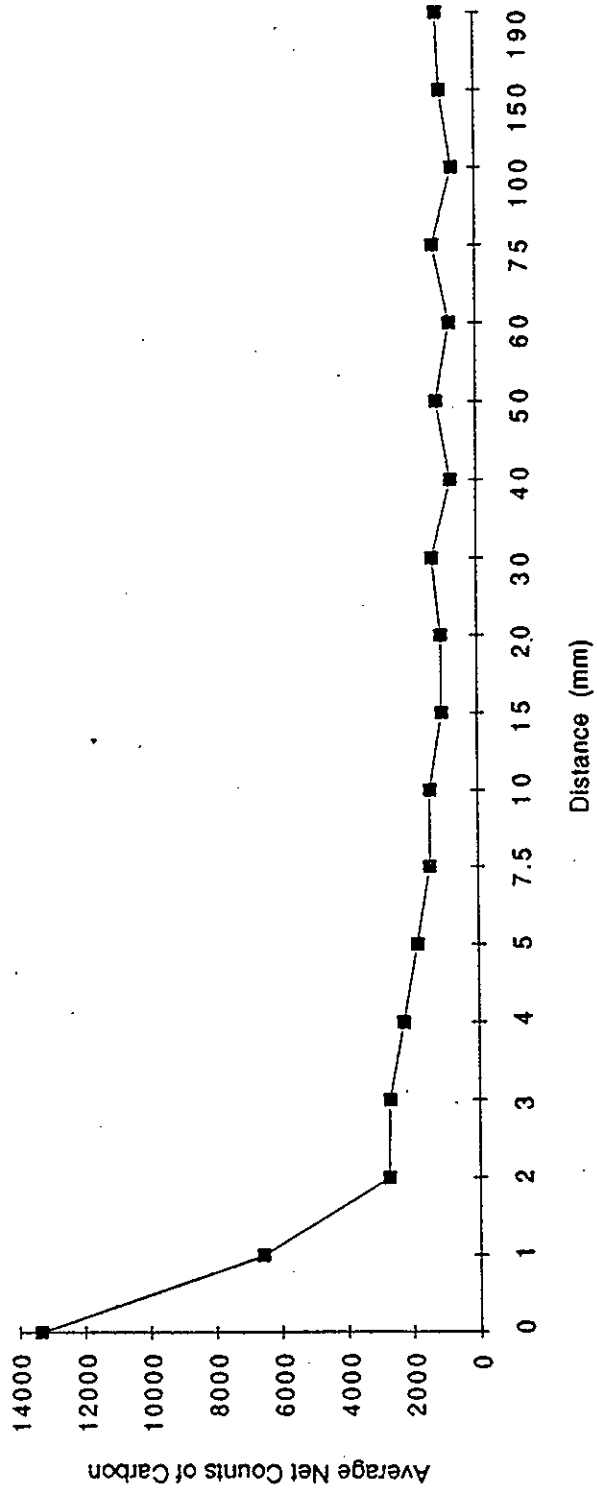

becomes depleted near the grout interface. The qualitative characterization of the iodine profile in one of the grout cylinders (Figure F-2) shows that iodine in the interior of the cylinder about an inch from the interface remains at its initial concentration. At the same time, the relative amounts of carbon are maximum at the interface (Figure F-3) and drop off into the interior of the cylinder. This evidence indicates that calcium carbonate and silica phases are forming in the pores of the grout at the interface and shutting off the diffusion of iodine from the interior. In essence, the permeability and diffusive properties of the grout material are being reduced in the grout reactive rind adjacent to the soil-grout interface, because interconnecting pores are being filled with secondary mineralization.

More rigorous experimental data must be developed to quantity the observations of these scoping studies. In particular, measurement of mass balance must be improved. Additionally, the effects of cracking in grouts, variable initial grout permeabilities, and advective flow of groundwater past the grout would be useful in evaluating the influence of natural mineralization reactions on contaminant release. Despite the qualitative nature of these data, the hypothesis that grout becomes less permeable with time under environmental conditions that occur at the Hanford Site is supported. Further, immobilization of contaminants may be considerably enhanced compared to the usual modeling assumption that contaminants are completely released from a waste form at release rates measured by standard leaching tests. Immobilization of large fractions of contaminants will reduce the expected groundwater concentrations and, therefore, dose estimates.

F.3 REFERENCES

Jenkins, J. F., 1993, "Corrosion Behavior of HY-80 Steel Type 304 Stainless Steel, and Inconel® Alloy 600 at 218-E-12B Burial Ground, Hanford, WA," Naval Facilities Engineering Service Center, Port Hueneme, California.

APPENDIX G1

CALIBRATION/TESTING OF VAM3D-CG COMPUTER CODE USING INJECTION TEST SITE DATA AT HANFORD

This page intentionally left blank.

APPENDIX G1

CALIBRATION/TESTING OF VAM3D-CG COMPUTER CODE USING INJECTION TEST SITE DATA AT HANFORD

A. H. Lu and R. Khaleel

ABSTRACT

A test facility comprised of an injection well at the center and a radial array of 32 monitoring wells was constructed in 1980 at the Department of Energy Hanford Site in southeastern Washington. The facility was used in late 1980 and early 1981 to conduct an infiltration and multiple tracer (i.e., chloride, nitrate, barium, rubidium, ^{85}Sr and ^{134}Cs) test, in which 45,000 L of liquid (in eleven increments) were injected at a depth of 4.7 m over a period of 133 days. Three-dimensional water content profiles, in layered, coarse sediments, were monitored to a depth of 18 m, by down-hole neutron probe measurements. The initial water contents were measured at 30-cm increments over the 300- to 1800-cm depths in all 32 observation wells. In situ gamma energy analysis data were collected to determine the distribution of radioactive tracers. The unique three-dimensional nature of the experiment, measurement of water content and radioactive tracers in situ, and the use of multiple injections provide an important data base to validate multidimensional, unsaturated zone flow and transport models.
A multidimensional, finite-element code is used to model the moisture plume at the injection site. Laboratory-measured moisture retention and unsaturated hydraulic conductivity data were obtained for the sediments. The model includes effects of layered heterogeneity, hysteresis, and saturation-dependent anisotropy. The preliminary results suggest that saturation-dependent anisotropy, enhanced by textural heterogeneities, is a significant process at the injection site. Extensive lateral spreading is suggested by both field data and modeling. Assuming a heterogeneous but isotropic medium for modeling result in predictions of significant vertical movement that did not occur during the field experiment.

G1.1.0 INTRODUCTION

The report summarizes the progress made during the Fiscal Year 1993 on the calibration/testing of the flow model for VAM3G-CG using the Injection Test Site in 200 East Area (Figure G1-1). The field experiment was conducted in 1980 and 1981 to provide data on the subsurface movement of water and contaminants at the Hanford site (Sisson and Lu, 1984).

The field data suggest an extensive lateral spreading of the moisture plume. Extensive lateral spreading has also been observed at other sites at Hanford (e.g., Routson et al., 1979; Price et al., 1979). Sisson and Lu compared field data from the Injection Site to those from a numerical model. Assuming a uniform isotropic media for the simulation resulted in predictions of moisture movement past the 18-m depth. This deep movement did not occur at the field site. The spreading was conjectured by Sisson and Lu as the result of sediment layering and anisotropy in hydraulic properties; they suggested that improved estimates of model parameters and model setup using information of the "natural" moisture content correlated with the site lithology should be considered a fruitful direction for further study.

As noted earlier, the field observations of Routson et al. (1979) and Price et al. (1979) suggest extensive lateral spreading of the moisture plume in Hanford sediments. Gelhar et al. (1985) suggest that the lateral migration is enhanced if the soil is stratified, the initial moisture content is low, the size of application area is small relative to the size of unsaturated zone, and the liquid application rate is low. These conditions are similar to those at the injection site. The dependence of lateral movement on moisture content suggests a moisture-dependent anisotropy of hydraulic conductivity. This is in accordance with the stochastic theory of Yeh et al. (1985a, b, c), who indicate that in stratified soils the effective hydraulic conductivity tensor is anisotropic with a tension-dependent degree of anisotropy. Other studies (e.g., Mualem, 1984; Mantoglou and Gelhar, 1987; Bear et al., 1987; McCord et al., 1991) also suggest that at higher tensions (low moisture contents) in stratified sediments lateral flow may be important. This is due to the fact that at a high tension, hydraulic conductivities of fine-textured soils are relatively high and water may prefer to spread laterally in finer soils than to move vertically through coarser soils.

VAM3D-CG computer code (Huyakorn and Panday, 1991) is a three-dimensional, variably saturated flow and transport code. The flow model is based on the pressure head form of Richards' equation, while the transport model is based on the advection-dispersion equation. The primary objective of this study is to test the applicability of VAM3D-CG computer code in simulating the moisture movement in the unsaturated subsurface sediments at the Injection Test Site. A second objective is to gain insight in field mechanisms, especially moisture-dependent anisotropy, in controlling lateral migration at the field site.

Figure G1-1. Location of Injection Experiment in 200 East Area of the Hanford Site.

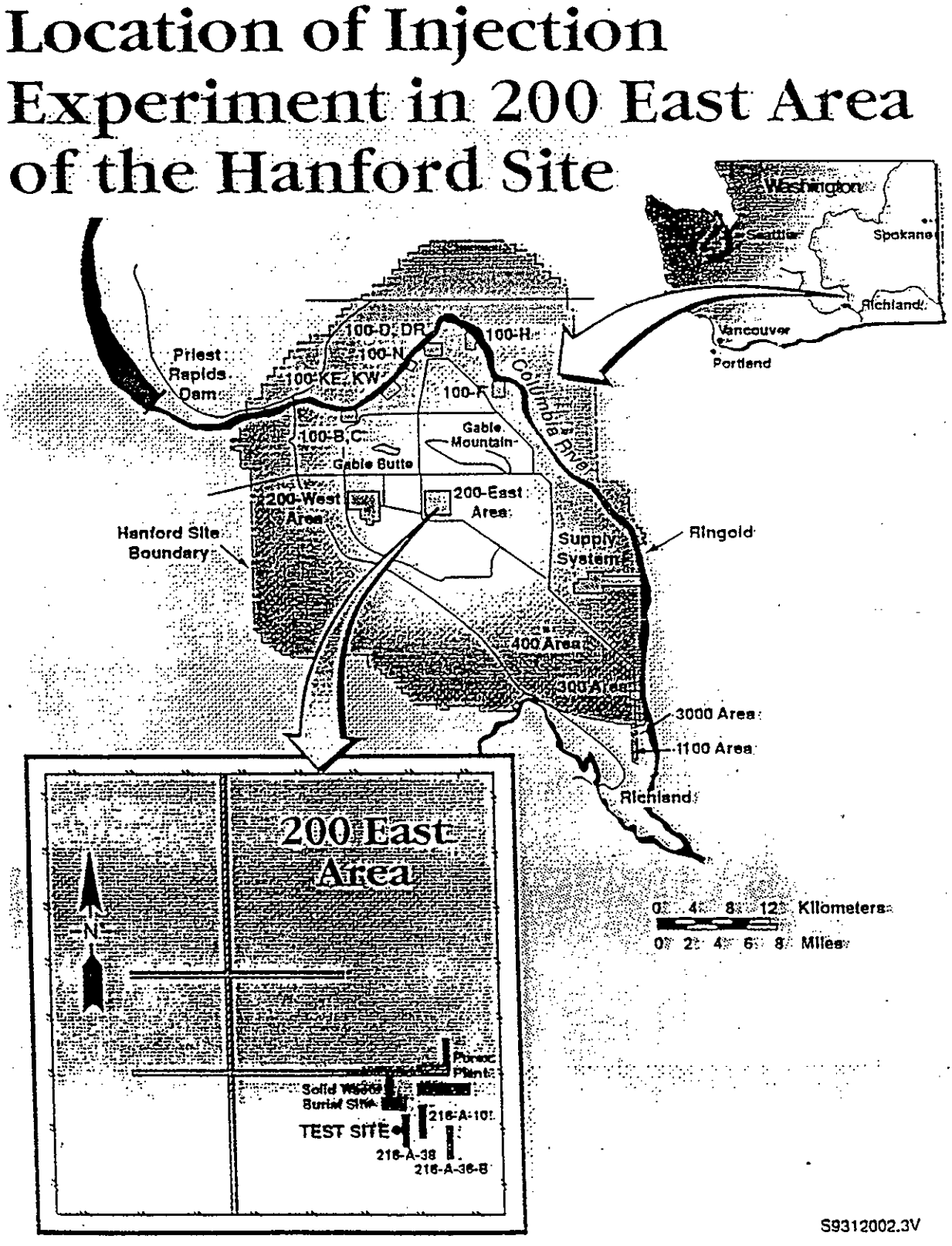

G1.2.0 FIELD DATA

G1.2.1 BRIEF DESCRIPTION OF FIELD EXPERIMENT

The field data for the Injection Test Site in the 200 East Area at Hanford Site are documented in Sisson and Lu (1984). A recent report (Fayer et al. 1993) combines the information in Sisson and Lu with unpublished laboratory and field data on the hydraulic properties of the sediments and core data collected at the end of the experiment. The entire experiment was conducted between 0- and 20-m depths, well within the Hanford Formation (about 60-m deep) and well above the water table (about 90-m deep). A plan view of the well system consisting of an injection well surrounded by 32 0.152-m (6-in) diameter observation wells is shown in Figure 2. A pump delivered each solution from a storage tank to the injection well, which was the only source of water and tracers to the sediments. Each observation well was constructed from three 6.1-m (20-ft) sections and one 1.52-m (5-ft) section of 0.152-m (6-in.)-diameter schedule 40 steel casing. The well numbering scheme is also shown in Figure G1-2.

Each injection consisted of filling the holding tank, adding the tracers, mixing the water and tracers, and then injecting the solution. About 3800 L (1000 gal) of water were delivered for each of ten consecutive weekly injections. An additional injection was executed nine weeks later. A 20-mL solution of the radiological tracers ^{85}Sr and ^{134}Cs were injected for first seven consecutive weekly injections. The tracer included calcium salts and additional sorbing tracers, barium and rubidium. ^{134}Cs was chosen because it is a gamma emitter and undergoes strong sorption by the sediments. ^{85}Sr was chosen because it is a gamma emitter but is moderately sorbed by sediments.

The cumulative volumes of liquid injection for injection 1 to 6 are presented in Figure G1-3. The observation that these lines are nearly parallel and straight indicates a nearly constant infiltration rate.

Field data was obtained by lowering sensors to the desired depths in the observation wells. The sensors used in the experiment included neutron probes, Geiger-Muller (GM) probes, gamma energy analysis probes, and gamma-gamma probes.

Three Campbell-Pacific Nuclear (CPN) neutron probes were used. The diameter of the probes was slightly less than 5.08-cm (2-in), smaller than the internal diameter of the 15.2-cm (6-in) well casing. A single calibration equation was generated for the three probes from data obtained from two sets of calibration standards (Sisson and Lu, 1984).

During installation of the observation wells, most of drilled sediments were deposited on the ground. The sediments from the selected depths in three wells, however, were collected in plastic bags as they were blown out of the wells. Eight samples were collected from well A-7 (E24-79), three samples were collected from well E-1 (E24-92), and six samples were collected from well E-7 (E24-95).

Plan View of Wells and Construction Details

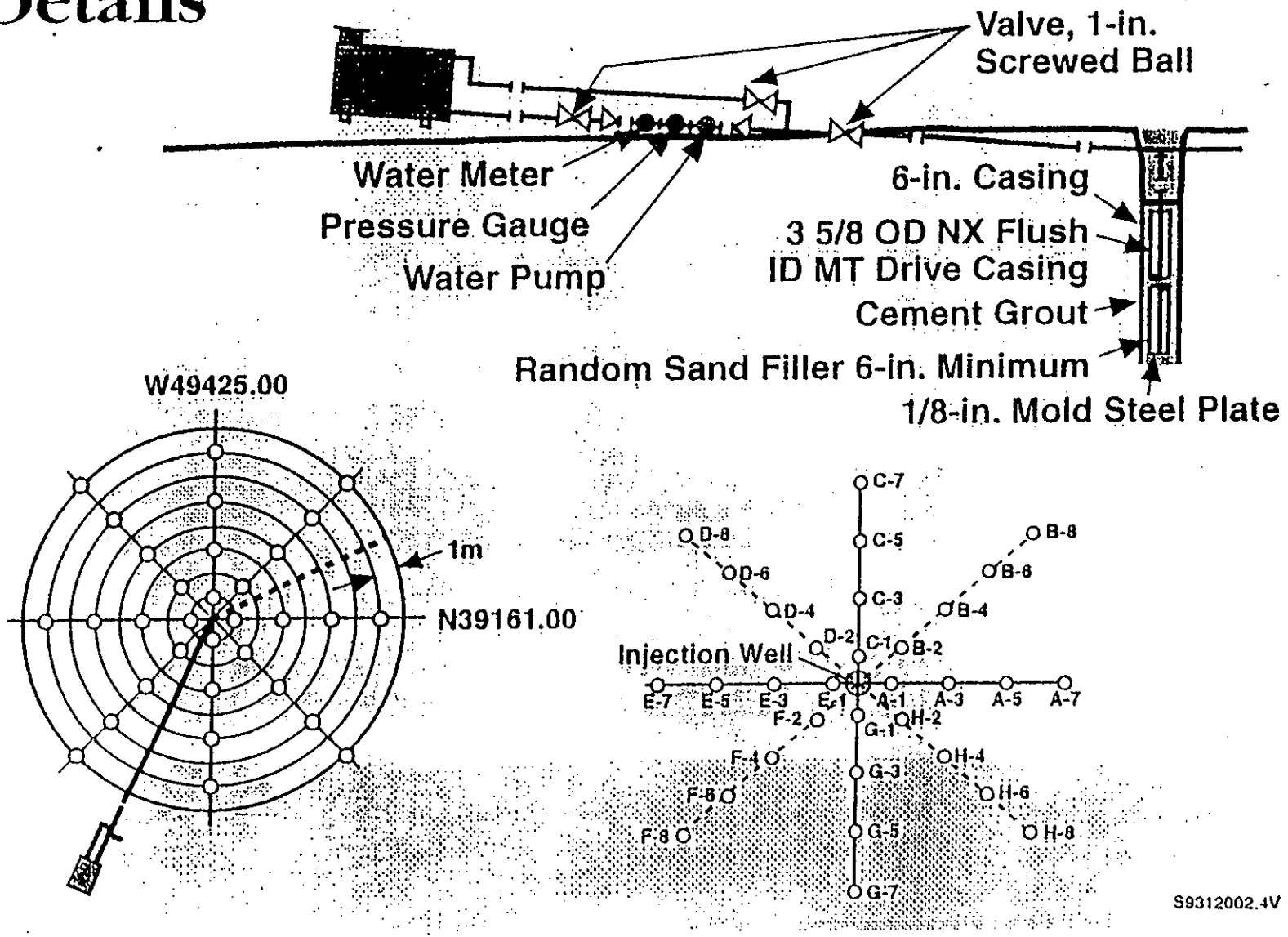

Figure G1-2. Plan View of Wells and Construction Details.

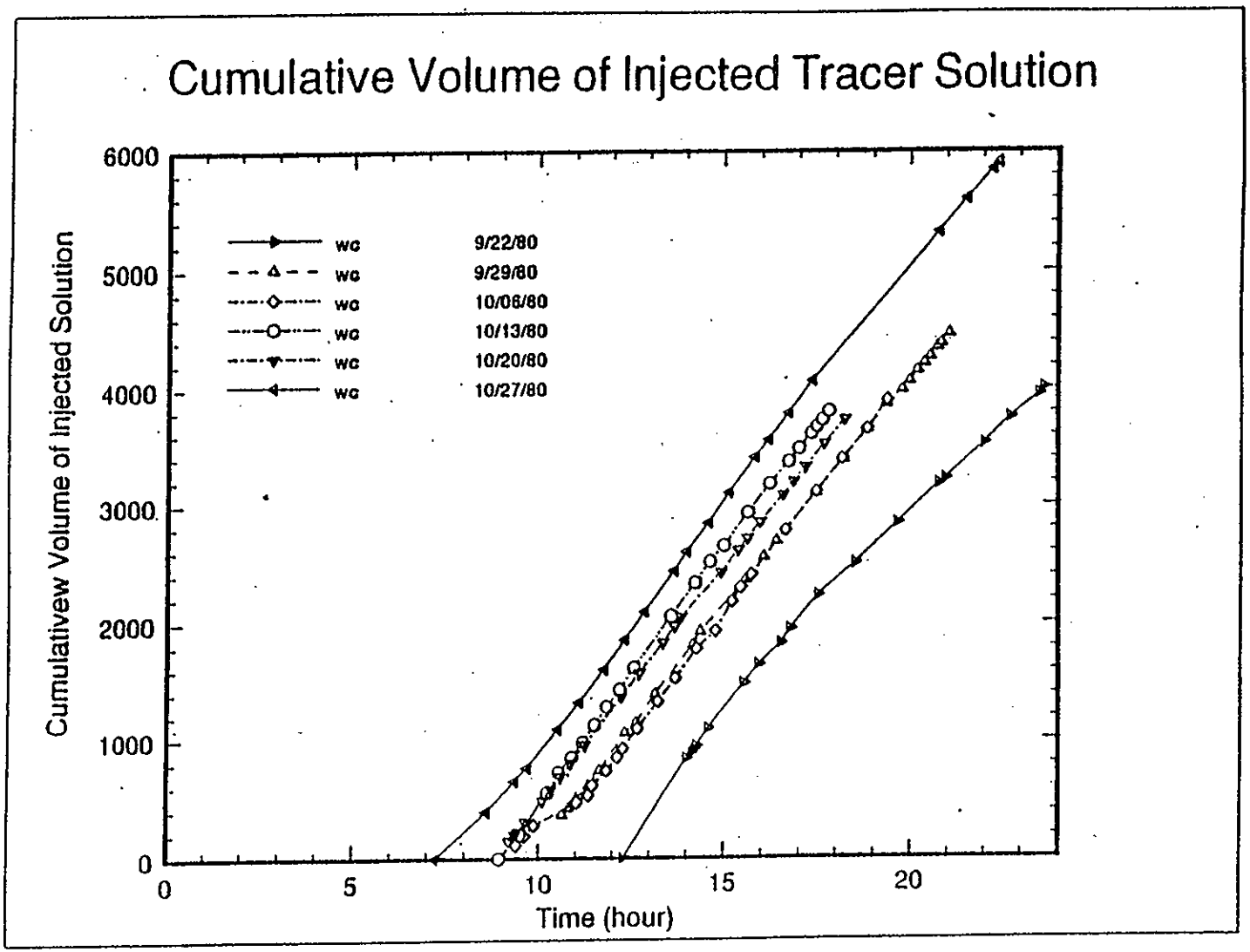

Figure G1-3. Cumulative Volume of Injected Tracer Solution.

West-East Lithologic Cross Section

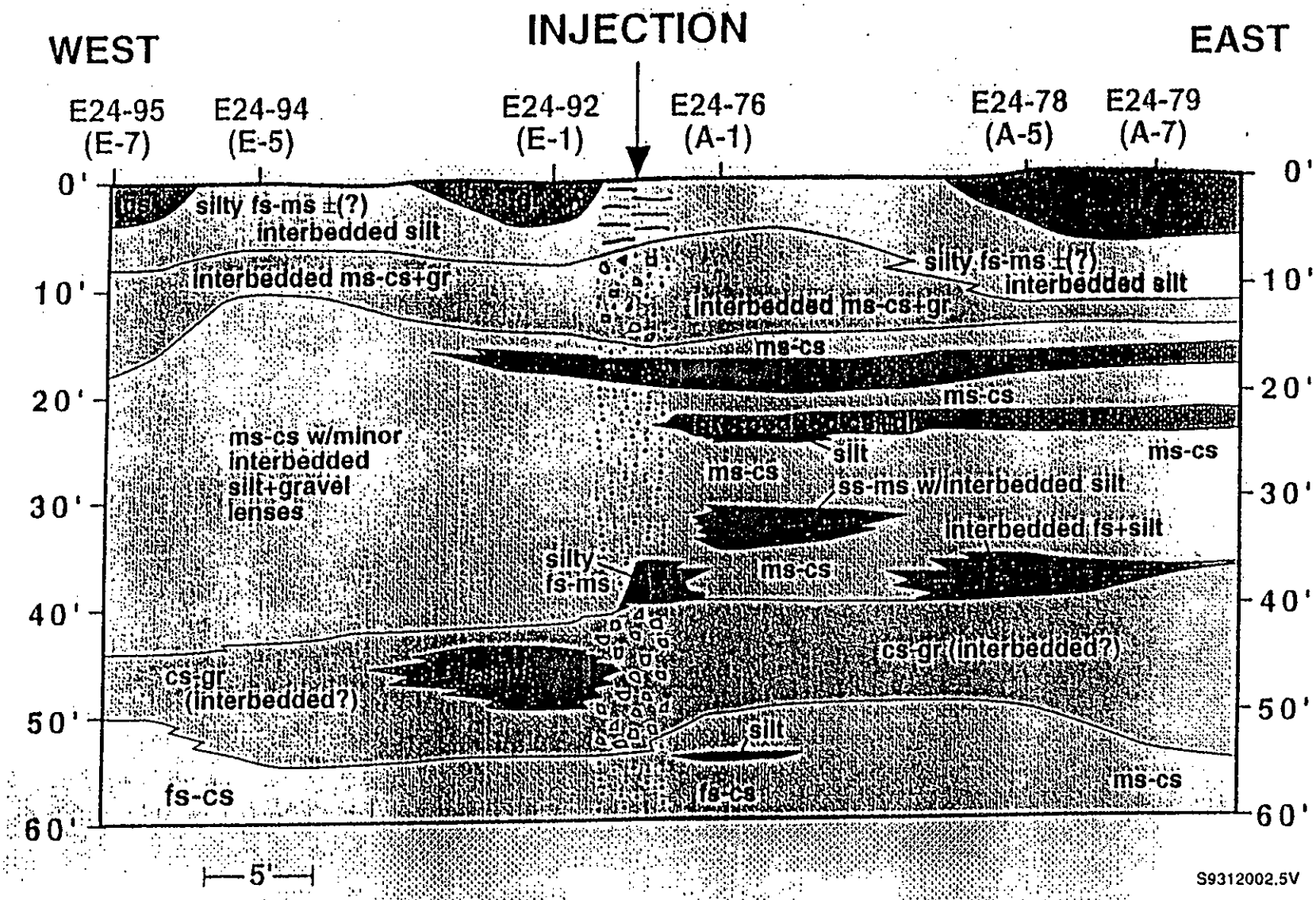

Figure G1-4. West-East Lithologic Cross Section.

G1.2.2 SITE LITHOLOGY

Figure G1-4 is lithologic cross sections sketched from the driller's logs. Figure G1-4 shows one of the cross sections, W-E cross section, based on the information from A and E well series.

In view of Figure G1-4, five general units or horizons are present. From top to the bottom their general characteristics are as follows.

The first interval consists of silty fine- to medium-grained sand. It is not clear from the logs if the silts occur mixed with the sands or as interbeds. On one of the cross sections, several boreholes show medium- to coarse-grained sand and gravel locally overlying this silty interval. The interval covers approximately from the land surface to about 3 m depth and varies from place to place.

The second interval is dominated by medium- to coarse-grained sand and gravel. Based on the examination of probable outcrop analog for this type of deposit, this material probably consists of variably interbedded horizons of sand and gravel. The scale of interbed in outcrops generally ranges from 0.5 to 2 ft. Many of these gravel and sand beds may display an "open-framework" texture. On the basis of the log descriptions, it is probable that much of this interval is open-framework gravel dominated. The interval covers approximately from about 3 m to 6 m depth and varies from place to place.

The third interval is comprised of a variety of deposits. In general it appears to be dominated by medium- to coarse-grained sand. This sand contains numerous lenticular interbeds of gravel and silty sand. Based on the examination of outcrops of potentially analogous deposits, this interval is very well stratified, displaying cross-bedding, horizontal bedding, and channel cut-and-fill. The interval covers approximately from about 6 m to 12 m depth and varies from place to place.

The fourth interval is dominated by coarse-grained sand and gravel. Several lenses containing little or no gravel and dominated by medium- to coarse-grained sand also are found. Outcrop analogs indicate strata such as this interval dominated by sand and containing both random, unbedded pebbles, and gravel interbeds. The interval covers approximately from about 12 m to 16 m depth and varies from place to place.

The lowest horizon consists of fine- to coarse-grained sand with minor interbedded silt. The sands, again based on outcrop analogs, are very well stratified. The interval covers approximately from about 16 m to 18 m depth and varies from place to place.

G1.2.3 INITIAL MOISTURE CONTENT

The selected initial moisture contents measured from 32 observation wells are plotted in Figures G1-5a through G1-5d. Figure G1-5a displays the moisture content profiles for wells A-1, A-3, A-5 and A-7. Figures G1-5b, G1-5c and G1-5d show the moisture content profiles for wells B-2, B-4, B-6 and B-8, C-1, C-3, C-5 and C-7, and D-2, D-4, D-6 and D-8, respectively.

Figures G1-5a, G1-5b, G1-5c, and G1-5d. Selected Initial Moisture Contents from Observation Wells.

Figure 5-b.

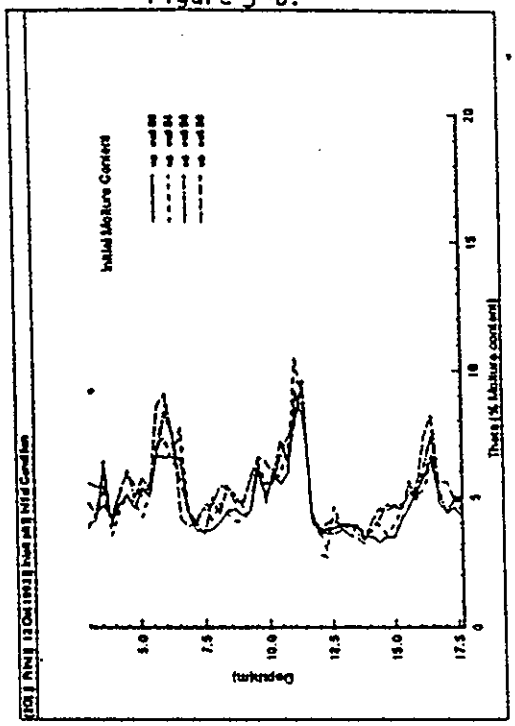

Figure 5-d.

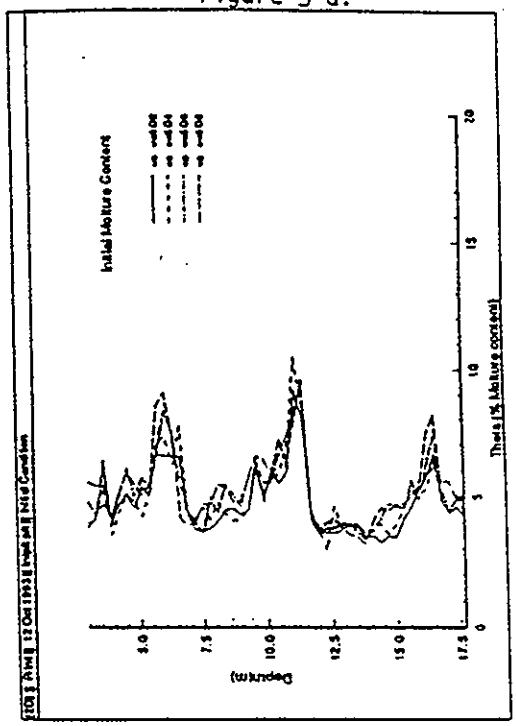

Figure 5-a.

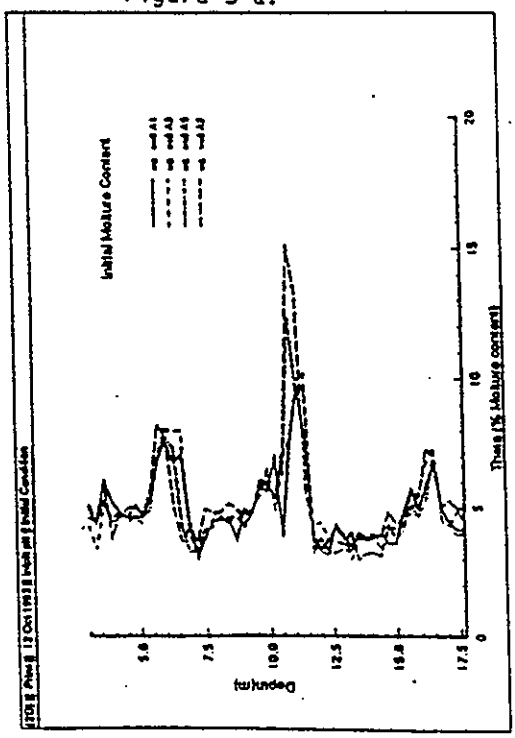

Figure 5-c.

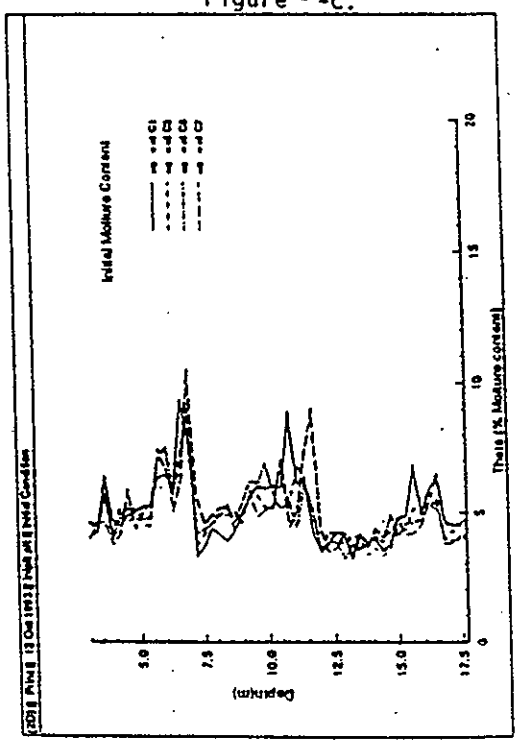

Field Initial Moisture Contents

The moisture profile data generally corresponds to observed geologic trends in the monitoring wells. Generally, increased moisture contents occur at two main lithologic changes: (a) where there are marked changes from one lithology to another, and (b) where significant silt-rich deposits, either silty sands or silt beds, occur. On most of the sections the uppermost increased moisture content areas, generally above 7.5 m, occur because of a combination of the preceding two factors. The major moisture increases observed between 10 and 12.5 m almost all correspond with zones where a significant number of silt-rich sands and silt interbeds occur. Most of the high moisture zones near the base of the sections, between 15 and 17.5 m, correspond to a change from coarse-grained sand and gravel above to fine- to coarse-grained sand below. A few logs suggest silt-rich zones may also be present and these could also be a factor contributing to the presence of this lowermost high moisture zone. At several locations there are high moisture zones that do not correspond to anything observed during drilling. It seems most likely that these zones, which are generally in the middle of the sections between 8 and 15 m, correspond to unlogged silt-rich intervals.

G1.2.4 FIELD DATA VISUALIZATION

Figure G1-6a shows the moisture contents as function of time at a radius of 1 m and a depth of 6 m. The time span in this plot is 150 days after the first injection began. The distinct response of the soil moisture content to the ten weekly injections is clearly apparent. After ten weekly injections, the moisture contents generally decline but at a slightly different rate. This indicates that the retention capabilities of the soils in the four wells are different. Figure G1-6b shows the data at a radius of 2 m and a depth of 6 m. A similar distinct response to the ten weekly injections is shown. Figure G1-6c shows the data at a radius of 3 m and a depth of 6 m. The moisture contents in the A well (east) are generally the highest, whereas those in the E well (west) the lowest. This suggests a preferential flow corresponding to probably variably silt-rich interbedded horizons or lenses. Figure G1-6d shows a similar feature with the most preferential flow being in the south-east (H well) and the lowest in the north-west (D well).

Figures G1-7a through G1-7d show the moisture contours at the cross sections- east-west, northeast-southwest, north-south, and northwest-southeast, respectively, at 59 days after the first injection began. Again, we see a preferential flow. The moisture plume are generally separated vertically into two layers. The second-layer plume shows a downward but mostly eastward enhancement (Figure G1-7a) and a downward but mostly south-eastward enhancement (Figure G1-7d). The high moisture contents generally corresponds to silt-rich deposits, either silty sands or silty beds.

G1.3.0 MODEL SET-UP

G1.3.1 STRATEGY OF CALIBRATION/TESTING

Approaches of this study were to: a. correlate the initial moisture data taken from the 32 observation wells and the lithology of the injection site.

Figures G1-6a, G1-6b, G1-6c, and G1-6d. Moisture Contents as a Function of Time.

Figure 6-a.

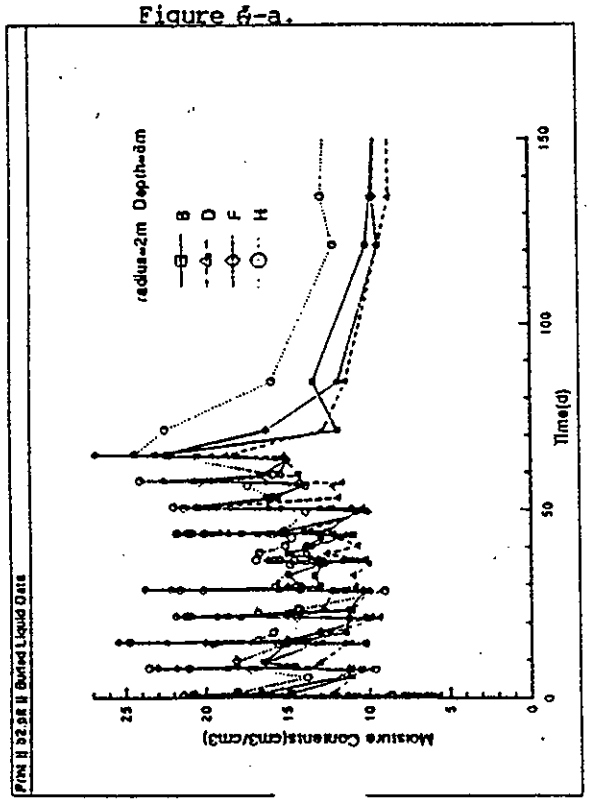

Figure 6-c.

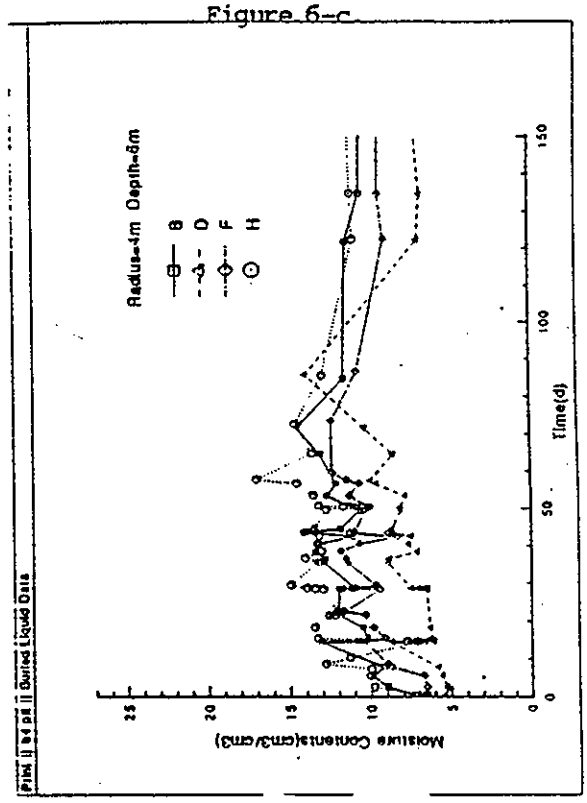

Figure 6-b.

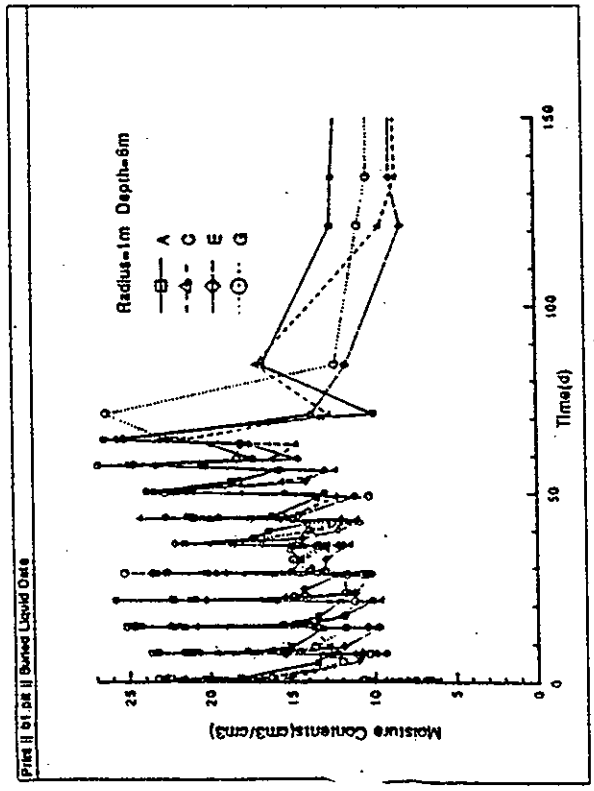

Figure 6-d.

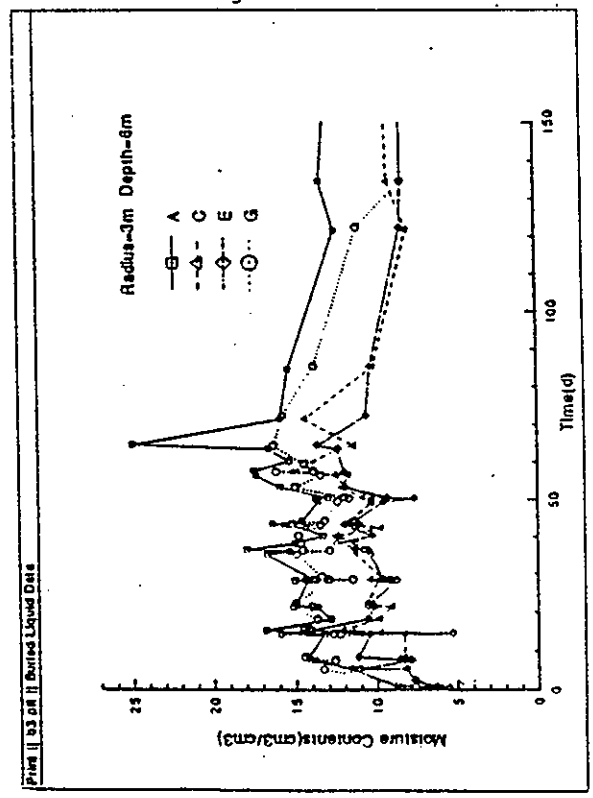

Figures G1-7a, G1-7b, G1-7c, and G1-7d. Moisture Content Cross Sections.

Figure 7-b.

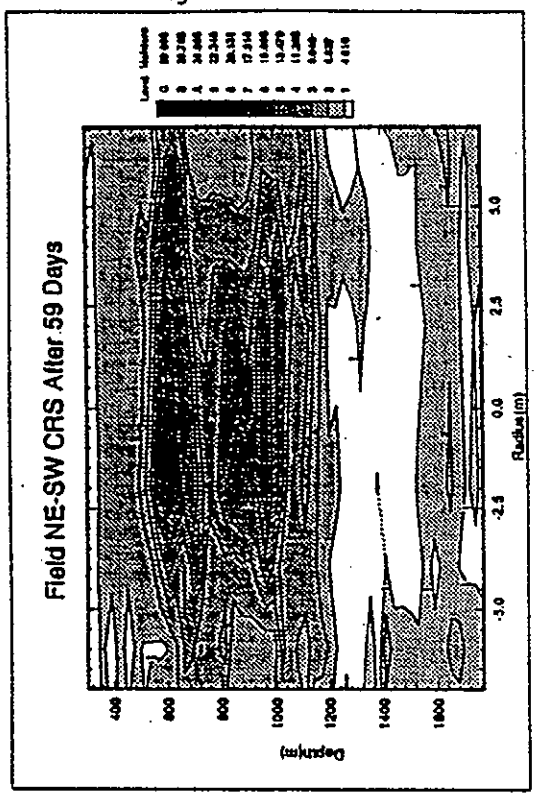

Figure 7-d.

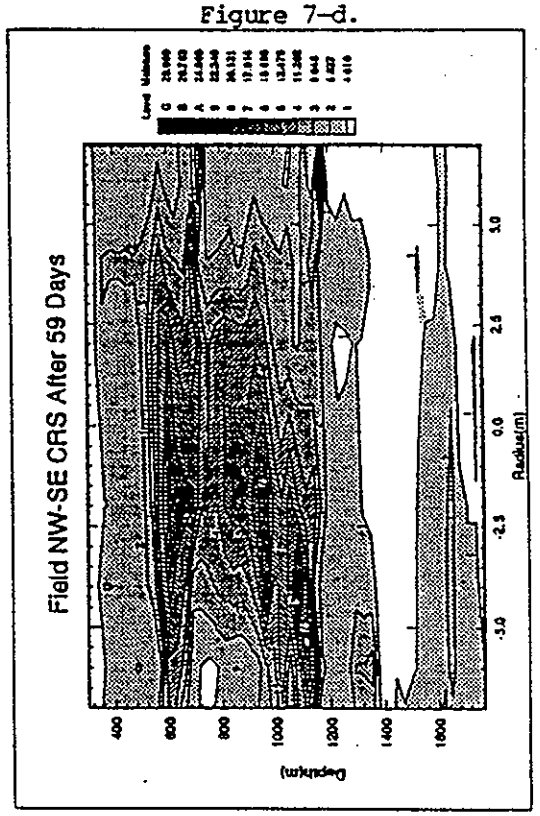

Figure 7-a.

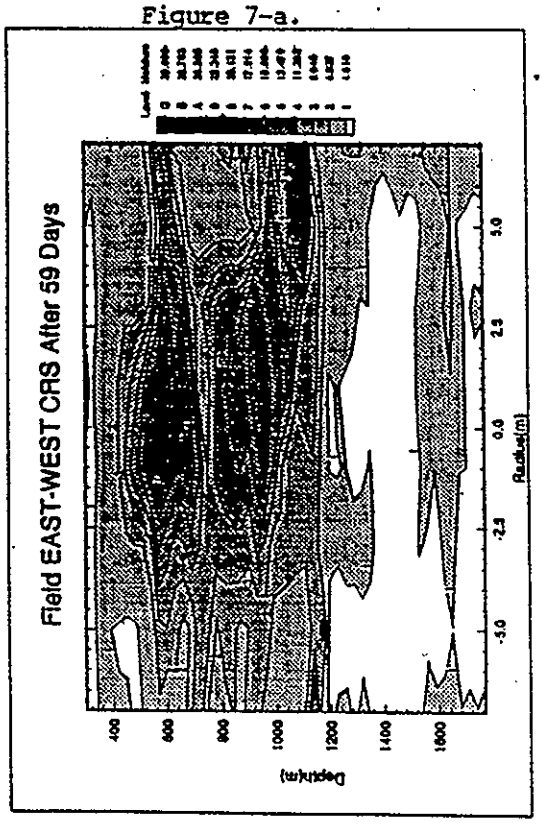

Figure 7-c.

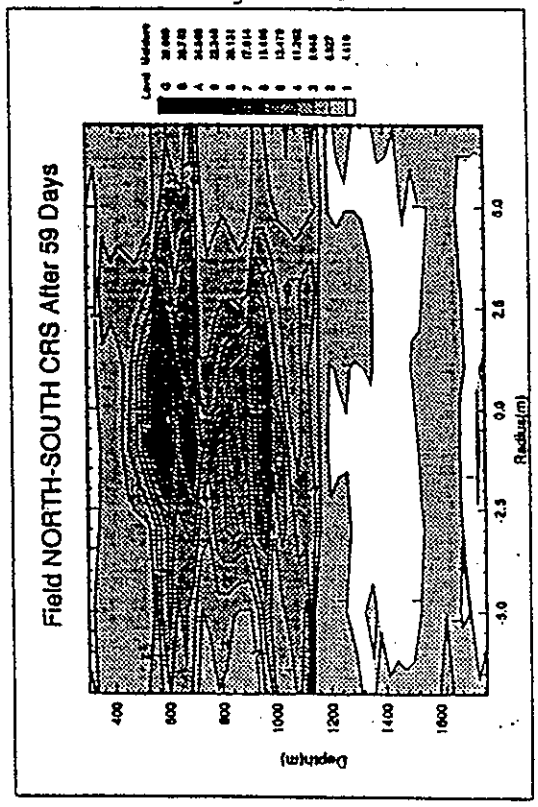

The lithology of the site was depicted based on driller's logs. This information was used to interpret the initial moisture contents and to set up model layers for the injection site; b. assign soil properties to each layer from available soil samples taken from the site at various depths; and c. analyze a number of different modeling scenarios which differ in processes. Among the physical processes modeled are isotropy, hysteresis, and saturation dependent anisotropy.

In this paper, focus was on the water movement. An accurate description of water movement is an essential first step in assessing the migration of solute which is of ultimate environmental concern.

G1.3.2 FINITE ELEMENT MESH

Figure 8 shows the finite element mesh used with soil type numbers. The elements were configured for axial symmetric flow in a cylindrical coordinate system with layers based on initial moisture contents and available characteristic curves analyzed from soil samples. The water was injected evenly at three nodal points at depths 4.5, 5.1, and 5.7 m on the left edge, respectively. At these injection elements, the water flux was specified so that the flux integrated over the surface equaled the rate of injection.

G1.3.3 SOIL CHARACTERISTICS

Construction of a geometric model to represent injection site is limited by the scale of geologic heterogeneity (see Figure G1-4) and amount of hydrologic data available to distinguish them. Ten soil samples were used to represent ten horizons. The intervals of each horizon were estimated from the observation of initial moisture contents shown in Figures G1-5a through G1-5d. Soil type numbers 1 and 2 correspond to the first lithologic interval. The soil type number 3 corresponds to the second lithologic interval. Soil type number 4, 5, and 6 correspond the third lithologic interval. Two high moisture spikes embodied in the interval (see Figures G1-5a through G1-5d) suggested that three soil types should be used. The soil type number 7 corresponds to the fourth lithologic interval. Soil type numbers 9 and 10 correspond to the fifth lithologic interval.

A total of 10 from 17 samples analyzed to generate the moisture retention and unsaturated hydraulic conductivity curves were used to represent 10 soil types. The laboratory-measured moisture retention data and unsaturated hydraulic conductivity were fitted simultaneously with the van Genuchten-Mualem equation using the computer code RETC (van Genuchten, 1978). An unsaturated flow apparatus (UFA™), based on the centrifuge technique, was used to measure the unsaturated hydraulic conductivities (Conca and Wright, 1990).

G1.3.4 MODEL INITIAL CONDITION

Model is a simplified reality. For each stratified layer, the heterogeneity is treated as an equivalent homogeneous system because of lacking of hydrologic data available to distinguish them. A direct employment

Figure G1-8. Axisymmetric Model for Injection Site Simulation Material Type Table.

(L2DGEOM 2.00)
(90993112759)

AXISYMMETRIC MODEL FOR INJECTION SITE SIMULATION
MATERIAL TYPE TABLE

90993110721

1	1	1	1	1	1	1	1	1	1	1	1	1	1	1	1
2	2	2	2	2	2	2	2	2	2	2	2	2	2	2	2
3	3	3	3	3	3	3	3	3	3	3	3	3	3	3	3
3	3	3	3	3	3	3	3	3	3	3	3	3	3	3	3
3	3	3	3	3	3	3	3	3	3	3	3	3	3	3	3
3	3	3	3	3	3	3	3	3	3	3	3	3	3	3	3
3	3	3	3	3	3	3	3	3	3	3	3	3	3	3	3
4	4	4	4	4	4	4	4	4	4	4	4	4	4	4	4
4	4	4	4	4	4	4	4	4	4	4	4	4	4	4	4
4	4	4	4	4	4	4	4	4	4	4	4	4	4	4	4
4	4	4	4	4	4	4	4	4	4	4	4	4	4	4	4
5	5	5	5	5	5	5	5	5	5	5	5	5	5	5	5
5	5	5	5	5	5	5	5	5	5	5	5	5	5	5	5
5	5	5	5	5	5	5	5	5	5	5	5	5	5	5	5
6	6	6	6	6	6	6	6	6	6	6	6	6	6	6	6
6	6	6	6	6	6	6	6	6	6	6	6	6	6	6	6
6	6	6	6	6	6	6	6	6	6	6	6	6	6	6	6
7	7	7	7	7	7	7	7	7	7	7	7	7	7	7	7
7	7	7	7	7	7	7	7	7	7	7	7	7	7	7	7
8	8	8	8	8	8	8	8	8	8	8	8	8	8	8	8
8	8	8	8	8	8	8	8	8	8	8	8	8	8	8	8
9	9	9	9	9	9	9	9	9	9	9	9	9	9	9	9
10	10	10	10	10	10	10	10	10	10	10	10	10	10	10	10

Y POSITION (M): 0.0, -2.0, -4.0, -6.0, -8.0, -10.0, -12.0, -14.0, -16.0, -18.0, -20.0

X POSITION (M): 0.0, 0.5, 1.0, 1.5, 2.0, 2.5, 3.0, 3.5, 4.0, 4.5, 5.0, 5.5, 6.0, 6.5, 7.0, 7.5, 8.0, 8.5, 9.0, 9.5

of the heterogeneous initial moisture contents did not produce a stable initial flow field. The unit gradient theory was used to estimate the model initial condition by assuming a constant recharge rate. Using the average initial moisture contents at various depths (see Figures 5a through 5d) and the characteristic curves, we estimate the recharge rate for the injection site to be less than 2 cm/year. The estimate was crude and uncertainty was large, but it showed a remarkable consistency for all the soil types, including the one showing the highest moisture spike.

A steady-state computer run using 2 cm/yr recharge rate was performed and the results were used as initial head input for calibration/testing run. The vertical moisture distribution of the model initial condition is shown in Figure G1-9. The model initial moisture content distribution provides a fairly good simulation for the highest moisture spike occurring at 10 m-12 m depth, but fail to show the high moisture spike occurring at 5 m-7.5 m depth. There were no samples taken at that depth for moisture characteristic curves.

G1.4.0 MODEL SCENARIOS

The preceding visualizations of the liquid movement suggest some inherent complexities in modeling the physical process itself. This is due to the fact that the system parameters are not constant, but vary in some manner about their nominal values.

As discussed earlier, the influence of spatial heterogeneities in soil properties on field-scale flow has been investigated by several researchers (Yeh et al., 1985a,b,c and Mantoglou and Gelhar, 1987). Yeh et al. (1985b) developed the following expression for anisotropy as a function of the pressure head:

$$a=\frac{(K_s k_r)_x}{(K_s k_r)_z}=\exp\left[\frac{\sigma_f^2+\sigma_\beta^2 H^2}{1+\lambda A \cos\gamma}\right] \qquad \text{(G1-1)}$$

where:

- $\sigma_{f_2}^2$ = variance of ln K_s random field,
- σ_β^2 = variance of the slope of the ln K vs. ψ relationship,
- H = mean value of ψ,
- λ = correlation length for both lnK_s and β random field in the direction perpendicular to stratification,
- A = mean slope of ln K vs. ψ, and
- γ = angle between the soil layer stratification and the horizontal.

$(K_s k_r)_x$, $(K_s k_r)_z$ are conductivities parallel and perpendicular to stratification, where K_s is the saturated conductivity and k_r is the relative conductivity. Equation (G1-1) was incorporated in the numerical flow code VAM2D (Kool and Wu, 1991) in a straight-forward manner. Provided the

Figure G1-9. Model Initial Moisture Contents.

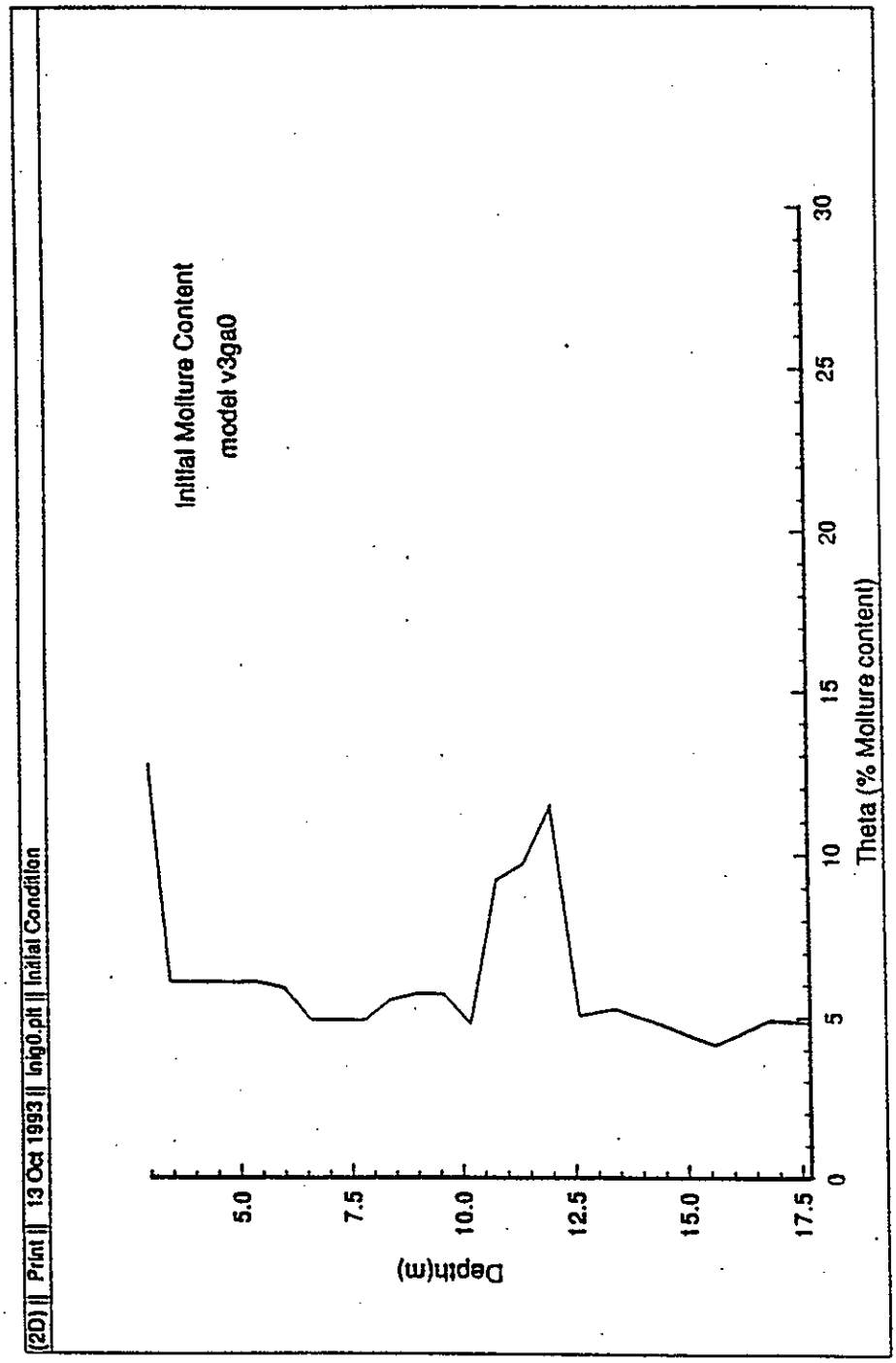

necessary statistical parameters are known, it allows evaluation of this aspect of the stochastic unsaturated flow theory in a deterministic flow simulation. Using equation (1), McCord et al. (1991) has reported a good qualitative agreement between the field observations of flow behavior in unsaturated soil and the model simulations.

VAM3D has been modified to simulate the effect of saturation dependent anisotropy on unsaturated flow by using equation (G1-1) to evaluate anisotropy as a function of pressure head (Huyakorn and Panday, 1992). This requires input values of variables σ_f^2, σ_β^2, λ and γ. The parameter A can be treated either as an input variable or be evaluated by VAM3D as the derivative of the $\ln[k_r(\psi)]$ relation.

In this study, simulation scenarios are postulated representing various conceptual models of key processes controlling flow at the injection site. Based on the field data and experience gained in previous modeling effort (Sisson and Lu, 1984), four different model simulation scenarios were evaluated.

1. Non-uniform, isotropic media with spatial variation of hydraulic properties and initial conditions reflecting initial field moisture contents as close as possible.

2. Same as scenario 1, except that the effects of hysteresis in the moisture retention curves are included in the model simulations.

3. Same as scenario 1, with the exception that the saturation-dependent anisotropy is included in the model simulation.

4. A variant of scenario 3 with a smaller correlation length.

G1.4.1 SCENARIO 1: NON-UNIFORM, ISOTROPIC MEDIA

Two sets of moisture retention data, drying and wetting, were analyzed in the laboratory. For drying (drainage) curves, an option was chosen in RETC run to fit model parameters to measured moisture retention and hydraulic conductivity data simultaneously. In this process, K_s value is not fixed. For wetting (imbibition) curves, an option was chosen to fit retention parameters to measured moisture retention data. The fitted retention parameters are subsequently used to predict the hydraulic conductivity functions. This option assumes that the initial estimates for K_s remain unaltered during the parameter optimization process. The fitted parameters for both drying and wetting curves are listed in Table G1-1. For one of the material types, #6, both drying and wetting moisture retention and hydraulic conductivity curves are displayed graphically in Figures G1-10-a and G1-10-b, respectively.

Only drying curves are used in scenario 1. The horizontal and vertical conductivities were assumed to be equal for all the soil types.

Table G1-1. Injection Test Site

Sample# (Mat.#)	2-2225 (5)	2-2226 (7)	2-2227 (9)	2-2228 (8)	2-2229 (10)	2-2230 (1)	2-2231 (2)	2-2232 (3)	2-2233 (4)	2-2234 (6)
Well #	299-E24-92	299-E24-92	299-E24-92	299-E24-95	299-E24-95	299-E24-79	299-E24-79	299-E24-79	299-E24-79	299-E24-79
Depth (m)	9.75	15.24	18.29	15.24	18.29	1.83	3.05	4.88	7.92	10.97
$\theta_{r\ dry\ \&\ wet}$	0.0350	0.0300	0.0240	0.0230	0.0250	0.0590	0.0540	0.0300	0.0310	0.0090
$\theta_{s\ dry}$	0.3822	0.3801	0.3924	0.4278	0.4408	0.3646	0.3055	0.4033	0.4488	0.3434
$\theta_{s\ wet}$	0.3053	0.2573	0.3190	0.2709	0.3455	0.3712	0.2755	0.3329	0.2933	0.2642
α_{dry} (1/cm)	0.0229	0.0701	0.0575	0.0669	0.0685	0.0078	0.0109	0.0658	0.0737	0.0746
α_{dry} (1/m)	2.29	7.01	5.75	6.69	6.85	0.78	1.09	6.58	7.37	7.46
α_{wet} (1/cm)	0.0512	0.1125	0.1005	0.1246	0.1545	0.0251	0.0299	0.1313	0.1063	0.1448
α_{wet} (1/m)	5.12	11.25	10.05	12.46	15.45	2.51	2.99	13.13	10.63	14.48
n	4.6584	2.5823	2.3647	2.8331	2.4275	2.0399	1.5362	2.1882	2.3498	1.5636
m = 1-1/n	0.7853	0.6128	0.5771	0.6470	0.5881	0.5098	0.3490	0.5430	0.5744	0.3604
K_s (cm/s)	4.47E-4	5.64E-3	6.54E-3	3.66E-3	1.22E-2	6.21E-5	6.56E-5	7.31E-3	4.91E-2	2.46E-3
K_s (m/yr)	141.0	1778.6	2062.5	1154.2	3847.4	19.6	20.69	2305.3	15484.2	775.8
Soil Type	Loamy Sand	Sandy Loam	Loamy Sand	Sandy Loam	Sandy Loam	Silt	Silt	Sandy Loam	Loamy Sand	Sandy Loam

Note: Gravel corrections have been made

Figure 10-a.

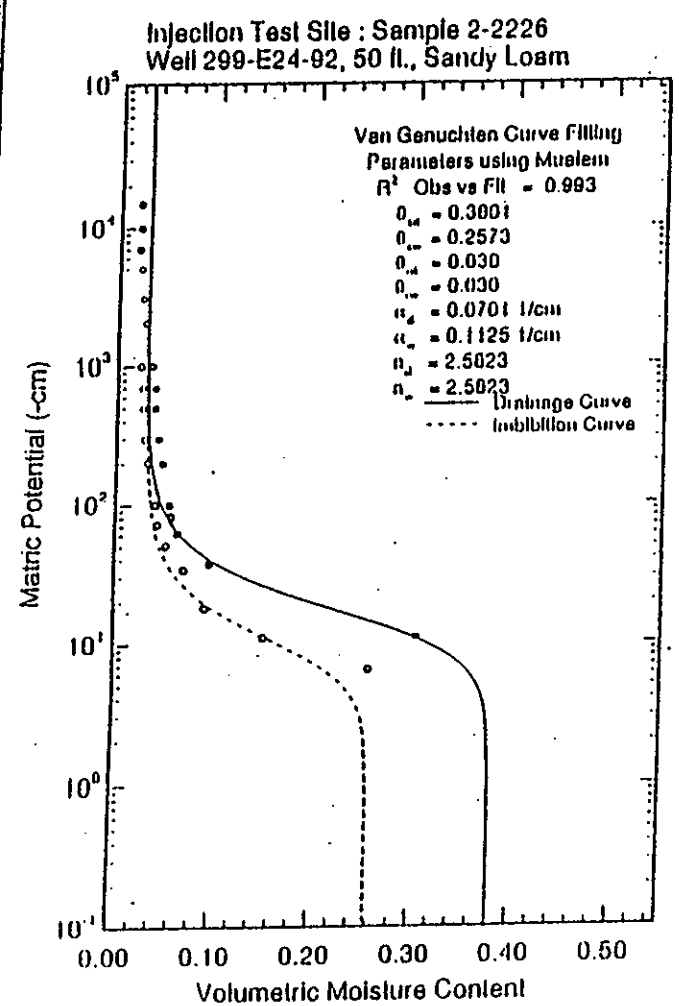

Figure 10-b.

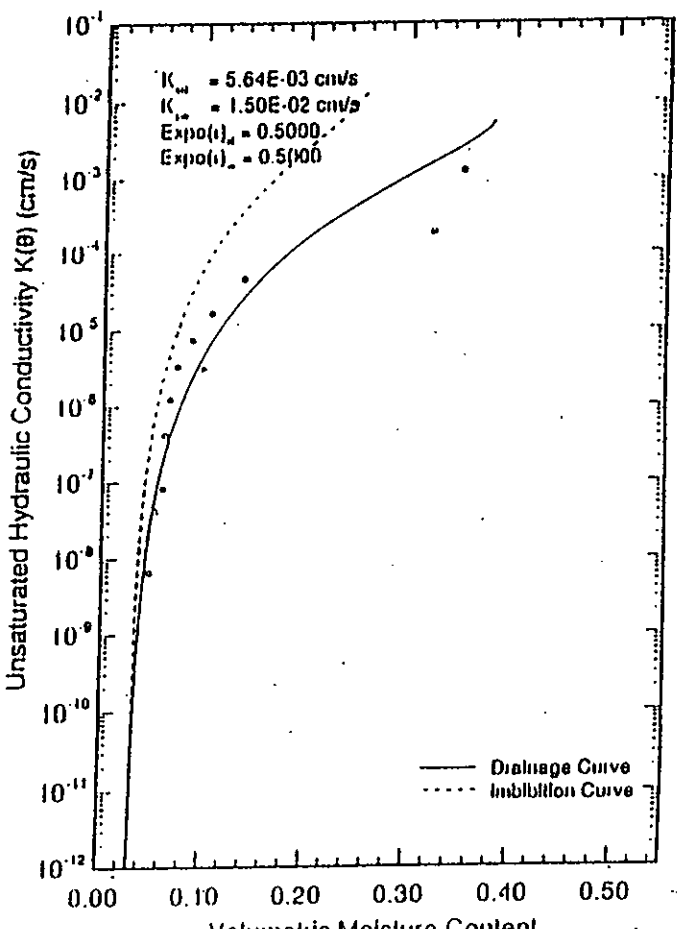

Figures G1-10a and G1-10b. Volumetric Moisture Content.

G1.4.2 SCENARIO 2: SAME AS 1, BUT WITH HYSTERESIS

This scenario was designed to evaluate the possible influence of soil moisture hysteresis on the infiltration and redistribution of water. The VAM3D computer code has the ability to model the hysteresis in the $\theta(\psi)$ relation, using the procedure described by Kool and Parker (1987). In addition to the retention curves and hydraulic conductivity curves (drying) used in scenario 1, a set of wetting curves are also used in the numerical simulation. The horizontal and vertical conductivities were again assumed to be identical for all the soil types.

G1.4.3 SCENARIO 3: SAME AS 1, BUT WITH SATURATION DEPENDENT ANISOTROPY

This scenario examines the effect of the saturation dependent anisotropy on the lateral spreading. Equation 1 provides an expression for the anisotropy ratio, but not for the actual, directional relative permeabilities themselves. To implement equation G1-1, McCord et al (1991) suggest the following empirical equations

$$k_x = K_s k_r^{\mu}; \quad k_z = K_s \frac{k_r^{\mu}}{a} \quad for \quad 0 < \mu \leq 1 \tag{G1-2}$$

They indicate that the approach worked well with μ=0.8 in a model of a very wet sand.

An empirical logarithmic interpolation procedure was developed by Kool and Wu (1991) which ensures that both K_x and K_z decrease with increasing suction head when they applied equation 1 in the Las Cruces soil. The algorithm has been implemented in VAM3D-CG and was employed in this study.

The σ_f^2 (see eq. G1-1) was estimated based on constant-head permeameter measurements of K_s in the laboratory for 17 samples taken from the injection site during drilling. The estimates for A and σ_β^2 were obtained using following procedure: a. transform the fitted unsaturated $K(\theta(\psi))$ data using $k(\theta(\psi))=k_s e^{-\beta\psi}$; b. obtain slope of ln K_r vs. ψ plot. Generally, two distinct β values can be inferred for each sample. The fit for one of samples is shown in Figure G1-11. The β value characterizing the wet end of the curve was used; and c. mean and variances for 17 β values were then obtained. The correlation length λ was estimated from the variogram using data set of saturated conductivity from the injection site. The variogram plot is presented in Figure G1-12.

The statistical parameters used in scenario 3 are:

σ_f^2=3.54; σ_β^2=3.50 m^{-2}; λ=2.50 m; and A=3.78 m^{-1}.

Figure G1-11. Kr vs. Psi Injection Test Site: Sample 1-1417.

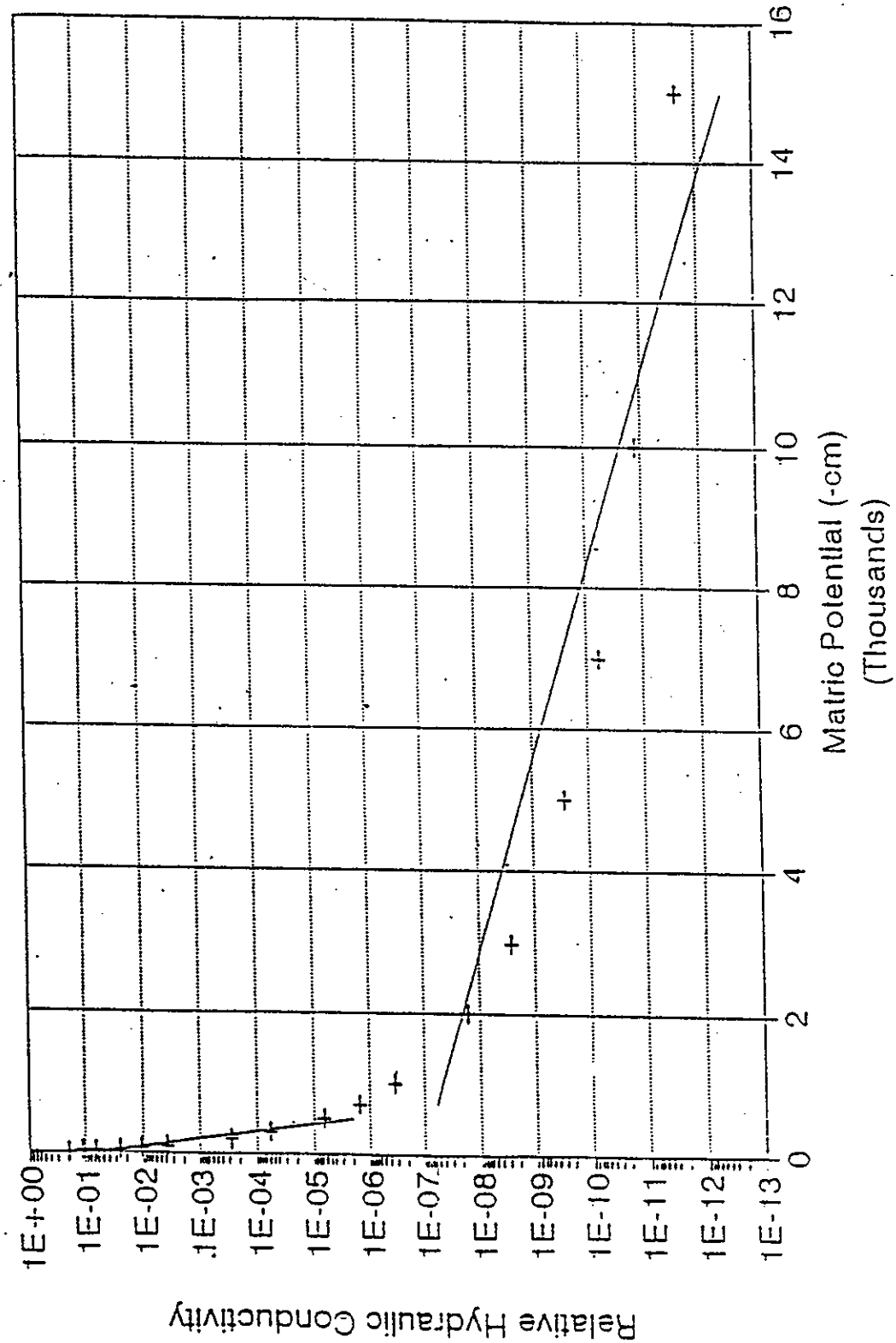

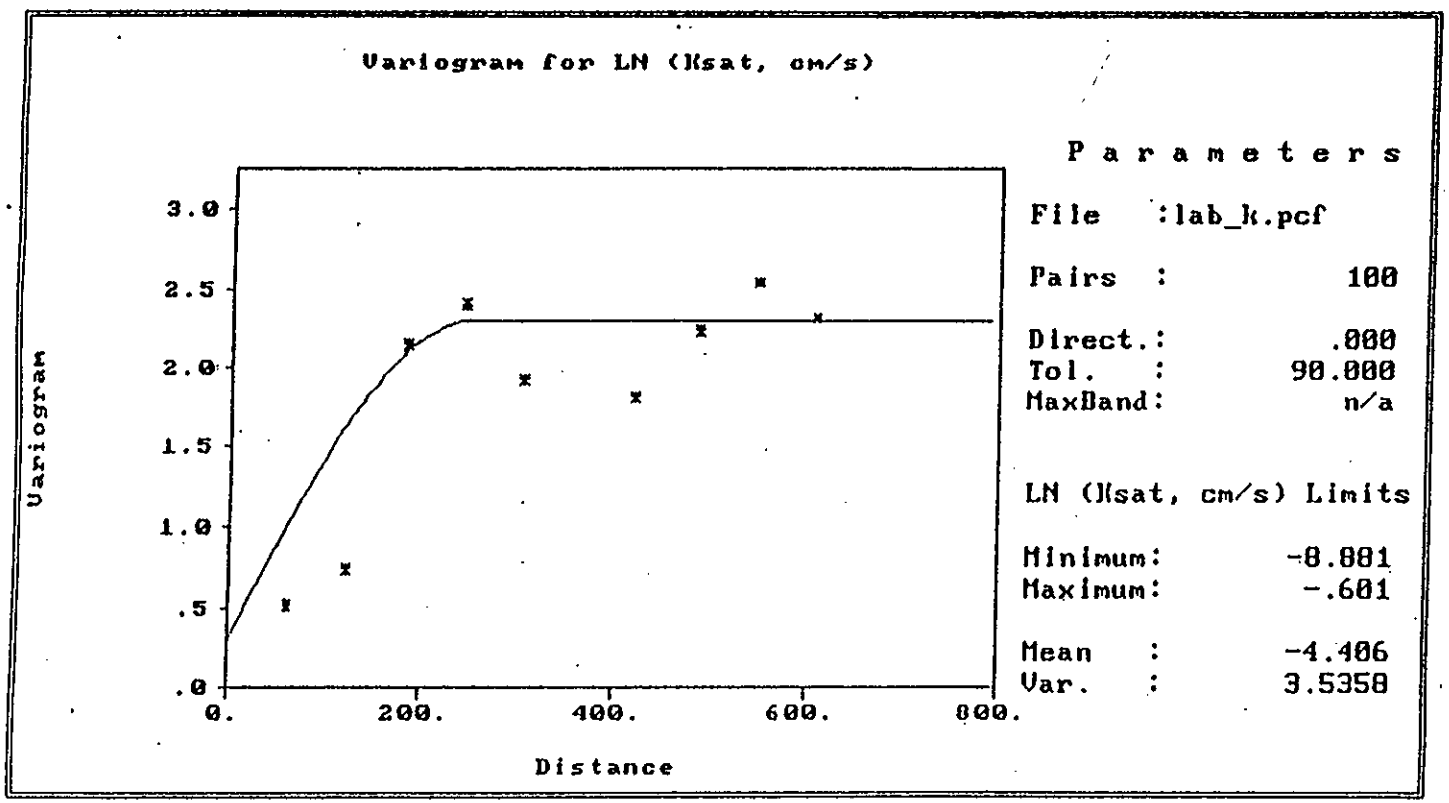

Figure G1-12. Variogram.

G1.4.4 SCENARIO 4: SAME AS SCENARIO 3, BUT WITH Λ=0.50 M

Since the data used for the variogram are scarce and the predicted anisotropy ratio is quite sensitive to the chosen values of λ, scenario 4 is a variant of scenario 3 using a smaller correlation length of λ=0.5 m. The other statistical parameters remain the same as scenario 3.

Examples of moisture-dependent anisotropy relations as modeled by VAM3D-CG for scenarios 3 and 4 are shown in Figures G1-13a and G1-13b, respectively. These figures show relative conductivity as a function of pressure head. The solid curve represents the isotropic case in which conductivity is given by the van Genuchten function. The dashed line and the dotted dashed line with triangle symbols represent an anisotropic case with the anisotropy ratio computed by equation (G1-1).

Figures G1-14a and G1-14b show the anisotropy ratios calculated by equation (G1-1) with two different correlation lengths, respectively.

G1.5.0 MODEL EVALUATION CRITERIA

Numerical results based on various model scenarios are compared with the field measurements. A visual comparison of field data and simulated results are presented as: (a) contour plots at chosen times; and (b) moisture content history plots at various radii and depths.

In addition to visual comparisons, spatial moments of water contents are computed and compared. This provides a quantitative measure of the goodness of fit of model predictions with the field data. To accommodate the fact that different initial water content distributions are used, we evaluate the flow simulations on the basis of the water content changes, Θ, rather than actual water contents, where

$$\Theta(r,z,t) = \theta(r,z,t) - \theta(r,z,t=0) \qquad \text{(G1-3)}$$

r and z are components of the cylindrical coordinates. The ij-th spatial moment of the water content change, $M_{ij}(t)$ in an axial symmetric model is defined as (Freyberg, 1986; Kool and Wu, 1991):

$$M_{ij}(t) = 2\pi\sum_{i=1}^{N} r_i\theta(r_i, z_i, t)\, r_i^k z_i^l V_i \qquad \text{(G1-4)}$$

where V_i is the volume associated with measurement i. Of special interest are the lower-order moments, i.e., the zero, first and second moments, respectively. The central moments of interest are computed from:

$$\Delta\theta = M_{00}/V_T \qquad \text{(G1-5a)}$$

Figures G1-13a and G1-13b. Moisture Dependent Anisotropy Relationships.

Figure 13-b.

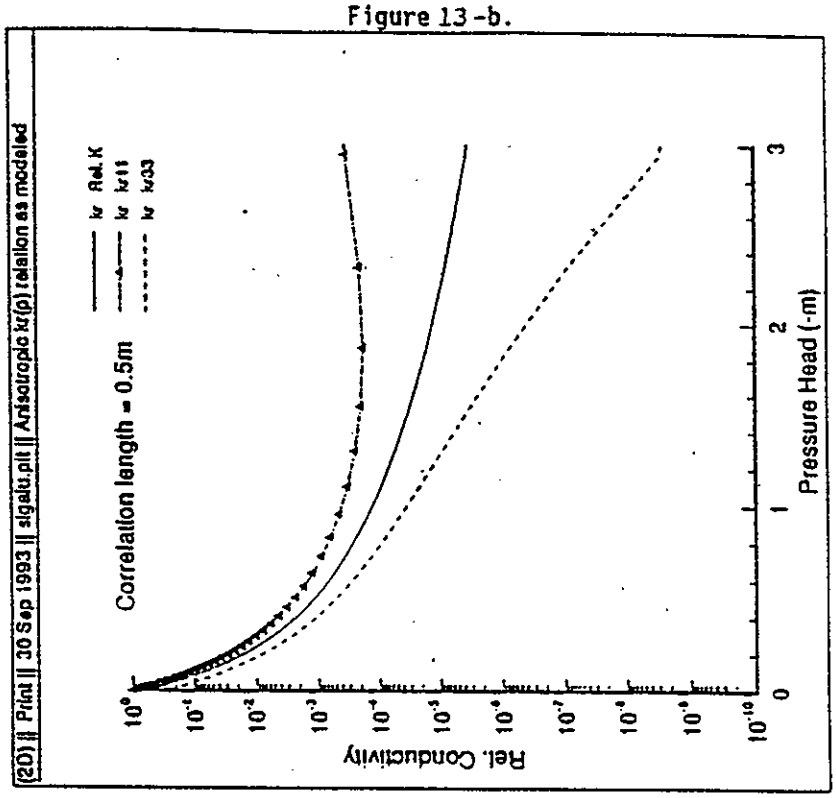

Figure 13-a.

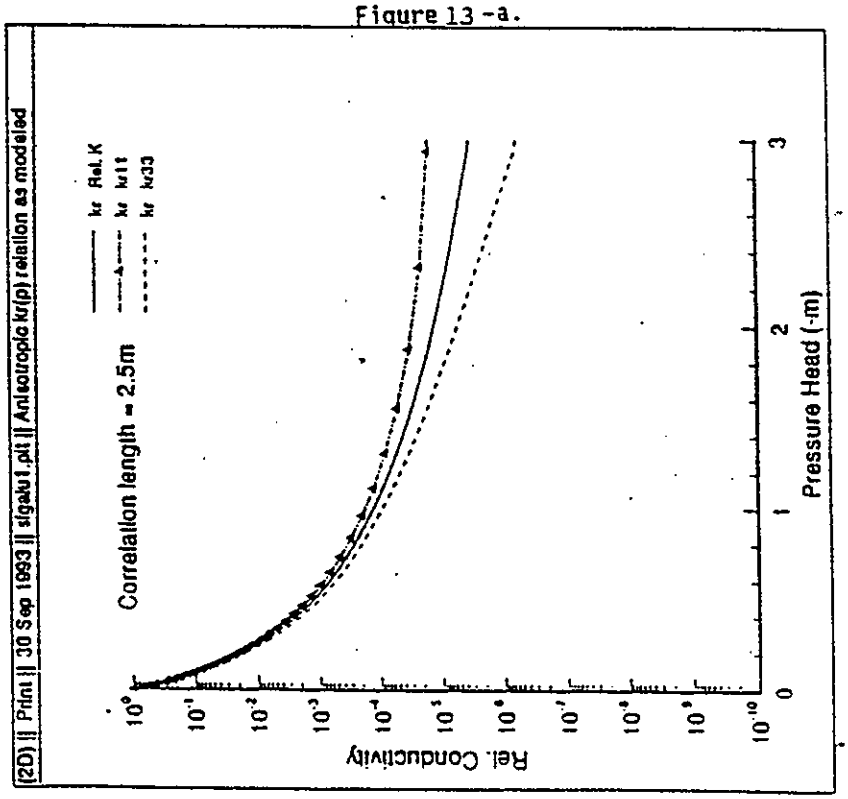

Figures G1-14a and G1-14b. Anisotropy Ratios for Two Different Correlations.

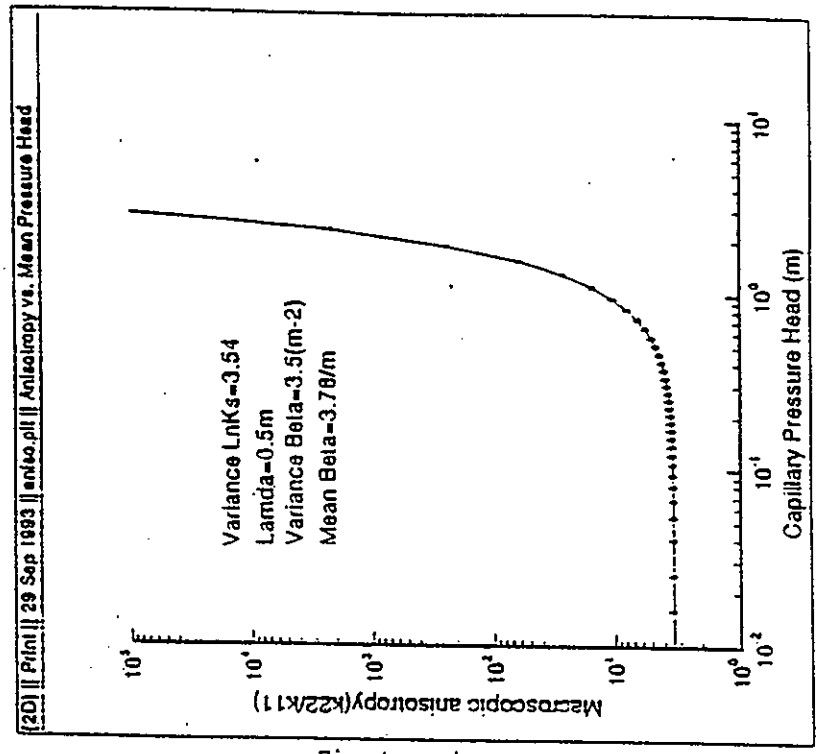

Figure 14-b.

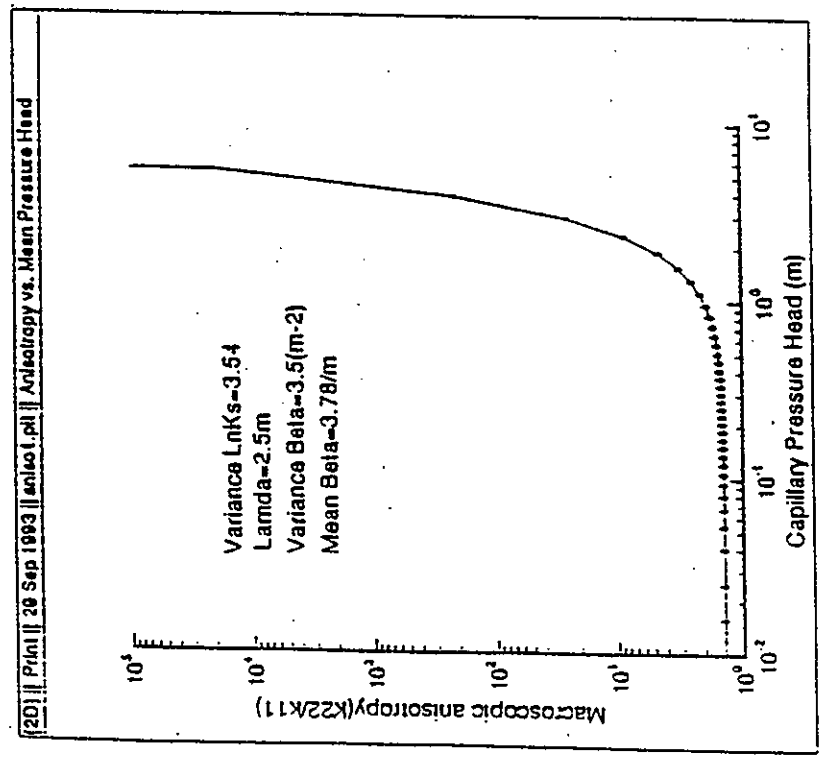

Figure 14-a.

$$r_c = M_{10}/M_{00} \tag{G1-5b}$$

$$z_c = M_{01}/M_{00} \tag{G1-5c}$$

$$\sigma_{rr}^2 = M_{20}/M_{00} - x_c^2 \tag{G1-5d}$$

$$\sigma_{zz}^2 = M_{02}/M_{00} - z_c^2 \tag{G1-5e}$$

The zero-order central moment $\Delta\Theta$ measures total mass change in the simulation domain. The first-order moments r_c and z_c indicate the change in location of the moisture plume's radial and vertical center of mass, respectively. The second-order non-central moments σ_{rr}^2 and σ_{zz}^2 measure spreading in the horizontal and vertical directions, respectively.

G1.6.0 MODEL RESULTS AND COMPARISONS

In this section, we compare the field data and the model prediction at various times and locations. The visual comparison is presented first and followed by spatial moment analyses. Ten different soil types were used for all simulation scenarios, but soil properties such as hysteresis and saturation dependent anisotropy were varied according to model scenario assumptions.

G1.6.1 VISUAL COMPARISON

For visual comparison, two different plots are presented: (a) the contour plots of average moisture contents measured at the field at four chosen times, followed by the corresponding predictions calculated by four model scenarios; and (b) the history plot comparisons of the field data with each scenario predictions at chosen depths and radii.

G1.6.1.1 Contour Plot Comparison

Figures G1-15a through G1-15d show the field-measured average moisture content contours at t=1.25, 13.2, 22.2, and 31.2 days, respectively, after the first injection began. The first five injections took place at time intervals, t=0.58 - 0.98 days, 7.45 - 7.89 days, 14.40 - 14.82 days, 21.38 - 21.75 days, and 28.39 - 28.77 days, respectively. Since an axial symmetric model was used, average field data were used for comparison. The average was obtained by summing up the moisture contents over four wells at the same radius and depth and dividing it by four. These figures indicate how the liquid migrates through the sediments in an axial average sense. Generally,

Figures G1-15a, G1-15b, G1-15c and G1-15d. Field-Measured Average Moisture Content Contours as a Function of Time.

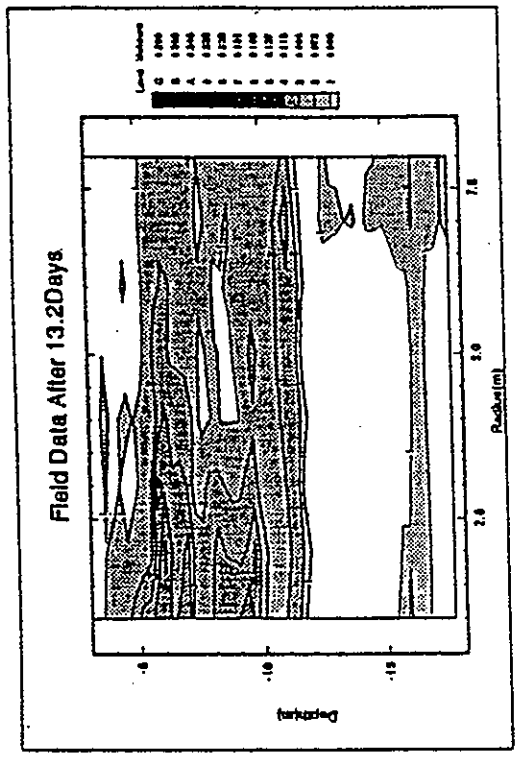

Figure 15-b.

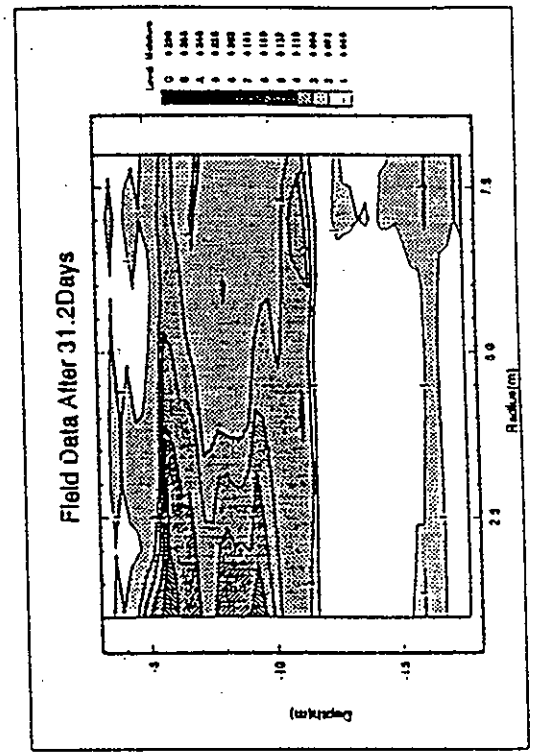

Figure 15-d.

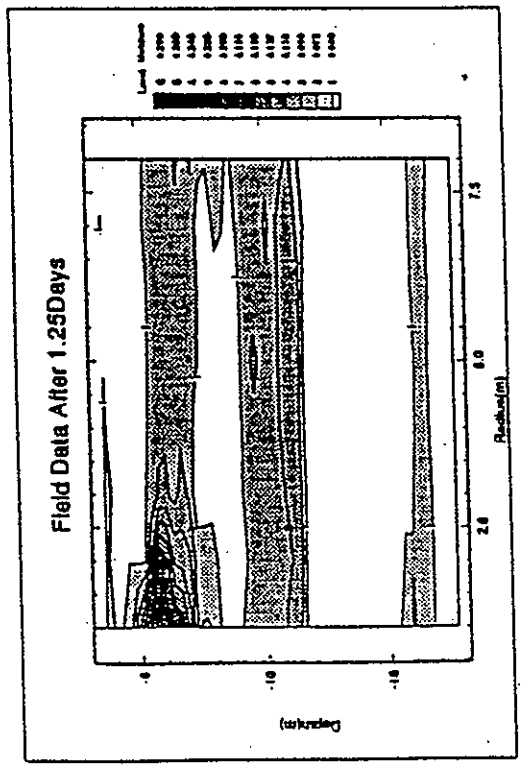

Figure 15-a.

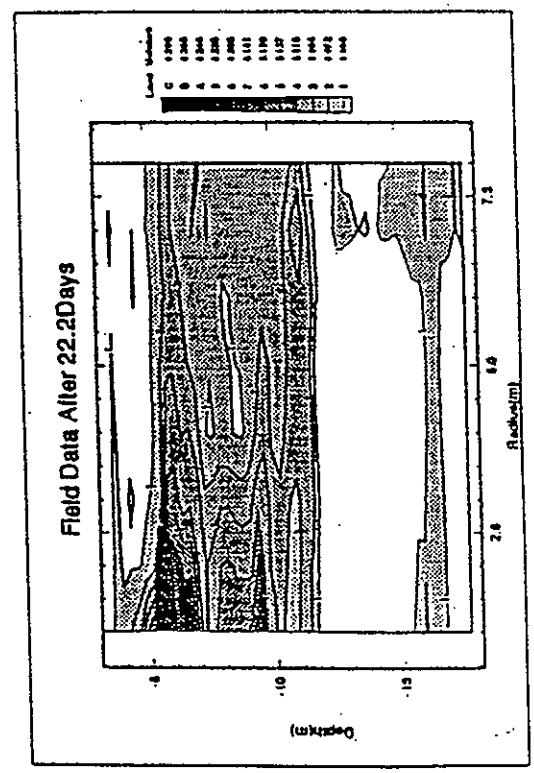

Figure 15-b.

we see that the moisture movement is anisotropic and stratified. An enhancement of lateral water movement occurs at intervals generally corresponding to the high initial moisture spikes. A downward break-through occurred at the region near the injection well where the moisture contents were high. As a result, a fingering of the moisture contours is exhibited, e.g., at t=13.2 days, the moisture contour (marked #2) has moved radially over 6 m at a depth of 5.4 m and over 3 m and 3.5 m at depths 8 m and 9.5 m, respectively. A similar fingering phenomenon occurs at higher moisture contours as well. At t=22.2 days, the moisture contour of #2 has progressed to the detected limit (r=8 m) and the lowest finger has migrated over 5 m.

We see a fast lateral water movement during and after the first two injections. The low moisture contour levels remained relatively steady after 22.2 days when the fourth injection had just completed. Compared to the contour plot at t=22.2 days, the upper part of the plume at t=31.2 days (two and half days after the fifth injection completed) remain relatively steady and the high moisture contours dissipated downward and then migrated laterally along the lower preferential paths. Up to this time, a vertical flow barrier has been seen at a depth of 11.5 m.

Figures G1-16a through G1-16d show the corresponding contour plots of the moisture contents calculated by scenario 1. Compared to the field data (see figures 15a through 15d), the model overpredicts the downward movement and underpredicts the horizontal spread of the moisture plume, especially at the depths of 5-7 m. At t=31.2 days, the model predicts that the moisture plume has moved down past the 17 m depth at a radius of 1 m. This deep movement did not occur. At t=31.2 days, the predicted moisture contents at the depths of 8-12 m are generally higher than the measured ones.

Figures G1-17a through G1-17d show the contour plots of moisture contents calculated by scenario 2. Compared to scenario 1, the inclusion of the hysteretic process resulted in some noticeable local variations, however, the results showed no significant change in size and shape of the moisture plume. It is seen that accounting for hysteresis does not enhance the lateral spreading. The model computed scanning curves in the moisture saturation vs. pressure head relation to determine the appropriate saturation path for every element in the model domain with reversals from wetting to drying, or vice versa occur. The wetting and drying curves were measured from laboratory tests. The hysteretic phenomenon was attributed to pore scale effect. Since the wetting and drying curves were employed regardless of directions (vertical or horizontal), it is not likely resulted in an anisotropic flow.

The stochastic theory (Mantoglou and Gelhar, 1987a,b,c) attributes the large-scale hysteresis to the spatial soil variability. In this interpretation, as demonstrated in the paper, a vertical flow plume in stratified soils could result in an enhanced lateral flow.

Figures G1-18a through G1-18d show the contour plots of moisture contents predicted by scenario 3. The simulation predicts a slightly larger degree of horizontal spread and a lesser downward movement of the moisture plume than those predicted by scenarios 1 and 2. Compared to the field data, the horizontal spread is still very much underpredicted by the model. It is because the anisotropy ratios are small for the moisture contours of level #2

Figures G1-16a, G1-16b, G1-16c, and G1-16d. Calculated Moisture Contour Plots by Scenario 1.

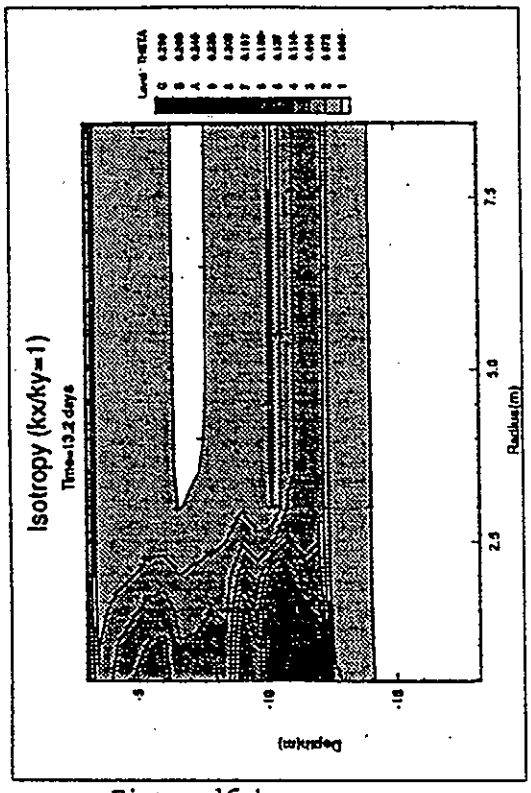

Figure 16-b.

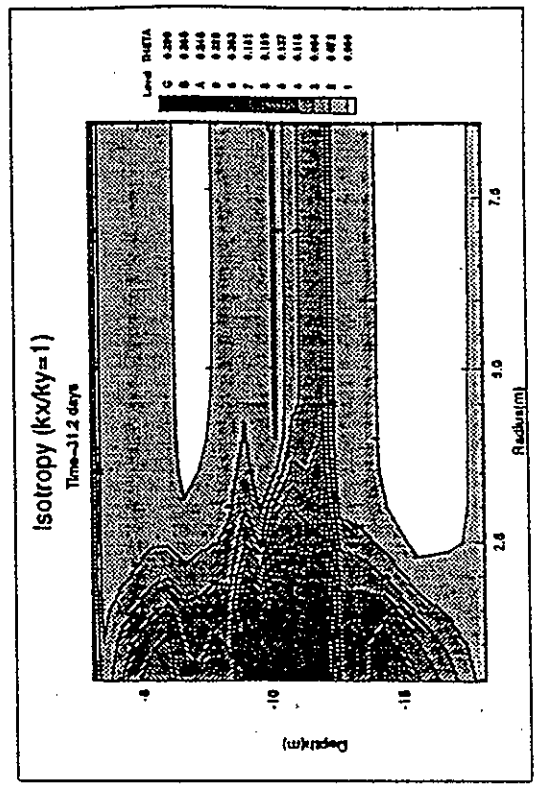

Figure 16-d.

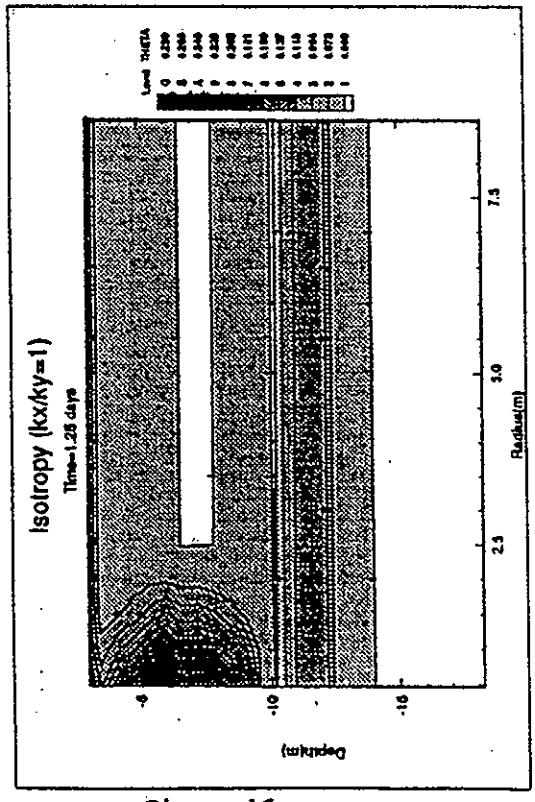

Figure 16-a.

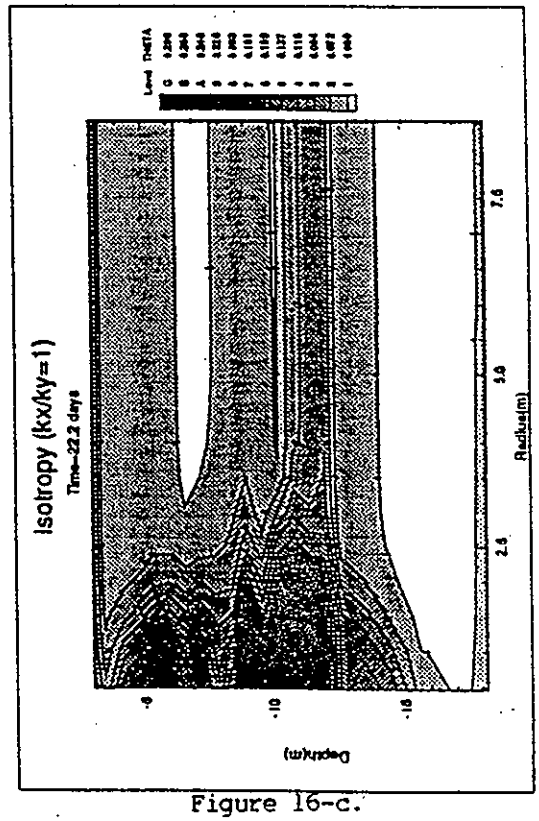

Figure 16-c.

Figures G1-17a, G1-17b, G1-17c, and G1-17d. Calculated Moisture Contour Plots by Scenario 2.

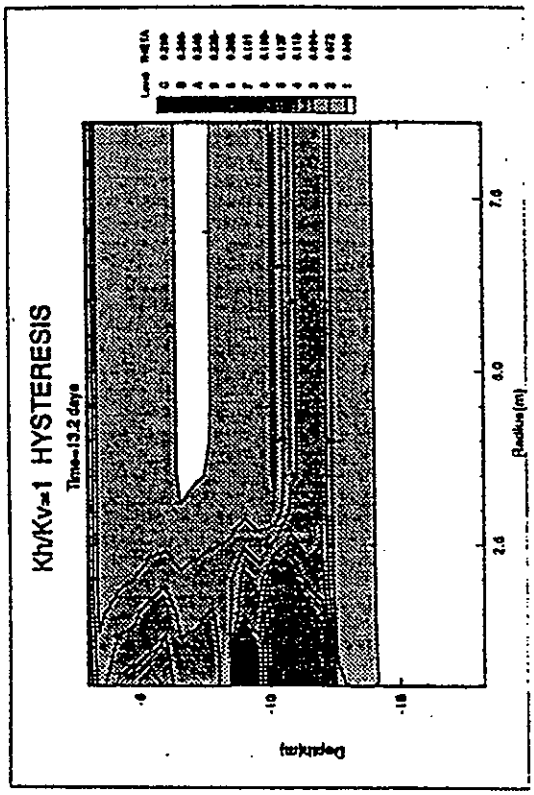

Figure 17-b.

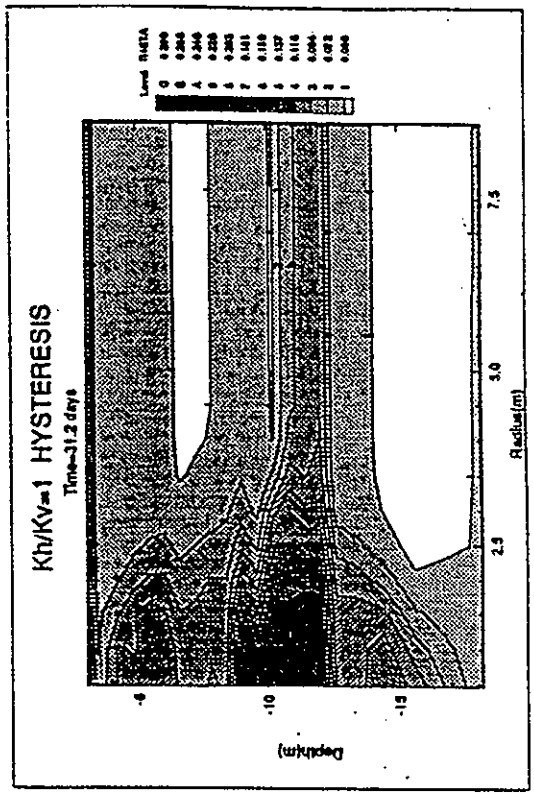

Figure 17-d.

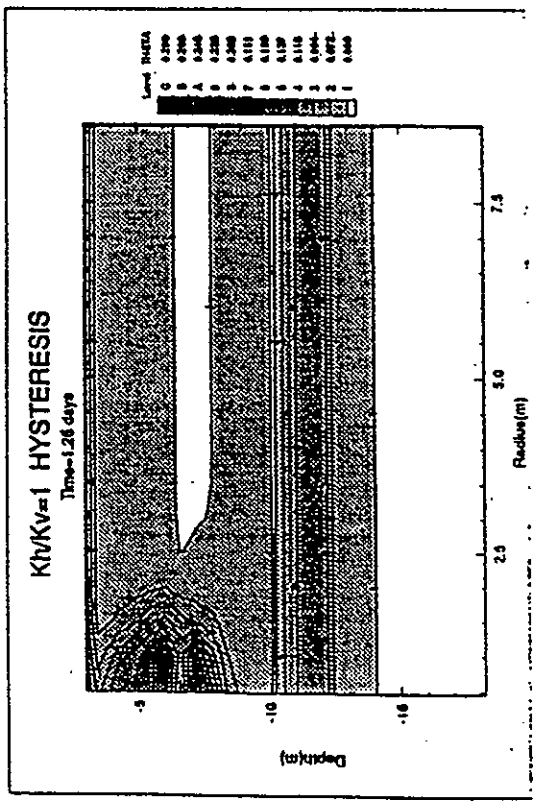

Figure 17-a.

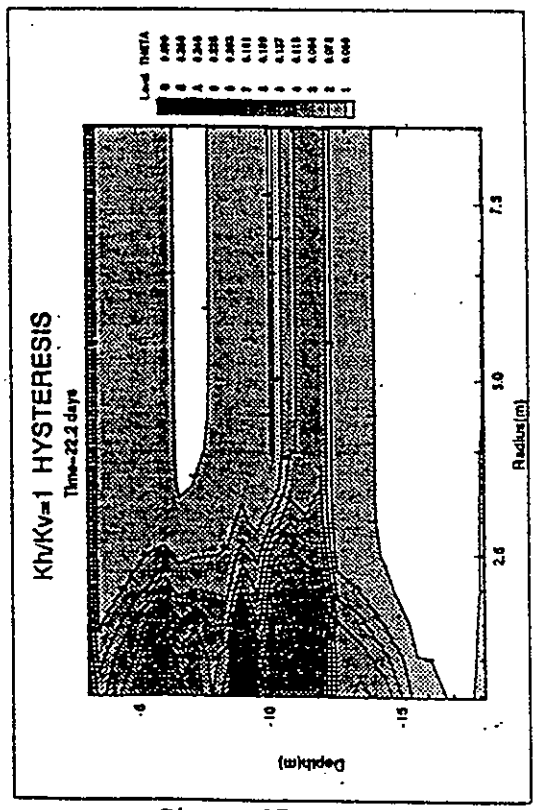

Figure 17-c.

Figures G1-18a, G1-18b, G1-18c, and G1-18d. Calculated Moisture Content Plots By Scenario 3.

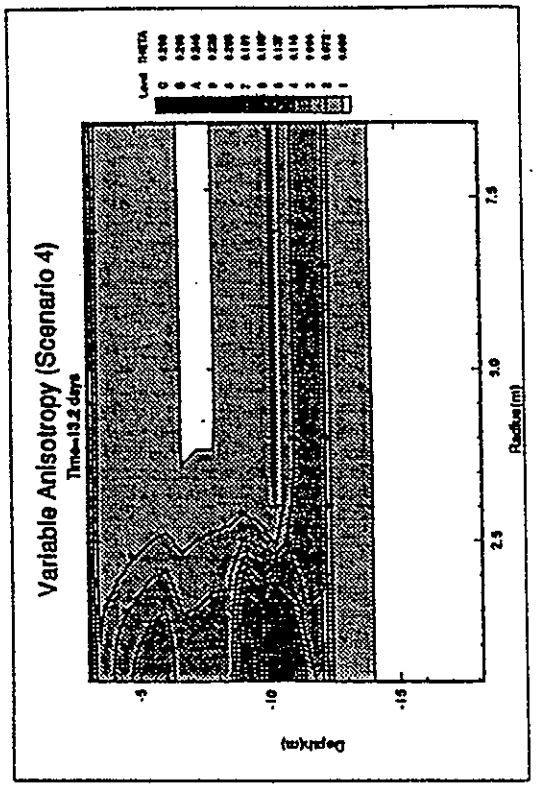

Figure 18-b.

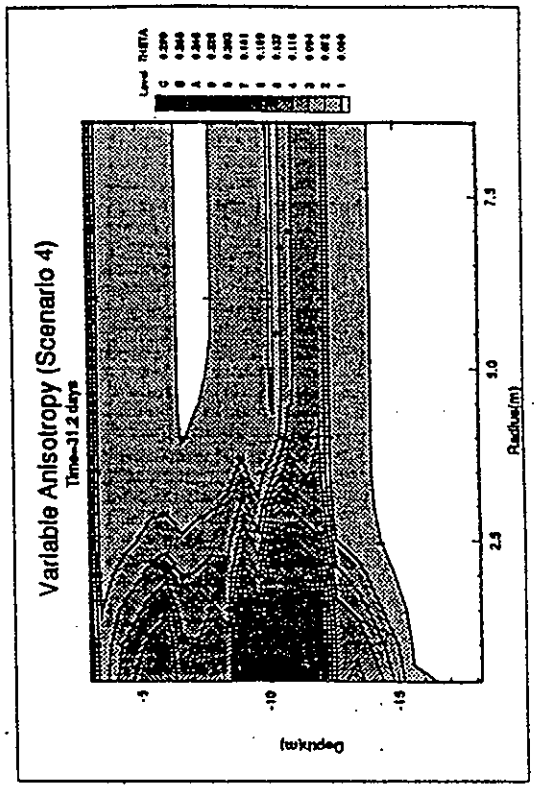

Figure 18-d.

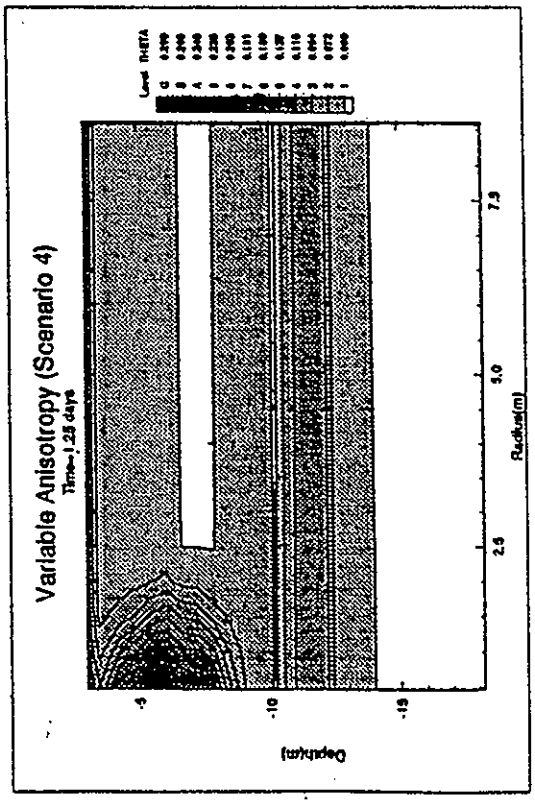

Figure 18-a.

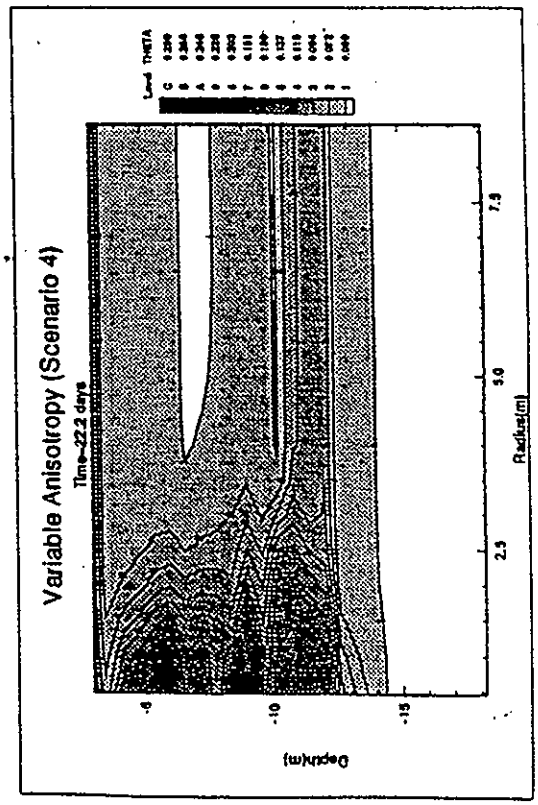

Figure 18-c.

and above. In view of Figure G1-10-a, the anisotropy ratios are less than two when the capillary pressure heads are less than 1 m, which corresponds to the moisture contours of level #2 and above for most retention curves used for the simulation. Compared to the field observation, smaller and fatter fingers appeared at later times due to the layers in which soil hydraulic properties were different.

Figures G1-19a through G1-19d show the contour plots of moisture contents predicted by scenario 4 which used a smaller correlation length and kept other parameters the same as that in scenario 3. The decrease in the correlation length from λ=2.5 m to λ=0.5 m resulted in a substantial increase of the anisotropy ratios (see Figure G1-10-b). The inclusion of this scenario is because of the limited samples, warranting a sensitivity run. Among the four scenarios considered, the scenario 4 predictions compare most favorably with the field data. However, compared to the field data, the horizontal spread is still underpredicted, especially at depths of 5-7 m.

G1.6.1.2 History Plot Comparison

The following comparisons are intended to examine the results of the four model scenarios in response to the infiltration and redistribution at chosen depths and radii.

Figures G1-20a through G1-20d and G1-21a through G1-21d show the comparison of calculated moisture contents by scenario 1 with the measured ones at the depths of 6.0 and 8.4 m, respectively. The measured data at four wells are displayed along with the results generated by the model. At each depth, the comparisons are made at radii of 1 m, 2 m, 3 m, and 4 m. At a depth of 6 m, the model shows a good agreement at a radius of 1 m. However, the model underpredicts at radii of 2 m, 3 m and 4 m. In these plots, we see that water was detected in an early time at wells B-4 and H-4 which are 4-m away from the injection well. Meanwhile, the water simulated by the model hasn't reached the wells which are 3-m away, even at the end of 35 simulation days. At a depth of 8.4 m, the model shows a good agreement at a radius of 1 m, a good to fair agreement at the radii of 2 m, 3 m and 4 m.

Figures G1-22a through G1-22d and G1-23a through G1-23d show a similar comparison of calculated moisture contents by scenario 2 with the measured ones. Scenario 2 includes the hysteretic process in the model simulation. Again, at a depth of 6 m, the model shows a good agreement at a radius of 1 m and underpredicts at radii of 2 m, 3 m and 4 m. At a depth of 8.4 m, the model shows a good agreement at a radius of 1 m, a good to fair agreement at the radii of 2 m, 3 m and 4 m. The peaks in response to the infiltration at radii of 1 m and 2 m are slightly different from that depicted in scenario 1. The wetting curve was selected by the code during the period of the infiltration, and the drying curve was selected during the redistribution. These local variations didn't result in a significant lateral migration.

Figures G1-24a through G1-24d and G1-25a through G1-25d show a comparison of calculated moisture contents by scenario 3 with the measured ones. Scenario 3 includes the saturation dependent anisotropy in the model calculation. At the depth of 6 m, the model shows a good agreement at r=1 m

Figures G1-19a, G1-19b, G1-19c, and G1-19d. Calculated Moisture Content Plots By Scenario 4.

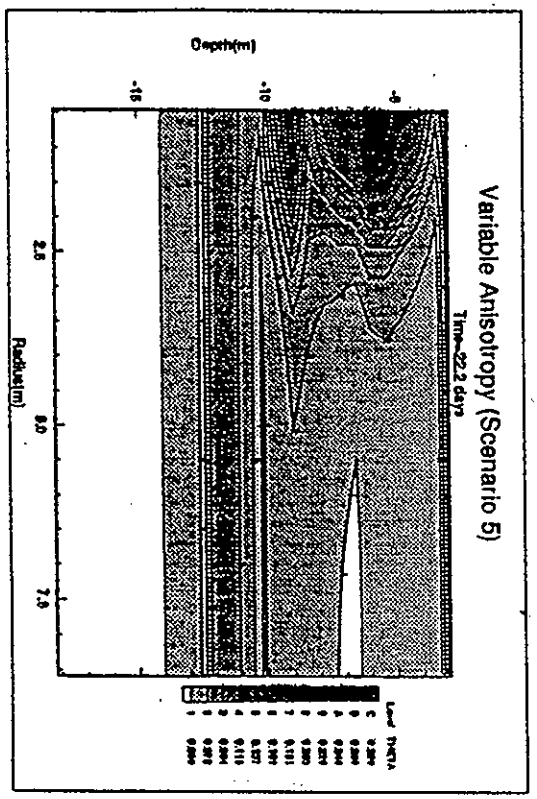

Figure 19-b.

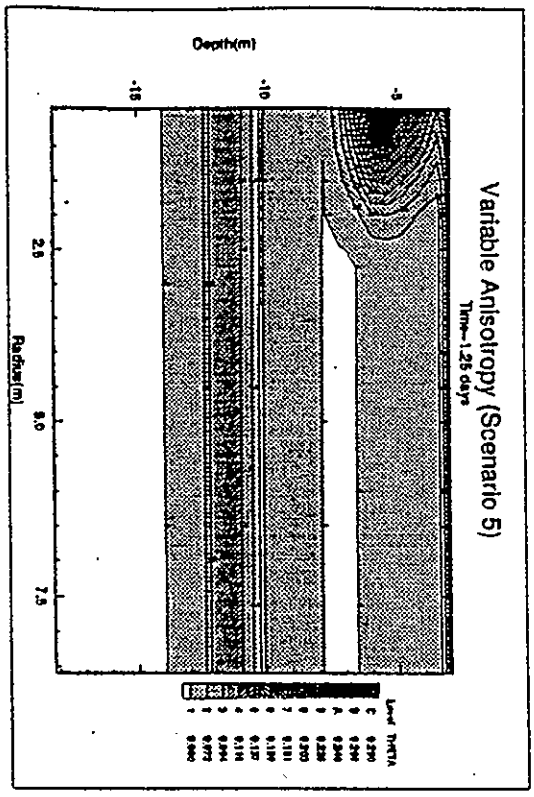

Figure 19-d.

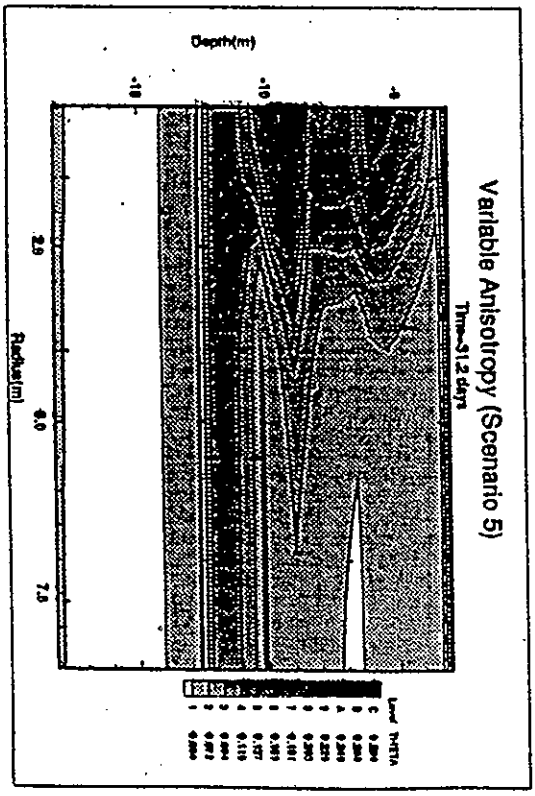

Figure 19-a.

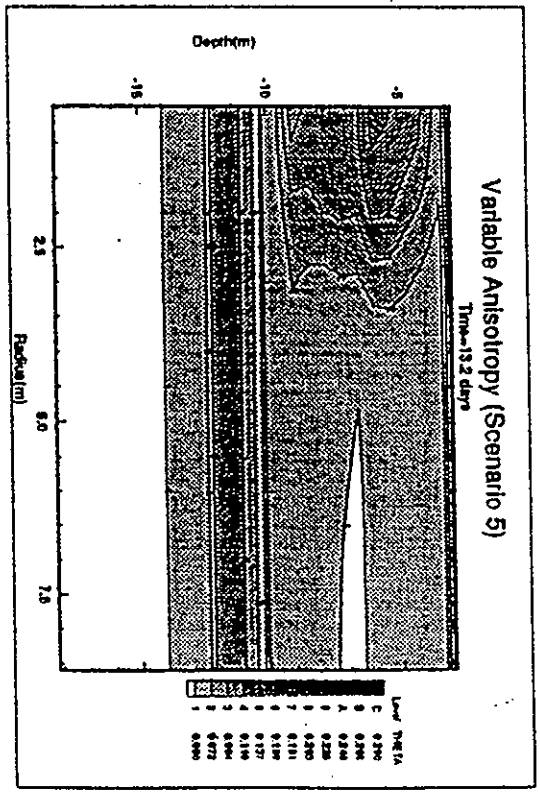

Figure 19-c.

Figures G1-20a, G1-20b, G1-20c, and G1-20d. Comparison of Calculated Versus Measured Moisture Contents at 6.0-m Depth and Radii of 1 m, 2 m, 3 m, and 4 m for Scenario 1.

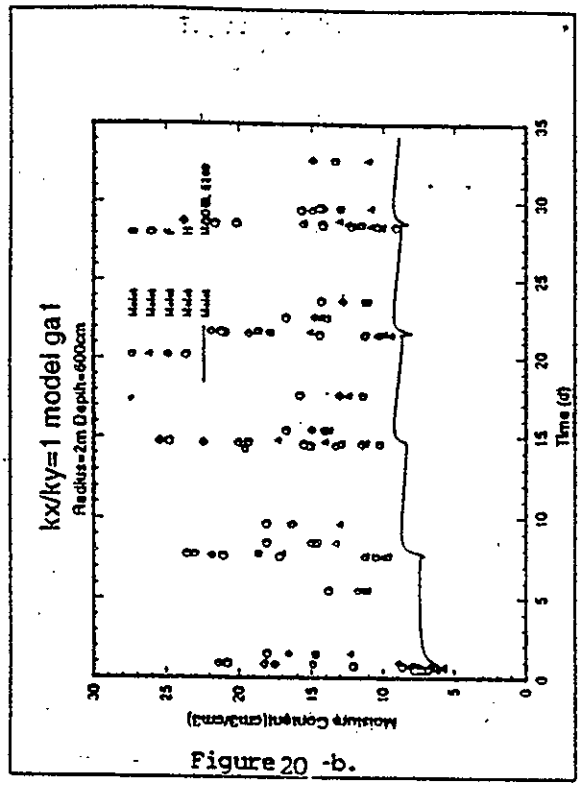

Figure 20 -b.

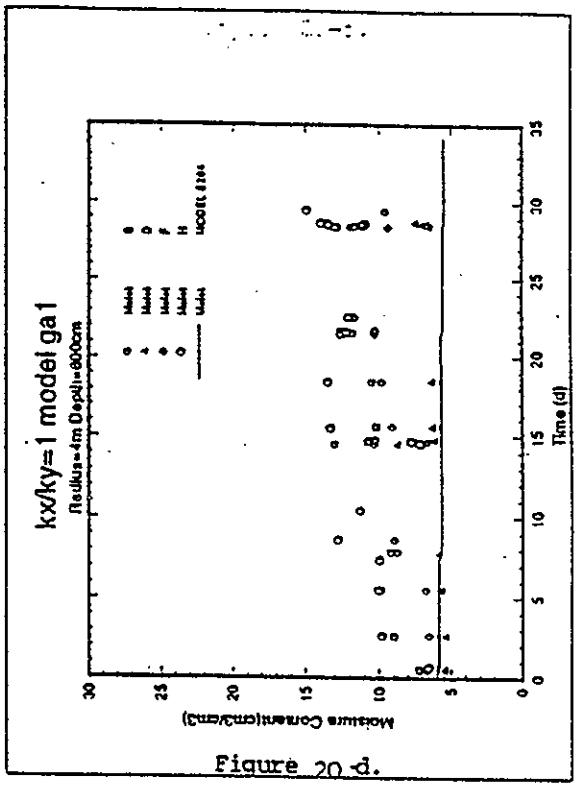

Figure 20 -d.

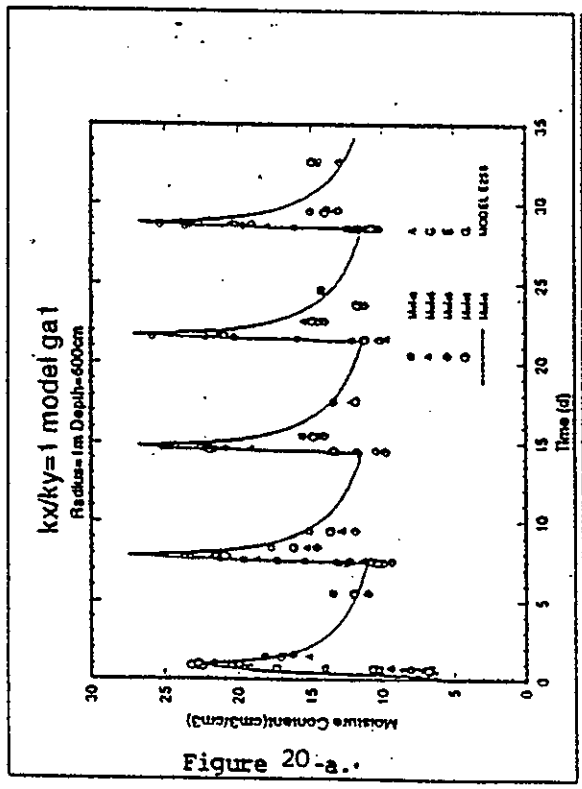

Figure 20 -a.

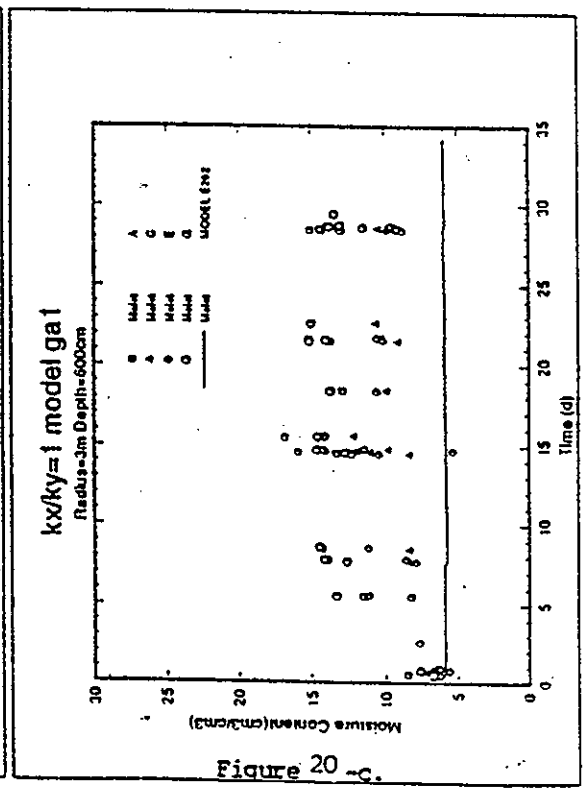

Figure 20 -c.

Figures G1-21a, G1-21b, G1-21c, and G1-21d. Comparison of Calculated Versus Measured Moisture Contents at 8.4-m Depth and Radii of 1 m, 2 m, 3 m, and 4 m for Scenario 1.

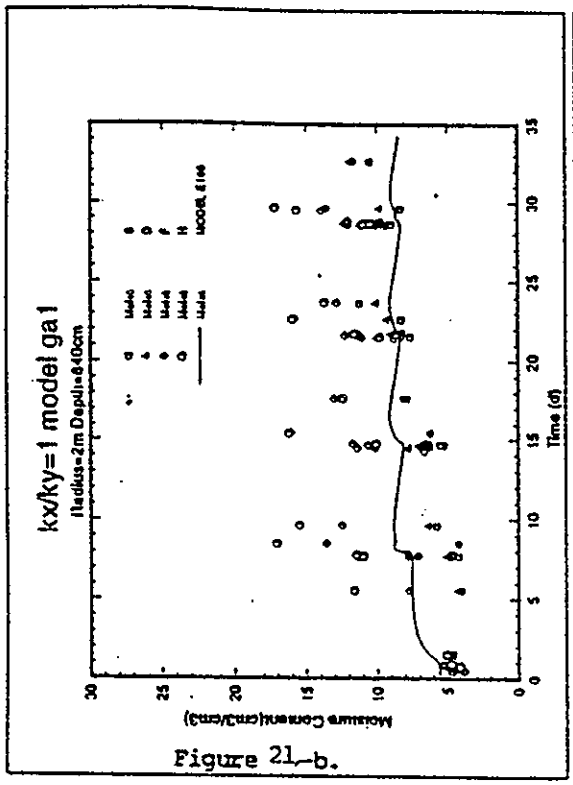

Figure 21-b.

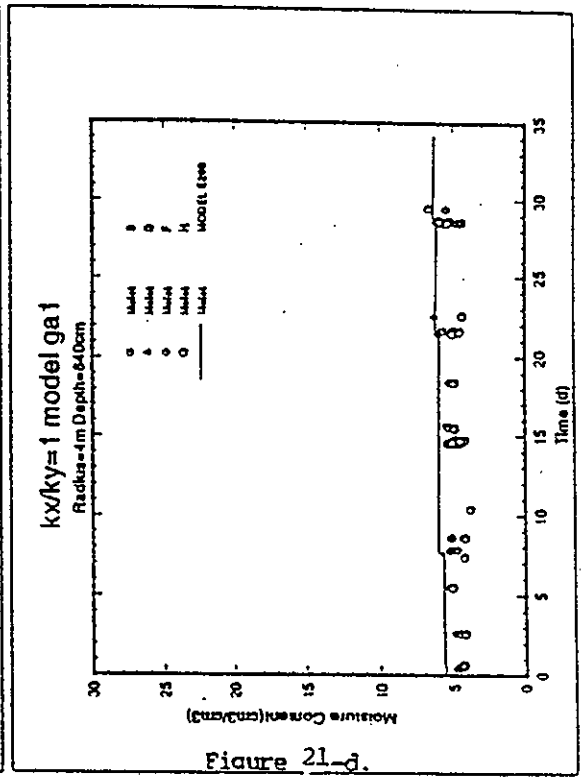

Figure 21-d.

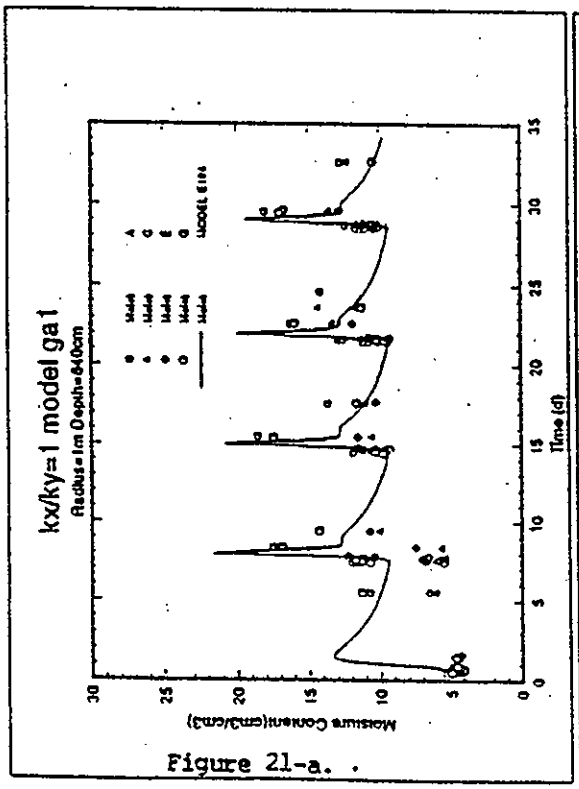

Figure 21-a.

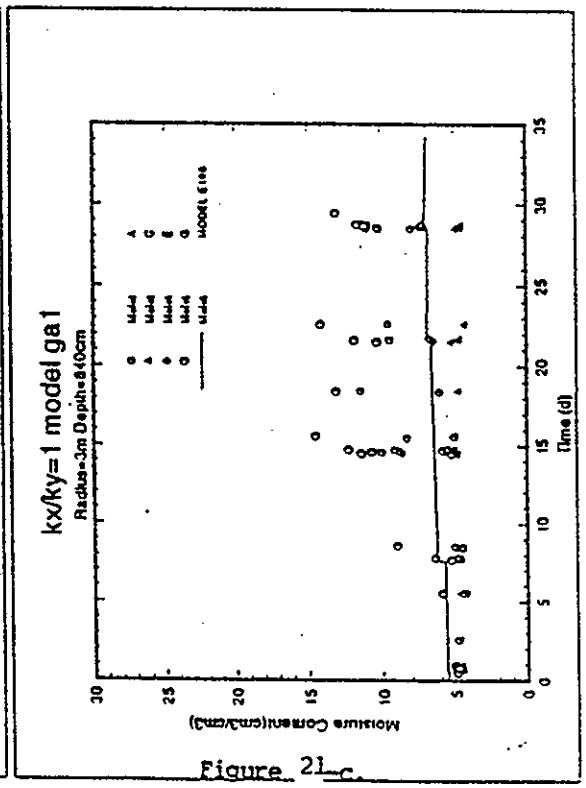

Figure 21-c.

Figures G1-22a, G1-22b, G1-22c, and G1-22d. Comparison of Calculated Versus Measured Moisture Contents at 6.0-m Depth and Radii of 1 m, 2 m, 3 m, and 4 m for Scenario 2.

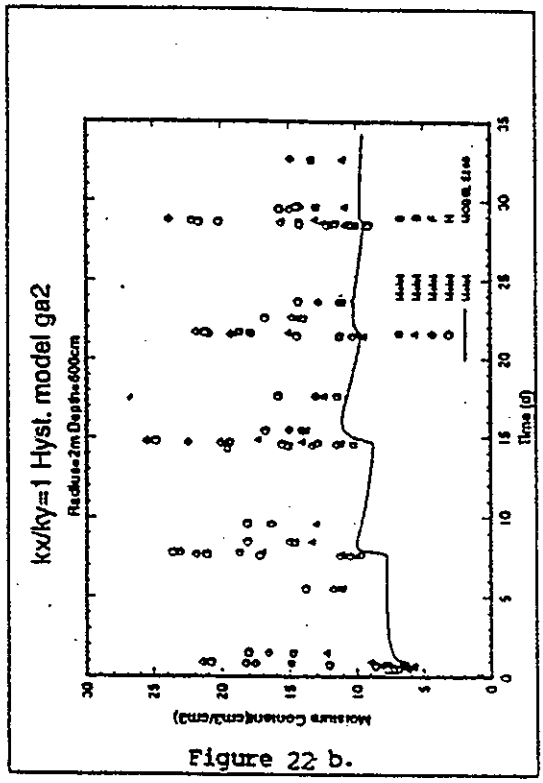

Figure 22 b.

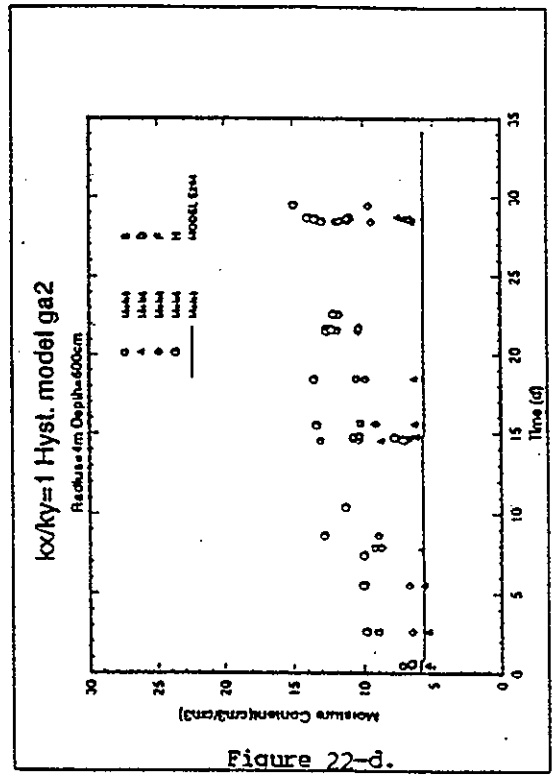

Figure 22-d.

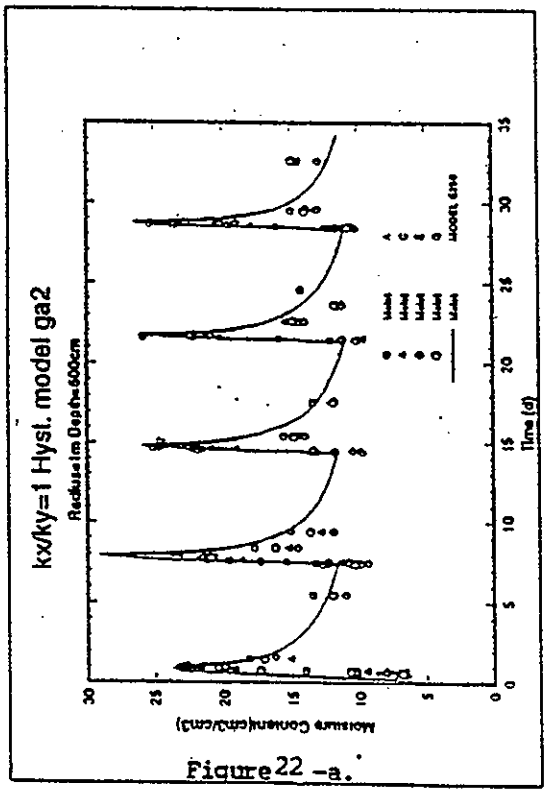

Figure 22 -a.

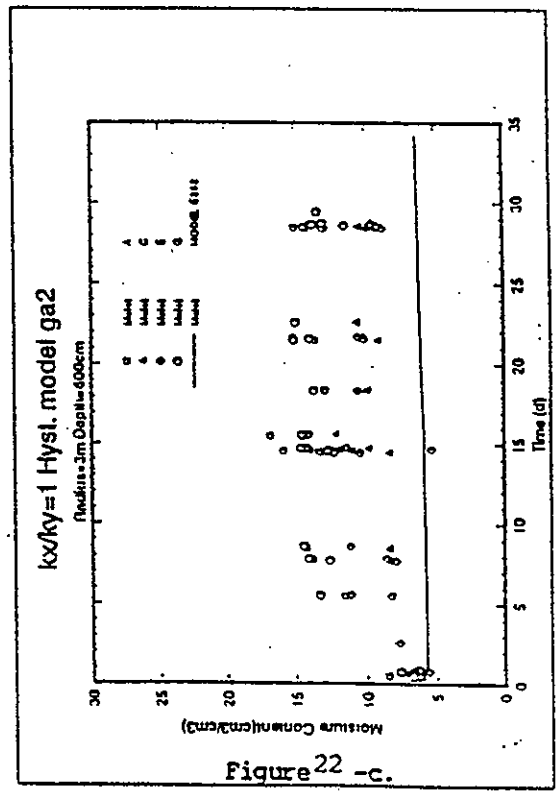

Figure 22 -c.

Figures G1-23a, G1-23b, G1-23c, and G1-23d. Comparison of Calculated Versus Measured Moisture Contents at 8.4-m Depth and Radii of 1 m, 2 m, 3 m, and 4 m for Scenario 2.

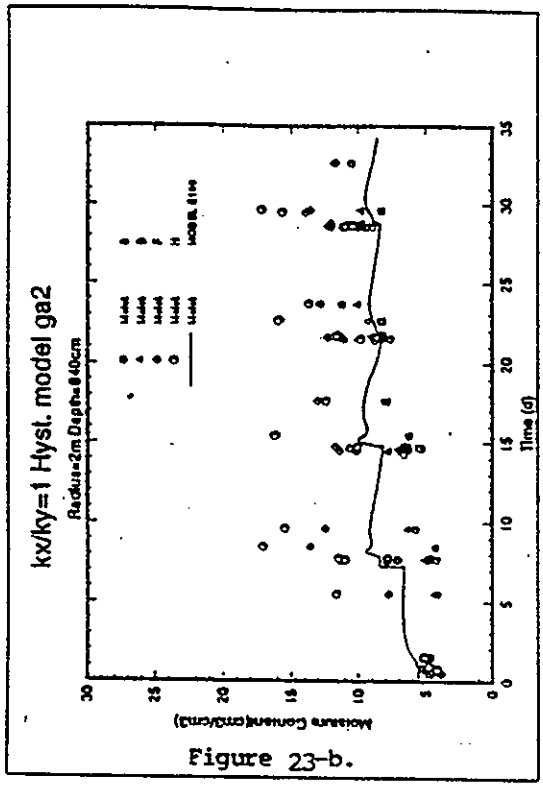

Figure 23-b.

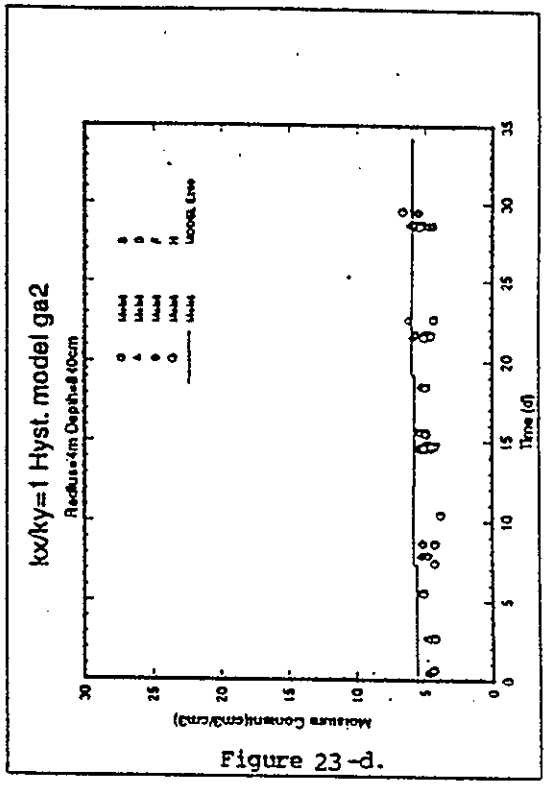

Figure 23-d.

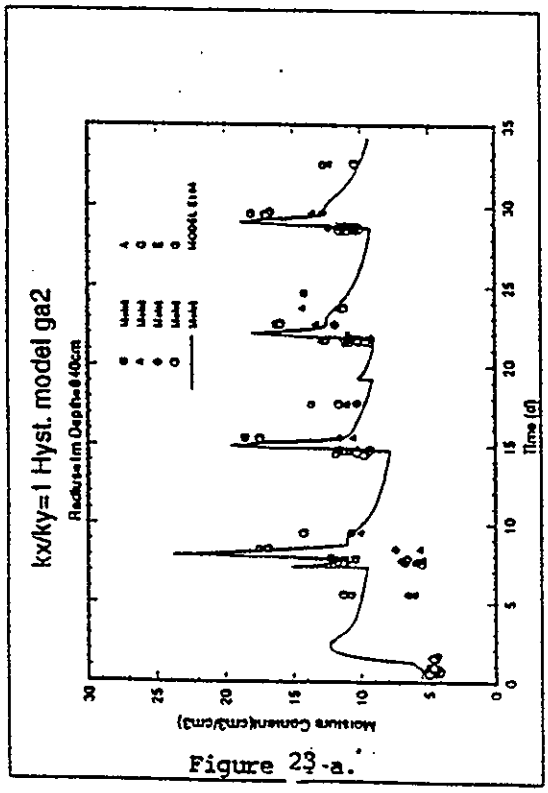

Figure 23-a.

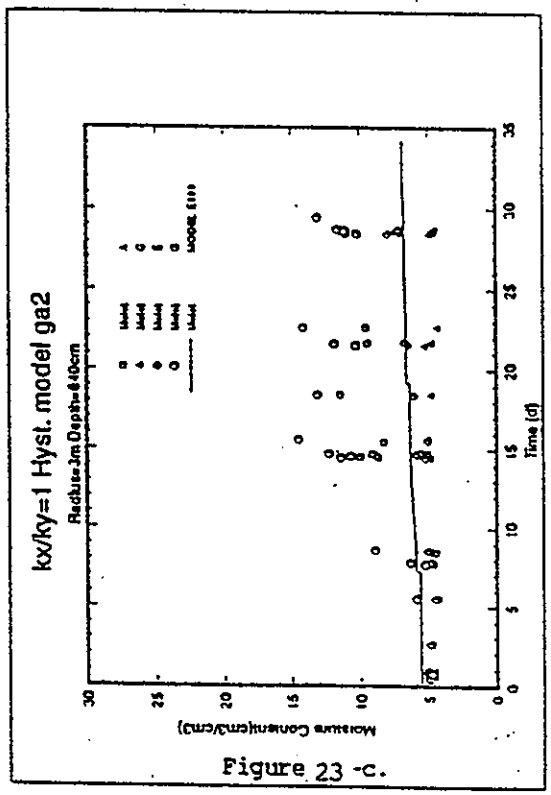

Figure 23-c.

Figures G1-24a, G1-24b, G1-24c, and G1-24d. Comparison of Calculated Versus Measured Moisture Contents at 6.0-m Depth and Radii of 1 m, 2 m, 3 m, and 4 m for Scenario 3.

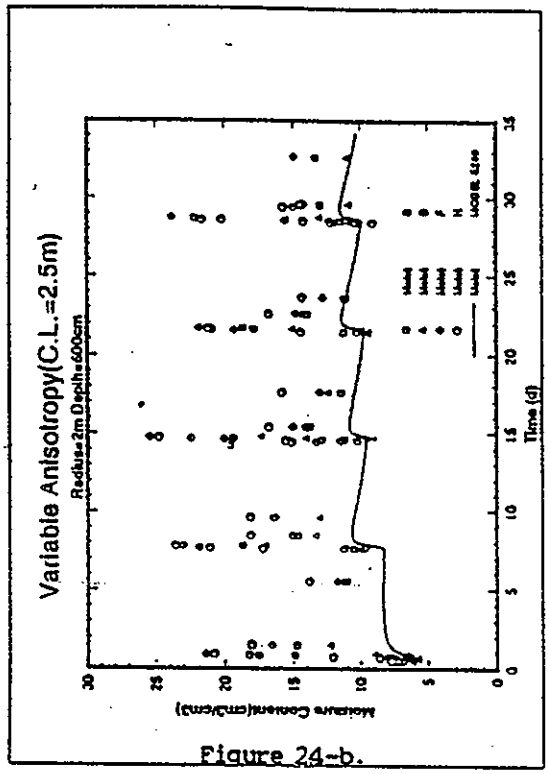

Figure 24-b.

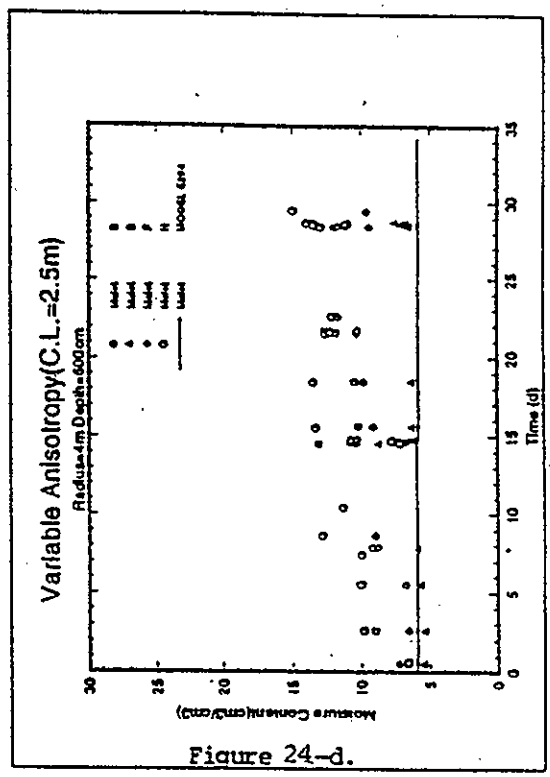

Figure 24-d.

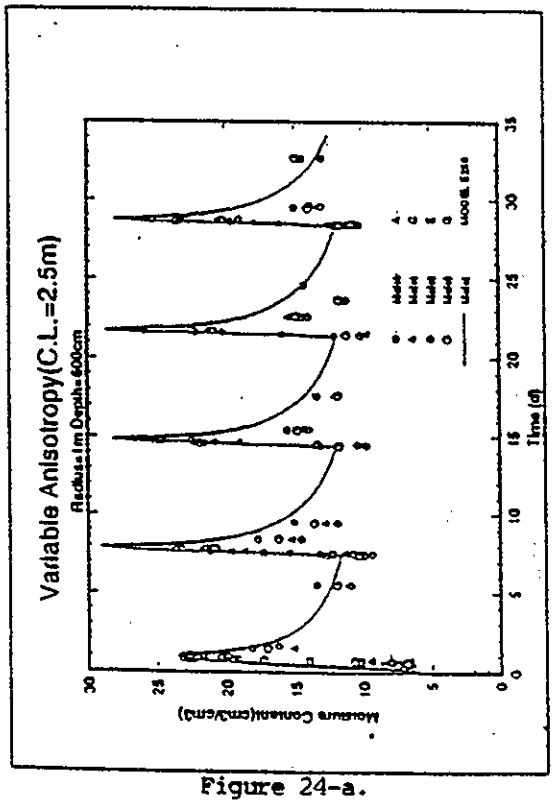

Figure 24-a.

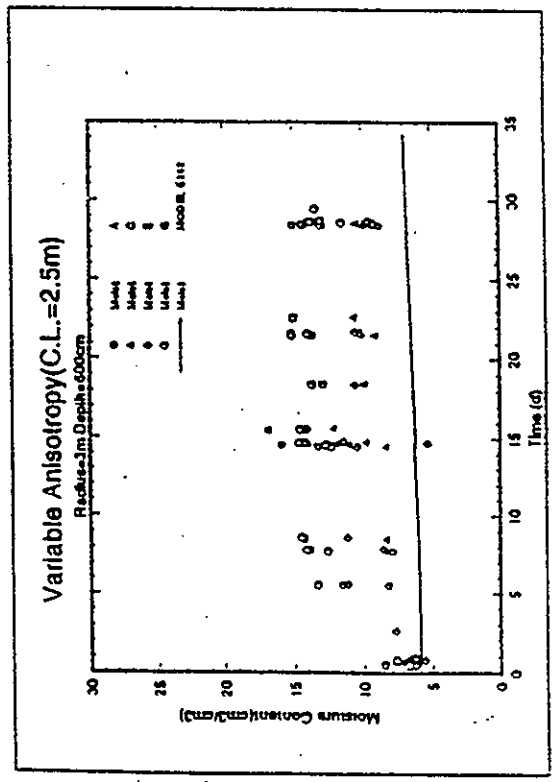

Figure 24-c.

Figures G1-25a, G1-25b, G1-25c, and G1-25d. Comparison of Calculated Versus Measured Moisture Contents at 8.4-m Depth and Radii of 1 m, 2 m, 3 m, and 4 m for Scenario 3.

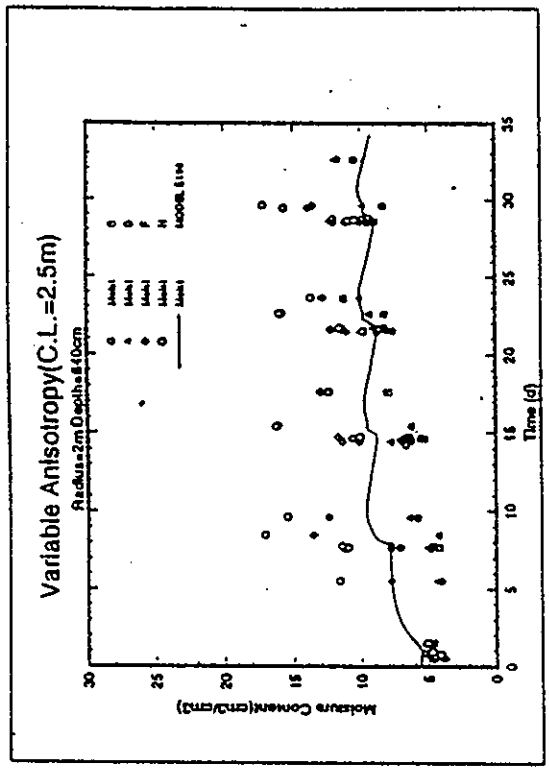

Figure 25-b.

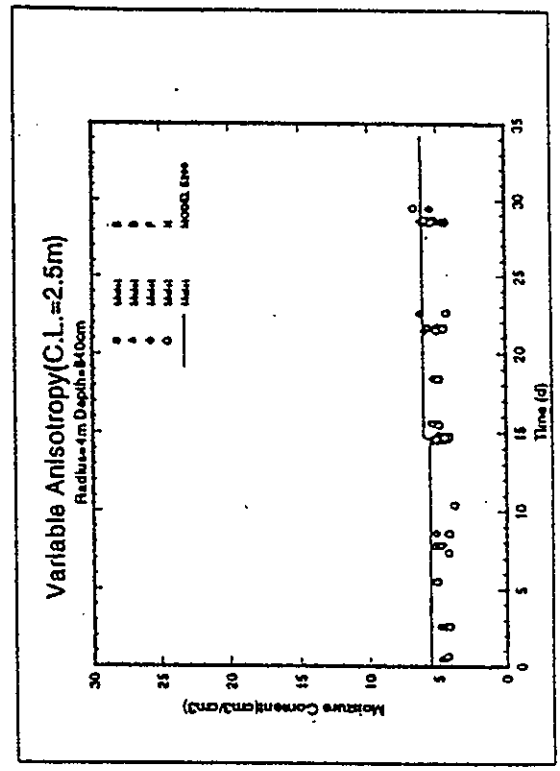

Figure 25-d.

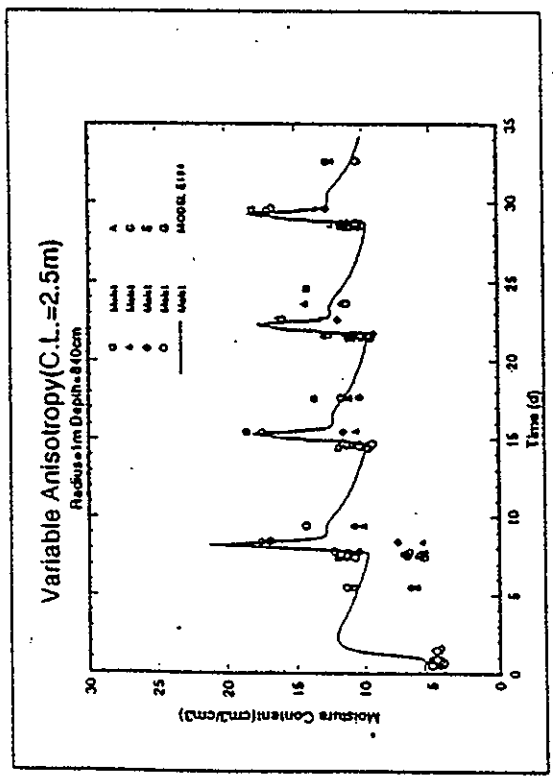

Figure 25-a.

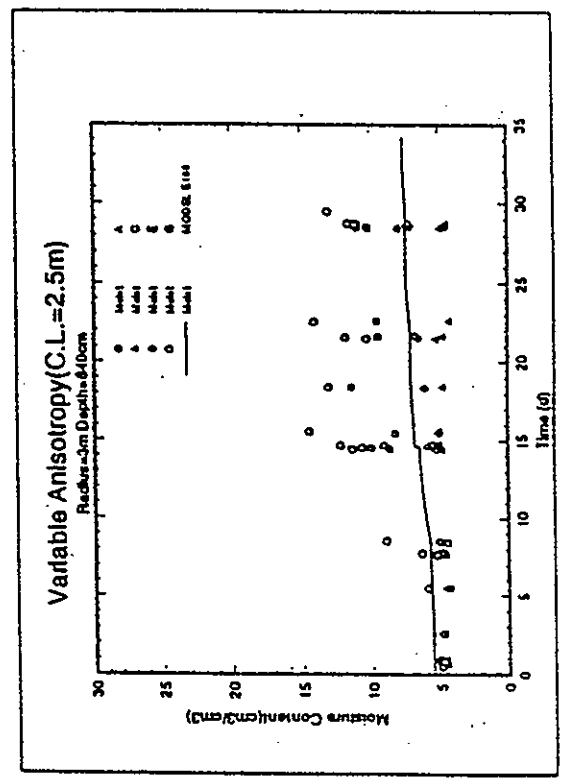

Figure 25-c.

and underpredicts at r=2, 3, and 4 m. At a depth of 8.4 m, the model shows good agreement at a radius of 1 m and some improvement at radii of 2 m and 3 m in comparison with scenarios 1 and 2.

Figures G1-26a through G1-26d and G1-27a through G1-27d show a comparison of calculated moisture contents based on scenario 4 with the measured ones. At a depth of 6 m, the model shows a good agreement at a radius of 1 m, a significant improvement at radii of 2 m and 3 m comparing to the other scenarios. At a depth of 8.4 m, the model shows an excellent to good agreement at all radii.

G1.6.1.3 Overview of Visual Comparison

A comparison of the four model scenarios with the field data suggests that scenario 4 provides the most favorable fit. Scenario 1 generally underpredicts the lateral movement of the moisture plume and overpredicts the vertical penetration. Scenario 2 shows a similar trend as scenario 1 but with noticeable local variations. The effect of hysteresis on the lateral water movement is insignificant. In the model simulation the hysteresis was not differentiated between the horizontal and vertical direction. However, the stochastic theory (Mantoglou and Gelhar, 1987) demonstrated that a vertical water movement in a stratified soil should exhibit a large-scale hysteretic phenomenon.

Inclusion of the process of saturation-dependent anisotropy in the model gave result which could partially account for the extensive lateral spreading of the plume which occurred in the field. The anisotropy ratio is sensitive to the correlation length. A better fit for scenario 4 with a smaller correlation length suggests that the soil textural heterogeneity is underestimated by the limited soil samples that are available.

G1.6.2 Spatial Moments Analysis

The following section provides a quantitative assessment, using spatial moment estimates, of a number of aspects of the preceding visual comparison of the moisture movement. Note that the moisture contents measured in the field show considerable variability in space which can be attributed to small-scale heterogeneities within the sediments. Spatial moments of the moisture plume distribution only provides a larger-scale, integrated measures of the water movement.

Figure G1-28 shows the zero-order moment calculations. In this calculation, the zero moment is the change of the integrated total mass over a cylindrical section with the depths from 3 m to 16 m and the radii from 0 to 8 m. For the field-measured data, we assume the moisture content of each annulus with a depth of 0.3 m is represented by the average of 4 measurements from the wells located at the middle radius of the annulus. The solid line represents the total volumetric water injected. Compared to the total mass injected, the integrated total mass for field-measured data is consistently higher by up to 35 percent. The reasons for the discrepancy are unclear. One kind of errors conjectured is the over-representation of the preferential flow region. The measured history plots presented in Figures G1-6a through G1-6d

Figure G1-26a, G1-26b, G1-26c, and G1-26d. Comparison of Calculated Versus Measured Moisture Contents at 6.0-m Depth and Radii of 1 m, 2 m, 3 m, and 4 m for Scenario 4.

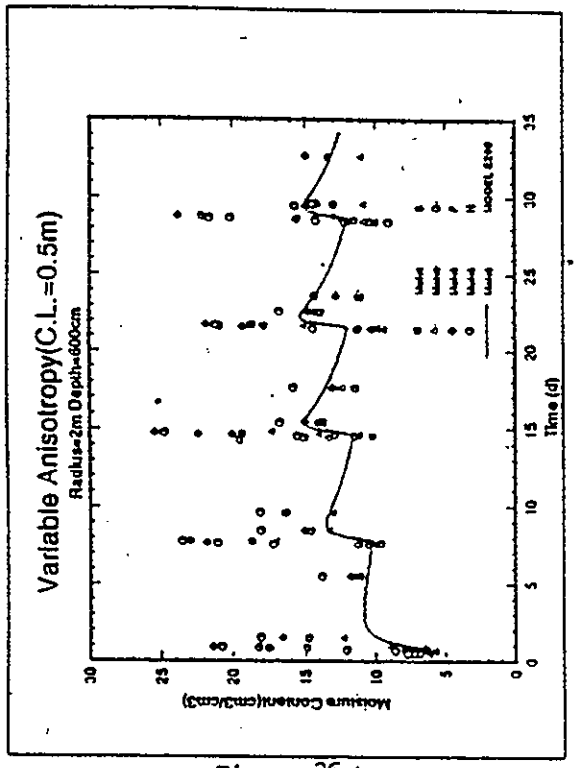

Figure 26-b.

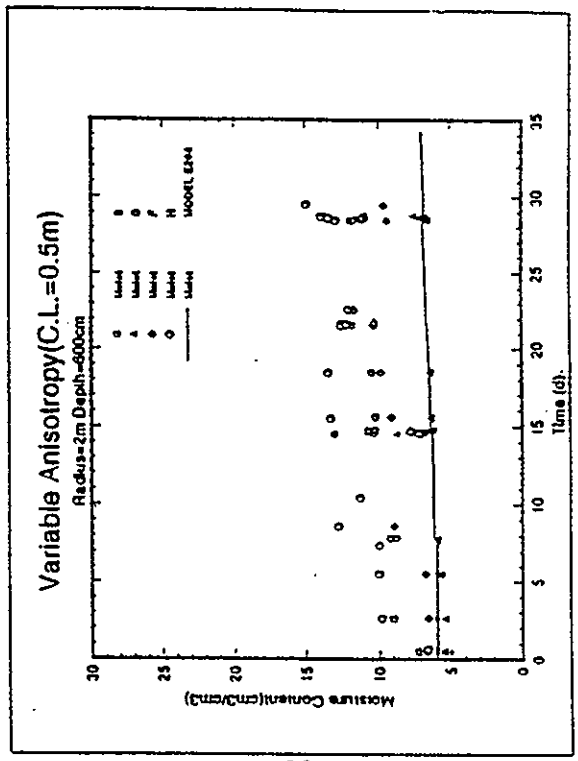

Figure 26-d.

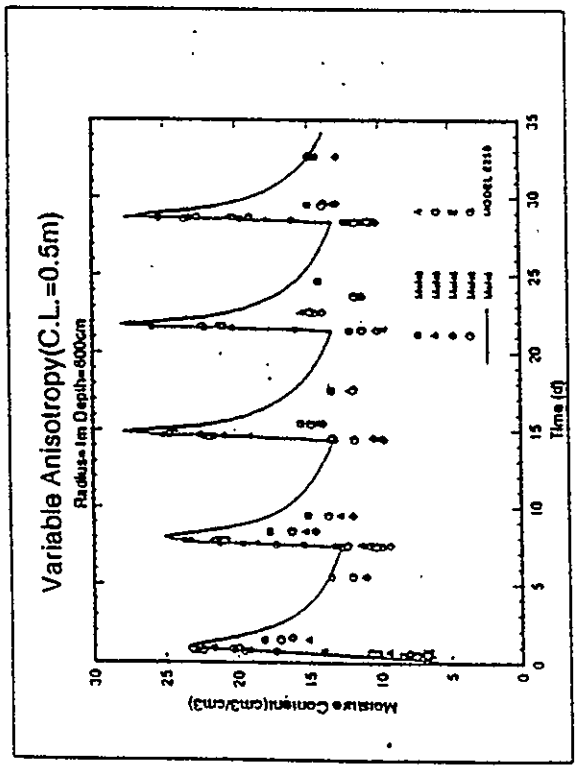

Figure 26-a.

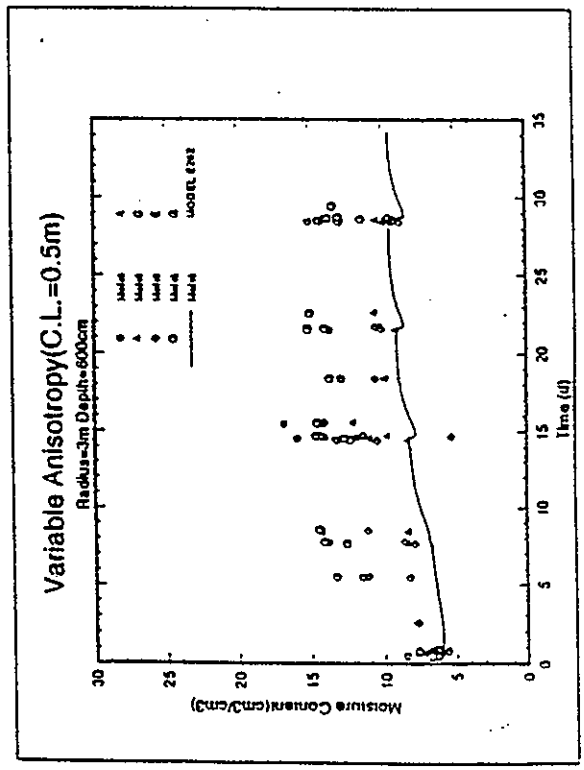

Figure 26-c.

Figure G1-27a, G1-27b, G1-27c, and G1-27d. Comparison of Calculated Versus Measured Moisture Contents at 8.4-m Depth and Radii of 1 m, 2 m, 3 m, and 4 m for Scenario 4.

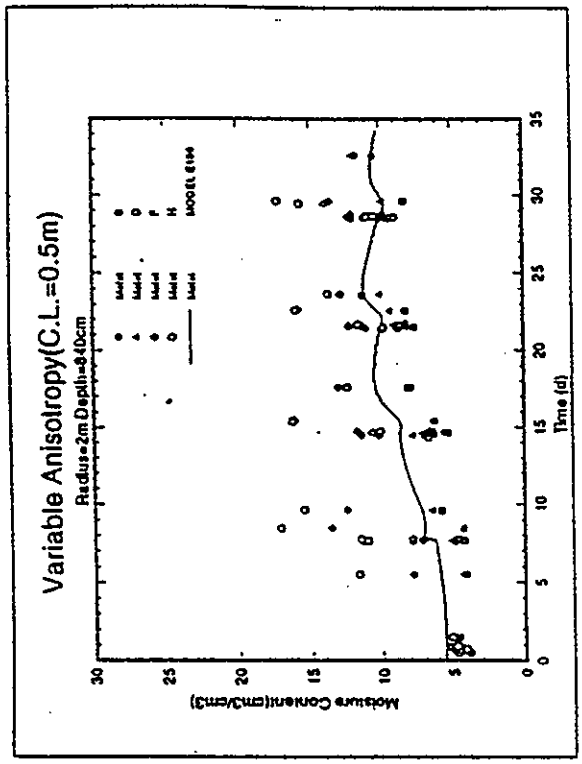

Figure 27-b.

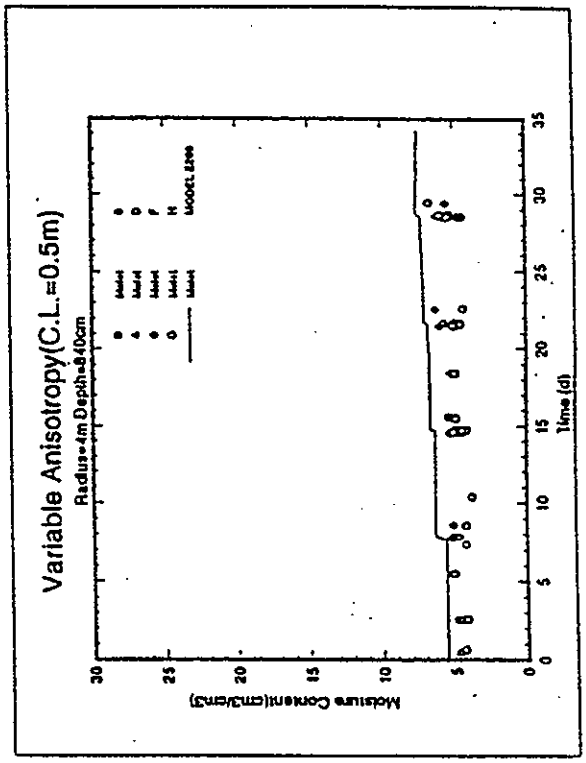

Figure 27-d.

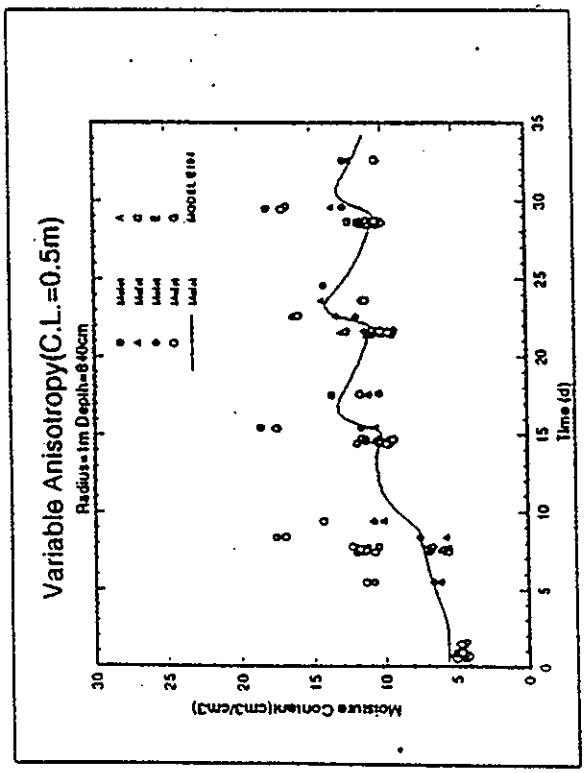

Figure 27-a.

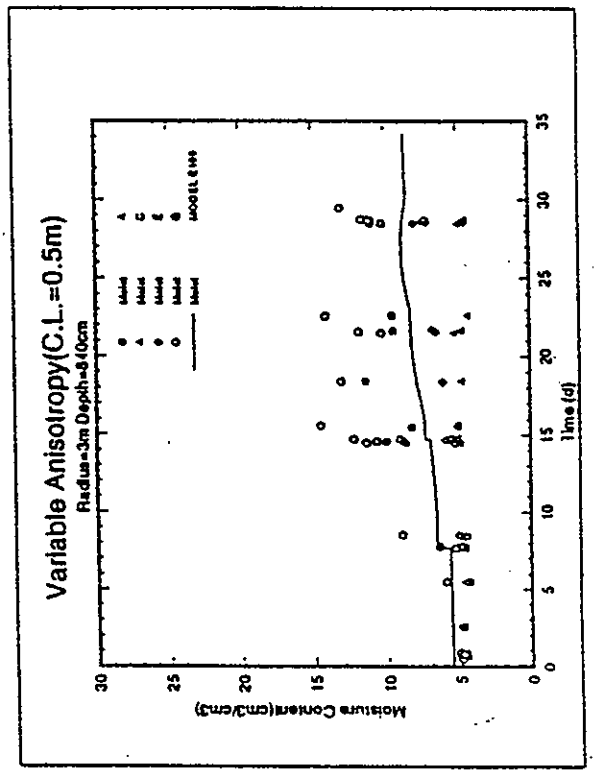

Figure 27-c.

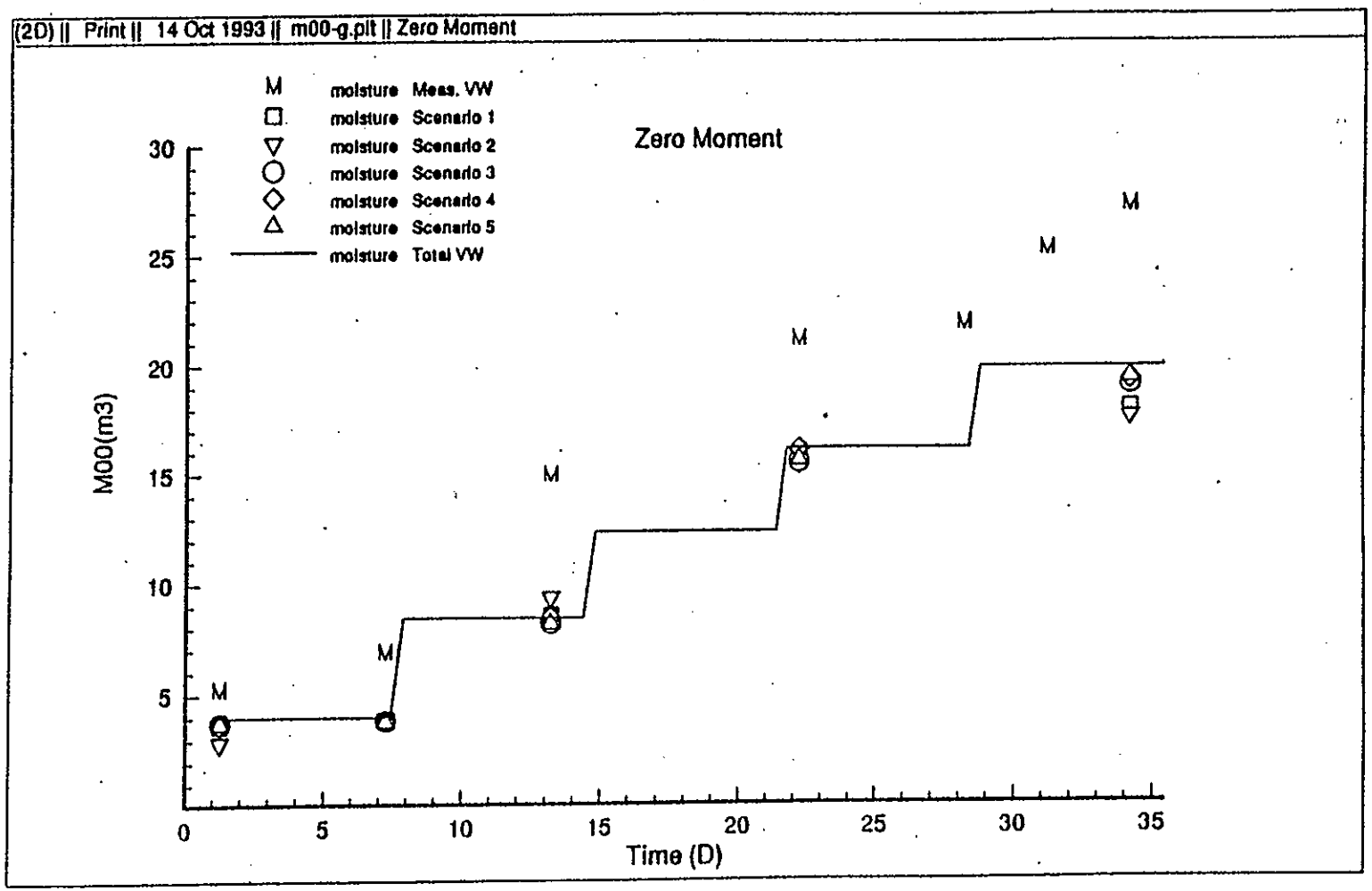

Figure G1-28. Zero Moment Calculations.

show a preferential flow in the wells at the east, south-east, and south; and much less flow in the wells at the north, north-west, and west. Since only four flow paths are intercepted and recorded at a radius of every meter, the average might be misrepresented by the higher moisture flow path. The other kinds of errors might be attributed to the calibration and measurements. The measurement was done manually by lowering sensors to the desired depths in each of the observation wells. Two measurement errors might have been generated: a. readings in a single observation well were recorded as one time; and b. the probe location (centered or decentralized) may affect its sensitivity. Quantifying the errors, however, is difficult.

Figure G1-29 shows a comparison of measured and calculated first-order moments. The first-order moments r_c and z_c indicate the change in location of moisture plume's center of mass in a cylindrical coordinates. Calculations were made at five different times: (a) 1.25 days, right after the first injection completed; (b) 7.25 days, the plume has gone six-day redistribution after the first injection completed; (c) 13.2 days, before the third injection begins; (d) 22.2 days, right after the 4th injection completed; and (e) 34.2 days, before the 6th injection took place.

The results are consistent with what the visual comparisons have shown. The center of mass of the field plume moved fast during and after first two injections and remained relatively steady afterwards.

A relatively steady movement was seen for the calculated center of mass for all scenarios. Scenarios 1 and 2 underpredict radial movement and overpredict the vertical downward movement of the plume's center of mass. Scenario 3 show a slight improvement in the lateral migration of the moisture plume. A significant improvement in the lateral spreading was seen in scenario 4 but still underpredicted compared to the field data. The degree of underprediction might slightly be overestimated in view of the zero-moment calculation which indicates a possible systematic error in the moisture content measurements.

The values of the first and second spatial moments at chosen times are presented in Table G1-2. The values of second moment confirmed conclusions from the previous discussions, i.e., the field data show more spatial variability and more spreading both horizontally and vertically than the calculated ones. However, the horizontal spreading of the plume calculated by scenario 4 is the most close fit to that observed in the field.

G1.7.0 CONCLUDING REMARKS

The preliminary results suggest that both structural layering and saturation-dependent anisotropy are significant processes at the injection site. Results of scenario 2 show that hysteresis is not a significant factor to cause an enhanced water lateral movement in this experiment, at least in the way hysteresis was treated in the model.

The initial moisture contents are consistent with the lithologic information gathered from the driller's logs. The enhanced lateral movement

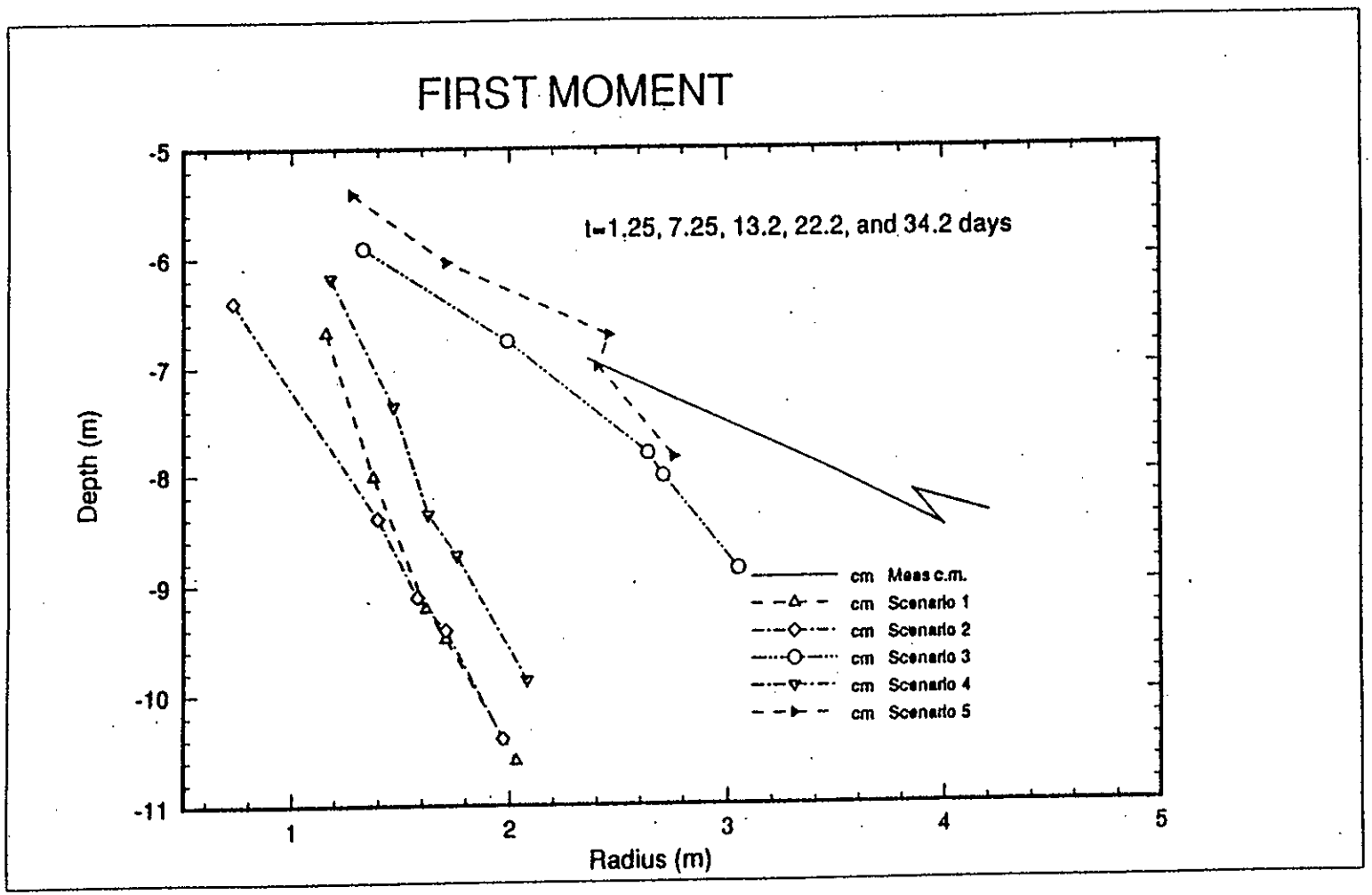

Figure G1-29. First Moment Calculation.

Table G1-2. Spatial Moments of Simulated and Observed Moisture Plumes.

Moments	Scenario				Field
	1	2	3	4	
t=1.25 days					
r_c (m)	1.26	0.735	1.18	1.28	2.36
z_c (m)	-6.68	-6.40	-6.18	-5.41	-6.93
$\sigma_{rr}^2(m^2)$	0.302	-1.90	2.75	3.26	2.10
$\sigma_{zz}^2(m^2)$	2.160	1.73	1.60	0.97	4.16
t=34.2 days					
r_c (m)	2.03	1.97	2.08	2.76	4.21
z_c (m)	-10.60	-10.40	-9.87	-7.85	-8.38
$\sigma_{rr}^2(m^2)$	0.87	0.68	0.79	2.27	3.89
$\sigma_{zz}^2(m^2)$	4.47	5.43	5.04	3.11	6.83

of the moisture plume is generally confined in two layers in which the initial moisture contents have high moisture spikes. The lithologic information suggests a finer but highly heterogeneous soil texture in these layers. The field data suggested that the downward break-through occurred in the region near the injection well where the moisture contents were high. As a result, the moisture contours exhibited a fingering phenomenon.

Inclusion of the process of saturation-dependent anisotropy in the model could partially account for the extensive lateral spreading of the plume which occurred in the field. The anisotropy ratio is sensitive to the correlation length. A better fit for Scenario 4 with a smaller correlation length suggests that the soil textural heterogeneity is underestimated by the limited soil samples that are available.

The spatial moment analyses showed a consistent conclusion with the visual comparisons. The zero moment analysis, which accounts for the change of the total water mass, indicated that the integrated field water mass was consistently higher (up to 35%) than the water mass injected. A poor calibration of the neutron probes were suspected. The first moment analysis showed that the field data exhibited a fast lateral spreading during the first two or three injections. And then the center of mass remained relatively steady. The second spatial moment analysis showed that the field data exhibited more spatial variability than the calculated ones. However, the horizontal spreading of the plume calculated by scenario 4 is the closest fit to that observed in the field.

A deficiency of the saturation-dependent anisotropy theory for this application was noted. The relative conductivities calculated with the anisotropy ratio computed from equation (G1-1) increase with decreasing pressure in the dry end of the curves.

REFERENCES

Bear, J., C. Braester, and P. C. Menier, 1987, "Effective and Relative Permeabilities of Anisotropic Porous Media," Transport in Porous Media, 2, pp.301,316.

Conca, J.L. and J. Wright, 1990, "Diffusion Coefficients in Gravel Under Unsaturated Conditions," Water Resour. Res., v. 26, pp. 1055-1066.

Fayer, M. J., J. B. Sisson, W. A. Jordan, A. H. Lu, P. R. Heller and T. J. Nicholson, "Subsurface Injection of Radioactive Tracers," NUREG/CR-5996, PNL-8499, February 1993.

Freyberg, D. L., "A Natural Gradient Experiment on Solute Transport in a Sand Aquifer, 2. Spatial Moments and the Advection and Dispersion of Nonreactive Tracers," Water Resour. Res., 22(13), 2031-2046, 1986.

Huyakorn, P. S. and S. Panday, "VAM3d-CG - Variably Saturated Analysis Model in Three-dimensions with Preconditioned Conjugate Gradient Matrix Solvers: Documentation and User's Guide, Version 2.2," HGL-89-02, July 1991.

Kool, J. B., and J. C. Parker, 1987, Development and Evaluation of Close-form Expressions for Hysteric Soil Hydraulic Properties, Water Resour. Res., 23: 105-114.

Kool, J. B., and Y. S. Wu, 1991, Validation and Testing of the VAM2D Computer Code, NUREG/CR-5795.

Mantoglou, A. M. and L. W. Gelhar, 1987a, "Stochastic Modeling of Large-Scale Transient Unsaturated Flow Systems," Water Resour. Res., 23(1), 37-46.

Mantoglou, A. M. and L. W. Gelhar, 1987b, "Capillary Tension Head Variance, Mean Soil Moisture Content, and Effective Specific Soil Moisture Capacity of Transient Unsaturated Flow in Stratified Soil," Water Resour. Res., 23(1), 47-56.

Mantoglou, A. M. and L. W. Gelhar, 1987c, "Effective Hydraulic Conductivities of Transient Unsaturated Flow in Stratified Soils," Water Resour. Res., 23(1), 57-67.

McCord, J. T., D. B. Stephens, and J. L. Wilson, "Hysteresis and State-Dependent Anisotropy in Modeling Unsaturated Hill Slope Hydrologic Processes," Water Resour. Res., 27(7), 1501-1518, 1991.

Mualem, Y., 1984, "Anisotropy of Unsaturated Soil," soil Sci. Soc. Am. J., pp. 513-522.

Price, S. M., R. B. Kasper, M. K. Additon, R. M. Smith and G. V. Last. 1979. "Distribution of Plutonium and Americium Beneath the 216-Z-1A Crib: A Status Report," Rockwell International Report RHO-ST-17, Richland, WA.

Routson, R. C., W. H. Price, D. J. Brown and K. R. Fecht. 1979, "High Level Waste Leakage from the 241-T-106 Tank at Hanford," Rockwell International Report RHO-ST-17, Richland, WA.

Sisson, J. B. and Allen H. Lu, "Field Calibration Of Computer Models For Application to Buried Liquid Discharges: A Status Report," RHO-ST-46 P, August 1984.

Van Genuchten, R., 1978, "Calculating the Unsaturated Hydraulic Conductivity with a New Close-Form Analytic Model," Report 78-WR-08, Water Resources Program, Department of Engineering, Princeton University, Princeton, New Jersey.

Yeh, T.-C. Jim, L. W. Gelhar, and A. L. Gutjahr, 1985a, "Stochastic Analysis of Unsaturated Flow in Heterogeneous Soils, 1. Statistically Isotropic Media," Water Resour. Res., 21(4), 447-456.

Yeh, T.-C. Jim, L. W. Gelhar, and A. L. Gutjahr, 1985b, "Stochastic Analysis of Unsaturated Flow in Heterogeneous Soils, 2. Statistically Anisotropic Media With Variable α," Water Resour. Res., 21(4), 457-464.

Yeh, T.-C. Jim, L. W. Gelhar, and A. L. Gutjahr, 1985c, "Stochastic Analysis of Unsaturated Flow in Heterogeneous Soils, 3. Observations and Applications," Water Resour. Res., 21(4), 465-471.

APPENDIX G2

VERIFICATION AND BENCHMARK TESTING OF THE VAM3D-CG FLOW AND TRANSPORT COMPUTER CODE FOR USE IN THE PERFORMANCE ASSESSMENT AT HANFORD

This page intentionally left blank.

APPENDIX G2

VERIFICATION AND BENCHMARK TESTING OF THE VAM3D-CG FLOW AND TRANSPORT COMPUTER CODE FOR USE IN THE PERFORMANCE ASSESSMENT AT HANFORD

Allen Lu and Dave Langford

ABSTRACT

Testing of the VAM3D-CG computer code, Version 2.4b, was conducted to establish confidence that the code is ready for use in performance assessment applications at the Hanford site. VAM3D-CG is a proprietary product of HydroGeologic, Inc., of Herndon, Virginia.

This report describes the technical basis, approach, and results of the testing. Verification (comparisons with known solutions) and benchmarking (code-to-code comparisons) were used to check the capabilities and limitations of the code to simulate diverse hydrological and geological conditions pertinent to performance assessment applications. Emphasis was on numerical stability and accuracy. Graphical comparisons and calculation of relative root mean square (RRMS) values were used as indicators of accuracy and consistency.

Three sets of testing problems were performed: 1. reproduction of the verification and benchmark testing problems published by the vendor (HydroGeologic, Inc.) in the user's manual, 2. two benchmark testing problems: a. a model of the vadose zone flow and transport due to the operation of the 216-U-17 crib in the 200 West Area. b. a cross section model consisting of a sloping clay layer. and 3. verification of the VAM3D-CG source code as installed on the Silicon Graphics, Inc. (SGI) workstation. The selected tests were performed to show that the VAM3D-CG code on the SGI produces the same results as those previously on the Cray computer which is no longer in service.

In general, the test results showed excellent agreement with the first and third sets of problems. Both maximum difference and RRMS values are negligible. The differences can be explained by rounding errors between the two computers.

For the second set of problems, the solutions showed very good overall agreement when plotted, even though VAM3D-CG and the benchmark code employ significantly different solution techniques. Although minor discrepancies exist, the two codes should perform equally well in terms of performance assessment applications at Hanford.

CONTENTS

G2.1.0 INTRODUCTION G2-6

G2.2.0 GOVERNING AND SUPPLEMENTARY EQUATIONS G2-7

G2.3.0 CODE DESCRIPTIONS G2-9

G2.4.0 PERFORMANCE INDICATORS G2-10

G2.5.0 VERIFICATION OF THE VAM3D-CG RESULTS WITH THE VENDOR'S PUBLISHED RESULTS G2-11
G2.5.1 TRANSIENT ONE-DIMENSIONAL HORIZONTAL FLOW IN A SOIL SLAB G2-12
G2.5.2 TRANSIENT VERTICAL INFILTRATION IN A SOIL COLUMN . . . G2-12
G2.5.3 TRANSIENT TWO-DIMENSIONAL FLOW IN A RECTANGULAR SOIL SLAB G2-13
G2.5.4 TRANSIENT TWO-DIMENSIONAL TRANSPORT IN A RECTANGULAR SOIL SLAB G2-14
G2.5.5 THREE-DIMENSIONAL TRANSPORT IN UNIFORM GROUNDWATER FLOW G2-14

G2.6.0 BENCHMARK TESTS: MODEL FOR THE 217-U-17 CRIB, 200 WEST AREA . G2-15
G2.6.1 OVERVIEW G2-15
G2.6.1.1 Problem Description G2-15
G2.6.1.2 Computational Grid G2-16
G2.6.1.3 Flow and Transport Parameters G2-16
G2.6.1.4 Problem History G2-21
G2.6.2 EXECUTION OF THE MODELS G2-21
G2.6.2.1 Steady State Flow Run (run1) G2-21
G2.6.2.2 Dynamic Flow Run (run2) G2-22
G2.6.2.3 Coupled Flow and Transport (run3) G2-22
G2.6.3 COMPARISON OF PORFLO-3 AND VAM3D-CG CONTOUR PLOTS . . . G2-22
G2.6.3.1 Flow Field Results G2-24
G2.6.3.2 Contaminant Transport Results G2-30
G2.6.4 CONCLUSIONS G2-30

G2.7.0 BENCHMARK TESTS: FLOW AROUND A CLAY CAP G2-35
G2.7.1 OVERVIEW G2-35
G2.7.1.1 Problem Description G2-35
G2.7.1.2 Computational Grid G2-35
G2.7.1.3 Material Properties G2-37
G2.7.2 EXECUTION OF THE MODELS G2-40
G2.7.3 COMPARISON OF PORFLO-3 AND VAM3D-CG CONTOUR PLOTS . . . G2-40
G2.7.4 CONCLUSIONS G2-43

G2.8.0 VERIFICATION OF THE VAM3D-CG SOURCE CODE AS INSTALLED ON THE SGI G2-43
G2.8.1 OVERVIEW G2-43
G2.8.2 TEST CASE ID: V3D7 (RUN # 2 IN THE REFERENCED DOCUMENT) G2-43
G2.8.3 TEST CASE ID: v3dt7cp (RUN # 2c IN REFERENCED DOCUMENT) G2-44
G2.8.4 TEST CASE ID: v3d7c (CONT. OF RUN # 2c) G2-46

CONTENTS (Cont)

G2.9.0 CONCLUSIONS G2-47

G10.0 REFERENCES G2-48

G2.1.0 INTRODUCTION

VAM3D-CG is a model of fluid flow and mass transport in saturated and unsaturated ground water systems. Modeling is performed in one, two, or three dimensions, using a finite element technique. A user's guide, published by the vendor, contains a full description of the software. VAM3D-CG (Huyakorn and Panday, 1993) is a proprietary product of HydroGeologic, Inc., of Herndon, Virginia.

The primary objective of this report is to examine the capabilities and limitations of VAM3D-CG, Version 2.4b in performance assessment applications at the Hanford Site. The examining process follows a general approach used in evaluating and/or certifying computer codes, i.e., verification (comparisons with known solutions) and benchmarking (code-to-code comparisons). Three sets of testing problems were performed and are presented in this report.

1. Verification of the VAM3D-CG Version 2.4b with the vendor's (HydroGeologic, Inc.) published results (Huyakorn and Panday, 1993);

2. Benchmarking the VAM3D-CG simulated results with the results simulated by PORFLO-3 Version 1.2 (Sagar and Runchal, 1990; Runchal and Sagar, 1992) - selected problems have the complexity and features relevant to the performance assessment applications at Hanford; and

3. Verification of the VAM3D-CG source code as installed on the Silicon Graphics, Inc. (SGI) workstation. Since the past Solid Waste Performance Assessment was performed on the Cray computer, selected tests (Wood et al., 1993) were performed to show that the VAM3D-CG code on SGI produces the same results as those on the Cray.

Because of their nonlinearity, analytical solutions to unsaturated flow equations are rare. Therefore, the verification of the accuracy with which VAM3D-CG approximates the solution to the unsaturated flow equation is performed by comparisons to other numerical approximations rather than by the standard use of analytical solutions. Only one analytical solution was selected by the vendor for verification in a saturated flow and transport problem.

Additional testing of the VAM3D-CG code using data from a field experiment (Sisson and Lu, 1984) is described by Lu and Khaleel (1993). The results from independent verification and benchmark testing of an earlier version of the VAM3D-CG code were reported by Huyakorn and Panday (1993). The 2D version (VAM2D) of VAM3D-CG was validated by Kool and Wu (1991) using the field data from the Las Cruces Trench Study.

This report is organized as follows. The governing equations used for unsaturated flow and contaminant transport modeling are presented in Section 2. Brief descriptions of the VAM3D-CG code are presented in Section 3. The performance indicators used as the acceptance criteria for the test problems are discussed in Section 4. Verification of VAM3D-CG results with the vendor's published results is described in Section 5. Benchmarking of the VAM3D-CG results for the 216-U-17 Crib with those obtained by PORFLO-3,

version 1.2, is discussed in Section 6. Benchmarking of the VAM3D-CG results for flow around a clay cap with those obtained by PORFLO-3, version 1.2, is discussed in Section 7. Section 8 contains the verification of the VAM3D-CG source code as installed on the SGI workstation. The conclusions are given in Section 9 and references are listed in Section 10.

G2.2.0 GOVERNING AND SUPPLEMENTARY EQUATIONS

To perform a variably saturated flow analysis, the VAM3D-CG code uses the pressure head or hydraulic head as the dependent variable if a rectangular grid is used. For an orthogonal curvilinear grid, the dependent variable is the hydraulic head. The governing equation for water flow in a variably saturated soil is written as:

$$\frac{\partial}{\partial x_i}[\rho_w K_{ij} k_{rw}(\frac{\partial \psi}{\partial x_j}+e_j)] = \frac{\partial}{\partial t}(\rho_w \phi S_w) - \rho_w q \qquad \text{(G2-2.1)}$$

where ρ_w = density of water
ψ = pressure head
K_{ij} = saturated hydraulic conductivity tensor
k_{rw} = relative permeability with respect to the water phase
x_i = (i=1,2,3) a set of orthogonal spatial coordinates
t = time
e_j = unit vector assumed to be vertically upward
S_w = water phase saturation
ϕ = effective porosity
q = volumetric flow rate via sources (or sinks) per unit volume.

The pressure head ψ and hydraulic head p are related as $p=\psi+z$ where z is in the vertical upward direction.

For a slightly compressible fluid, equation (2.1) can be written in the form:

$$\frac{\partial}{\partial x_i}[K_{ij} k_{rw}(\frac{\partial \psi}{\partial x_j}+e_j)] = (S_w S_s + \phi \frac{dS_w}{d\psi})\frac{\partial \psi}{\partial t} - q \qquad \text{(G2-2.2)}$$

The specific storage coefficient is defined as

$$S_s = \rho_w g(\phi\beta + \alpha) \qquad \text{(G2-2.3)}$$

where g is the gravitational constant and α and β are coefficients of compressibility of the porous medium and water, respectively.

In order to solve the variably saturated flow problem, two supplementary equations need to be specified, i.e., the relationships of

relative permeability versus water saturation, and pressure head versus water saturation. These functions are given by (Brooks and Corey, 1966):

$$k_{rw}=S_e^n \tag{G2-2.4}$$

and (van Genuchten, 1976):

$$k_{rw}=S_e^{1/2}[1-(1-S_e^{1/\gamma})^{\gamma}]^2 \tag{G2-2.5}$$

where n and γ are empirical parameters and S_e is the effective water saturation defined as $S_e=(S_w-S_{wr})/(1-S_{wr})$ with S_{wr} being referred to as the residual water saturation.

The relationship of pressure head versus water saturation is described by the following function (van Genuchten, 1976; Mualem, 1976):

$$\frac{S_w-S_{wr}}{1-S_{wr}}=\frac{1}{[1+(\alpha|\psi-\psi_a|)^{\beta}]^{\gamma}} \qquad for\,\psi<\psi_a \tag{G2-2.6}$$

$$=1 \qquad for\,\psi\geq\psi_a$$

where α and β are empirical parameters, ψ_a is the air entry pressure head value, and S_{wr} is the residual water saturation. The parameters β and γ are usually related $\gamma=1-1/\beta$. The Brooks-Corey and van Genuchten functions for the moisture retention and relative permeability characteristics can be measured in the laboratory for a given soil.

The governing equation for three-dimensional transport of a non-conservative component in a variably saturated soil takes the form

$$\frac{\partial}{\partial x_i}\left(D_{ij}\frac{\partial c}{\partial x_j}\right)-\frac{\partial}{\partial x_i}(v_i c)=\frac{\partial}{\partial t}[\phi S_w c+\rho_s(1-\phi)c_s]-qc^* \tag{G2-2.7}$$

$$+\lambda[\phi S_w c+\rho_s(1-\phi)c_s] \qquad i,j=1,2,3$$

where D_{ij} = hydrodynamic dispersion tensor
c = solute concentration in the fluid
v_i = Darcy velocity
ρ_s = density of solid grains
C_s = adsorbed concentration
λ = first-order decay coefficient
c^* = solute concentration in the injected fluid.

Assuming the relation between adsorbed and solution concentration is described by a linear equilibrium, equation (2.7) can be expressed as

$$\frac{\partial}{\partial x_i}\left(D_{ij}\frac{\partial c}{\partial x_j}\right)-\frac{\partial}{\partial x_i}(v_i c)=\frac{\partial}{\partial t}(\phi S_w R c)+\lambda\phi S_w R c-qc^* \qquad \text{(G2-2.8)}$$

where R is the retardation defined as

$$R=1+\frac{\rho_s(1-\phi)k_d}{\phi S_w}=1+\frac{\rho_B k_d}{\phi S_w} \qquad \text{(G2-2.9)}$$

with the bulk density ρ_B being defined as $(1-\phi)\rho_s$.

The hydrodynamic dispersion tensor components are computer derived using the following constitutive relations for homogeneous systems (Scheidegger, 1961):

$$D_{ij}=\alpha_T|V|\delta_{ij}+(\alpha_L-\alpha_T)\frac{v_i v_j}{|V|}+\tau D^{\circ}\delta_{ij} \qquad \text{(G2-2.10)}$$

where α_L and α_T are longitudinal and transverse dispersivities, respectively, δ_{ij} is the Kronecker delta, D° is the bulk molecular diffusion coefficient, and τ is the tortuosity.

G2.3.0 CODE DESCRIPTIONS

The VAM3D-CG code is briefly described in this section. Detailed descriptions of the numerical methods implemented in the code are given in the users' manual (Hyyakorn and Panday, 1993).

VAM3D-CG version 2.4b is a three-dimensional finite element model used for simulating saturated-unsaturated groundwater flow and transport with variable water table positions and highly non-linear soil moisture conditions. The Galerkin and upstream weighted residual procedures are employed for solving the flow and transport equations (equations G2-2.1 or G2-2.2 and G2-2.7 or G2-2.8, respectively). Preconditioned Conjugate Gradient (PCG) and ORTHOMIN techniques are used to solve the large symmetric and asymmetric matrix equations. Element matrices are generated using influence coefficient formulas, thus avoiding costly numerical integration. The code can easily be adapted for one-, two- or three-dimensional applications, including axisymmetric configurations.

VAM3D-CG was placed under configuration management in mid 1993. This ensures the source and executable codes are carefully controlled, and the results are traceable to the code which created them. The current effort

examines version 2.4b of the source code, dated August 13, 1993 (the vender has released multiple revisions of version 2.4b).

The bulk of the tests which follow were run on an SGI workstation, under the operating system IRIX Release 4.0.5C, System V. This includes most of the VAM3D-CG results and all of the PORFLO-3 results. Additional runs were made on a Cray XMP12-32 computer, operating under UNICOS 6.0, in an effort to verify the installation of VAM3D-CG as it was moved to the SGI.

When VAM3D-CG was moved to the SGI environment, two changes were made to the code. First, a traceability record was added to the top of the output files. File traceability is often a necessary feature, when then results must be archived for a number of years, or when multiple versions of the modeling code are released. Second, the system dependent routines were separated from the numeric modeling software. This allows the code to be moved between operating systems, without making modifications to the source code files which do the actual computation.

G2.4.0 PERFORMANCE INDICATORS

Various performance indicators can be used to evaluate the accuracy of the results generated by the numerical models. Quantitative indicators of model performance include maximum difference, maximum relative difference, root mean square error and relative root mean square error. The relative root mean square error (RRMS) was adopted as the performance indicator for the first and third sets of the test problems. The RRMS indicator is defined by the following formula:

$$RRMS = \sqrt{\frac{\sum_{i=1}^{k} ((r_i - n_i)/r_i)^2}{k}} \qquad \text{(G2-3.1)}$$

where r_i = reference solution at point i

n_i = numerical solution at point i by the VAM3D-CG version 2.4b on the SGI

k = number of comparison points.

For the first set of testing problems, the reference solutions are the results calculated by the vendor using a different version of the VAM3D-CG code. For the third set of problems, the reference solutions are the results calculated by the VAM3D-CG version 2.4b on the Cray XMP12-32 operating under UNICOS 6.0.

Magnusen et al (1990) used the RRMS error as a performance indicator for comparing numerical and analytical solutions. They defined four

performance categories: 1. Excellent - RRMS ≤ 0.01, 2. Good - RRMS ≤ 0.05, 3. Acceptable - RRMS ≤ 0.10, and 4. unacceptable - RRMS ≥ 0.10.

In this application, since we verify different versions of the VAM3D-CG operating on different computers, small errors are expected. Thus, we define arbitrarily the acceptable RRMS ≤ 0.01.

For the second set of problems, significant differences were expected in the results near the source term and boundaries between the VAM3D-CG code and the benchmarked code, PORFLO-3 Version 1.2. The RRMS performance indicator was not used as an acceptance criteria. Some of the reasons these differences occurred were:

- Different geometries (PORFLO-3 uses a finite difference scheme, while VAM3D-CG uses a finite element. Consequently, the nodal locations do not match between the models).

- Different handling of boundary conditions (e.g., PORFLO-3 places its first computational node well within the domain, while VAM3D-CG places that node on the boundary).

- Different material boundaries (PORFLO-3 places the material boundaries mid-way between nodes, while VAM3D-CG places them on the nodes).

- Different calculation methods (e.g., PORFlO-3 uses the concept of internodal conductivity and results in several averaging methods at users' choice, while the VAM3D-CG approximates the hydraulic conductivity as a function of space over the area or volume of the finite element).

Instead, graphical comparisons were made as the primary comparison for the two benchmark testing problems. Although only a subjective judgement on the degree of agreement between the two codes can be made, overall agreement in terms of the prediction of the ultimate performance objectives should be emphasized.

G2.5.0 VERIFICATION OF THE VAM3D-CG RESULTS WITH THE VENDOR'S PUBLISHED RESULTS

The following testing problems described in the user's guide were rerun to verify accuracy of the new code version 2.4b on the SGI workstation:

- Transient one-dimensional horizontal flow in a soil slab
- Transient vertical infiltration in a soil column
- Transient two-dimensional flow in a rectangular soil slab
- Transient two-dimensional transport in a rectangular soil slab
- Three-dimensional transport in uniform groundwater flow.

A detailed description of these testing problems, values of the physical parameters used in the simulations, numerical results, and

comparisons between the vendor's version and Version 2.4b, are presented. RRMS values in the section use a threshold of 1.0e-3 cm for pressure head and 1.0e-3 g/cm^3 for concentration (data points below this limit are not compared).

G2.5.1 TRANSIENT ONE-DIMENSIONAL HORIZONTAL FLOW IN A SOIL SLAB

1. Problem Description

The purpose of this problem is to test the implementation of the Galerkin finite element formulation and the nonlinear iterative schemes for a case where there is no gravity effect. A rectangular grid comprised of 2 x 2 x 21 nodes was used for simulation. Fixed pressure head values equal 0.0 cm on one end, and -83.33 cm on the other end. The soil was assumed to be homogeneous and isotropic with a saturated hydraulic conductivity of 1 cm/d and a porosity of 0.45. Twenty time steps were taken with Δt = 0.01 days.

The soil moisture characteristics used in the simulation correspond to the Brooks-Corey equation with n=1 and S_{wr}=0.3333 (see eq. G2-2.4). The selected water saturation function corresponds to the van Genuchten equation with α=-0.01 cm^{-1}, β=1, and γ=-1. ψ_a is assumed to be 0.0 cm (eq. G2-2.6).

The pressure head profiles and the water saturation profiles computed by VAM3D-CG were compared by the vendor to those computed by the UNSAT2 (Table G2-1), a two-dimensional Galerkin finite element code, documented in Neuman et al. (1974) and David and Neuman (1983). The vendor concluded a good agreement between the two numerical solutions. The VAM3D-CG input and output files, p421.dat and p421.out, were provided by the vendor.

Table G2-1. Comparison of the Vendor's Version with Version 2.4b Numeric Data.

Time (Days)	Range of Variable Pressure Head (cm)	Max. Difference (cm)	RRMS
0.1	-83.330 --- 0.0	1.0e-3	1.896e-5
0.2	-83.330 --- 0.0	1.0e-3	6.962e-6

In this section, the RRMS values use a threshold of 1.0e-3 cm for pressure-head value and 1.0e-3 g/cm^3 for concentration. Values at the boundary nodes were excluded from RRMS calculation.

G2.5.2 TRANSIENT VERTICAL INFILTRATION IN A SOIL COLUMN

1. Problem Description

This problem is concerned with the one-dimensional infiltration in an unsaturated zone. It was selected to test the nonlinear finite element formulation for a case that included gravity effects. A rectangular grid

comprised of 41 x 2 x 2 nodes was used for simulation. Initially, the values of the pressure head of the soil column were -70.0 cm. The value of the pressure head at the lower end was maintained at zero. A no-flow boundary conditions was applied at the top end. 15 time steps were taken with Δt = 0.01 days.

The soil moisture characteristics used in the simulation corresponds to the Brooks-Corey equation with n=1 and S_{wr}=0.3333. The selected water saturation function corresponds to the van Genuchten equation with α=-0.01 cm^{-1}, β=1, and γ=-1. ψ_a is assumed to be 0.0 cm.

Results were compared by the vendor with both UNSAT2 and VAM2D solutions (Table G2-2). From the graphics, the vendor concluded that the solution from the VAM3D-CG agrees well with both UNSAT2 and VAM2D solutions. The VAM3D-CG input and output files, p422.dat and 422.out, were provided by the vendor.

Table G2-2. Comparison of the Vendor's Version with Version 2.4b Numeric Data.

Time (Days)	Range of Variable Pressure Head (cm)	Max. Difference (cm)	RRMS
0.1	-90.00 --- 0.0	5.40e-2	7.652e-4
0.2	-90.00 --- 0.0	3.70e-2	5.338e-4

G2.5.3 TRANSIENT TWO-DIMENSIONAL FLOW IN A RECTANGULAR SOIL SLAB

1. Problem Description

The purpose of this problem is to test the finite element formulation for a two-dimensional unsaturated flow involving gravity, and a prescribed head and flux boundary condition. A rectangular grid comprised of 11 x 16 x 2 nodes was used for simulation. Initial pressure head values were -90.0 cm, boundary conditions: ψ = 6-y for 6 cm $\leq$ y $\leq$ 10 cm on the left upper corner nodes, -90 cm on all right side nodes, and no flow for all other boundary nodes. The soil properties were kept the same as those used in Section 5.2. Time step values were generated within the code using the algorithm: Δt_1 = 0.01 days, $\Delta t_k = 1.2 * \Delta t_{k-1} \leq 0.05$ days for k=2,...,15.

The vendor compared VAM3D-CG results with those obtained from the UNSAT2 code (Table G2-3), and they agreed well. VAM3D-CG input and output files, p423.dat and p423.out, were provided by the vendor.

Table G2-3. Comparison of the Vendor's Version with Version 2.4b Numeric Data.

Time (Days)	Range of Variable Pressure head (cm)	Max. Difference (cm)	RRMS
0.074	-90.00 --- 0.0	3.00e-3	1.703e-5
0.254	-90.00 --- 0.0	2.00e-3	8.645e-4

G2.5.4 TRANSIENT TWO-DIMENSIONAL TRANSPORT IN A RECTANGULAR SOIL SLAB

1. Problem Description

This problem corresponds to the two-dimensional unsaturated flow problem described in 5.3. It is concerned with the transport of a nonconservative solute in a rectangular soil slab. Boundary conditions for the transport were on the upper left five nodes with all values 1.0. Initial conditions were 0.0 g/cm^3. Parameters used were: longitudinal dispersivity, α_L = 1 cm; transverse dispersivity, α_T = 0.0 cm; apparent molecular diffusion, D_0 = 0.01 cm^2/d; Decay coefficient, λ = 0.001 d^{-1}; bulk density, ρ_B = 1.46 g/cm^3; and distribution coefficient, k_d = 0.308 cm^3/g.

The solution obtained is compared by the vendor with the corresponding Galerkin solution obtained by using the FEMWASTE code (Yeh and ward, 1981). The vendor concluded that the overall agreement between the two numerical solutions was reasonable (Table G2-4). The VAM3D input and output files, p433.dat and p433.out, were provided by the vendor.

Table G2-4. Comparison of the Vendor's Version with Version 2.4b Numeric Data.

Time (Days)	Range of Variable Conc. (g/cm^3)	Max. Difference (g/cm^3)	RRMS
0.074	0.001 --- 1.0	1.0e-5	7.761e-5
0.258	0.001 --- 1.0	1.0e-5	6.573e-5

G2.5.5 THREE-DIMENSIONAL TRANSPORT IN UNIFORM GROUNDWATER FLOW

1. Problem Description

The purpose of this problem was to verify the transport finite element formulation in VAM3D-CG by comparing the results with the analytical solution and the other two numerical models for a full three-dimensional transport problem. The problem concerned contaminant transport from a small volume source (land disposal) situated on top of a shallow unconfined aquifer. The transport occurred in the saturated zone of the aquifer with steady uniform groundwater flow. The Darcy velocity flow was assumed to be 1.61 x 10^{-2} m/d

parallel to the horizontal axis. The source term was a constant contaminant mass flux at a rate of 140.8 g/d.

Because of its symmetry with respect to the x-y plane, only one half of the region was modeled. A rectangular grid comprised of 2,430 (30 x 9 x 9) nodes was selected. Nodal spacings were constant in the y and z directions. The values of Δy and Δz are 2.5 m and 3.7 m, respectively. The x-coordinates of the grid line selected were -36, -19, -10, -4, 0, 4, 10,17, 24, 31, 38, 46, 54, 62, 70, 78, 96, 105, 114, 123, 132, 141, 150, 159, 168, 177, 186, 195, and 204 m, respectively. 20 time steps were taken with Δt = 100 days. Parameters used were: longitudinal dispersivity, α_L = 4 m; transverse dispersivity, α_T = 0.8 m; and porosity, ϕ = 0.35.

A general analytical solution for such a problem can be found in Yeh (1981). The solution was implemented into a computer code referred to by the vendor as the AT123D analytical model. Results computed by VAM3D-CG were compared by the vendor with the AT123D and additional three-dimensional finite element codes, MAST3D and STACE3D. The vendor concluded that these numerical solutions exhibited reasonable agreement with the analytical solution (Table G2-5). The VAM3D-CG input and output files, p432.dat and p432.out, were provided by the vendor.

Table G2-5. Comparison of the Vendor's Version with Version 2.4b Numeric Data.

Time (Days)	Range of Variable Conc. (g/cm^3)	Max. Difference (g/cm^3)	RRMS
1,000	0.001 --- 1367	1.0e-7	4.810e-7
1,400	0.001 --- 1367	1.0e-4	7.476e-7
2,000	0.001 --- 1368	1.0e-5	7.169e-7

G2.6.0 BENCHMARK TESTS: MODEL FOR THE 217-U-17 CRIB, 200 WEST AREA

G2.6.1 OVERVIEW

This problem is based on a model of vadose zone flow and transport due to operation of the 216-U-17 crib in the 200 West Area. The model was originally implemented with PORFLO-3, version 1.2 (Runchal et al., 1992; Kline, 1993) and is described in the Groundwater Impact Assessment (GIA) report for the 216-U-17 Crib (Reidel et at, 1993). All numeric values used in this effort have been taken from that document. The results from VAM3D-CG are compared with the PORFLO-3 results, to benchmark the correctness of VAM3D-CG (Huyakorn et. al., 1993).

A lengthy series of 216-U-17 crib simulations was performed in support of the GIA. This problem represents only one of those models. It is presented here solely for the purpose of benchmarking.

G2.6.1.1 Problem Description

The 216-U-17 Crib is waste water disposal site for operations in the 200 Area. The floor of the crib is about 3 m wide, 3 m below the ground surface, and 46 m (150 ft) in length. The crib is backfilled with gravel, and covered with a polyethylene barrier. Waste water enters the crib through a perforated fiberglass reinforced pipe which is buried in the gravel. The pipe measures 46 m in length by 15.24 cm (6 in) in diameter. From the entry point at the west end of the crib, the pipe slopes downward 0.2%.

The discharge into the crib was substantially below the design capacity. Therefore, for the purposes of this modeling, the fluid source is assumed to be at the uppermost 20 m of the discharge pipe.

The spatial domain for the model (See Figure G2-1) extends downward from the mean elevation of the pipe. Several layers of sedimentary soil and rock are present below the Crib. The water table lies 65 m below the ground surface, and the domain extends 30 m down into the water table. The model extends 100 m to both the east and west from the west end of the crib (Reidel et al, 1993).

Flow modeling began by determining a steady state flow field under the crib, before operation began. The steady flow field was the starting point for simulation of coupled (simultaneous) flow and transport. The particular case used for the present study of the counterpart VAM3D-CG model is identified in Section 5.1.4.1.1 of the GIA report (Reidel et al, 1993).

Both PORFLO-3 and VAM3D-CG used a hydraulic head formulation of the pressure equation. These were converted to pressure head prior to plotting.

G2.6.1.2 Computational Grid

The computational grid for VAM3D-CG was taken directly from the PORFLO-3 grid. The nodes of the finite element grid were placed mid-way between the nodes of the finite difference grid. Thus, each cell of the PORFLO-3 grid was translated into a finite element, except boundary cells. Material boundary locations were preserved by this construction, and both models had the same grid resolution.

For VAM3D-CG, the grid had 3705 elements and 7656 nodes. All elements were regular quadrilaterals, arranged in a 57 by 65 rectangular grid. The grid is plotted in Figure G2-2, while material boundaries are plotted in Figure G2-3. A two dimensional model was used. The thickness of the model, Δy, was set to 2 m. A fully three dimensional solution was generated, using finite element connectivity.

G2.6.1.3 Flow and Transport Parameters

The flow properties are listed in Table G2-6. The hydraulic conductivities were taken as isotropic. The specific storage was set uniformly to 0.2 m^{-1} for all materials. A van Genuchten model was used for the unsaturated flow characteristics. The porosity used was taken from the diffusive porosity in the PORFLO-3 model.

VAM3D-CG allows the van Genuchten gamma to be specified directly. These values were set to zero, which forces the code to compute gamma from the beta values, $\gamma=(1-1/\beta)$.

Figure G2-1. Idealized Longitudinal Cross-Section of Stratigraphy Under the 216-U-17 Crib.

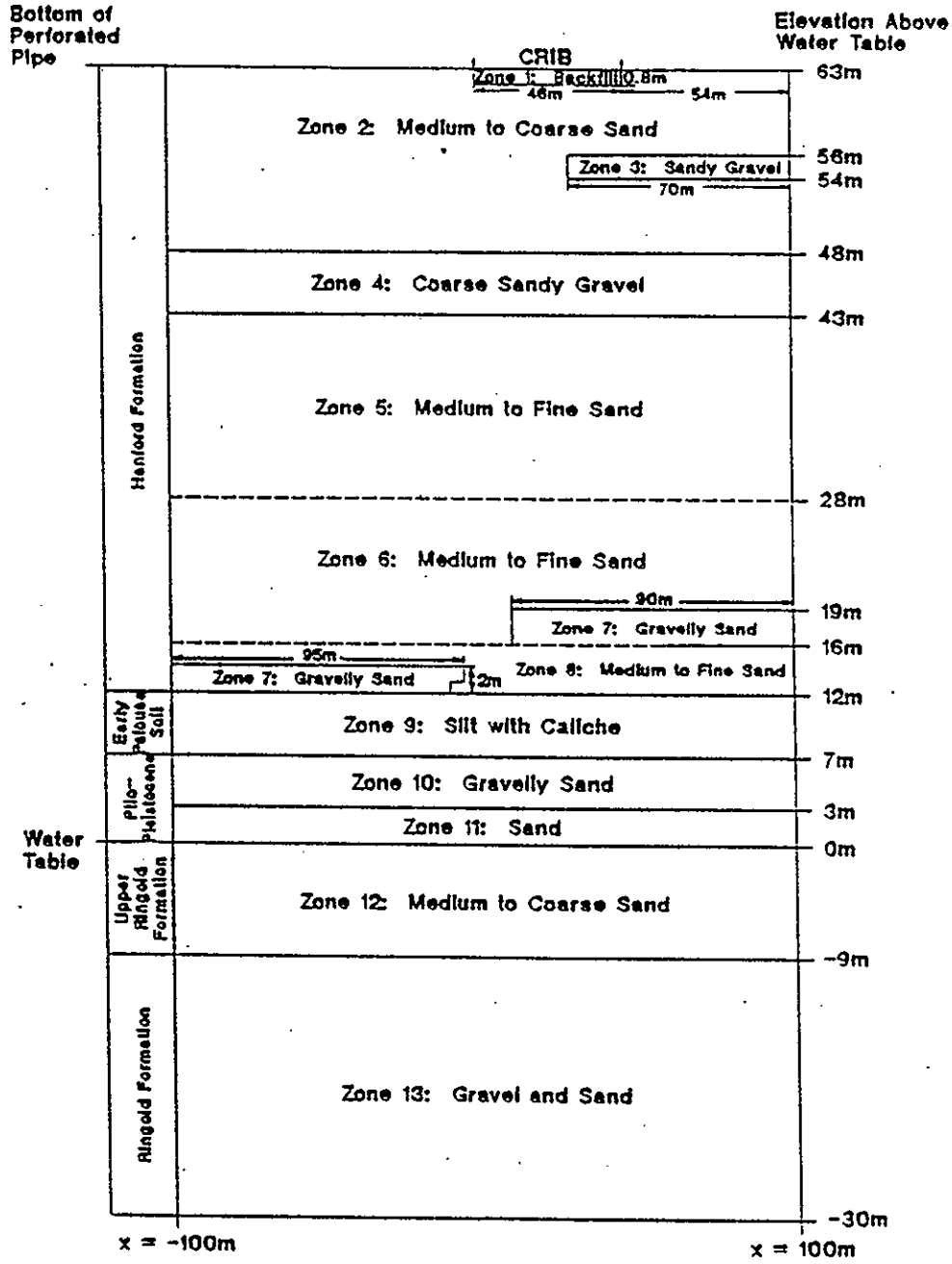

Figure G2-2. Cross Section of the Finite Element Grid.

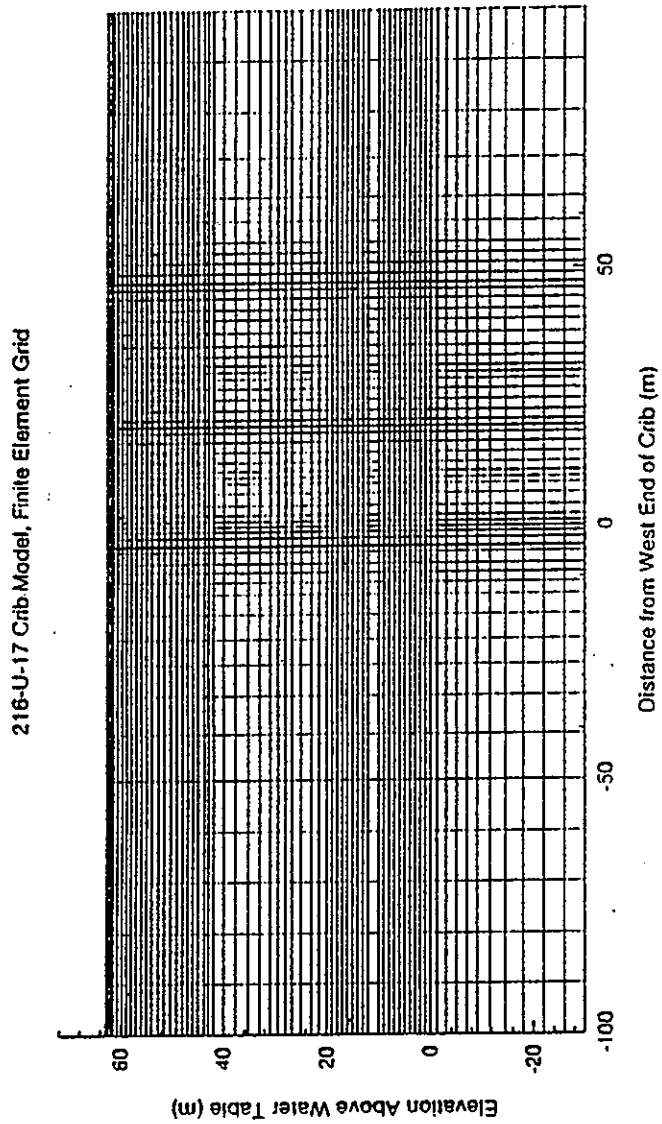

Figure G2-3. Cross Section of Material Boundaries.

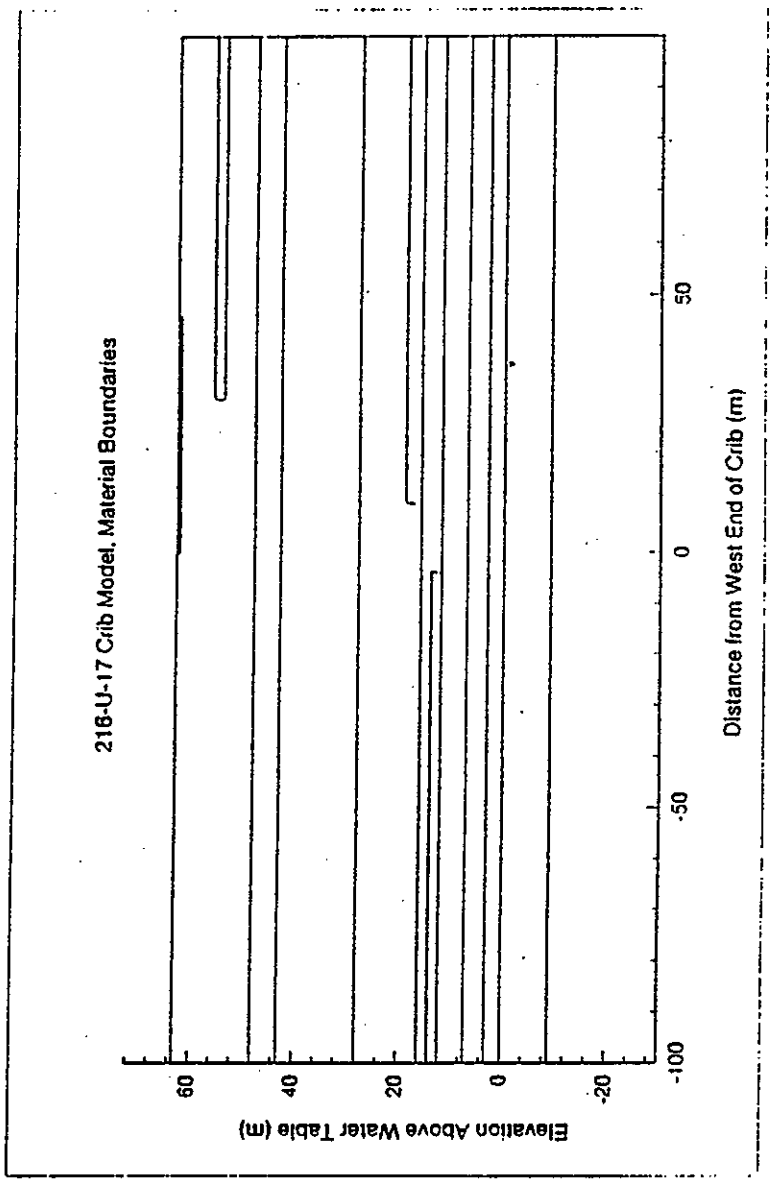

Fig. 6.3

The nominal rain water recharge rate was set to 10 cm/yr. When crib operation begins, the crib receives a constant water recharge flux of 109.5 m/yr, evenly spread over the floor of the crib source zone (x=0 to x=20). The contaminant boundary concentrations are set to unity along the fluid flux boundary, to model the inflow of contaminants into the domain.

For the transport properties, identical values were assumed for all of the material zones. These are listed in Table G2-7.

For the PORFLO-3 runs, the flow properties were averaged at cell interfaces using a geometric mean. The transport properties were averaged using a harmonic mean.

Table G2-6. Flow Parameters.

Zone	Hyd Cond (m/yr)	Porosity	Residual Saturation	alpha (1/m)	beta
1	6.224E+02	0.3660	8.000E-03	8.547E+01	1.343E+00
2	7.200E-01	0.3420	2.300E-02	7.770E+00	1.683E+00
3	7.637E+02	0.3720	0.000E+00	2.320E+00	1.189E+00
4	8.520E+03	0.4960	1.020E-01	2.786E+01	1.371E+00
5	3.950E+01	0.4270	4.100E-02	1.060E+01	1.473E+00
6	3.950E+01	0.4270	4.100E-02	1.060E+01	1.473E+00
7	3.471E+03	0.3720	1.900E-02	1.368E+01	1.288E+00
8	3.950E+01	0.4270	4.100E-02	1.060E+01	1.473E+00
9	2.610E+01	0.4490	6.000E-02	5.800E-01	3.145E+00
10	8.390E+00	0.5160	0.000E+00	1.470E+00	1.196E+00
11	1.638E+01	0.3350	0.000E+00	1.470E+00	1.397E+00
12	1.073E+01	0.4180	4.100E-02	8.826E+00	2.387E+00
13	8.521E+02	0.2620	8.800E-02	8.826E+00	2.387E+00

Table G2-7. Transport Parameters.

Zone	Alpha L (m)	Alpha T (m)	Diffusivity (m^2/yr)	Decay (1/yr)	Sorption
All	1.00	0.100	3.00E-02	0.00	0.00

G2.6.1.4 Problem History

This model was originally executed by PORFLO-3 in 1990, using a more coarse grid. That model showed some oscillatory wetting-drying behavior under the crib. The more recent model (Reidel et al, 1993) employed a finer grid and did not show the oscillatory behavior. The current effort with VAM3D-CG duplicates the finer grid model. This provides a benchmark for the techniques used by VAM3D-CG. Version 2.4b of VAM3D-CG was used for the modeling.

The VAM3D-CG model was originally constructed and executed as an integration test of the VAM3D-CG pre processor, PREPRO. That input and output was used extensively in this effort.

The original VAM3D-CG input material types were modified, in order to be consistent with the material zoning used in the PORFLO-3 executions. One boundary flux value was found to be incorrect (node 7565) in the original input file in PORFLO-3. The error was about 15% at one node out of 116 nodes. This was corrected, but the results did not change noticeably on the output graphs.

G2.6.2 EXECUTION OF THE MODELS

Three runs of VAM3D-CG were made with this problem. The first generated initial conditions for the flow field. A second run modeled only fluid flow, to ensure the results were comparable with PORFLO-3. The third run modeled coupled fluid flow and mass transport.

G2.6.2.1 Steady State Flow Run (run1)

This sets up a steady state flow field under the crib to act as initial conditions for the transient flow. The crib itself was assigned hydraulic properties equal to the surrounding soils.

The top of the domain was assigned a uniform fluid flux value of 10 cm/yr. The sides of the domain, in the unsaturated zone, were set to zero flux boundaries. In the saturated zone, the heads were set to 0.04 on the east end of the domain, and 0.0 on the west end of the domain. The bottom boundary was assigned fixed values, linearly interpolated from the east to west boundary values.

Initial conditions were set by estimating the appropriate head for the given recharge rate, assuming a unit gradient driving force. These were placed into an initial conditions file (TAPE8) for input to VAM3D-CG. This file was taken from the original VAM3D-CG integration tests. The flow model was executed for 700 years (1740 time steps), when a near steady state solution was reached.

The results of this run were used as initial conditions for the transient flow and transport models. Note that the initial pressures used in the PORFLO-3 comparisons are taken from the first time step of the coupled flow and transport model, and not from this steady state run.

G2.6.2.2 Dynamic Flow Run (run2)

VAM3D-CG was set up to run the dynamic flow fields, using the steady state flow field as initial conditions.

The boundary conditions remained unchanged, except the region above the crib. The source boundary extends from x=0 to x=20, and is 2 m (= Δy) in width. For the corresponding PORFLO-3 model, crib operation discharged 2,190 m^3/yr of fluid into a boundary area of 20 m^2, for a boundary flux of 109.5 m/yr. The same fluid flux was used for the source boundary for VAM3D-CG. For the remainder of the crib, boundary fluid flux is set to zero, due to the polyethylene barrier over the crib. The boundary conditions are displayed in Figure G2-4.

The model was run for ten years. The initial time steps were set to 1.0E-7 yr, and increased to 0.005 yr. In the finished model, an additional 0.2 yr of modeling time was added, to ensure a plot file record was written after the final time of 10 years. A total of 1,449 time steps were taken.

The flow field was plotted, and compared with results from PORFLO-3. The plotted time values were not identical. However, within the limit of a visual comparison between the plots, both codes produced substantially similar results.

G2.6.2.3 Coupled Flow and Transport (run3)

The fluid flow model was again run, with the addition of simultaneous mass transport. The boundary and initial conditions for fluid flow remained as before. Initial conditions for concentration were set to zero.

Boundary conditions for concentration were set to zero at the bottom of the domain, and zero diffusive flux along the east and west sides of the domain. Above the effluent source zone (x=0 to x=20), boundaries were set to a fixed value of 1. The transport equation is linear, and the results can be scaled to any desired boundary value.

For the remaining boundary above the crib (x=20 to x=46), the concentrations were set to a zero diffusive flux value. The boundary nodes outside the crib (x<0 and x>46) were set to fixed values of zero. This avoids a false boundary source due to the rain water recharge in that region.

Time stepping for the coupled flow and transport model were the same as for the flow model.

G2.6.3 COMPARISON OF PORFLO-3 AND VAM3D-CG CONTOUR PLOTS

Contour plotting was selected as the primary comparison between the PORFLO-3 and VAM3D-CG models. This produces only a subjective judgement on the agreement between the two codes. However, PORFLO-3 uses a finite difference scheme, while VAM3D-CG uses finite elements. Since the nodal coordinates to not match between the models, they are of limited value in direct data comparisons.

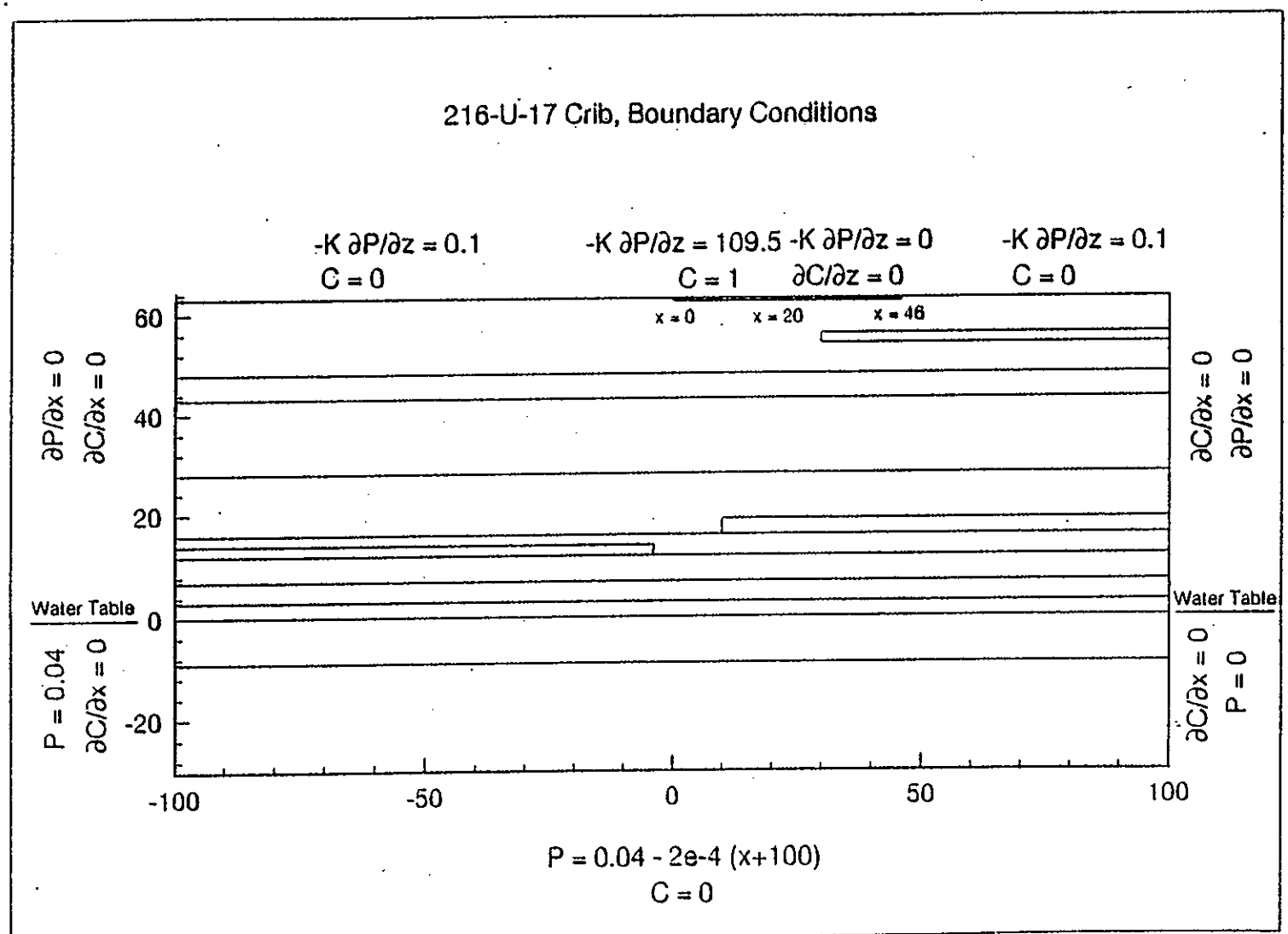

Figure G2-4. 216-U-17 Crib, Boundary Conditions.

Where data gradients are small, contour plots tend to exaggerate minor difference between data sets. This also makes it difficult to compare regions where the data are nearly constant. Therefore, the comparison between plots must be done judiciously.

Some systematic differences are expected in the contour plotting of the results. Graphics processing normally uses linear interpolation between values at the nodes of a model. However, PORFLO-3 places the material boundaries mid-way between nodes. Accurate interpolation of the data would also include material properties within adjoining cells.

In VAM3D-CG, the state variables are modeled to a quadratic accuracy within each element, which is one order higher than the plotting. In addition, VAM3D-CG does not permit an easy method for plotting data at predetermined times. Therefore, the VAM3D-CG results are plotted at times which differ slightly from those of PORFLO-3.

6.3.1 Flow Field Results

The fluid pressures are plotted in Figures G2-5 through G2-8. Each figure shows the corresponding results between the two models. Plotting times for PORFLO-3 were 0, 1, 3, and 5 years. For VAM3D-CG, results were plotted at times 3.5E-6, 0.99, 3.05, and 5.12 years.

Some very minor differences in the initial conditions are noted between PORFLO-3 and VAM3D-CG. These could be due to differences in the finite difference and finite element modeling techniques, or in the data interpolation schemes. Also, one or both of the models might not have reached a true steady state when the dynamic model initial conditions were generated. The differences are very minor, and not considered significant.

At time 1.0, the flow fields are very similar. The wetting fronts are in nearly the same positions, although VAM3D-CG generates higher pressure values behind the wetting front. In the plots, the VAM3D-CG data is 0.01 years behind the PORFLO-3 data.

At time 3.0, the flow fields are very nearly equivalent. The PORFLO-3 wetting front lags slightly behind the VAM3D-CG front at the west end of the domain. All other contours shown match up fairly well.

At time 5.0, the wetting fronts again match up very well. The saturated pressures show some minor differences at the west end of the crib, but otherwise agree for the range of pressures shown. Near the bottom of the unsaturated zone, the PORFLO-3 contours are slightly lower than the VAM3D-CG contours. PORFLO-3 apparently responds to the approaching fluid column faster than VAM3D-CG. This may result from a small amount of numeric diffusion, but the difference is small.

Plots of the fluid saturations were made at time 5.0 for both models. These are shown in Figure G2-9. These also match up fairly well. Some conspicuous discrepancies are present, but these are probably very minor differences which are accentuated by the use of contour curves.

Figure G2-5. Comparison of Fluid Pressure Results Between PORFLO-3 and VAM3D-CG at 0 Years.

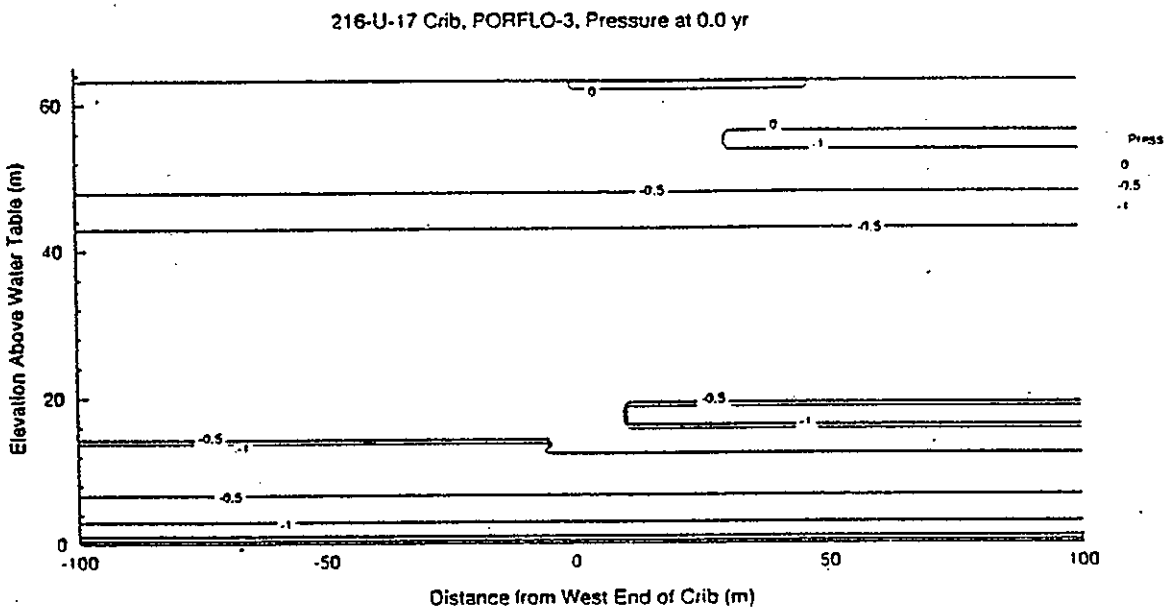

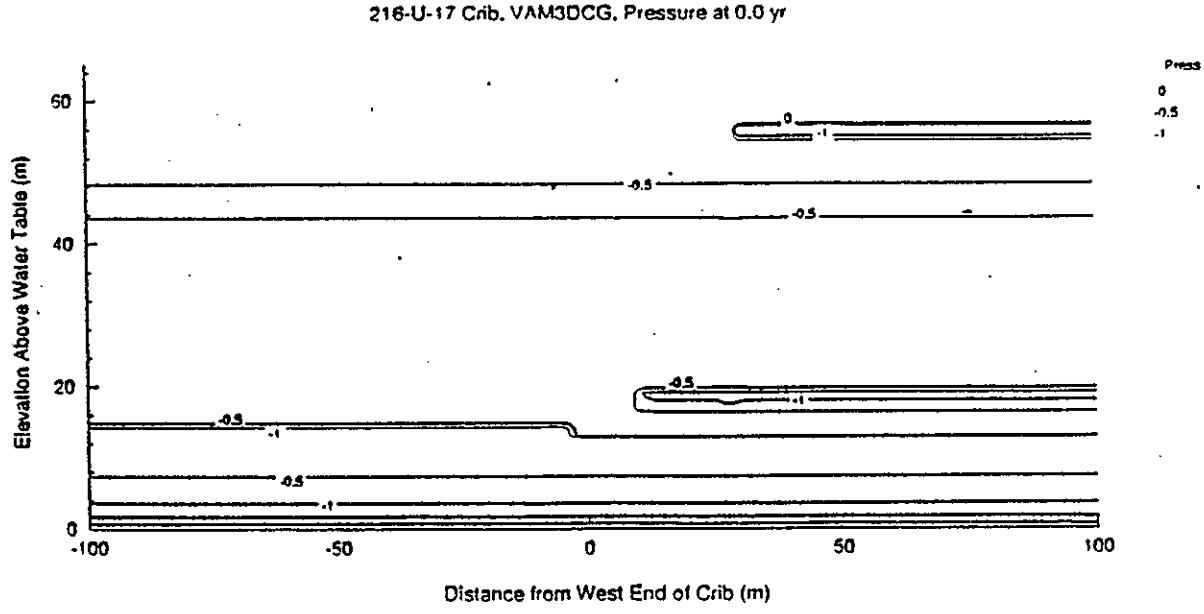

Figure G2-6. Comparison of Fluid Pressure Results Between PORFLO-3 and VAM3D-CG at 1 Year.

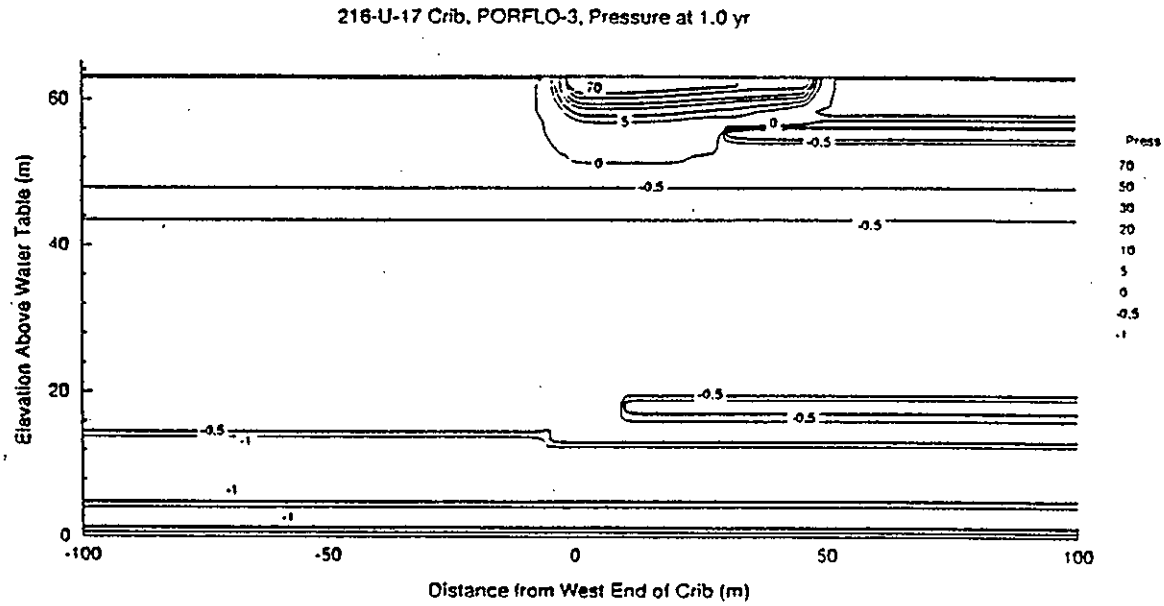

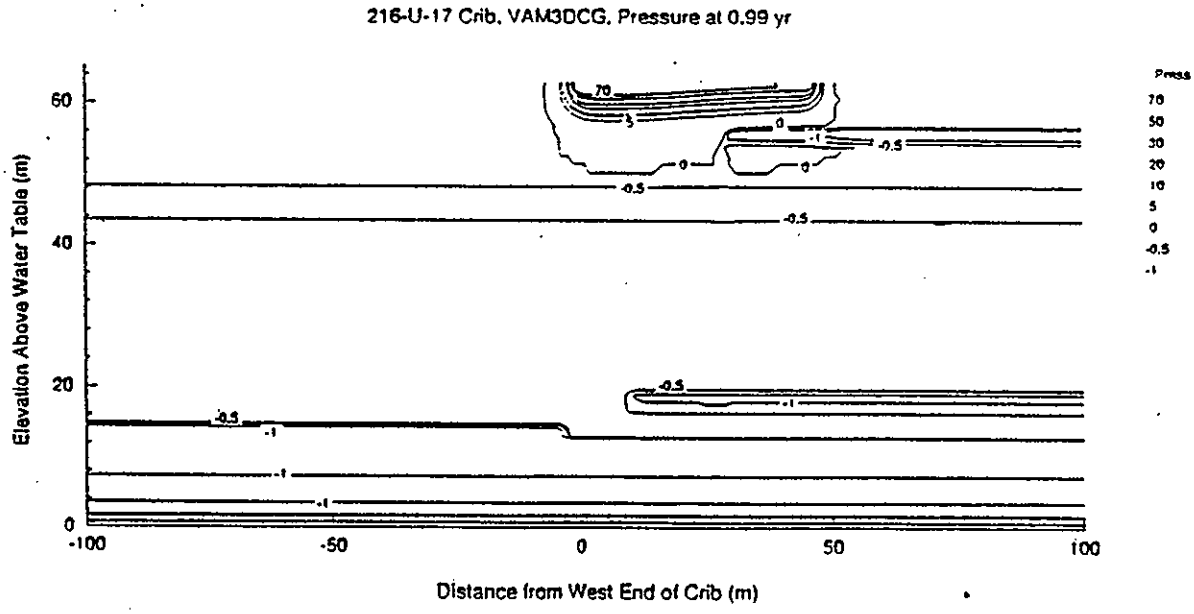

Figure G2-7. Comparison of Fluid Pressure Results Between PORFLO-3 and VAM3D-CG at 3 Years.

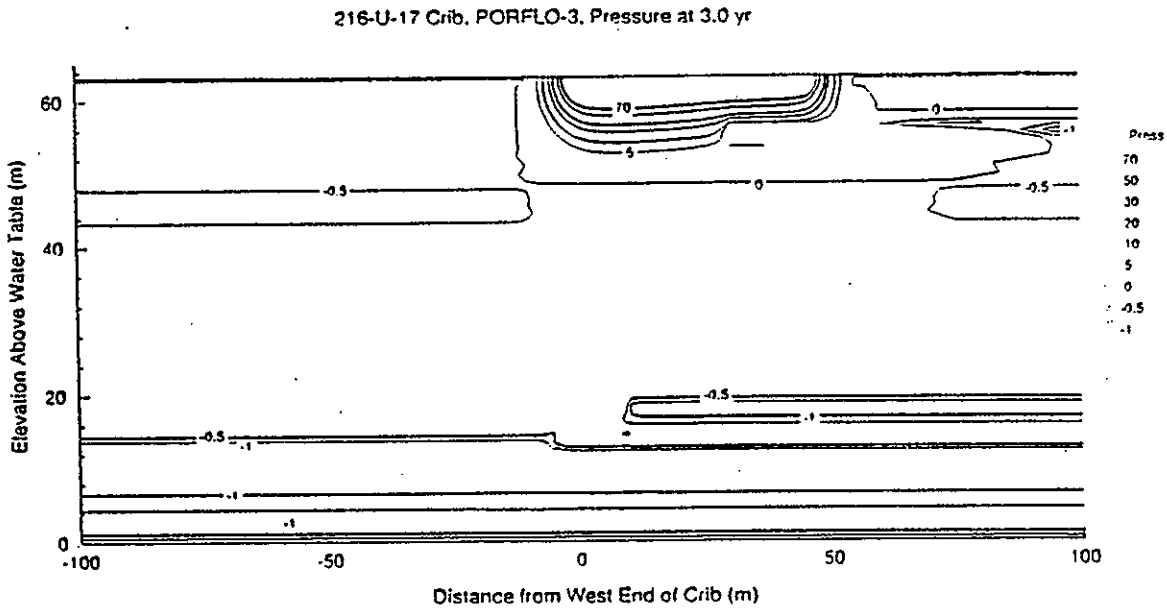

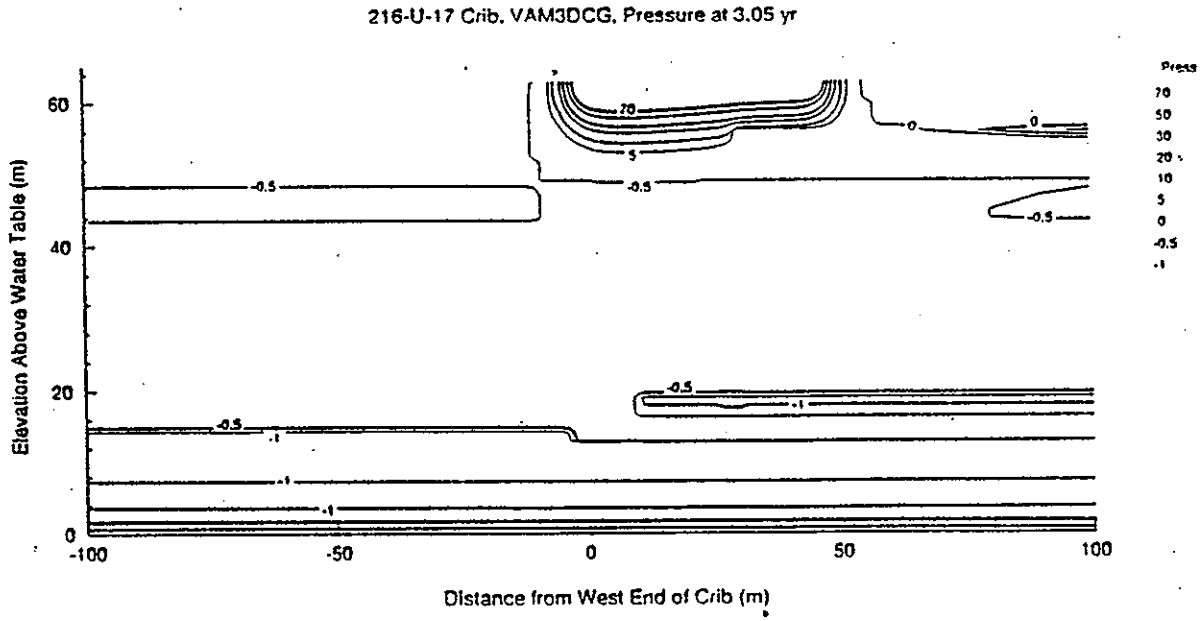

Figure G2-8. Comparison of Fluid Pressure Results Between PORFLO-3 and VAM3D-CG at 5 Years.

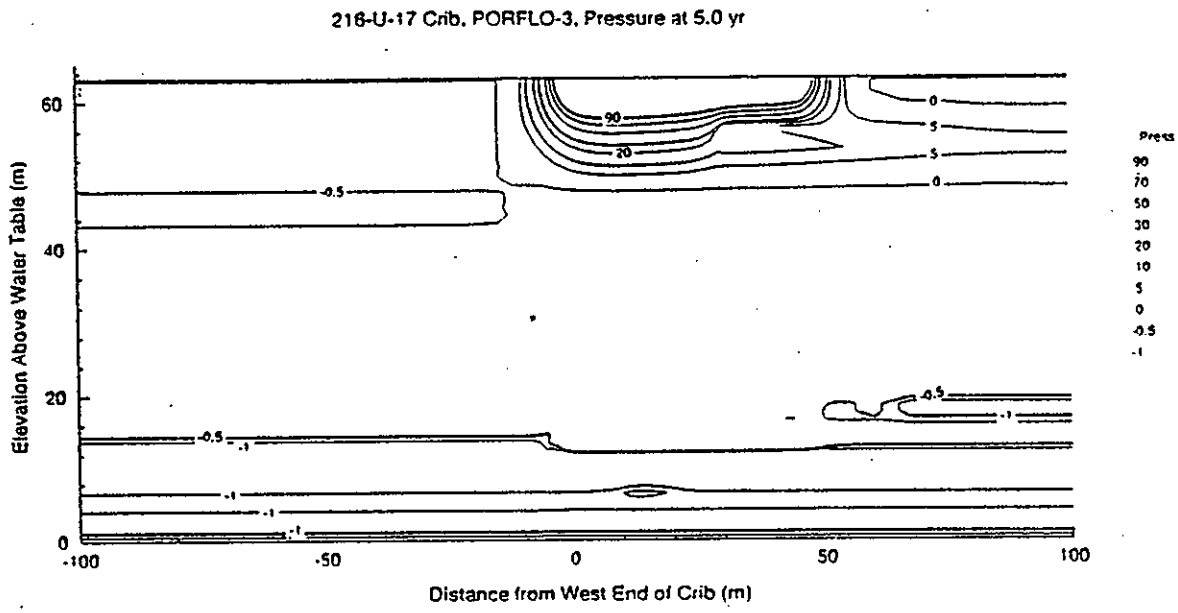

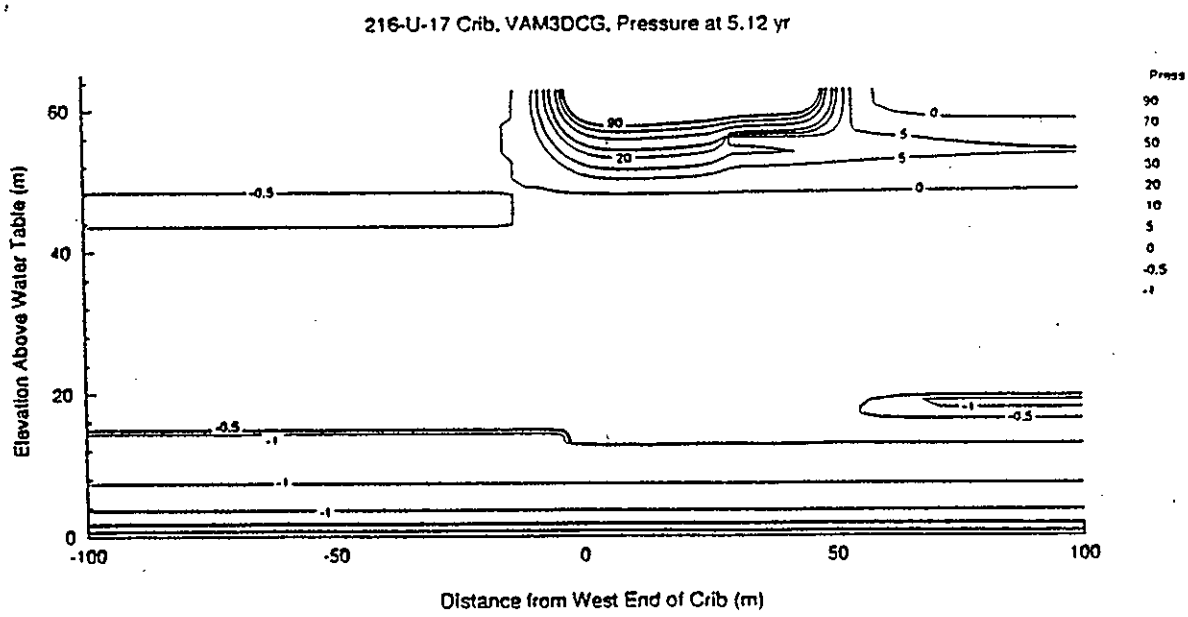

Figure G2-9. Comparison of Saturation Percentage Between PORFLO-3 and VAM3D-CG at 5 Years.

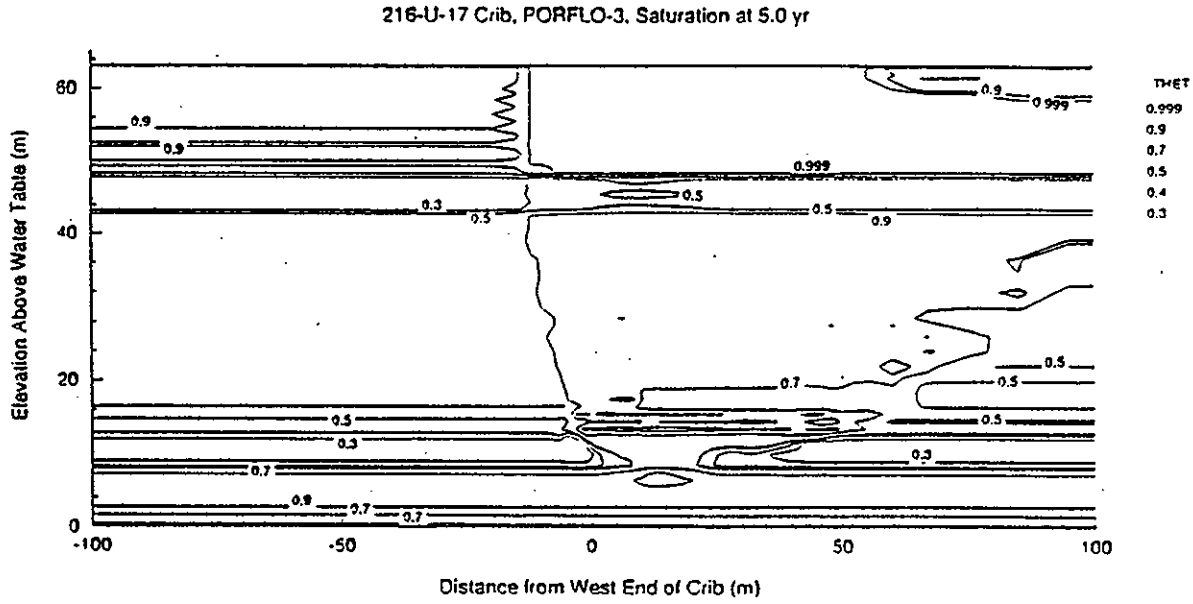

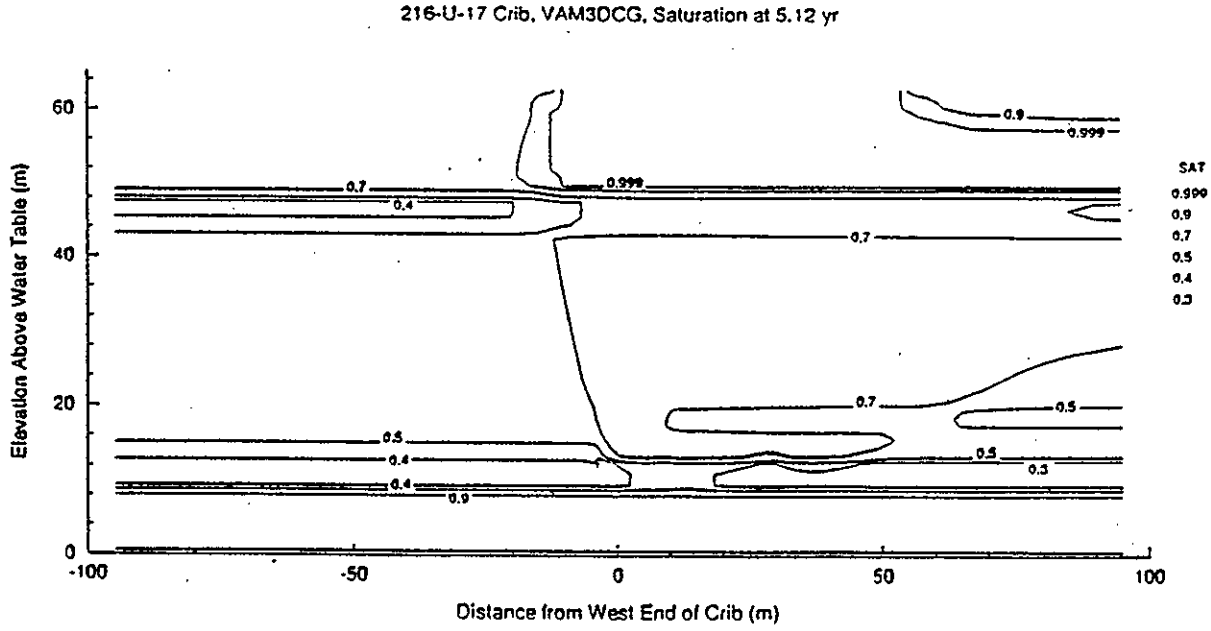

G2.6.3.2 Contaminant Transport Results

The concentrations contours are plotted in Figures G2-10 through G2-12. Results were taken from the same times as those used for the pressure plots.

When the VAM3D-CG results were plotted, the contours at very small concentration values were found to be "unstable." The 0.0001 contour at time 0.99 wandered about the plot, and included many disconnected islands. This is not unusual in a finite element model, especially when the Peclet number limitation is approached. Small contour values which displayed this behavior were omitted from the VAM3D-CG plots.

At time 1.0, a reasonable match between contour curves is seen. Both models show an inordinate diffusion towards the zero concentration boundary nodes along the top of the domain, as expected. PORFLO-3 moves the contaminant into the domain slightly faster, except towards the sandy gravel layer (zone 3) below and to the west of the crib.

At time 3.0, the match is good below the crib and to the east of the crib. In the region towards the sandy gravel layer (zone 3), VAM3D-CG moves the contaminant faster than does PORFLO-3. In both models, relatively small concentration values are involved.

At time 5.0, the overall match is still good. PORFLO-3 has moved the contaminant down farther. However, only the smaller contour levels show a significant difference. As with the flow equation, this may be due to a small amount of numeric diffusion. The simulation time values also differ slightly (5.0 versus 5.12 years). The material moving through the sandy gravel layer is now very nearly the same in both models.

PORFLO-3 also appears to be better enforcing the no flux boundary condition at the west boundary. This may be a plotting artifact: VAM3D-CG models the elements using quadratic accuracy, while the plotting interpolation is linear.

G2.6.4 CONCLUSIONS

This problem involves a complex, two dimensional model. The programs PORFLO-3 and VAM3D-CG employ significantly different solution techniques. However, the solutions show very good overall agreement when plotted.

A reasonable acceptance criteria cannot be stated for the numeric data comparisons, due to differences in grid structures. A subjective criteria would at best involve the location of the wetting and transport fronts in the computed solutions.

From the graphics, the wetting fronts (Pressure = 0.0) are usually within a 1 m of each other vertically, and a few meters horizontally. They are much closer over most of their lengths. The few exceptions are likely to be regions where the pressure gradients are low, and small differences in pressure create large placement errors in the contour curves.

Figure G2-10. Comparison of Concentration Contours Between PORFLO-3 and VAM3D-CG at 1 Year.

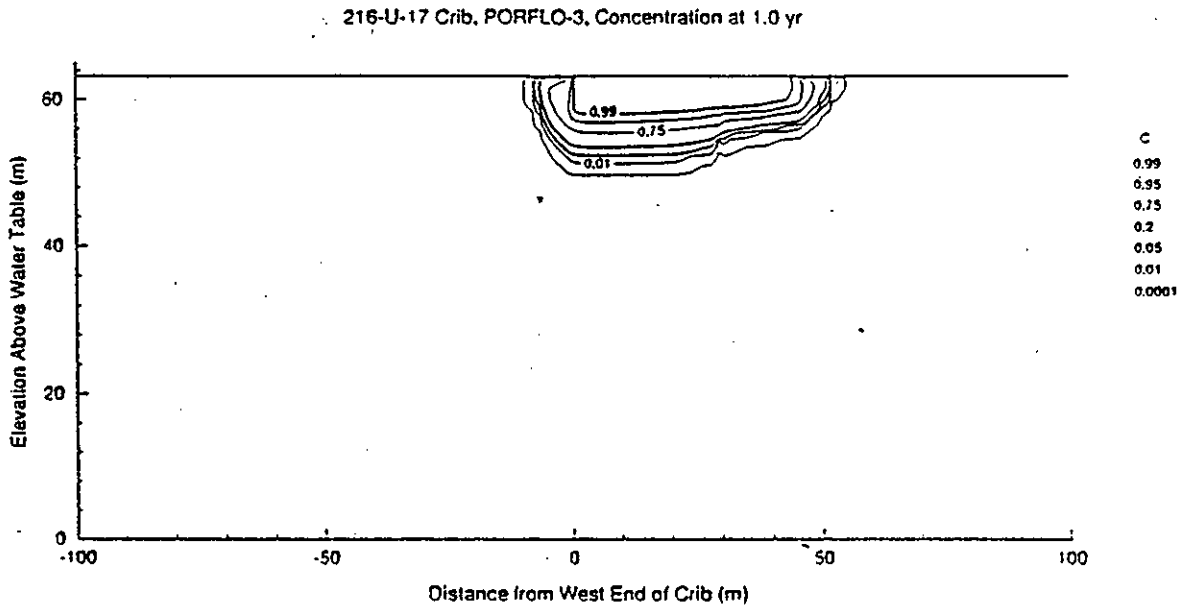

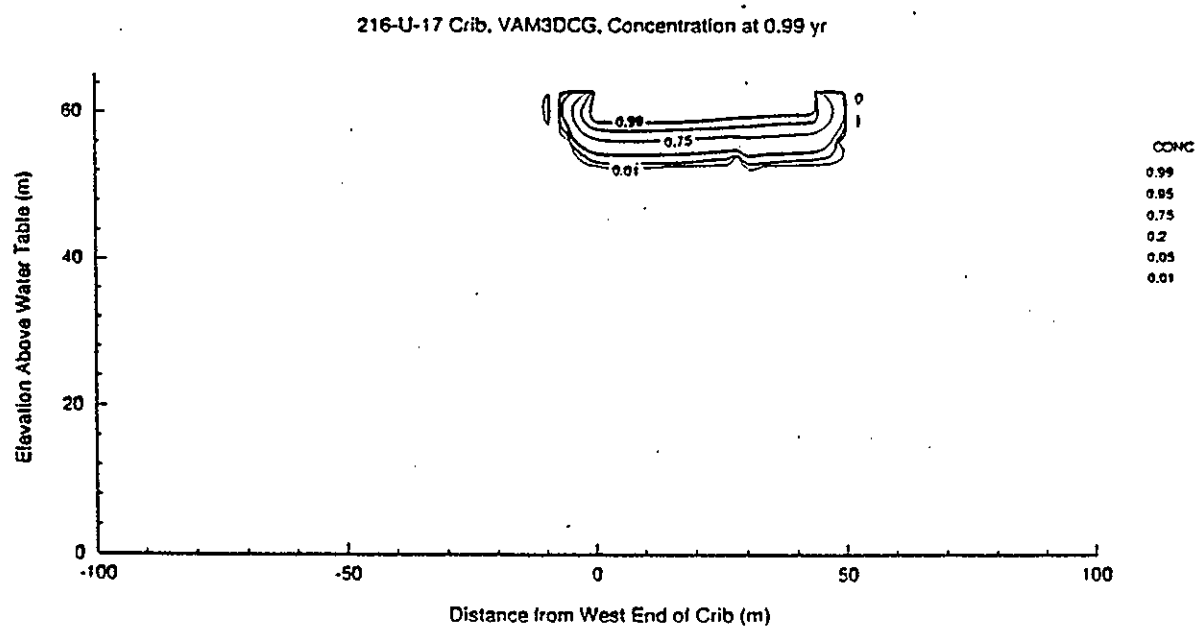

Figure G2-11. Comparison of Concentration Contours Between PORFLO-3 and VAM3D-CG at 3 Years.

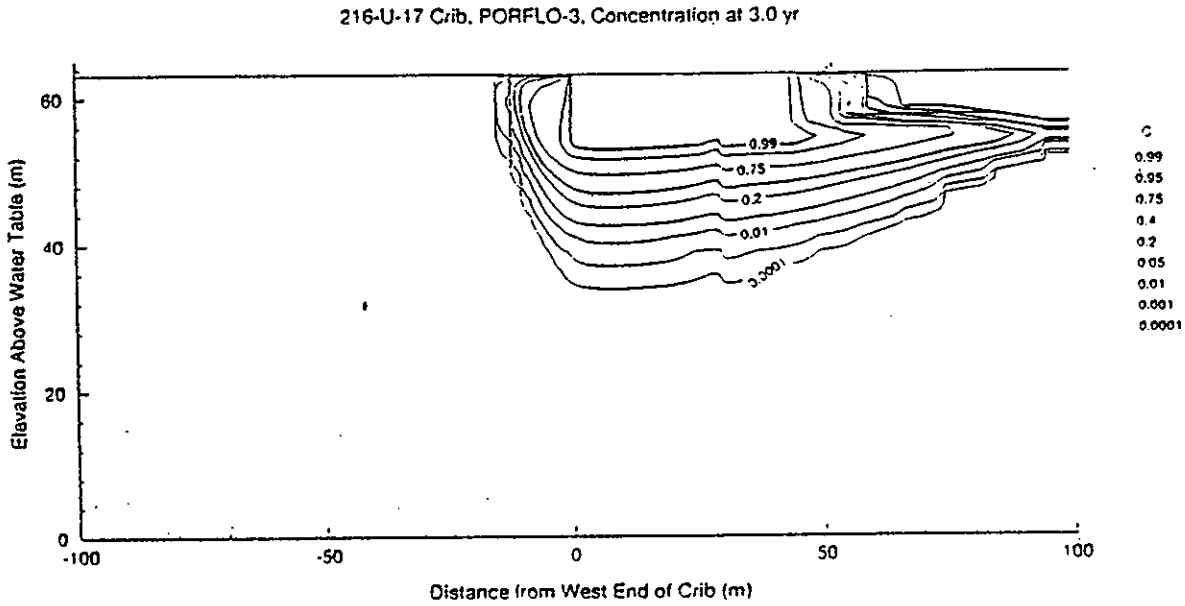

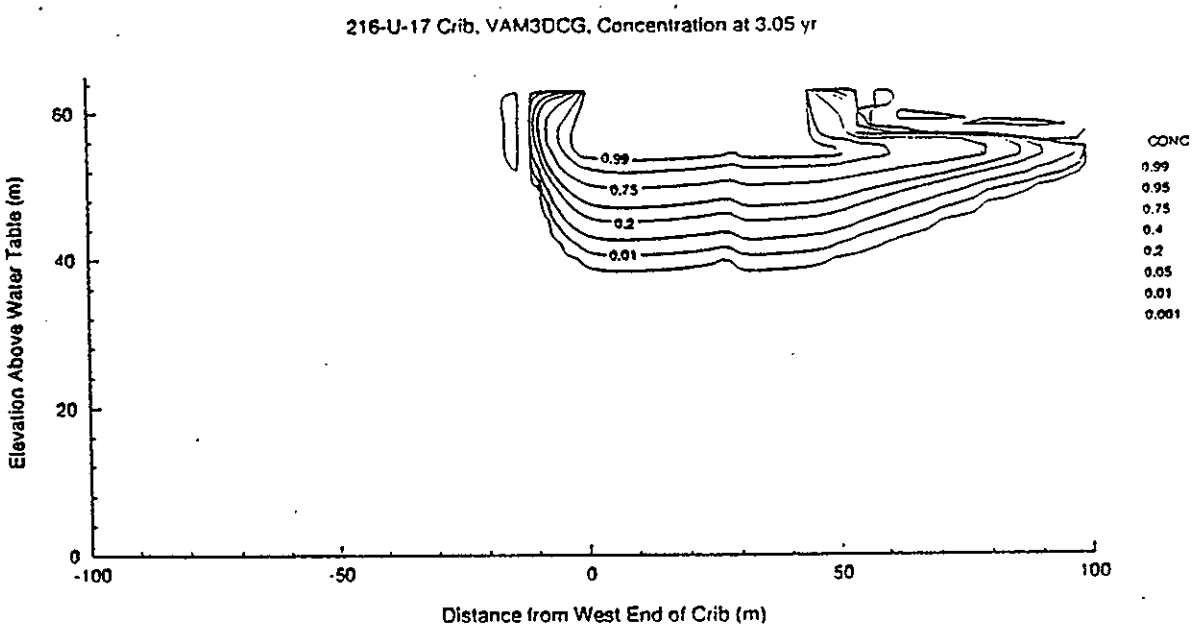

Figure G2-12. Comparison of Concentration Contours Between PORFLO-3 and VAM3D-CG at 5 Years.

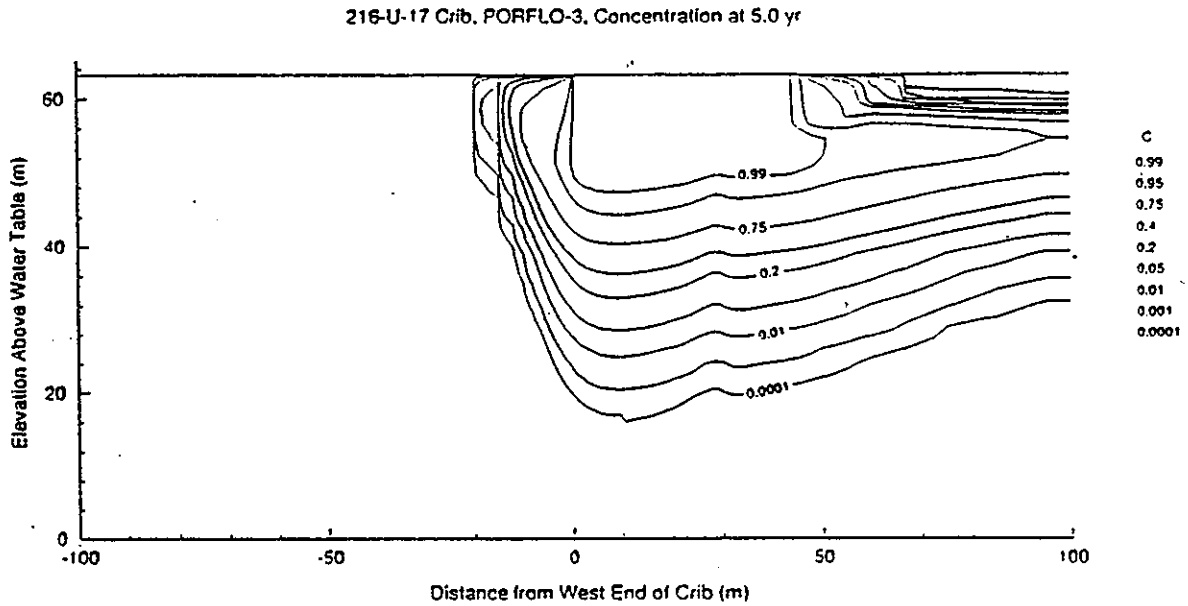

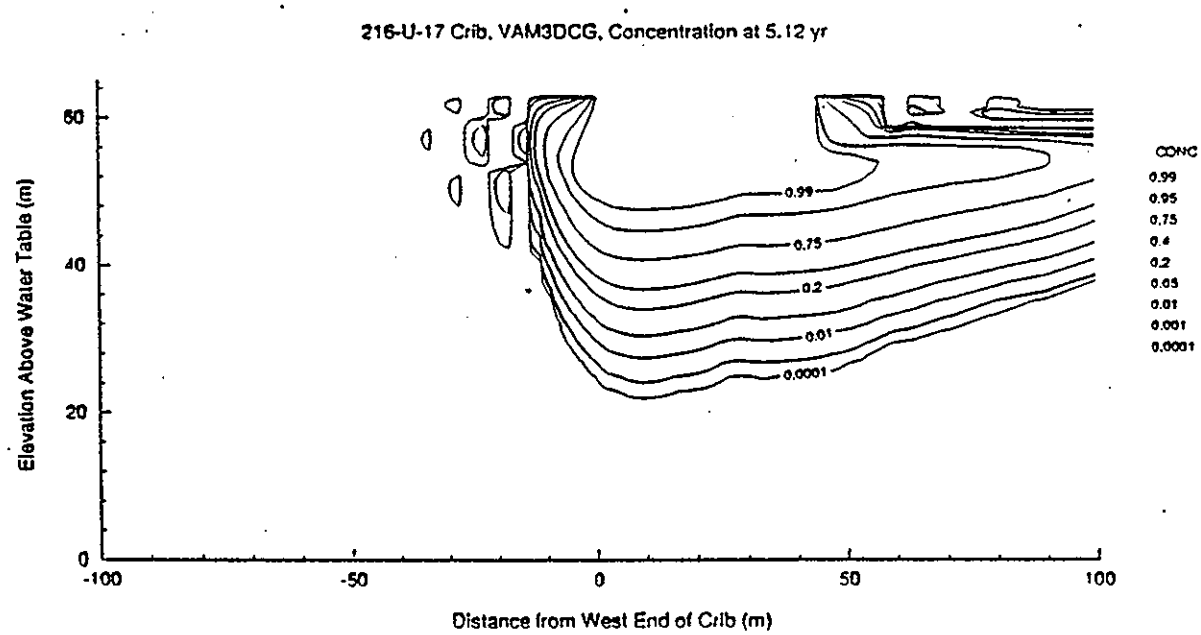

The transport fronts were examined by looking at the C=0.2 and C=0.75 contours. Higher and lower values tend to be in low gradient regions, where the small differences in concentration lead to larger errors in the placement of contour curves. As before, these curves are usually within 1 m vertically, a few meters horizontally, and generally much better. The main exceptions are at early times, where:

a) The front has recently passed the interface between the crib and the sandy soil.

b) The front is approaching the partial sandy gravel layer (zone 3).

Since the contaminant transport properties are uniform, these discrepancies are probably due to differences in the flow fields. Again, this may result from the averaging of hydraulic properties at the boundaries of a thin layer. Once the front passes through a thin layer, the comparison is fairly good (which may be indicative of a good averaging scheme).

By the chosen criteria, the comparison of PORFLO-3 and VAM3D-CG is fairly good. Results from either model should be reasonably accurate. The major differences found between PORFLO-3 and VAM3D-CG are:

1) PORFLO-3 appears to move low levels of material (fluid and contaminants) through the domain slightly faster than VAM3D-CG. This may be due to minor numeric diffusion inherent to that model.

2) VAM3D-CG does not compute entirely stable contaminant concentrations at the lower concentration values. This is typical of finite element models, especially when the element resolution is marginal.

3) In this problem, a narrow material zone (zone 3) caused temporary difference in the transport rates across that zone, when concentrations were low. This difference disappeared at later times, when concentration values increased. This may result from differences in the modeling of the interface between elements (cells).

4) The peak pressures computed by VAM3D-CG were higher than those computed by PORFLO-3. This may be due to large pressure gradients crossing a narrow zone (zone 1), and the treatment of the boundary between two zones of highly differing material properties. This is a localized problem, and the overall transport across the domain does not appear to be significantly affected.

Items 1 through 3 may be important if the first arrival of a contaminant must be determined. For very small concentration values, PORFLO-3 reports faster arrival times. Although VAM3D-CG computes slower arrival times, it does not give stable concentration values.

Items 3 and 4 are significant when a model employs thin layers of materials, and adjacent zones have large differences in properties. Each zone in a grid must have enough cells (elements) to model the expected behavior. In particular, PORFLO-3 averages at material boundaries must not be allowed to affect the overall performance of the model. One should probably avoid using data (e.g., fluxes) near such a boundary, especially at early times.

All of these discrepancies are minor, and may result from using slightly under-resolved computational grids. However, both codes tend to be run in that mode, since they execute significantly faster with fewer nodes.

G2.7.0 BENCHMARK TESTS: FLOW AROUND A CLAY CAP

G2.7.1 OVERVIEW

This problem models unsaturated fluid flow through and around a sloping clay layer, that is embedded within a coarse sandy material. This is part of the cover required by the Resource and Conservation Recovery Act (RCRA) for hazardous waste landfills in Title 40 of the Code of Federal Regulations (40 CFR).

The model has previously been executed by PORFLOW (version 2.394) for benchmarking against other codes (e.g., TRACR3D). Those results have been published (Kincaid et. al., 1993). In the present effort, the VAM3D-CG output is compared against results from PORFLO-3, version 1.2.

G2.7.1.1 Problem Description

Figure G2-13 shows the conceptual configuration of the model. The domain is 36 m wide and 6 m deep, consisting of backfill soil. A sloping clay layer is embedded within the backfill, which is 28 m long by 0.6 m thick.

Water enters the system along the upper boundary, with a recharge rate of 0.1 cm/yr. A no flow condition is enforced along the side boundaries, while the bottom boundary has a fixed pressure value. A steady state solution is sought for the problem. Both VAM3D-CG and PORFLO-3 were executed in a dynamic mode, allowing the solution to develop for 1,000 years.

The lower boundary was set to a pressure head of -4.815 m. This corresponds to a volumetric water content of 0.04058 in the backfill soil, and is consistent with a nominal flow rate of 0.1 cm/yr. The initial conditions are uniform water saturations of 0.265958 in the backfill (pressure = -0.675), and 0.9241 in the clay cap (pressure = -8.9284). The backfill is thus somewhat wetter than the steady state solution, while the clay is somewhat drier.

7.1.2 Computational Grid

The simulation was performed in two dimensions, using a vertical cross section. The problem was run three times; twice with VAM3D-CG and once with PORFLO-3. The first execution with VAM3D-CG used regular rectangular elements, with a stair stepping approximation to the clay cap. The second VAM3D-CG execution used curvilinear elements to portray the cap. PORFLO-3 is a finite difference model, and is restricted to a rectangular grid.

Figure G2-13. Clay Cap Model, Conceptual Domain.

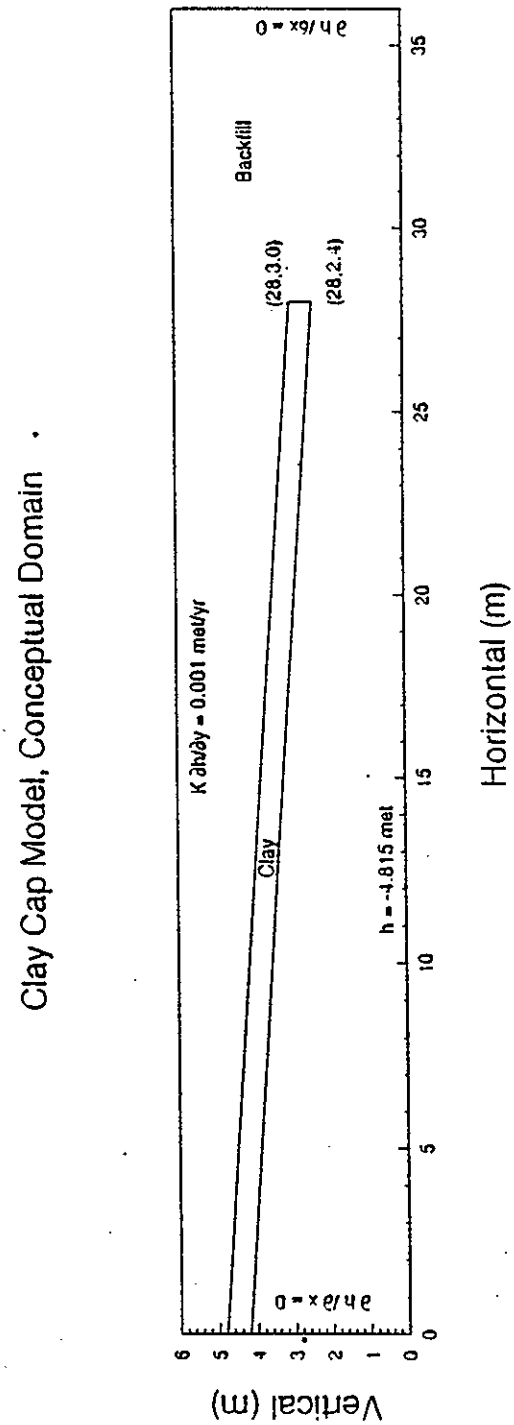

The VAM3D-CG stair stepped model is shown in Figures G2-14 and G2-15. A total of 2160 elements and 4550 nodes are used. All elements in the grid were 0.4 m wide. Above and below the layer containing the clay cap, the elements were 0.3 m high. Within the horizontal layer containing the cap, each element was 0.2 m high. The stair stepping is distinctly different than that used by the PORFLO-3 model. This should provide insight into the relative errors expected in the 'stepped' region, due to the steps.

The curvilinear grid for the second execution used 1,137 elements and 2,442 nodes. Fifteen "pinch nodes" were used to reduce the grid resolution where possible. Curvilinear elements were constructed to model the clay layer as a slanting structure in the domain, rather than as stair stepped. The results of this model were generally in agreement with the orthogonal grid model, but showed some non physical perturbations. These may have been due to input errors, VAM3D-CG errors, and/or post processing errors. Since the error(s) involved could not be traced, those results are not presented here.

The PORFLO-3 grid was a uniform and rectangular array of 6072 grid cells (92 x 3 x 22, 1,800 computational cells). Each cell was 0.4 m wide (Δx) by 0.3 m high (Δz). The model depth (Δy) was 1 m.

G2.7.1.3 Material Properties

Material properties are shown in Table G2-8. A van Genuchten model for unsaturated flow was implemented. The van Genuchten gamma was set to the default value of $(1-1/\beta)$. Hydraulic conductivities were taken as isotropic.

Table G2-9 indicates the pressure heads, moisture content, and total hydraulic conductivities corresponding to the initial saturation values, for the specified material properties.

Table G2-8. Material Properties for the Clay Cap Model.

Material	Storage	alpha (1/m)	beta	Hyd Cond (m)	Resid. Sat	Porosity
Backfill	0.2	8.6	1.742	9467.	0.018	0.376
Clay	0.2	0.054	1.324	0.002966	0.00	0.448

Table G2-9. Initial Conditions for the Clay Cap Model.

Material	Moisture Content	Total Hyd K (m/yr)	Pressure (m)	Saturation
Backfill	0.132129	1.81097	0.675000	0.265958
Clay	0.413997	2.08506E-4	8.92876	0.924100

Figure G2-14. Finite Element Grid, Orthogonal Clay Cap Model.

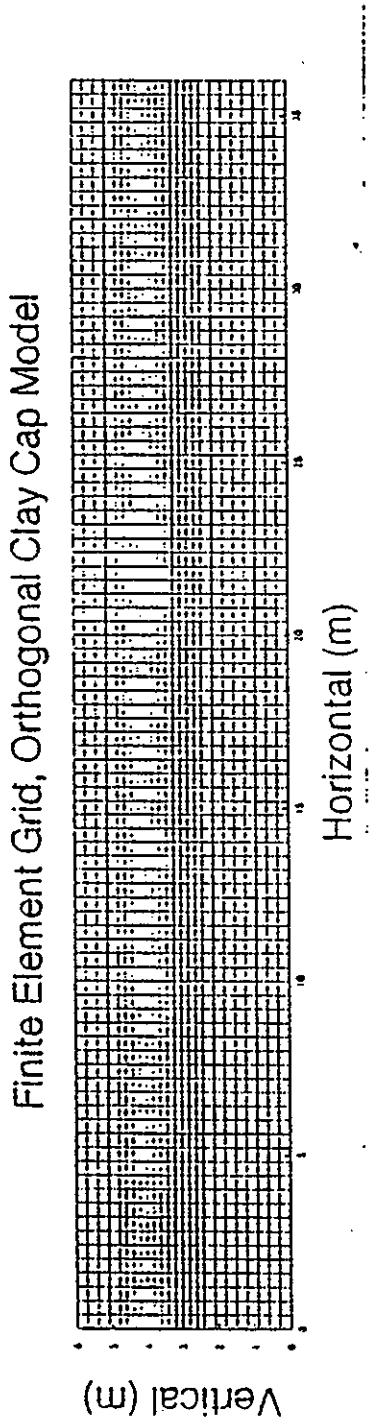

Figure G2-15. Material Boundaries, Orthogonal Clay Cap Model.

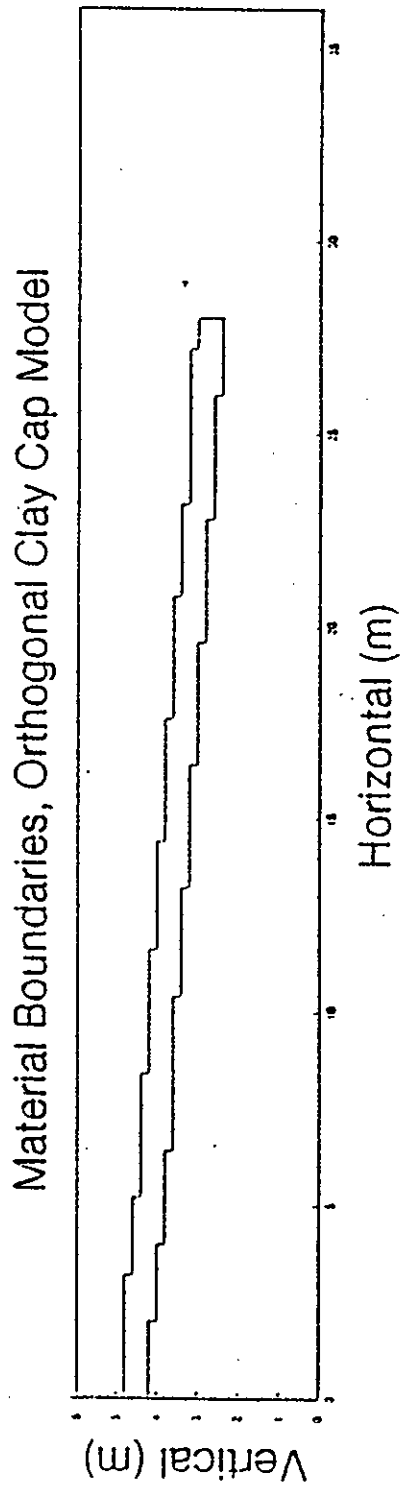

G2.7.2 EXECUTION OF THE MODELS

VAM3D-CG was executed using the pressure formulation of the flow equations. The storage term was computed directly as the time derivative of the saturation. Full three dimensional modeling and finite element connectivity were used.

PORFLO-3 generated hydraulic heads as the output variable. These were converted to pressure heads for the comparison between the models.

Both PORFLO-3 and VAM3D-CG were run for 1000 years. Both models required very small initial time steps, on the order of 1.0E-5. Both models also developed convergence difficulties at later times, between 0.1 and 5.0 years. The plotted pressure heads at 1000 years indicate that a steady state solution has not quite been reached.

The rectangular VAM3D-CG model required just over 5,000 cpu seconds to execute 321 time steps. The curvilinear grid reduced this to roughly 1,500 cpu seconds for 285 steps, although the savings does not offset the extra analyst time required to build the input data set. PORFLO-3 required 467 cpu seconds for 224 time steps. No attempt was made to optimize the time stepping for each model. The VAM3D-CG output file indicates much larger time steps could be taken after the initial instabilities were past.

G2.7.3 COMPARISON OF PORFLO-3 AND VAM3D-CG CONTOUR PLOTS

Contour plots of the VAM3D-CG and PORFLO-3 pressure head results are shown in Figure G2-16. Similar plots for saturation are given in Figure G2-17.

The pressure heads displayed in Figure G2-16 show relatively good agreement. Different stair stepping schemes were used to represent the sloped clay cap layer in each model. This is particularly noticeable at the ψ=-4.2 m contour level above the clay layer. While the pressure contours do follow each other relatively well, one must be cautious when using a stair stepped model, as pressure values near the steps can be locally inaccurate.

The PORFLO-3 domain remains slightly drier than the VAM3D-CG domain. This difference is not serious, but is noticeable when the plots are laid over each other. Contour plotting does tend to exaggerate the differences between data sets, especially when the gradients are small. The likely cause of the difference is the nodal averaging schemes at the boundaries between material types. PORFLO-3 uses a harmonic mean hydraulic conductivity, while the finite element model VAM3D-CG need not compute such averages.

The saturation curves are shown in Figure G2-17. These curves are not very useful, since the steady state saturations in the each material are determined largely by the boundary conditions. The curves follow the material boundaries; the porous backfill is relatively dry, while the clay is relatively wet.

Figure G2-16. Contour Plots of VAM3D-CG and PORFLO-3 Pressure Head Results for the Clay Cap.

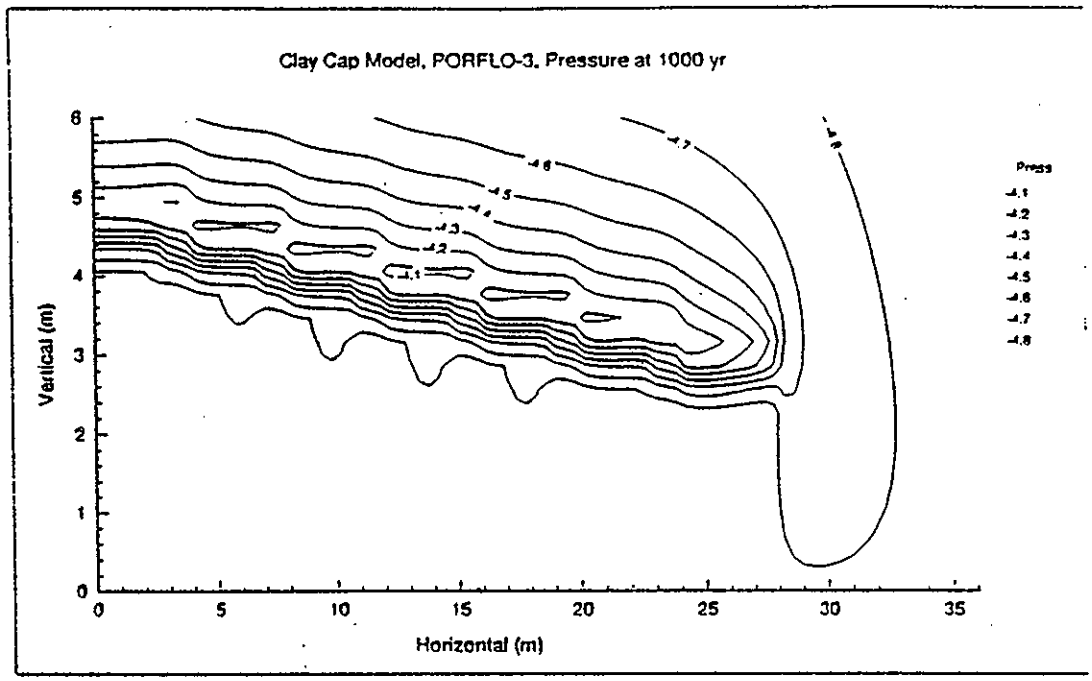

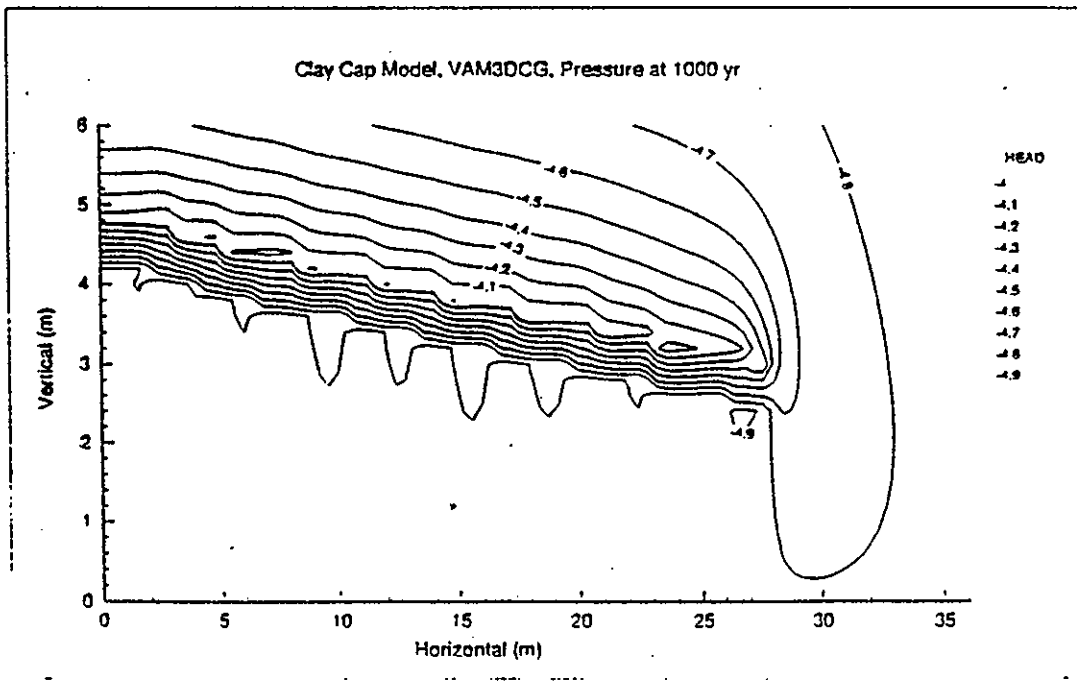

Figure G2-17. Contour Plots of VAM3D-CG and PORFLO-3 Saturation Curves for the Clay Cap.

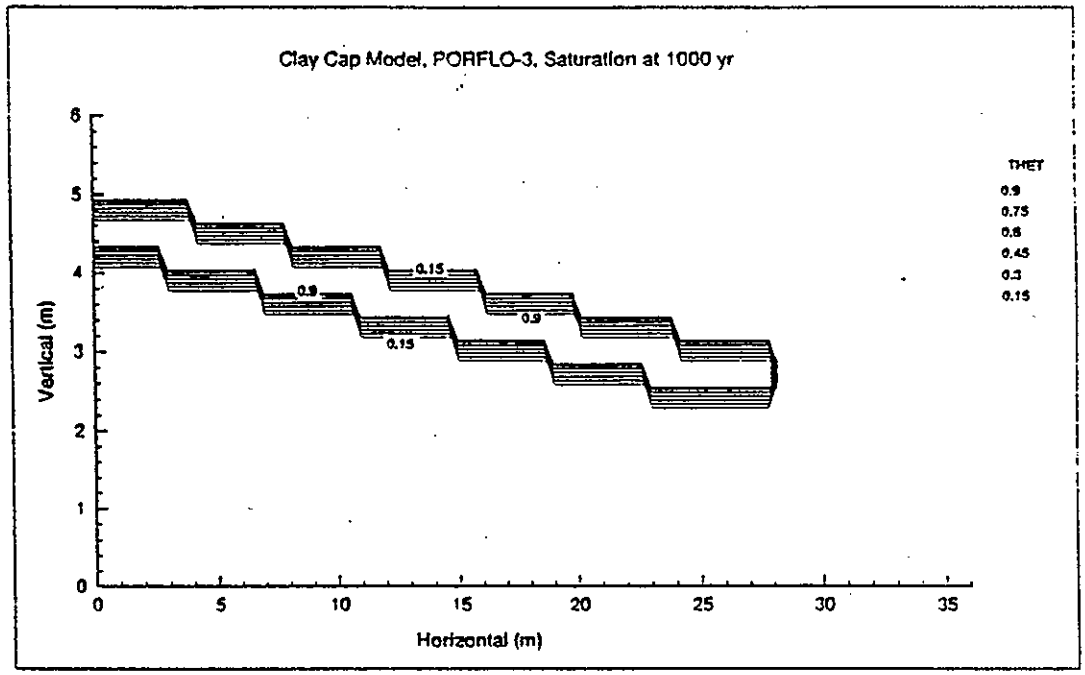

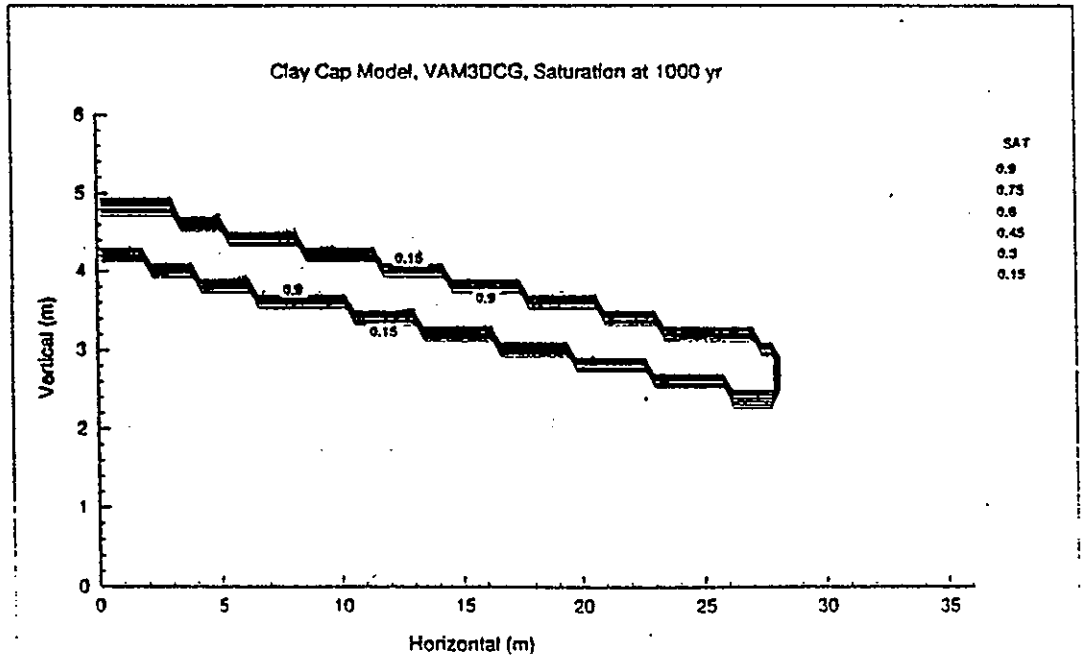

G2.7.4 CONCLUSIONS

This problem models the steady state response of a single, low conductivity layer embedded within a higher conductivity material. The saturated conductivities of the two materials differ by roughly six orders of magnitude. However, both models compute substantially identical results.

The primary differences in the results from the two models include:

1) The PORFLO-3 domain remains slightly drier than the VAM3D-CG domain, as shown by the plots. This is probably due to the conductivity averaging scheme used by PORFLO-3 at material boundary interfaces. The PORFLO-3 grid resolution may be marginal, as in many places the clay layer is only two cells wide.

2) The differences in the stair stepping produce local difference in the head values. The stair stepping scheme produces inaccurate heads near the material boundary, which must be considered if flow or heads in that region are important to the overall model.

3) The transients below the clay layer are not necessarily reproducible between models. Since the unsaturated flow equation is non linear, some solutions will produce "chaotic" behavior.

These differences are very minor. Overall, VAM3D-CG compares quite favorably with PORFLO-3.

G2.8.0 VERIFICATION OF THE VAM3D-CG SOURCE CODE AS INSTALLED ON THE SGI

G2.8.1 OVERVIEW

The newly received version 2.4b of the VAM3D-CG on the SGI is compared with the previous version on the Cray. Three test cases are included. These cases were originally part of analyses (Run numbers 2 and 2c) performed in the preliminary draft of this document. The first case is a steady-state flow run. The second case is the corresponding transport run. The third case is a continual run of case 2 after the source term was completely depleted from the trench.

G2.8.2 TEST CASE ID: V3D7 (RUN # 2 IN THE REFERENCED DOCUMENT)

1. Problem Description

Conceptually, this problem was a steady infiltration of 0.5 cm/yr of recharge water into a 160-m thick, saturated-unsaturated soil column. A five layer stratigraphy representing the vadose zone and the unconfined aquifer beneath the W-5 burial ground was modeled. The model layout used the geologic information gathered from borehole 299-W7-9. As shown in Figure G2-18, a rectangular soil slab with an open trench on the top is selected for simulation.

A total of four moisture characteristic curves (see Table G2-10) representing four upper units (Hanford, Early Palouse, Plio-Pleistocene, and Upper-Ringold) were selected for the model simulations. The laboratory-measured moisture retention data and unsaturated hydraulic conductivity were fitted simultaneously with the van Genuchten-Mualem equation using the computer code RETC. The four formation types, Hanford, Early Palouse, Plio-Pleistocene, and Upper-Ringold are referred to as material types 1, 2, 3, and 4, respectively (Table G2-10). Since no samples were available in the middle Ringold unit, material type 5 is the same as material type 4.

Table G2-10. Hydraulic Characteristics.

Sample #	Formation Type (Mat.#)	Depth (m)	Θ_s	Θ_r	α (1/m)	β	K_s (m/yr)	ρ_b (g/cm^3)
0-069	Hanford (1)	3.05	0.301	0.000	9.45	1.2515	6496.4	2.29
0-072	E.P (2)	19.82	0.391	0.056	0.90	2.0877	517.12	1.81
0-082	Plio (3)	24.70	0.455	0.127	4.86	1.3520	1892.2	1.43
0-107	U. R. (4)	40.40	0.317	0.025	9.16	1.807	5203.4	1.59

where α and β are van Genuchten parameters, θ_s and θ_r are the saturated and residual moisture contents, respectively, and ρ_b is the soil bulk density.

The results of the comparison are shown in G2-11.

Table G2-11. File Differences:

Time (year)	Range of Variable Pressure Head (m)	Max Difference (m)	RRMS
Steady state	-8.533 --- 86.70	-1.192e-7	4.419e-9

G2.8.3 TEST CASE ID: v3dt7cp (RUN # 2c IN REFERENCED DOCUMENT)

1. Problem Description

The purpose of this problem concerns the transport of a nonconservative contaminant with K_d=10. A transient-flux boundary condition was imposed at the bottom of the trench. The flux was chosen to reflect a 0.5 cm/yr infiltration rate with moderate dispersion. The model uses flow field from problem v3d7. 600 time steps (0.5 yr), from zero to 300 years were taken.

Figure G2-18. Materials for Solidwaste Geometry.

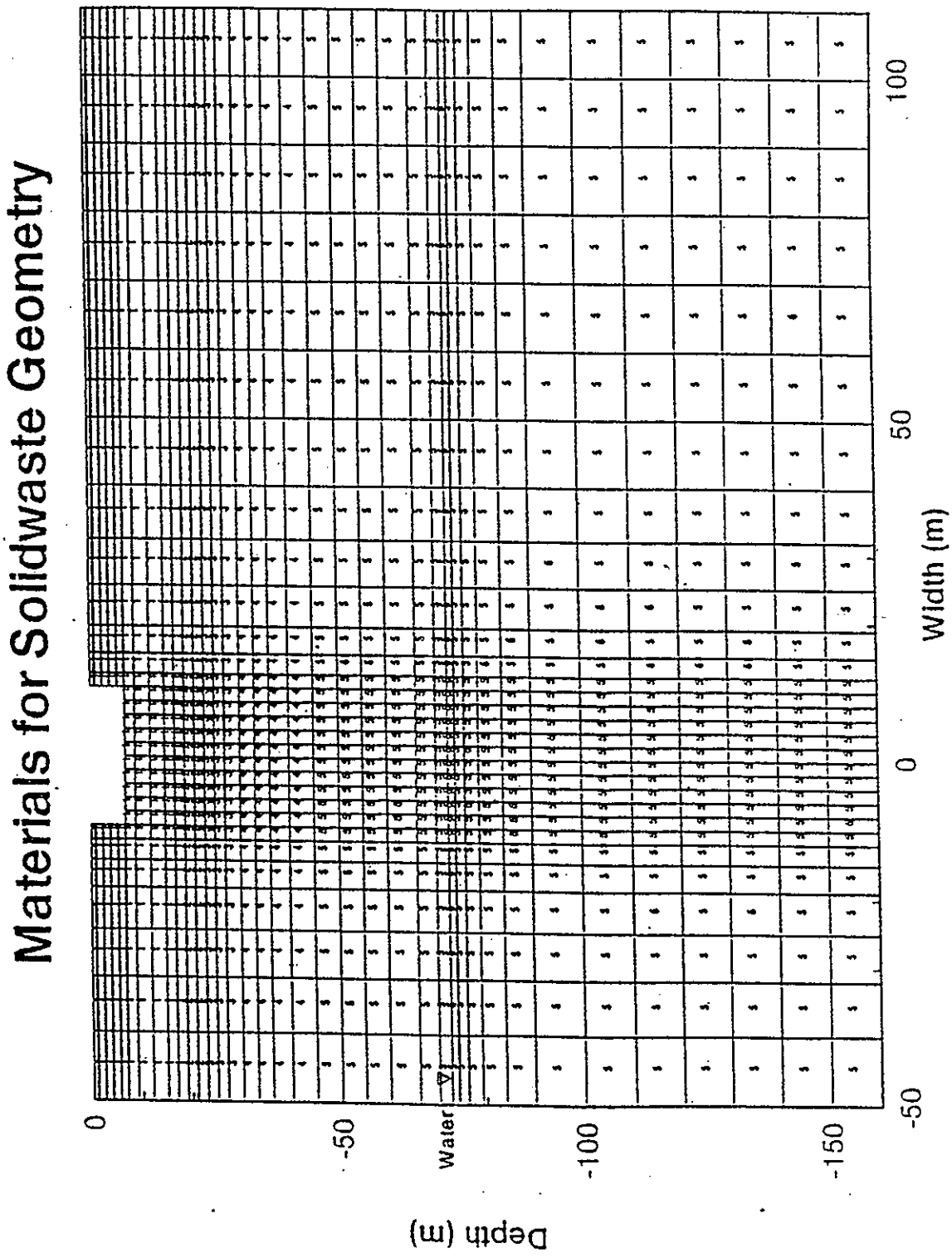

A longitudinal dispersivity of 1.0 m, a transverse (lateral) dispersivity of 0.1 m and an effective molecular diffusion coefficient of 2.95 x 10^{-7} cm^2/sec (9.30 x 10^{-4} m^2/yr) were used in the simulations. The results of the comparison are shown in Table G2-12.

Table G2-12. File Differences:

Time (year)	Range of variable Conc. (Ci/m^3)	Max Difference Conc. (Ci/m^3)	RRMS
30.0	1.46e-6 -- 1.46e-3	-1.323e-23	0.0
150.0	4.99e-6 -- 4.99e-3	-1.694e-21	0.0
300.0	4.39e-6 -- 4.39e-3	-2.220e-16	0.0

Comments: RRMS values use a threshold of 1.0e-3 times max value (data points below this limit are not compared).

G2.8.4 TEST CASE ID: v3d7c (CONT. OF RUN # 2c)

1. Problem Description

Since the contaminants have a long resident time in the unsaturated and saturated zones due to a high K_d value, the model uses the final results from problem v3dt7cp as the initial conditions and continues the simulation. The model simulates transport from 300 to 800,300 years. The model uses flow field from problem v3d7 and the final results from problem v3dt7cp as initial conditions. 800 time steps (1000.0 yr) were taken. The results of the comparison are shown in Table G2-13.

Table G2-13. File Differences:

Time (year)	Range of Variable Conc. (Ci/m^3)	Max Difference Conc. (Ci/m^3)	RRMS
50,300	1.52e-7 -- 1.52e-4	3.683e-12	3.997e-9
400,300	1.97e-9 -- 1.97e-6	-1.776e-15	5.635e-9
800,300	1.12e-13 - 1.12e-13	-2.608e-18	1.260e-7

For the problems in this section, both maximum difference and RRMS values are negligible. The differences can be explained by rounding errors between the two computers.

G2.9.0 CONCLUSIONS

Three sets of testing problems were selected to examine the general capabilities and limitations of the VAM3D-CG Code. The first set of test problems was used to show that the VAM3D-CG Version 2.4b code on the SGI produces the same results as those published by the vendor in the users' manual. The test problems were originally selected for the verification of numerical schemes and the demonstration of the major capabilities of the VAM3D-CG code.

The third set of test problems was selected to show that the VAM3D-CD Version 2.4b on the SGI workstation produces the same results as those previously on the Westinghouse Hanford Cray computer which is no longer in service.

The test results showed excellent agreement with the first and third sets of problems. In these comparisons, both maximum difference and RRMS values are negligible. The differences can generally be explained as rounding errors between computers.

The second set of test problems was selected to examine the abilities of the VAM3D-CG code to accurately solve the flow and transport problems relevant to the performance assessment applications at Hanford. For this purpose, a comparison was made with the PORFLO-3 code for the simulation of two problems.

For the second set of problems, a reasonable acceptance criteria cannot be stated for the numeric data comparisons, due to the differences in grid structures. A subjective criteria would at best involve the location of the wetting and transport fronts in the computed solutions.

For the 216-U-17 Crib problem, the solutions showed very good overall agreement when plotted, even though VAM3D-CG and PORFLO-3 employ significantly different solution techniques. The main difference occurs at an early time when the front has recently passed the interface between the crib and the sandy soil and the front is approaching the partial sandy gravel layer (zone 3).

This may result from differences in the modeling of the interface between materials. The PORFLO-3 uses an averaging scheme at material boundaries, while the VAM3D-CG code does not need to compute such averages. The differences are generally enhanced when a model employs thin layers of materials, and adjacent zones have large differences in properties. To minimize the impact on the overall performance of the model, each zone in a grid must have enough elements to model the expected behavior.

For the clay cap problem, the steady state response of a single, low conductivity layer embedded within a higher conductivity material was modeled. The saturated conductivities of the two materials differ by rough six orders of magnitude. However, both models compute substantially identical results.

Though the overall agreement in the results are satisfactory, minor differences exist at several locations. The differences can again be attributed to the conductivity averaging scheme used by the PORFLO-3 at material boundary interfaces.

Although minor discrepancies exist on both benchmark testing problems, the two codes should perform equally well in terms of performance assessment applications at Hanford.

G10.0 REFERENCES

Brooks, R. H., and A. T. Corey, 1966, Properties of Porous Media Affecting Fluid Flow, ASCE J. Irrig. Drain. Div., 92(IR2): 61-88.

Davis, L. A., and S. P. Neuman, 1983, Documentation and User's Guide: UNSAT1-Variably Saturated Flow Model, U.S. Nuclear Regulatory Commission, NUREG/CR-3390, Washington, D.C.

Huyakorn, P. S. and S. Panday, 1993, "VAM3D-CG - Variably Saturated Analysis Model in Three-Dimensions with Preconditioned Conjugate Gradient Matrix Solvers, Version 2.4b, Documentation and User' Guide," HydroGeoLogic, Inc. Herndon, VA.

Kincaid, C. T., J. W. Shade, G. A. Whyatt, M. G. Piepho, K. Rhoads, J. A. Voogd, J. H. Westsik, Jr., M. D. Freshley, K. A. Blanchard, and B. G. Lauzon, 1993, "Performance Assessment of Grouted Double-Shell Tank Waste Disposal at Hanford," WHC-SD-WM-EE-004, Rev. 0.

Kline, N. W., 1993, "Certification of Version 1.2 of the PORFLO-3 Code For the Hanford Cray Computer," WHC-SD-ER-CSWD-003, Rev. 0.

Magnuson, S. O, R. G. Baca, and A. J. Sondrup, 1990, "Independent Verification and Benchmark Testing of the PORFLO-3 Computer Code, Version 1.0," EGG-BG-9175, Idaho National Engineering Laboratory, Idaho Falls, Idaho.

Mualem, Y., 1984, "Anisotropy of Unsaturated Soil," soil Sci. Soc. Am. J., pp. 513-522.

Neuman, S. P., R. A. Feddes, and E. Bresler, 1974, Finite Element Simulation of Flow in Saturated-unsaturated Soils Considering Water Uptake by Plants, Hydrodynamics an Hydraulic Engineering Laboratory Report for Project No. ALO-SWC-77, Haifa, Israel.

Lu, A. H. and R. Khaleel, "Calibration/Testing of VAM3D-CG Computer Code Using Injection Test site Data at Hanford," Internal Letter: J.A. Rawlins to M.J. Lauterbach,"Fiscal Year 1993 M-29-02 Milestone Document," 25350-JAR93-059, October 14, 1993.

Reidel, S. P., V. G. Johnson, and N. W. Kline, 1993, "Groundwater Impact Assessment for the 216-U-17 Crib, 200 West Area," WHC-EP-0664, Westinghouse Hanford Company, Richland, WA.

Runchal, A. K., and B. Sagar, 1992, PORFLOW: A Model for Fluid Flow, Heat, and Mass Transport in Multifluid, Multiphase, Fractured or Porous Media - Users Manual, Version 2.4. ACRi/016/REV.G, Analytical and Computational Research, Inc., Los Angeles, California.

Sagar, B. and A. K. Runchal, 1990, "PORFLO-3: A mathematical Model for Fluid Flow, Heat, and Mass Transport in Variably Saturated Geological Media, Theory and Numerical Methods, Version 1.0," WHC-EP-0042, Westinghouse Hanford Company, Richland, WA.

Scheidegger, A. E., 1961, General Theory of Dispersion in Porous Media, J. Geophys. Res., v. 66, pp. 3273-3278.

Sisson, J. B. and Allen H. Lu, "Field Calibration of Computer Models for Application to Buried Liquid Discharges: A Status Report," RHO-ST-46 p, August 1984.

Van Genuchten, R., 1978, "Calculating the Unsaturated Hydraulic conductivity with a New Close-Form Analytic Model," Report 78-WR-08, Water Resources Program, Department of Engineering, Princeton University, Princeton, New Jersey.

Wood M. I., R. Khaleel, P. D. Rittman, A. H. Lu, R. J. Serne, and K. J. Cantrell, 1993, "Performance Assessment for the Disposal of Low-Level Waste in the 218-W-5 Burial Ground," WHC-EP-0645 Draft.

Yeh, G. T. and D. S. Ward, 1981, FEMWASTE: A Finite-element Model of Waste Transport Through Saturated-unsaturated Porous Media, Rep. ORNL-5601, Oak Ridge National Lab., Oak Ridge, Tennessee, 137pp.

Yeh, G. T., 1981, AT123D: Analytical Transient One-, Two- and Three-dimensional Simulation of Transport in the Aquifer System, Oak Ridge National Lab., Tennessee, Report no. ORNL-5602.

APPENDIX H

RESPONSE TO PEER REVIEW PANEL COMMENTS

This page intentionally left blank.

RESPONSE TO PEER REVIEW PANEL COMMENTS

In this appendix, specific responses are given to comments provided by the Peer Review Panel (PRP) in their review of the preliminary draft of this performance assessment (PA) analysis (Letter, Wilhite to Coleman, October 12, 1993). Where appropriate, specific answers are drawn from additional analyses completed for the final PA. References are given to sections in the document where the topic is discussed more fully.

Comment: **The PRP appreciates the warm reception extended by the hosts and the openness of discussion.**

Response: None required.

Comment: **The PRP commends the PA preparers on the extent of the draft PA. The calculation and presentation of results beyond the assumed 10,000-yr time of compliance strengthens the completeness of the analysis.**

Response: None required.

Comment: **The PRP observes that there has been no technical editing of the draft PA. There are many minor editorial comments which the PRP will not address in this review. However, the PRP advises that careful attention to technical editing is necessary in producing the final PA.**

Response: Care has been taken to improve the quality of technical editing.

Comment: **The PA needs to acknowledge all other low-level (including mixed-waste) disposal facilities at the Hanford Site and the plans for PA of these facilities.**

Response: Additional solid low-level waste and mixed low-level waste facilities the Hanford Site exist or are planned for use. The following were not explicitly discussed in the preliminary draft but are addressed in the final PA:

1. Currently operating burial grounds contiguous to Burial Ground 218-W-5; for example: 218-W3A, 218-W-3AE, and 218-W-4C. Disposal of waste in these burial grounds has been incorporated in this analysis. The basis for this decision is spatial closeness of the burial grounds which would result in a single contaminant waste plume emanating from the collective burial grounds. Some hydrogeologic differences do exist in the surface portions of the Hanford formation soils. The importance of these differences are addressed through sensitivity analyses of hydrogeologic parameter influences on travel time and peak concentrations (Section 4.2.2.3.3). In particular, in the near-surface Hanford formation in 216-W-3A and 216-W-3AE, the particle size distribution is dominated by

gravel and cobble sized boulders compared to coarse sand in 216-W-5. The sensitivity analyses show that the only significant change is a slight increase in travel time and no significant change in peak concentrations.

2. Nearly constructed mixed waste facility in Burial Ground 216-W-5: A RCRA compliant mixed waste disposal facility is nearly completed in the southern portion of Burial Ground 218-W-5. In this PA analysis, the facility is treated as if it were a low-level waste trench (Section 2.6). The justification for this assumption is two-fold. First, no credit is taken for any of the design features of the mixed waste facility, such as the liner leachate collection system. The facility cover will ultimately function in the same fashion as the covers for the low-level waste trenches. Second, the waste to be placed in the trench is currently projected to be contaminated soils. Thus, it is expected that the hazardous constituents will be primarily metals. It is not expected that these constituents will have any significant effect on radionuclide behavior. Consequently, the radioactive components of the mixed waste can be treated as constituents of low-level waste.

3. The Environmental Restoration Disposal Facility (ERDF): The ERDF is a potentially large single mixed waste facility located just south of and between the 200 East and 200 West Areas on the Hanford Plateau. It is intended for the disposal of waste generated by the Comprehensive Environmental Response, Compensation, and Liability Act (CERCLA) cleanup of Hanford waste sites, primarily in the 100 Areas and the 300 Area. A separate PA analysis is being completed for this facility. The preliminary PA report is scheduled to be sent to the PRP early in fiscal year 1995.

4. Active solid waste burial grounds are present in the northeast and northwest corners of the 200 East Area. A separate PA analysis will be completed for these burial grounds. The preliminary PA report is scheduled to be sent to the PRP early in fiscal year 1996.

Comment: **The potential for contaminant plumes from other current or planned low-level waste disposal facilities adding to those from 218-W-5 must be considered.**

Response: Numerous contaminant plumes are present in the unconfined aquifer beneath the 200 Area Plateau that have resulted from the disposal of wastewater from various processing facilities into ponds, cribs and ditches. Radionuclides present in the plumes include ^{3}H, ^{129}I, ^{106}Ru, ^{99}Tc, and uranium (see Appendix A for areal maps). The analyses for these liquid effluents are compiled in the report *Liquid Effluent Study Final Project Report*, WHC-EP-0367 (August 1990). The averaged infiltration rate, f, from 27 disposal sites is 5.45×10^{-4} cm/s. The infiltration rate was estimated on the basis of the rate of effluent disposal and the area of the disposal facility. Compared to the infiltration rate of

1.58×10^{-7} cm/s (high recharge case, 5 cm/yr) from 218-W-5 LLW disposal facility, the infiltration rate for liquid effluent is three orders of magnitude higher. The travel time for these liquid effluents is on an order of months, not years, through vadose zone. As a result, the major portion of the radionuclides released has entered an unconfined aquifer. Evaluation of estimated plume development from the 200 West Area Burial Grounds (Section 4.3.3) with current contaminant plumes indicates that current unconfined aquifer plumes will dissipate before the arrival of the solid waste plume.

Other potential plumes may occur beneath the 200 Area Plateau as the result of solid waste disposal in other locations on the Plateau. These include (1) solid waste burial grounds in the 200 East Area, (2) A commercial low-level waste disposal facility (U.S. Ecology) just south of the 200 Areas, (3) an ERDF adjacent to U.S. Ecology, and (4) a potential LLW facility east of the 200 East Area resulting from remediation of the double-shell tanks. An increase in potential dose as a result of interaction between contaminant plumes from the 200 West Area Burial Grounds and others requires mixing of plumes along the same groundwater flowpath. Flowpaths (see Figure 4-14) estimated from the water table map 1944 (Section 4.3.3) indicate that a possible mixing of plumes results from solid waste burial grounds in the 200 West Area and 200 East Area.

However, the peak concentration of a plume from West Area to the East Area will be diminished by a factor of about 8 due to the dispersive process. The estimate is conservative because the values of dispersivities which were used correspond to a scale of tens of meters. For a large scale (about 8 km from 200 West Area to 200 East Area) the values of dispersivities are expected to increase. A separate PA analysis for the 200 East Area will be performed and should make a correction if the two plumes are additive.

The mixing with the plumes from other disposal sites is not expected to occur.

Comment: **The potential for exposure from the air pathway must be addressed.**

Response: Three radionuclides are considered capable of transport in the vapor state under ambient conditions: ^{14}C, ^{3}H, and ^{222}Rn. An analysis has been conducted to consider the dose potential from this pathway for each of these isotopes (Section 4.3.1). Both intruder and offsite dose have been considered. The results indicate that these pathways have an influence only in the case of ^{3}H vapor transport to an inadvertent intruder in the postexcavation scenario. The waste acceptance criterion for Category 1 ^{3}H (concentration limit) has been adjusted accordingly.

Comment: **Although the draft PA discussed sensitivity extensively, there was no discussion of uncertainty. The final PA will need to discuss uncertainty.**

Response: Separate discussions are provided in the analysis to distinguish sensitivity and uncertainty analyses for intruder and groundwater pathways. For the intruder analyses, sensitivity and uncertainty analyses are provided in Sections 4.1.2 and 4.1.3, respectively. For the groundwater analyses, sensitivity and uncertainty analyses are provided in Sections 4.2.2 and 4.2.5, respectively. In the sensitivity analyses, parameters are systematically varied to determine the effect each has on dose estimates. In the uncertainty analyses, ranges of dose variability around the base case estimates are calculated as a function of expected ranges in key parameter values.

Comment: **The effect of variation in the chemical and physical form of radionuclides in the waste on radionuclide migration must be discussed.**

Response: Chemical and physical form of radionuclides in waste is important only for those radionuclides whose mobility in the disposal facility environment (i.e., release characteristics) is significantly changed by these characteristics (e.g., ^{14}C, ^{237}Np, ^{99}Tc, uranium in grout and radionuclides in activated metal such as ^{14}C). The solubility of uranium, in soil, and grout, and the diffusion control of uranium release in grout are utilized in this analysis (Section 4.4.2.1). Also, the immobilization of ^{14}C by grout and an activated metal matrix has been used in the evaluation of some special wastes (Appendix F).

Comment: **The PRP applauds the approach of using the PA to establish waste acceptance criteria (WAC). However, the linkage between intruder-based and groundwater-based limits needs to be clearly established.**

Response: A primary goal of the PA analysis is to support the development of a disposal system that satisfies dose limit criteria for both intruder and groundwater pathways. The analyses are used to establish WAC that take the form of concentration and inventory limits for a given set of facility and site-specific conditions. In this analysis, each isotope was evaluated to determine limits. It was assumed that two sets of limits were conceivable for every isotope corresponding to intruder and groundwater limits. The two types of limits are not linked in any way because the scenarios do not share common assumptions. If a given radionuclide must satisfy both types of limits, then one of the limits would end up being more limiting, but each would be part of the WAC. This relationship is described in Section 4.4.3. As it turns out, only the long-lived groundwater mobile radionuclides are required to satisfy both types of criteria.

Comment: **The final PA should have some detailed discussion of how PA results will be implemented in the WAC.**

Response: The application of PA results to quantification of WAC are listed in a WAC document (WHC-EP-0063), which regulates the acceptability of waste for disposal at the Hanford low-level burial grounds. The details of what appears in this document are summarized in Section 5.3. The primary components are a listing of intruder concentration limits and groundwater dose limits. In addition, other requirements from the PA analysis are also provided such as depth of burial requirements, stability requirements, and waste form requirements.

Comment: **The potential for a few high-concentration packages to cause the groundwater limits to be exceeded, even though a total facility inventory is not exceeded, should be discussed.**

Response: A groundwater release and transport analysis has been done in which the total quantity of a radionuclide is placed on one node in the sample trench as opposed to homogenous distribution in the trench (Section 4.2.2.4.1). The results indicate that as long as the total curie content for a given radionuclide remains the same in the same segment of trench, parallel to flow, regardless of trench length, the peak groundwater concentrations remain the same.

Comment: **The PRP is concerned that the projected land use for Burial Ground 218-W-5 may not be consistent with regional land use. For example, if large-scale irrigation is practiced, the estimate of maximum recharge of 5 cm/yr may not be conservative.**

Response: Large-scale irrigation is practiced in land contiguous to the Hanford Site and it is conceivable that similar agricultural practices could evolve on the Hanford Site over time. Certainly, in the near future, there will be no agricultural practice onsite and a joint committee of U.S. Department of Energy (DOE) staff, state environmental staff, and concerned citizens have issued a report recommending that the 200 Area Plateau be used as a permanent waste disposal site. These intentions do not eliminate the possibility that large-scale agriculture may occur at the site. If this were to occur, it is likely that water for irrigation would be pumped from the Columbia River. Several cases were considered in which differential infiltration was assumed with the undisturbed facility cover reducing the allowable infiltration rate relative to the surrounding soil (Section 4.2.2.2). The results indicate that the cover infiltration rate dominates the surrounding soil infiltration rate when calculating the peak concentration and therefore dose. Thus, it is concluded that only small increases in dose are possible if large-scale irrigation does in fact substantially increase the infiltration rate.

Comment: **Plans for developing a closure plan for the burial ground must be discussed.**

Response: A discussion of burial ground closure plans is provided (Section 5.3). At a minimum, a RCRA-type cover will be required for the mixed waste facilities. Low-level waste facilities will utilize some of the features of the Hanford Barrier, the minimum being a vegetative soil cover which is the primary control of infiltration.

Comment: **The draft PA suffers from a lack of integration and interpretation of results. This is a critical section of a PA and must be included in the final document.**

Response: A section (4.4) has been added to more clearly define the integration and interpretation of the results. Much of this discussion was in Sections 4.2 to 4.4 of the preliminary draft and has been reorganized. The integration and interpretation section includes four focal points: (1) identification of significant mechanisms and parameters influencing radionuclide release, (2) identification of major uncertainties in the analyses, (3) identification of conservatisms incorporated in the scenario development, and (4) a summary of the development of WAC.

Comment: **In view of the uncertainty in the waste to be disposed in the 218-W-5 facility, the PRP is concerned that care must be exercised in establishing and implementing WAC and generator characterization/certification plans to ensure that performance objectives are not exceeded.**

Response: As described in a previous response, an interface has been established between PA-driven WAC and the disposal operator and generator through the development of the Westinghouse WAC manual. The document is updated as needed and is expected to incorporate PA requirements as needed.

Comment: **The "base cases" presented in the draft PA need to be justified as best estimate cases.**

Response: Much of the primary information for justifying the base cases is present in the draft PA. The discussion has been reorganized to focus on the rationale for justifying the base case as the best estimate case. Best estimates are most important for critical parameters affecting radionuclide release and transport. Best estimate parameter values are based on the concept that a higher dose is calculated than could actually occur under real condition. The values are also chosen such that a worst case or improbably high dose is not calculated. The critical parameters are infiltration rate, source-term release rates, hydrogeologic parameters and geochemical reactions in the vadose zone. Infiltration rates affect travel time in the vadose zone and radionuclide flux out of the facility. Hydrogeologic parameters affect travel time. Geochemical factors affect travel time and groundwater concentrations. Selection of infiltration rates is

based on an extensive data set from numerous lysimeter experiments that establish the importance of soil and vegetation types in controlling infiltration and also quantify ranges of expected values. Hydrogeologic parameters are based on the only available set of moisture content permeability data for the vadose zone and filed measurements for the unconfined aquifer. Values have been chosen within ranges of potential values that result in faster travel times and higher peak radionuclide concentrations. Sorption coefficients are bracketed by orders of magnitude and the lower end of the bracket is chosen that is appropriate for each radionuclide.

The one exception to this philosophy was the selection of a very high infiltration rate for the Category 1 facility. The purpose of this assumption was to identify waste that could be disposed in the most cost-efficient fashion and still satisfy the performance objectives. The analysis suggests that a large amount of waste that has been disposed and is likely to be disposed will fall into this category. It remains to be seen whether or not this option is exercised in the operation and closure of the burial ground.

Comment: **The discussion of flooding on pages 2-11 and 2-12 is not clear. Is a 100-yr flood or the probable maximum flood being considered?**

Response: The flood is a maximum probable flood. The discussion is clarified in the text (Section 2.2.1).

Comment: **The potential for deep-rooted vegetation to increase recharge or to translocate contaminants needs to be discussed.**

Response: The probability that deep-rooted natural vegetation can increase recharge is considered to be very low. Under normal conditions, when a deep-rooted plant is healthy, it removes water from the soil through transpiration and is a primary effective means of minimizing infiltration. The lysimeter studies referred to in the text document this mechanism.

If deep-rooted plants do penetrate waste, transfer of radionuclides from the waste material to the soil horizon can happen. For the intruder, the significance of this pathways is assessed by comparing contamination in the soil by root uptake the contamination caused by exhumation of waste and mixing in soil (postdrilling and postexcavation scenario). Because relatively few species are deep-rooted and abundant (sagebrush being the primary plant species), the relative quantity of radionuclides translocated to the surface is expected to be much less than the assumption of direct exhumation of waste. Consequently, the potential dose from biotic transport must be less than that calculated for the postdrilling scenario. The other types of vegetation to consider are typical crops. A standard burial cover system is expected to exceed 3 m in depth and few, if any, crops will have root systems that can get to the waste. Consequently, dose from this mechanism is expected to be inconsequential.

Comment: **The anticipated low recharge rate may give opportunity for upward migration of contaminants and this has not been considered. The potential for upward migration and subsequent impact on resuspension or other pathways should be considered.**

Response: A simple analytical approach has been taken to estimate the relative upward movement of contaminants by diffusion versus the downward movement by advection (Section 4.3.2). The results indicate that even under extremely low infiltration rates, maximum transport upward (regardless of time) is less than a meter for completely mobile radionuclides (Kd=0). It is expected that covers can be engineered to essentially prevent erosion. It is also expected that periodic high precipitation events will occur that would negate any upward movement by diffusion. Therefore, this pathway is of no consequence.

Comment: **Graphical depiction of results (such as contaminant plume maps) will aid in understanding of the results.**

Response: Plume maps are added to illustrate the results.

Comment: **Calibration/verification of VAM3D using data from the injection test in 200 East Area (or other data) should be pursued and discussed in the final document. Some effort to validate the models used is essential to providing confidence in the model results. The use of such data may aid in assigning dispersivities.**

Response: A discussion of the calibration/verification efforts to date is provided in Appendix G.

Comment: **Additional support is needed for the spatial averaging of properties. The PRP is concerned about the potential for preferential flow paths in the vadose zone that may significantly shorten travel times.**

Response: Two types of potential preferential flow paths are recognized in the analysis. The first is the secondary channel that apparently existed during the deposition of the Hanford formation. This channel runs on a north-south axis through Burial Grounds 216-W-3A to 216-W-4C. The stratigraphic data shown in Appendix A indicates that the channel had a scouring effect only on the soil layer directly beneath the Hanford formation, the early Palouse formation. To assess the effects on peak groundwater concentrations, a sensitivity study was completed (Section 4.2.2.3.3) in which the gravel hydrologic properties of the gravel dominated soil of the channel sediments was substituted in the Hanford formation for the sand properties used in the base case. The changes in peak concentrations were slight.

The second potential preferential path is the clastic dike which is a vertical feature that occurs sporadically in the Hanford formation (although none are reported in the 200 West Burial Grounds) whose hydrologic properties are not well known but could serve as a conduit for more rapid transport through the vadose

zone. A sensitivity study was completed (Section 4.2.2.3.4) in which a dike filled with gravel occurred directly beneath a trench. The analysis indicates that no significant change in peak concentration occurs at the 100-m well downstream from which water is assumed to be drawn. Therefore, it is concluded this preferential flow path is also not significant.

Comment: **The final PA needs to consider the regional hydrogeology and the scale of hydrogeologic features as the discretization and assignment of properties in the groundwater model are discussed. The PA should establish that the model represents the site being studied.**

Response: A more detailed description of regional hydrology is provided in Section 2.1.7 and Appendix A. The additional data is used to demonstrate that the model is representative of regional characteristics. The most important point is that the expected general direction of hydrologic flow in the aquifer is uniform across the site.

Comment: **The PRP is concerned that Burial Ground 218-W-5 has not been simulated in the model. For example, it has been assumed that the maximum groundwater concentration will be at 100 m from the trench rather than using the model to determine the point of maximum concentration. Also there has been no consideration given to the impact of multiple trenches.**

Response: The observation from current modeling is that increased distance leads to increased dilution of the contaminant plume because of dispersive properties. Thus, concentrations at 100 m will exceed those at further distances. Unless there is some hydrogeologic feature that could concentrate groundwater contaminants, this assumption holds true. From Figure 4-14, the flowpaths show nearly one-dimensional flow in the area adjacent to the 200 West Area LLBG and thus support this assumption. The groundwater flows dominantly from west to east at the Hanford Site. This is the conceptual basis for an adoption of a 2-dimensional layer case model.

Multiple trenches are present in the 200 West Burial Grounds. The modeling analysis considered one trench orthogonally oriented to the direction of flow with a 1-m width perpendicular to flow and 20 m parallel to flow. A unit concentration (Ci) of any radionuclide was assumed as the initial inventory. Subsequently, a dose from release and transport to the compliance point is calculated. A back calculation is completed to determine the inventory in that trench which equates to the dose limit. To apply this limit to multiple trenches in the 200 West Area Burial Grounds, the width of the trench perpendicular to the expected primary direction of groundwater flow is determined and each meter of width is allowed the total activity quantified in the calculation, regardless the length of the trench. There is some additional activity allowed in the trenches as their length

parallel to the direction of groundwater flow increases. This additional amount has not been assumed in the calculation of acceptable inventory.

Comment: **The development of the conceptual groundwater model must be made clear. Consideration must be given to the regional hydrogeology, seasonal precipitation, transient effects, etc. The logical process of formulating the conceptual model into the calculational model must be discussed.**

Response: To give a more complete description of the conceptual model, a more detailed description of the regional geohydrologic conditions is given (Section 2.1.7). The discussion of the regional characteristics is tied to the assumptions used in the conceptual model such as the decision to use a layer cake approach, the quantification of the hydraulic gradient, a description of the evolution of the groundwater system from pre-Hanford conditions to present conditions to expected conditions as the impact of Hanford activities decreases with time. A description and rationale for conservatisms assumed in the model are also provided to increase confidence in the conservatism of the dose calculations. Additional sensitivity analyses have been done to evaluate the variability of additional parameters of the conceptual model (i.e., hydraulic conductivity and hydraulic gradients).

Comment: **The sensitivity of model results to changes in hydraulic conductivity values must be assessed. The representation of field hydraulic conductivity by laboratory-determined conductivity values must be justified.**

Response: Additional analyses have been completed in which saturated hydraulic conductivity values for all stratigraphic units has been increased (Section 4.2.2.3.1). This is a reasonable approach because hydraulic conductivity field measurements are typically one or two orders of magnitude higher than laboratory measurements. The results indicate that a relative reduction in groundwater concentration and, therefore, potential dose, occurs because the diluting volume in the unconfined aquifer increases by a factor of 10 and dominates all other effects.

Comment: **The discussion of flow and transport in the saturated zone must be amplified. For example, what is the extent of vertical dispersion?**

Response: In the analysis, a conservative approach has been taken by assuming very little dispersion (see figures of plume distribution in Appendix C). Also, the estimate of groundwater concentration is taken from a series of nodes at the top of the unconfined aquifer that essentially captures the groundwater plume. Thus, a maximum groundwater concentration is estimated.

Comment: **The choice of modeling approach (i.e., two-dimensional versus one-dimensional or three-dimensional) must be justified.**

Response: In order to adequately estimate the contaminant transport in the partially saturated vadose zone and the unconfined aquifer, a two-dimensional approach was preferred over a one-dimensional approach. The flow field can be characterized satisfactorily using a two-dimensional approach since the velocity in vadose zone is dominantly vertical and the velocity in the unconfined aquifer is dominantly from west to east. An insufficient database is available to support a three-dimensional analysis. Furthermore, the two-dimensional approach permits less dispersion and tends to increase groundwater concentration estimates.

Comment: **Plans for monitoring to assess the performance of the facility should be discussed. The discussion should indicate how contaminants from Burial Ground 218-W-5 will be differentiated from those arising from other facilities.**

Response: As discussed in an earlier response, the primary concern is that contaminants from this facility might mix with other contaminant plumes and, in the process, enhance radionuclide concentrations and potential. As discussed in the previous question, plumes presently in the groundwater resulting from liquid waste disposal should have dissipated before solid waste plumes reach the unconfined aquifer. Thus, there should be no need to differentiate between these plumes. An evaluation of potential mixing of the 200 West Area LLBG plume with other LLW disposal site plumes has been provided (Section 4.4.3). Indications that the combination of low potential for mixing and dispersion effects should eliminate significant concentration increases. In any event, potential plumes from other disposal sites are downstream of the 200 West Area LLBG.

Measurement of contaminants from the 200 West Area Burial Grounds are potentially detectable in downstream groundwater monitoring wells. However, several factors inhibit actual measurement of these contaminants. First, the lowest travel time calculated for nonsorbing radionuclides is more than 100 yr under extremely conservative conditions (high infiltration rate). This calculation also does not include the effects of containers which have some finite short-term lifetime that increases the length of travel time. In addition, the quantity of long-lived mobile radionuclides actually in the disposal facilities is not large and actual dispersion effects which can only be considered qualitatively in the PA analysis probably prevent these nuclides from reaching the groundwater table in the near term or at least in measurable quantities.

The discussion in Chapter 5 links development of monitoring systems with the burial ground closure program. Emphasis is placed on the use of lysimeters and/or moisture probes in the cover as the primary monitoring approach.

This page intentionally left blank.